

HUMAN SECTIONAL ANATOMY

Atlas of body sections, CT and MRI images

THIRD EDITION

Harold Ellis ● Bari M Logan ● Adrian K Dixon

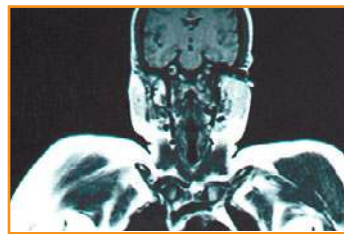
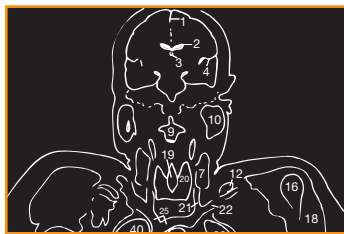
HUMAN SECTIONAL ANATOMY

This page intentionally left blank

HUMAN SECTIONAL ANATOMY

Atlas of body sections, CT and MRI images

THIRD EDITION



● **HAROLD ELLIS**
CBE MA DM MCh FRCS
FRCOG

Professor
Applied Clinical Anatomy
Group
Applied Biomedical Research
Guy's Hospital
London, UK

● **BARI M LOGAN**
MA FMA Hon MBIE
MAMAA

Formerly University Prosector
Department of Anatomy
University of Cambridge
Cambridge, UK
and
Formerly Prosector
Department of Anatomy
The Royal College of Surgeons
of England
London, UK

● **ADRIAN K DIXON**
MD FRCP FRCR FRCS
FMedSci

Professor
Department of Radiology
University of Cambridge
and
Honorary Consultant
Radiologist
Addenbrooke's Hospital
Cambridge, UK
and
Fellow, Peterhouse

Hodder Arnold

A MEMBER OF THE HODDER HEADLINE GROUP

First published in Great Britain in 1991 by Butterworth-Heinemann
Second edition 1999
This third edition published in 2007 by Hodder Arnold
Hodder Arnold, an imprint of Hodder Education and a member of the Hodder Headline Group,
an Hachette Livre UK Company
338 Euston Road, London NW1 3BH

<http://www.hoddereducation.com>

© 2007 Harold Ellis, Bari M Logan and Adrian Dixon

All rights reserved. Apart from any use permitted under UK copyright law, this publication may only be reproduced, stored or transmitted, in any form, or by any means, with prior permission in writing of the publishers or in the case of reprographic production in accordance with the terms of licences issued by the Copyright Licensing Agency. In the United Kingdom such licences are issued by the Copyright Licensing Agency: Saffron House, 6–10 Kirby Street, London EC1N 8TS

Whilst the advice and information in this book are believed to be true and accurate at the date of going to press, neither the authors nor the publisher can accept any legal responsibility or liability for any errors or omissions that may be made. In particular (but without limiting the generality of the preceding disclaimer) every effort has been made to check drug dosages; however, it is still possible that errors have been missed. Furthermore, dosage schedules are constantly being revised and new side-effects recognized. For these reasons the reader is strongly urged to consult the drug companies' printed instructions before administering any of the drugs recommended in this book.

British Library Cataloguing in Publication Data
A catalogue record for this book is available from the British Library

Library of Congress Cataloging-in-Publication Data
A catalog record for this book is available from the Library of Congress

ISBN 978 0 340 91222 5

1 2 3 4 5 6 7 8 9 10

Commissioning Editor:	Sarah Burrows
Development Editor:	Naomi Wilkinson
Project Editor:	Francesca Naish
Production Controller:	Lindsay Smith
Cover Designer:	Helen Townson
Indexer:	Laurence Errington

Typeset in 11 on 13pt Meridien by Phoenix Photosetting, Lordswood, Chatham, Kent
Printed and bound in India

What do you think about this book? Or any other Hodder Arnold title?
Please visit our website: www.hoddereducation.com

• <i>Preface</i>	<i>viii</i>
• <i>Introduction</i>	<i>ix</i>
The importance of cross-sectional anatomy	<i>ix</i>
Orientation of sections and images	<i>xi</i>
Notes on the atlas	<i>xii</i>
• <i>References</i>	<i>xiii</i>
• <i>Acknowledgements</i>	<i>xiv</i>
• <i>Interpreting cross-sections: helpful hints for medical students</i>	<i>xv</i>

■ BRAIN	Series of Superficial Dissection [A–H]	2
	<i>Selected images</i>	
	3D Computed Tomograms [A–C]	8

■ HEAD	Axial sections [1–19 Male]	10
	<i>Selected images</i>	
	Axial Magnetic Resonance Images [A–C]	48
	Coronal sections [1–13 Female]	50
	Sagittal section [1 Male]	76
	TEMPORAL BONE/INNER EAR	
	Coronal sections [1–2 Male]	78
	<i>Selected images</i>	
	Axial Computed Tomogram [A] Temporal Bone/Inner Ear	80

■ NECK	Axial sections [1–9 Female]	82
	Sagittal section [1 Male]	100

■ THORAX	Axial sections [1–10 Male]	102
	Axial sections [1] Female Breast	122
	<i>Selected images</i>	
	Reconstructed Computed Tomograms, Images [A–C]	124
	Axial Computed Tomograms [A–D] Mediastinum	126
	Coronal Magnetic Resonance Images [A–C]	128
	Reconstructed Computed Tomograms, Images [A–E]	130
	Reconstructed 3D Computed Tomograms, Images [A–B]	132

■ ABDOMEN	Axial sections [1–8 Male]	134
	Axial sections [1–2 Female]	150
	<i>Selected images</i>	
	3D Computed Tomography Colonogram [A]	154
	Coronal Computed Tomograms [A–C]	156
	Axial Computed Tomograms [A–F] Lumbar Spine	158
	Coronal Magnetic Resonance Images [A–B] Lumbar Spine	160
	Sagittal Magnetic Resonance Images [A–D] Lumbar Spine	162
<hr/>		
■ PELVIS		
	MALE – Axial sections [1–11]	164
	<i>Selected images</i>	
	Coronal Magnetic Resonance Images [A–C]	186
	FEMALE – Axial sections [1–7]	188
	<i>Selected images</i>	
	Axial Magnetic Resonance Images [A–B]	202
	Coronal Magnetic Resonance Images [A–C]	204
	Sagittal Magnetic Resonance Image [A]	206
<hr/>		
■ LOWER LIMB		
	HIP – Coronal section [1 female]	208
	<i>Selected images</i>	
	3D Computed Tomograms Pelvis [A–B]	210
	THIGH – Axial sections [1–3 Male]	212
	KNEE – Axial sections [1–3 Male]	215
	KNEE – Coronal section [1 Male]	218
	KNEE – Sagittal sections [1–3 Female]	220
	LEG – Axial sections [1–2 Male]	226
	ANKLE – Axial sections [1–3 Male]	228
	ANKLE – Coronal section [1 Female]	232
	ANKLE/FOOT – Sagittal section [1 Male]	234
	FOOT – Coronal section [1 Male]	236

■ UPPER LIMB

SHOULDER – Axial section [1 Male]	238
SHOULDER – Coronal section [1 Male]	240
<i>Selected images</i>	
3D Computed Tomograms Shoulder [A–B]	242
ARM – Axial section [1 Male]	244
ELBOW – Axial sections [1–3 Male]	245
ELBOW – Coronal section [1 Female]	248
FOREARM – Axial sections [1–2 Male]	250
WRIST – Axial sections [1–3 Male]	252
WRIST/HAND – Coronal section [1 Female]	256
WRIST/HAND – Sagittal section [1 Female]	258
HAND – Axial sections [1–2 Male]	260
• <i>Index</i>	262

Preface

The study of sectional anatomy of the human body goes back to the earliest days of systematic topographical anatomy. The beautiful drawings of the sagittal sections of the male and female trunk and of the pregnant uterus by Leonardo da Vinci (1452–1519) are well known. Among his figures, which were based on some 30 dissections, are a number of transverse sections of the lower limb. These constitute the first known examples of the use of cross-sections for the study of gross anatomy and anticipate modern technique by several hundred years. In the absence of hardening reagents or methods of freezing, sectional anatomy was used seldom by Leonardo (O'Malley and Saunders, 1952). Andreas Vesalius pictured transverse sections of the brain in his *Fabrica* published in 1543 and in the seventeenth century portrayals of sections of various parts of the body, including the brain, eye and the genitalia, were made by Vidius, Bartholin, de Graaf and others. Drawings of sagittal section anatomy were used to illustrate surgical works in the eighteenth century, for example those of Antonio Scarpa of Pavia and Peter Camper of Leyden. William Smellie, one of the fathers of British midwifery, published his magnificent *Anatomical Tables* in 1754, mostly drawn by Riemsdyk, which comprised mainly sagittal sections; William Hunter's illustrations of the human gravid uterus are also well known.

The obstacle to detailed sectional anatomical studies was, of course, the problem of fixation of tissues during the cutting process. De Riemer, a Dutch anatomist, published an atlas of human transverse sections in 1818, which were obtained by freezing the cadaver. The other technique developed during the early nineteenth century was the use of gypsum to envelop the parts and to retain the organs in their anatomical position – a method used by the Weber brothers in 1836.

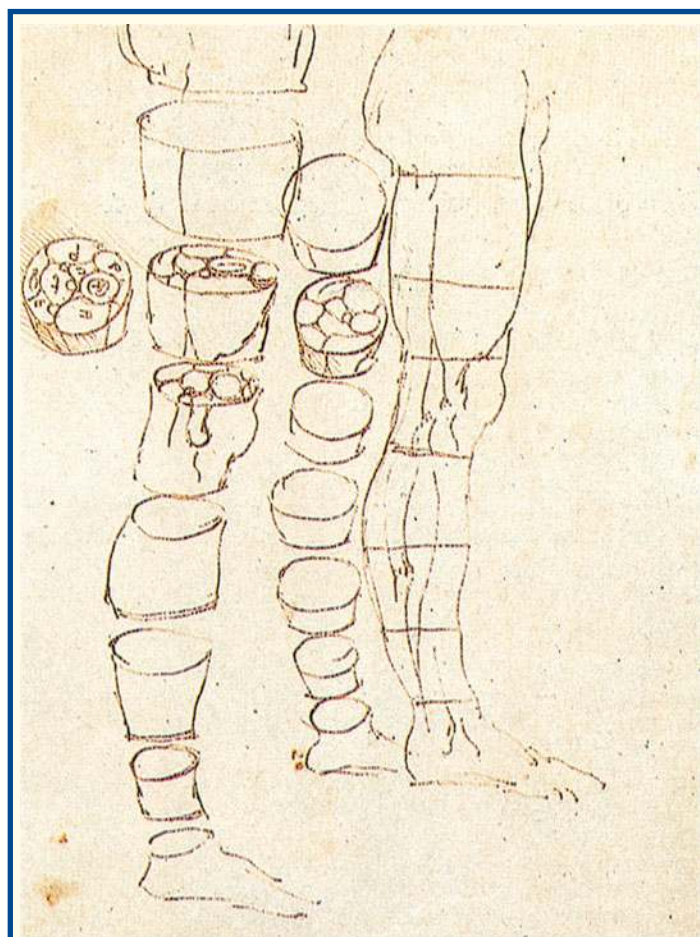
Pirogoff, a well-known Russian surgeon, produced his massive five-volume cross-sectional anatomy between 1852 and 1859, which was illustrated with 213 plates. He used the freezing technique, which he claimed (falsely, as noted above) to have introduced as a novel method of fixation.

The second half of the nineteenth century saw the publication of a number of excellent sectional atlases, and photographic reproductions were used by Braun as early as 1875.

Perhaps the best known atlas of this era in the United Kingdom was that of Sir William Macewen, Professor of Surgery in Glasgow, published in 1893. Entitled *Atlas of Head Sections*, this comprised a series of coronal, sagittal and transverse sections of the head in the adult and child. This was the first atlas to show the skull and brain together in detail. Macewen

intended his atlas to be of practical, clinical value and wrote in his preface 'the surgeon who is about to perform an operation on the brain has in these cephalic sections a means of refreshing his memory regarding the position of the various structures he is about to encounter'; this from the surgeon who first proved in his treatment of cerebral abscess that clinical neurological localization could be correlated with accurate surgical exposure.

The use of formalin as a hardening and preserving fluid was introduced by Gerota in 1895 and it was soon found that thorough perfusion of the vascular system of the cadaver enabled satisfactory sections to be obtained of the formalin-hardened material. The early years of the twentieth century saw the publication of a number of atlases based on this technique. Perhaps the most comprehensive and beautifully executed of these was *A Cross-Section Anatomy* produced by Eycleshymer and Schoemaker of St Louis University, which was first published in 1911 and whose masterly historical introduction in the 1930 edition provides an extensive bibliography of sectional anatomy.



Leonardo da Vinci. The right leg of a man measured, then cut into sections (Source: The Royal Collection © 2007 Her Majesty Queen Elizabeth II).

Introduction

■ The importance of cross-sectional anatomy

Successive authors of atlases on sectional anatomy have emphasized the value to the anatomist and the surgeon of being able to view the body in this dimension. It is always difficult to consider three dimensions in the mind's eye; to be able to view the relationships of the viscera and fascial planes in transverse and vertical section helps to clarify the conventional appearances of the body's structure as seen in the operating theatre, in the dissecting room and in the textbook.

The introduction of modern imaging techniques, especially ultrasound, computed tomography (CT) and magnetic resonance imaging (MRI), has enormously expanded the already considerable importance of sectional anatomy. The radiologist, neurologist, internist, chest physician and oncologist, as well as specialists in the various fields of surgery, have had to re-educate themselves in the appearances and relationships of anatomical structures in transverse and vertical section. Indeed, precise diagnosis, as well as the detailed planning of therapy (for example, the ablative surgery of extensive cancer) and of interventional radiology, often depends on the cross-sectional anatomical approach.

This atlas combines three presentations of cross-sectional anatomy – that of the dissecting room, CT and MRI. The series are matched to each other as closely as possible on opposite pages. Students of anatomy, surgeons, clinicians and radiologists should find the illustrations of anatomical cross-sections (obtained by the most modern techniques of preparation and photographic reproduction) and the equivalent cuts on imaging (obtained on state-of-the-art apparatus) both interesting and rewarding.

Preservation of cadavers

Preservation of the cadavers used for the sections in this atlas was by standard embalming technique, using two electric motor pumps set at a maximum pressure rate of 15 p.s.i. Preservative fluid was circulated through the arterial system via two cannulae inserted into the femoral artery of one leg. A partial flushing of blood was effected from the accompanying femoral vein by the insertion of a large-bore drainage tube.

After the successful acceptance of 20 L of preservative fluid, local injection by automatic syringe was carried out on those areas that remained unaffected. On average, approximately 30 L of preservative fluid was used to preserve each cadaver.

Following preservation, the cadavers were stored in thick-gauge polythene tubes and refrigerated to a temperature of 10.6 °C at 40 per cent humidity for a minimum of 16 weeks before sectioning. This period allowed the preservative solution to saturate the

body tissues thoroughly, resulting in a highly satisfactory state of preservation.

The chemical formula for the preservative solution (Logan *et al.*, 1989) is:

Methylated spirit 64 over proof	12.5 L
Phenol liquefied 80%	2.5 L
Formaldehyde solution 38%	1.5 L
Glycerine BP	3.5 L
Total	= 20 L

The resultant working strengths of each constituent is:

Methylated spirit	55%
Glycerine	12%
Phenol	10%
Formaldehyde solution	3%

The advantages of this particular preservative solution are that (i) a state of soft preservation is achieved; (ii) the low formaldehyde solution content obviates excessive noxious fumes during dissection; (iii) a degree of natural tissue colour is maintained, which benefits photography; and (iv) mould growth does not occur on either whole cadavers thus preserved or their subsequent prosected and stored parts.

Safety footnote

Since the preparation of the anatomical material for this book, in 1988, there have been several major changes to health and safety regulations concerning the use of certain chemical constituents in preservative (embalming) fluids. It is important, therefore, to seek local health and safety guidance if intending to adopt the above preservative solution.

Sectioning

In order to produce the 119 cross-sections illustrated in this atlas, five preserved cadavers, two male and three female, were utilised in addition to five upper and five lower separate limbs and two temporal bone specimens.

The parts to be sectioned were deep-frozen to a temperature of –40 °C for a minimum of 3 days immediately before sectioning.

Sectioning was carried out on a purpose-built AEW 600 stainless-steel bandsaw (AEW Delford Systems, Gresham House, Pinetrees Business Park, Salhouse Road, Norwich, Norfolk, NR7 9BB, England). The machine is equipped with a 10 horse power, three-phase electric motor capable of producing a constant blade speed of 6000 feet/minute.

A fine-toothed (four skip) stainless-steel blade was used, 19 mm in depth and precisely 1 mm in thickness (including tooth set).

The design and precision manufacture of the machine results, during operation, in the loss of only 1 mm of material between each section.

Sections were taken from the cadavers to the following thickness of cut:

Head	1 cm serial
Temporal bones	at selected levels
Neck	1.5 cm serial
Thorax	2 cm serial
Abdomen	2 cm serial
Pelvis male	2 cm serial
Pelvis female	2 cm serial
Lower limb	at selected levels
Upper limb	at selected levels

Computed tomography

Since the invention of CT by Hounsfield (1973), there has been renewed interest in sectional anatomy. Despite the high cost, CT systems are now used widely throughout more affluent countries. Radiologists in particular have had to go through a rapid learning process. Several excellent sectional CT anatomy books have been written. More modern CT technology allows a wider range of structures to be demonstrated with better image quality, due mainly to improved spatial resolution and shorter data-acquisition times. Spiral CT techniques have lowered data acquisition time further still, allowing a volume acquisition during a single breath-hold – hence, the justification for yet another atlas that correlates anatomical and CT images. The development of multidetector CT allows multiple thin sections to be acquired during a single breath-hold. The computer can then assimilate this volume of data, from which coronal, sagittal and 3D images can be extracted.

Most of the images in this volume have been obtained on Siemens (Forchheim, Germany) CT systems in Addenbrooke's Hospital, Cambridge. Imaging protocols have continued to evolve from the original descriptions (e.g. Dixon, 1983a), particularly with the advent of spiral data acquisition. Oral contrast medium is often given for abdominopelvic studies; thus, the stomach and small bowel sometimes appear opaque. Intravenous contrast medium provides additional information and thus, in some sections, vessels appear opaque.

Precise correlation between the cadaveric sections and the clinical images is very difficult to obtain in practice. No two patients are quite the same shape. The distribution of fat, particularly in the abdomen, varies from patient to patient and between the sexes (Dixon, 1983b). Furthermore, there are the inevitable physiological discrepancies between cadaveric slices and images obtained in vivo. These are especially

noticeable in the juxta-diaphragmatic region. In particular, the vertebral levels do not quite correlate because of the effect of inspiration; all intrathoracic structures are better displayed on images obtained at suspended inspiration. Furthermore, in order to obtain as precise a correlation as possible, some CT images may not be quite of optimal quality. A further difficulty encountered when attempting to correlate the two sets of images is caused by the fact that CT involves ionizing radiation. The radiation dose has to be kept to the minimum that answers the clinical problem; thus, it is not always possible to find photogenic examples of the anatomy shown in the cadavers for all parts of the body.

Some knowledge of the X-ray attenuation of normal structures is useful to assist interpretation of the images. The Hounsfield scale extends from air, which measures –1000 HU (Hounsfield units), through pure water at 0 HU, to beyond +1000 HU for dense cortical bone. Most soft tissues are in the range +35 to +70 HU (kidney, muscle, liver, etc.). Fat provides useful negative contrast at around –100 HU. The displayed image can appear very different depending on the chosen window width (the spread of the grey scale) and the window level (the centre of the grey scale). These differences are especially apparent in Axial section 8 of the thorax, where the images are displayed both at soft-tissue settings (window 400, level +20 HU) and at lung settings (window *c.*1250, level –850 HU). Such image manipulation merely requires alteration of the stored electronic data at the viewing console, where any parameters can be chosen. The hard-copy photographic record of the electronic data is always a rather poor representation. Indeed, in clinical practice, it may be difficult to display all structures and some lesions on hard-copy film.

Magnetic resonance imaging

The evolution of MRI to its present status from long-established chemical magnetic resonance techniques has been gradual. A key milestone occurred when Lauterbur (1973) first revealed the imaging potential of MRI. Clinical images followed quickly, initially from Aberdeen and Nottingham (e.g. Hawkes *et al.*, 1980). Research by various manufacturers led to a plethora of techniques, moving towards shorter and shorter acquisition times, which are now approaching those of CT. Most of the MR images in this volume were obtained on GE (Milwaukee, USA) MR systems in Addenbrooke's Hospital, Cambridge.

The physics of MRI are substantially more complex than CT, even though the principles of picture elements (pixels) derived from volume elements (voxels) within the body are similar, along with the partial volume artefacts that can occur. Much of the computing and viewing software is similar; indeed, many manufacturers allow viewing of CT and MR images on the same viewing console.

Central to an MRI system is a very strong magnet, usually between 0.2 and 3.0 Tesla (T). 1 T = 10 000

Gauss; the earth's magnetic field strength is approximately 0.5 Gauss.

When the patient is in the magnet, the hydrogen protons within the body align their spins according to the strength and direction of the magnetic field. The hydrogen protons within the water of the body are particularly suitable for magnetic resonance techniques. At 1.0 T, protons within hydrogen nuclei resonate at approximately 42.6 MHz. The protons can be excited so that the net magnetism of the spins is flipped by the application of a radiofrequency signal. Gradient magnetic fields are applied to vary the precessional frequency. The emitted signal is detected as an echo to provide spatial information and data about the chemical environment of the protons within the voxel, etc.

Some common imaging sequences are:

- *Proton density images*: conventionally acquired using a long repetition time (TR; *c.*2000 ms between signals) and a short echo time (TE; *c.*20 ms) before readout. These provide a map of the distribution of hydrogen protons (mainly within water).
- *T1-weighted images*: conventionally acquired with short TR (*c.*700 ms) and short TE (*c.*20 ms). They are useful for demonstrating the anatomy. The T1 time of the tissue refers to the time taken for the longitudinal magnetism to decay following the radiofrequency (RF) pulse and involves energy loss to the lattice in the chemical environment.
- *T2-weighted images*: conventionally acquired using long TR (e.g. 2000 ms) and long TE (80+ ms). These images often show oedema and fluid most clearly and are good for demonstrating lesions. The T2 time of the tissue refers to the time taken for the transverse magnetism to decay following the RF pulse. It involves the way in which the spin of one proton interacts with the spins of neighbouring protons.
- *Fast imaging sequences*: in order to complete acquisitions quickly (e.g. within a breath-hold), numerous techniques have been devised. These include gradient echo sequences, whereby the magnetization is never allowed to recover fully. Other techniques involve a rapid succession (train) of RF pulses and echoes, requiring advanced computer processing.
- *Tissue-specific techniques*: the different environments of protons (fat, water, flowing blood, etc.) mean that protocols can be adapted to accentuate certain features. Fat can be suppressed by the application of a RF pulse at the resonant frequency of fat followed by a gradient pulse to null the signal from fat. Images can also be generated to show either static fluid or flowing blood.

Because of the range of possible sequences, the appearances of the resulting images vary considerably. It is important to realize that the grey scale of the image reflects the intensity of the

returning signal. There are no absolute values, such as in CT.

In general, fat returns high signal and appears bright (white), unless fat suppression is used (see above).

There is not sufficient water vapour in air to produce a signal. Therefore, air always returns very little signal and appears dark (black). Dense cortical bone also appears black; cortical bone has very tightly bound protons within its structure, and the lack of mobility results in reduced signal. Medullary bone contains a lot of fatty marrow and thus usually appears bright. Sequences can be performed so that blood within the vessels will return high signal; this is the basis of magnetic resonance angiography.

In the magnetic resonance images presented here, the sequence(s) have been chosen to demonstrate certain anatomical features to best effect. Thus, the precise parameters and the appearance vary extensively. On occasions, a proton density image and corresponding T2-weighted image are displayed side by side for optimal demonstration of anatomical features.

■ Orientation of sections and images

A concerted effort over recent years has meant that axial cross-sectional and coronal images are now viewed in a standard conventional manner. Hitherto, there was wide variation, which led to considerable confusion and even medicolegal complications.

All axial cross-sectional images in clinical practice are now viewed as shown in **Figure A**; that is, from 'below' and 'looking up'. This is the logical method, in so far that the standard way in which a doctor approaches the examination of the supine patient is from the right-hand foot end of a couch. The image is thus in the correct orientation for the doctor's palpating right hand. For example, the doctor has to 'reach across' the image in order to find the spleen, exactly as he or she would during the clinical examination of the abdomen. Similarly, for the head, the right eye is the one more accessible for right-handed ophthalmoscopy. Thus, all axial sections should be considered, learned and even displayed with an orientation logo shown in **Figure B**. This is the same orientation as that used for other images (e.g. chest X-ray). Here, again, the right of the patient is on the viewer's left, just as if the clinician was about to shake hands with the patient.

There is now worldwide agreement over this matter with regard to axial imaging. Furthermore, many anatomy books have adopted this approach so that students learn this method from the outset. Ideally, embryologists and members of all other disciplines concerned with anatomical orientation should, ultimately, conform to this method.

The orientation logo in **Figure B** is suitable for the head, neck, thorax, abdomen and pelvis. In the limbs, however, when only one limb is displayed, further clarification is required. All depends on whether a right or left limb is being examined. To

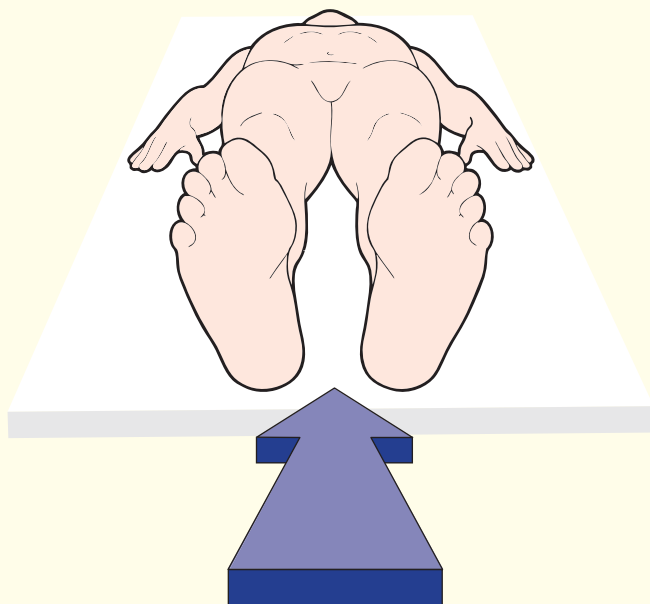


Figure A. View from below looking up

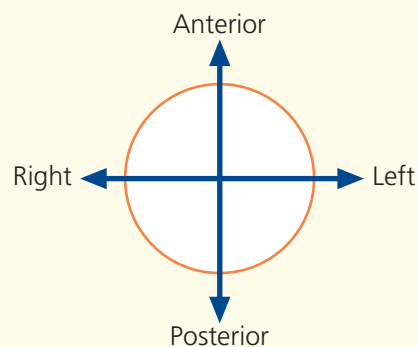


Figure B.

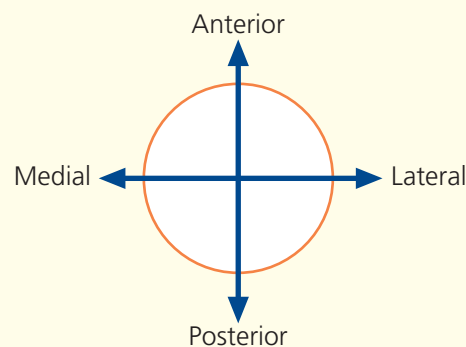


Figure C.

assist this quandary, a medial and a lateral marker is provided in **Figure C**. In this book, a left limb has been used throughout. Again, viewing is as from 'below'.

The orientation of coronal images has also been standardized so that they are viewed with the patient's right on the left, exactly as for a chest X-ray or when talking to the patient face to face.

There is no firm standardization of sagittal images. Various manufacturers display their images in different ways. Although there is a certain logic in viewing from the patient's right side, the visual approach for a clinician examining a patient on a couch, the majority of manufacturers display sagittal images viewed from the left. Thus, in this book most sagittal images are viewed from the left side of the patient.

Figure D, line A: the radiographic baseline used for axial head sections and images in this atlas has been selected as that running from the inferior orbital margin to the external auditory meatus. This allows most of the brain to be demonstrated without excessive bony artefact.

Figure D, line B: for sections and images of the neck and the rest of the body, a true axial plane has been used.

■ Notes on the atlas

This atlas presents various sections of the cadaver with corresponding radiological images. The logical sequence should enable the student to find the desired anatomical level with ease.

The numbers placed on the colour photographs and on the line drawings that accompany each

radiological image match, and the key to these numbers is given on the accompanying list on each page spread. Where numbers are in coloured boxes on the key, these refer to features that are apparent only on the radiological image.

Brief notes accompany each section and refer to important anatomical and radiological features.

In the majority of sections, bilateral structures have been labelled only on one side. This has been done in order to allow readers to have an unobscured view of

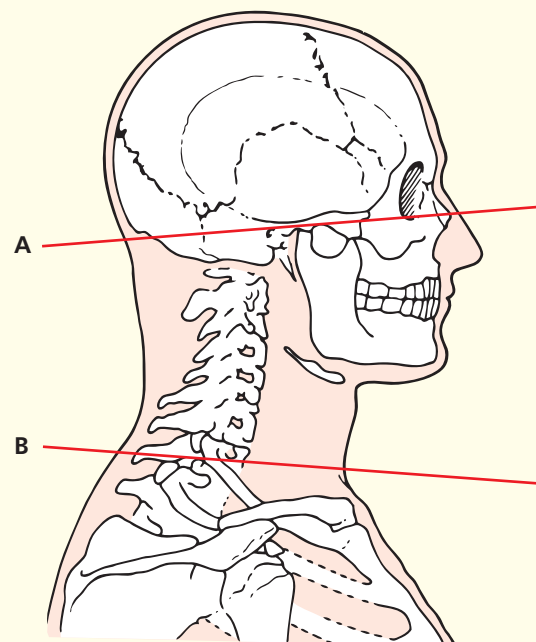


Figure D. Axial head sections

structures and to put their own anatomical knowledge to the test.

A series of views of a minimally dissected brain is provided in order to clarify the orientation of cerebral topography in the series of head sections.

The colour photographs of the brain dissections and of the sections of the upper and lower limb are of natural size. Those of the head and neck sections have been reduced slightly, and still greater reduction has been used in the thorax, abdomen and pelvis series in order to fit the page format.

Several spreads of selected images (e.g. mediastinum) have been included in order to show the features of important anatomical areas in more detail than can be demonstrated easily in cadavers and standard imaging.

Terminology

Terminology conforms to the International Anatomical Terminology – *Terminologia Anatomica* – created in 1988 by the Federative Committee on Anatomical Terminology (FCAT) and approved by the 56 member associations of the International Federation of Associations of Anatomists (IFAA).

Important changes to note are:

The Greek adjective ‘peroneal’ is now replaced by the Latin ‘fibular’ for various muscles, vessels, nerves and structures of the lower limb, e.g. Fibularis tertius instead of Peroneus tertius; Fibular artery instead of Peroneal artery; Common fibular nerve instead of Common peroneal nerve.

For this new edition, the term ‘peroneal’ is included italicized in brackets in order to help identify change, e.g. Common fibular (*peroneal*) nerve.

Note also that flexor accessories is now known as ‘quadratus plantae’.

References

- Dixon, A.K. (1983a) *Body CT: A Handbook*. Churchill Livingstone, Edinburgh.
- Dixon, A.K. (1983b) Abdominal fat assessed by computed tomography: sex difference in distribution. *Clinical Radiology* 34, 189–91.
- Eycleshymer, A.C. and Schoemaker, D.M. (1930) *A Cross-Section Anatomy*. Appleton, New York.
- Federative Committee on Anatomical Terminology (1988) *Terminologia Anatomica: International Anatomical Terminology*. Thieme, New York.
- Hawkes, R.C., Holland, G.N., Moore, W.S and Worthington, B.S. (1980) Nuclear magnetic resonance tomography of the brain. *Journal of Computer Assisted Tomography* 4, 577–80.
- Hounsfield, G.N. (1973) Computerized transverse axial scanning (tomography). *British Journal of Radiology* 46, 1016–102.
- Lauterbur, P.C. (1973) Image formation by induced local interaction: examples employing nuclear magnetic resonance. *Nature* 242, 190–91.
- Logan, B.M., Watson, M. and Tattersall, R. (1989) A basic synopsis of the ‘Cambridge’ procedure for the preservation of whole human cadavers. *Institute of Anatomical Sciences Journal* 3, 25.
- Logan, B.M., Liles, R.P. and Bolton, I. (1990) A photographic technique for teaching topographical anatomy from whole body transverse sections. *Journal of Audio Visual Media in Medicine* 13, 45–8.
- O’Malley, C.D. and Saunders, J.B. (1952) *Leonardo da Vinci on the Human Body*. Schuman, New York.

Acknowledgements

Dissecting room staff

For skilled technical assistance in the preservation and sectioning of the cadavers

Mr M Watson, Senior Technician
Mr R Tattersall, Technician
Ms L Nearn, Technician
Mrs C Bester, Technician
Mr M O'Hannan, Porter

Department of Anatomy, University of Cambridge

Audiovisual unit

For photographic expertise

Mr J Bashford
Mr R Liles LMPA
Mr I Bolton
Mr A Newman

Department of Anatomy, University of Cambridge

For the excellent artwork and graphics

Mrs Rachel Chesterton and Ms Emily Evans

Printing of colour photographs

Streamline Colour Labs, Cambridge

Secretarial

For typing of manuscript

Miss J McLachlan
Miss AJJ Burton
Miss S Clark
Mrs K Frans

Departments of Anatomy and Radiology, University of Cambridge

Annotation of central nervous system (brain and head sections)

Professor Roger Lemon

The Sobell Department of Neurophysiology, Institute of Neurology, London

Dr Catherine Horner

Lecturer in Neurobiology, Department of Anatomy, University of Cambridge

Annotation of head and limb sections

Dr Ian Parkin

Clinical Anatomist, Department of Anatomy, University of Cambridge

Computed tomography and magnetic resonance imaging

For performing many of the procedures

Mrs B Housden DCR
Mrs L Clements DCR
Mrs C Sims DCR
Mr D Gibbons DCR

and many other radiographers at Addenbrooke's Hospital, Cambridge.

Many radiological colleagues provided useful advice.

Dan Gibbons also kindly constructed many of the 3D generated CT images.

Production of the atlas

The authors would also like to thank the staff at Hodder Arnold Health Sciences for their help and advice in the production of this atlas, in particular:

Sarah Burrows, Commissioning Editor
Naomi Wilkinson, Development Editor
Francesca Naish, Project Editor
Joanna Walker, Production Manager
Lindsay Smith, Production Controller.

Interpreting cross-sections: helpful hints for medical students

When first confronted with an anatomical cross-section or a corresponding CT/MRI image, students are often overwhelmed by the amount of structural information on display to be identified. This apprehension may be overcome by adopting a logical approach to interpretation by appreciating the 'tight-packed' compartmental composition of a cross-section. The following series of 'build-up' pictures (A–L) of an anatomical axial cross-section have been created in order to illustrate this strategy of thought.



The above is an axial cross-section through the abdomen of an adult male subject.

Many important key structures are displayed, but where to begin identifying them in a logical sequence?

First establish:

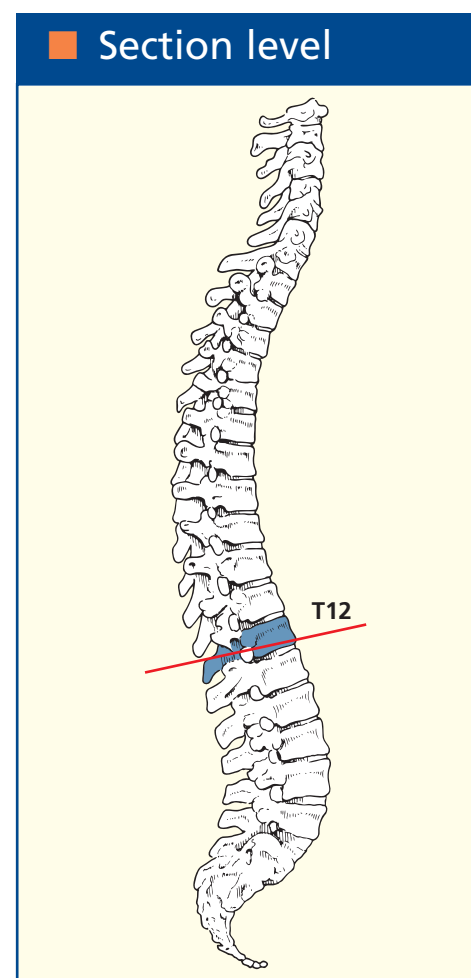
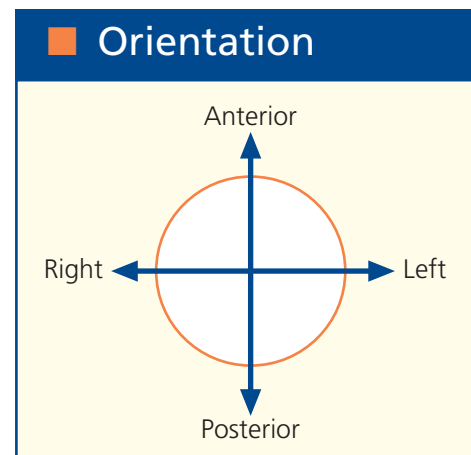
1. View:

Is the view looking up or down?
The orientation guide will solve this.

2. Section level:

Where does the slice pass through the body of the subject?
The section level guide will solve this.

Now begin a logical tour of the section, beginning over the page with picture A and build up your knowledge through the sequence of pictures to L.

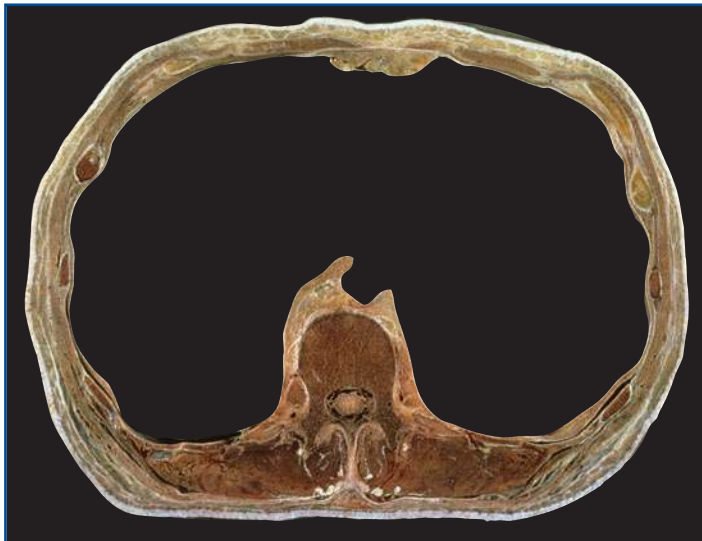




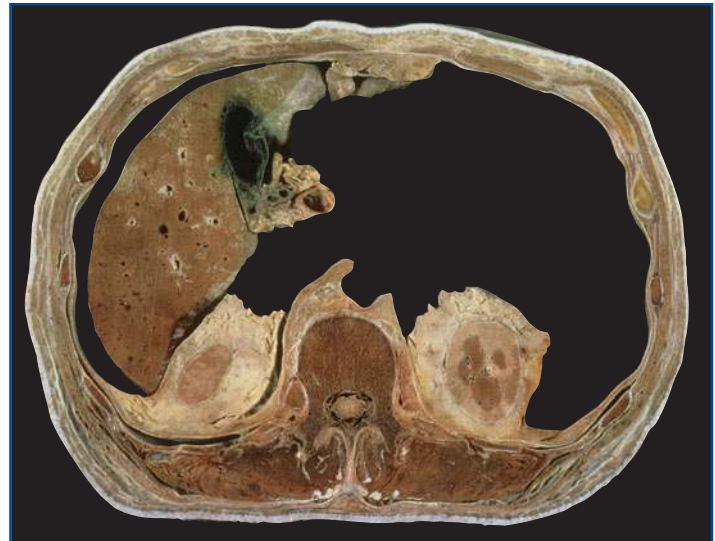
A Vertebral body of twelfth thoracic vertebra, spine, transverse process and laminae, spinal cord within the meninges.



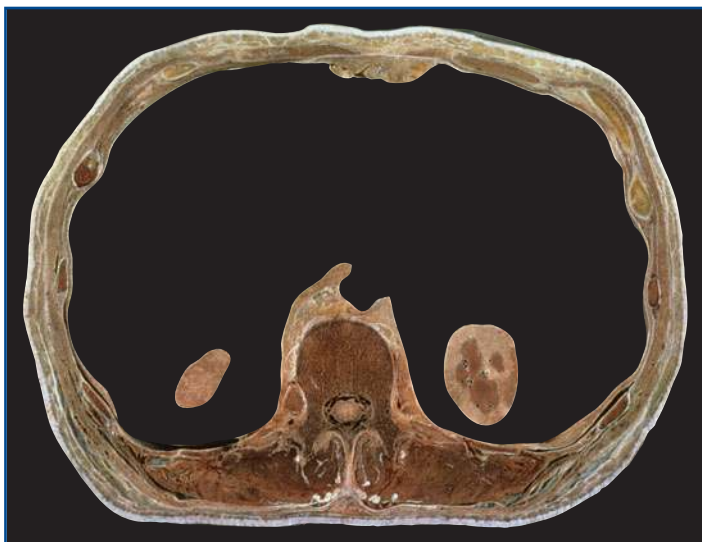
D Para and perirenal (perinephric) fat capsules surrounding the kidneys.



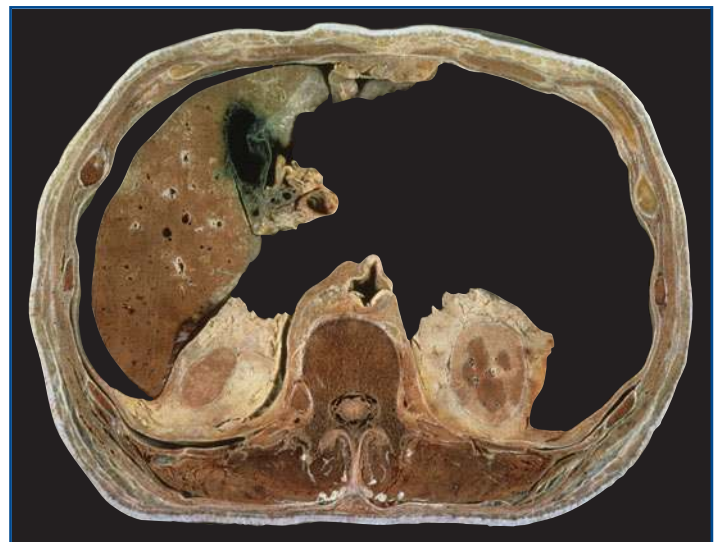
B Outer skin of abdominal wall and back, muscles of the abdominal wall, ribs, intercostal muscles, erector spinae muscles of back, psoas muscles. Appreciate the size of the abdominal cavity.



E Liver (green bile staining from the gall bladder), gall bladder, common bile duct, hepatic artery and portal vein (the largest of the three components of the portal triad).



C Left and right kidney; disparate in size because the left is positioned higher than the right within the abdomen.



F Aorta (misshapen in this subject due to arteriosclerosis). At this level (T12), it is just emerging behind the median arcuate ligament into the abdominal cavity.



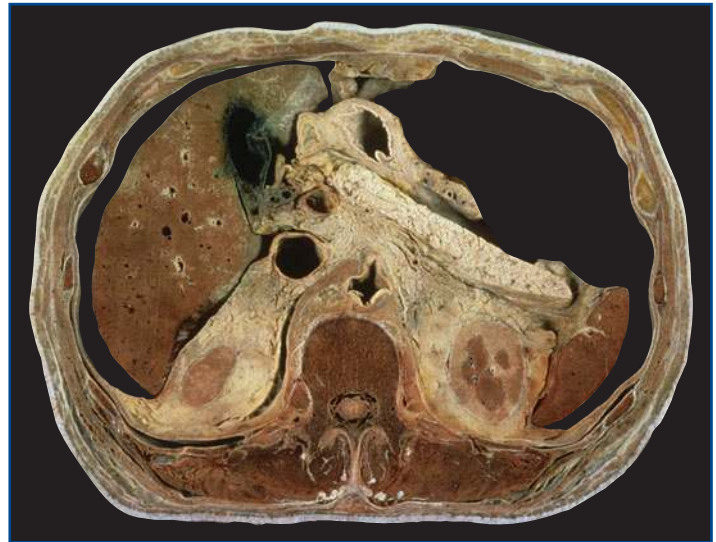
G Inferior vena cava separated from the portal triad by the epiploic foramen (foramen of Winslow).



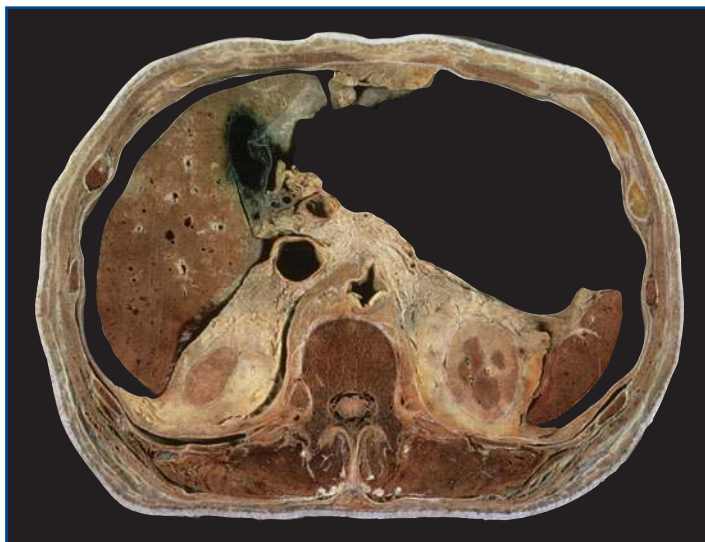
J The pancreas (head, body and tail).



H Adipose tissue containing small blood vessels, lymph nodes, lymphatics and the fine nerves of the sympathetic trunk.



K Stomach, part of pylorus with part of first part of the duodenum, right gastro-epiploic blood vessels within omentum.



I The spleen.



L Large bowel (portion of transverse and descending colon, the splenic flexure), surrounded by greater omentum.

A detailed account of a similar section to this with an accompanying CT can be found on pages 136–139.

This page intentionally left blank

HUMAN SECTIONAL ANATOMY

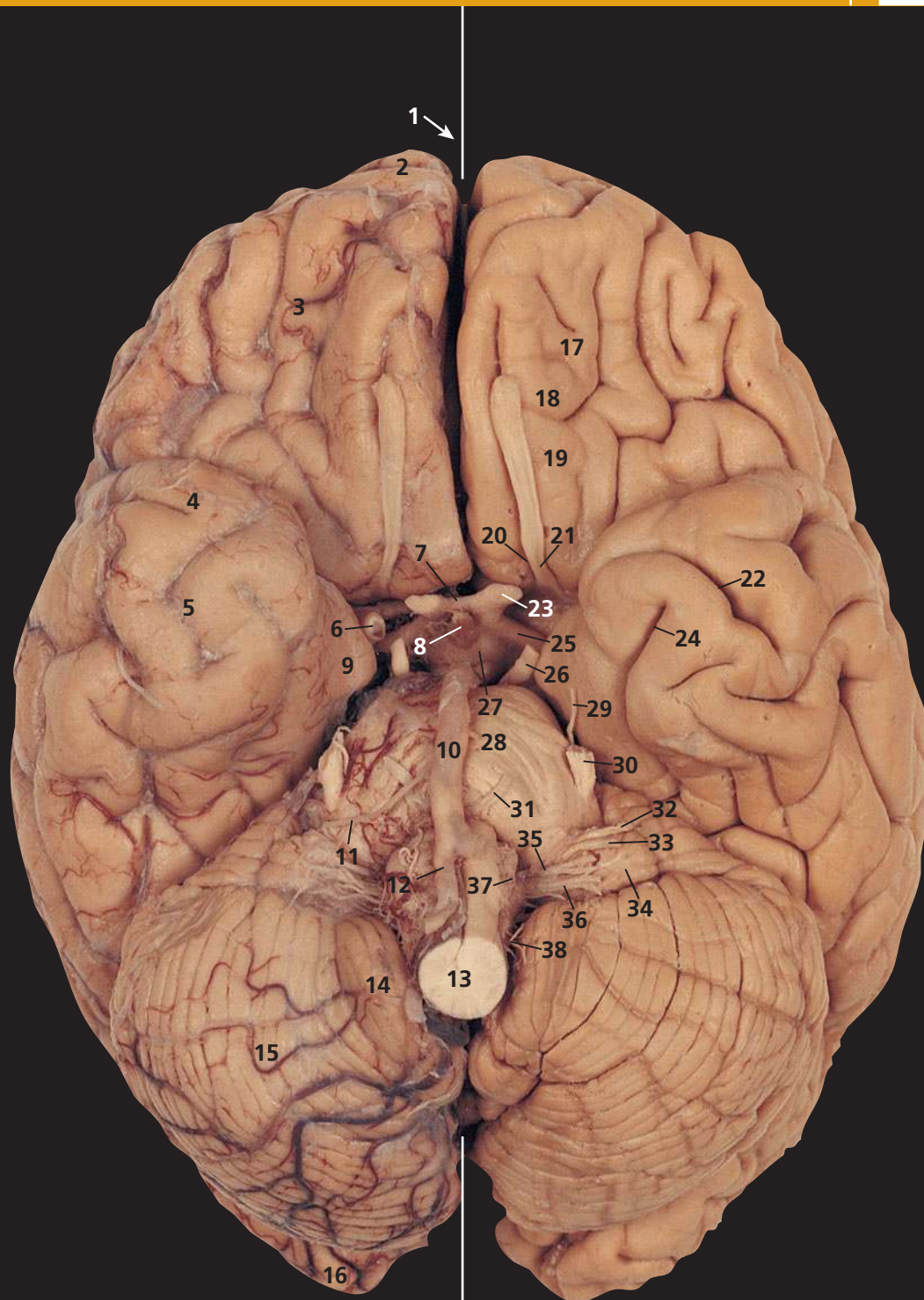


A Left cerebral hemisphere. From above, with the arachnoid mater and blood vessels removed

- 1 Longitudinal cerebral fissure (arrowed)
- 2 Frontal pole
- 3 Middle frontal gyrus
- 4 Superior frontal sulcus
- 5 Precentral gyrus
- 6 Central sulcus
- 7 Postcentral gyrus
- 8 Postcentral sulcus
- 9 Inferior parietal lobe
- 10 Parieto-occipital fissure
- 11 Occipital gyri

B Right cerebral hemisphere. From above, with the arachnoid mater and blood vessels intact

- 12 Arachnoid granulations
- 13 Superior cerebral veins

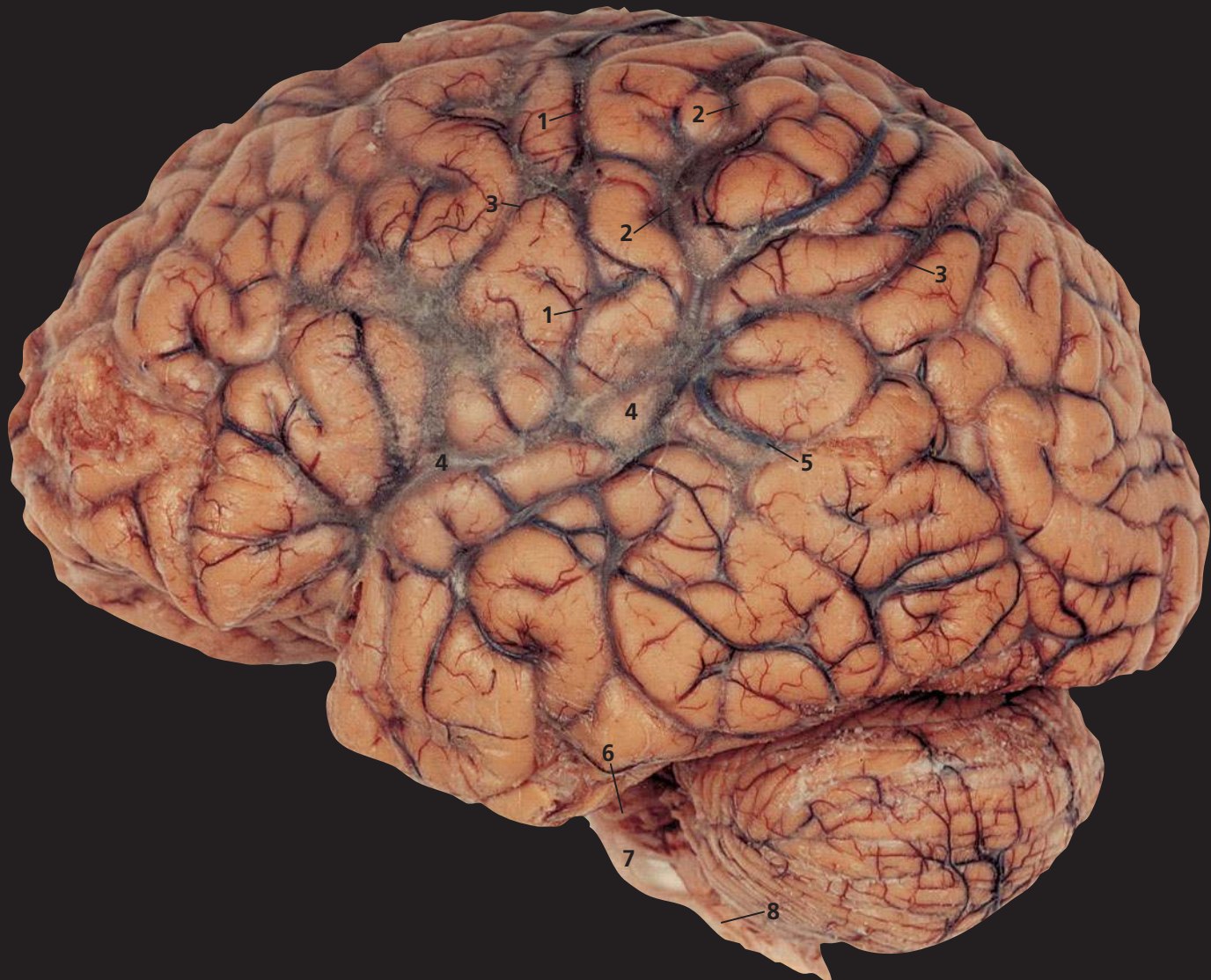


C Right cerebral hemisphere, cerebellum and brain stem. From below, with the arachnoid mater and blood vessels intact

- 1 Longitudinal cerebral fissure (arrowed)
- 2 Frontal pole
- 3 Inferior surface of frontal pole
- 4 Temporal pole
- 5 Inferior surface of temporal pole
- 6 Internal carotid artery
- 7 Optic chiasma
- 8 Infundibulum
- 9 Parahippocampal gyrus
- 10 Basilar artery
- 11 Labyrinthine artery
- 12 Right vertebral artery
- 13 Medulla oblongata
- 14 Tonsil of cerebellum
- 15 Cerebellar hemisphere
- 16 Occipital pole

D Left cerebral hemisphere, cerebellum and brain stem. From below, with the arachnoid mater and blood vessels removed

- 17 Orbital gyri
- 18 Olfactory bulb
- 19 Olfactory tract (I)
- 20 Medial olfactory stria
- 21 Lateral olfactory stria
- 22 Inferior temporal sulcus
- 23 Optic nerve (II)
- 24 Collateral sulcus
- 25 Optic tract
- 26 Oculomotor nerve (III)
- 27 Mamillary body
- 28 Pons
- 29 Trochlear nerve (IV)
- 30 Trigeminal nerve (V)
- 31 Abducent nerve (VI)
- 32 Facial nerve (VII)
- 33 Vestibulocochlear nerve (VIII)
- 34 Flocculus
- 35 Glossopharyngeal nerve (IX)
- 36 Vagus nerve (X)
- 37 Hypoglossal nerve (XII)
- 38 Accessory nerve (XI)



- E From the left, with the arachnoid mater and blood vessels intact
- 1 Rolandic artery (in central sulcus)
 - 2 Superior anastomotic vein (Troland)
 - 3 Superior cerebral veins
 - 4 Lateral fissure
 - 5 Inferior anastomotic vein (Labbé)
 - 6 Superior cerebellar artery
 - 7 Basilar artery
 - 8 Vertebral artery



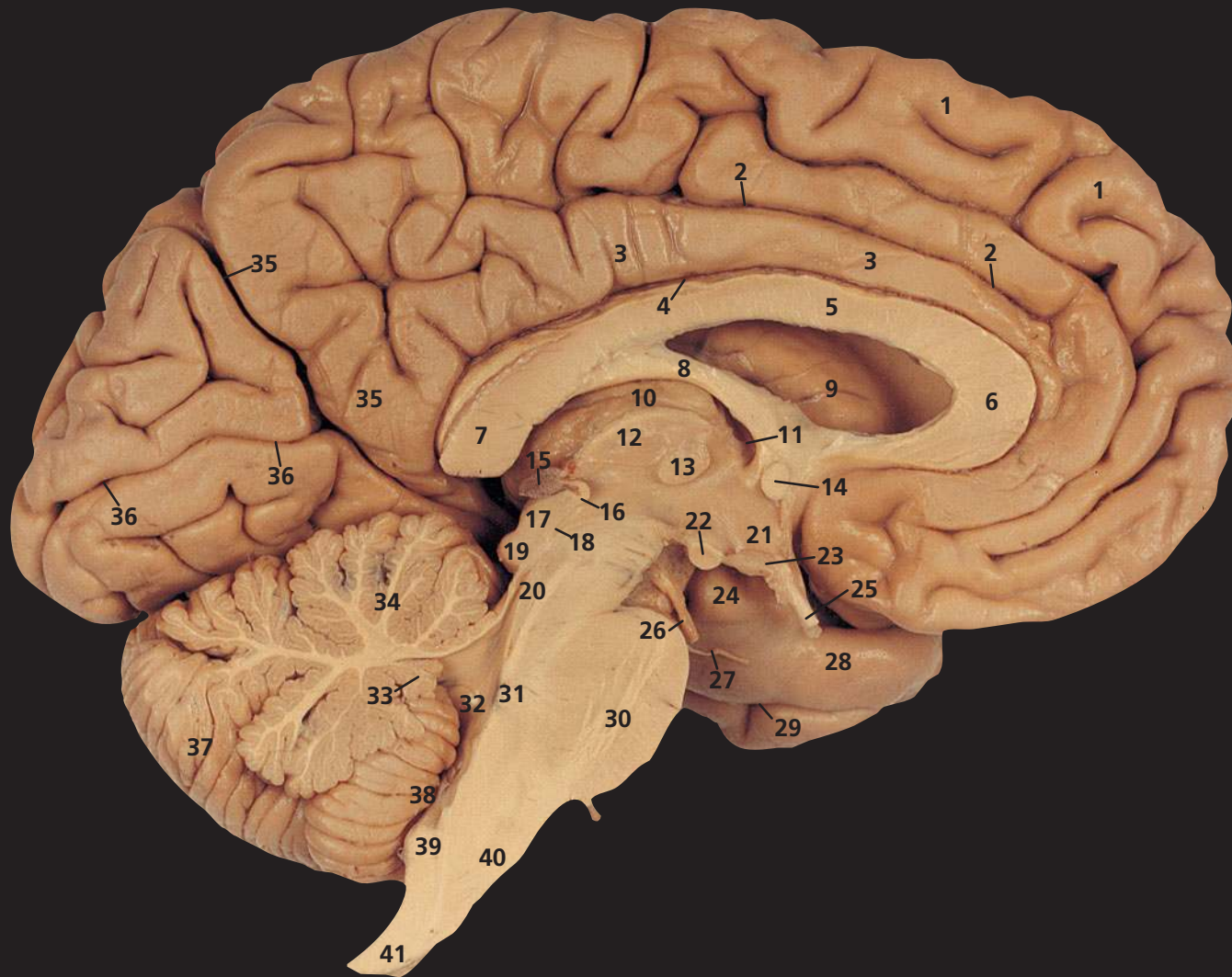
F From the left, with the arachnoid mater and blood vessels removed

- | | |
|----------------------------|----------------------------------------|
| 1 Central sulcus | 12 Superior temporal sulcus |
| 2 Precentral gyrus | 13 Middle temporal gyrus |
| 3 Postcentral gyrus | 14 Inferior temporal sulcus |
| 4 Precentral sulcus | 15 Inferior temporal gyrus |
| 5 Inferior frontal sulcus | 16 Parieto-occipital fissure (arrowed) |
| 6 Superior frontal gyrus | 17 Lunate sulcus |
| 7 Inferior frontal gyrus | 18 Anterior occipital sulcus |
| 8 Orbital gyri | 19 Pons |
| 9 Postcentral sulcus | 20 Flocculus |
| 10 Lateral fissure | 21 Cerebellar hemisphere |
| 11 Superior temporal gyrus | 22 Medulla oblongata |



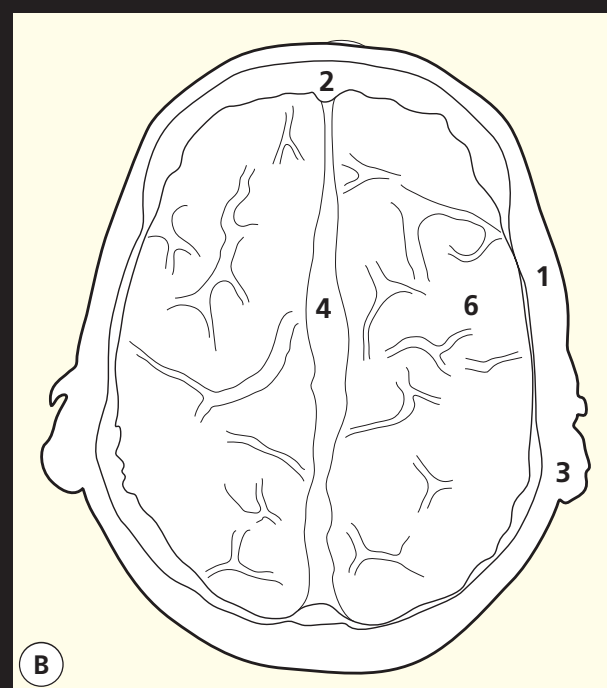
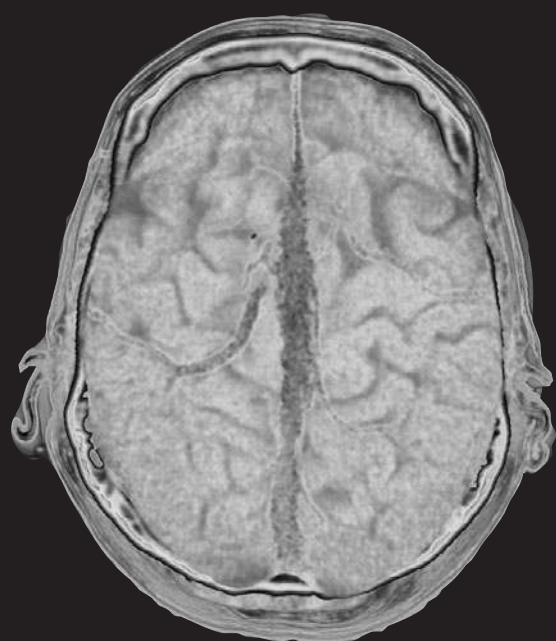
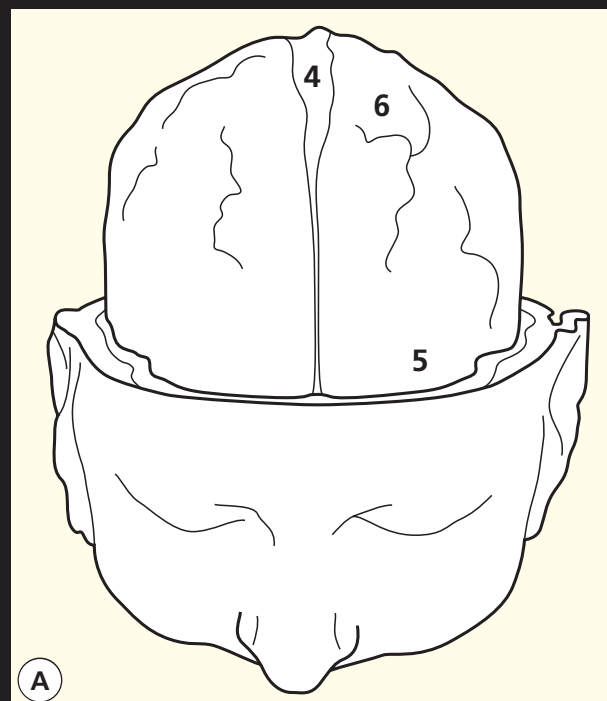
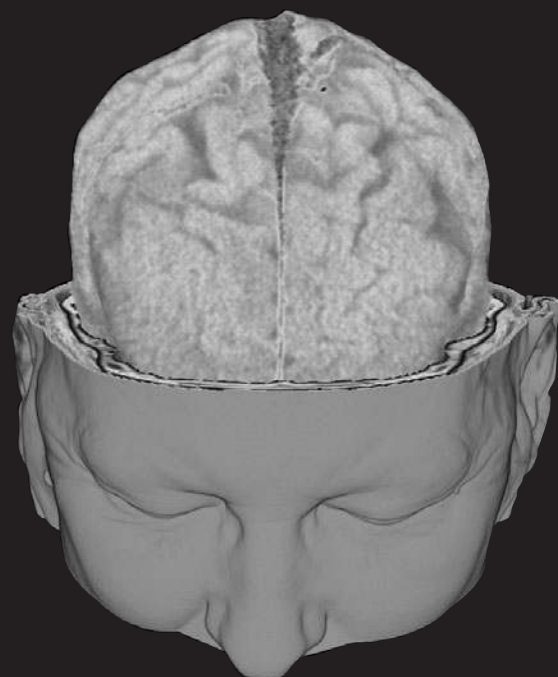
G Median sagittal section. The left half, from the right, with the arachnoid mater and blood vessels intact

- 1 Callosomarginal artery
- 2 Pericallosal artery
- 3 Calcarine artery
- 4 Posterior inferior cerebellar artery
- 5 Anterior cerebellar artery
- 6 Orbital artery
- 7 Basilar artery
- 8 Anterior inferior cerebellar artery
- 9 Left vertebral artery



H Median sagittal section. The left half, from the right, with the arachnoid mater and blood vessels removed

- | | | |
|-------------------------------------------------------|---------------------------|---------------------------------|
| 1 Superior frontal gyrus | 14 Anterior commissure | 29 Rhinal sulcus |
| 2 Cingulate sulcus | 15 Pineal body | 30 Pons |
| 3 Cingulate gyrus | 16 Posterior commissure | 31 Pontine tegmentum |
| 4 Callosal sulcus | 17 Superior colliculus | 32 Fourth ventricle |
| 5 Corpus callosum – body | 18 Aqueduct (of Sylvius) | 33 Nodulus |
| 6 Corpus callosum – genu | 19 Inferior colliculus | 34 Anterior lobe of cerebellum |
| 7 Corpus callosum – splenium | 20 Mesencephalon | 35 Parieto-occipital fissure |
| 8 Fornix | 21 Hypothalamus | 36 Calcarine sulcus |
| 9 Caudate nucleus (head) in wall of lateral ventricle | 22 Mamillary body | 37 Cerebellar hemisphere |
| 10 Choroid plexus, third ventricle | 23 Infundibulum | 38 Tonsil of cerebellum |
| 11 Interventricular foramen (Monro) | 24 Uncus | 39 Inferior cerebellar peduncle |
| 12 Thalamus | 25 Optic nerve (II) | 40 Pyramid |
| 13 Massa intermedia | 26 Oculomotor nerve (III) | 41 Medulla oblongata |
| | 27 Trochlear nerve (IV) | |
| | 28 Parahippocampal gyrus | |

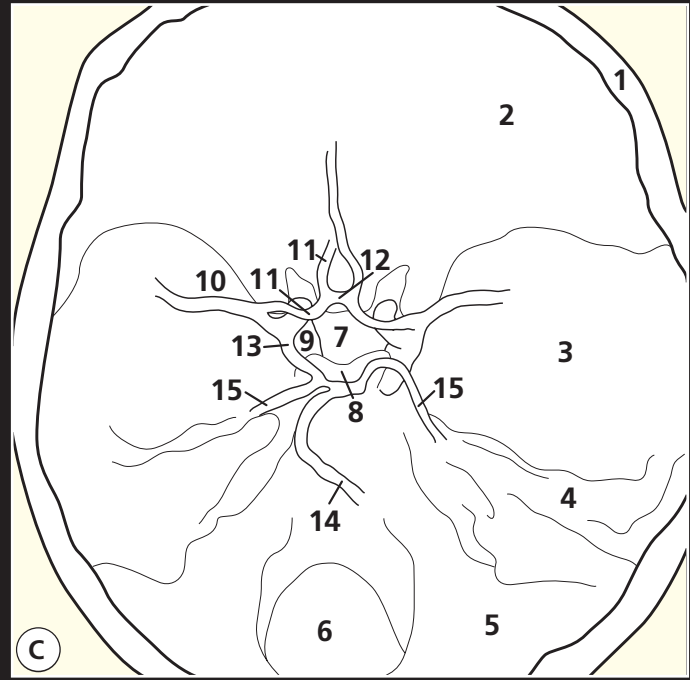
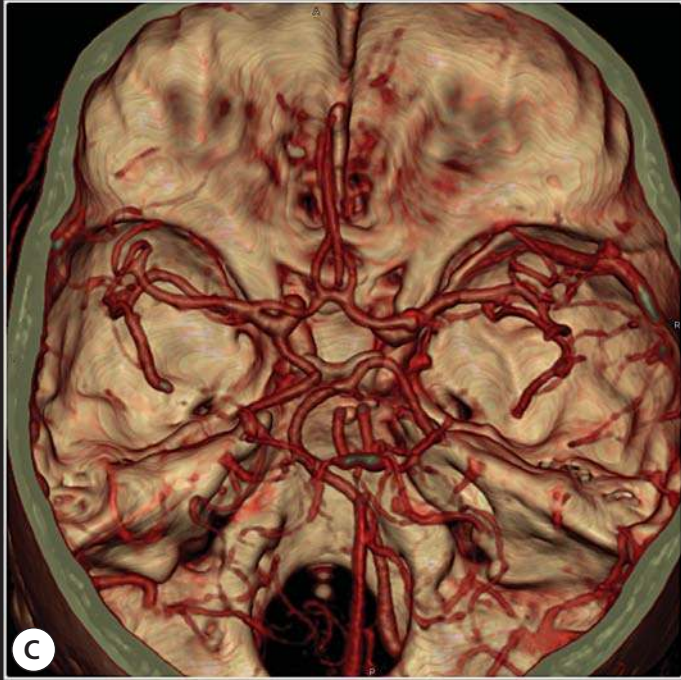


1 Skin and subcutaneous tissue
2 Frontal bone
3 Pinna

4 Superior sagittal sinus
5 Frontal lobe
6 Parietal lobe

Notes

These edited 3D CT images neatly show the relationship of the brain to the skull and facial bones. The skin, subcutaneous tissues, scalp and meninges have been stripped away electronically in order to show the relations to best effect. The frontal perspective is self explanatory. The 'axial' image is in effect viewed from 'above'. A few of the appropriate landmarks have been labelled.

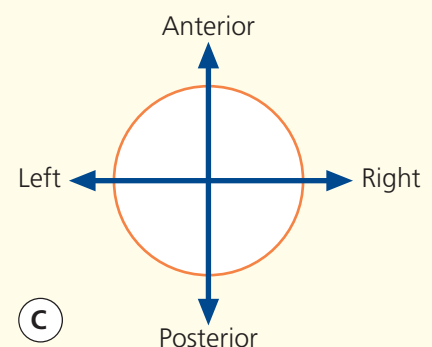
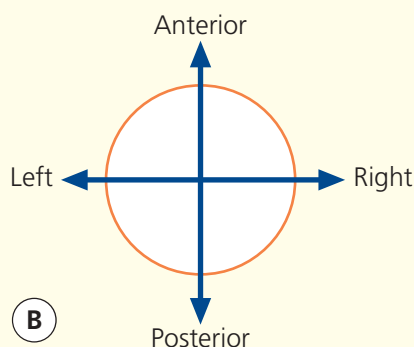
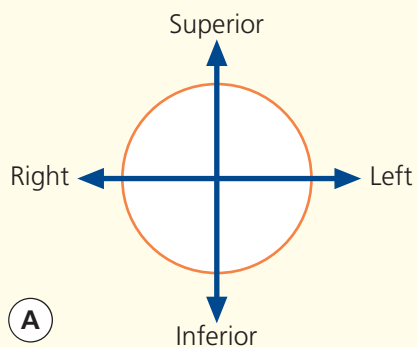


- 1 Skull vault
- 2 Anterior cranial fossa
- 3 Middle cranial fossa
- 4 Petrous ridge of temporal bone
- 5 Posterior cranial fossa

- 6 Foramen magnum
- 7 Pituitary fossa
- 8 Posterior clinoid process
- 9 Internal carotid artery
- 10 Middle cerebral artery

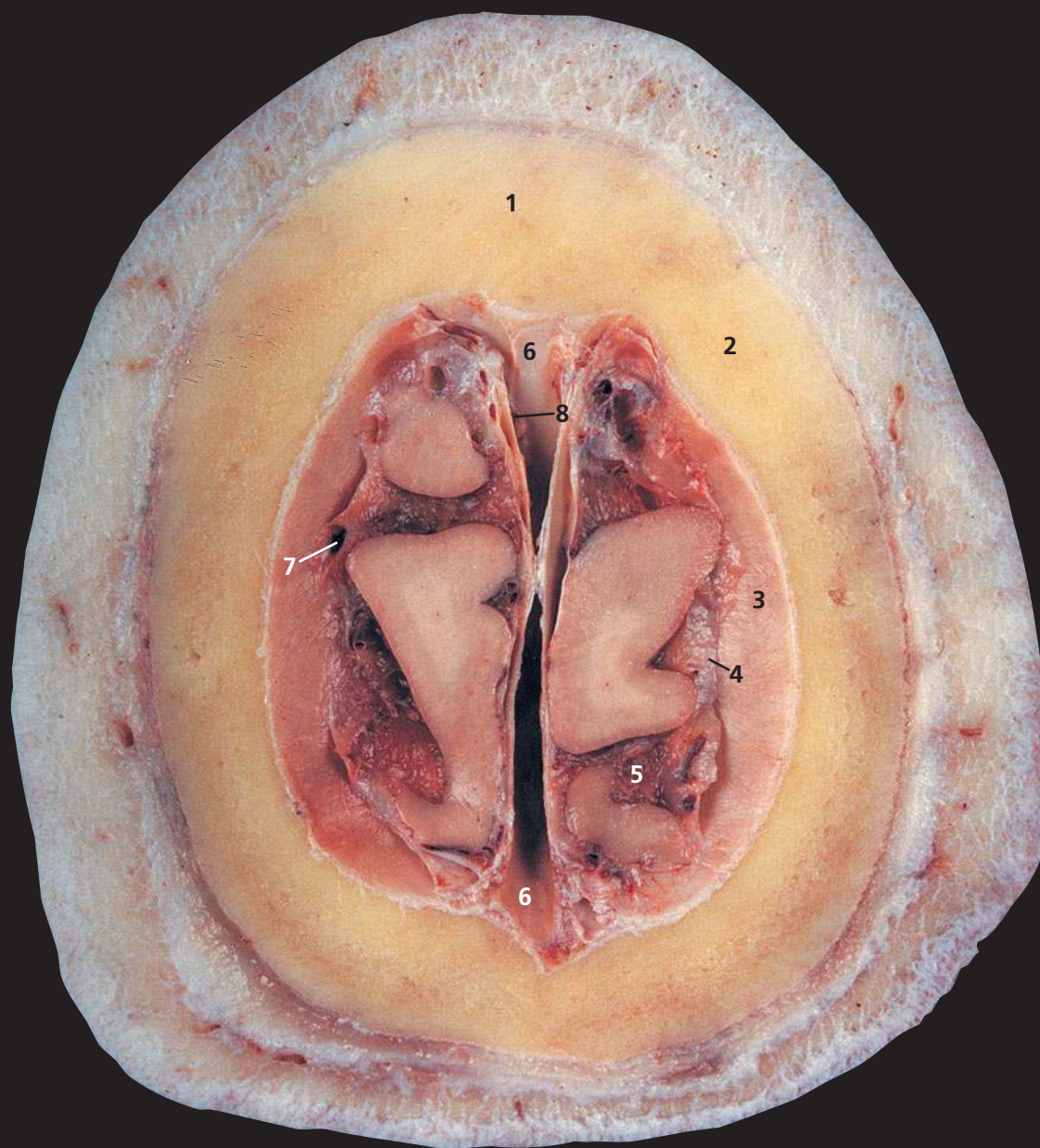
- 11 Anterior cerebral artery
- 12 Anterior communicating artery
- 13 Posterior communicating artery
- 14 Basilar artery
- 15 Posterior cerebral artery

Orientation



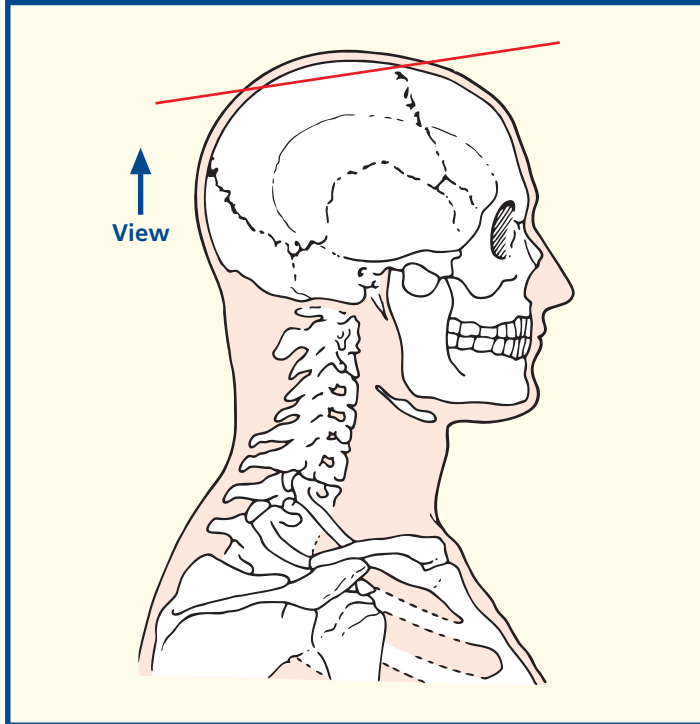
Notes

3D CT angiogram showing the vessels forming the circle of Willis in relation to the fossae formed by the base of the skull. This particular type of image is viewed from 'above'. Despite careful technique there is a little contamination with overlying vessels, which slightly confuses the image. Nevertheless the major vessels can be identified clearly and this image reveals how variable the circle of Willis can be. For example one of the two vertebral arteries is dominant as they come through the foramen magnum (6) to create the basilar artery (14). The right posterior communicating artery (13) is large and is the main contributor to the posterior cerebral artery (15) on this side. Note the close relation of the circle of Willis to the pituitary fossa (7) and posterior clinoid process (8). Note also how the internal carotid arteries (9) ascend on either side of the pituitary fossa. Aneurysms in this region can affect the pituitary, the optic chiasm and numerous cranial nerves.



- 1 Frontal bone
- 2 Parietal bone
- 3 Dura mater
- 4 Arachnoid mater
- 5 Pia mater
- 6 Superior sagittal sinus
- 7 Superior cerebral vein
- 8 Arachnoid granulation

Section level



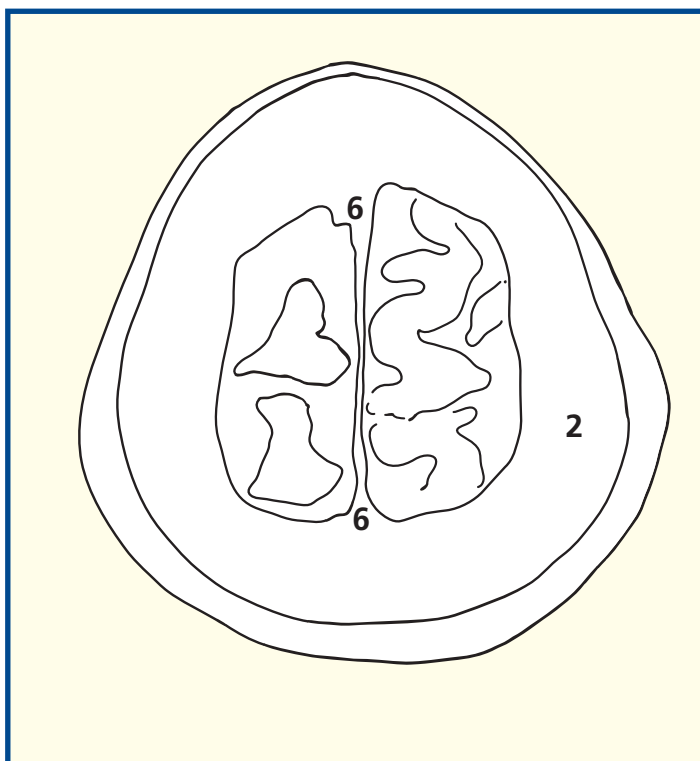
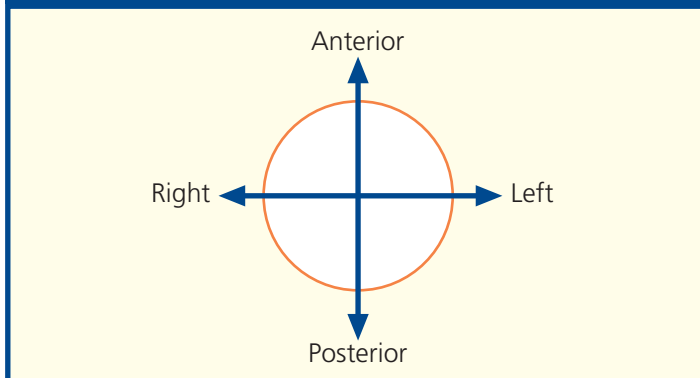
Notes

This section passes through the apex of the skull vault and traverses the parietal bones (2) and the superior portion of the frontal bone (1).

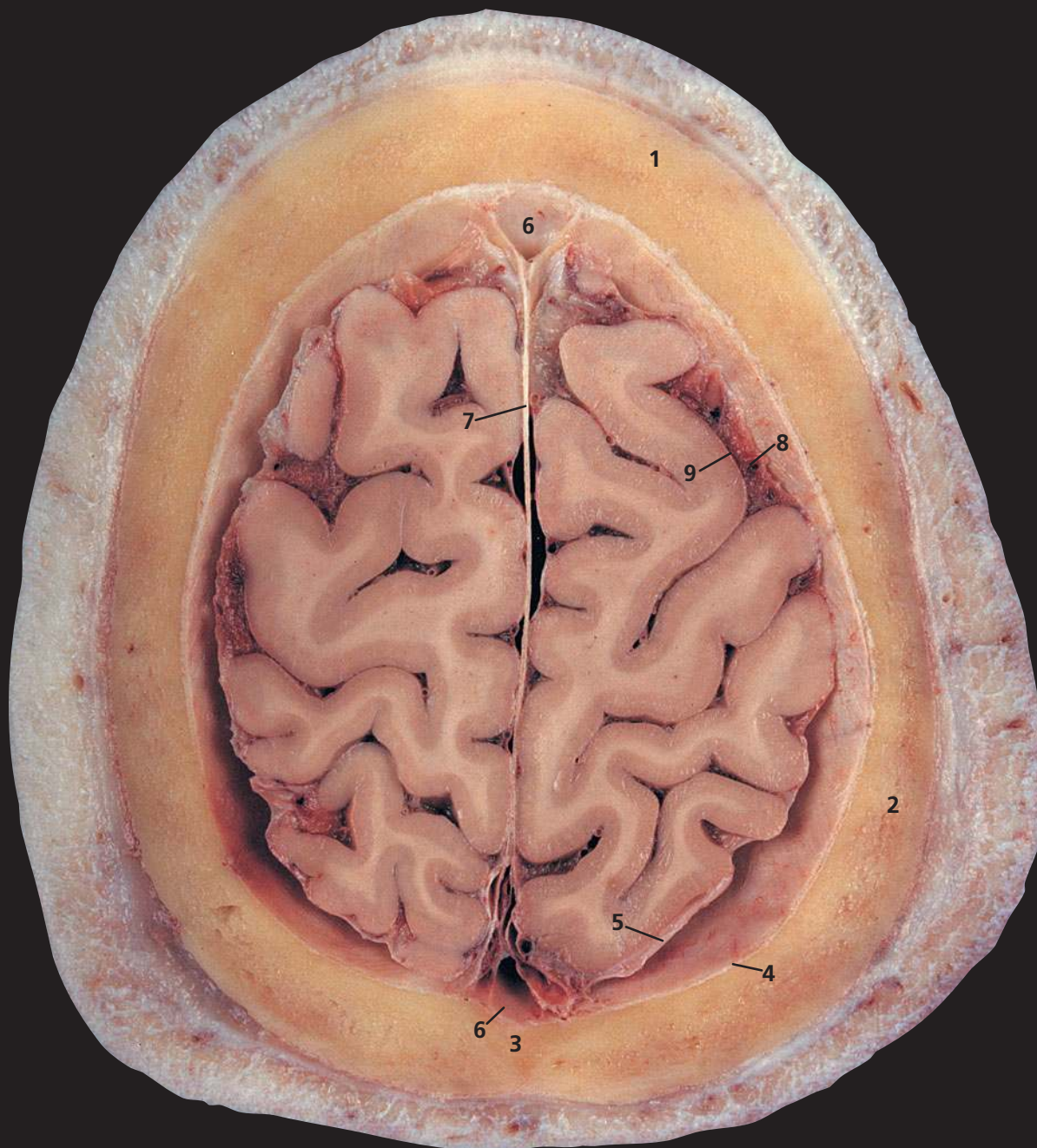
Between the inner and outer tables of the bones of the skull vault lie trabecular bone, termed diploe, which contains red bone marrow. This is highly vascular and a common site for blood-borne metastatic tumour deposits and multiple myeloma. Diploic veins (see (8) on page 18) occupy channels in this trabecular bone. These are absent at birth but begin to appear at about 2 years of age. They are large and thin-walled, being merely endothelium supported by elastic tissue, and they communicate with meningeal veins, dural sinuses and the pericranial veins. Radiographically they may appear as relatively transparent bands 3–4 mm in diameter.

The dura mater, which lines the inner aspect of the skull, comprises an outer, or endosteal, layer, or endocranium (3) (which is, in fact, the periosteum, which lines the inner aspect of the skull) and an inner, or meningeal, layer (4). Most of the intracranial venous sinuses are formed as clefts between these two layers, as demonstrated in this section by the superior sagittal sinus (6). The exceptions to this rule are the inferior sagittal sinus and the straight sinus, which are clefts within the meningeal layer.

Orientation

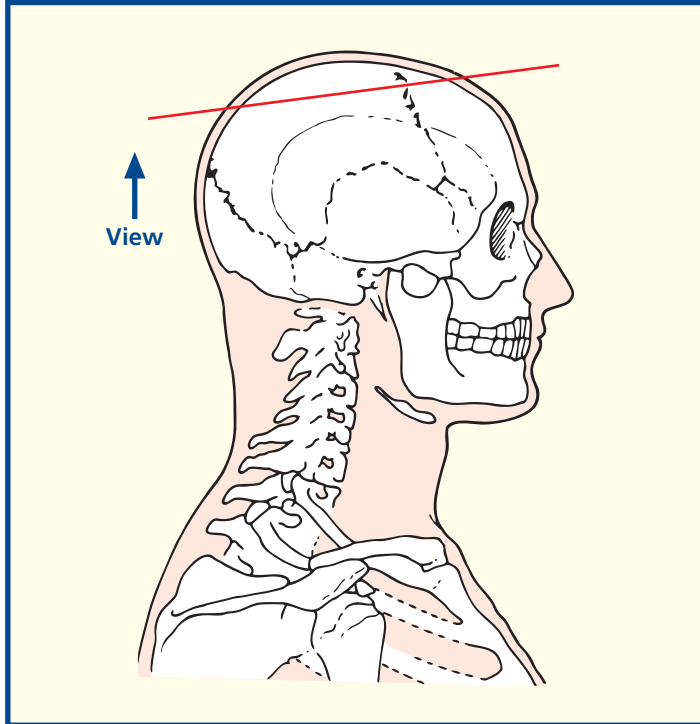


Axial computed tomogram (CT)



- 1 Frontal bone
- 2 Parietal bone
- 3 Sagittal suture
- 4 Dura mater
- 5 Arachnoid mater
- 6 Superior sagittal sinus
- 7 Falx cerebri
- 8 Subarachnoid space
- 9 Pia mater

Section level



Notes

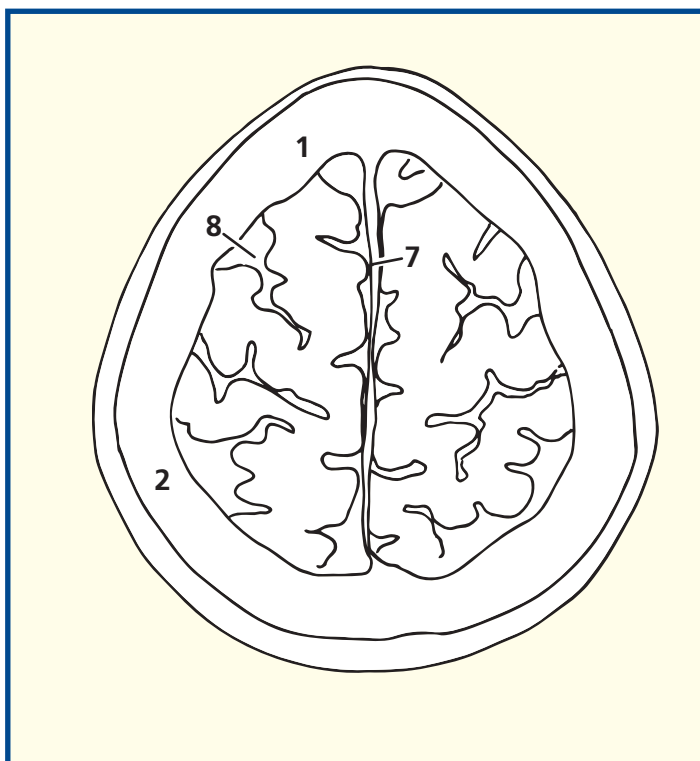
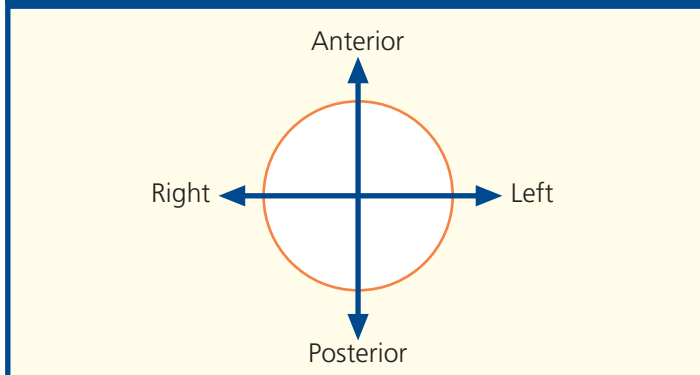
This section, at a deeper plane through the skull vault, demonstrates the falx cerebri (7), which is formed as a double fold of the inner, meningeal, layer of the dura mater (5) and which forms the dural septum between the cerebral hemispheres.

The inner layer of the dura is lined by the delicate arachnoid mater. The pia mater (9) is vascular and invests the brain, spinal cord, cranial nerves and spinal nerve roots. It remains in close contact with the surface of the brain, including the depths of the cerebral sulci and fissures.

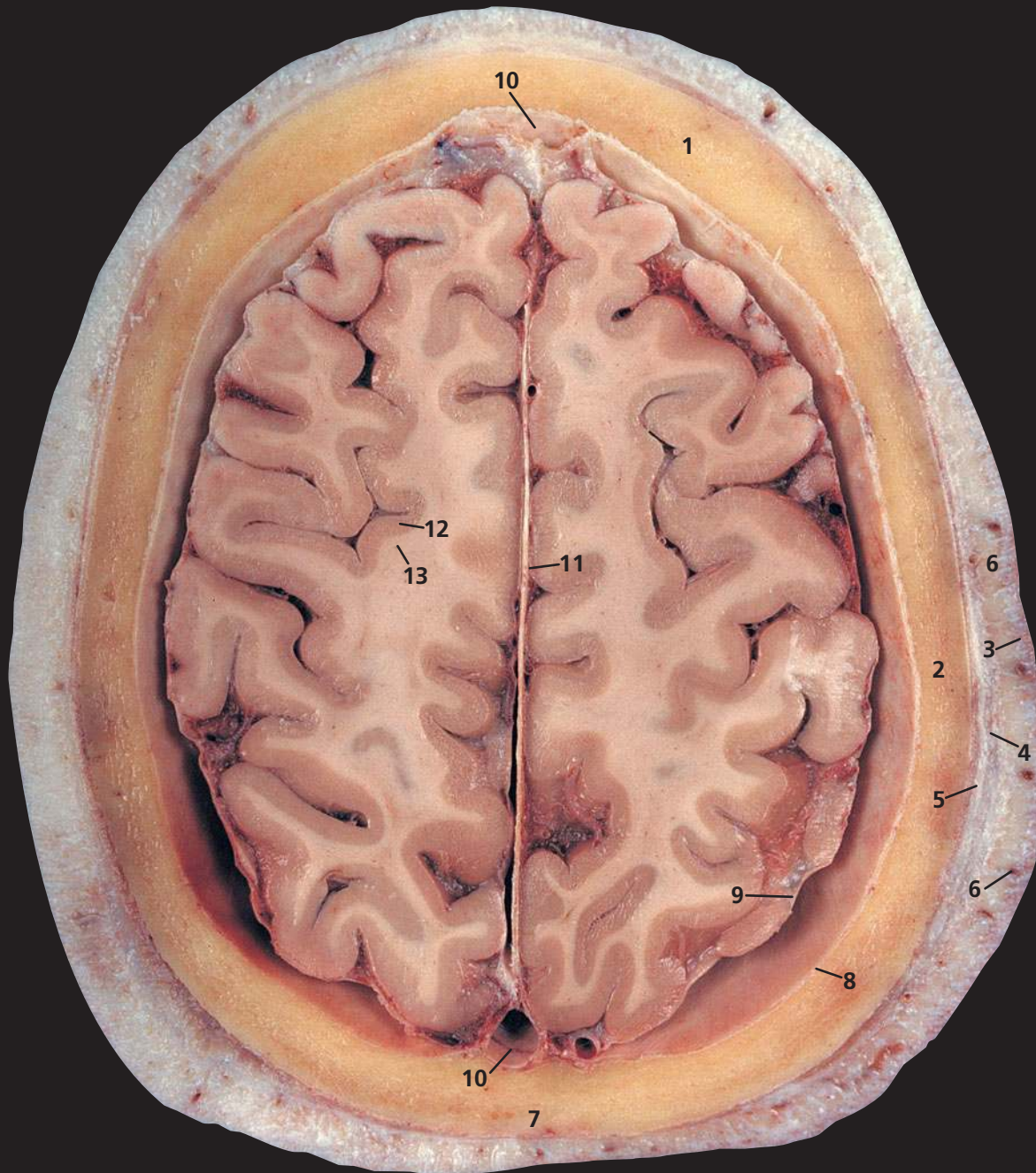
Over the convexities of the brain, the pia and arachnoid are in close contact. Over the cerebral sulci and the cisterns of the brain base, the pia and arachnoid are separated by the subarachnoid space (8), which contains cerebrospinal fluid. This space is traversed by a fine spider's web of fibres (*arachnoid*: pertaining to the spider).

The total volume of cerebrospinal fluid in the adult is approximately 150 mL, of which some 25 mL is contained in the ventricular system, 25 mL in the spinal theca and the remaining 100 mL in the cerebral subarachnoid space.

Orientation

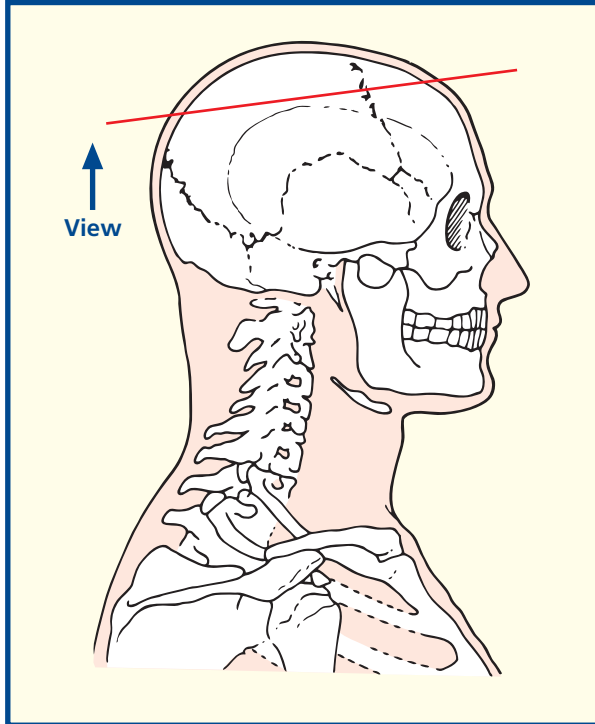


Axial computed tomogram (CT)



- | | |
|-----------------------------------------------|----------------------------|
| 1 Frontal bone | 7 Sagittal suture |
| 2 Parietal bone | 8 Dura mater |
| 3 Skin and dense subcutaneous tissue | 9 Arachnoid mater |
| 4 Epicranial aponeurosis (galea aponeurotica) | 10 Superior sagittal sinus |
| 5 Pericranium | 11 Falx cerebri |
| 6 Branches of superficial temporal artery | 12 Grey matter |
| | 13 White matter |

Section level



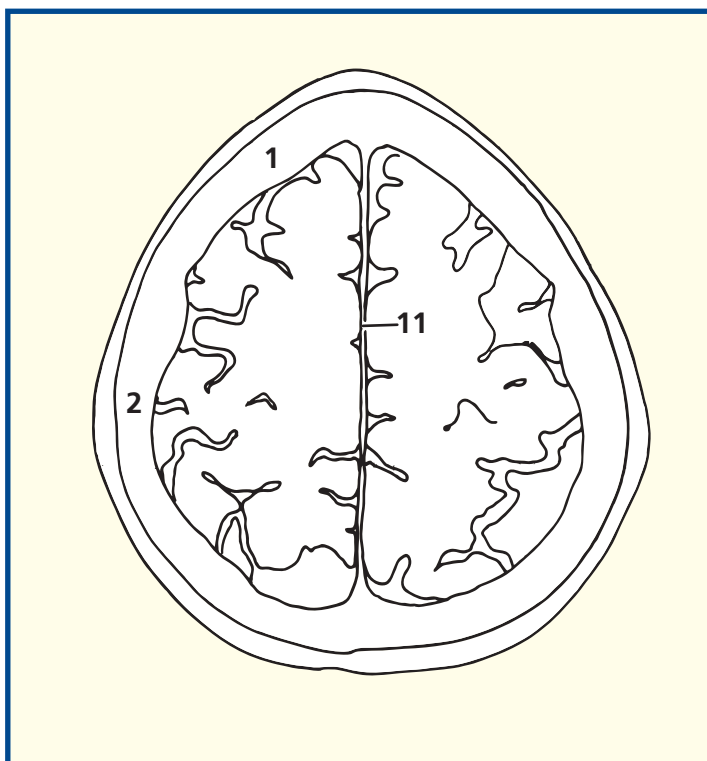
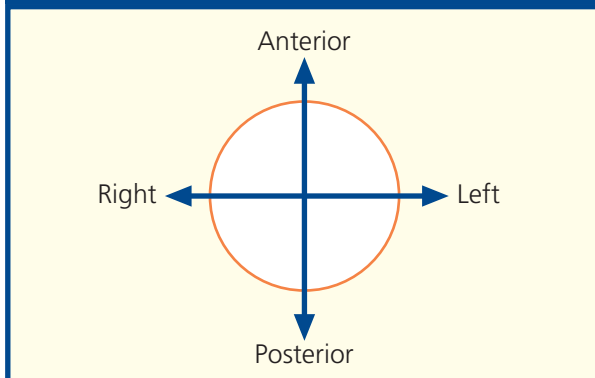
Notes

This section, through the upper parts of the cerebral hemispheres, gives a clear picture of the distinction between the outer grey matter (**12**), which contains nerve cells, and the inner white matter (**13**), made up of nerve fibres. This is in contradistinction to the arrangement of the spinal cord, with the central grey and surrounding white matter.

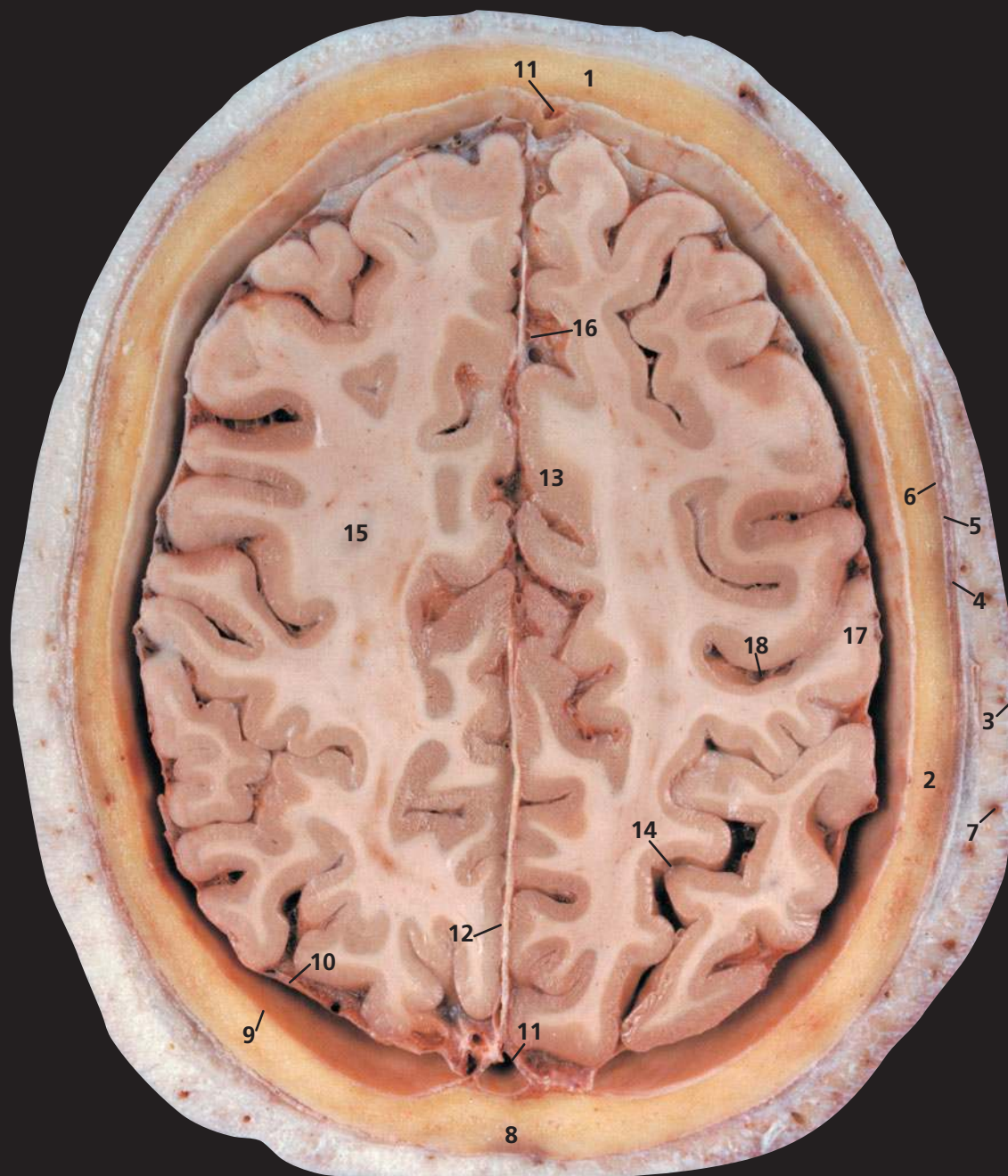
Note the five layers of the scalp – skin, underlying dense connective tissue (**3**), dense epicranial aponeurosis, or galea aponeurotica (**4**), which is separated by a film of loose areolar connective tissue from the outer periosteum of the skull, the pericranium (**5**). The pericranium is densely adherent to the surface of the skull and passes through the various foramina, where it becomes continuous with the outer endosteal layer of the dura (**8**) and is also continuous with the sutural ligaments that occupy the cranial sutures.

Each of these layers is of clinical significance. The scalp is richly supplied with sebaceous glands and is the commonest site of epidermoid cysts. The connective tissue is made up of lobules of fat bound in tough fibrous septa. The blood vessels of the scalp lie in this layer; when the scalp is lacerated, the divided vessels retract between these septa and cannot be picked up with artery forceps in the usual way – they can be controlled by firm digital pressure against the skull on either side of the laceration. The aponeurotic layer is the occipitofrontalis, which is fibrous over the dome of the scalp but muscular in the occipital and frontal regions (see **(2)** on p. 24 and **(2)** on p. 26). The underlying loose areolar connective tissue accounts for the mobility of the scalp on the underlying bone. It is in this plane that surgical mobilization of scalp flaps is performed. Blood in this layer tracks forward into the orbits to produce periorbital haematomas. The periosteum adheres to the suture lines of the skull, so that a collection of blood or pus beneath this layer outlines the affected bone. This may produce the cephalohaematoma seen in birth injuries involving the skull.

Orientation

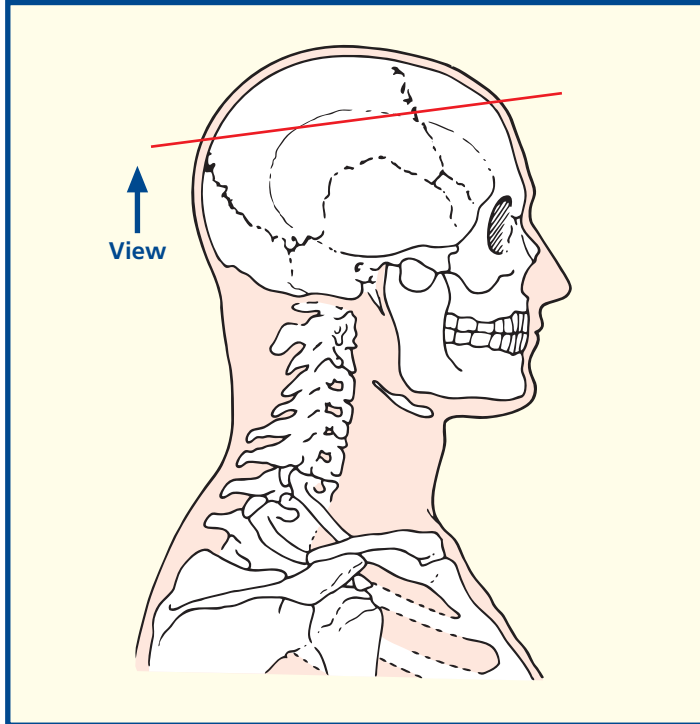


Axial computed tomogram (CT)



- | | |
|-----------------------------------------------|----------------------------------------|
| 1 Frontal bone | 9 Dura mater |
| 2 Parietal bone | 10 Arachnoid mater |
| 3 Skin and dense subcutaneous tissue | 11 Superior sagittal sinus |
| 4 Epicranial aponeurosis (galea aponeurotica) | 12 Falx cerebri |
| 5 Temporalis | 13 Cingulate gyrus |
| 6 Pericranium | 14 Parieto-occipital sulcus |
| 7 Branch of superficial temporal artery | 15 Corona radiata |
| 8 Sagittal suture | 16 Anterior cerebral artery (branches) |
| | 17 Postcentral gyrus |
| | 18 Central sulcus |

Section level



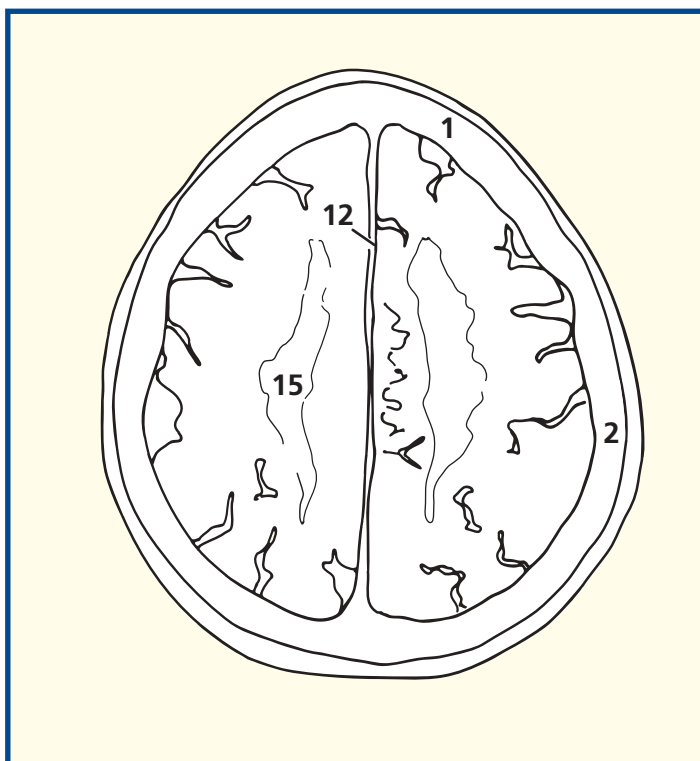
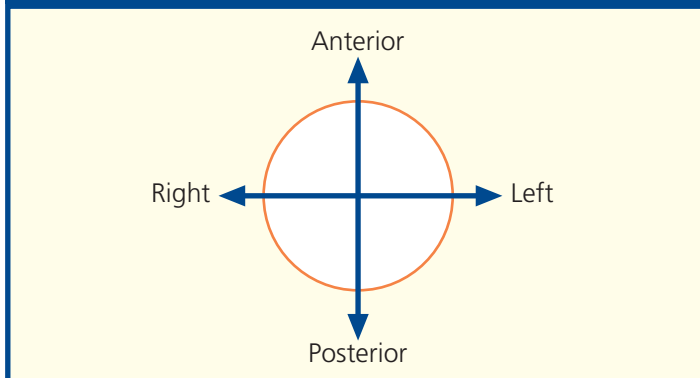
Notes

This section allows some of the main gyri and sulci of the cerebrum to be identified. Cross-reference should be made to the photographs of the external aspects and sagittal section of the brain for orientation.

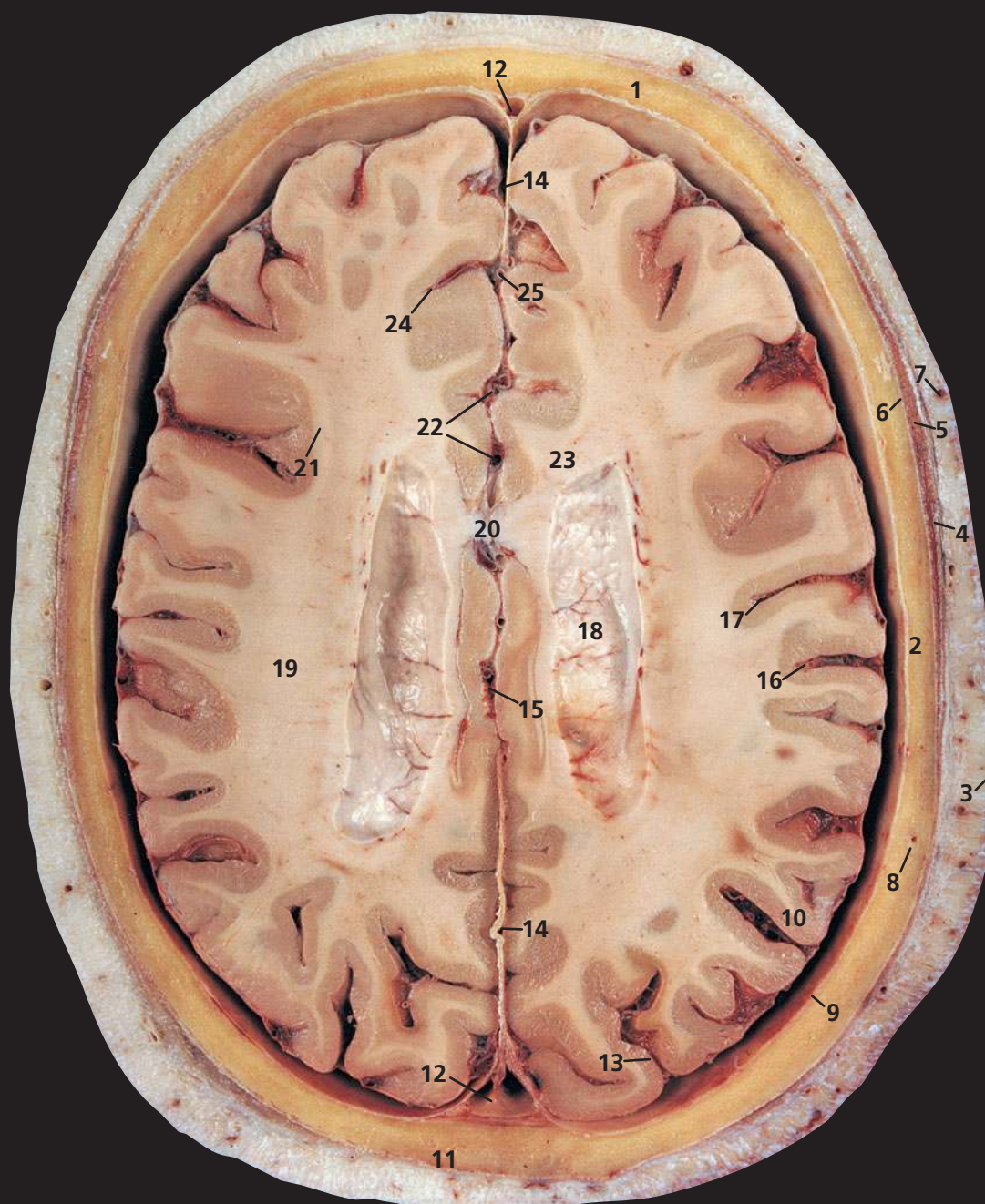
The corona radiata (**15**) comprises a fan-shaped arrangement of afferent and efferent projection fibres, which join the grey matter to lower centres. On the computed tomography (CT) image, it appears as a curved linear area of low attenuation termed the centrum semiovale.

The superficial temporal artery, of which the parietal branch can be seen at (**7**), is the smaller terminal branch of the external carotid artery, the other being the maxillary artery. The middle terminal branch can be seen immediately in front of (**4**). The blood supply to the scalp is the richest of all areas of the skin and there are free anastomoses between its various branches. It is for this reason that a partially avulsed scalp flap is usually viable.

Orientation

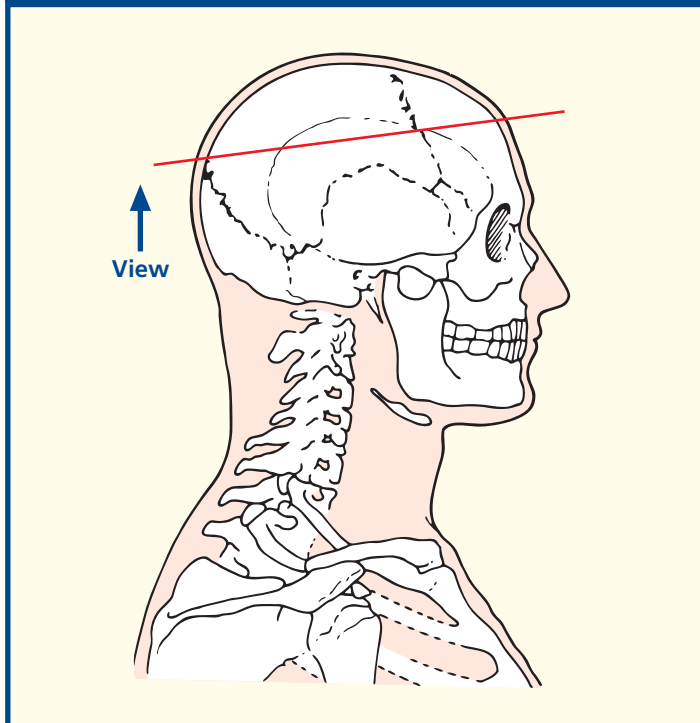


Axial computed tomogram (CT)



- | | | |
|-------------------------------------------|--------------------------------------|-----------------------------------------------------|
| 1 Frontal bone | 9 Dura mater | 19 Corona radiata |
| 2 Parietal bone | 10 Arachnoid mater | 20 Corpus callosum |
| 3 Skin and dense subcutaneous tissue | 11 Sagittal suture | 21 Longitudinal fasciculus (corticocortical fibres) |
| 4 Temporal fascia | 12 Superior sagittal sinus | 22 Anterior cerebral artery (branches) |
| 5 Temporalis | 13 Lunate sulcus | 23 Forceps minor |
| 6 Pericranium | 14 Falx cerebri | 24 Cingulate sulcus |
| 7 Branches of superficial temporal artery | 15 Cingulate gyrus | 25 Inferior sagittal sinus |
| 8 Diploic vein | 16 Postcentral sulcus | |
| | 17 Central sulcus | |
| | 18 Roof of body of lateral ventricle | |

Section level



Notes

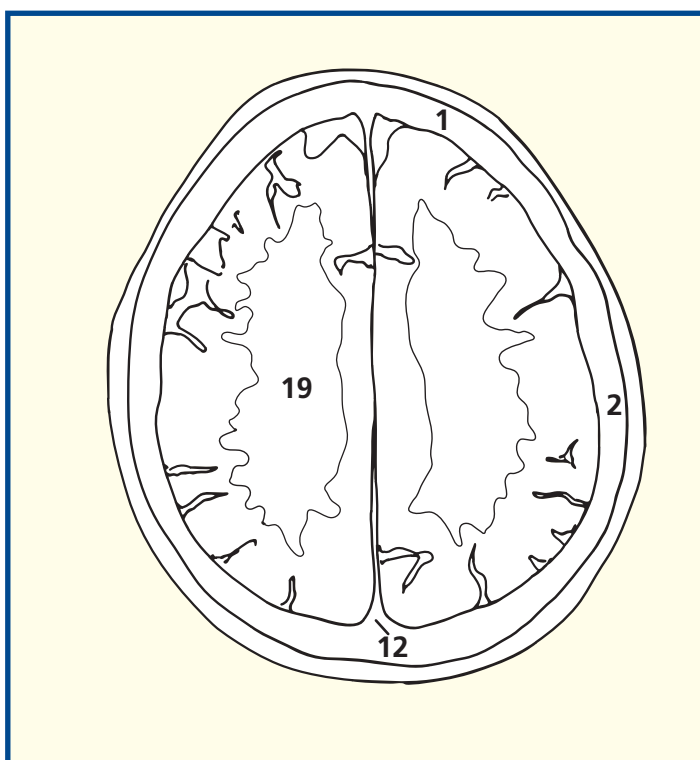
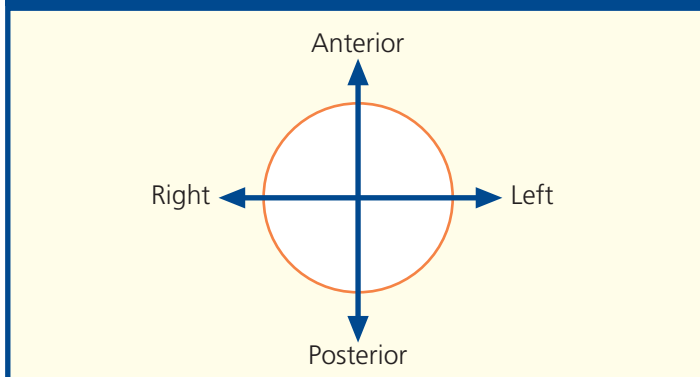
This section passes through the roof of the lateral ventricle (18).

The central sulcus, or fissure of Rolando (17), is the most important of the sulcal landmarks, since it separates the precentral (motor) gyrus from the postcentral (sensory) gyrus. It also helps demarcate the frontal and parietal lobes of the cerebrum.

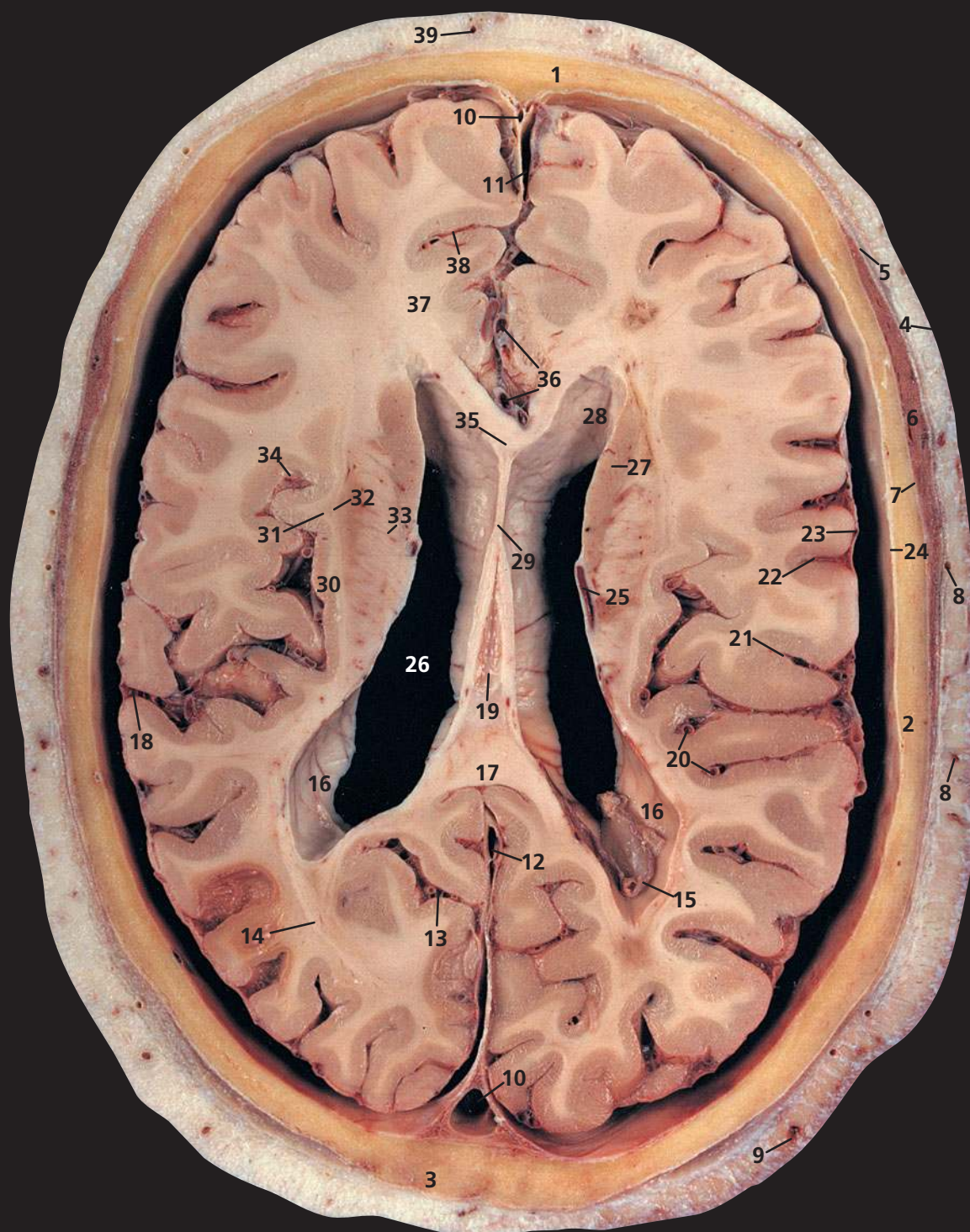
Again, the corona radiata (19), or centrum semiovale, is well seen in both the section and the CT image.

The corpus callosum (20) – and seen also on p. 7, in (5), (6) and (7) – is the largest fibre pathway of the brain. It links the cortex of the two cerebral hemispheres and roofs much of the lateral ventricles. Its anterior portion is termed the genu; its body is termed the trunk, which is arched and convex superiorly. It ends posteriorly as the splenium, which is its thickest part – see p. 20 (17). Congenital absence of the corpus callosum, or its surgical division, results in surprisingly little disturbance of function.

Orientation

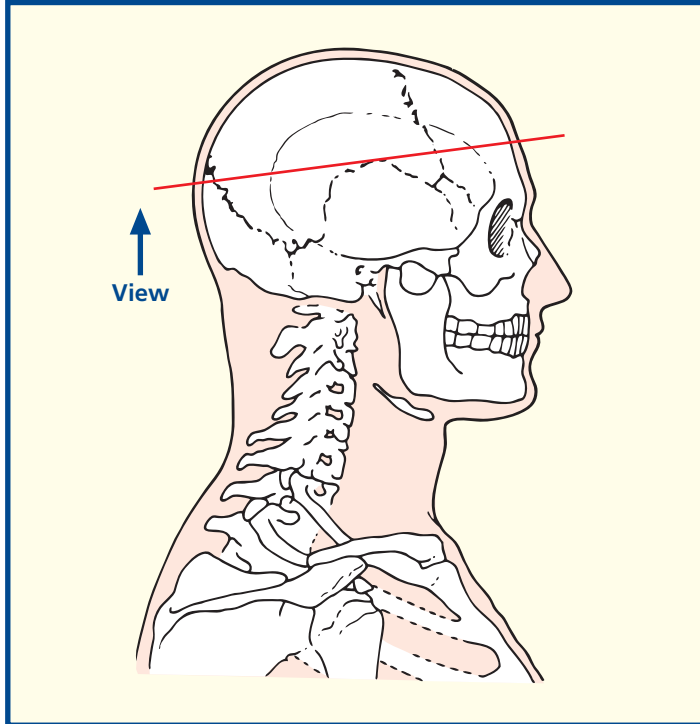


Axial computed tomogram (CT)



- | | | |
|-----------------------------------------------|--------------------------------------|----------------------------------------|
| 1 Frontal bone | 13 Parieto-occipital sulcus | 27 Body of caudate nucleus |
| 2 Parietal bone | 14 Optic radiation | 28 Frontal horn of lateral ventricle |
| 3 Sutural bone | 15 Choroid plexus | 29 Septum pellucidum |
| 4 Skin and dense subcutaneous tissue | 16 Posterior horn lateral ventricle | 30 Insula |
| 5 Epicranial aponeurosis (galea aponeurotica) | 17 Splenium of corpus callosum | 31 Claustrum |
| 6 Temporalis | 18 Lateral sulcus (Sylvian fissure) | 32 Putamen |
| 7 Pericranium | 19 Third ventricle | 33 Internal capsule |
| 8 Branches of superficial temporal artery | 20 Middle cerebral artery (branches) | 34 Circular sulcus |
| 9 Occipital vein | 21 Postcentral sulcus | 35 Genu of corpus callosum |
| 10 Superior sagittal sinus | 22 Central sulcus | 36 Anterior cerebral artery (branches) |
| 11 Falx cerebri | 23 Arachnoid mater | 37 Forceps minor |
| 12 Straight sinus | 24 Dura mater | 38 Cingulate sulcus |
| | 25 Thalamostriate vein | 39 Supra-orbital artery |
| | 26 Body of lateral ventricle | |

Section level



Notes

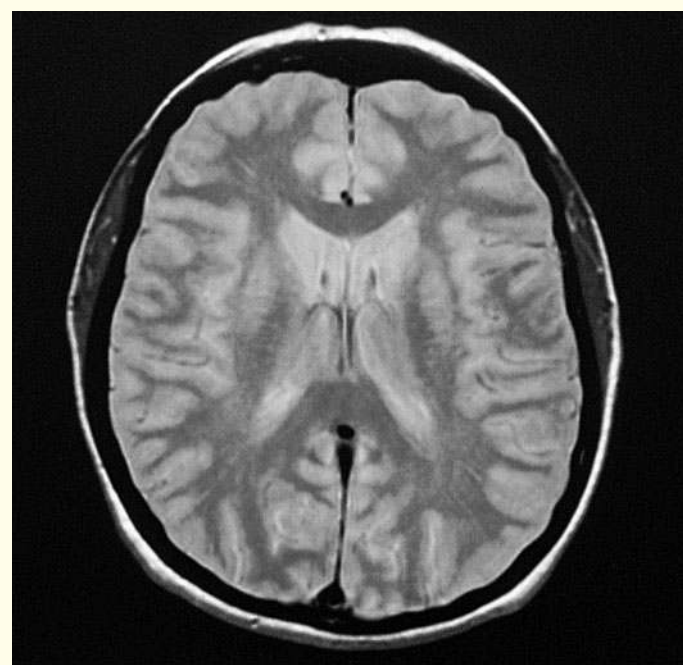
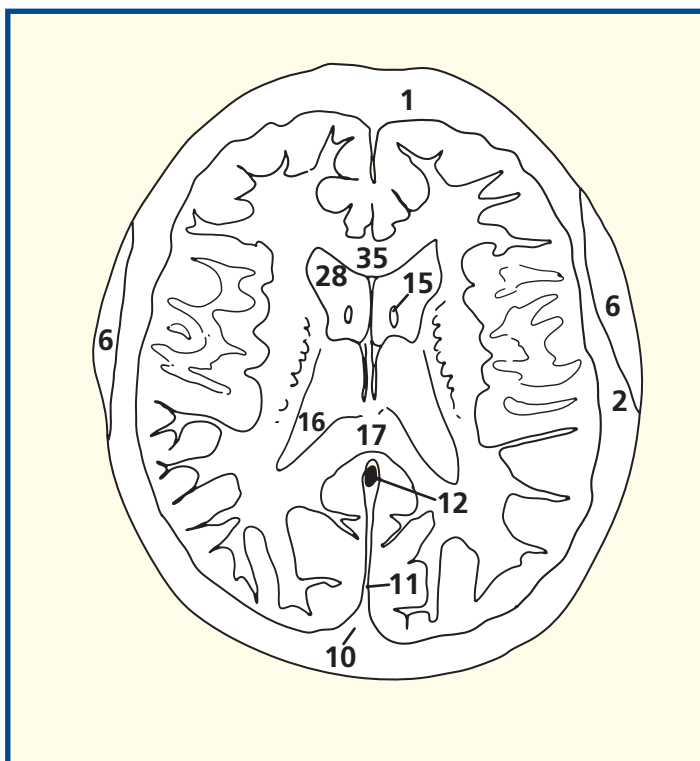
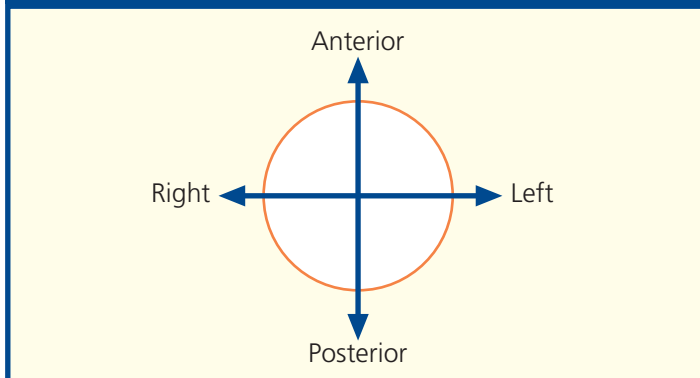
This section passes through the bodies of the lateral ventricles (26) and the third ventricle (19).

The lateral ventricles comprise a frontal horn (28) and body (26), which continues with the posterior or occipital horn (16), which, in turn, enters the inferior horn within the temporal lobe. This will be seen in later sections. The lateral ventricles are separated almost completely from each other by the septum pellucidum (29) but communicate indirectly via the third ventricle (19), a narrow slit-like cavity.

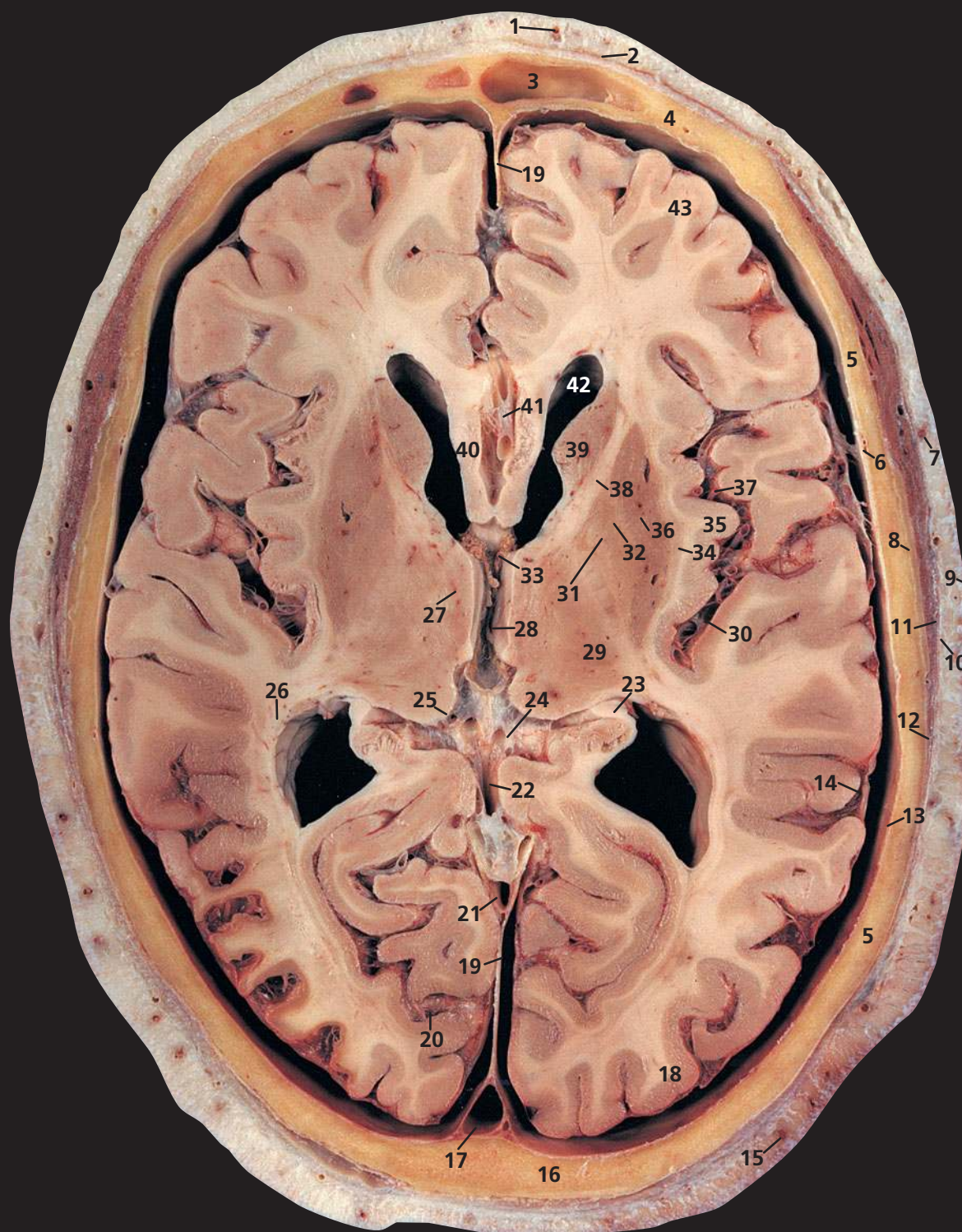
The choroid plexuses of the lateral ventricles (15), which are responsible for the production of most of the cerebrospinal fluid extend from the inferior horn, through the body to the interventricular foramen, where they become continuous with the plexus of the third ventricle.

In addition to the centres of ossification of the named bones of the skull, other centres may occur in the course of the sutures, which give rise to irregular sutural (Wormian) bones (3). They occur most frequently in the region of the lambdoid suture, as here, but sometimes they may be seen at the anterior, or more especially, the posterior fontanelle. They are usually limited to two or three in number, but they may occur in greater numbers in congenital hydrocephalic skulls and other congenital anomalies.

Orientation

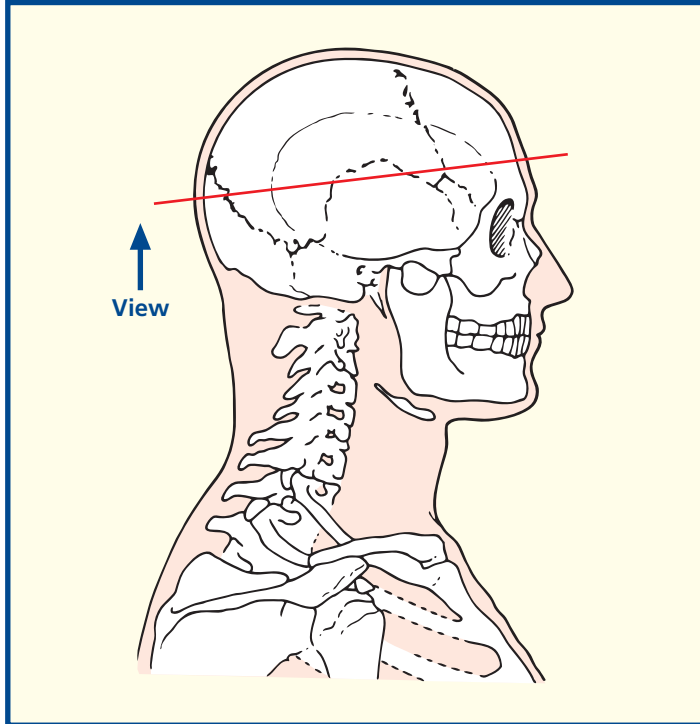


Axial magnetic resonance image (MRI)



- | | | |
|------------------------------------------------|--------------------------------------|-------------------------------------------------------|
| 1 Supra-orbital artery | 15 Occipital artery | 31 Globus pallidus – internal segment |
| 2 Frontal belly of occipitofrontalis | 16 Squamous part of occipital bone | 32 Globus pallidus – external segment |
| 3 Frontal sinus | 17 Superior sagittal sinus | 33 Choroid plexus in interventricular foramen (Monro) |
| 4 Frontal bone | 18 Occipital lobe | 34 Claustrum |
| 5 Parietal bone | 19 Falx cerebri | 35 Insula |
| 6 Middle meningeal artery and vein | 20 Calcarine sulcus | 36 Putamen |
| 7 Branch of temporal artery | 21 Straight sinus | 37 Middle cerebral artery (branches) |
| 8 Sliver of squamous part of temporal bone | 22 Great cerebral vein | 38 Anterior limb of internal capsule |
| 9 Skin and dense subcutaneous tissue | 23 Fornix | 39 Caudate nucleus – head |
| 10 Epicranial aponeurosis (galea aponeurotica) | 24 Internal cerebral vein (branches) | 40 Corpus callosum |
| 11 Temporalis | 25 Pulvinar of thalamus | 41 Anterior cerebral artery |
| 12 Pericranium | 26 Optic radiation | 42 Frontal horn of lateral ventricle |
| 13 Dura mater | 27 Medial nucleus of thalamus | 43 Frontal lobe |
| 14 Arachnoid mater | 28 Third ventricle | |
| | 29 Ventroposterior thalamic nucleus | |
| | 30 Circular sulcus | |

Section level



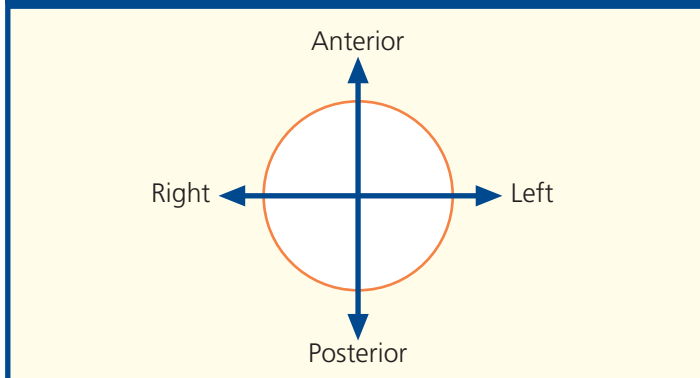
Notes

This section passes through the apex of the squamous part of the occipital bone (16) and the frontal sinus (3). These are paired but are rarely symmetrical, while the septum between them is usually deviated from the midline. They vary greatly in size, as may be appreciated from viewing a number of skull radiographs. Each lies posterior to the superciliary arch and extends upwards above the medial part of the eyebrow and back on to the medial part of the orbital roof. Sometimes they are divided by incomplete bony septa; rarely, one or both may be absent. Each drains into the anterior part of the middle meatus on the lateral wall of the nasal cavity via the frontonasal duct.

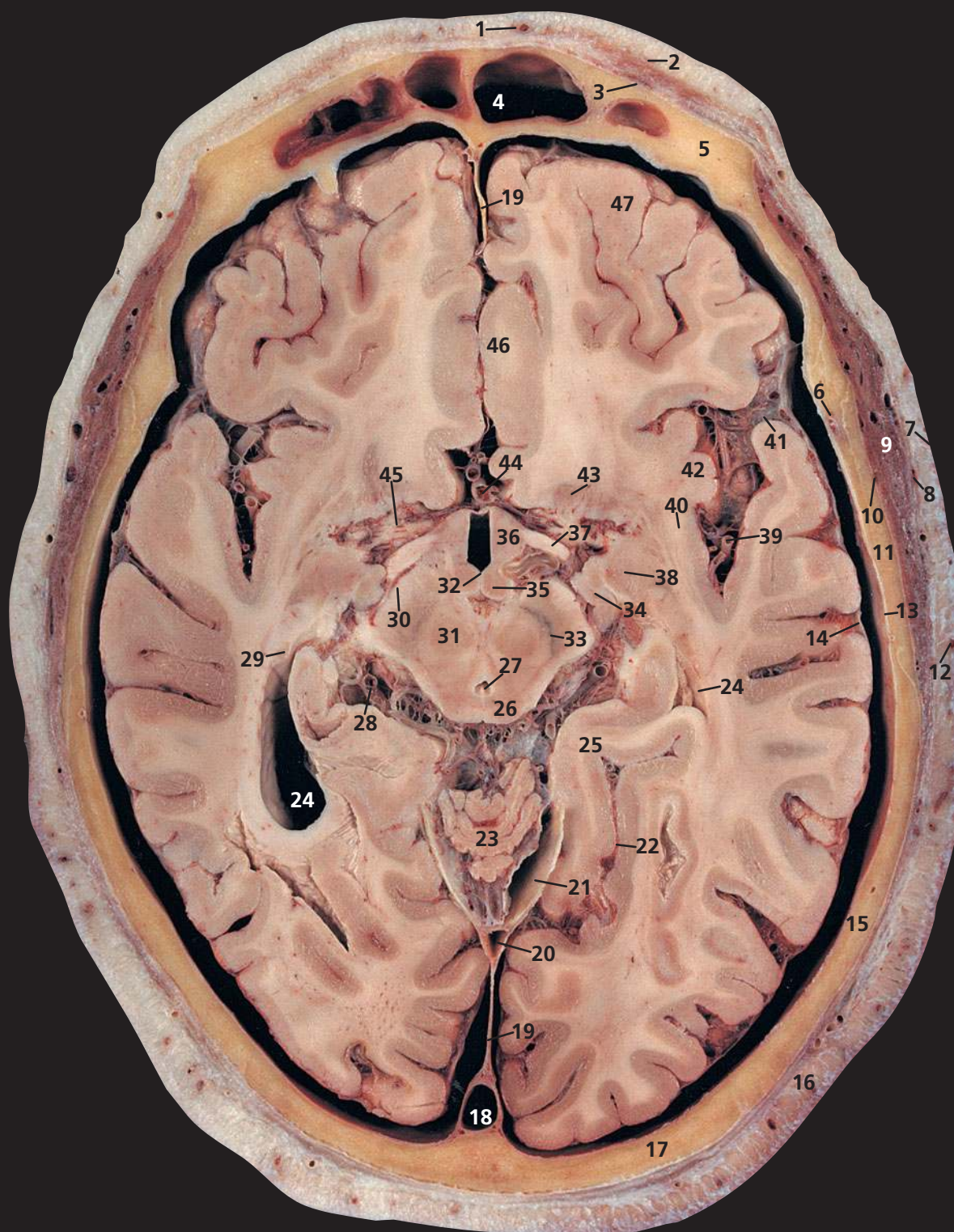
The interventricular foramen of Monro (33) is well demonstrated and drains the lateral ventricle on both sides into the third ventricle (28), thus providing a linkage between the ventricular systems within the two cerebral hemispheres.

This section also demonstrates the components of the basal ganglia, the claustrum (34), and the lentiform nucleus, made up of the globus pallidus (31, 32) and putamen (36). The latter is largely separated from the head of the caudate nucleus (39) by the anterior limb of the internal capsule (38).

Orientation

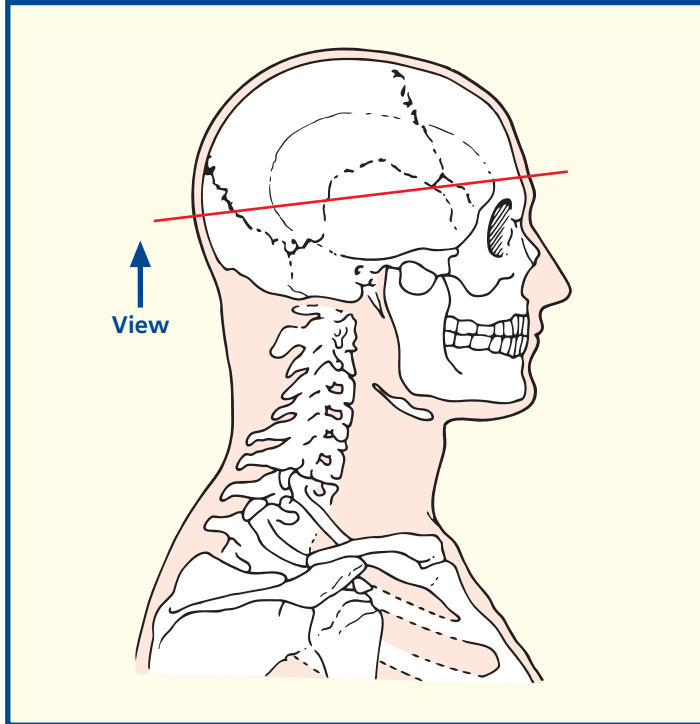


Axial magnetic resonance image (MRI)



- | | | | |
|-----------------------------------------------|------------------------------------|--------------------------------------|----------------------------------|
| 1 Supra-orbital artery | 12 Superficial temporal artery | 26 Superior colliculus | 40 Claustrum |
| 2 Orbital part of occipitofrontalis | 13 Dura mater | 27 Aqueduct of Sylvius | 41 Lateral sulcus (Sylvius) |
| 3 Frontal belly of occipitofrontalis | 14 Arachnoid mater | 28 Posterior cerebral artery | 42 Insula |
| 4 Frontal sinus | 15 Parietal bone | 29 Tail of caudate nucleus | 43 Nucleus accumbens septi |
| 5 Frontal bone | 16 Occipital artery | 30 Cerebral peduncle | 44 Anterior cerebral artery |
| 6 Middle meningeal artery and vein | 17 Squamous part of occipital bone | 31 Red nucleus | 45 Anterior perforated substance |
| 7 Skin and dense subcutaneous tissue | 18 Superior sagittal sinus | 32 Third ventricle | 46 Cingulate gyrus |
| 8 Epicranial aponeurosis (galea aponeurotica) | 19 Falx cerebri | 33 Substantia nigra | 47 Orbitofrontal cortex |
| 9 Temporalis | 20 Straight sinus | 34 Cornu ammonis (hippocampus) | |
| 10 Pericranium | 21 Tentorium cerebelli | 35 Mamillary body | |
| 11 Squamous part of temporal bone | 22 Collateral sulcus | 36 Hypothalamus | 48 Cisterna ambiens |
| | 23 Vermis of cerebellum | 37 Optic tract | 49 Temporal lobe |
| | 24 Lateral ventricle | 38 Amygdala | 50 Interpeduncular cistern |
| | 25 Parahippocampal gyrus | 39 Middle cerebral artery (branches) | |

Section level



Notes

This section passes through the upper part of the squamous temporal bone (11) and traverses the midbrain at the level of the cerebral peduncle (30) and the red nucleus (31).

The red nucleus (31) has a pinkish tinge, which is visible only in fresh tissue. The colour is produced by a ferric iron pigment present in the neurons of the red nucleus.

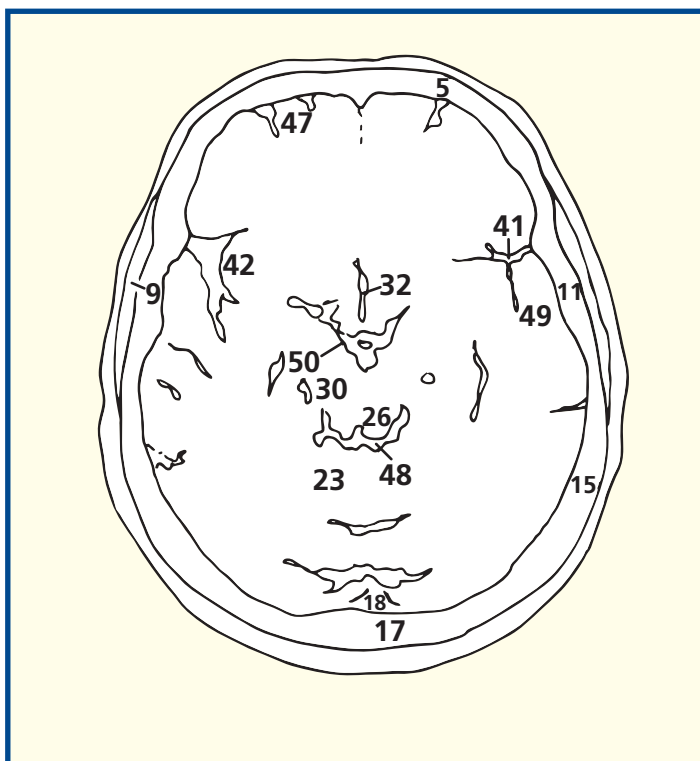
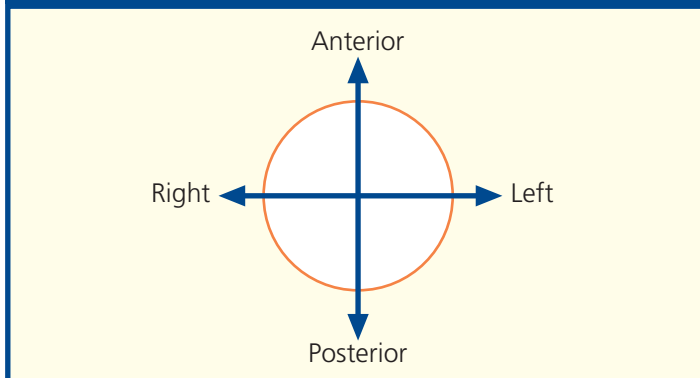
The aqueduct of Sylvius (27) is the communication between the third ventricle (see Axial section 7) and the fourth ventricle (see Axial section 10).

The colliculi, two superior (26) and two inferior, blend to form the tectum over the aqueduct (27). This is sometimes termed the quadrigeminal plate, hence an alternative name for the cisterna ambiens (48) is the quadrigeminal cistern. Other names for this include superior cistern and cistern of the great cerebral vein. As this cistern contains the great cerebral vein and the pineal body, it is an important anatomical landmark.

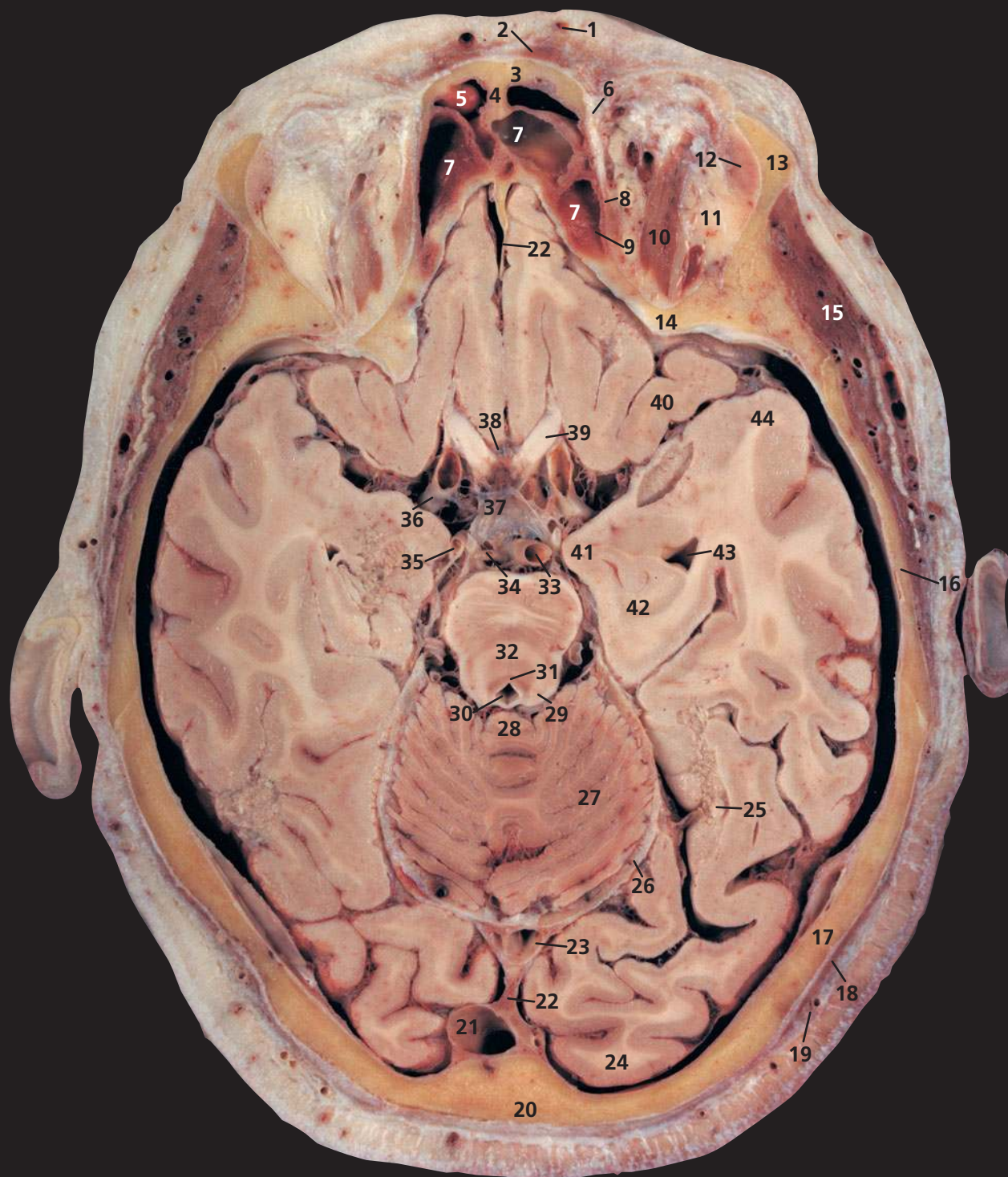
The squamous part of the temporal bone (11) is the thinnest bone of the calvarium (although, in contrast, its petrous part is the densest). It is, however, 'protected' by the thick overlying temporalis muscle (9).

The middle meningeal artery (6) is a branch of the maxillary artery, and its accompanying vein, and may be torn, either together or individually, in fractures of the temporal bone. This constitutes the commonest cause of a traumatic extradural haematoma.

Orientation

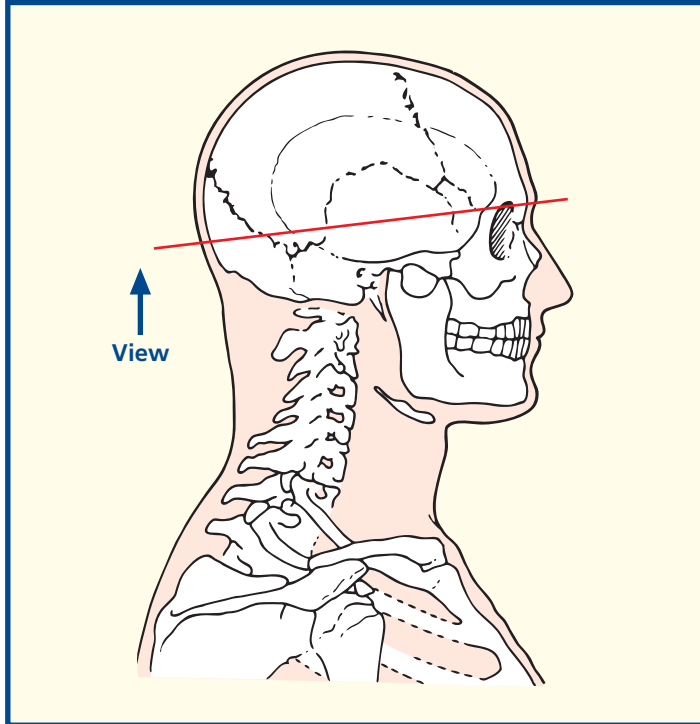


Axial computed tomogram (CT)



- | | | | |
|------------------------------------------------------------|------------------------------------------------|------------------------------------------------|---------------------------------------|
| 1 Supra-orbital artery | 14 Lesser wing of sphenoid bone | 27 Anterior lobe of cerebellum | 40 Orbitofrontal cortex |
| 2 Frontal belly of occipitofrontalis | 15 Temporalis | 28 Cerebellar vermis | 41 Uncus of parahippocampal gyrus |
| 3 Frontal bone | 16 Temporal bone | 29 Inferior colliculus | 42 Hippocampus |
| 4 Frontal crest | 17 Parietal bone | 30 Aqueduct of Sylvius | 43 Temporal horn of lateral ventricle |
| 5 Frontal sinus | 18 Posterior belly of occipitofrontalis | 31 Locus coeruleus | 44 Temporal pole |
| 6 Trochlea | 19 Occipital artery | 32 Decussation of superior cerebellar peduncle | 45 Vitreous humour |
| 7 Ethmoidal air cells | 20 Occipital bone | 33 Basilar artery | 46 Lens |
| 8 Superior oblique | 21 Superior sagittal sinus | 34 Superior cerebellar artery | 47 Middle cerebral artery |
| 9 Orbital plate of ethmoid bone | 22 Falx cerebri | 35 Posterior cerebral artery | |
| 10 Superior rectus underlying levator palpebrae superioris | 23 Straight sinus | 36 Internal carotid artery | |
| 11 Orbital fat | 24 Occipital pole | 37 Pituitary infundibulum | |
| 12 Lacrimal gland | 25 Floor of lateral ventricle (occipital horn) | 38 Optic chiasma | |
| 13 Zygomatic process of frontal bone | 26 Tentorium cerebelli (outer edge) | 39 Optic nerve (II) | |

Section level



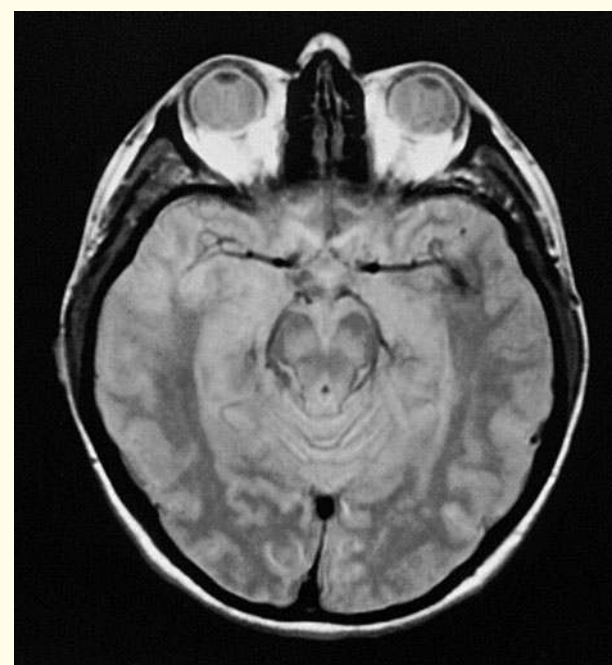
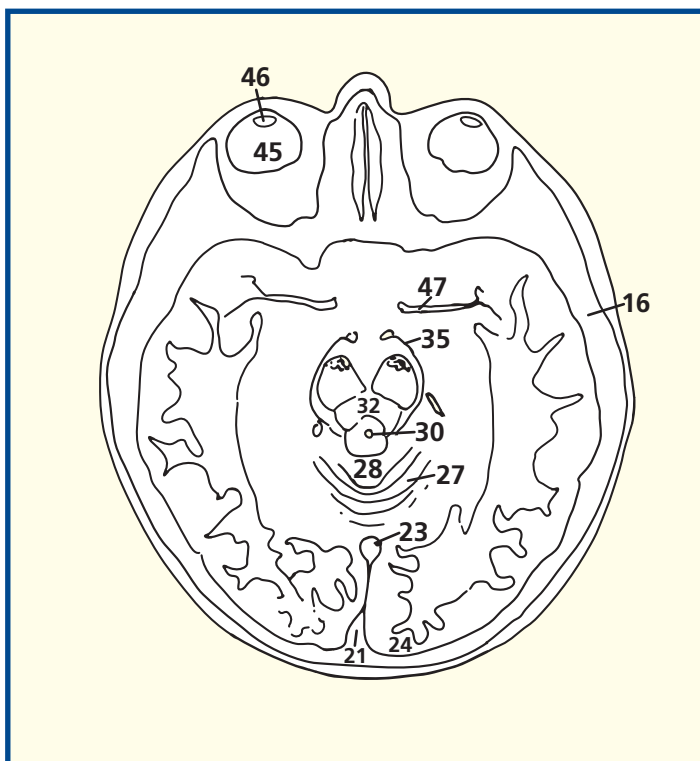
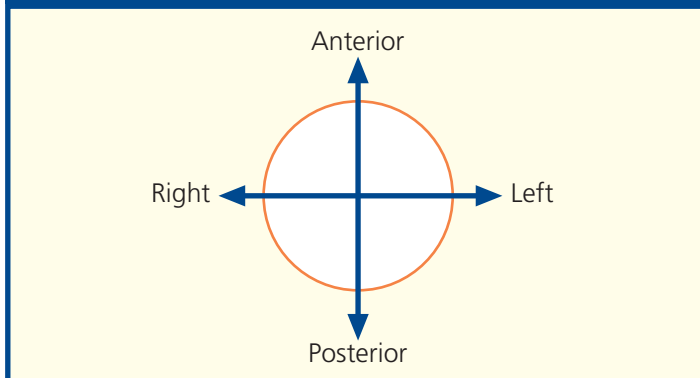
Notes

This section traverses the upper part of the orbits, the midbrain at the level of the inferior colliculus (29) and the anterior lobe of the cerebellum (27).

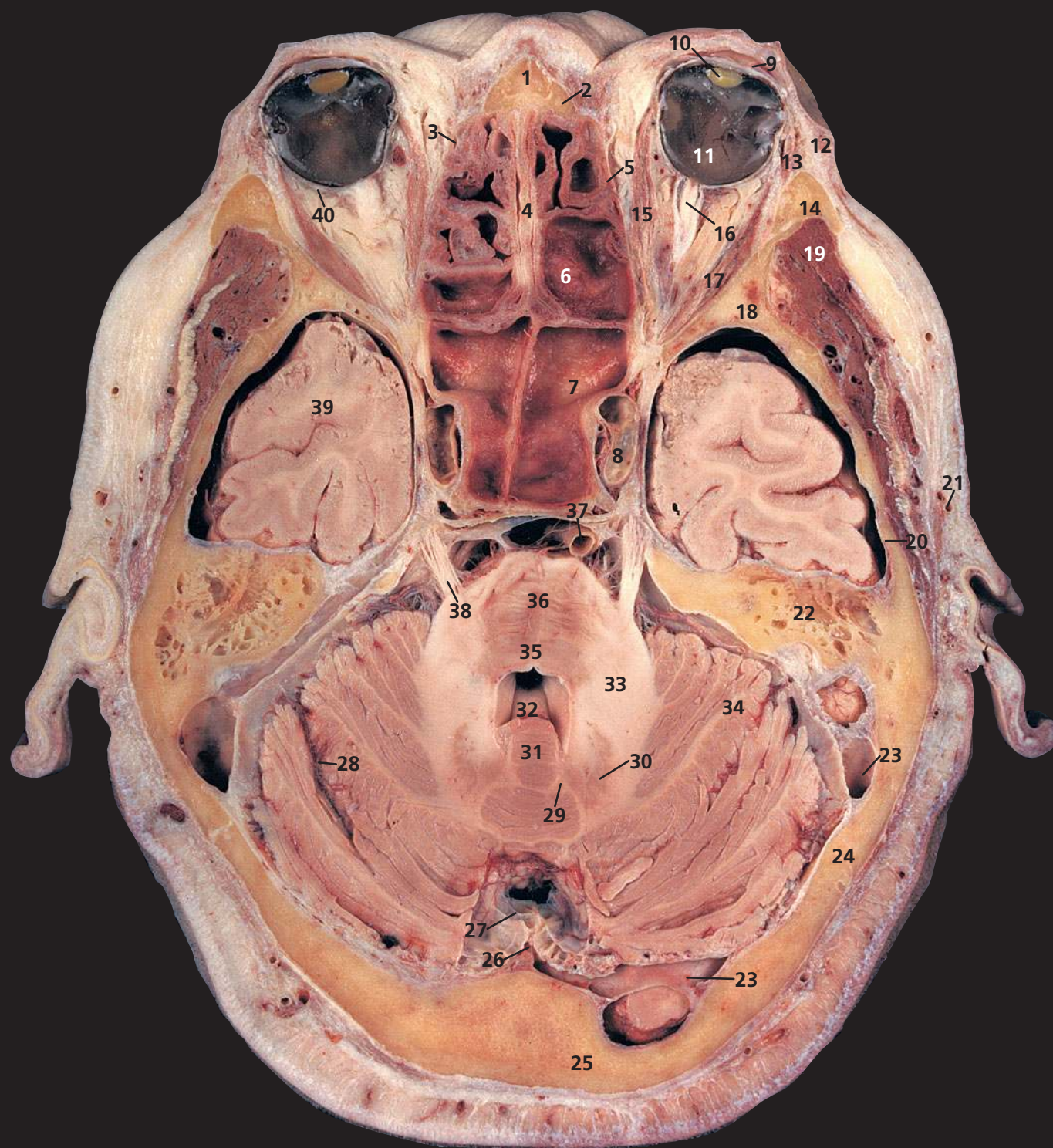
The straight sinus (23) lies in the sagittal plane of the tentorium cerebelli (26) at its attachment to the falx cerebri (22). It receives both the inferior sagittal sinus and the great cerebral vein, and drains posteriorly, usually into the left, but occasionally into the right, transverse sinus.

The optic nerves (39) have an intracranial course of about 10 mm. They unite at the optic chiasma (38), which lies immediately anterior to the infundibulum of the hypophysis cerebri, or pituitary gland (37). See also Coronal section 8 on p. 64.

Orientation



Axial magnetic resonance image (MRI)



- 1 Nasal bone
- 2 Frontal process of maxilla
- 3 Nasolacrimal duct
- 4 Perpendicular plate of ethmoid bone
- 5 Orbital plate of ethmoid bone
- 6 Posterior ethmoidal air cells
- 7 Sphenoidal sinus
- 8 Internal carotid artery within cavernous sinus
- 9 Cornea
- 10 Lens
- 11 Vitreous humour

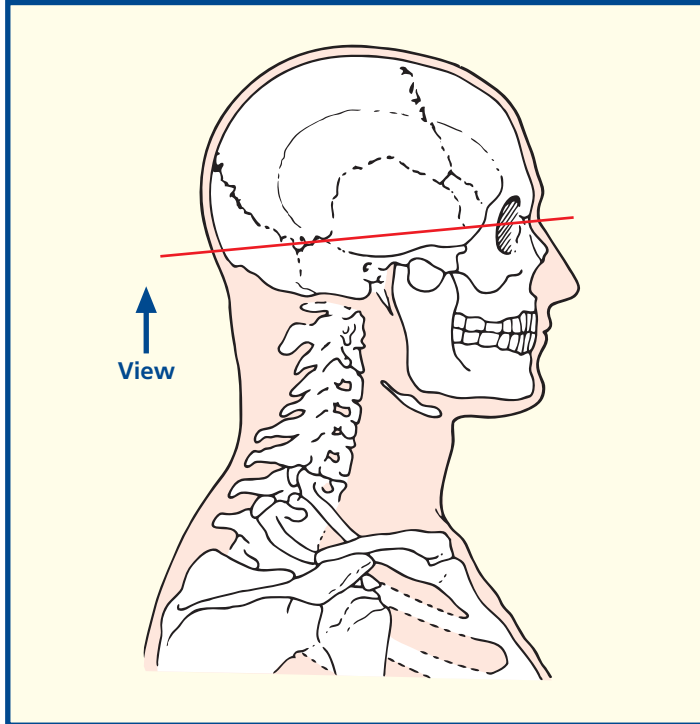
- 12 Orbicularis oculi – orbital part
- 13 Orbicularis oculi – palpebral part
- 14 Frontal process of zygomatic bone
- 15 Medial rectus
- 16 Optic nerve (II)
- 17 Lateral rectus
- 18 Greater wing of sphenoid bone
- 19 Temporalis
- 20 Squamous part of temporal bone
- 21 Superficial temporal artery and vein

- 22 Mastoid air cells
- 23 Transverse sinus
- 24 Parietal bone
- 25 Squamous part of occipital bone
- 26 Falx cerebelli
- 27 Superior sagittal sinus
- 28 Posterolateral fissure
- 29 Emboliform (interposed) nucleus
- 30 Dentate nucleus
- 31 Vermis of cerebellum
- 32 Fourth ventricle
- 33 Middle cerebellar peduncle

- 34 Hemisphere of cerebellum
- 35 Pontine tegmentum
- 36 Pontine nuclei
- 37 Basilar artery
- 38 Trigeminal nerve (V)
- 39 Temporal lobe
- 40 Sclera

- 41 Crista galli of ethmoid
- 42 Petrous part of temporal bone
- 43 Internal auditory meatus

Section level



Notes

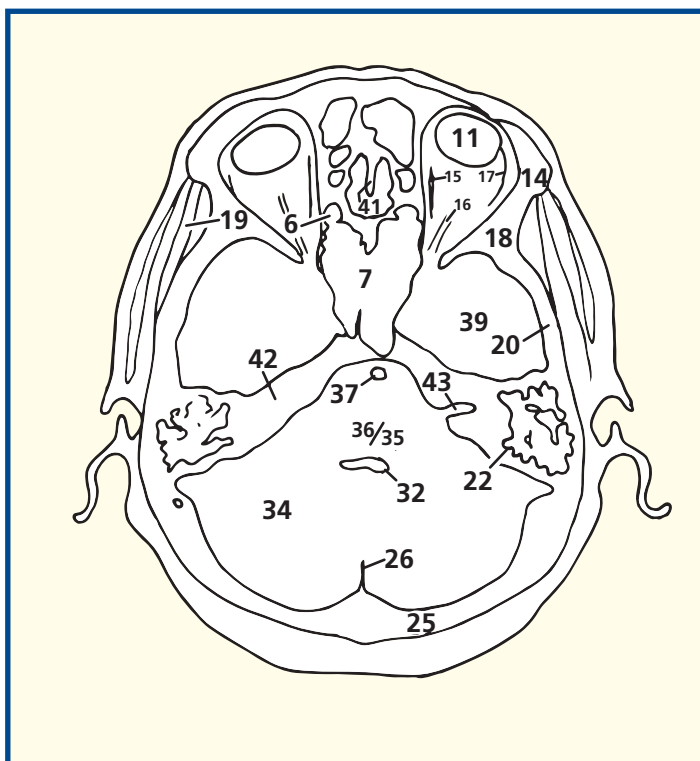
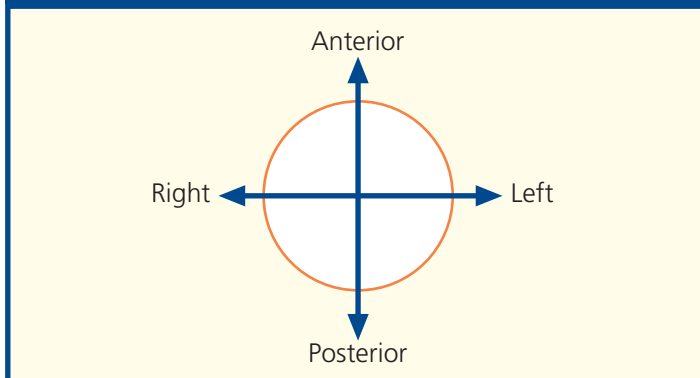
This section transects the eyeballs, the sphenoid sinus (7) and the pons (36) at the level of the middle cerebellar peduncles (33).

The structure of the orbit in horizontal section can be appreciated in this section. The eyeball with its cornea (9), lens (10) and vitreous humour (11) contained within the tough sclera (40), and the optic nerve (16) lie surrounded by the extrinsic muscles (15, 17). The slit-like nasolacrimal duct (3) drains downwards into the inferior meatus.

The fourth ventricle (32) lies above the tegmentum of the pons (35) and below the vermis of the cerebellum (31).

The ethmoidal air cells, or sinuses (6), are made up of some eight to ten loculi suspended from the outer extremity of the cribriform plate of the ethmoid bone and bounded laterally by its orbital plate. They thus occupy the upper lateral wall of the nasal cavity. The cells are divided into anterior, middle and posterior groups by bony septa. The middle group bulge into the middle meatus to form an elevation, the bulla ethmoidalis, into which they open. The anterior cells drain into the hiatus semilunaris, which is a groove below the bulla. The posterior cells drain into the superior meatus.

Orientation

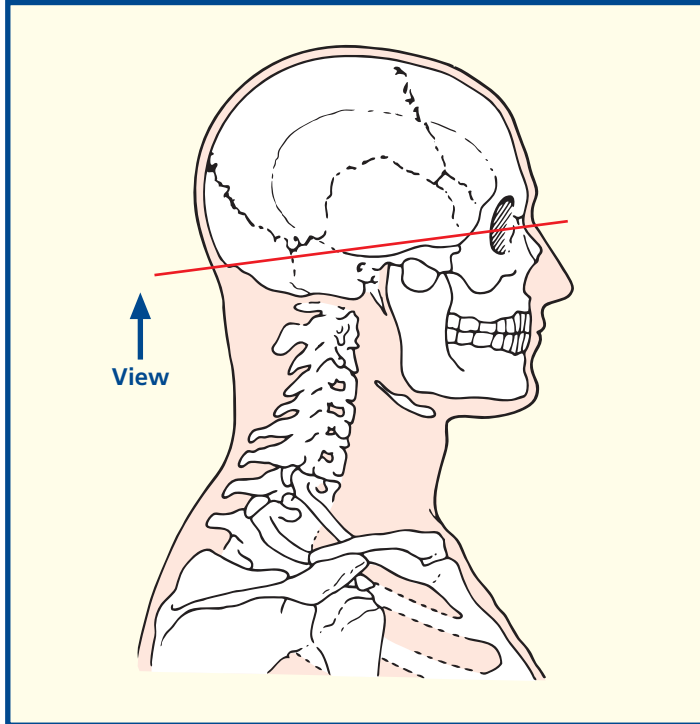


Axial computed tomogram (CT)



- | | | | |
|----------------------------------------|--------------------------------------|-----------------------------------------|----------------------------------------------|
| 1 Inferior rectus | 14 Apex of maxillary antrum | 25 Transverse sinus | 37 Basilar artery |
| 2 Nasolacrimal duct | 15 Frontal process of zygomatic bone | 26 Occipital artery and vein | 38 Abducent nerve (VI) |
| 3 Cartilage of nasal septum | 16 Temporalis | 27 Trapezius | 39 Trigeminal nerve (V) |
| 4 Nasal bone | 17 Greater wing of sphenoid bone | 28 External occipital protuberance | 40 Labyrinthine artery |
| 5 Frontal process of maxilla | 18 Middle meningeal artery | 29 Falx cerebelli | 41 Facial nerve (VII) |
| 6 Lacrimal bone | 19 Petrous part of temporal bone | 30 Vermis | 42 Vestibulocochlear (auditory) nerve (VIII) |
| 7 Upper eyelid | 20 Internal carotid artery | 31 Middle cerebellar peduncle | 43 Cochlea |
| 8 Orbicularis oculi | 21 Sphenoidal sinus | 32 Fourth ventricle with choroid plexus | 44 Stapes |
| 9 Sclera | 22 Septum of sphenoidal sinus | 34 Inferior cerebellar peduncle | 45 External auditory meatus |
| 10 Vitreous humour | 23 Cerebellar hemisphere | 35 Flocculus | 46 Tympanic membrane and handle of malleus |
| 11 Orbital plate of ethmoid bone | 24 Mastoid air cells | 36 Pyramidal tract | 47 Auditory tube (Eustachian) |
| 12 Ethmoidal air cells | | | |
| 13 Perpendicular plate of ethmoid bone | | | |

Section level



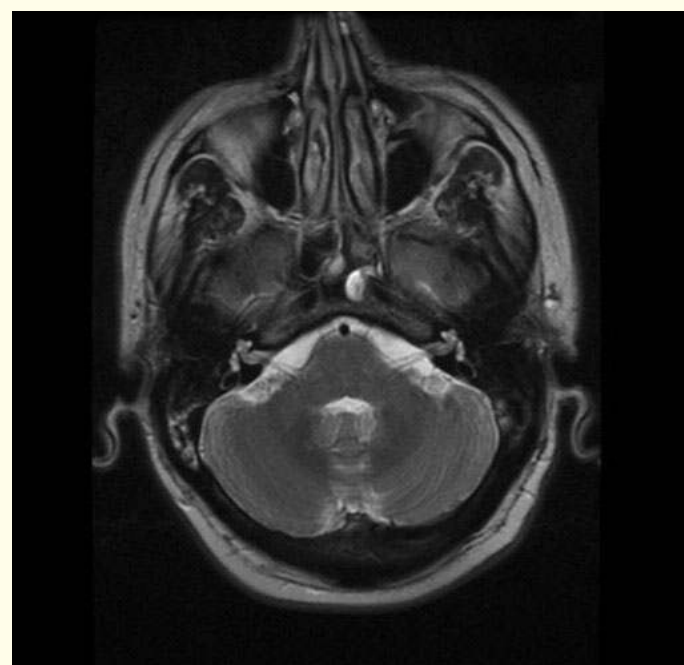
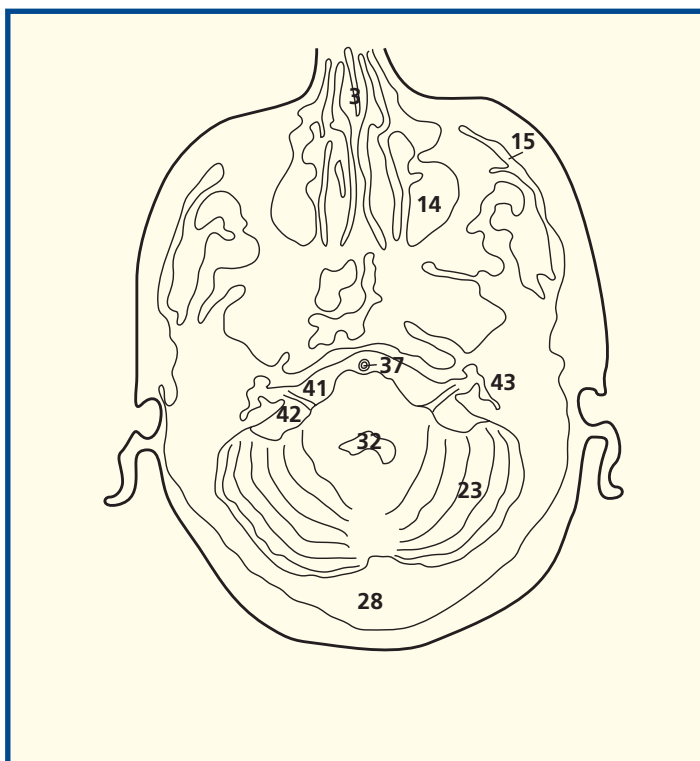
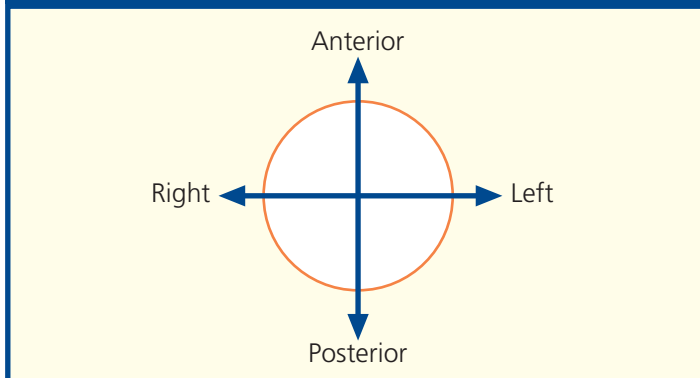
Notes

This section passes through the upper part of the nasal cavity, the medulla oblongata (33) and, posteriorly, through the external occipital protuberance (28).

The sphenoidal sinus (21) is unusually large in this specimen. It is divided by a median septum (22) and drains anteriorly into the nasal cavity at the sphenoidal recess.

Note the relations of the labyrinthine artery (40), a branch of the basilar artery (37), the facial nerve (41) and the vestibulocochlear (or auditory) nerve (42) as they enter the internal auditory meatus of the temporal bone together with the close relationships of the trigeminal nerve (V) (39) and the cerebellum (35). As an acoustic neuroma of the vestibulocochlear nerve enlarges, it stretches the adjacent cranial nerves V and VII anteriorly and also presses on the cerebellum and brain stem to produce the cerebello-pontine angle syndrome. Rather surprisingly, facial nerve weakness with unilateral taste loss is uncommon – occurring in less than five per cent of cases – although the facial nerve is at risk in surgical removal of the tumour.

Orientation

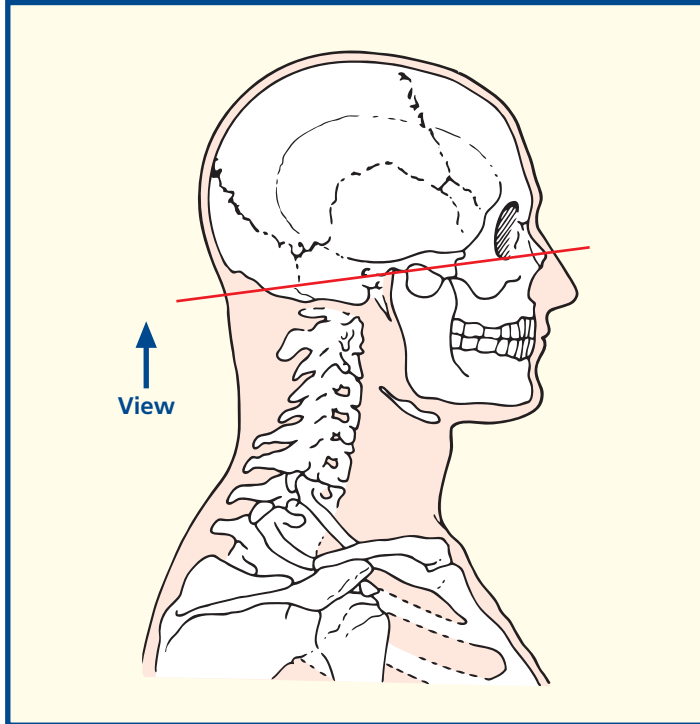


Axial magnetic resonance image (MRI)



- | | | | |
|---------------------------------------|----------------------------------------------|-----------------------------------------------|--------------------------------------------------------------------------|
| 1 Cartilage of nasal septum | 15 Trigeminal nerve (V) | 26 Vermis | 39 Bulb of internal jugular vein |
| 2 Nasolacrimal duct | 16 Articular disc of temporomandibular joint | 27 Cerebellar hemisphere | 40 Glossopharyngeal nerve (IX), vagus nerve (X) and accessory nerve (XI) |
| 3 Orifice of maxillary sinus | 17 Head of mandible | 28 Tonsil of cerebellum | 41 Internal carotid artery |
| 4 Maxillary sinus | 18 Superficial temporal artery and vein | 29 Fourth ventricle (median aperture of roof) | 42 Basi-occiput |
| 5 Maxillary artery | 19 External auditory meatus | 30 Anterior inferior cerebellar artery | 43 Longus capitis |
| 6 Sphenoidal sinus | 20 Mastoid air cells | 31 Glossopharyngeal nerve (IX) | 44 Auditory (Eustachian) tube |
| 7 Vomer | 21 Sternocleidomastoid | 32 Hypoglossal nerve (XII) | |
| 8 Middle nasal concha | 22 Occipital artery and vein | 33 Pyramidal tract | |
| 9 Maxilla | 23 Trapezius | 34 Medulla | |
| 10 Orbicularis oculi | 24 Occipital bone – squamous part | 35 Inferior olive | |
| 11 Zygomatic bone | 25 Falx cerebelli | 36 Vertebral artery | |
| 12 Temporalis and tendon | | 37 Vagus nerve (X) | |
| 13 Zygomatic process of temporal bone | | 38 Sigmoid sinus | |
| 14 Lateral pterygoid | | | |
| | | | 45 Pterygopalatine fossa (apex) |
| | | | 46 Foramen ovale |

Section level



Notes

This section transects the maxillary sinus (4) and the basi-occiput (42) and passes through the external auditory meatus (19).

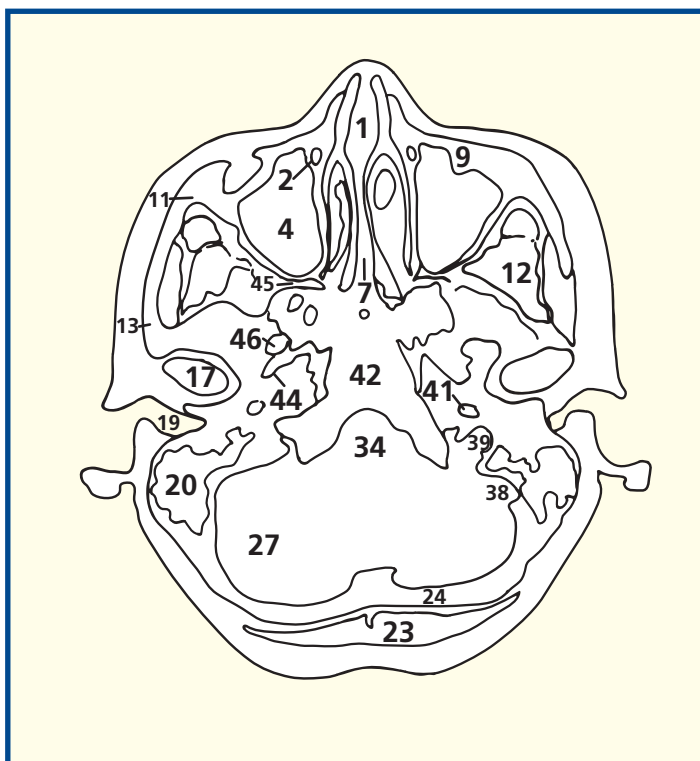
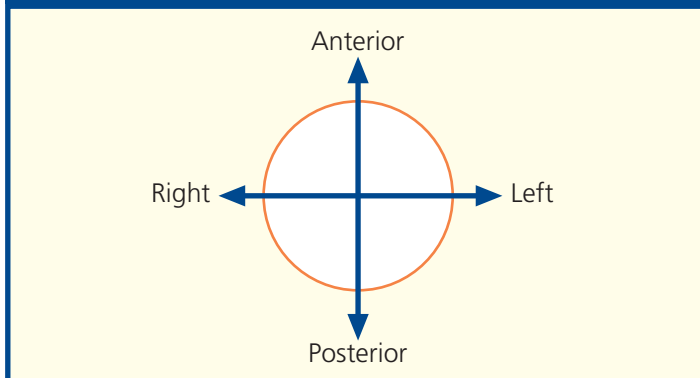
At this level, the vertebral arteries (36) are running cranially from their entry into the skull at the foramen magnum to form the basilar artery.

The sigmoid sinus (38) runs forward to emerge from the skull at the jugular foramen, at which it becomes the bulb of the internal jugular vein (39). Exiting through the jugular foramen anterior to the vein lie, from anterior to posterior, the glossopharyngeal, vagus and accessory cranial nerves (40).

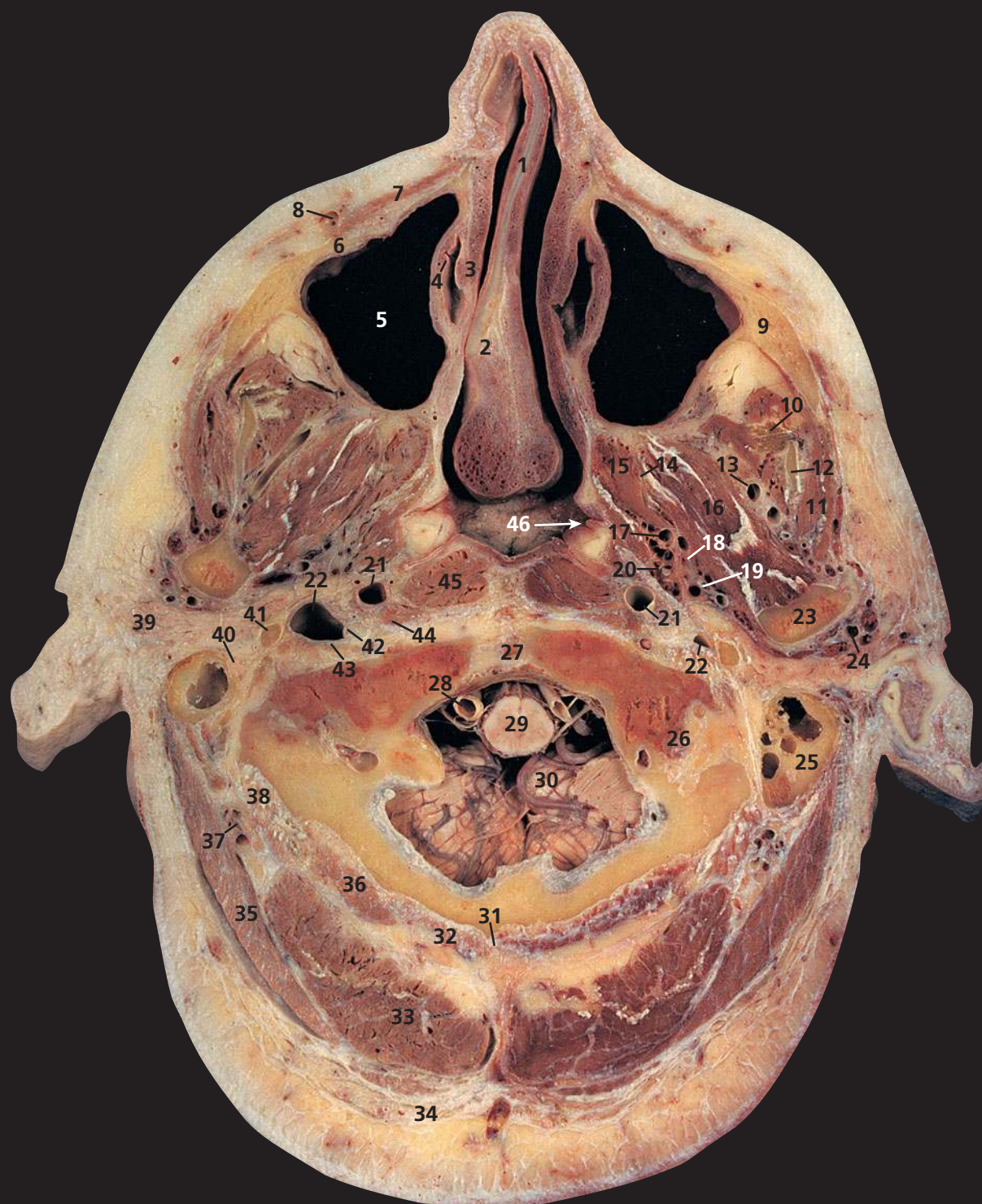
The maxillary nerve (Vⁱⁱ) passes into the pterygopalatine fossa (45 on this CT image) having traversed the foramen rotundum. The mandibular nerve (Vⁱⁱⁱ) leaves the skull via the foramen ovale (46).

The maxillary sinus (4) is the largest of the air sinuses, is pyramidal in shape and occupies the body of the maxilla. Medially, the sinus drains through its orifice (3) into the middle meatus below the middle concha (8). The ostium is placed high up on this wall and is thus located inefficiently from a mechanical point of view; drainage depends mainly on the effectiveness of the cilia that line the walls of the sinus.

Orientation

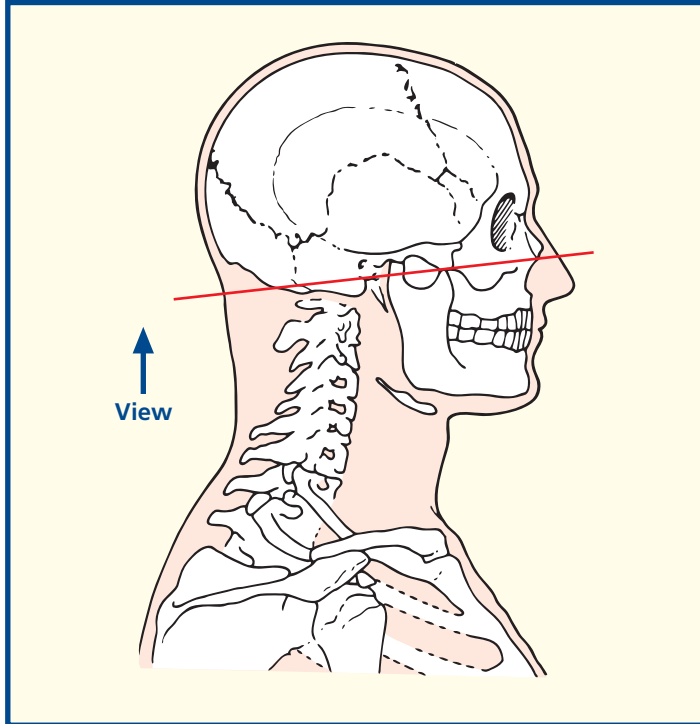


Axial computed tomogram (CT)



- | | | | |
|---------------------------------|-------------------------------------------------|-----------------------------------|--------------------------------------------------------------------------|
| 1 Cartilage of nasal septum | 14 Lateral pterygoid plate of sphenoid | 26 Base of occipital condyle | 38 Obliquus capitis superior |
| 2 Vomer | 15 Medial pterygoid | 27 Basilar part of occipital bone | 39 Parotid gland |
| 3 Inferior nasal concha | 16 Lateral pterygoid | 28 Vertebral artery | 40 Facial nerve (VII) |
| 4 Orifice of nasolacrimal duct | 17 Pterygoid artery and pterygoid venous plexus | 29 Spinal cord | 41 Styloid process |
| 5 Maxillary sinus | 18 Lingual nerve (V ⁱⁱⁱ) | 30 Tonsil of cerebellum | 42 Glossopharyngeal nerve (IX), vagus nerve (X) and accessory nerve (XI) |
| 6 Maxilla | 19 Inferior alveolar nerve (V ⁱⁱⁱ) | 31 External occipital crest | 43 Hypoglossal nerve (XII) |
| 7 Levator labii superioris | 20 Chorda tympani | 32 Rectus capitis posterior minor | 44 Rectus capitis anterior |
| 8 Facial vein | 21 Internal carotid artery | 33 Semispinalis capitis | 45 Longus capitis |
| 9 Zygomatic bone | 22 Internal jugular vein | 34 Trapezius | 46 Opening of auditory (Eustachian) tube |
| 10 Tendon of temporalis | 23 Neck of condylar process of mandible | 35 Splenius capitis | |
| 11 Masseter | 24 Superficial temporal artery | 36 Rectus capitis posterior major | |
| 12 Coronoid process of mandible | 25 Mastoid air cells | 37 Occipital artery and vein | |
| 13 Maxillary artery and vein | | | 47 Nasopharynx |
| | | | 48 Parapharyngeal space |
| | | | 49 Pharyngeal recess |

Section level



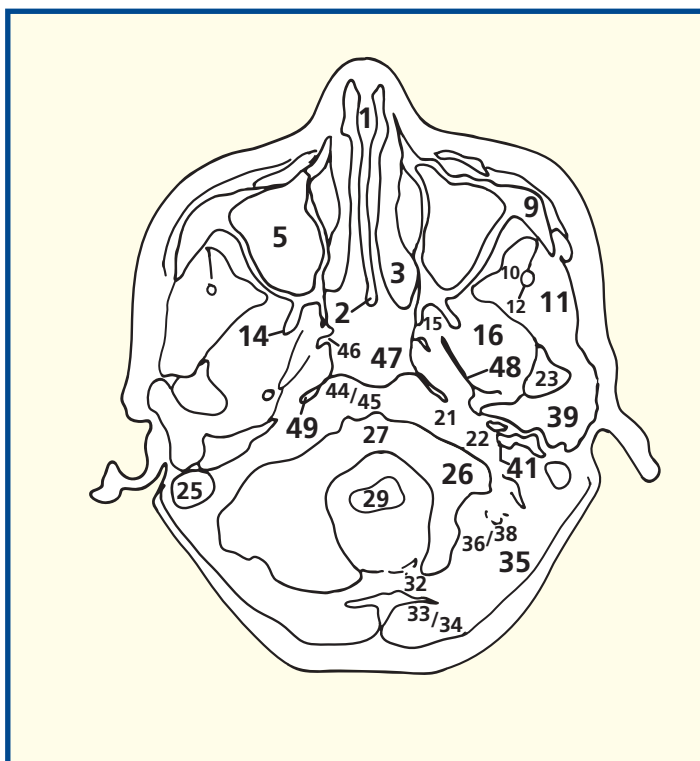
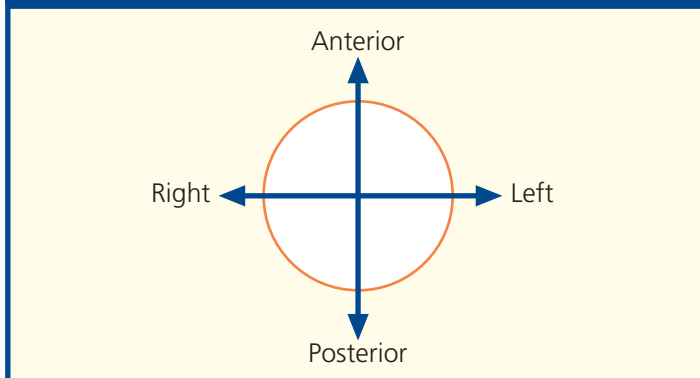
Notes

This section traverses the nasal septum (1) at the level of the inferior nasal concha (3), beneath which opens the nasolacrimal duct (4). This is the only structure that drains into the inferior meatus of the nasal cavity. Its termination is guarded by a mucosal valve, which prevents reflux from the nose. Posteriorly, the plane passes through the uppermost part of the spinal cord (29) and the cerebellar tonsil (30).

The internal jugular vein (22) in this specimen is small, especially on the left side. The chorda tympani (20) is seen here as it emerges from the petrotympanic fissure to join the lingual nerve (18) about 2 cm below the base of the skull. It subserves taste sensation to the anterior two-thirds of the tongue and supplies secretomotor fibres to the submandibular and sublingual salivary glands.

The tonsil of the cerebellum (30), on the inferior aspect of the cerebellar hemisphere, lies immediately above the foramen magnum. Withdrawal of cerebrospinal fluid at lumbar puncture in a patient with raised intracranial pressure is dangerous as it may result in potentially lethal herniation of the tonsils through this bony ring.

Orientation

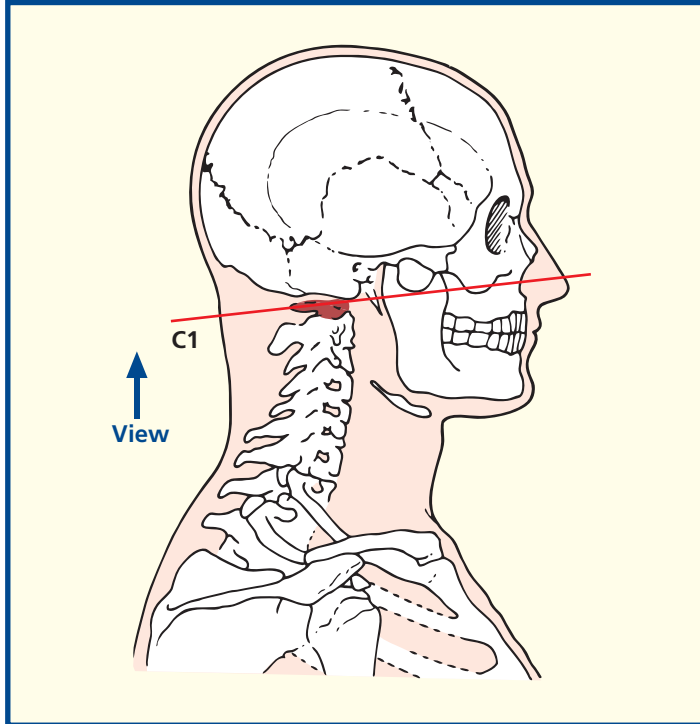


Axial computed tomogram (CT)



- | | | | |
|----------------------------------------------------------------|-----------------------------------------|----------------------------------------------------------------|----------------------------------------------------|
| 1 Cartilage of nasal septum | 17 Maxillary artery | 31 Spinal root of accessory nerve (XI) | 42 Nasopharynx |
| 2 Facial vein | 18 Styloid process | 32 Spinal cord within dural sheath | 43 Internal carotid artery |
| 3 Inferior nasal concha | 19 External carotid artery | 33 Spinal dura mater | 44 Glossopharyngeal nerve (IX) and vagus nerve (X) |
| 4 Horizontal plate of palatine bone | 20 Retromandibular vein | 34 Vertebral artery | 45 Sympathetic chain |
| 5 Maxillary sinus | 21 Posterior belly of digastric | 35 Atlanto-occipital joint | 46 Internal jugular vein |
| 6 Levator labii superioris | 22 Anastomotic vertebral vein | 36 Condyle of occipital bone | 47 Parotid gland |
| 7 Zygomaticus major | 23 Sternocleidomastoid | 37 Alar ligament | 48 Stylopharyngeus |
| 8 Maxilla | 24 Splenius capitis | 38 Transverse ligament of atlas (first cervical vertebra) | 49 Accessory nerve (XI) |
| 9 Buccal pad of fat | 25 Trapezius | 39 Dens of axis (odontoid process of second cervical vertebra) | 50 Pterygoid venous plexus |
| 10 Lateral pterygoid | 26 Semispinalis capitis | 40 Anterior arch of atlas (first cervical vertebra) | 51 Tensor veli palatini |
| 11 Medial pterygoid | 27 Rectus capitis posterior major | 41 Longus capitis | 52 Soft palate |
| 12 Temporalis | 28 Ligamentum nuchae | | |
| 13 Masseter | 29 Posterior atlanto-occipital membrane | | |
| 14 Ramus of mandible | 30 Posterior arch of atlas | | |
| 15 Lingual nerve (V ⁱⁱⁱ) | | | |
| 16 Inferior alveolar artery vein and nerve (V ⁱⁱⁱ) | | | |
| | | | 53 Pharyngeal recess |
| | | | 54 Parapharyngeal space |

Section level



Notes

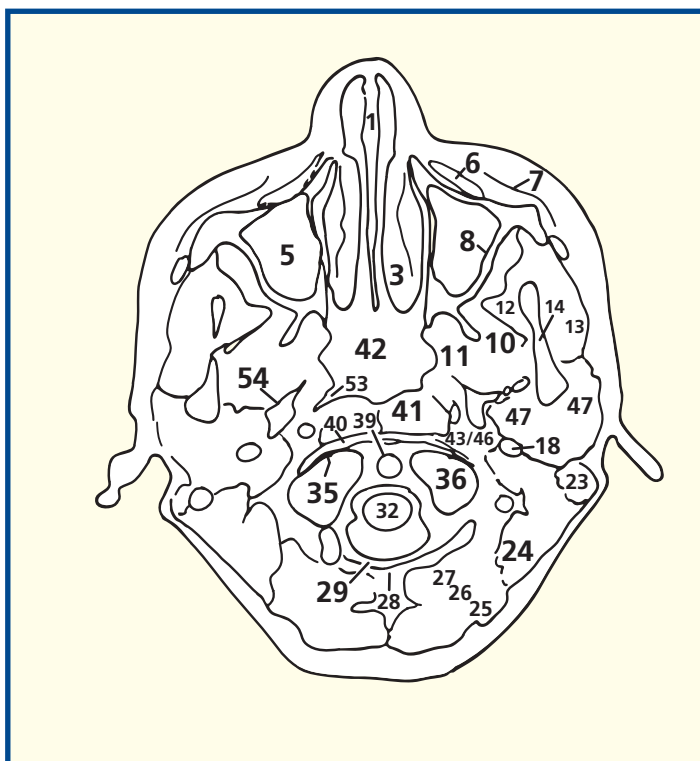
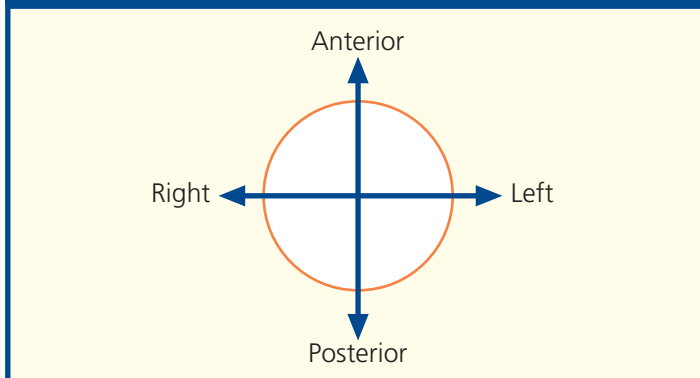
This section traverses the nasal cavity through its inferior meatus below the inferior concha (3), the hard palate at the horizontal plate of the palatine bone (4) and the tip of the dens of the axis, the second cervical vertebra (39).

The external carotid artery (19) divides at the neck of the mandible into the superficial temporal artery and the maxillary artery (17).

Note that the outer endosteal layer of the dura mater of the skull blends with the pericranium at the foramen magnum. The dural sheath surrounding the spinal cord (32) represents the continuation of the inner meningeal layer of the cerebral dura (see Axial section 1).

Note that the large vertebral canal of the atlas (first cervical vertebra), demonstrated well in this section between the posterior atlanto-occipital membrane (29) and the anterior arch of the atlas (40), and seen well also in the Axial section 15, can be conveniently divided by the 'rule of three' into three roughly equal areas – that occupied by the cervical spinal cord (32), that occupied by the dens of the axis (39) and that occupied by the dural sheath and the extradural space.

Orientation



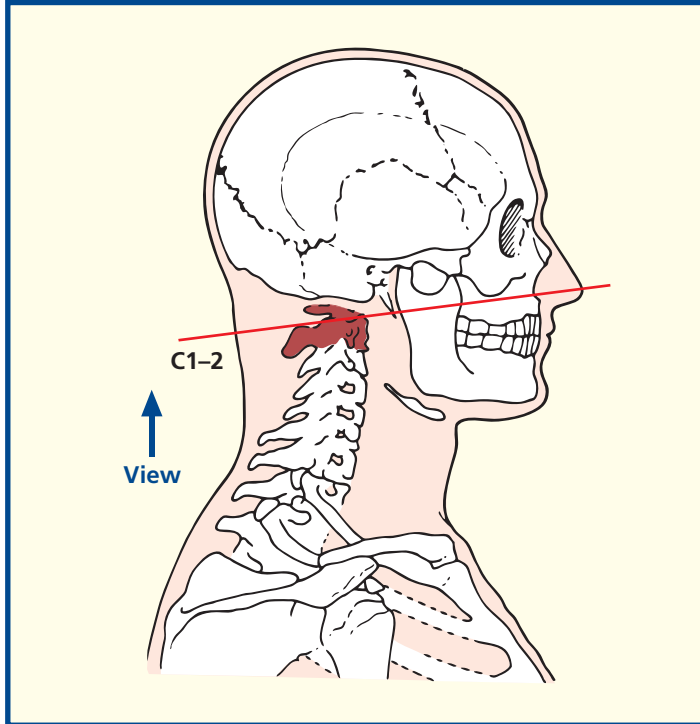
Axial computed tomogram (CT)



- | | | | |
|---------------------------------------------------------------|------------------------------------------------------|----------------------------------------------------------------|-------------------------------------------------------------------------------------------------|
| 1 Nasopalatine nerve (V ⁱⁱ) within incisive canal | 16 Retromandibular vein | 30 Dorsal root ganglion of second cervical nerve | 40 Internal carotid artery |
| 2 Orbicularis oris | 17 Parotid gland | 31 Spinal cord within dural sheath | 41 Vertebral artery |
| 3 Levator angulis oris | 18 External carotid artery | 32 Transverse ligament of atlas | 42 Transverse process of atlas (first cervical vertebra) |
| 4 Maxillary antrum | 19 Dermoid cyst of scalp | 33 Dens of axis (odontoid process of second cervical vertebra) | 43 Internal jugular vein |
| 5 Zygomaticus major | 20 Trapezius | 34 Lateral mass of atlas (first cervical vertebra) | 44 Styloid process, with origins of styloglossus and stylohyoid and glossopharyngeal nerve (IX) |
| 6 Buccinator | 21 Splenius capitis | 35 Longus capitis | 45 Stylopharyngeus |
| 7 Alveolar process of maxilla | 22 Semispinalis capitis | 36 Longus colli | |
| 8 Hard palate | 23 Ligamentum nuchae | 37 Anterior arch of atlas (first cervical vertebra) | |
| 9 Soft palate | 24 Spine of axis | 38 Nasopharynx | |
| 10 Temporalis | 25 Obliquus capitis inferior | 39 Vagus nerve (X) and hypoglossal nerve (XII) | |
| 11 Medial pterygoid | 26 Longissimus capitis | | |
| 12 Lingual nerve (V ⁱⁱⁱ) | 27 Sternocleidomastoid | | |
| 13 Ramus of mandible | 28 Posterior belly of digastric | | |
| 14 Inferior alveolar vein and nerve | 29 Posterior arch of atlas (first cervical vertebra) | | |
| 15 Masseter | | | |

- 46 Levator and tensor veli palatini
- 47 Parapharyngeal space
- 48 Inferior nasal concha
- 49 Cartilage of nasal septum

Section level



Notes

This section traverses the hard (8) and soft (9) palate, the nasopharynx (38), the dens (33) and the spine of the axis (24). The CT image is rather more cranial.

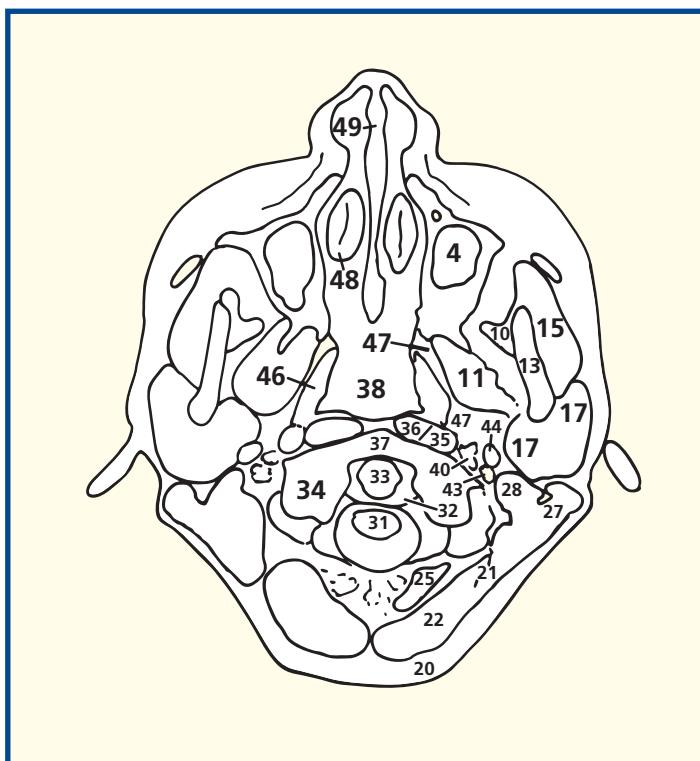
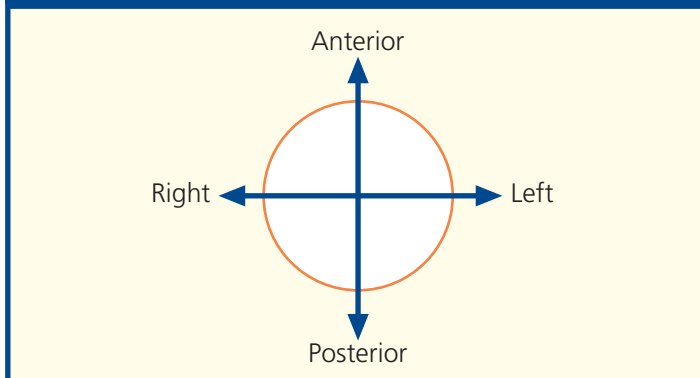
Flexion and extension of the skull (nodding movements of the head) take place at the atlanto-occipital joint between the upper facet of the lateral mass of the atlas (34) and the corresponding facet on the occipital bone. Rotation of the skull (looking to the left and right) takes place at the atlanto-axial articulation between the dens (33) and the facet on the anterior arch of the atlas (37). The transverse ligament of the atlas (32) is dense and is the principal structure in preventing posterior dislocation of the dens.

Obliquus capitis inferior (25) forms the lower outer limb of the suboccipital triangle. The vertebral artery (41), on emerging from the foramen transversarium of the atlas, enters this triangle on its ascending course to the foramen magnum.

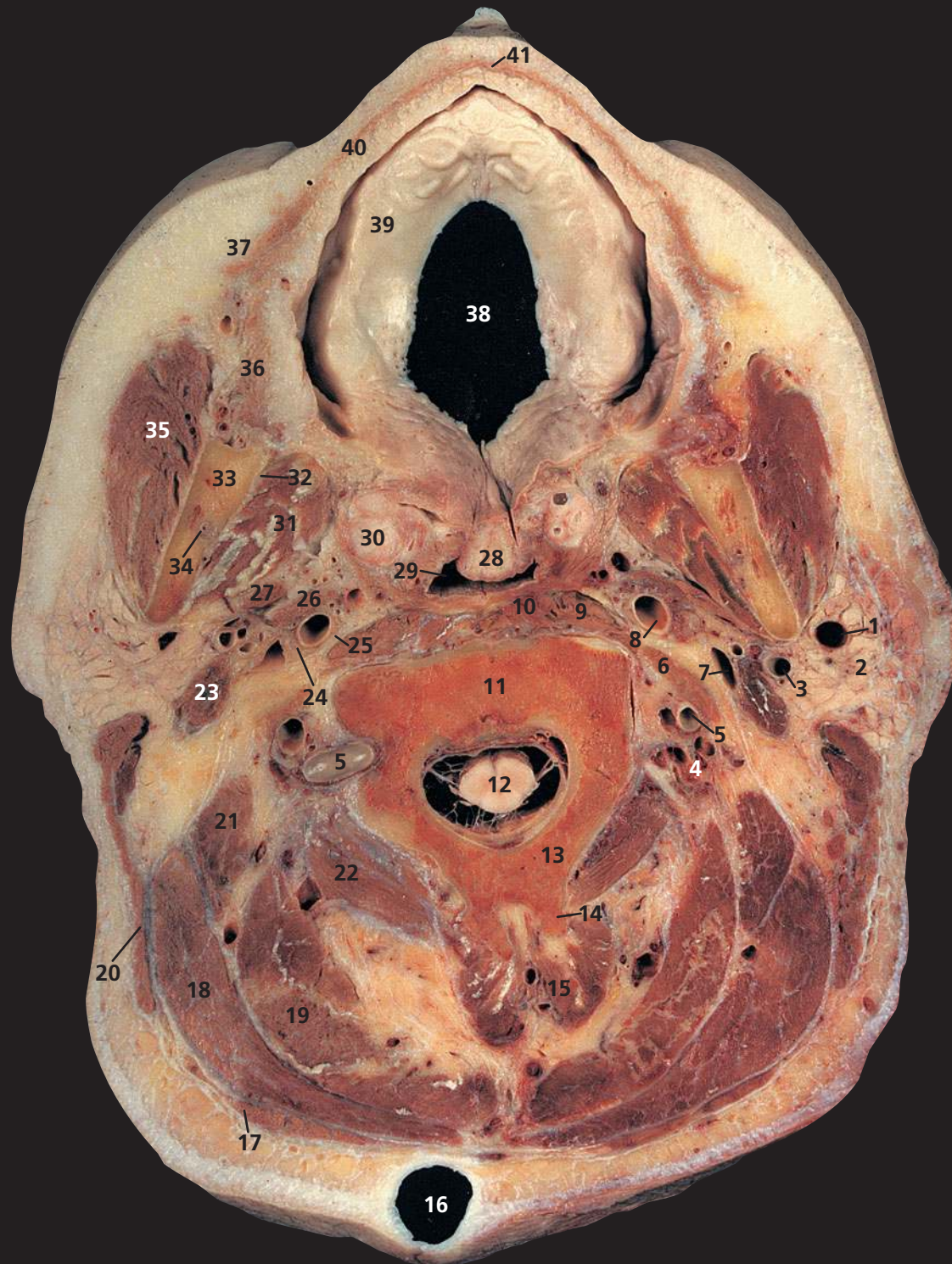
The maxillary antrum, or sinus (4), may be somewhat asymmetrical between the two sides – here it projects more inferiorly on the left side. The floor of the sinus relates to the roots of the upper teeth – at least the upper second premolar and first molar. The sinus may extend forwards, however, as far as the canine and behind to the third molar.

Note that this subject has a large dermoid cyst of the scalp (19).

Orientation

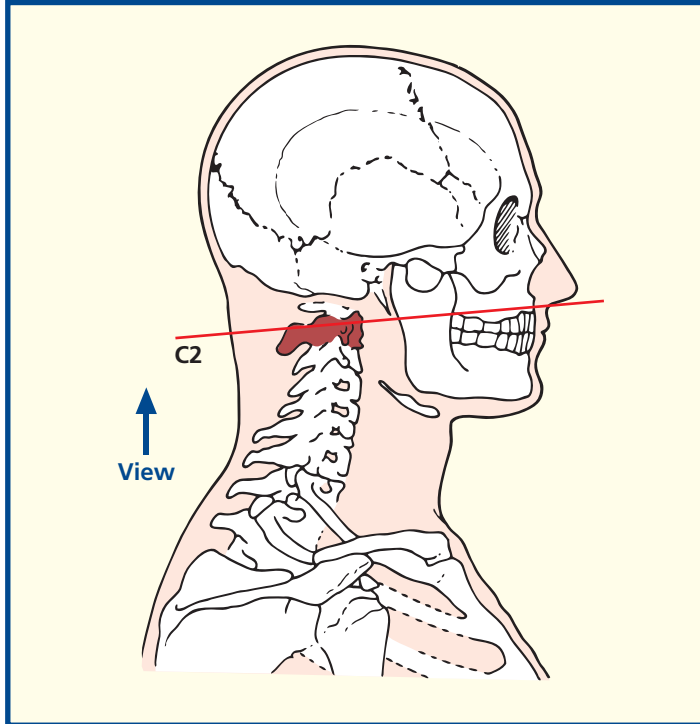


Axial computed tomogram (CT)



- | | | | |
|----------------------------------------------|----------------------------------------------------|-----------------------------------------------------------------------------------------|----------------------------------------------------------------|
| 1 Retromandibular vein | 15 Semispinalis cervicis | 27 Styloglossus and stylohyoid (posteriorly) | 40 Orbicularis oris |
| 2 Parotid gland | 16 Dermoid cyst of scalp | 28 Base of uvula | 41 Mucous gland of lip |
| 3 External carotid artery | 17 Trapezius | 29 Nasopharynx | 42 Hard palate |
| 4 Vertebral vein | 18 Splenius capitis | 30 Palatine tonsil | 43 Soft palate |
| 5 Vertebral artery | 19 Semispinalis capitis | 31 Medial pterygoid | 44 Styloid process |
| 6 Scalenus medius | 20 Sternocleidomastoid | 32 Lingual nerve (V ⁱⁱⁱ) | 45 Parapharyngeal space |
| 7 Internal jugular vein | 21 Longissimus capitis | 33 Ramus of mandible | 46 Anterior arch of atlas |
| 8 Internal carotid artery | 22 Obliquus capitis inferior | 34 Inferior alveolar artery, vein and nerve (V ⁱⁱⁱ) within mandibular canal | 47 Dens of axis (odontoid process of second cervical vertebra) |
| 9 Longus capitis | 23 Posterior belly of digastric | 35 Masseter | 48 Posterior arch of atlas (first cervical vertebra) |
| 10 Longus colli | 24 Vagus nerve (X) and hypoglossal nerve (XII) | 36 Buccinator | 49 Foramen transversarium |
| 11 Body of axis (second cervical vertebra) | 25 Sympathetic chain | 37 Levator anguli oris | |
| 12 Spinal cord within dural sheath | 26 Stylopharyngeus and glossopharyngeal nerve (IX) | 38 Mouth | |
| 13 Lamina of axis (second cervical vertebra) | | 39 Alveolar margin | |
| 14 Spine of axis (second cervical vertebra) | | | |

Section level



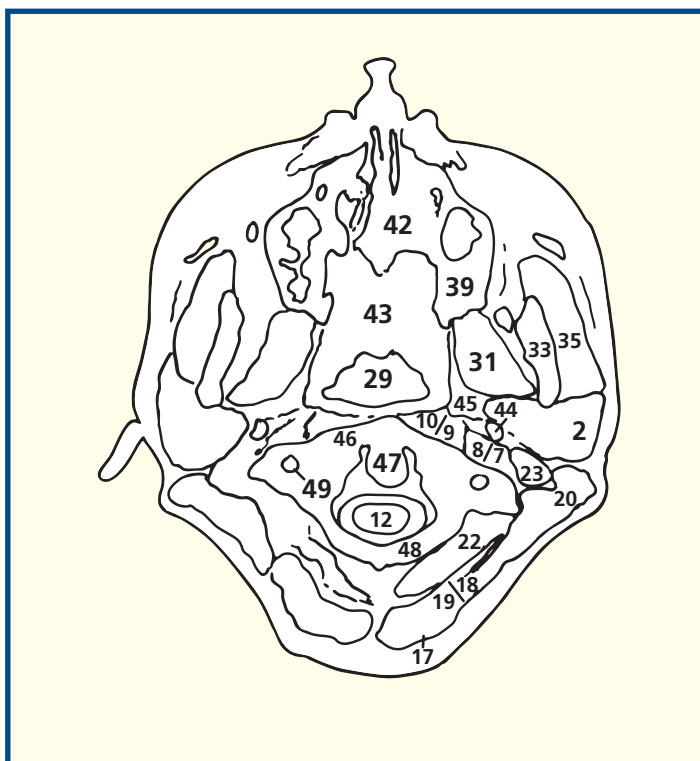
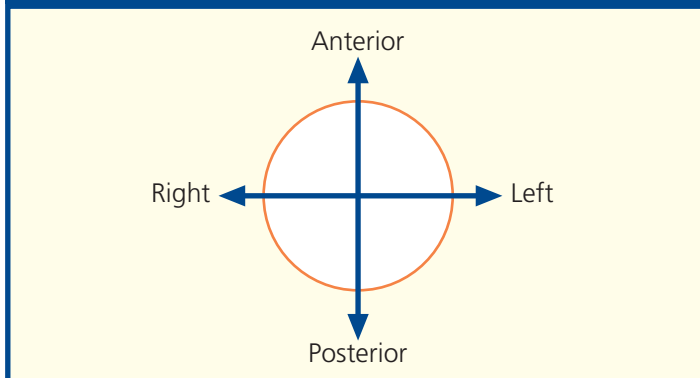
Notes

This section passes through the alveolar margin (39) of the upper jaw and through the body of the axis (11). The CT image is at a more cranial level.

The vertebral artery (5) on the right side of this specimen is tortuous and bulges laterally between the transverse processes of the atlas and axis, a not uncommon feature in arteriosclerotic subjects. Each cervical vertebra bears its characteristic foramen transversarium (49) within its transverse process. The vertebral artery, with its accompanying vein, ascends through the foramina of C6 to C1 to gain access to the foramen magnum. Not uncommonly, the foramen transversarium is bifid, the larger opening of the two being for the vertebral artery and the smaller for the vein. Sympathetic fibres from the superior cervical ganglion (C1, 2, 3, 4) accompany the artery.

The lips are lined by mucous membrane enclosing orbicularis oris (40), the labial vessels and nerves, fibrofatty connective tissue and the labial mucous glands (41). These lie between the mucosa and underlying muscle, are about 0.5 cm in diameter and resemble mucous salivary glands. Their ducts drain into the vestibule of the mouth. These glands, like those studded over the oral aspect of the palate, are occasional sites of pleomorphic adenomas, which are similar to those seen more commonly in the parotid gland.

Orientation

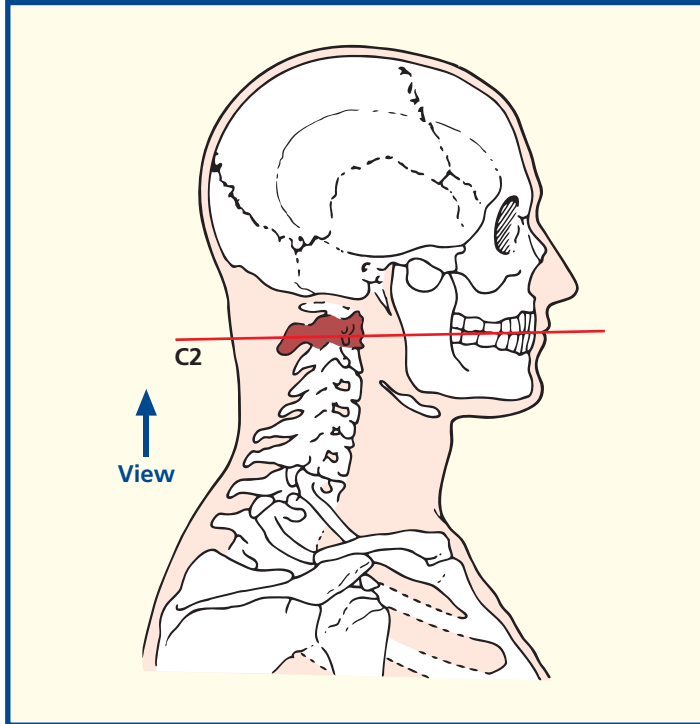


Axial computed tomogram (CT)



- | | | | |
|---------------------------------------------------------------------------------------|------------------------------------------------------------------|------------------------------------------------|--------------------------------|
| 1 Upper lip | 15 Splenius capitis | 25 Scalenus medius | 39 Digastric (posterior belly) |
| 2 Orbicularis oris | 16 Deep cervical vein | 26 Longus capitis | 40 External carotid artery |
| 3 Tongue | 17 Trapezius | 27 Longus colli | 41 Styloglossus |
| 4 Buccinator | 18 Semispinalis cervicis | 28 Constrictor of pharynx | 42 Stylohyoid |
| 5 Facial artery and vein | 19 Spine of axis (second cervical vertebra) | 29 Uvula | 43 Posterior auricular artery |
| 6 Lingual nerve (V ⁱⁱⁱ) | 20 Lamina of axis (second cervical vertebra) | 30 Oropharynx | 44 Retromandibular vein |
| 7 Ramus of mandible | 21 Spinal cord within dural sheath | 31 Palatopharyngeal arch with palatopharyngeal | 45 Parotid gland |
| 8 Masseter | 22 Inferior articular process of axis (second cervical vertebra) | 32 Palatoglossal arch with palatoglossus | |
| 9 Inferior alveolar artery vein and nerve (V ⁱⁱⁱ) within mandibular canal | 23 Vertebral artery and vein | 33 Palatine tonsil | |
| 10 Medial pterygoid | 24 Body of axis (second cervical vertebra) | 34 Stylopharyngeus | |
| 11 Sternocleidomastoid | | 35 Internal carotid artery | |
| 12 Levator scapulae | | 36 Vagus nerve (X) | |
| 13 Longissimus capitis | | 37 Internal jugular vein | |
| 14 Semispinalis capitis | | 38 Accessory nerve (XI) | |
| | | | 46 Nasopharynx |
| | | | 47 Parapharyngeal space |
| | | | 48 Alveolar process of maxilla |

Section level



Notes

This section traverses the upper lip (1), the tongue (3), the uvula (29) and the axis (19, 20, 22, 24). The plane of the CT image is slightly more cranial.

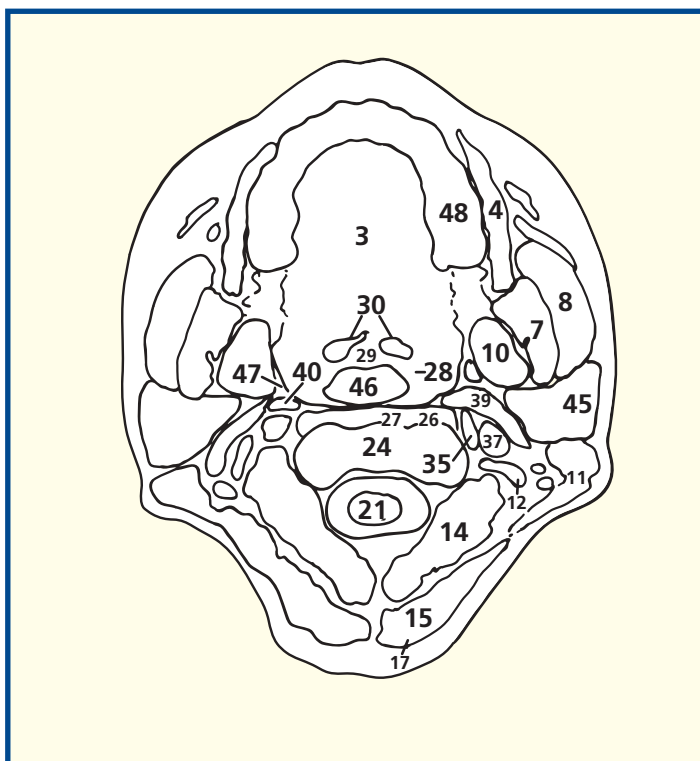
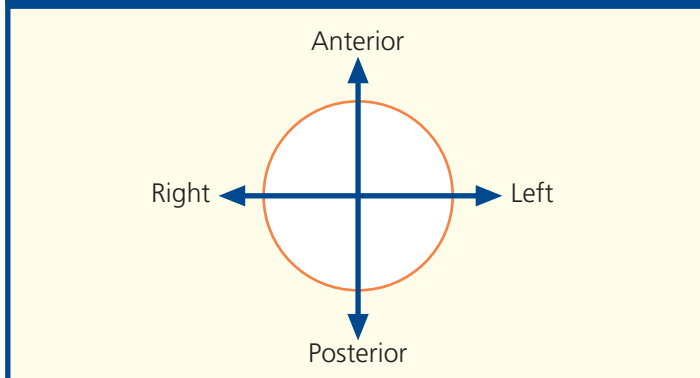
The palatine tonsil (33) lies in the tonsillar fossa between the anterior and posterior pillars of the fauces. The anterior pillar, or palatoglossal arch (32), forms the boundary between the buccal cavity and the oropharynx (30); it fuses with the lateral wall of the tongue and contains the palatoglossus muscle. The posterior pillar, or palatopharyngeal arch (31), blends with the wall of the pharynx and contains the palatopharyngeus muscle.

The tonsil consists of a collection of lymphoid tissue covered by a squamous epithelium, a unique histological combination that makes it easy to identify it under the microscope. From late puberty onwards, the lymphoid tissue undergoes progressive atrophy.

The prominent deep cervical vein (16) is a useful landmark in separating the deeply placed semispinalis cervicis muscle (18) from the more superficially placed semispinalis capitis (14); this is seen again in Axial section 18.

The intrinsic muscles of the tongue (3) are well shown and comprise longitudinal transverse and cervical bands. Acting alone or in combination, they give the tongue its precise and highly varied mobility, which is important in both speech and swallowing.

Orientation

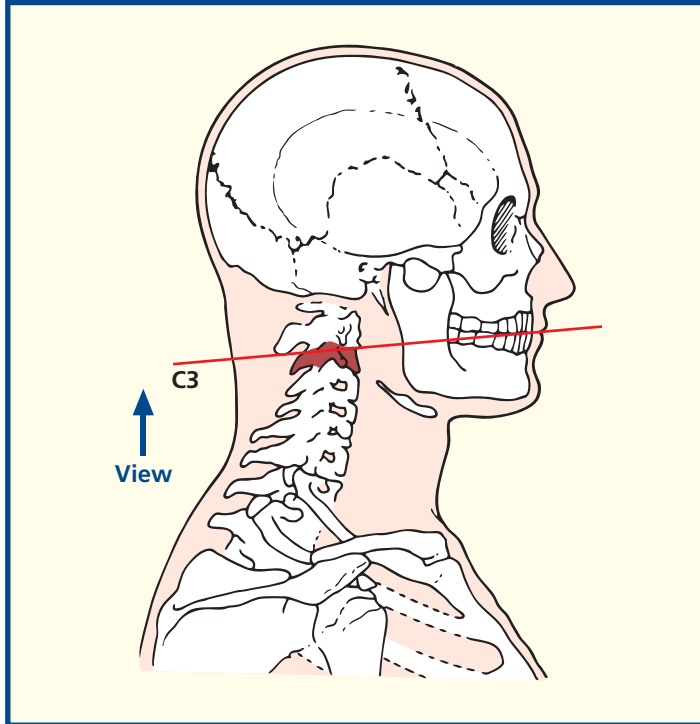


Axial computed tomogram (CT)



- | | | | |
|------------------------------------|----------------------------|----------------------------|---------------------------|
| 1 Upper lip | 14 Splenius cervicis | 26 Anterior primary | 37 Stylohyoid |
| 2 Lower lip | 15 Longissimus capitis | ramus of third cervical | 38 Tendon of digastric |
| 3 Orbicularis oris | 16 Deep cervical vein | nerve | 39 Parotid gland |
| 4 Buccinator | 17 Semispinalis cervicis | | 40 Submandibular |
| 5 Transverse intrinsic | 18 Semispinalis capitis | 27 Longus capitis | salivary gland |
| muscle of tongue | 19 Splenius capitis | 28 Longus colli | 41 Styloglossus entering |
| 6 Facial artery and vein | 20 Ligamentum nuchae | 29 Part of intervertebral | tongue |
| 7 Ramus of mandible | 21 Trapezius | disc between second | 42 Oropharynx |
| 8 Inferior alveolar artery | 22 Spine of third cervical | and third cervical | |
| vein and nerve (V ⁱⁱⁱ) | vertebra | | |
| within mandibular | 23 Spinal cord within | 30 Vagus nerve (X) | 43 Genioglossus |
| canal | dural sheath | 31 Accessory nerve (XI) | 44 Constrictor of pharynx |
| 9 Masseter | 24 Body of third cervical | 32 Deep cervical lymph | 45 Base of tongue |
| 10 Medial pterygoid | vertebra | node | 46 Mylohyoid |
| 11 Retromandibular vein | 25 Vertebral artery and | 33 Sternocleidomastoid | 47 Hyoglossus |
| 12 Scalenus medius | vein within foramen | 34 Internal jugular vein | 48 External jugular vein |
| 13 Levator scapulae | transversarium | 35 Internal carotid artery | |
| | | 36 External carotid artery | |

Section level



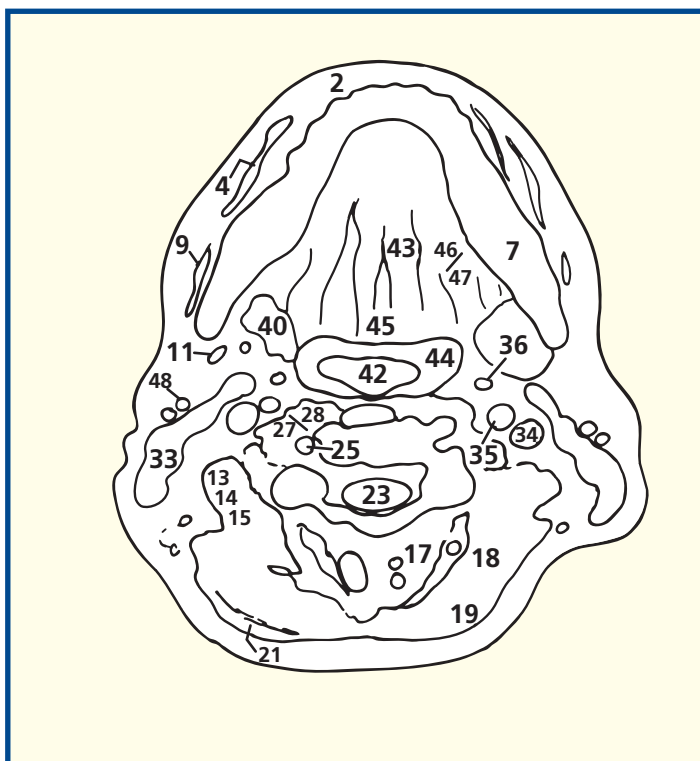
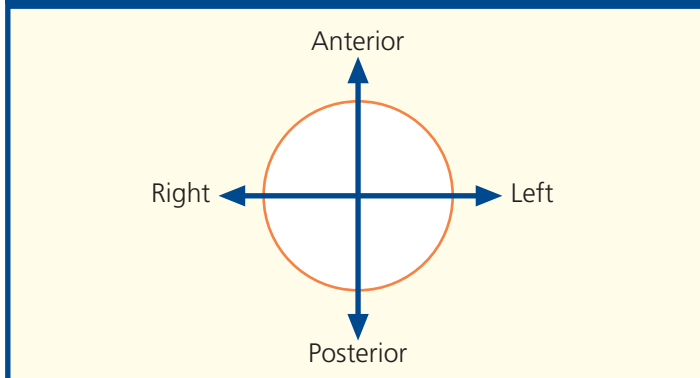
Notes

This section passes between the lips (1 and 2), the body of the third cervical vertebra (24) and the spine of the third cervical vertebra (22). The CT image is from a different subject and comes from the series that traverse the neck. This is because few cranial CT runs extend as caudal as this level. Moreover, artefacts from the amalgam of dental fillings often obscure this region. Bolus enhancement with intravenous iodinated contrast medium has opacified the major vessels (34–36) and assists in their identification.

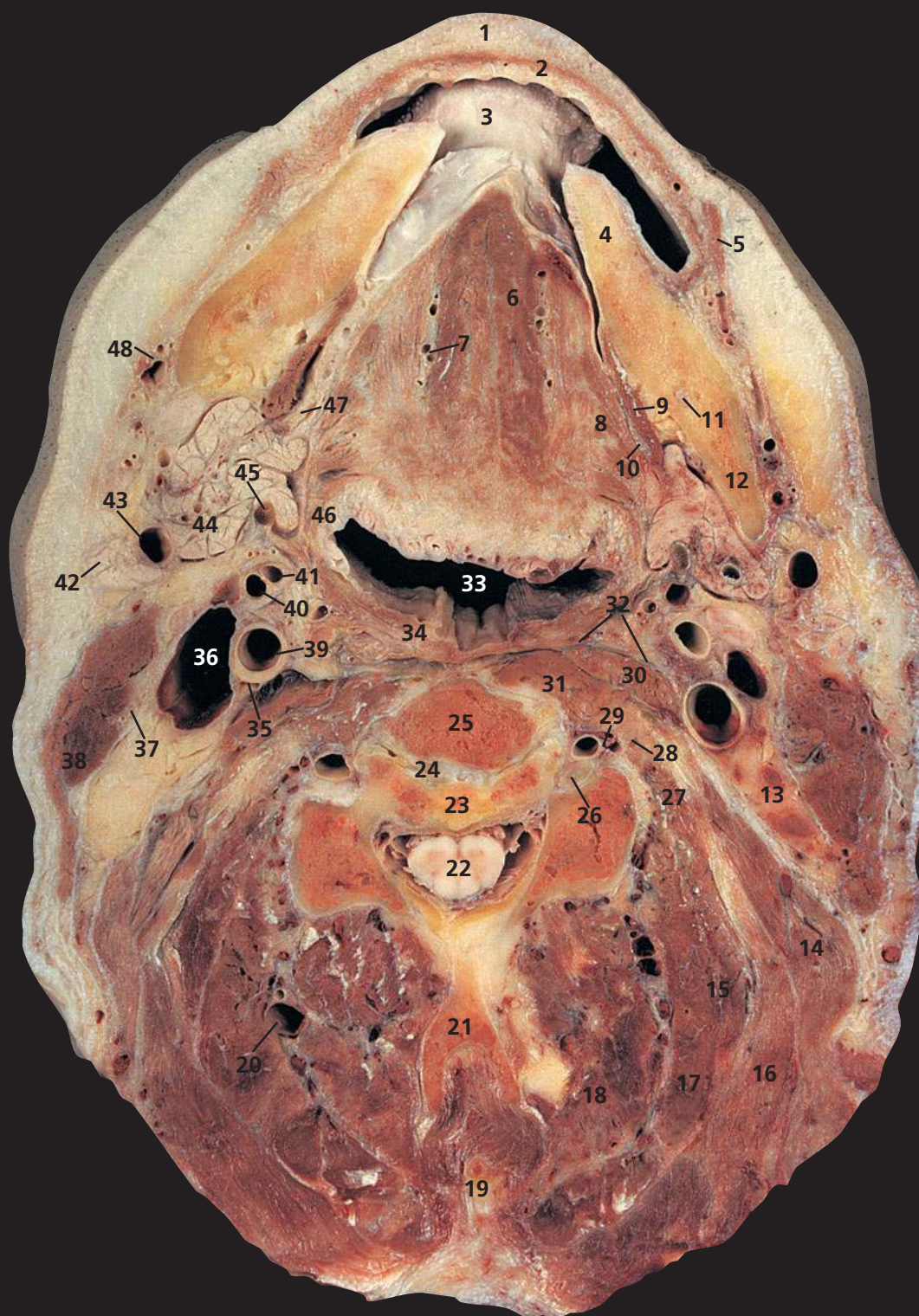
The submandibular salivary gland (40) lies against the ramus of the mandible (7) at its angle, separated by the medial pterygoid muscle (10). Its close relationship to the parotid gland (39) is well demonstrated; it is separated from the latter only by the fascial sheet of the stylomandibular ligament.

The foramen transversarium (25), lying within the transverse process, is the characteristic feature of all seven of the cervical vertebrae. That of the seventh cervical vertebra, the vertebra prominens, is often of small size because it transmits only small accessory vertebral veins and not the vertebral artery, which usually enters at the sixth cervical vertebra. The artery is surrounded by a plexus of sympathetic nerve fibres and is accompanied by the smaller vertebral vein. Not infrequently, the foramen transversarium will be seen to be double – the smaller compartment in such examples conveys the vein.

Orientation

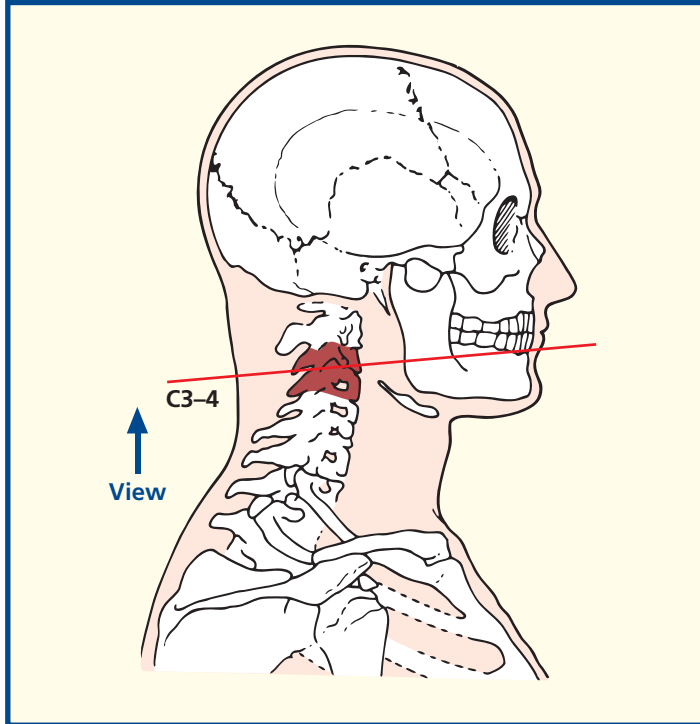


Axial computed tomogram (CT)



- | | | | |
|------------------------------------------------------------------------|----------------------------------------------------------------------------|------------------------------------------------------------|----------------------------------------------------|
| 1 Lower lip | 16 Splenius capitis | of fourth cervical | 40 External carotid artery |
| 2 Orbicularis oris | 17 Semispinalis capitis | nerve | 41 Origin of facial artery |
| 3 Under surface of tongue | 18 Semispinalis cervicis | 27 Scalenus medius | 42 Parotid gland |
| 4 Body of mandible | 19 Ligamentum nuchae | 28 Scalenus anterior | 43 Retromandibular vein |
| 5 Depressor anguli oris | 20 Deep cervical vein | origin | 44 Submandibular salivary gland – superficial lobe |
| 6 Genioglossus | 21 Spine of fourth cervical vertebra | 29 Vertebral artery and vein within foramen transversarium | 45 Tendon of digastric |
| 7 Lingual artery and vein | 22 Spinal cord within dural sheath | 30 Longus capitis | 46 Styloglossus |
| 8 Hyoglossus | 23 Part of body of fourth cervical vertebra | 31 Longus colli | 47 Deep lobe of submandibular salivary gland |
| 9 Mylohyoid | 24 Part of intervertebral disc between third and fourth cervical vertebrae | 32 Prevertebral fascia | 48 Facial artery and vein |
| 10 Lingual nerve (V ⁱⁱⁱ) | 25 Part of body of third cervical vertebra | 33 Oropharynx | |
| 11 Inferior alveolar nerve (V ⁱⁱⁱ) within mandibular canal | 26 Dorsal root ganglion | 34 Constrictor muscles of pharynx | |
| 12 Ramus of mandible | | 35 Vagus nerve (X) | 49 Platysma |
| 13 Cervical lymph nodes | | 36 Internal jugular vein | 50 Hyoid bone |
| 14 Levator scapulae | | 37 Accessory nerve (XI) | 51 External jugular vein |
| 15 Splenius cervicis | | 38 Sternocleidomastoid | |
| | | 39 Internal carotid artery | |

Section level



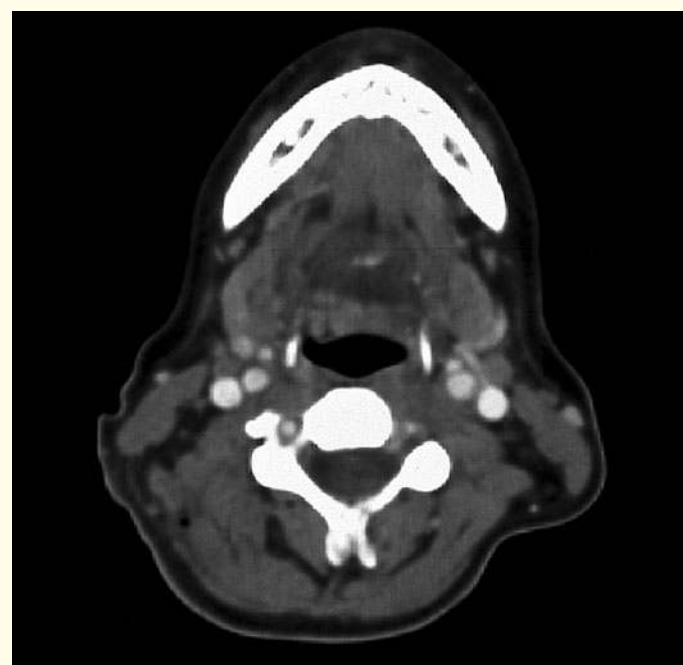
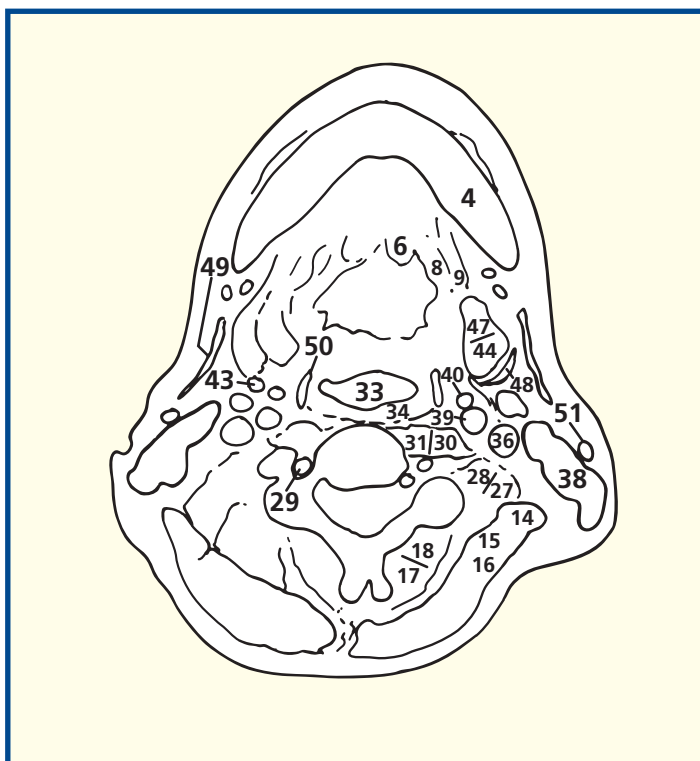
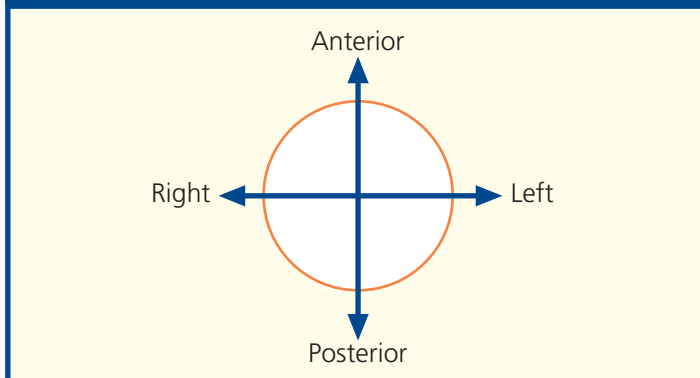
Notes

This section passes through the upper border of the lower lip (1), genioglossus at the base of the tongue (6) and the cartilaginous disc between the third and fourth cervical vertebrae (24).

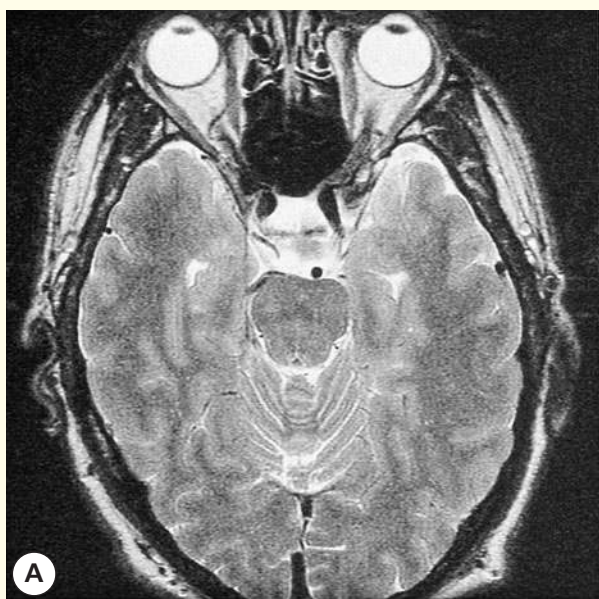
The prevertebral fascia (32) invests the front of the bodies of the cervical vertebrae, the prevertebral muscles (30, 31) and the scalene muscles (27, 28). It forms an almost avascular transverse plane behind the pharynx (33) and the great vessels (36, 39). It extends from the skull base above to the superior mediastinum below, where it blends with the anterior longitudinal vertebral ligament. It provides an avascular plane for the anterior surgical approach to the cervical vertebrae. It is deep to this fascia that tuberculous pus will track from an infected cervical vertebra.

The facial artery at its origin from the external carotid artery (40) is seen at (41). It arches over the submandibular salivary gland (44) to cross the lower border of the mandible (4), where its pulse is palpable (48).

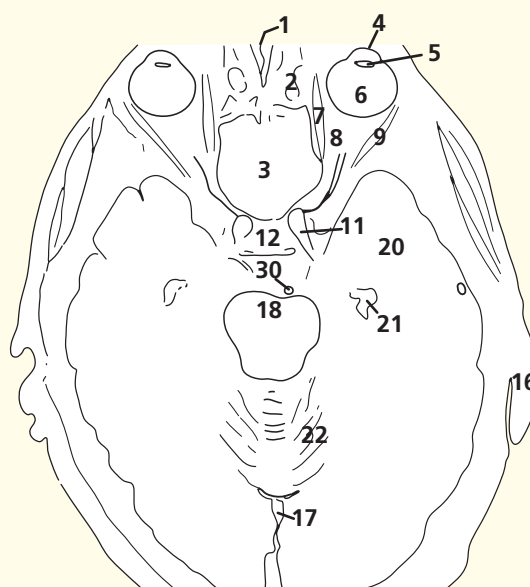
Orientation



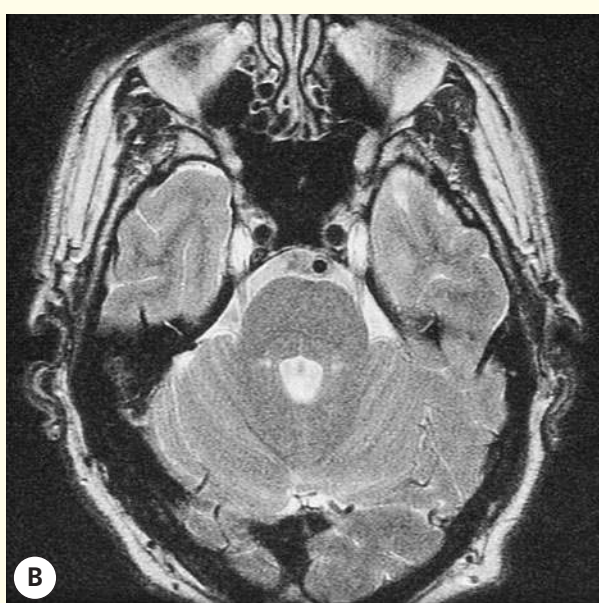
Axial computed tomogram (CT)



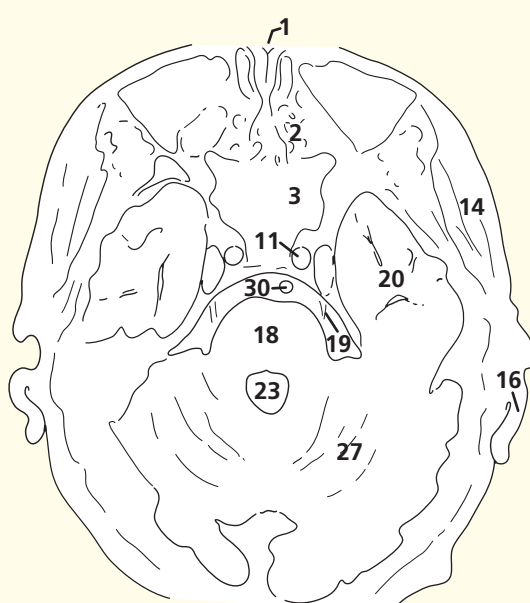
A Axial magnetic resonance image (MRI)



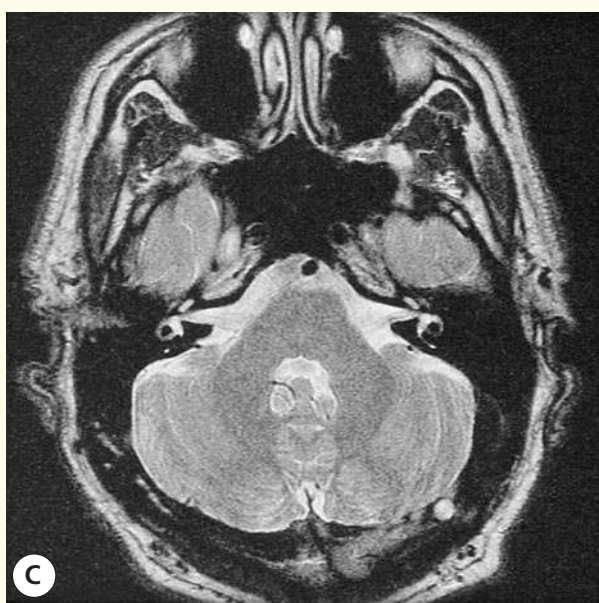
A



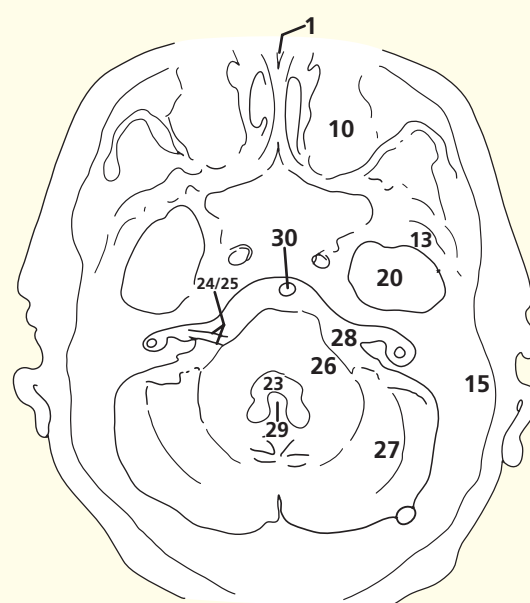
B Axial magnetic resonance image (MRI)



B

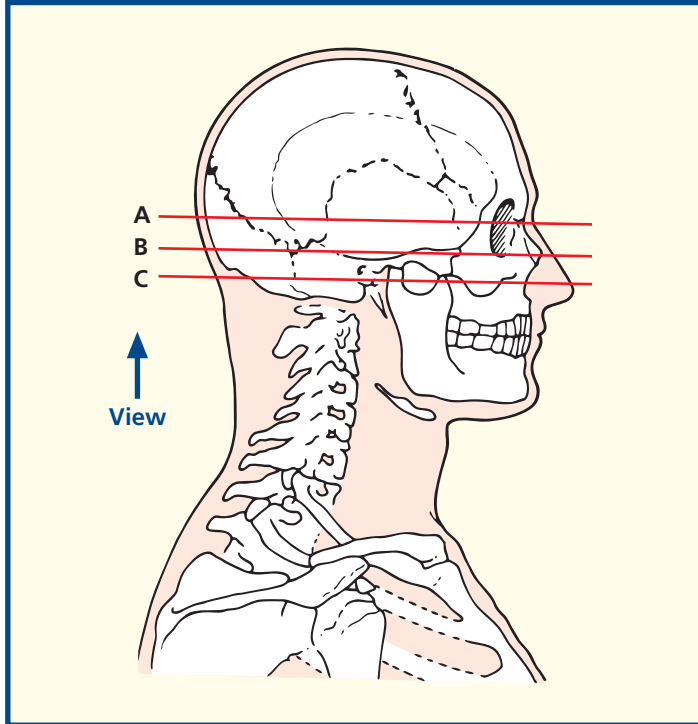


C Axial magnetic resonance image (MRI)

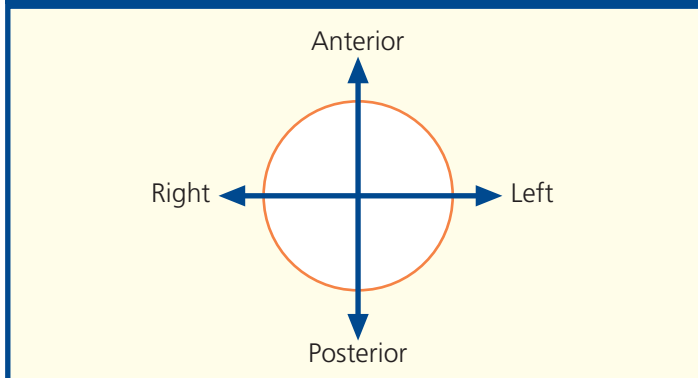


C

Section level



Orientation



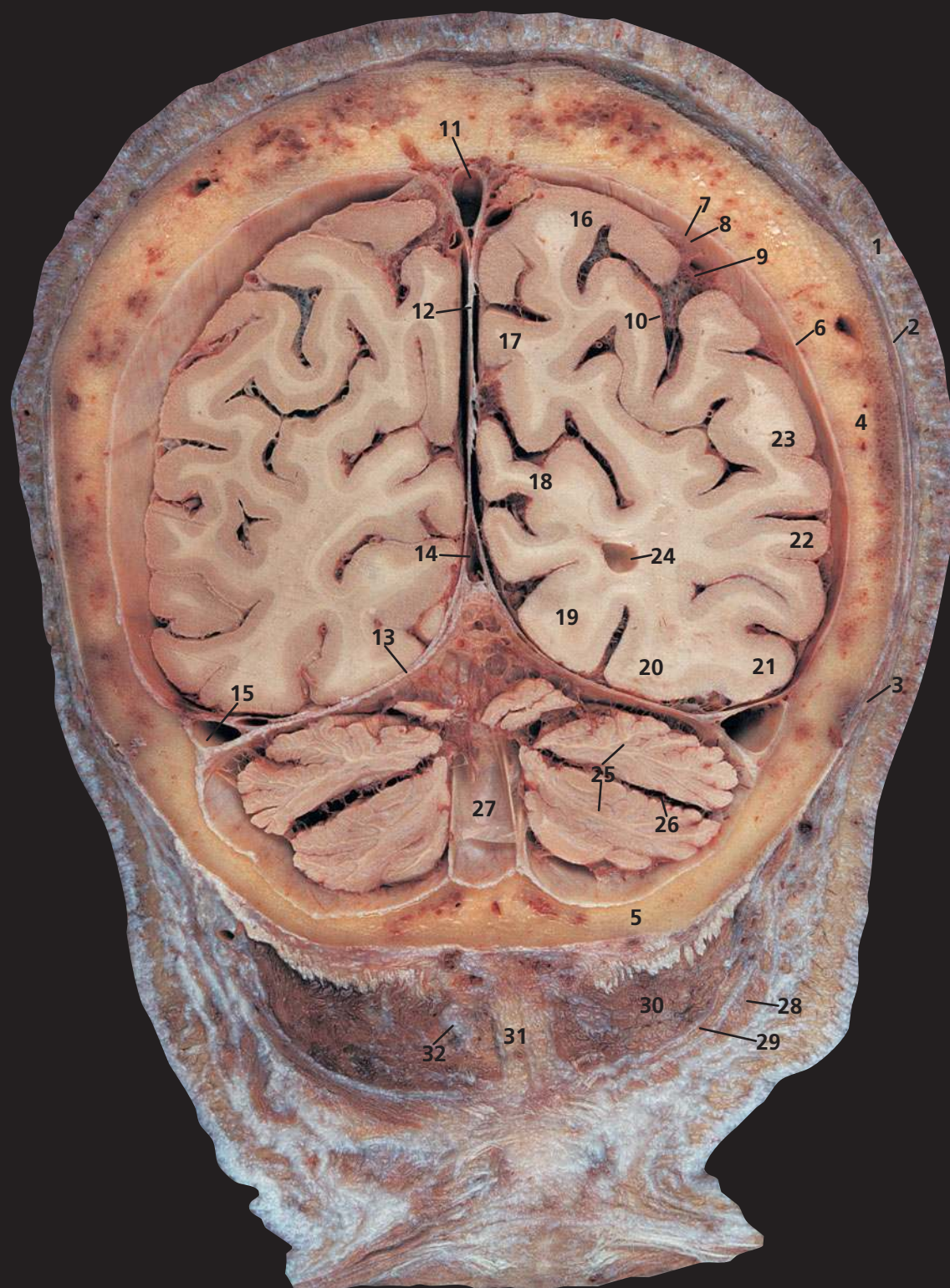
Notes

These three axial T2-weighted images show many important structures at the base of the brain, along with the orbits and sinuses. The water content of the globe provides good contrast with the lens. On this sequence, the fluid in the globe and cerebrospinal spaces yields similar signal intensity to the fat within the orbit. The T2 weighting also demonstrates the emerging nerves within the cerebrospinal fluid to good effect. Demonstration of a normal VIII (vestibulocochlear) nerve and fluid entering the internal auditory canal (meatus) effectively excludes a neuroma here. Possible lesions at this site (the cerebello-pontine angle) provide one of the commonest referrals for magnetic resonance imaging (MRI). On the spin-echo sequence used here, flowing arterial blood returns no signal and thus appears black; in this way, the internal carotid and basilar arteries are well visualized. Air-containing structures, such as the sphenoidal sinus, also appear black.

The pons is seen well on these images, and areas of infarction and other lesions should be looked for on T2-weighted images. The fourth ventricle is another important landmark in this region; it should be central and symmetrical.

- 1 Nasal bone
- 2 Ethmoidal air cells
- 3 Sphenoidal sinus
- 4 Cornea
- 5 Lens
- 6 Vitreous humour
- 7 Medial rectus
- 8 Optic nerve (II)
- 9 Lateral rectus
- 10 Maxillary sinus
- 11 Internal carotid artery – within cavernous sinus (b11)
- 12 Pituitary fossa
- 13 Greater wing of sphenoid bone
- 14 Temporalis
- 15 Mastoid

- 16 Pinna
- 17 Straight sinus
- 18 Pons
- 19 Trigeminal nerve (V)
- 20 Temporal lobe of brain
- 21 Temporal horn of lateral ventricle
- 22 Anterior lobe of cerebellum
- 23 Fourth ventricle
- 24 Facial nerve (VII)
- 25 Vestibulocochlear (auditory) nerve (VIII)
- 26 Middle cerebral peduncle
- 27 Cerebellar hemisphere
- 28 Internal auditory meatus
- 29 Vermis of cerebellum
- 30 Basilar artery

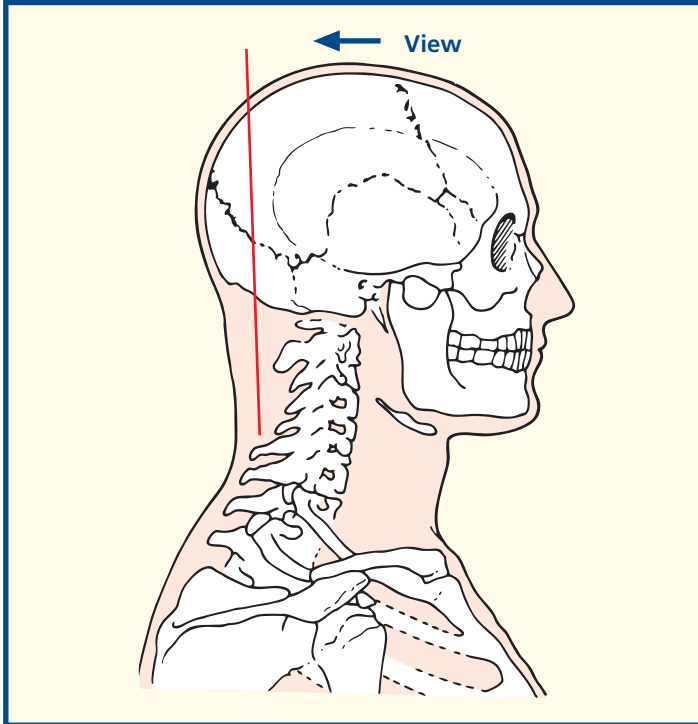


- 1 Skin and dense subcutaneous tissue
- 2 Epicranial aponeurosis (galea aponeurotica)
- 3 Occipital belly of occipitofrontalis
- 4 Parietal bone
- 5 Occipital bone
- 6 Dura mater
- 7 Subdural space
- 8 Arachnoid mater
- 9 Subarachnoid space

- 10 Pia mater
- 11 Superior sagittal sinus
- 12 Falx cerebri
- 13 Tentorium cerebelli
- 14 Straight sinus
- 15 Transverse sinus
- 16 Superior parietal lobule
- 17 Precuneus
- 18 Cuneus
- 19 Lingual gyrus
- 20 Medial occipitotemporal gyrus
- 21 Lateral occipitotemporal gyrus

- 22 Middle temporal gyrus
- 23 Inferior parietal lobule
- 24 Posterior horn of lateral ventricle
- 25 Cerebellar hemisphere
- 26 Horizontal fissure of cerebellum
- 27 Internal occipital crest
- 28 Trapezius
- 29 Splenius capitis
- 30 Semispinalis capitis
- 31 Ligamentum nuchae
- 32 Greater occipital nerve

Section level



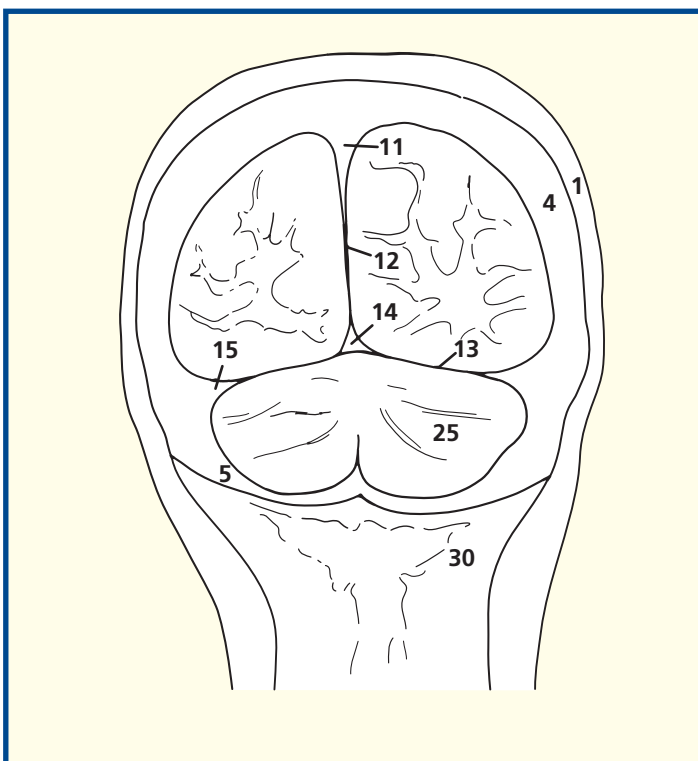
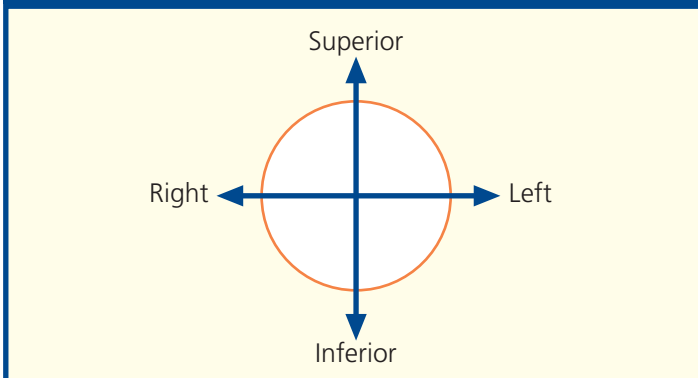
Notes

This coronal section passes through the posterior part of the occipital bone (5) immediately anterior to the external occipital protuberance. It passes through the posterior extremity of the posterior, or occipital, horn of the lateral ventricle (24).

In this, as in all subsequent sections, cross-reference should be made between a coronal section with the photographs of the external aspects and sagittal section of the brain for orientation of the positions of the main sulci and gyri (see pages 2–7).

On this proton-density magnetic resonance image, flowing blood in the venous sinuses appears black (low signal intensity) because the protons that were excited have moved out of the slice before measurement (creating a flow void).

Orientation

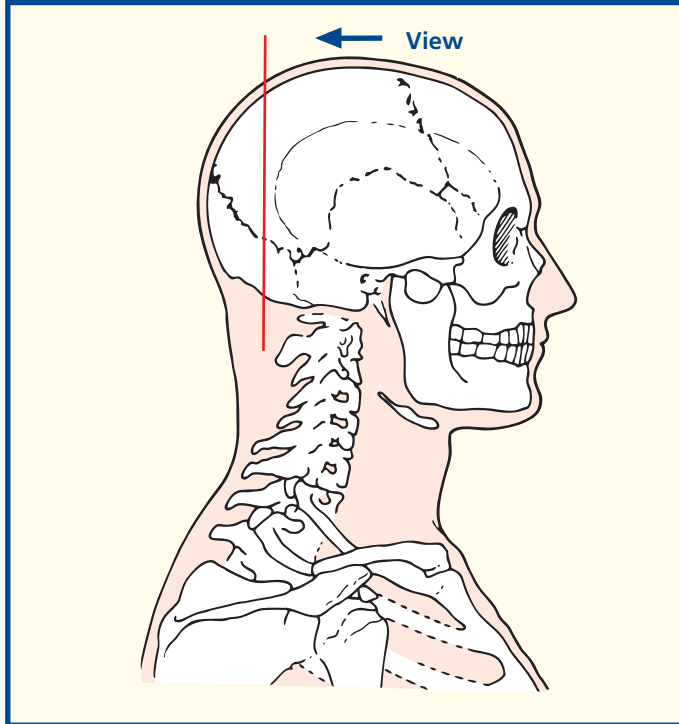


Coronal magnetic resonance image (MRI)

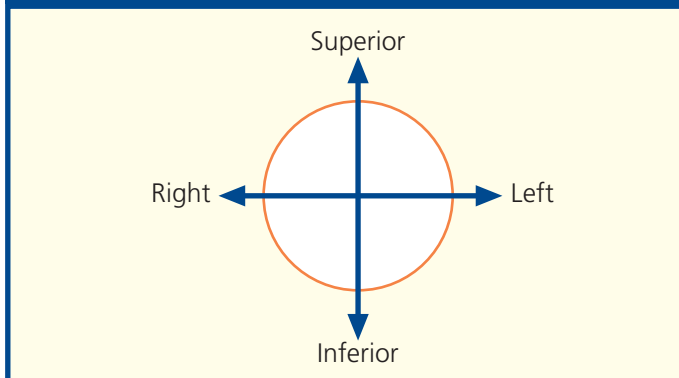


- | | | |
|----------------------------------------|----------------------------------------|-----------------------------------|
| 1 Skin and dense subcutaneous tissue | 12 Falx cerebri | 24 Transverse sinus |
| 2 Pericranium | 13 Precuneus | 25 Cerebellar hemisphere |
| 3 Parietal bone | 14 Superior parietal lobule | 26 Superior vermis |
| 4 Occipital bone | 15 Inferior parietal lobule | 27 Inferior vermis |
| 5 Occipital belly of occipitofrontalis | 16 Middle temporal gyrus | 28 Falx cerebelli |
| 6 Dura mater | 17 Lateral occipitotemporal gyrus | 29 Internal occipital crest |
| 7 Subdural space | 18 Medial occipitotemporal gyrus | 30 Rectus capitis posterior minor |
| 8 Arachnoid mater | 19 Lingual gyrus | 31 Semispinalis capitis |
| 9 Subarachnoid space | 20 Cuneus | 32 Splenius capitis |
| 10 Pia mater | 21 Cingulate gyrus | 33 Trapezius |
| 11 Superior sagittal sinus | 22 Posterior horn of lateral ventricle | 34 Greater occipital nerve |
| | 23 Tentorium cerebelli | 35 Ligamentum nuchae |
| | | 36 Semispinalis cervicis |

Section level



Orientation

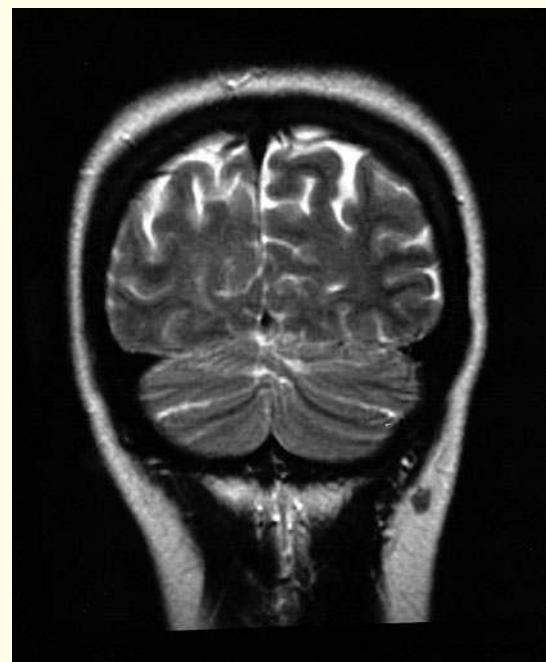
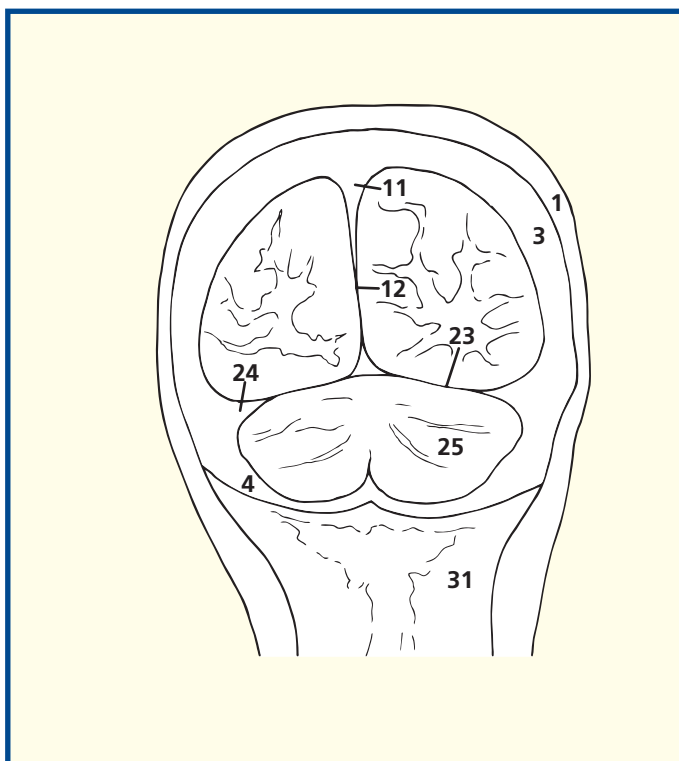


Notes

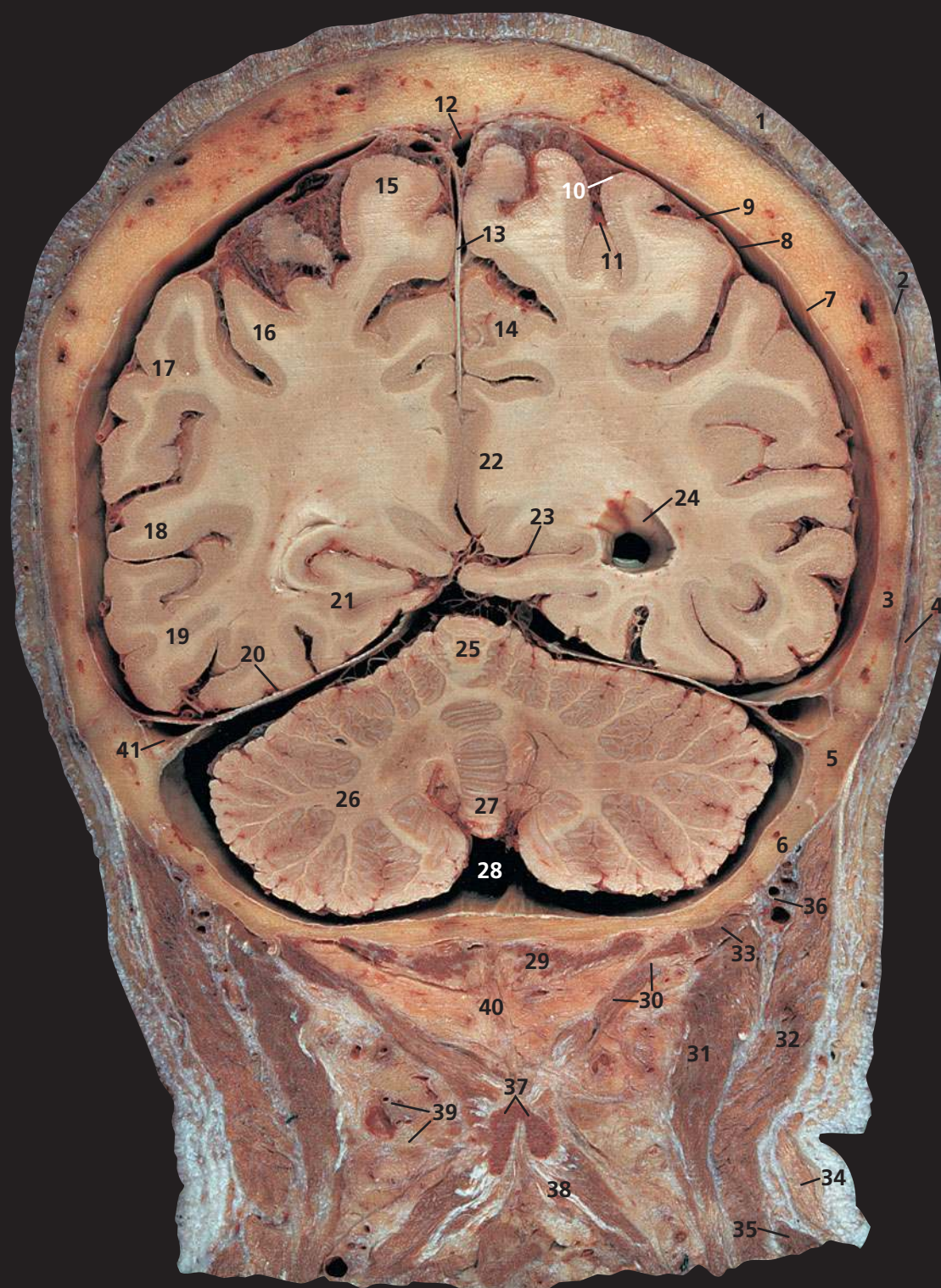
The makeup of the layers of the scalp can be appreciated in this and subsequent sections. It comprises hair-bearing skin, lying on dense, highly vascular connective tissue (1); note the large vessels seen in many of the sections. This, in turn, is adherent to a tough aponeurosis, which is the aponeurotic sheet joining the occipital belly of occipitofrontalis (5) to the frontalis muscle. The former arises from the superior nuchal line, while the latter inserts into the fascia above the eyebrows. The occipital part is supplied by the auricular, and the frontal part by the temporal, branch of the facial nerve (VII). Paralysis of the facial nerve is followed by inability to wrinkle the forehead on the affected side. Beneath the aponeurosis lies a layer of loose areolar tissue, which again can be appreciated in these sections. It is in this plane that avulsion of the scalp can take place in tearing injuries and in which a flap of scalp can be turned down during surgical exposure of the skull. The final layer, the periosteum, is closely adherent to the skull.

This T2-weighted image is through the same position as in the MRI image in coronal section 1. The cerebrospinal fluid in the subarachnoid space (9) now yields high signal intensity (white), providing contrast with the gyri.

The various layers of the meninges are demonstrated well (6, 8, 10). Haemorrhage around these layers is a serious event. An extradural haematoma develops between bone (3) and the dura mater (6) and usually arises soon after trauma that ruptures a meningeal vessel. A subdural haematoma collects in the subdural space (7), usually due to venous bleeding following minor trauma in the elderly. Subarachnoid haemorrhage develops suddenly in the subarachnoid space (9), usually following the spontaneous rupture of a cerebral artery, or berry aneurysm.



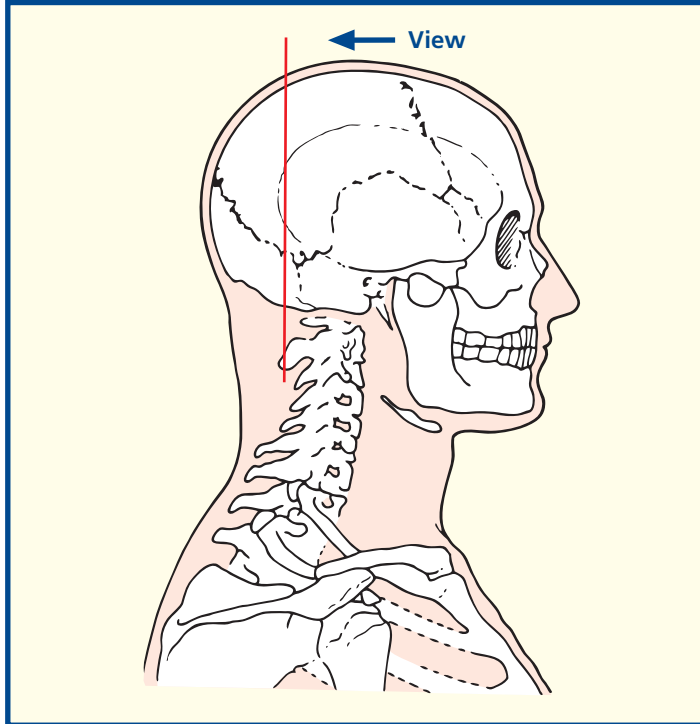
Coronal magnetic resonance image (MRI)



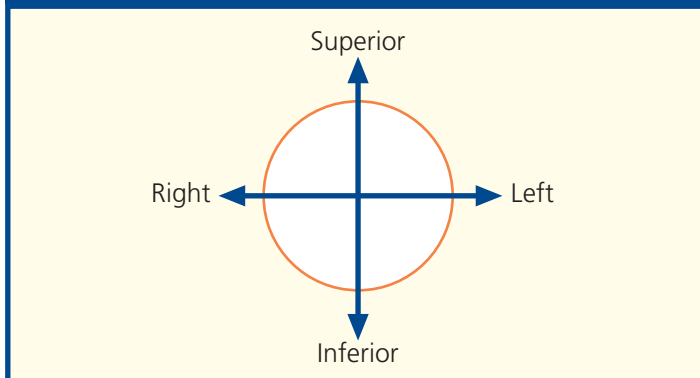
- | | | |
|-----------------------------------------------|----------------------------------------|-----------------------------------|
| 1 Skin and dense subcutaneous tissue | 13 Falx cerebri | 28 Cerebello-medullary cistern |
| 2 Epicranial aponeurosis (galea aponeurotica) | 14 Precuneus | 29 Rectus capitis posterior minor |
| 3 Parietal bone | 15 Superior parietal lobule | 30 Rectus capitis posterior major |
| 4 Occipital belly of occipitofrontalis | 16 Inferior parietal lobule | 31 Semispinalis capitis |
| 5 Occipital margin of temporal bone | 17 Superior temporal gyrus | 32 Splenius capitis |
| 6 Occipital bone | 18 Middle temporal gyrus | 33 Superior oblique |
| 7 Dura mater | 19 Inferior temporal gyrus | 34 Trapezius |
| 8 Subdural space | 20 Tentorium cerebelli | 35 Levator scapulae |
| 9 Arachnoid mater | 21 Lingual gyrus | 36 Occipital artery and vein |
| 10 Subarachnoid space | 22 Cingulate gyrus | 37 Bifid spine of axis |
| 11 Pia mater | 23 Calcarine sulcus | 38 Semispinalis cervicis |
| 12 Superior sagittal sinus | 24 Posterior horn of lateral ventricle | 39 Occipital lymph nodes |
| | 25 Superior vermis | 40 Ligamentum nuchae |
| | 26 Cerebellar hemisphere | 41 Transverse sinus |
| | 27 Inferior vermis | |

42 Small infarct (see notes)

Section level



Orientation



Notes

This and neighbouring sections give clear views of the structure of the superior sagittal sinus (12) and the transverse sinus (41), which are formed as clefts between the outer (endosteal) and inner (meningeal) layers of the dura mater.

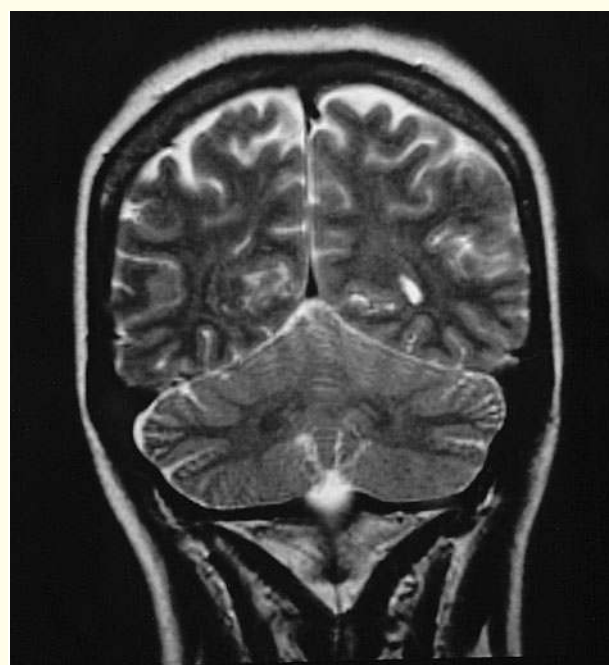
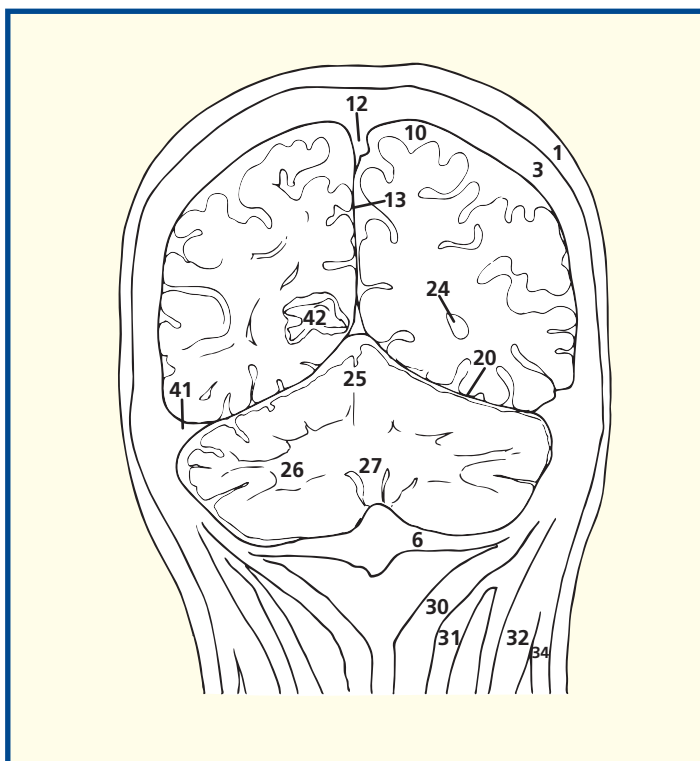
The internal structure of the cerebellum (26) can be appreciated in this section, with its superficial highly convoluted cortex over a dense core of white matter, which contains the deep cerebellar nuclei. The highly branched appearance of the cerebellum in section is given the fanciful name of ‘arbor vitae’ – tree of life.

The bifid spine of the axis (37) gives attachment to semispinalis cervicis (38), rectus capitis posterior major (30) and the ligamentum nuchae (40), as well as the inferior oblique, which can be seen in the next section.

The small occipital lymph nodes (39) are of clinical significance in that they are classically enlarged in rubella (German measles) and some forms of cancer.

This T2-weighted magnetic resonance image shows cerebrospinal fluid (white) in the subarachnoid space (10) surrounding the gyri and within the posterior horn of the left lateral ventricle (24).

The magnetic resonance image shows a small area of abnormal high signal intensity (42) medially in the occipital lobe. The clinical features and radiological features were those of a small infarct.

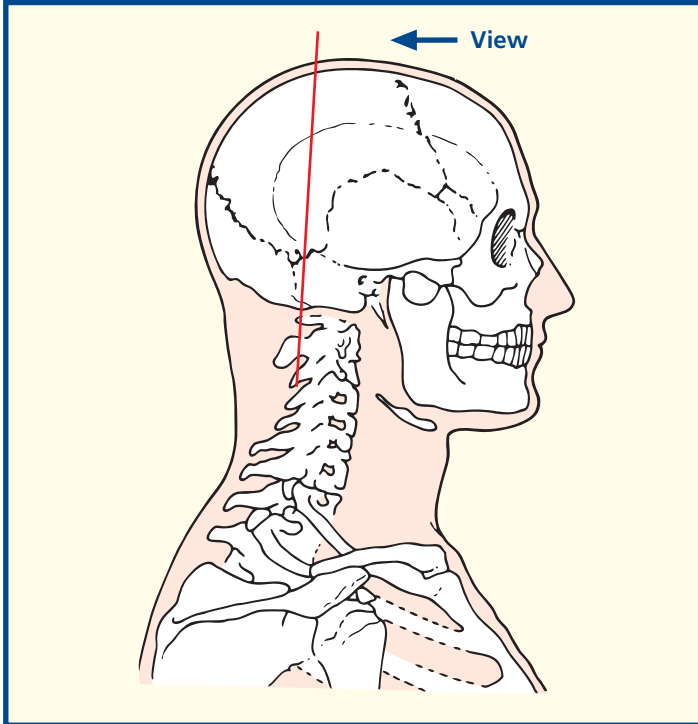


Coronal magnetic resonance image (MRI)



- | | | | |
|-----------------------------------------------|----------------------------------------|-----------------------------------------------------------|-----------------------------------|
| 1 Skin and dense subcutaneous tissue | 15 Lateral occipitotemporal gyrus | 27 Tentorium cerebelli | 39 Posterior tubercle of atlas |
| 2 Epicranial aponeurosis (galea aponeurotica) | 16 Medial occipitotemporal gyrus | 28 Cerebellar hemisphere | 40 Bifid spinous process of axis |
| 3 Dura mater | 17 Parahippocampal gyrus | 29 Superior vermis | 41 Superior oblique |
| 4 Subdural space | 18 Fimbria of hippocampus | 30 Superior medullary vellum | 42 Rectus capitis posterior major |
| 5 Arachnoid mater | 19 Tapetum | 31 Fourth ventricle | 43 Inferior oblique |
| 6 Subarachnoid space | 20 Posterior horn of lateral ventricle | 32 Cerebello-medullary cistern | 44 Sternocleidomastoid |
| 7 Pia mater | 21 Splenium of corpus callosum | 33 Tonsil of cerebellum | 45 Splenius capitis |
| 8 Superior sagittal sinus | 22 Cingulate gyrus | 34 Dentate nucleus | 46 Levator scapulae |
| 9 Falx cerebri | 23 Paracentral lobule | 35 Parietal bone | 47 Longissimus capitis |
| 10 Postcentral gyrus | 24 Cingulate sulcus | 36 Mastoid air cells within petrous part of temporal bone | 48 Semispinalis capitis |
| 11 Inferior parietal lobule | 25 Optic radiation | 37 Occipital bone | 49 Semispinalis cervicis |
| 12 Superior temporal gyrus | 26 Great cerebral vein | 38 Posterior atlanto-occipital membrane | 50 Transverse sinus |
| 13 Middle temporal gyrus | | | |
| 14 Inferior temporal gyrus | | | |

Section level



Notes

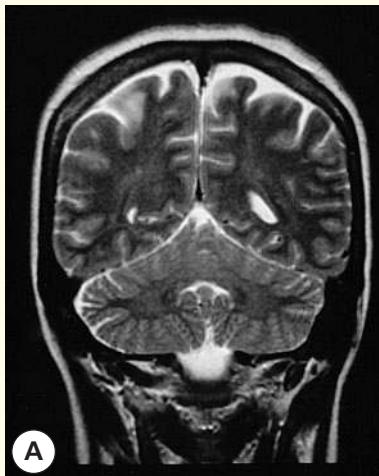
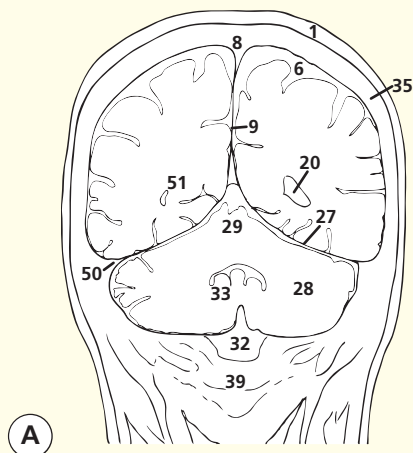
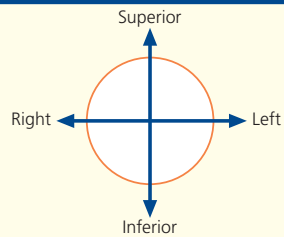
This section passes through the posterior part of the opening in the tentorium cerebelli (27). Note the great cerebral vein (26), a short median vessel formed by the union of the two internal cerebral veins. It passes backwards to open into the anterior end of the straight sinus, which lies at the junction of the falx cerebri (9) with the tentorium cerebelli.

The dentate nucleus of the cerebellum (34) is the largest and most lateral of the four cerebellar nuclei. Fibres from this nucleus form the bulk of the superior cerebellar peduncle.

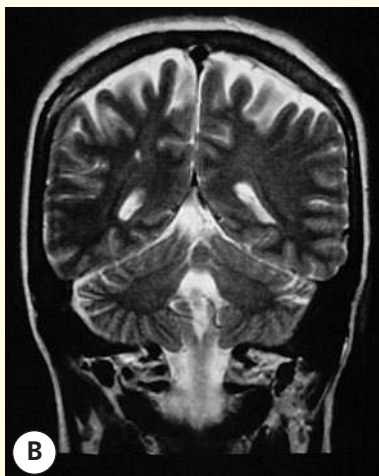
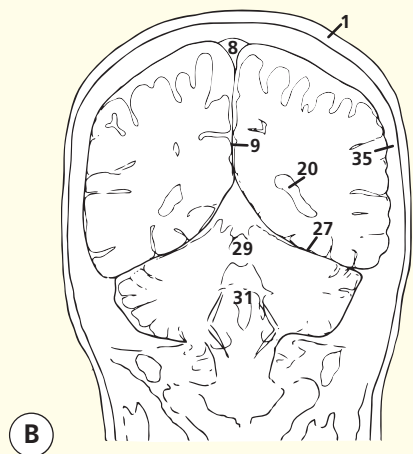
On the two T2-weighted images shown here, the extent of the cerebrospinal fluid is well demonstrated in image (A), especially in the subarachnoid space (6) around the gyri, but also in the cisterns around the base of the brain (32).

Also to be seen in image (A) is a small infarct (51); this is an area where there has been damage caused by interruption to the blood supply, most commonly due to a small embolus.

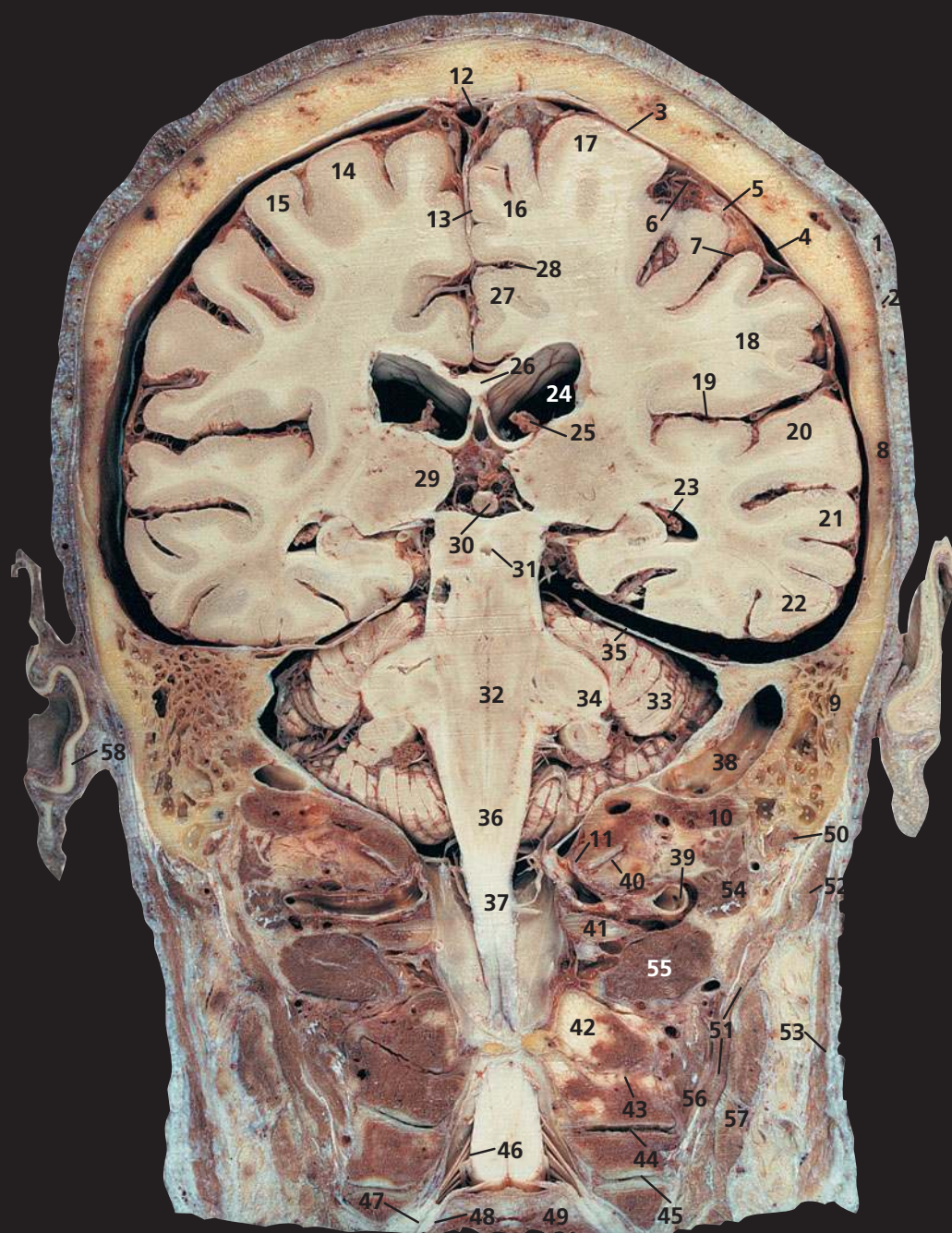
Orientation



Coronal magnetic resonance image (MRI)

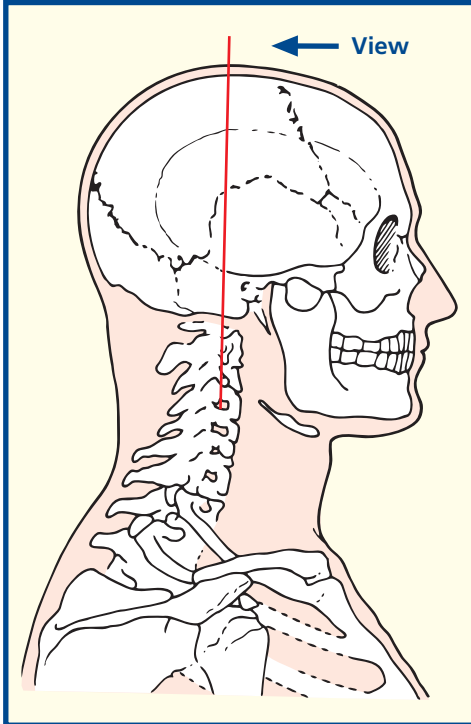


Coronal magnetic resonance image (MRI)



- | | | | |
|----------------------------------------------------------|-----------------------------------------------------------------------|---------------------------------------------|------------------------------------------------------------|
| 1 Skin and dense subcutaneous tissue | 18 Supramarginal gyrus | 33 Cerebellar hemisphere | 46 Dorsal nerve root C5 |
| 2 Epicranial aponeurosis (galea aponeurotica) | 19 Lateral sulcus | 34 Middle cerebellar peduncle | 47 Dorsal root ganglion C5 |
| 3 Dura mater | 20 Superior temporal gyrus | 35 Tentorium cerebelli | 48 Ventral nerve root C5 |
| 4 Subdural space | 21 Middle temporal gyrus | 36 Termination of medulla oblongata | 49 Body of fifth cervical vertebra |
| 5 Arachnoid mater | 22 Inferior temporal gyrus | 37 Commencement of spinal cord | 50 Posterior belly of digastric |
| 6 Subarachnoid space | 23 Choroid plexus within posterior horn of lateral ventricle (see 25) | 38 Sigmoid sinus | 51 Longissimus capitis |
| 7 Pia mater | 24 Body of lateral ventricle | 39 Vertebral artery entering foramen magnum | 52 Splenius capitis |
| 8 Parietal bone | 25 Choroid plexus within body of lateral ventricle (see 23) | 40 Atlanto-occipital joint | 53 Sternocleidomastoid |
| 9 Mastoid air cells within petrous part of temporal bone | 26 Corpus callosum | 41 Posterior arch of atlas | 54 Superior oblique |
| 10 Occipital bone | 27 Cingulate gyrus | 42 Lamina of axis | 55 Inferior oblique |
| 11 Margin of foramen magnum | 28 Cingulate sulcus | 43 Facet joint between C2/3 vertebrae | 56 Semispinalis capitis |
| 12 Superior sagittal sinus | 29 Thalamus | 44 Facet joint between C3/4 vertebrae | 57 Levator scapulae |
| 13 Falx cerebri | 30 Pineal gland | 45 Facet joint between C4/5 vertebrae | 58 Auricular cartilage of ear |
| 14 Precentral gyrus | 31 Aqueduct (of Sylvius) | | |
| 15 Postcentral gyrus | 32 Pons | | |
| 16 Para central lobule | | | |
| 17 Precentral gyrus | | | |
| | | | 59 Occipital condyle |
| | | | 60 Dens of axis (odontoid peg of second cervical vertebra) |

Section level



Notes

This section provides an excellent view of the foramen magnum (11) in the coronal section. It can be appreciated that the medulla oblongata (36) terminates at its superior margin and the spinal cord (37) commences at its inferior margin.

The vertebral artery (39) passes over the posterior arch of the atlas (41) to enter the skull through the foramen magnum. The first cervical dorsal spinal ramus lies between the artery and posterior arch. Muscular branches of the artery supply the deep muscles of this region and anastomose with the occipital, ascending and deep cervical arteries.

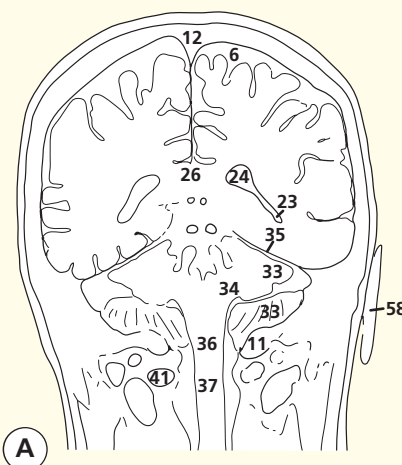
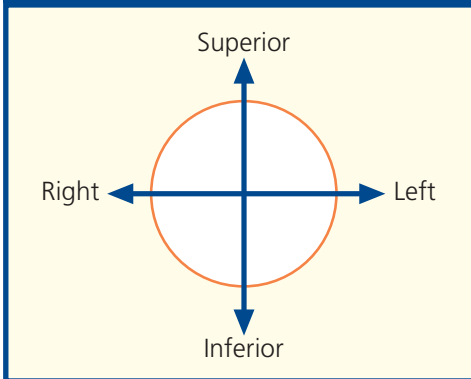
Formation of the fifth cervical spinal nerve from its dorsal (46) and ventral (48) roots is seen clearly. Note that the dorsal root ganglion (47) lies within the intervertebral foramen between the fourth and fifth (49) cervical vertebrae.

The nerve roots in the cervical spine emerge cranial to their numbered vertebra (i.e. C5 roots emerge between C4 and C5; C8 emerges between C7 and T1).

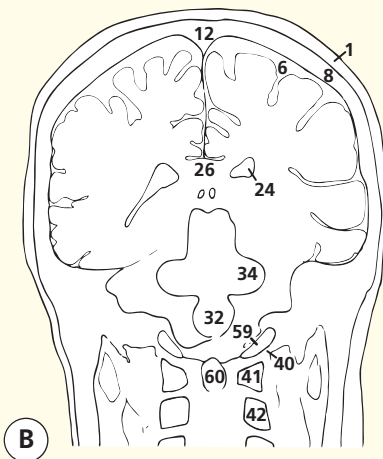
In the thoracic, lumbar and sacral spine, roots emerge caudal to their numbered vertebra (i.e. L5 emerges between L5 and S1).

Note the close relationship between the pons (32), medulla oblongata (36) and the atlanto-occipital joints (40) and dens of the axis (odontoid peg) (60). This explains why injuries at the C1/C2 level are so serious and diseases that affect this region, e.g. rheumatoid arthritis eroding the dens of the axis (odontoid peg) and weakening ligaments, can be so disabling.

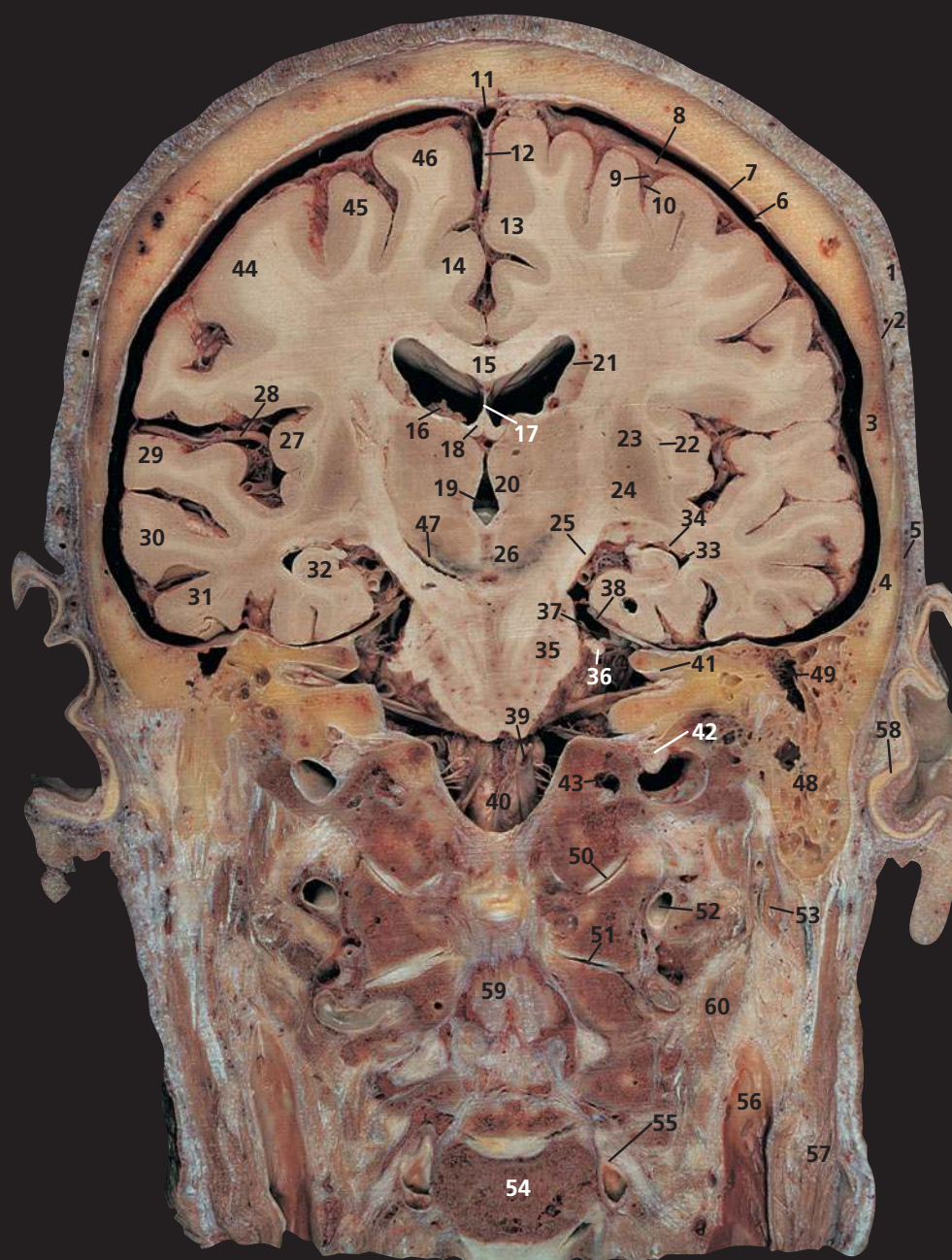
Orientation



Coronal magnetic resonance image (MRI)

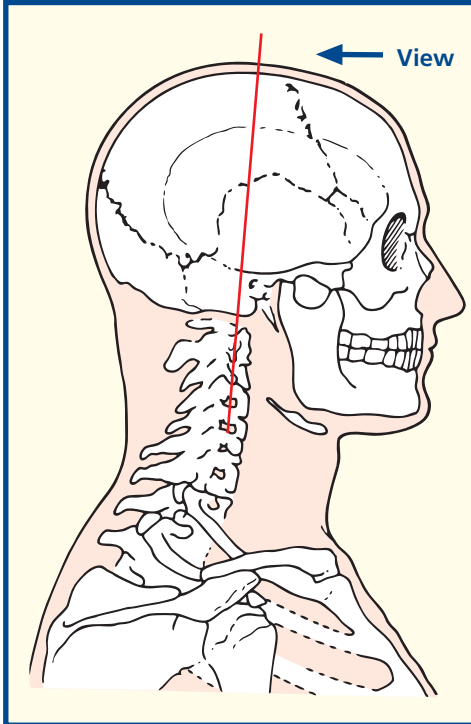


Coronal magnetic resonance image (MRI)



- | | | | |
|-----------------------------------------------|--------------------------------------------------------------------|--------------------------------------------------------------------------------------------------------------------------------------------------------|--------------------------------------------------------------------|
| 1 Skin and dense subcutaneous tissue | 22 Claustrum | 41 Facial nerve (VII) and vestibulocochlear nerve (VIII) entering internal auditory meatus within petrous part of temporal bone | 49 Mastoid antrum within petrous part of temporal bone |
| 2 Epicranial aponeurosis (galea aponeurotica) | 23 Putamen | 42 Glossopharyngeal nerve (IX), vagus nerve (X) and cranial part of accessory nerve (XI) entering jugular foramen within petrous part of temporal bone | 50 Atlanto-occipital joint |
| 3 Parietal bone | 24 Globus pallidus | 43 Hypoglossal nerve (XII) entering hypoglossal canal within petrous part of temporal bone | 51 Atlanto-axial joint |
| 4 Temporal bone | 25 Posterior limb of internal capsule | 44 Postcentral gyrus | 52 Vertebral artery within foramen transversarium of axis (see 39) |
| 5 Temporalis | 26 Mamillary body | 45 Precentral gyrus | 53 Posterior belly of digastric |
| 6 Dura mater | 27 Insula | 46 Superior frontal gyrus | 54 Body of C4 vertebra |
| 7 Subdural space | 28 Lateral cerebral fissure and branches of middle cerebral artery | 47 Substantia nigra | 55 C4 dorsal root ganglion |
| 8 Arachnoid mater | 29 Superior temporal gyrus | 48 Mastoid air cells within mastoid process of the petrous part of temporal bone | 56 Internal jugular vein |
| 9 Subarachnoid space | 30 Middle temporal gyrus | | 57 Sternocleidomastoid |
| 10 Pia mater | 31 Inferior temporal gyrus | | 58 Auricular cartilage of ear |
| 11 Superior sagittal sinus | 32 Hippocampus | | 59 Dura of spinal canal |
| 12 Falx cerebri | 33 Inferior horn of lateral ventricle | | 60 Levator scapulae |
| 13 Medial frontal gyrus | 34 Tail of caudate nucleus | | |
| 14 Cingulate gyrus | 35 Pons | | |
| 15 Body of corpus callosum | 36 Trigeminal nerve (V) | | |
| 16 Choroid plexus within lateral ventricle | 37 Trochlear nerve (IV) | | |
| 17 Septum pellucidum | 38 Free margin of tentorium cerebelli | | |
| 18 Fornix | 39 Vertebral artery (see 52) | | |
| 19 Third ventricle | 40 Medulla oblongata | | |
| 20 Thalamus | | | |
| 21 Caudate nucleus | | | |
| | | | 61 Lateral ventricle |
| | | | 62 Basilar artery |
| | | | 63 Body of second cervical vertebra |

Section level



Notes

The posterior limb of the internal capsule (25) is transected in this section and can be seen descending into the pons (35). Medial to the internal capsule can be seen the tail of the caudate nucleus (21) and the thalamus (20), while laterally lies the lentiform nucleus, made up of the putamen (23) and, more medially, the globus pallidus (24). Lateral to the lentiform nucleus lies the claustrum (22), sandwiching the narrow external capsule between the two.

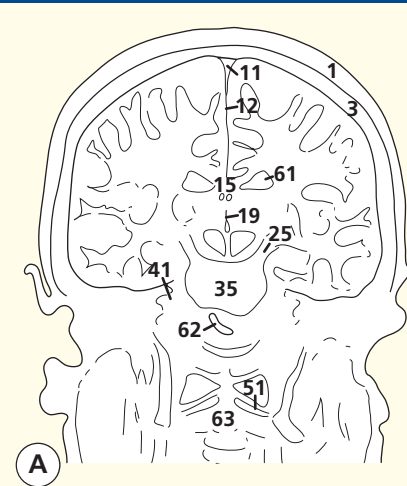
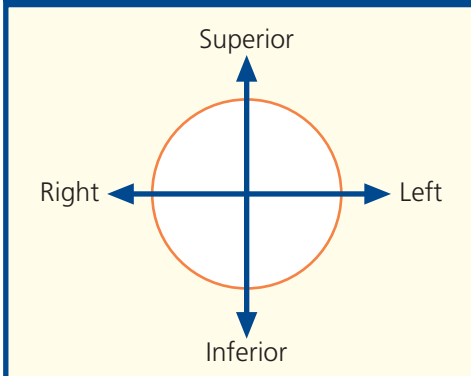
The squamous part of the temporal bone (4) is the thinnest part of the calvarium. Contrast it with the densest part of the skull – the well-named petrous temporal bone (49).

The internal auditory meatus is cut along its length and demonstrates the facial nerve (VII) and vestibulocochlear, or auditory, nerve (VIII) lying within it (41).

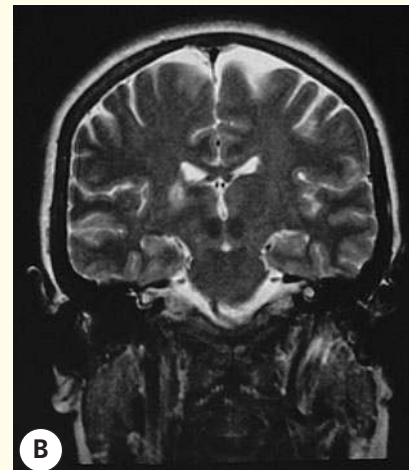
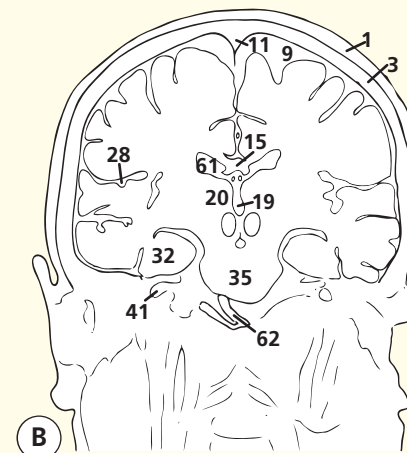
MRI is an excellent method of demonstrating small acoustic neurinomata, which develop close to the internal auditory meatus. It is now possible to diagnose these benign tumours long before the bony meatus becomes enlarged.

These two magnetic resonance images, obtained at the same anatomical plane, graphically demonstrate the different information that can be obtained using different magnetic resonance parameters: image (A) is the proton-density image whereas image (B) is the T2-weighted image from a dual-echo acquisition.

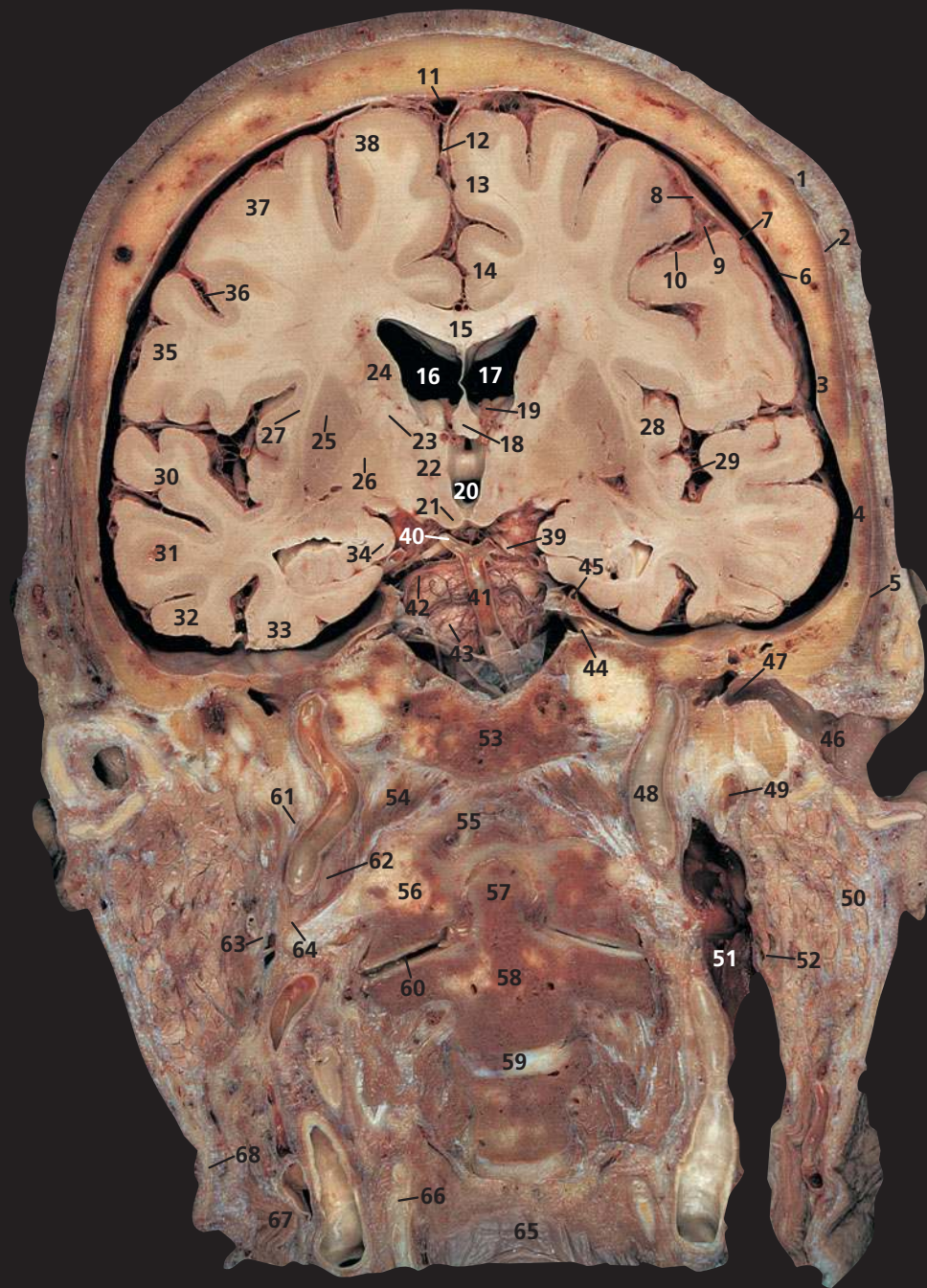
Orientation



Coronal magnetic resonance image (MRI)

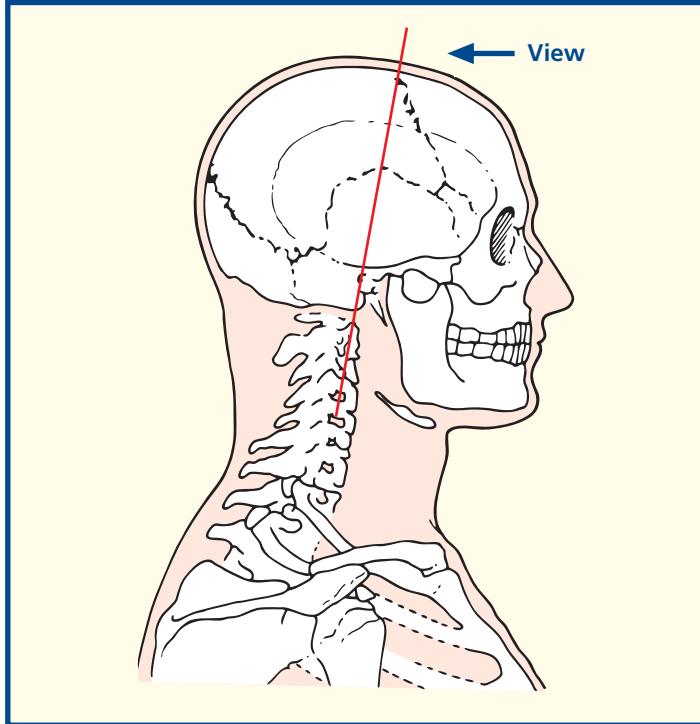


Coronal magnetic resonance image (MRI)



- | | | | |
|-----------------------------------------------|--------------------------------------------------------------------|---------------------------------------|------------------------------------------------------------|
| 1 Skin and dense subcutaneous tissue | 19 Choroid plexus with floor of lateral ventricle | 35 Postcentral gyrus | 54 Rectus capitis anterior |
| 2 Epicranial aponeurosis (galea aponeurotica) | 20 Third ventricle | 36 Central sulcus | 55 Anterior atlanto-occipital membrane |
| 3 Parietal bone | 21 Mamillary body | 37 Precentral gyrus | 56 Anterior arch of atlas |
| 4 Squamous part of temporal bone | 22 Thalamus | 38 Superior frontal gyrus | 57 Dens of axis (odontoid peg of second cervical vertebra) |
| 5 Temporalis | 23 Anterior limb of internal capsule | 39 Oculomotor nerve (III) | 58 Body of axis |
| 6 Dura mater | 24 Caudate nucleus | 40 Posterior cerebral artery | 59 C2/3 intervertebral disc |
| 7 Subdural space | 25 Putamen | 41 Basilar artery | 60 Atlanto-axial joint |
| 8 Arachnoid mater | 26 Globus pallidus | 42 Superior cerebral artery | 61 Glossopharyngeal nerve (IX) |
| 9 Subarachnoid space | 27 Claustrum | 43 Pons | 62 Vagus nerve (X) |
| 10 Pia mater | 28 Insula | 44 Trigeminal nerve (V) | 63 Spinal accessory nerve (XI) |
| 11 Superior sagittal sinus | 29 Lateral cerebral fissure and branches of middle cerebral artery | 45 Free margin of tentorium cerebelli | 64 Hypoglossal nerve (XII) |
| 12 Falx cerebri | 30 Superior temporal gyrus | 46 External auditory meatus | 65 Posterior wall of pharynx |
| 13 Medial frontal gyrus | 31 Middle temporal gyrus | 47 Tympanic membrane | 66 Thyroid cartilage |
| 14 Cingulate gyrus | 32 Inferior temporal gyrus | 48 Internal carotid artery | 67 Sternocleidomastoid |
| 15 Body of corpus callosum | 33 Lateral occipitotemporal gyrus | 49 Styloid process | 68 Platysma |
| 16 Body of lateral ventricle | 34 Parahippocampal gyrus adjacent (lateral) to hippocampus | 50 Parotid gland | |
| 17 Septum pellucidum | | 51 Internal jugular vein | |
| 18 Fornix | | 52 Digastric | |
| | | 53 Base of occipital bone (clivus) | |

Section level

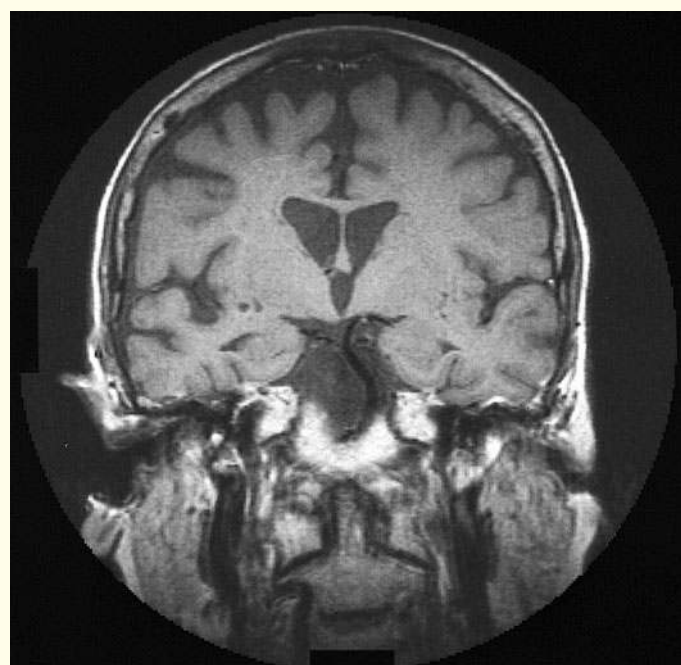
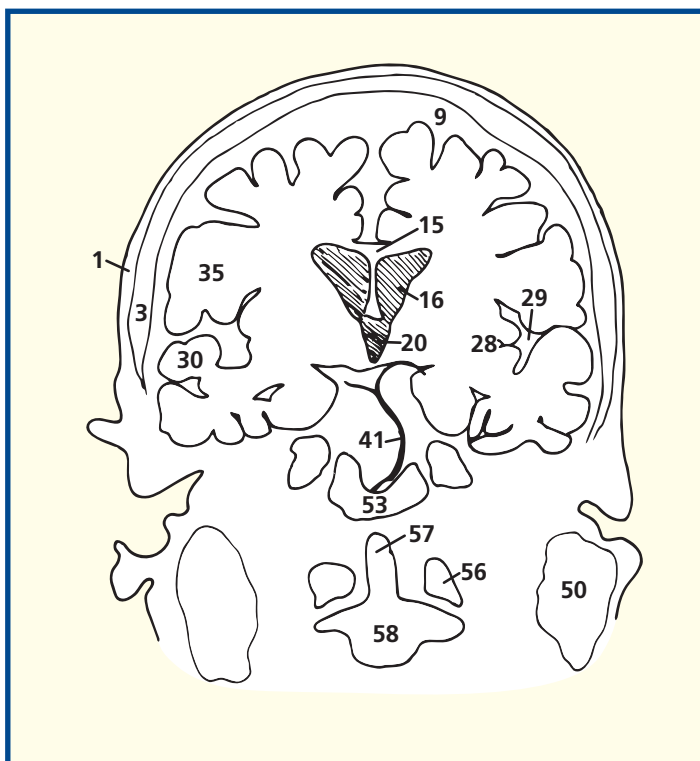
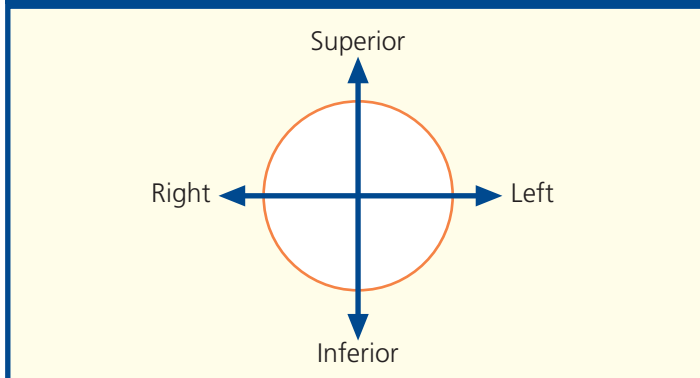


Notes

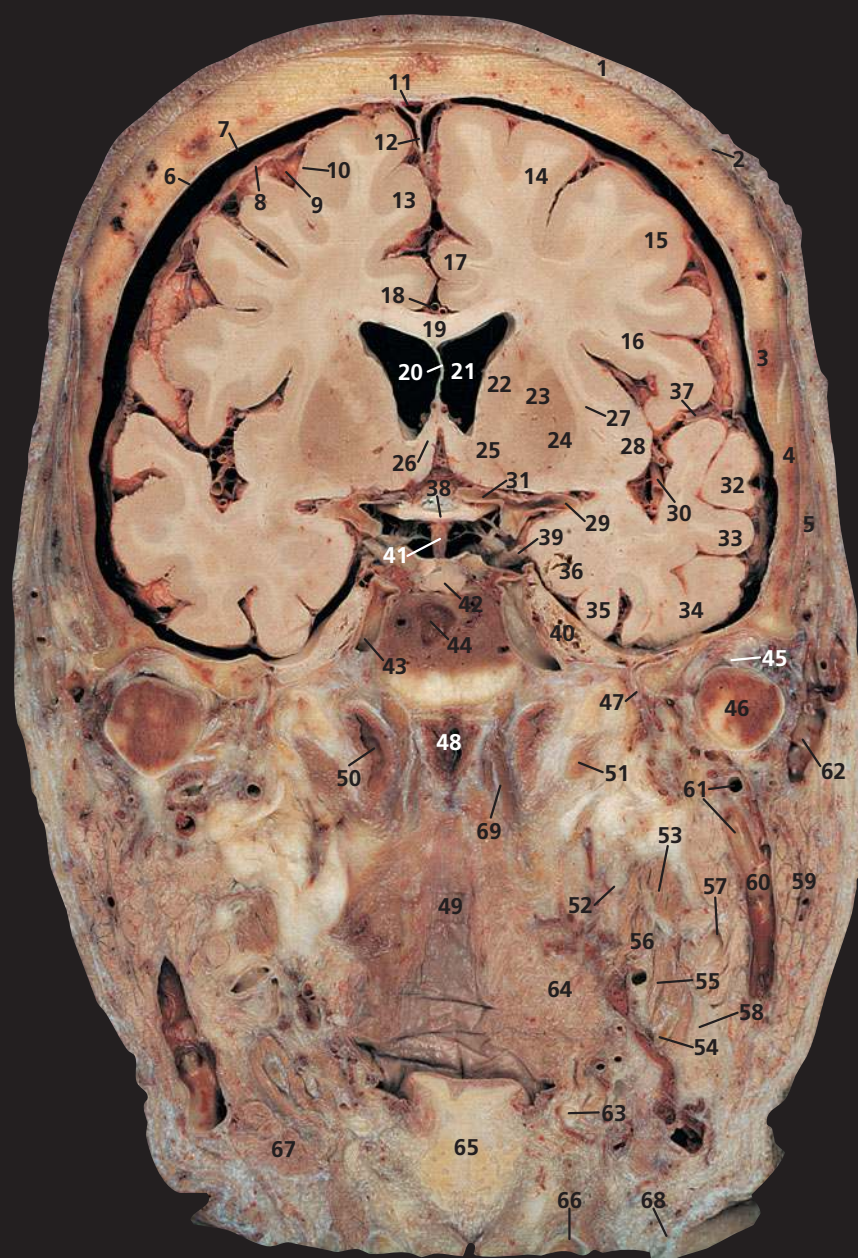
This section passes through the external auditory meatus (46). This is about 37 mm long and has a peculiar S-shaped course, being directed first medially upwards and backwards, then medially and backwards, and finally medially forwards and downwards. The outer third of the canal is cartilaginous and somewhat wider than the medial osseous portion. It leads to the tympanic membrane, or eardrum (47), which faces laterally downwards and forwards.

This section provides a clear view of the dens (57) in coronal section and articulation with the anterior arch of the atlas (56). It also illustrates the importance of the transverse ligament of atlas keeping the dens of the axis (odontoid peg of second cervical vertebra) (57) in intimate contact with the atlas (first cervical vertebra).

Orientation

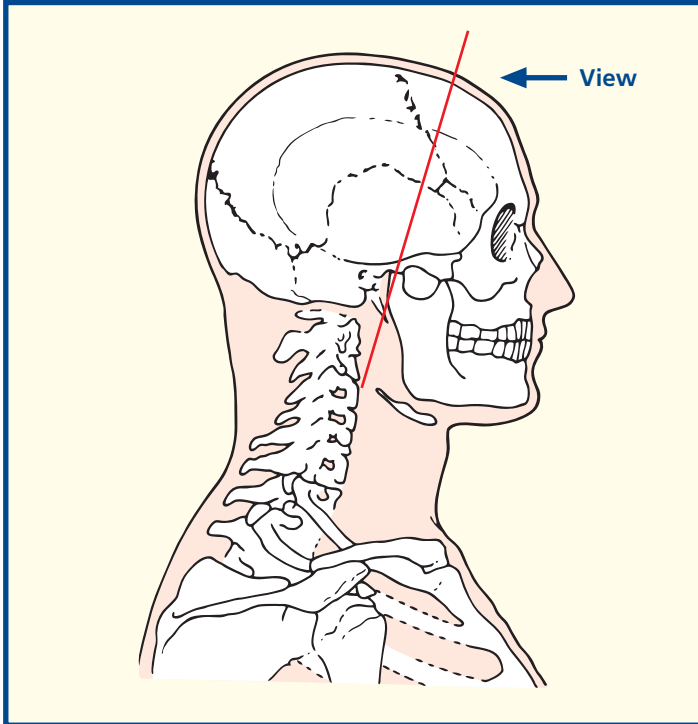


Coronal magnetic resonance image (MRI)



- | | | | |
|-----------------------------------------------|------------------------------------------------|---------------------------------------------------------------------|---------------------------------------------------|
| 1 Skin and dense subcutaneous tissue | 22 Head of caudate nucleus | 39 Oculomotor nerve (III) | 52 Internal carotid artery |
| 2 Epicranial aponeurosis (galea aponeurotica) | 23 Lentiform nucleus | 40 Trigeminal ganglion | 53 Styloglossus |
| 3 Parietal bone | 24 Putamen | 41 Pituitary stalk | 54 Tendon of digastric |
| 4 Squamous part of temporal bone | 25 Nucleus accumbens | 42 Pituitary gland within pituitary fossa (sella turcica) | 55 Stylohyoid |
| 5 Temporalis | 26 Anterior column of fornix | 43 Internal carotid artery within cavernous sinus | 56 Stylopharyngeus |
| 6 Dura mater | 27 Claustrum | 44 Body of sphenoid bone and sphenoidal sinus | 57 External carotid artery |
| 7 Subdural space | 28 Insula | 45 Intra-articular disc of temporomandibular joint | 58 Hypoglossal nerve (XII) |
| 8 Arachnoid mater | 29 Origin of middle cerebral artery (see 30) | 46 Head of mandible | 59 Parotid gland |
| 9 Subarachnoid space | 30 Middle cerebral artery branches (see 29) | 47 Middle meningeal artery within foramen spinosum of sphenoid bone | 60 Retromandibular vein |
| 10 Pia mater | 31 Origin of anterior cerebral artery (see 18) | 48 Posterior wall of nasopharynx | 61 Maxillary artery and vein |
| 11 Superior sagittal sinus | 32 Superior temporal gyrus | 49 Posterior wall of oropharynx | 62 Superficial temporal vein |
| 12 Falx cerebri | 33 Middle temporal gyrus | 50 Auditory (Eustachian) tube | 63 Greater horn of hyoid bone |
| 13 Medial frontal gyrus | 34 Inferior temporal gyrus | 51 Levator veli palatini | 64 Constrictor muscles of pharynx |
| 14 Superior frontal gyrus | 35 Lateral occipitotemporal gyrus | | 65 Cartilage of epiglottis |
| 15 Middle frontal gyrus | 36 Medial occipitotemporal gyrus | | 66 Superior margin of lamina of thyroid cartilage |
| 16 Inferior frontal gyrus | 37 Lateral sulcus | | 67 Submandibular gland |
| 17 Cingulate gyrus | 38 Optic chiasma (II) | | 68 Platysma |
| 18 Pericallosal artery | | | 69 Longus capitis |
| 19 Body of corpus callosum | | | |
| 20 Septum pellucidum | | | |
| 21 Lateral ventricle | | | |

Section level



Notes

The plane of this section passes through the head of the mandible (46) and the temporomandibular joint. The articular surfaces of the joint are covered with fibrocartilage (not hyaline cartilage as is usual in a synovial joint). The joint contains a prominent fibrocartilaginous intra-articular disc (45), which divides it into an upper and lower compartment.

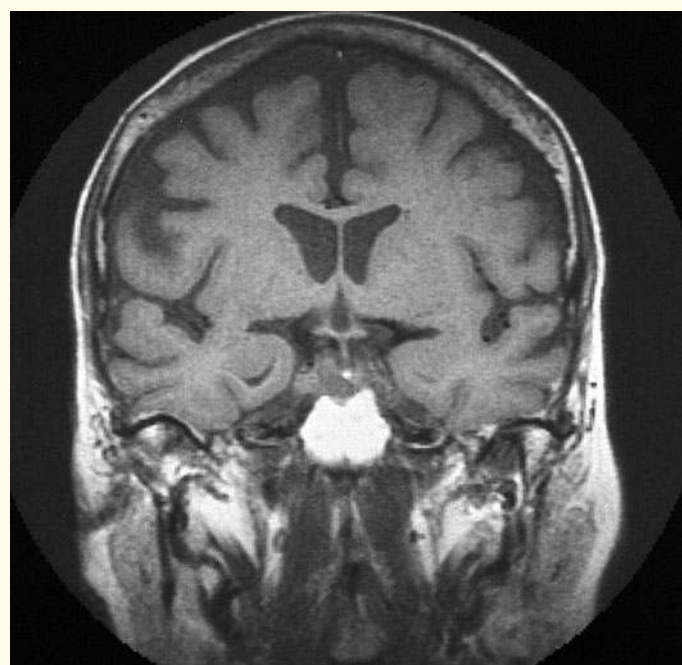
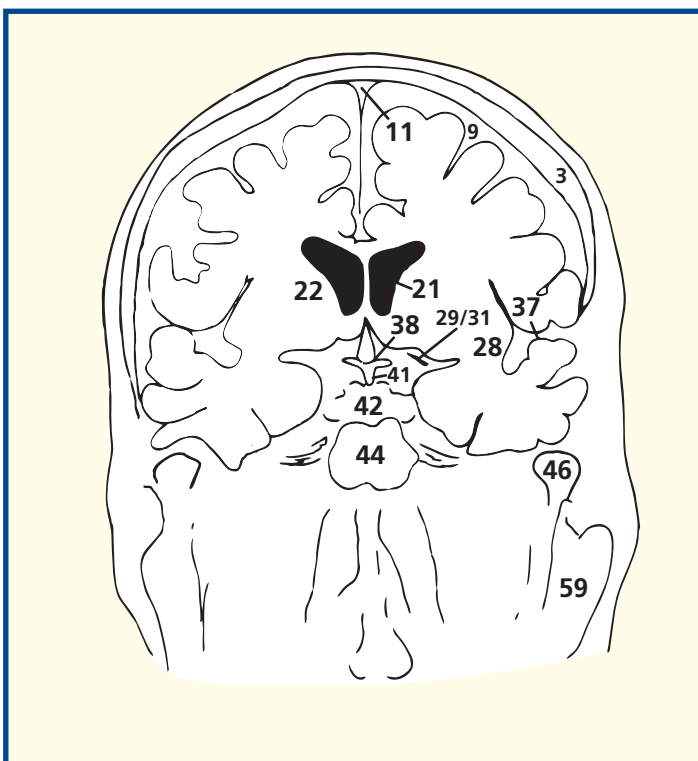
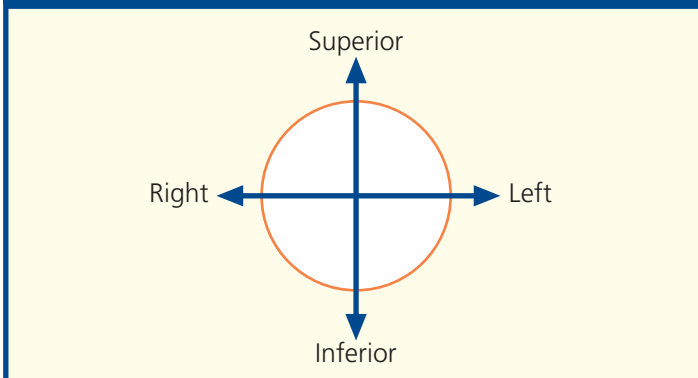
The parotid gland (59) and the submandibular salivary gland (67) are in contact with each other, separated only by a sheet of fascia, the stylomandibular ligament.

The anterior limb of the internal capsule relates medially to the head of the caudate nucleus (22) and laterally to the putamen (24). See also the note on the posterior limb of the internal capsule in Coronal section 6.

The pituitary gland (42) can be seen lying within its fossa, in close relationship to the optic chiasma. An enlarging tumour of the pituitary gland classically produces the visual disturbance of bitemporal hemianopia because of pressure on the medial aspect of the chiasma. The modern pernasal trans-sphenoidal fibre-optic approach for pituitary surgery via the sphenoid sinus (44) can be appreciated in this section.

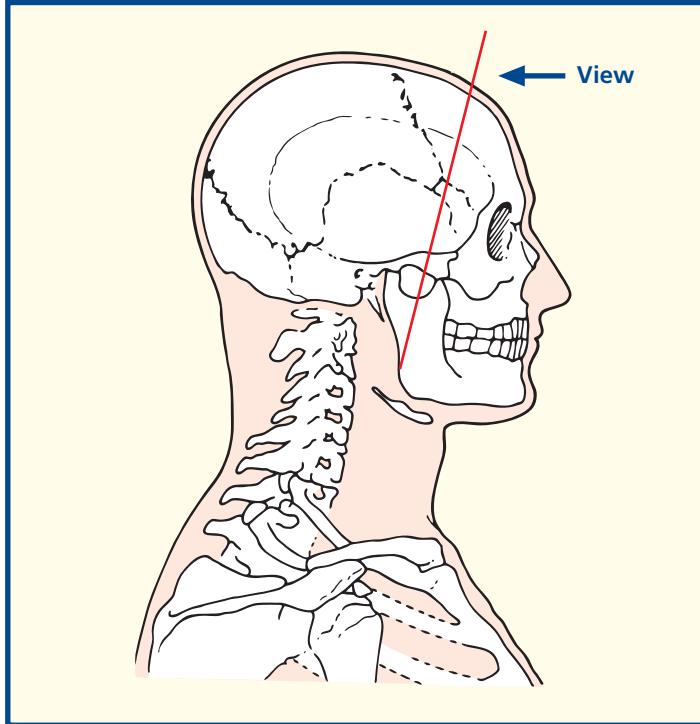
On this T1-weighted magnetic resonance image, the sphenoid (44) is very bright because there is virtually no sinus aeration; this is very variable. The bright signal reflects a high narrow content of bone.

Orientation



Coronal magnetic resonance image (MRI)

Section level



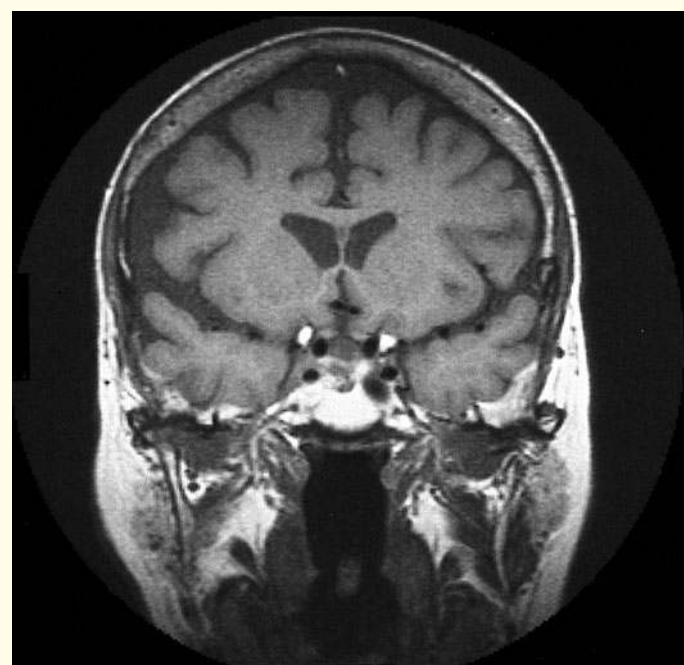
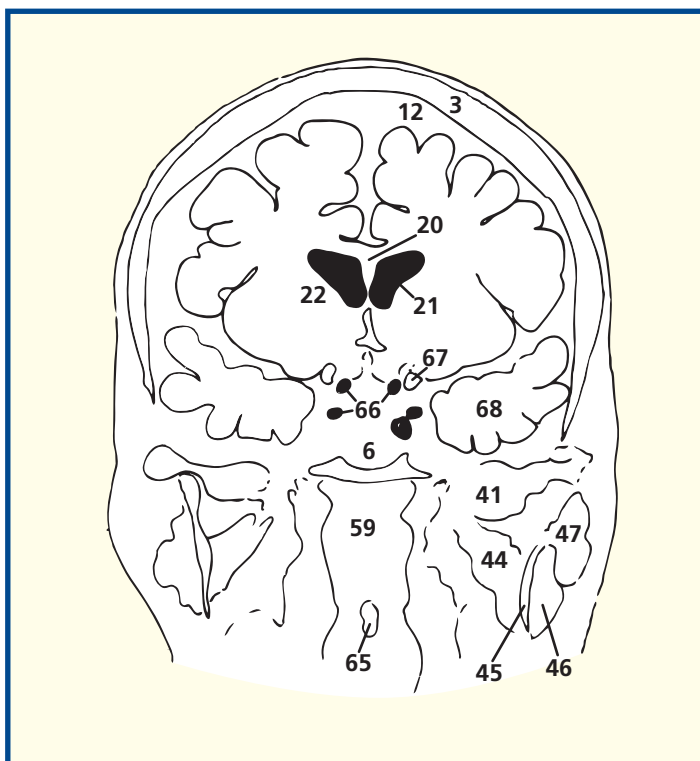
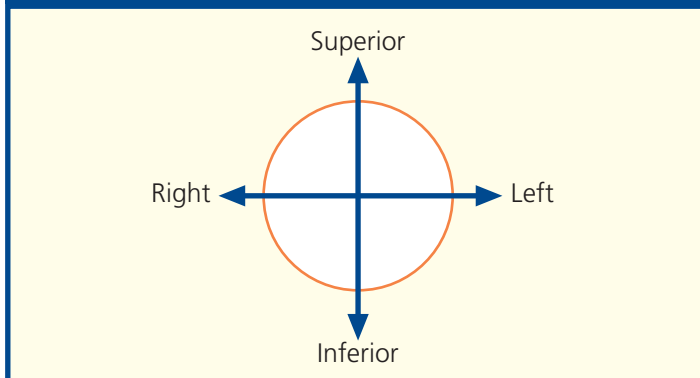
Notes

The line of this section passes through the zygomatic process of the temporal bone (5), the posterior part of the tongue (57) and the body of the hyoid bone (53). We peer into the nasopharynx (59) with the termination of the auditory, or Eustachian, tube (60) just visible.

The oculomotor nerve (III) (33) passes through the sharp edge of the tentorium cerebelli to enter the cavernous sinus (37). The cerebral hemisphere, compressed by an extradural or subdural clot, presses upon the nerve at the tentorial edge and produces dilation of the pupil; hence, the neurosurgical aphorism, 'explore the side with the dilated pupil'. Damage to the internal carotid artery within the cavernous sinus (37), usually as a result of trauma, may produce a carotico-cavernous fistula and results in a pulsating exophthalmos.

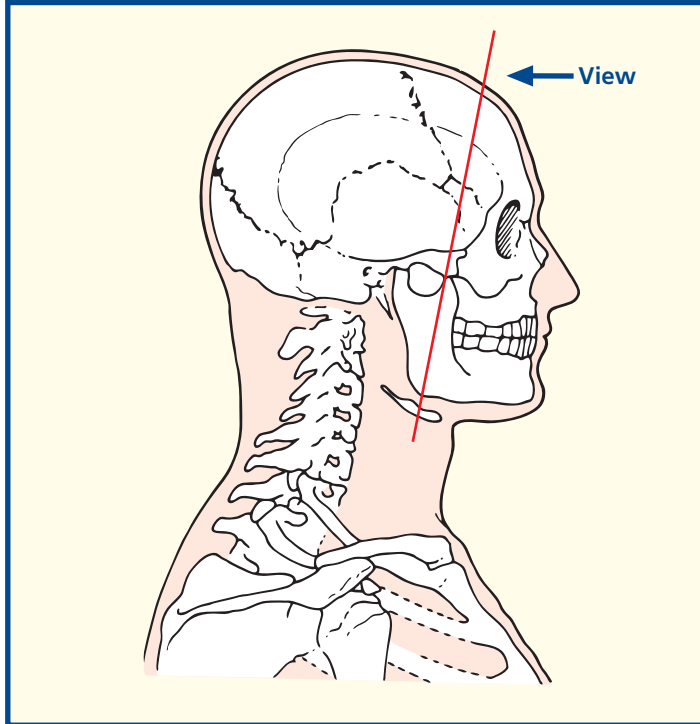
The intrinsic muscles of the tongue (57) comprise longitudinal, transverse and vertical bands of muscle. These, acting alone or in combination, give the tongue its precise and highly variable mobility in speech and swallowing. Their nerve supply is the hypoglossal nerve (XII).

Orientation



Coronal magnetic resonance image (MRI)

Section level



Notes

Do not be deceived! This section passes through the tip of the temporal lobe of the cerebrum (23), lying inferior to the lesser wing of the sphenoid (19) and not the orbit. Note that the plane of this section lies immediately anterior to the anterior horn of the lateral ventricle.

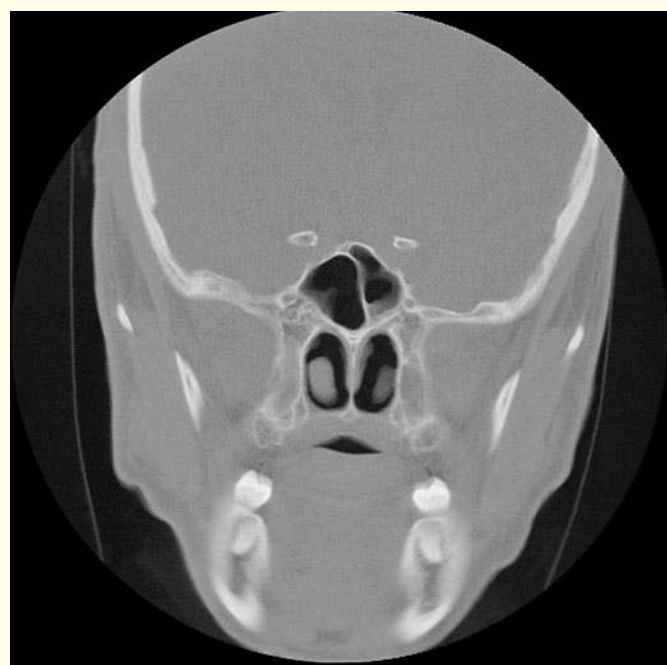
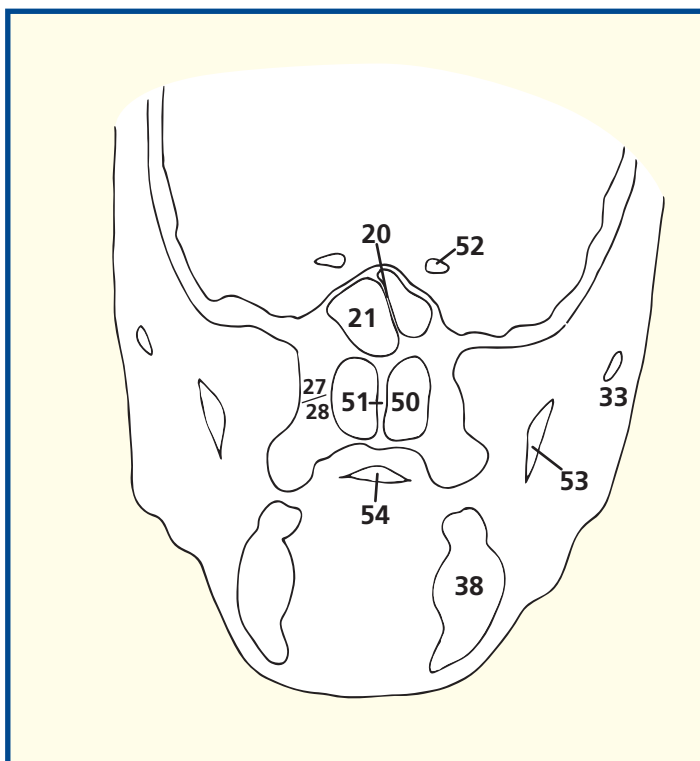
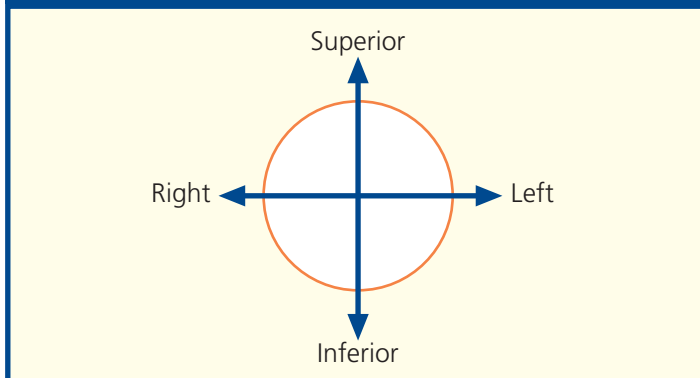
The parotid duct (36) can be palpated easily in the living subject by tensing the masseter muscle (34) and feeling along the upper part of the anterior border of this muscle just inferior to the zygomatic arch (33). The accessory parotid gland, or pars accessoria (35), is usually completely detached from the main gland and lies between the parotid duct and the zygomatic arch. It accounts for an occasionally very anteriorly placed parotid tumour.

The paired sphenoidal sinuses (21) lie within the body of the sphenoid bone and vary quite considerably in size and shape. They are rarely symmetrical, one often being much larger than the other and extending across the midline behind the other. Occasionally one overlaps the other sinus superiorly. Usually the septum (20) between the two sinuses is intact, although occasionally these communicate with each other.

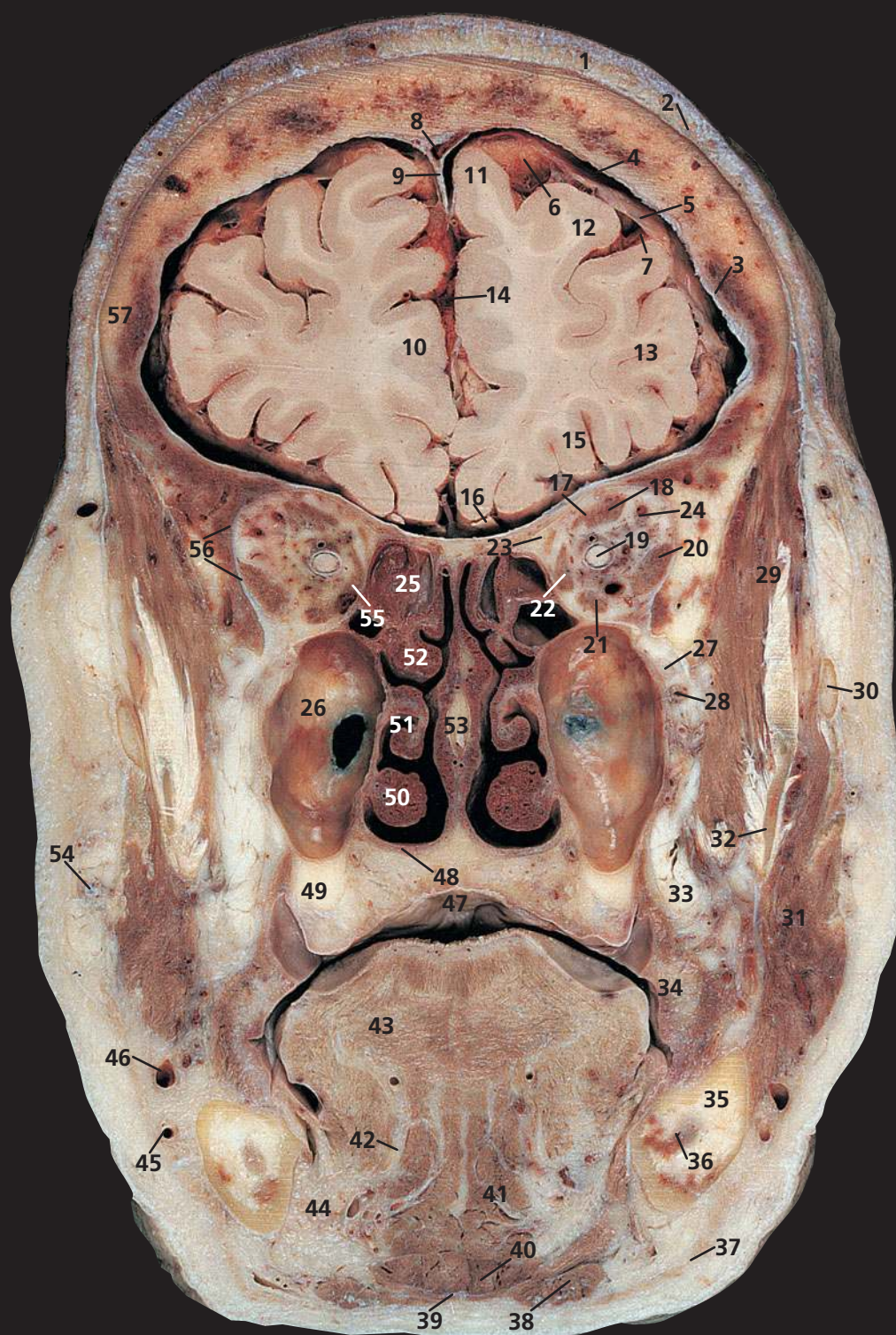
As well as the main salivary glands, many other accessory salivary glands are found, some in the tongue, some between the crypts of the palatine tonsils and some on the inner aspects of the lip and cheeks. Large numbers are found in the posterior hard palate and the soft palate (49). They are mainly mucous in type and are occasional sites for the development of a pleomorphic salivary tumour.

The CT image is purposefully displayed at optimal setting for bony structure.

Orientation

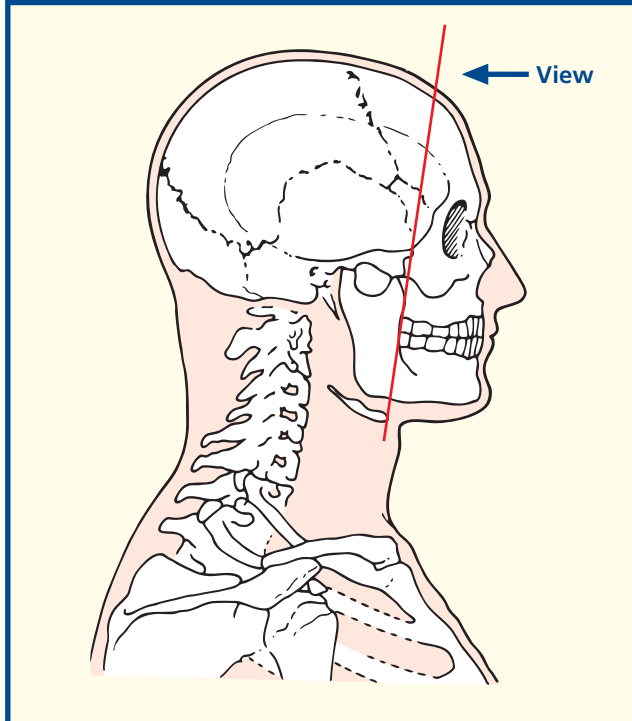


Coronal computed tomogram (CT)

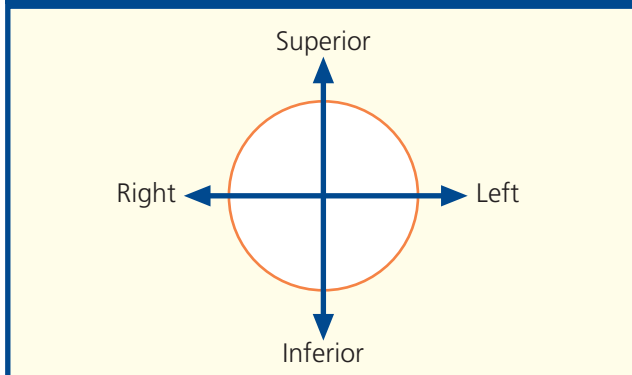


- | | | | | |
|-----------------------------------------------|-------------------------------------|------------------------------------------------|----------------------------------------------------|----------------------------------------------------|
| 1 Skin and dense subcutaneous tissue | 11 Superior frontal gyrus | 23 Superior oblique | 37 Platysma | 50 Inferior nasal concha |
| 2 Epicranial aponeurosis (galea aponeurotica) | 12 Middle frontal gyrus | 24 Branches of ophthalmic artery and vein | 38 Anterior belly of digastric | 51 Middle nasal concha |
| 3 Dura mater | 13 Inferior frontal gyrus | 25 Ethmoidal air cells | 39 Mylohyoid | 52 Superior nasal concha |
| 4 Subdural space | 14 Longitudinal fissure | 26 Maxillary sinus | 40 Geniohyoid | 53 Nasal septum |
| 5 Arachnoid mater | 15 Orbital gyri | 27 Maxillary nerve | 41 Genioglossus | 54 Parotid duct |
| 6 Subarachnoid space | 16 Olfactory tract (I) | 28 Maxillary artery | 42 Lingual artery | 55 Orbital part of ethmoid bone |
| 7 Pia mater | 17 Levator palpebrae superioris | 29 Temporalis | 43 Transverse fibres of intrinsic muscle of tongue | 56 Greater wing of sphenoid bone – orbital surface |
| 8 Superior sagittal sinus | 18 Superior rectus | 30 Zygomatic arch | 44 Sublingual gland | 57 Frontal bone |
| 9 Falx cerebri | 19 Optic nerve (II) in dural sheath | 31 Masseter | 45 Facial artery | |
| 10 Medial frontal gyrus | 20 Lateral rectus | 32 Ramus of mandible | 46 Facial vein | |
| | 21 Inferior rectus | 33 Buccal pad of fat | 47 Soft palate | |
| | 22 Medial rectus | 34 Buccinator | 48 Horizontal plate of palatine bone | |
| | | 35 Body of mandible | 49 Tuberosity of maxilla | |
| | | 36 Inferior alveolar nerve in mandibular canal | | |
| | | | | 58 Zygoma |
| | | | | 59 Dental artefacts (see notes) |

Section level



Orientation



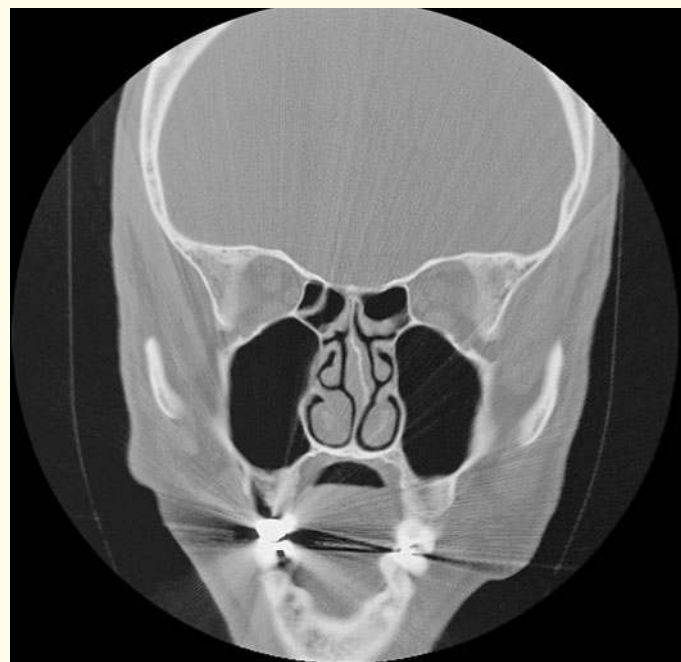
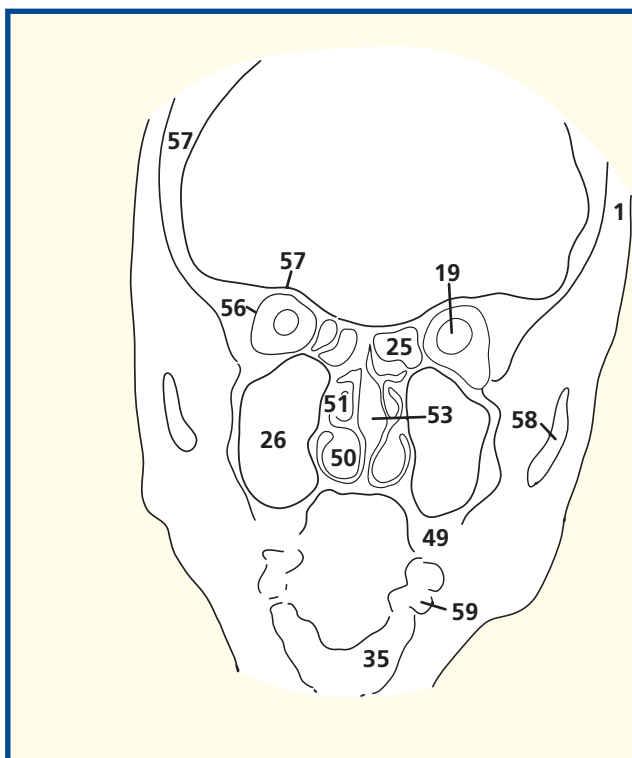
Notes

This section does indeed pass through the posterior part of the cavity of the orbit and demonstrates the close packing of the extrinsic muscles (**17, 18, 20–23**) and blood vessels (**24**) with the orbital fat and optic (II) nerve (**19**). Note that the optic nerve is surrounded by an extension of the dura mater and is, therefore, bathed in cerebrospinal fluid. Raised intracranial pressure is thus transmitted in the cerebrospinal fluid along the sheath and results in the changes of papilloedema.

The ethmoidal air cells, or sinuses (**25**), are small, thin-walled cavities in the ethmoidal labyrinth. They range in number from three large to 18 small cells on either side and are separated from the orbit by the paper-thin orbital plate of the ethmoid. Orbital cellulitis can thus easily result from ethmoid sinusitis (see (**54**) in Coronal section 13).

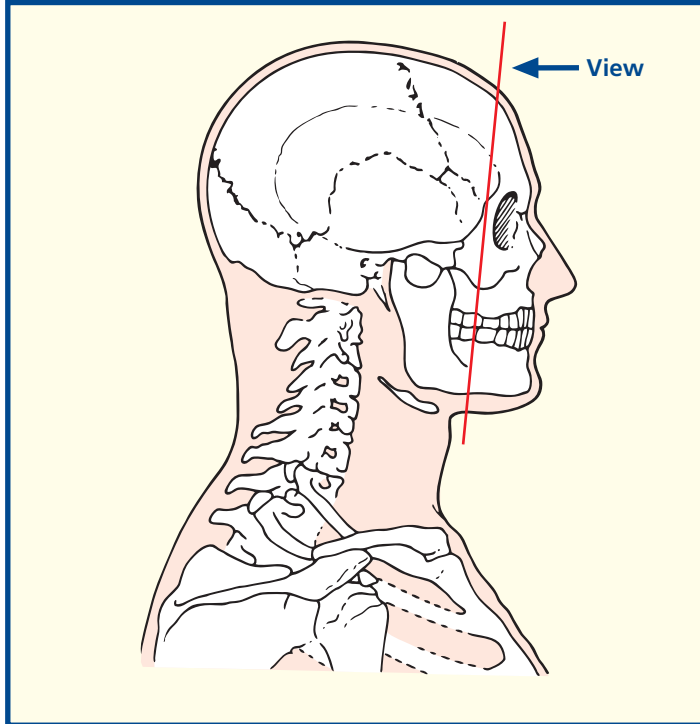
The three nasal conchae (still often referred to by ear, nose and throat (ENT) surgeons as the turbinate bones) project downwards like three scrolls from the lateral wall of the nasal cavity. The lowest, the inferior (**50**), is the largest and broadest. It is a separate bone, unlike the middle (**51**) and superior (**52**), which are part of the ethmoid bone (**55**). The middle and superior conchae are joined anteriorly, but diverge away from each other posteriorly so that the superior concha can be visualized only at posterior rhinoscopy and is invisible on viewing through the anterior nares. Beneath each concha is a space, termed the superior, middle and inferior meatus, respectively.

Metallic material used in dental fillings creates substantial problems for coronal CT. Even with careful positioning and gantry angulation, problems may be unavoidable: On the image, note the distortion created by the presence of a metallic dental filling.



Coronal computed tomogram (CT)

Section level



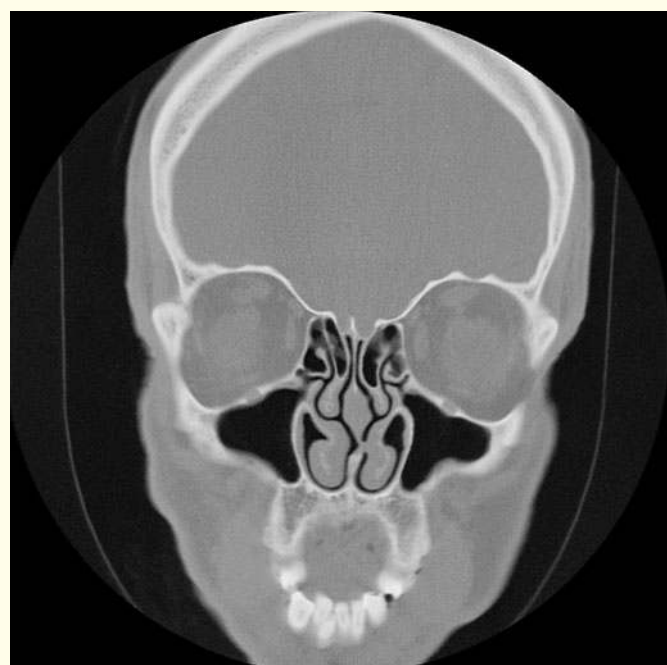
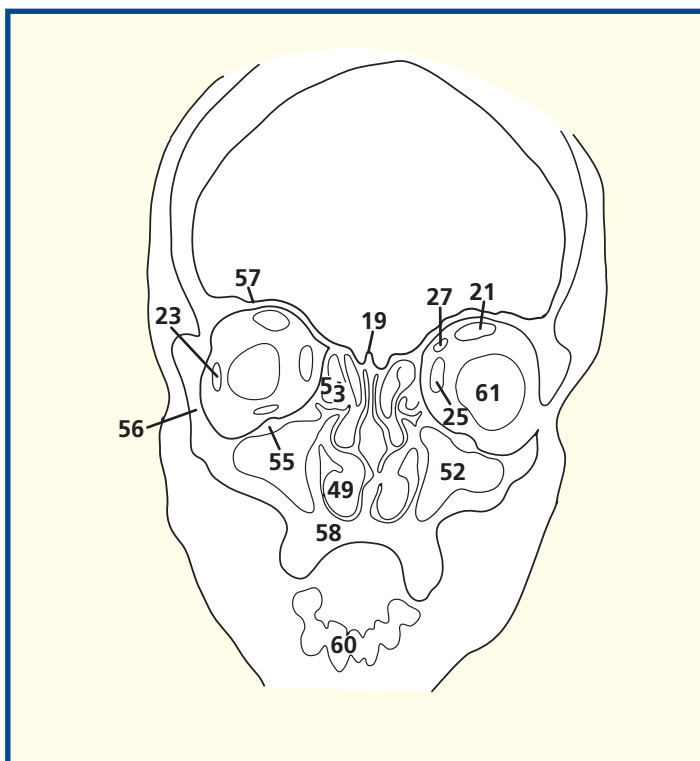
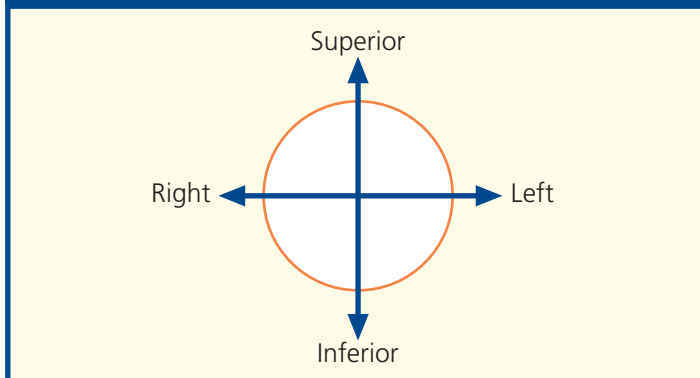
Notes

From the roof of the nasal cavity, some 20 olfactory nerve (I) filaments on each side perforate the dura and arachnoid over the cribriform plate and pass upwards through the subarachnoid space to enter the olfactory bulb (18). From here, the olfactory tract passes posteriorly on the inferior surface of the frontal lobe. Fractures crossing the anterior cranial fossa, with tearing of the overlying dura, may result in cerebrospinal rhinorrhoea, watery fluid draining into the nose. Untreated, this communication between the nasal cavity and the subarachnoid space inevitably results in meningitis.

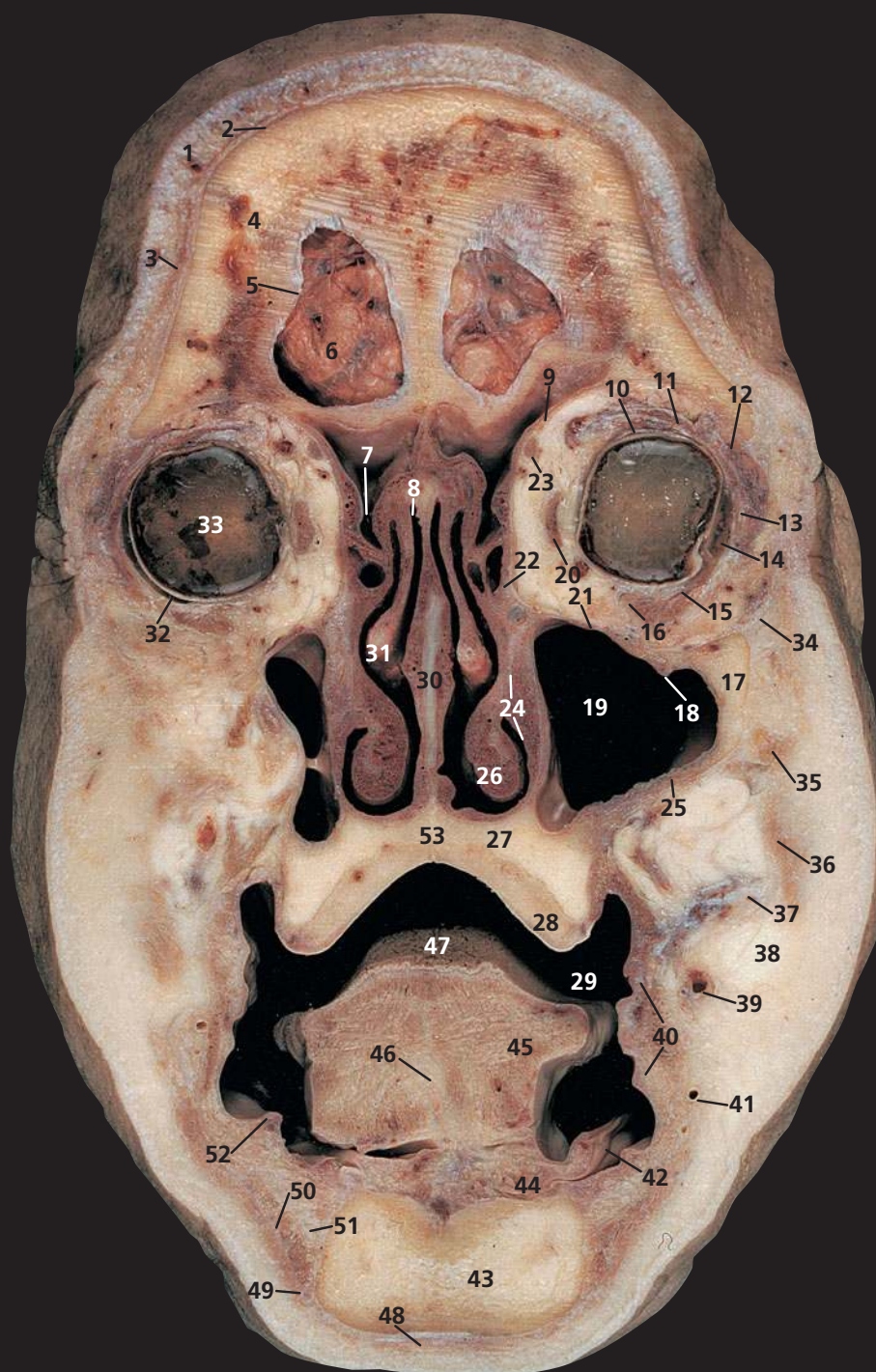
The maxillary sinus, or antrum (52), occupying most of the body of the maxilla, is the largest of the nasal accessory sinuses. In dentulous subjects, conical elevations, which correspond to the roots of the first and second molar teeth, project into the floor of the sinus, which they occasionally perforate. Less commonly, the roots of the two premolars, the third molar and, rarely, the canine may also project into the sinus. Upper dental infection may thus involve the sinus, and dental extraction may result in an oromaxillary fistula. The sinus opens into the nasal cavity in the lowest part of the hiatus semilunaris below the middle concha (51). A second orifice is often present in or just below the hiatus.

CT in the coronal plane is used to demonstrate the anatomy of the maxillary sinus and its drainage into the nasal cavity. Some ENT surgeons now perform flexible endoscopic sinus surgery (FESS) to improve matters. This CT projection is also useful for assessing fractures of the floor of the orbit.

Orientation

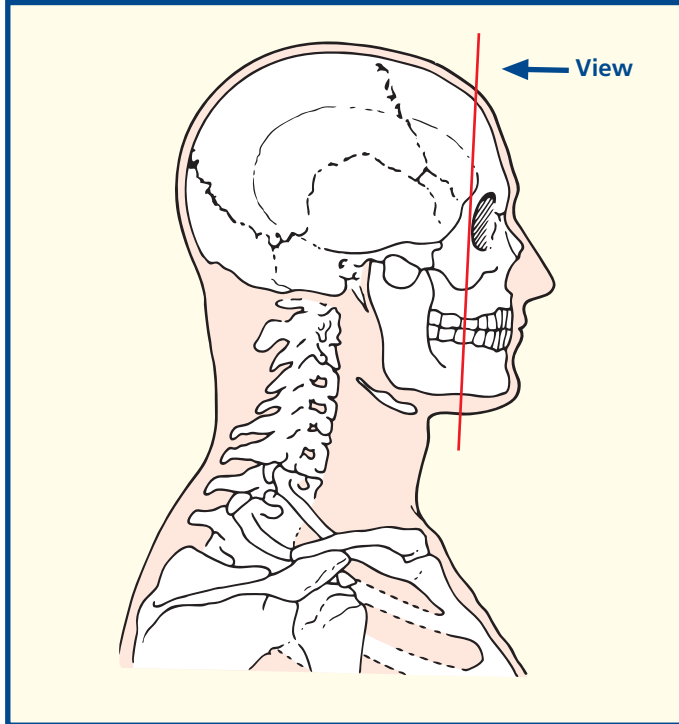


Coronal computed tomogram (CT)



- | | | | |
|----------------------------------------------------------------------------------------------------------|-------------------------------------------------------------------------|--------------------------------|-----------------------------------|
| 1 Skin and dense subcutaneous tissue | 12 Lacrimal gland (orbital part) | 26 Inferior nasal concha | 44 Sublingual gland |
| 2 Epicranial aponeurosis (galea aponeurotica) | 13 Lacrimal gland (palpebral part) | 27 Palatine process of maxilla | 45 Genioglossus |
| 3 Occipital belly of occipitofrontalis | 14 Lateral rectus | 28 Alveolar process of maxilla | 46 Median septum of tongue |
| 4 Frontal bone | 15 Inferior oblique | 29 Vestibule of mouth | 47 Dorsum of tongue |
| 5 Dura mater | 16 Inferior rectus | 30 Nasal septum | 48 Platysma |
| 6 Frontal lobe of brain covered with arachnoid mater and blood vessels within the anterior cranial fossa | 17 Orbital margin of zygomatic bone | 31 Middle nasal concha | 49 Depressor anguli oris |
| 7 Infundibulum draining frontal sinus | 18 Infra-orbital artery and nerve within infra-orbital canal of maxilla | 32 Scleral layer of orbit | 50 Depressor labii inferioris |
| 8 Roof of nasal cavity | 19 Maxillary sinus | 33 Vitreous humour | 51 Mental nerve |
| 9 Orbital part of frontal bone | 20 Medial rectus | 34 Orbicularis oculi | 52 Sublingual papilla |
| 10 Superior rectus | 21 Orbital surface of maxilla | 35 Zygomaticus minor | 53 Hard palate |
| 11 Levator palpebrae superioris | 22 Lacrimal bone | 36 Zygomaticus major | |
| | 23 Tendon of superior oblique | 37 Parotid duct | |
| | 24 Nasolacrimal duct | 38 Buccal fat pad | |
| | 25 Maxilla | 39 Facial vein | |
| | | 40 Buccinator | |
| | | 41 Facial artery | |
| | | 42 Mucous membrane of mouth | |
| | | 43 Mandible | |
| | | | 54 Orbital margin of ethmoid bone |
| | | | 55 Crista galli of ethmoid bone |

Section level



Notes

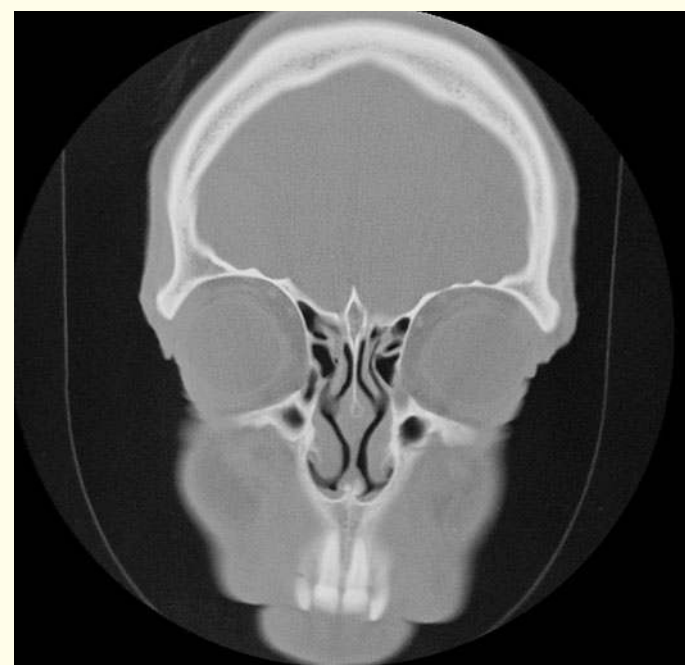
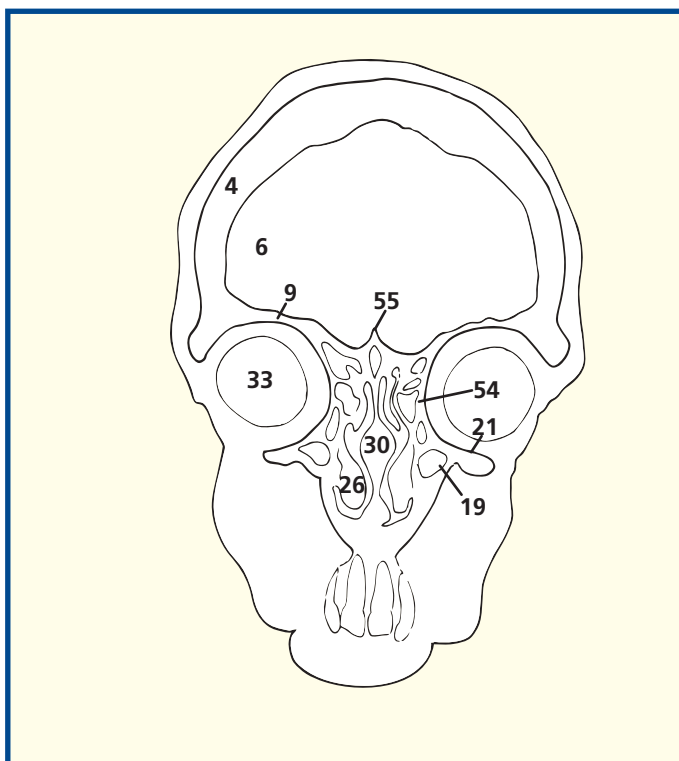
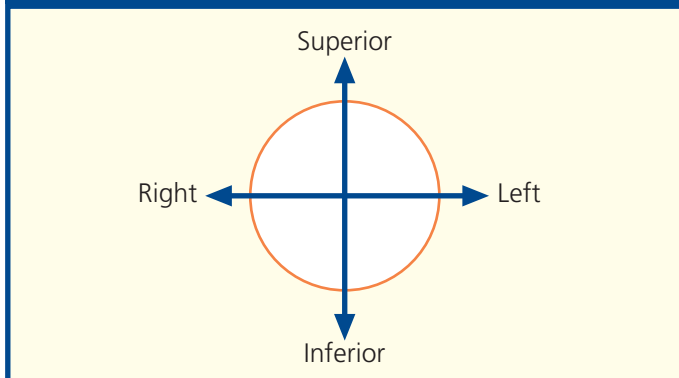
The orbital part of the lacrimal gland (12) lies in the lacrimal fossa on the lateral part of the roof of the orbit supported by the lateral margin of levator palpebrae superioris (11). It projects around the lateral margin of this muscle and turns forward to form the palpebral part of the gland (13), which is visible through the superior fornix of the conjunctiva. Its dozen or so ducts drain into the superior fornix.

The nasolacrimal duct (24), about 2 cm in length, runs downwards and laterally to open into the inferior meatus below the inferior nasal concha (26), about 2 cm behind the nostril. Its mucosa is raised into several folds, which act as valves. These prevent air and nasal mucus being forced up the duct into the lacrimal sac when blowing the nose.

The buccal pad of fat (38) protrudes in front of the masseter to lie on the buccinator (40) immediately inferior to the parotid duct (37). Its estimated volume is 10 cm³. It is well developed in babies, where it forms a prominent elevation over the external surface of the face (the sucking pad). This helps to prevent collapse of the cheeks in vigorous sucking. It persists through life and is relatively 'protected', in that it does not decrease, even in emaciated subjects.

Note the paper-thin (lamina papyracea) orbital margin of the ethmoid bone (54). This portion and the relatively thin orbital margin of maxilla are liable to be damaged by a blow-out injury; the globe, being tougher, transmits injury to the walls of the orbit following trauma that is not absorbed by the bony margins. Squash balls are a particular culprit. The extrinsic eye muscles may get trapped between the fracture margins.

Orientation

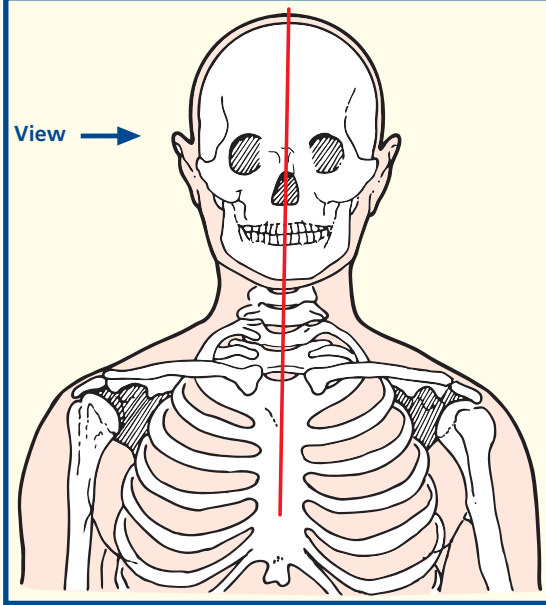


Coronal computed tomogram (CT)



- | | | | |
|--------------------------------|-----------------------------------------------------------------|------------------------------------------------------------|-----------------------------------------------------|
| 1 Occipital bone | 21 Oculomotor nerve (III) | 38 Middle nasal concha | 66 Anterior arch of atlas (first cervical vertebra) |
| 2 Falx cerebri | 22 Posterior cerebral artery | 39 Middle meatus | 67 Lateral ventricle |
| 3 Superior sagittal sinus | 23 Midbrain | 40 Inferior nasal concha | |
| 4 Parietal bone | 24 Pineal body | 41 Inferior meatus | |
| 5 Frontal bone | 25 Superior colliculus | 42 Hard palate | |
| 6 Frontal sinus | 26 Inferior colliculus | 43 Central incisor (upper and lower) | |
| 7 Crista galli of ethmoid bone | 27 Aqueduct (of Sylvius) connecting third and fourth ventricles | 44 Lip (upper and lower) | |
| 8 Sphenoidal sinus | 28 Pons | 45 Body of mandible | |
| 9 Genu of corpus callosum | 29 Fourth ventricle | 46 Sublingual gland | |
| 10 Body of corpus callosum | 30 Cerebellum | 47 Genioglossus | |
| 11 Splenium of corpus callosum | 31 Tentorium cerebelli | 48 Dorsum of tongue | |
| 12 Septum pellucidum | 32 Straight sinus | 49 Geniohyoid | |
| 13 Anterior lobe gyrus | 33 Transverse sinus | 50 Mylohyoid | |
| 14 Body of fornix | 34 Basilar artery | 51 Body of hyoid bone | |
| 15 Third ventricle | 35 Clivus (basi-occipital and basi-sphenoid bones) | 52 Epiglottis | |
| 16 Hypothalamus | 36 Superior nasal concha | 53 Valleculla | |
| 17 Mamillary body | 37 Superior meatus | 54 Oral part of pharynx (oropharynx) | |
| 18 Optic chiasm | | 55 Dens of axis (odontoid peg of second cervical vertebra) | |
| 19 Pituitary stalk | | | |
| 20 Pituitary gland | | | |

Section level



Notes

Note that the nasal septum has been removed from this section in order to display the nasal conchae on the lateral wall.

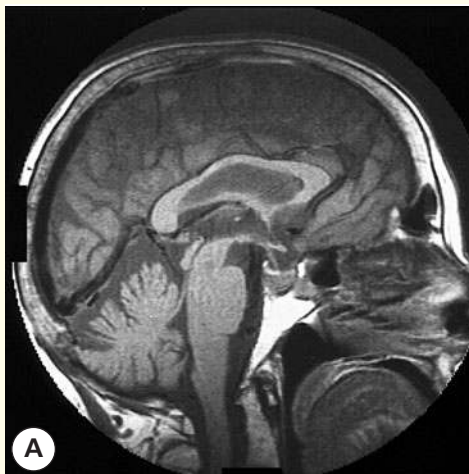
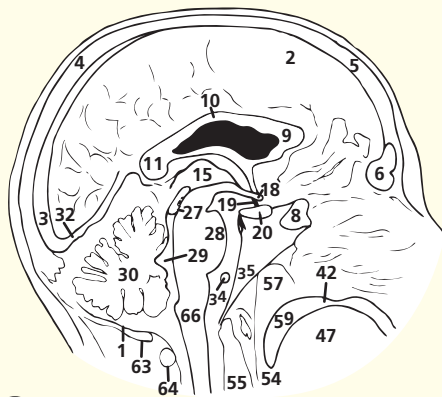
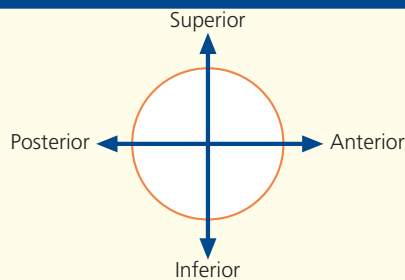
The roof of the hard palate (42) lies at the level of the atlas (first cervical vertebra). Note that a clear anteroposterior view of the dens of the axis (second cervical vertebra) can be obtained on radiological examination by asking the patient to open the mouth widely.

This section illustrates the approach to the pituitary gland (20) via the transnasal trans-sphenoidal sinus (8) route at fibre-optic endoscopic surgery.

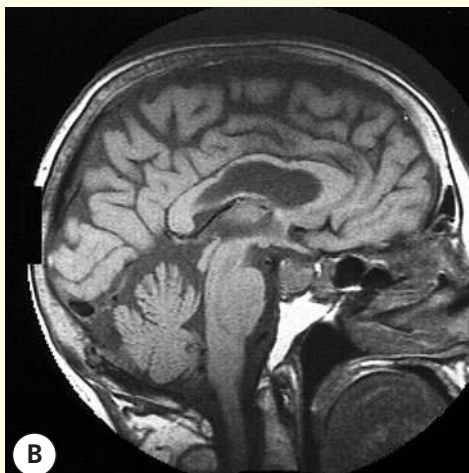
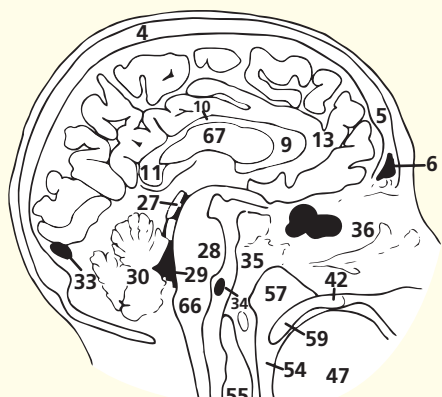
The frontal sinuses (6) vary considerably in size and are rarely symmetrical, the septum between the two usually being deviated to one or the other side. Each may be divided further by incomplete bony septa. Occasionally, one or both may be absent.

These two sagittal T1-weighted magnetic resonance images are very close to the median sagittal plane. Indeed, image (A) is so midline that the falx cerebri has been traversed. Image (B) is minimally lateral to the median sagittal plane and thus cerebral gyri and sulci are visible. The anatomy of the cerebral aqueduct and fourth ventricle is demonstrated well. So too is the important close relationship of the pituitary gland to the optic chiasm.

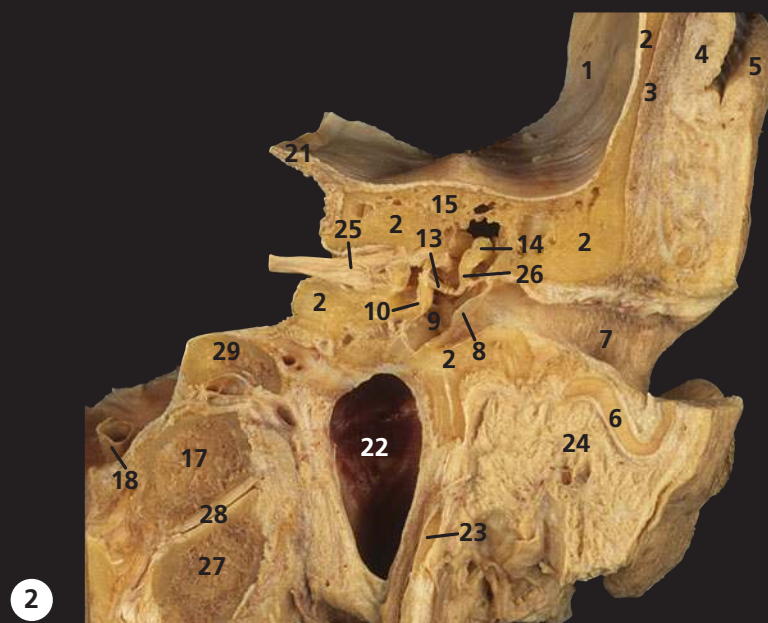
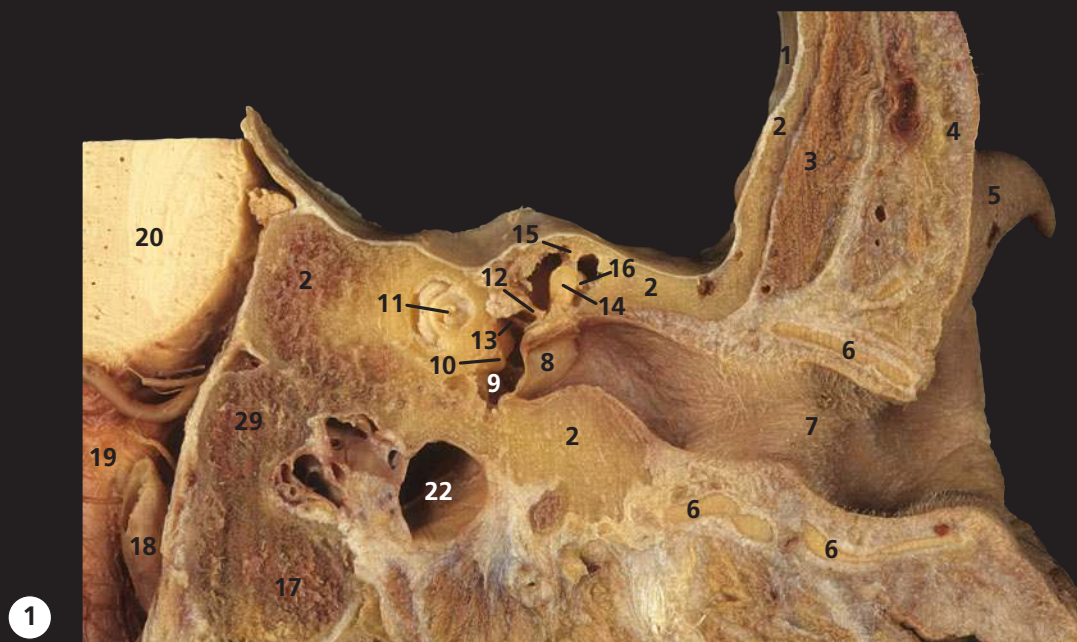
Orientation



Sagittal magnetic resonance image (MRI)

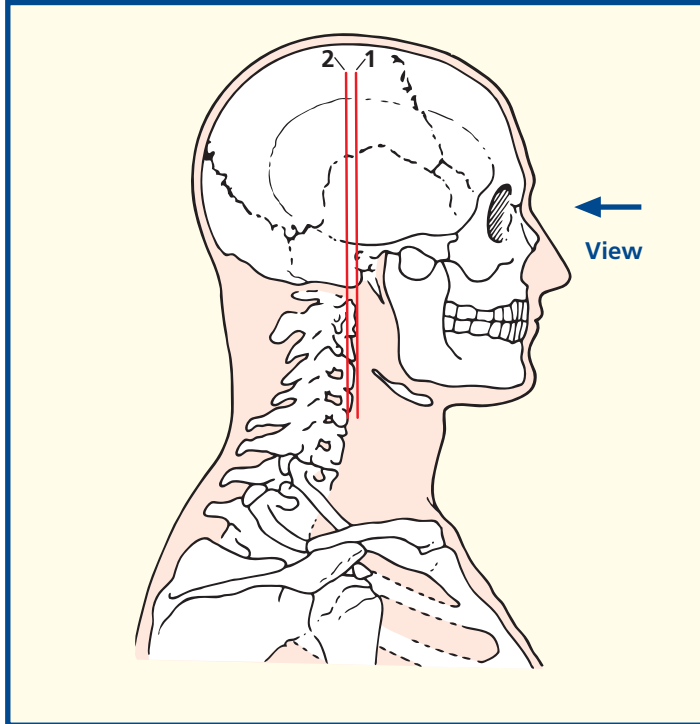


Sagittal magnetic resonance image (MRI)



- | | | |
|--------------------------------------|---------------------------------------|----------------------------------------------------------------------------------------------|
| 1 Dura mater | 12 Tendon of tensor tympani | 23 Styloid process |
| 2 Temporal bone | 13 Stapes | 24 Parotid gland |
| 3 Temporalis | 14 Head of malleus | 25 Facial nerve (VII) and vestibulocochlear nerve (VIII) within the internal acoustic meatus |
| 4 Skin and dense subcutaneous tissue | 15 Tegmen tympani | 26 Long limb of incus |
| 5 Helix of left ear | 16 Body of malleus | 27 Atlas (first cervical vertebra) |
| 6 Auricular cartilage of ear | 17 Occipital condyle | 28 Atlanto-occipital joint |
| 7 External acoustic meatus | 18 Vertebral artery | 29 Occipital bone |
| 8 Tympanic membrane | 19 Medulla oblongata | |
| 9 Cavity of middle ear | 20 Pons | |
| 10 Promontory of middle ear | 21 Free margin of tentorium cerebelli | |
| 11 Cochlea | 22 Internal jugular vein | |

Section level



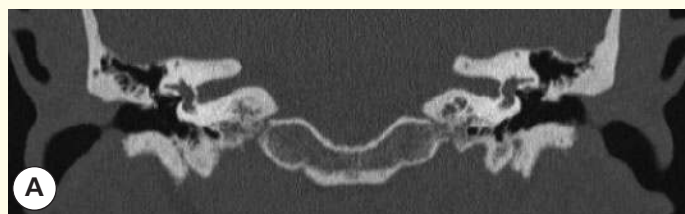
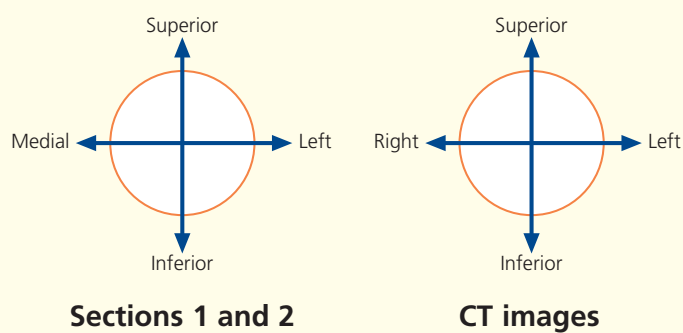
Notes

The external acoustic meatus (7) extends inwards to the tympanic membrane (8). The meatus is about 37 mm in length and has a peculiar S-shaped course, being directed first medially superiorly and anteriorly, then medially and backwards and then, at its termination, medially, anteriorly and inferiorly. The outer third of the canal is cartilaginous and somewhat wider than the inner osseous portion. The tympanic membrane (eardrum) separates the middle ear (9) from the external meatus. It is oval in outline and faces laterally, inferiorly and anteriorly. It is about 12 mm in its greatest (vertical) diameter and is slightly concave outwards. The middle ear, or tympanic cavity (9), is a slit-like cavity in the petrous temporal bone (2) and contains the three auditory ossicles. These are the malleus, whose body, or handle (16), is attached to the tympanic membrane, and a head (14) which articulates with the incus (26), which, in turn, articulates with the stapes (13). The base of the stapes is firmly adherent to the oval window, or fenestra vestibuli, of the inner ear. This comprises a complicated bony labyrinth that encloses the membranous labyrinth. This comprises the utricle and saccule, which communicate with the semicircular canals and the cochlea, respectively (11).

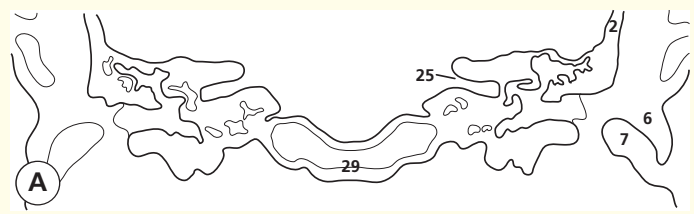
The intimate relationship of the facial nerve (VII) and the vestibulocochlear nerve (VIII) as they enter the internal auditory meatus (25) in the petrous part of the temporal bone (2) is demonstrated.

See also Coronal sections 5–7.

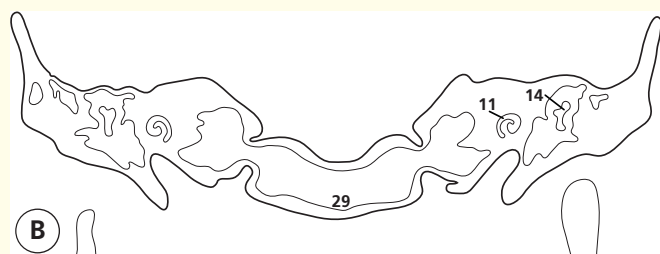
Orientation

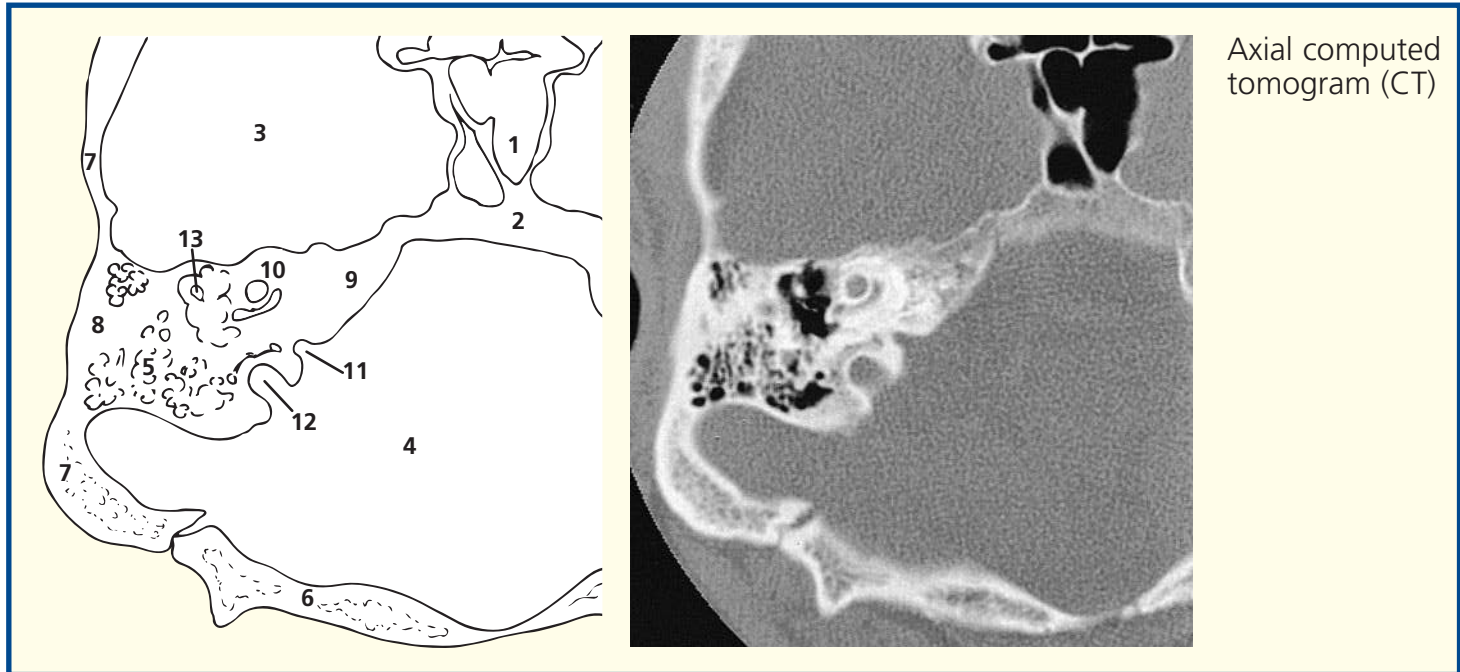


Coronal computed tomogram (CT)



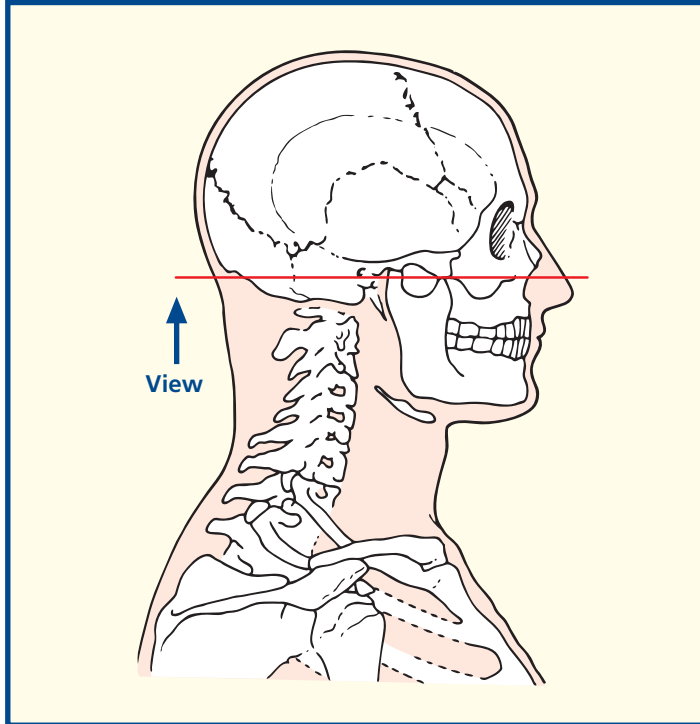
Coronal computed tomogram (CT)





- | | |
|-------------------------------------------------------|----------------------------------------|
| 1 Sphenoidal sinus | 8 Temporal bone (mastoid part) |
| 2 Basi-sphenoid joining basi-occiput (forming clivus) | 9 Temporal bone (apex of petrous part) |
| 3 Temporal lobe of brain (in middle cranial fossa) | 10 Cochlea |
| 4 Posterior cranial fossa | 11 Internal auditory meatus |
| 5 Mastoid air cells (within temporal bone) | 12 Superior aspect jugular bulb |
| 6 Occipital bone | 13 Malleus |
| 7 Temporal bone (petromastoid part) | |

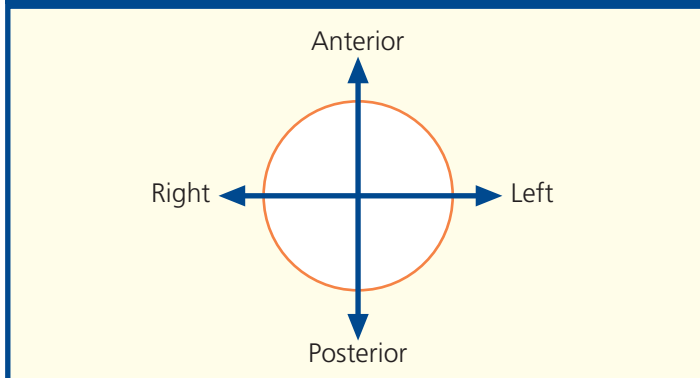
Section level

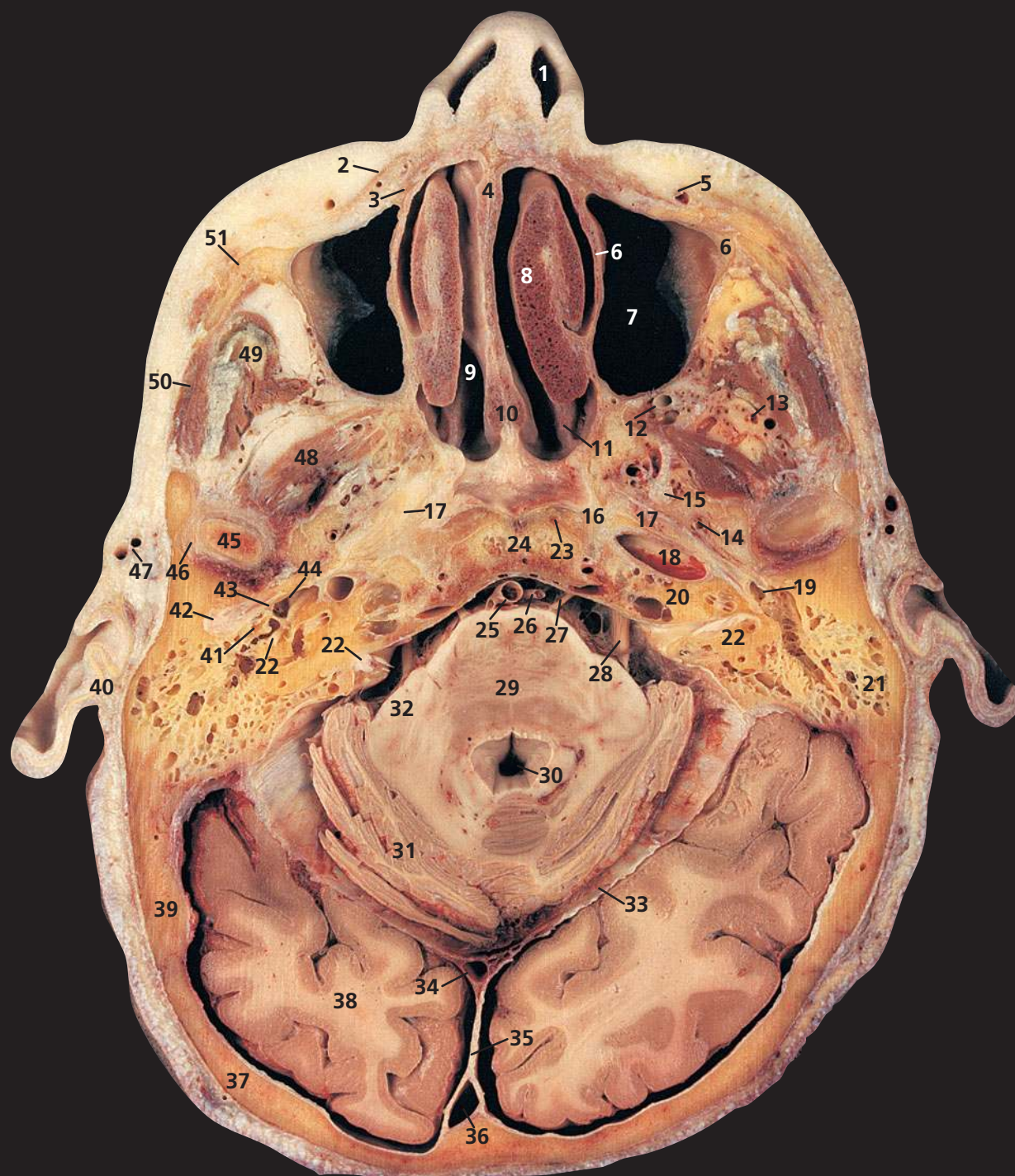


Notes

This thin section CT image has been reconstructed using a bony algorithm and displayed at settings to demonstrate the bony structures. Hence the bone texture is well seen (and the detail of cerebral tissue absent). Such high resolution images are essential to study the anatomy of the inner ear before complex surgery.

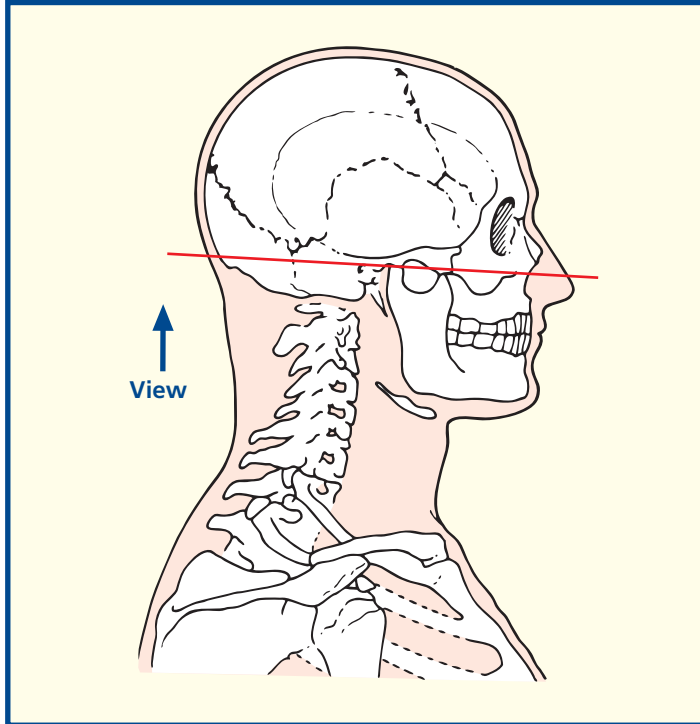
Orientation





- | | | | |
|-----------------------------------------|-----------------------------------------------------------|-----------------------------------|-----------------------------------------|
| 1 Vestibule of nose | 16 Greater wing of sphenoid | 30 Fourth ventricle | 46 Temporomandibular joint |
| 2 Levator labii superioris alaeque nasi | 17 Cartilaginous roof of auditory (Eustachian) tube | 31 Cerebellum | 47 Superficial temporal artery and vein |
| 3 Levator labii superioris | 18 Internal carotid artery | 32 Middle cerebellar peduncle | 48 Lateral pterygoid |
| 4 Cartilage of nasal septum | 19 Junction of internal auditory tube and tympanic cavity | 33 Tentorium cerebelli | 49 Temporalis and tendon |
| 5 Facial vein | 20 Petrous temporal bone | 34 Straight sinus | 50 Masseter |
| 6 Maxilla | 21 Mastoid air cells | 35 Falx cerebri | 51 Zygomatic process of maxilla |
| 7 Maxillary sinus (antrum of Highmore) | 22 Facial nerve (VII) | 36 Superior sagittal sinus | |
| 8 Inferior nasal concha | 23 Longus capitis | 37 Occipital bone (squamous part) | |
| 9 Middle meatus | 24 Body of sphenoid | 38 Occipital lobe of cerebrum | |
| 10 Vomer | 25 Basilar artery | 39 Squamous part of temporal bone | |
| 11 Middle nasal concha | 26 Anterior inferior cerebellar artery | 40 Pinna of ear | |
| 12 Maxillary artery | 27 Abducent nerve (VI) | 41 Malleus and incus | |
| 13 Pterygoid branch of maxillary artery | 28 Trigeminal nerve (V) | 42 External auditory meatus | |
| 14 Middle meningeal artery | 29 Pons cerebri | 43 Tympanic membrane | |
| 15 Mandibular nerve (V ⁱⁱⁱ) | | 44 Cavity of middle ear | |
| | | 45 Head of mandible | |
| | | | 52 Internal jugular vein (at origin) |
| | | | 53 Occipital bone (basilar part) |
| | | | 54 Postnasal space |
| | | | 55 Coronoid process of mandible |
| | | | 56 Medulla oblongata |

Section level



Notes

This section passes through the vestibule of the nose (1), the inferior nasal concha (8), the temporomandibular joint (46), the pons (29) and the occipital lobe of the cerebrum (38).

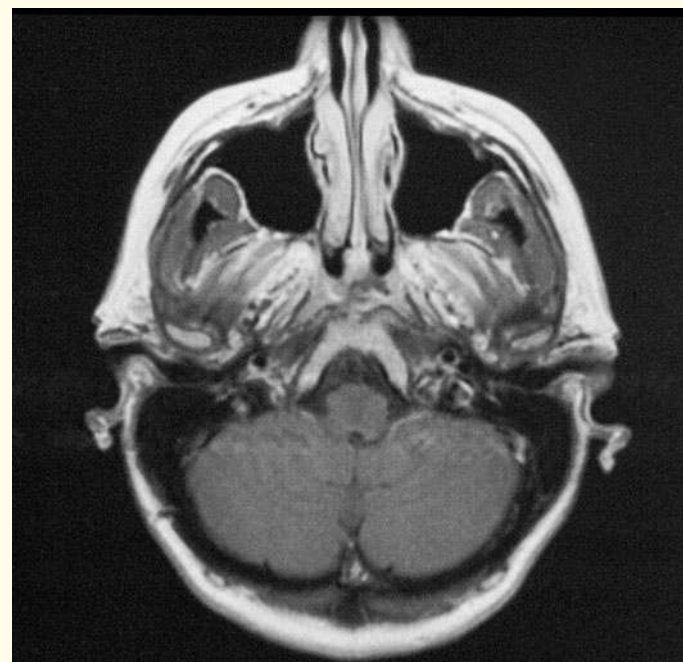
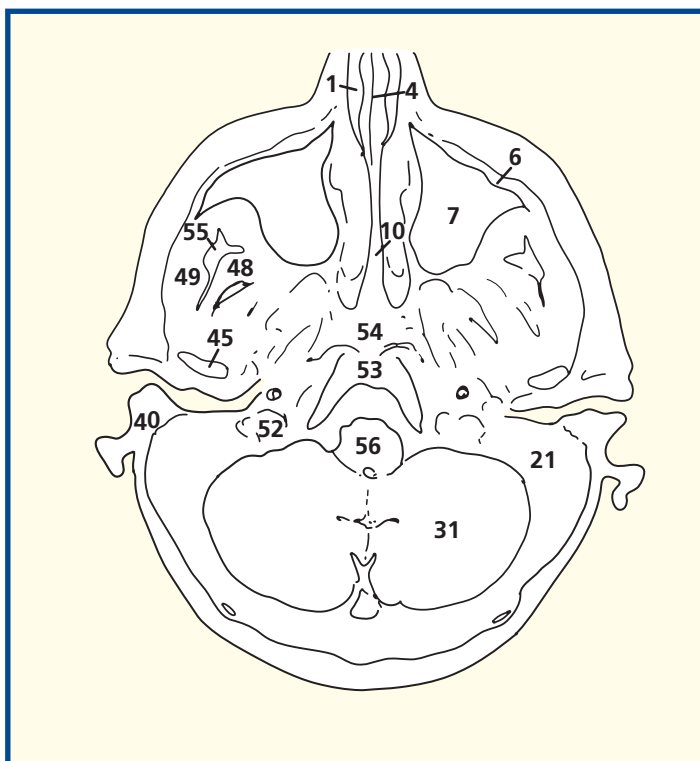
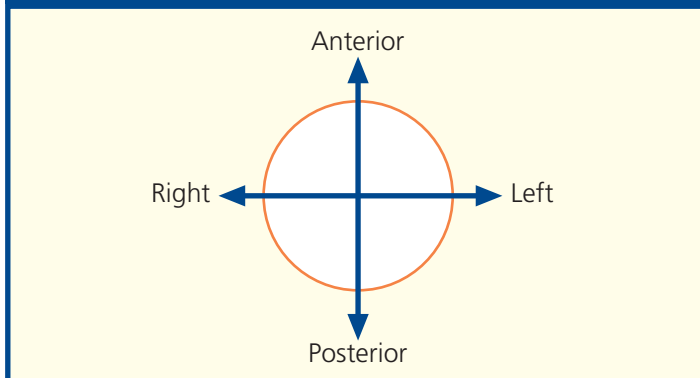
The angulation of this magnetic resonance image does not tally exactly with this section; some of the anatomical features of the neck on this and subsequent sections are therefore better seen on other images.

The maxillary sinus (the antrum of Highmore) within the maxilla (7) is demonstrated well. Its orifice lies at a higher plane and drains into the middle meatus (9) below the bulla ethmoidalis. The fact that the opening of this antrum is situated at this high level accounts for the poor drainage and consequent frequency of infection.

Note that the lateral pterygoid muscle (48) inserts not only into a depression on the front of the neck of the mandible but also into the articular capsule of the temporomandibular joint (46) and its articular disc.

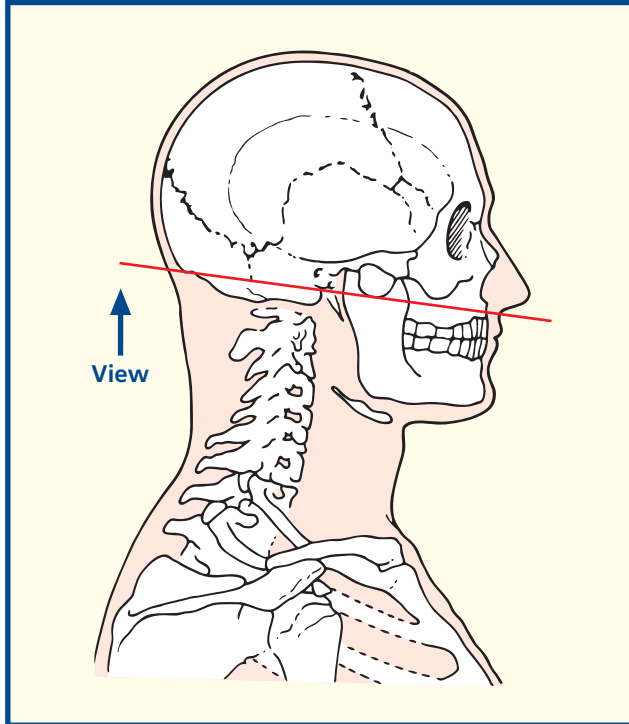
The postnasal space (54) lies between the nasopharynx and the basi-occiput (53) together with the anterior arch of the atlas. As well as containing the prevertebral muscles, this space contains variable quantities of lymphoid tissue (the pharyngeal tonsil, or adenoids). The size of the space is assessed readily on a lateral radiograph of the region. It is usually very narrow in adults (see Section 4, page 88) but can be very prominent in young children, whose adenoids are often very large.

Orientation

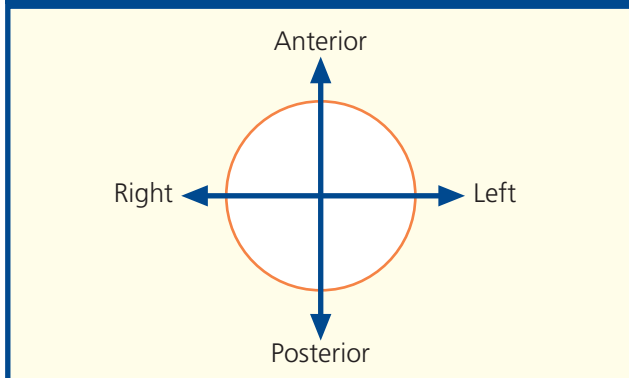


Axial magnetic resonance image (MRI)

Section level



Orientation



Notes

This section passes through the alveolar process of the maxilla (6) to reveal the hard palate (5) in its entirety. It then traverses the upper part of the ramus of the mandible (15), the mastoid air cells (50), the medulla oblongata (39), the cerebellum (30) and the posterior tip of the occipital lobe (32).

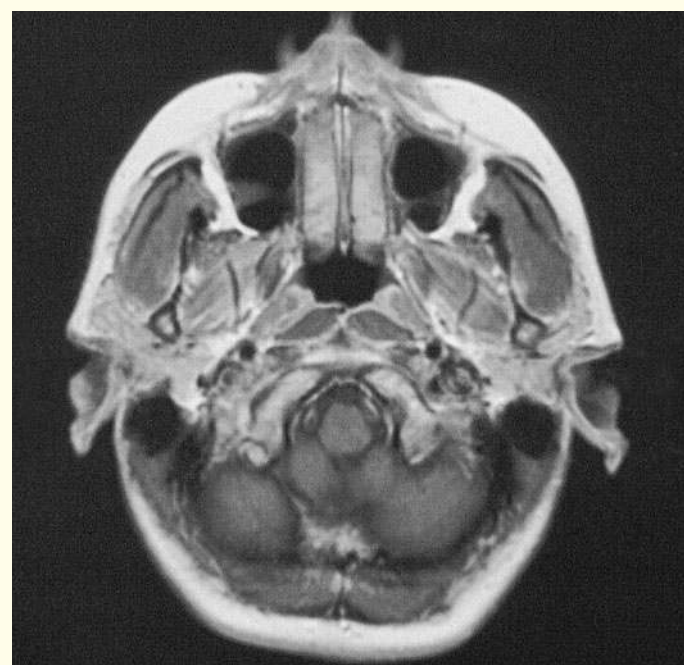
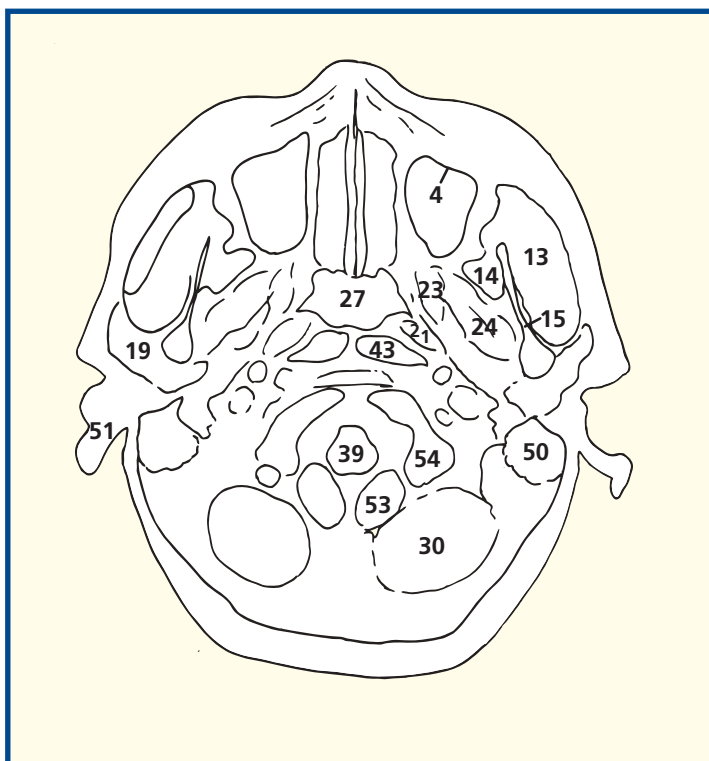
The floor of the maxillary sinus is formed by the alveolar process of the maxilla; several conical elevations, corresponding to the roots of the first and second molar teeth, project into the floor. An example of this is demonstrated here (4). Indeed, the floor is sometimes perforated by one or more of these molar roots.

This section gives a good view of the parotid duct (9) as it arches medially to penetrate the buccinator (11) and to enter the mouth at the level of the second upper molar tooth. The parotid duct is accompanied by a small, more or less detached, part of the gland that lies above the duct as it crosses the masseter; this is named the accessory part of the gland (12).

This section passes through the junctional zone between the falx cerebri, separating the occipital lobes of the brain (32), the falx cerebelli, separating the lobes of the cerebellum (30) and the tentorium cerebelli, which roofs the cerebellum. The straight sinus (31) is seen in section as it lies in the line of the junction of the falx cerebri and the tentorium cerebelli. The transverse sinus (37) lies in the attached margin of the tentorium cerebelli.

The facial nerve (48) (within the stylomastoid foramen) is demonstrated well in its immediate lateral relationship to the root of the styloid process (47).

Note that the orifice of the auditory tube (25) lies anterior to a depression – the pharyngeal recess (28). This helps to keep the orifice of the tube clear of secretions in the supine position.

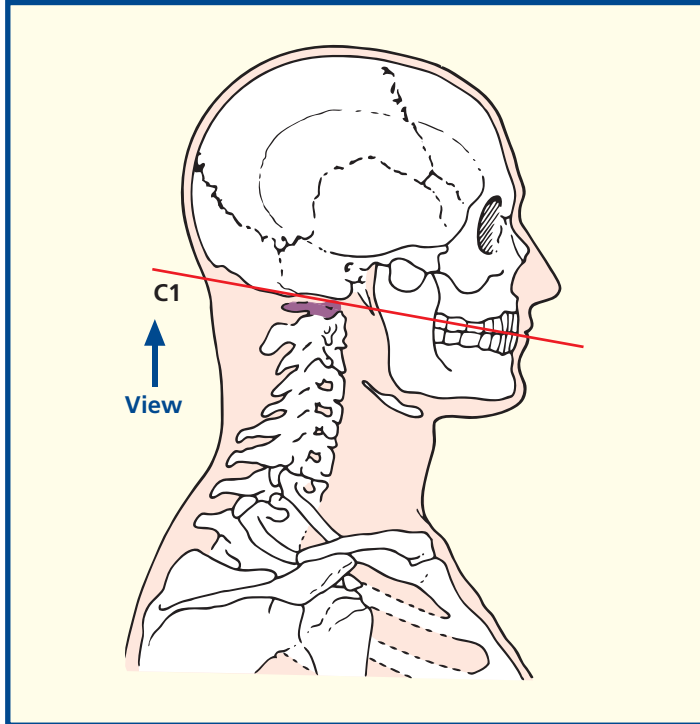


Axial magnetic resonance image (MRI)



- | | | | |
|----------------------------------------------------------------------------------------|----------------------------------------------------------------|-----------------------------------------------|-----------------------------------------------------|
| 1 Upper lip | 17 Anterior arch of atlas (first cervical vertebra) | 28 Atlanto-axial joint | 41 Internal jugular vein |
| 2 Orbicularis oris | 18 Longus capitis | 29 Sternocleidomastoid | 42 Accessory nerve (XI) and hypoglossal nerve (XII) |
| 3 Vestibule of mouth | 19 Lateral mass of atlas (first cervical vertebra) | 30 Mastoid air cells of temporal bone | 43 Vagus nerve (X) |
| 4 Alveolus | 20 Facial nerve (VII) | 31 Posterior belly of digastric | 44 Sympathetic chain |
| 5 Buccinator | 21 Roof of third part of vertebral artery | 32 Longissimus capitis | 45 Internal carotid artery |
| 6 Superior labial artery | 22 Rectus capitis lateralis | 33 Splenius capitis | 46 Glossopharyngeal nerve (IX) |
| 7 Facial artery and vein | 23 Atlanto-occipital joint | 34 Squamous part of occipital bone | 47 Superior constrictor muscle of pharynx |
| 8 Masseter | 24 Fourth part of vertebral artery | 35 Trapezius | 48 Styloid process |
| 9 Ramus of mandible | 25 Membrana tectoria | 36 Internal occipital crest of occipital bone | 49 External carotid artery |
| 10 Inferior alveolar artery vein and nerve (V ⁱⁱⁱ) within mandibular canal | 26 Superior longitudinal band of cruciform ligament | 37 Hemisphere of cerebellum | 50 Retromandibular vein at bifurcation |
| 11 Lingual nerve (V ⁱⁱⁱ) | 27 Dens of axis (odontoid process of second cervical vertebra) | 38 Tonsil of cerebellum | 51 Parotid gland |
| 12 Medial pterygoid | | 39 Spinal cord | |
| 13 Tensor veli palatini | | 40 Spinal root of accessory nerve | |
| 14 Soft palate | | | |
| 15 Nasopharynx | | | |
| 16 Anterior atlanto-occipital membrane | | | |

Section level



Notes

This section passes through the mouth at the level of the upper alveolus (4), the dens of the axis (27) at the articulation (28) with the anterior arch of the atlas (17) and posteriorly traverses the internal occipital crest of the occipital bone (36).

The radiographer obtains a clear anteroposterior view of the dens of the atlas (27) as it lies on the anterior arch of the axis (17) via the open mouth of the patient.

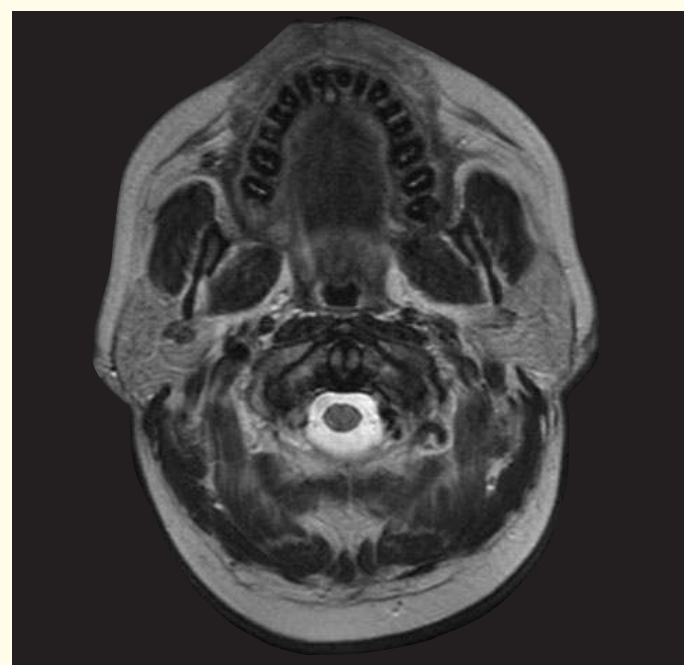
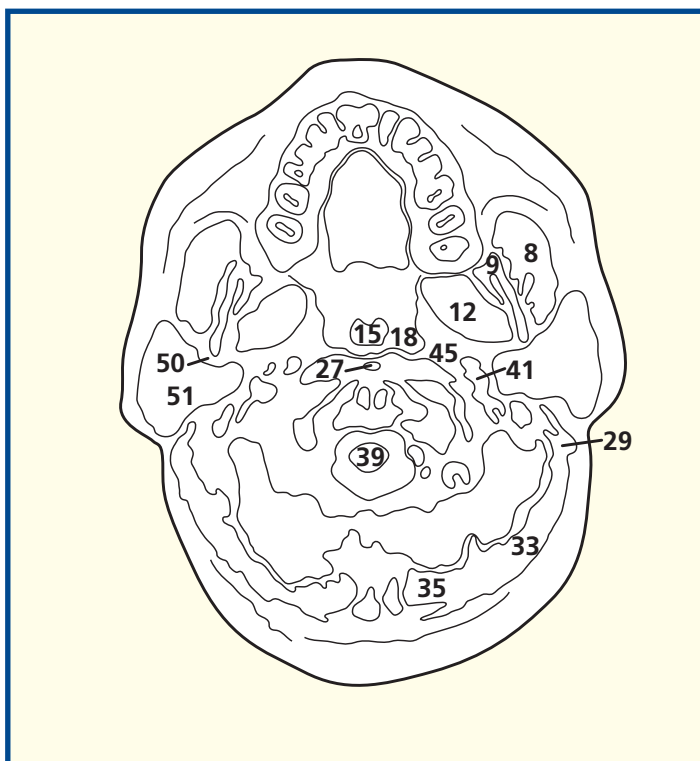
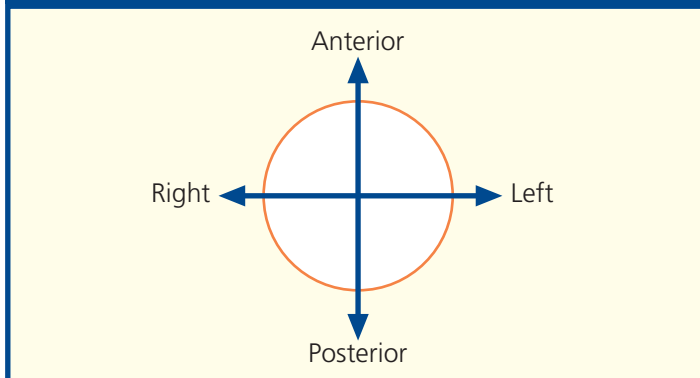
The third part of the vertebral artery (21) can be seen as it curves posterior to the lateral mass of the atlas (19) as it ascends to enter the vertebral canal by passing below the lower border of the posterior atlanto-occipital membrane. The fourth part (24) ascends anterior to the roots of the hypoglossal nerve.

Note how the last four cranial nerves (42, 43, 46) lie 'line astern' between the internal carotid artery (45) and the internal jugular vein (41) at the base of the skull.

The retromandibular vein (50) separates the parotid gland (51) into a superficial and deep lobe; it also demarcates the plane through which the facial nerve (20) and branches run.

The surgeon, in performing a subtotal superficial parotidectomy, establishes this plane, immediately superficial to the facial nerve.

Orientation

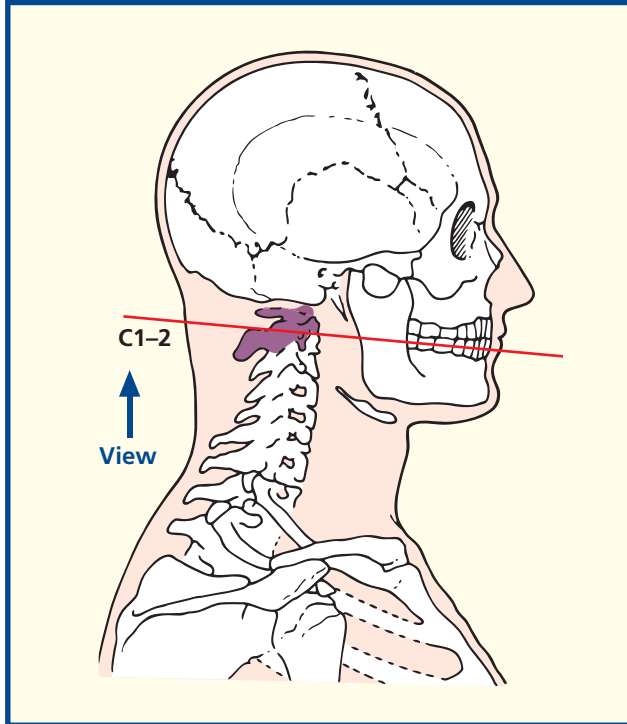


Axial magnetic resonance image (MRI)

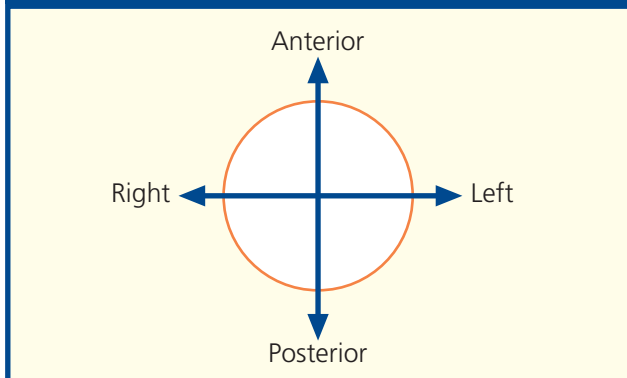


- | | | | |
|--------------------------------------------------------------------------------------------|----------------------------------------|------------------------------------------------------------|-------------------------------------------|
| 1 Orbicularis oris in lower lip | 14 Styloglossus | 30 Ligamentum nuchae | 42 Vagus nerve (X) |
| 2 Depressor anguli oris | 15 Medial pterygoid | 31 Obliquus capitis inferior | 43 Facial nerve (VII) |
| 3 Buccinator | 16 Masseter | 32 Posterior arch of atlas (first cervical vertebra) | 44 Parotid gland |
| 4 Anterior facial artery | 17 Internal carotid artery | 33 Occipital vein | 45 Glossopharyngeal nerve (IX) |
| 5 Mucosa of lower lip | 18 External carotid artery | 34 Spinal cord within dural sheath | 46 Palatopharyngeus |
| 6 Median raphe of tongue | 19 Stylohyoid | 35 Dorsal root ganglion of second cervical nerve | 47 Tonsillar fossa |
| 7 Intrinsic transverse muscle of tongue | 20 Posterior auricular artery and vein | 36 Anterior primary ramus of second cervical nerve | 48 Palatoglossus |
| 8 Intrinsic superior longitudinal muscle of tongue | 21 External jugular vein | 37 Vertebral artery and vein within foramen transversarium | 49 Longus capitis |
| 9 Facial vein | 22 Internal jugular vein | 38 Body of axis (second cervical vertebra) | 50 Longus colli |
| 10 Ramus of mandible | 23 Posterior belly of digastric | 39 Sympathetic chain | 51 Superior constrictor muscle of pharynx |
| 11 Inferior alveolar artery vein and nerve (V ⁱⁱⁱ) within the mandibular canal | 24 Sternocleidomastoid | 40 Accessory nerve (XI) | 52 Nasopharynx |
| 12 Mylohyoid | 25 Splenius capitis | 41 Hypoglossal nerve (XII) | 53 Uvula |
| 13 Lingual nerve (V ⁱⁱⁱ) | 26 Trapezius | | 54 Oropharynx |
| | 27 Semispinalis capitis | | |
| | 28 Rectus capitis posterior minor | | |
| | 29 Rectus capitis posterior major | | |
| | | | 55 Retromandibular vein |

Section level



Orientation



Notes

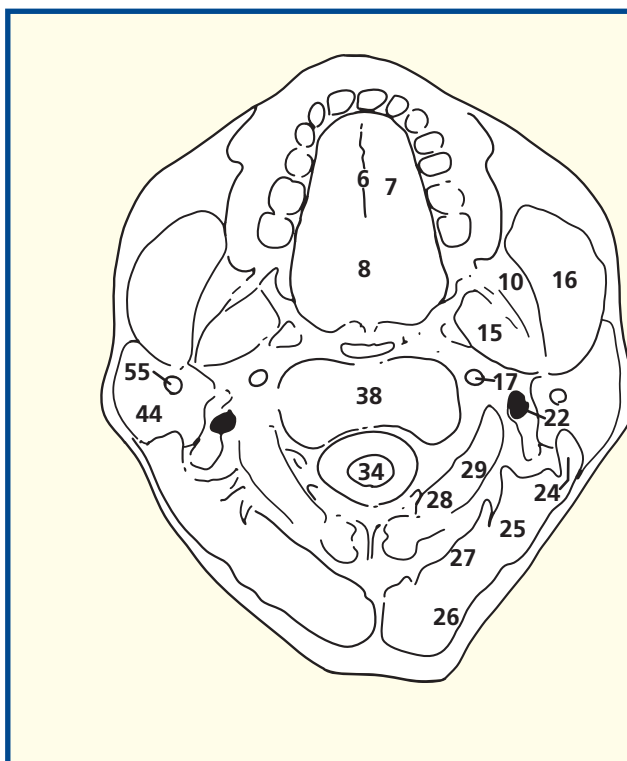
This section passes through the tongue (6) and the body of the axis, the second cervical vertebra (38).

This section gives a useful appreciation of the inferior alveolar nerve and its accompanying vessels within the mandibular canal (11). An inferior alveolar nerve block, performed by injecting local anaesthetic at a point immediately medial to the anterior border of the ramus of the mandible and approximately 1 cm above the occlusal surface of the third molar tooth, will provide anaesthesia of all the teeth in that hemi-mandible as far as, and including, the first incisor. The skin and mucosa of the lower lip will also become numb (the mental branch of the nerve), and there is loss of sensation over the side of the tongue due to involvement of the adjacent, anteriorly placed, lingual nerve (see Axial Section 13, page 34). Note also the vertebral artery in its second part, together with its accompanying vein, within the foramen transversarium (37). The further course of this artery, in its third and fourth parts, can be seen in Axial section 3.

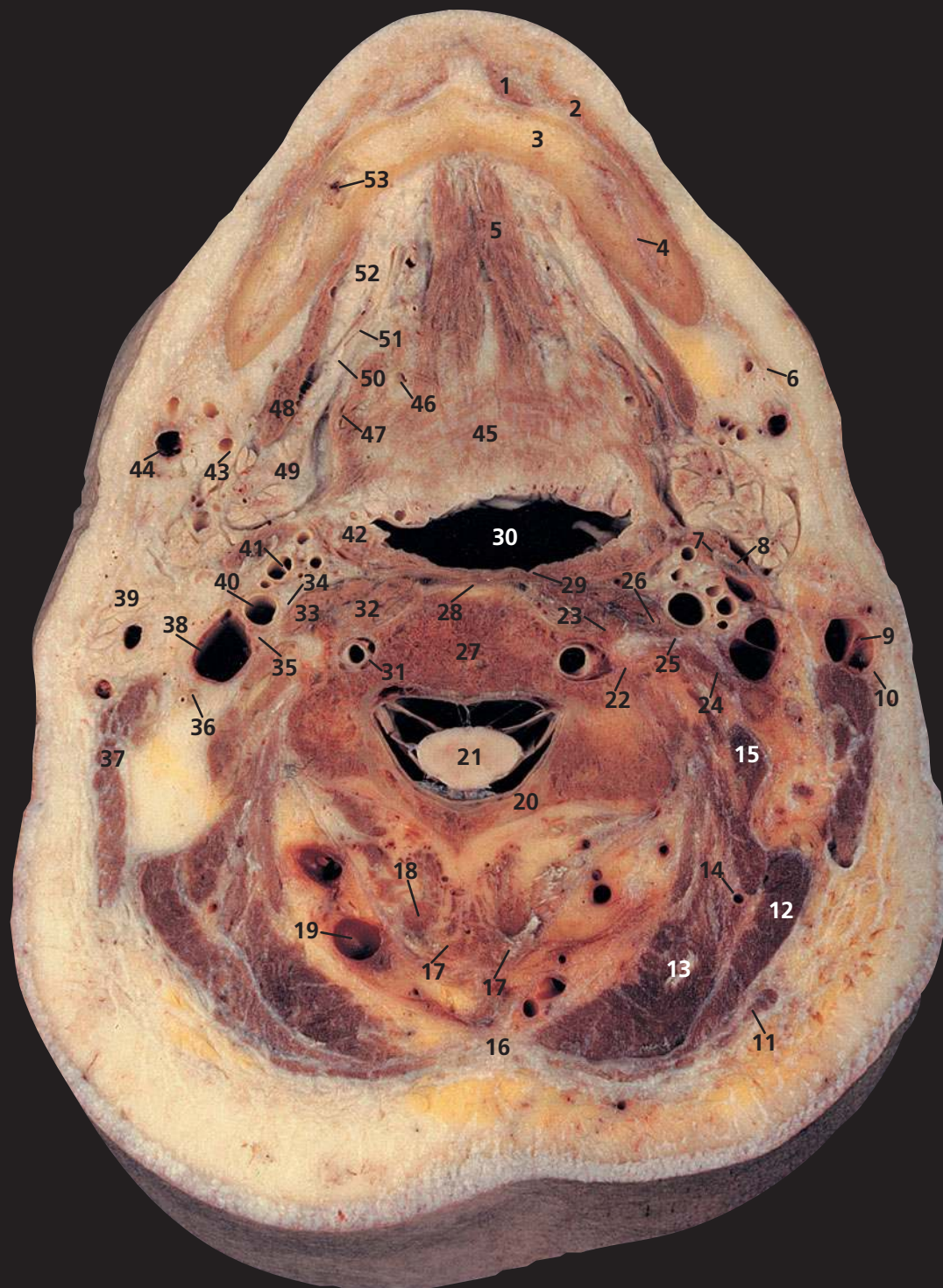
Note how close the posterior wall of the nasopharynx (52) lies to the body of the axis (38), and also to the anterior arch of the atlas in the previous section. The prevertebral space is thus normally very narrow on a lateral radiograph of the adult cervical spine (see Section 1, page 82).

This magnetic resonance image shows the parotid gland (44) very well. Note again how the retromandibular vein (55) separates the gland into superficial and deep portions.

The medial pterygoids are shown to good effect. The fat lying medially to these muscles in the parapharyngeal space shows up well on both MRI and CT imaging. Loss of this fat plane is an important sign when assessing the extent of tumours in this region.

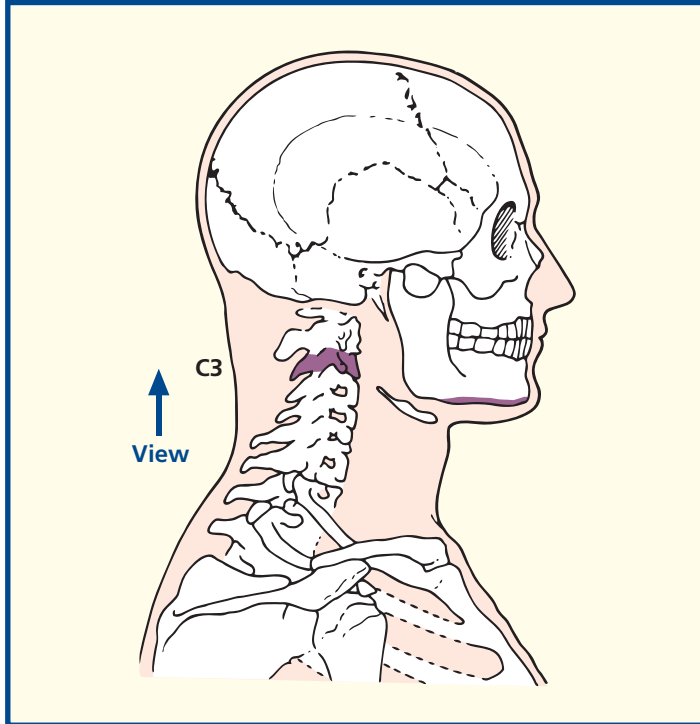


Axial magnetic resonance image (MRI)



- | | | | |
|-----------------------------------------------|------------------------------------------------------------------------|------------------------------------------------------------|---------------------------------------------------------------------|
| 1 Mentalis | 17 Bifid spine of third cervical vertebra | 27 Body of third cervical vertebra | 40 Internal carotid artery |
| 2 Orbicularis oris | 18 Semispinalis cervicis | 28 Anterior longitudinal ligament | 41 External carotid artery |
| 3 Mandible | 19 Occipital vein | 29 Superior constrictor muscle of pharynx | 42 Palatine tonsil |
| 4 Inferior alveolar nerve (V ⁱⁱⁱ) | 20 Lamina of third cervical vertebra | 30 Oropharynx | 43 Facial artery |
| 5 Genioglossus | 21 Spinal cord within dural sheath | 31 Vertebral artery and vein within foramen transversarium | 44 Facial vein |
| 6 Platysma | 22 Posterior tubercle of transverse process of third cervical vertebra | 32 Longus colli | 45 Intrinsic transverse muscle of tongue |
| 7 Posterior belly of digastric | 23 Anterior tubercle of transverse process of third cervical vertebra | 33 Longus capitis | 46 Lingual artery |
| 8 Stylohyoid ligament | 24 Scalenus medius | 34 Vagus nerve (X) | 47 Hyoglossus |
| 9 External jugular vein | 25 Anterior primary ramus of third cervical nerve | 35 Sympathetic chain | 48 Mylohyoid |
| 10 Great auricular nerve | 26 Scalenus anterior | 36 Accessory nerve (XI) | 49 Submandibular gland |
| 11 Trapezius | | 37 Sternocleidomastoid | 50 Lingual nerve (V ⁱⁱⁱ) |
| 12 Splenius | | 38 Internal jugular vein | 51 Submandibular duct |
| 13 Semispinalis capitis | | 39 Parotid gland | 52 Sublingual gland |
| 14 Occipital artery | | | 53 Inferior alveolar artery, vein and nerve within mandibular canal |
| 15 Levator scapulae | | | |
| 16 Ligamentum nuchae | | | |

Section level



Notes

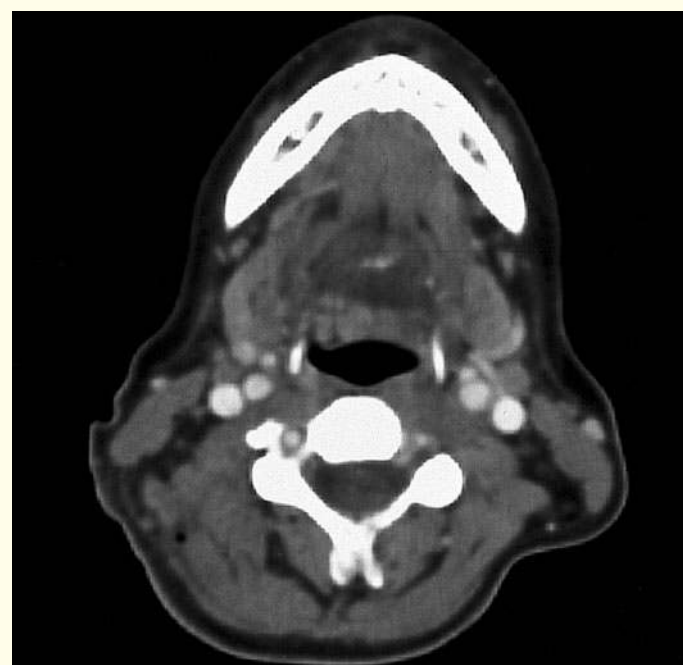
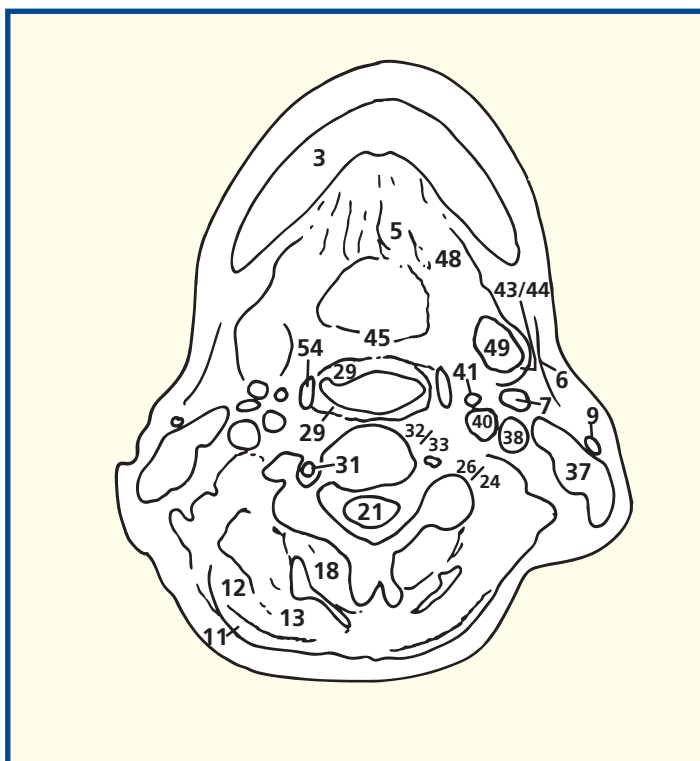
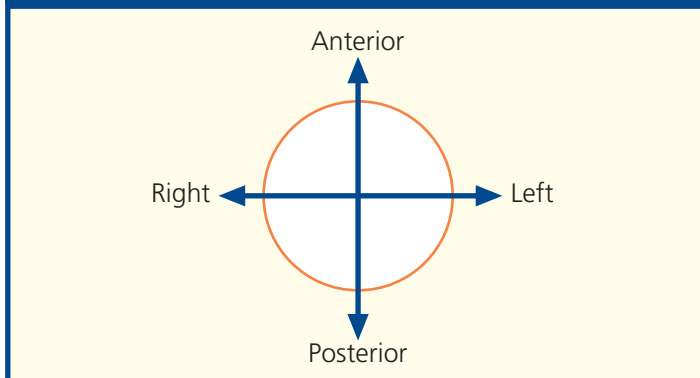
This section passes through the lower border of the body of the mandible (3), the oropharynx (30) and the third cervical vertebra (27).

It demonstrates how the parotid gland (39) projects deeply towards the side wall of the oropharynx (30). Indeed, a tumour of the deep portion of the gland may project into the tonsillar fossa and bulge the palatine tonsil (42) medially. An aneurysm of the internal carotid artery (40) similarly bulges into the tonsillar fossa medially and will give the unusual sign of visible pulsation of the palatine tonsil.

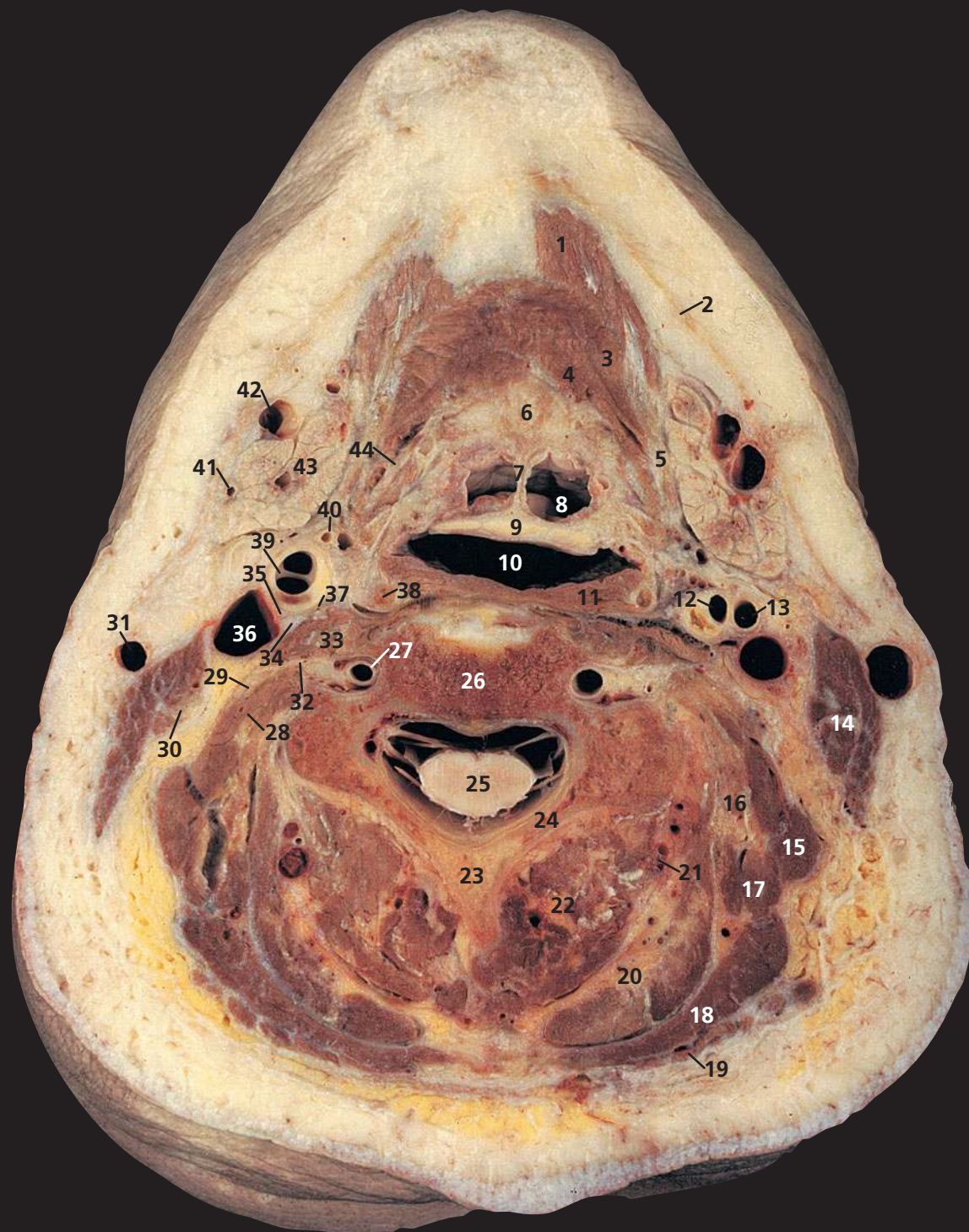
The vertebral vein (31) is smaller than the artery. Quite often it lies in its own compartment of the foramen transversarium. Sympathetic fibres from the superior cervical ganglion (C1,2,3,4) are conveyed as a plexus along the vertebral artery.

Genioglossus (5) is a triangular muscle placed close to, and parallel with, the median plane. It arises from the upper genial tubercle on the inner surface of the symphysis of the mandible (3) and spreads out in a fan-like form to enter the whole undersurface of the tongue from its root to its apex. It has the unique action of protruding the tongue, and this is used in the clinical testing of paralysis of the hypoglossal nerve (XII) (see Axial section 3, page 86).

Orientation

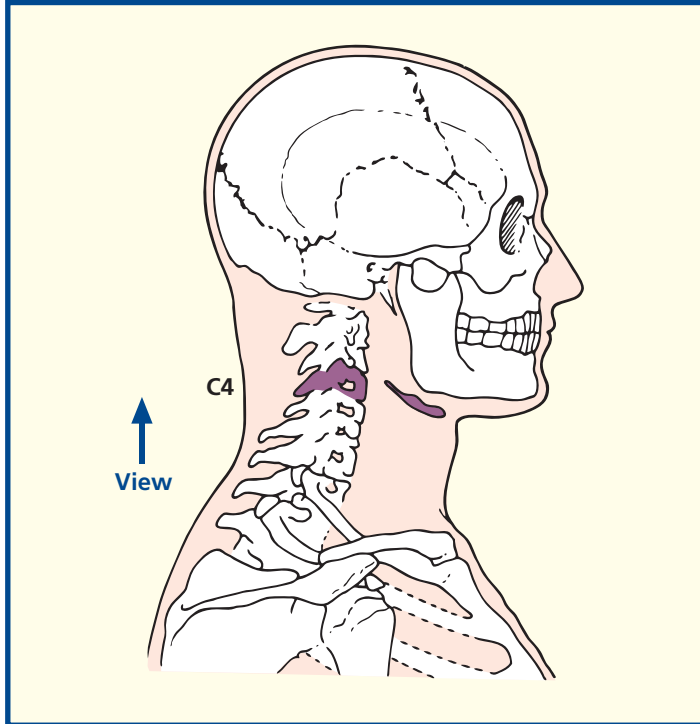


Axial computed tomogram (CT)



- | | | | |
|-----------------------------------------|---------------------------------------|------------------------------------------------------------|-----------------------------------------------|
| 1 Anterior belly of digastric | 14 Sternocleidomastoid | 26 Body of fourth cervical vertebra | 38 Hyoid |
| 2 Platysma | 15 Levator scapulae | 27 Vertebral artery and vein within foramen transversarium | 39 Right common carotid artery at bifurcation |
| 3 Mylohyoid | 16 Longissimus capitis and cervicis | 28 Scalenus medius | 40 Superior thyroid artery |
| 4 Hyoglossus | 17 Splenius cervicis | 29 Anterior primary ramus of third cervical nerve | 41 Facial artery |
| 5 Tendon of digastric | 18 Splenius capitis | 30 Accessory nerve (XI) | 42 Facial vein |
| 6 Base of tongue | 19 Trapezius | 31 External jugular vein | 43 Submandibular salivary gland |
| 7 Glosso-epiglottic fold | 20 Semispinalis capitis | 32 Anterior primary ramus fourth cervical nerve | 44 Lingual artery |
| 8 Vallecula | 21 Deep cervical artery and vein | 33 Scalenus anterior | |
| 9 Epiglottis | 22 Semispinalis cervicis | 34 Phrenic nerve | |
| 10 Laryngopharynx | 23 Spine of fourth cervical vertebra | 35 Vagus nerve (X) | |
| 11 Middle constrictor muscle of pharynx | 24 Lamina of fourth cervical vertebra | 36 Internal jugular vein | |
| 12 Left internal carotid artery | 25 Spinal cord within dural sheath | 37 Sympathetic chain | |
| 13 Left external carotid artery | | | |
| | | | 45 Mandible |
| | | | 46 Common carotid artery |
| | | | 47 Pre-epiglottic space |
| | | | 48 Superior cornu of thyroid cartilage |
| | | | 49 Aryepiglottic fold |
| | | | 50 Piriform fossa |

Section level



Notes

This section passes through the body of the fourth cervical vertebra (26), just shaving the inferior margin of the hyoid bone (38).

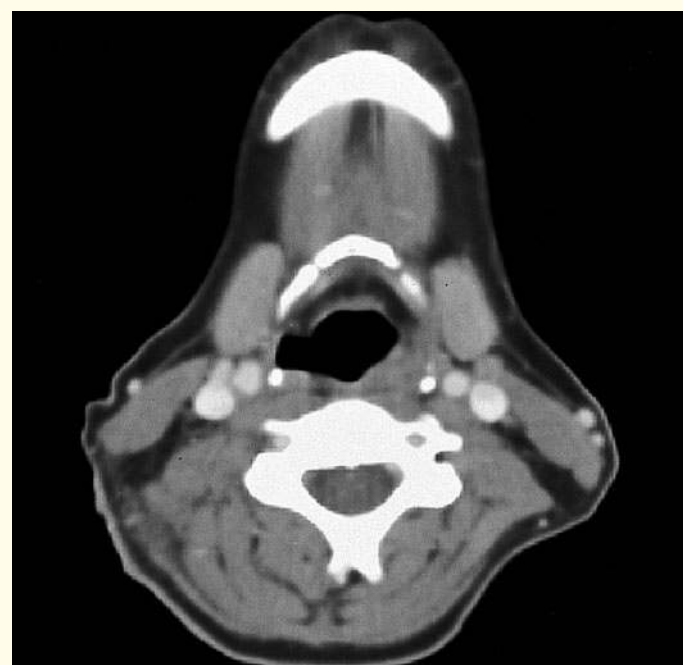
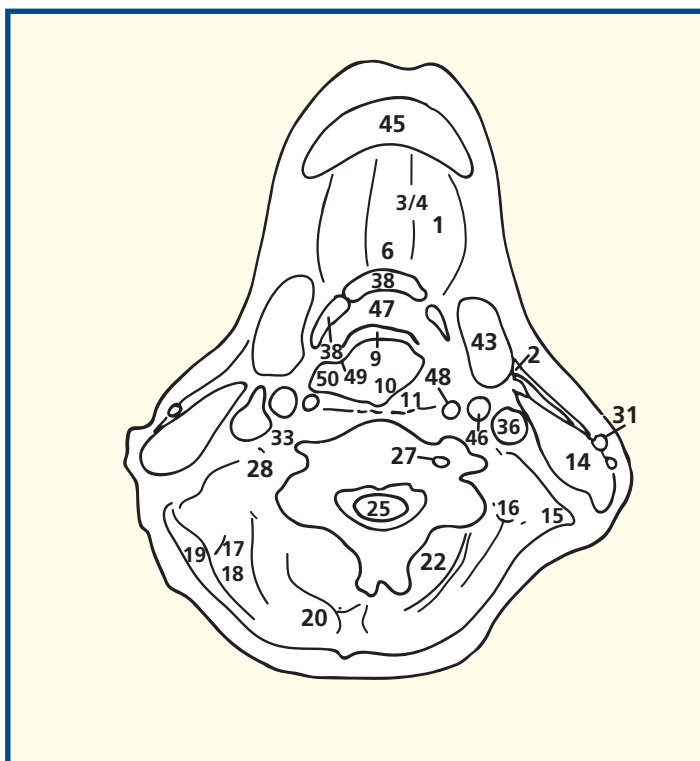
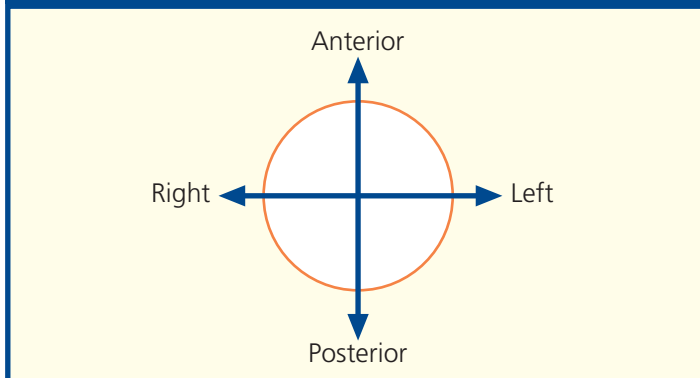
The fourth cervical vertebra marks the level of bifurcation of the common carotid artery. On the right side this is just occurring (39), and on the left it has already taken place (12, 13). Note the marked atheromatous thickening of the internal carotid artery. On the CT image the plane passes through the common carotid arteries.

The external jugular vein (31) is the only structure of prominence lying in the superficial fascia of the posterior triangle of the neck. Immediately above the clavicle it pierces the deep fascia to enter the subclavian vein, as the only tributary of this vessel. Occasionally it is double (see 39, Thorax, Axial section 1, page 102).

The way in which the lingual artery (44) passes deep to the hyoglossus muscle (4) to supply the tongue is demonstrated. On CT imaging, precise definition of the various intrinsic muscles of the tongue is difficult unless the fat planes are very pronounced.

The precise shape of the laryngopharynx (10), and indeed the whole airway system of the head and neck, depends on the phase of respiration, phonation etc. In practice, gentle inspiration is the most appropriate phase for routine CT imaging, but attempts at phonation and the Valsalva manoeuvre may be helpful.

Orientation

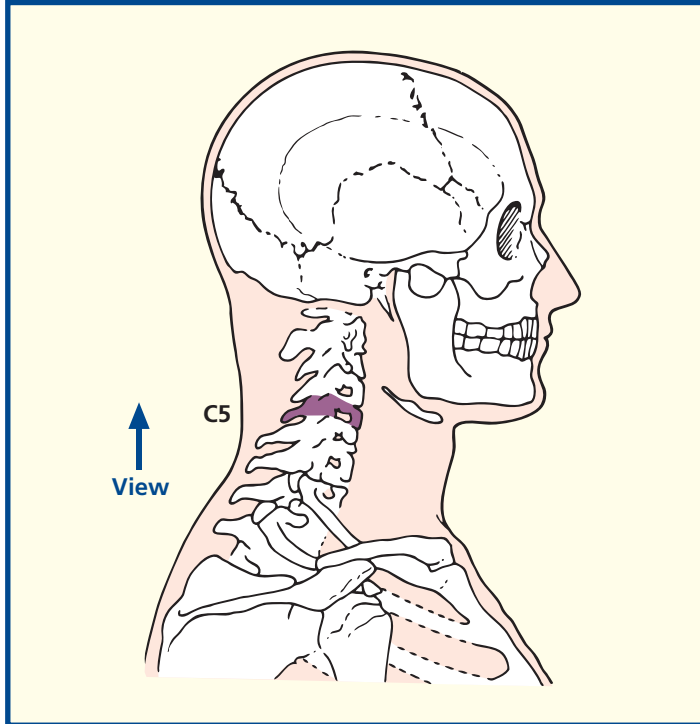


Axial computed tomogram (CT)



- | | | | |
|-------------------------------------------|------------------------------------------------------------|--------------------------------------|-----------------------------------------|
| 1 Sternohyoid | 15 External jugular vein | 28 Semispinalis capitis | 41 Sympathetic chain |
| 2 Omohyoid | 16 Sternocleidomastoid | 29 Erector spinae | 42 Scalenus anterior |
| 3 Thyrohyoid | 17 Internal jugular vein | 30 Spine of fifth cervical vertebra | 43 Phrenic nerve |
| 4 Lamina of thyroid cartilage | 18 Common carotid artery | 31 Lamina of fifth cervical vertebra | 44 Submandibular salivary gland |
| 5 Laryngopharynx | 19 Vagus nerve (X) | 32 Spinal cord within dural sheath | 45 Anterior jugular vein |
| 6 Corniculate cartilage | 20 Prevertebral fascia | 33 Ligamentum denticulatum | |
| 7 Vestibule of larynx | 21 Anterior tubercle of fifth cervical vertebra | 34 Trapezius | 46 Inferior horn of thyroid cartilage |
| 8 Epiglottis | 22 Ventral ramus of fifth cervical nerve | 35 Levator scapulae | 47 Arytenoid cartilage |
| 9 Pre-epiglottic space (fat filled) | 23 Posterior tubercle of fifth cervical vertebra | 36 Deep cervical artery and vein | 48 Cricoid cartilage |
| 10 Inferior constrictor muscle of pharynx | 24 Vertebral artery and vein within foramen transversarium | 37 Scalenus medius | 49 Vocal fold |
| 11 Platysma | 25 Accessory nerve (XI) | 38 Body of fifth cervical vertebra | 50 Anterior border of thyroid cartilage |
| 12 Investing fascia of neck | 26 Splenius cervicis | 39 Longus colli | |
| 13 Superior thyroid artery and vein | 27 Splenius capitis | 40 Longus capitis | |
| 14 Common facial vein | | | |

Section level



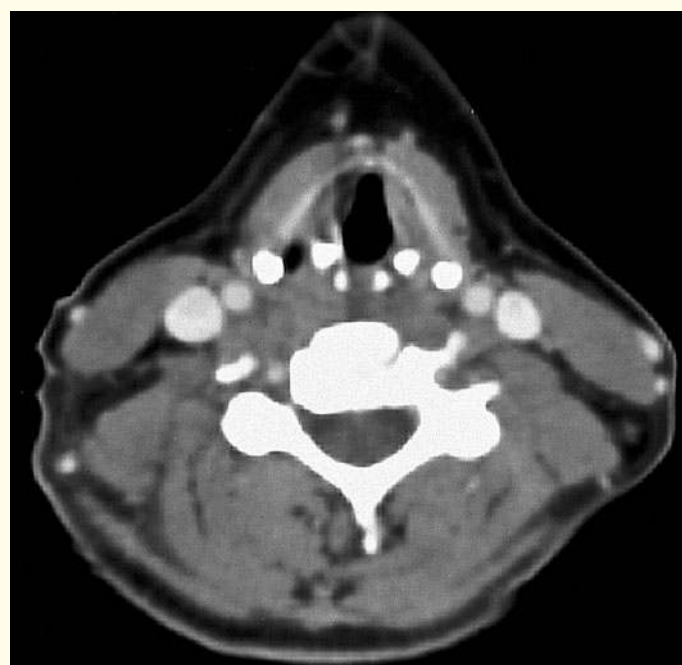
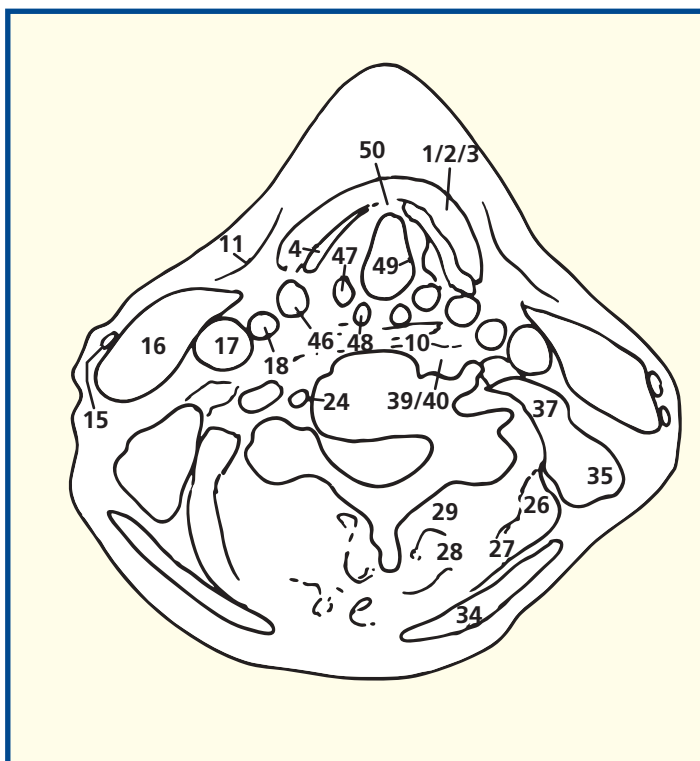
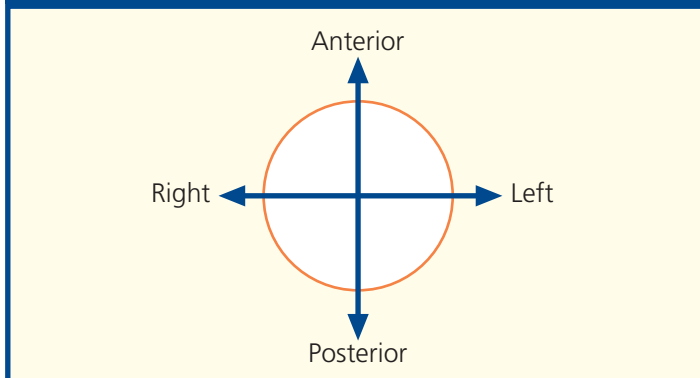
Notes

This section passes through the body of the fifth cervical vertebra (38) and the lamina of the thyroid cartilage (4).

The attachment of the stem of the cartilage of the epiglottis (8) to the angle formed by the two laminae of the thyroid cartilage (4) is demonstrated at this level. Apart from the apices of the arytenoids, the epiglottis (8) is the only laryngeal cartilage made of yellow elastic cartilage. On either side of the epiglottis can be seen the groove of the vallecula. In deglutition, the epiglottis acts like a stone jutting into a waterfall: it deviates the food bolus to pass either side along the vallecula, thus keeping it away from the laryngeal orifice. The vallecula is a common site for impaction of a sharp swallowed object, such as a fish bone.

This section gives an excellent demonstration of the ligamentum denticulatum (33). This is a narrow fibrous sheet situated on each side of the spinal cord. Its medial border is continuous with the pia mater at the side of the spinal cord, while its lateral border presents a series of triangular tooth-like processes whose points are fixed at intervals to the dura mater. There are 21 such processes on each side; the last lies between the exits of the twelfth thoracic and first lumbar nerves.

Orientation



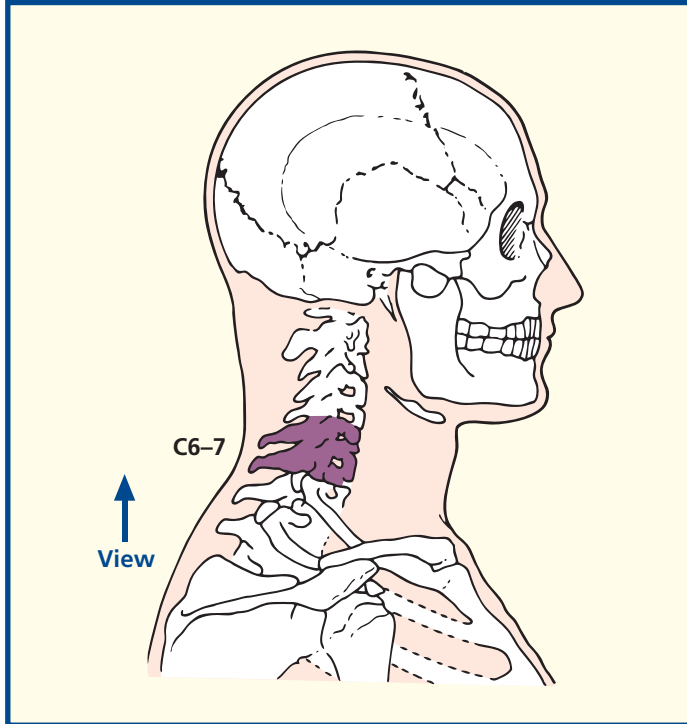
Axial computed tomogram (CT)



- | | | | |
|------------------------------------------|---------------------------------------------------|--------------------------------------------------------|------------------------------------------------------------|
| 1 Anterior border of thyroid cartilage | 15 Anterior jugular vein | 31 Splenius capitis | and seventh cervical vertebrae |
| 2 Vocal fold | 16 Sternohyoid | 32 Semispinalis | |
| 3 Lateral cricoarytenoid | 17 Sternocleidomastoid | 33 Ligamentum nuchae | |
| 4 Lamina of thyroid cartilage | 18 External jugular vein | 34 Tip of spinous process of seventh cervical vertebra | 42 Superior articular facet of seventh cervical vertebra |
| 5 Cricothyroid | 19 Phrenic nerve | 35 Erector spinae | 43 Vertebral artery and vein within foramen transversarium |
| 6 Lateral lobe of thyroid gland | 20 Scalenus anterior | 36 Lamina of sixth cervical vertebra | 44 Prevertebral fascia |
| 7 Superior thyroid artery and vein | 21 Ventral ramus of fifth cervical nerve | 37 Spinal cord within dural sheath | 45 Sympathetic trunk |
| 8 Laryngopharynx | 22 Scalenus medius | 38 Dorsal nerve root of seventh cervical nerve | 46 Vagus nerve (X) |
| 9 Inferior constrictor muscle of pharynx | 23 Ventral ramus of sixth cervical nerve | 39 Ventral nerve root of seventh cervical nerve | 47 Common carotid artery |
| 10 Posterior cricoarytenoid | 24 Longus capitis | 40 Inferior articular facet of sixth cervical vertebra | 48 Internal jugular vein |
| 11 Cricoid cartilage | 25 Longus colli | 41 Interarticular facet joint between sixth | 49 Accessory nerve (XI) |
| 12 Inferior cornu of thyroid cartilage | 26 Body of sixth cervical vertebra | | 50 Platysma |
| 13 Sternothyroid | 27 Dorsal root ganglion of seventh cervical nerve | | |
| 14 Omohyoid | 28 Splenius cervicis | | |
| | 29 Levator scapulae | | |
| | 30 Trapezius | | |

51 Outline of subglottic space

Section level



Notes

This section passes through the body of the sixth cervical vertebra (26) and traverses the cricoid cartilage (11). The cricoid is the only complete ring of cartilage throughout the respiratory system, but the plane of this section is above the narrow arch of the cricoid and only passes through its posterior lamina.

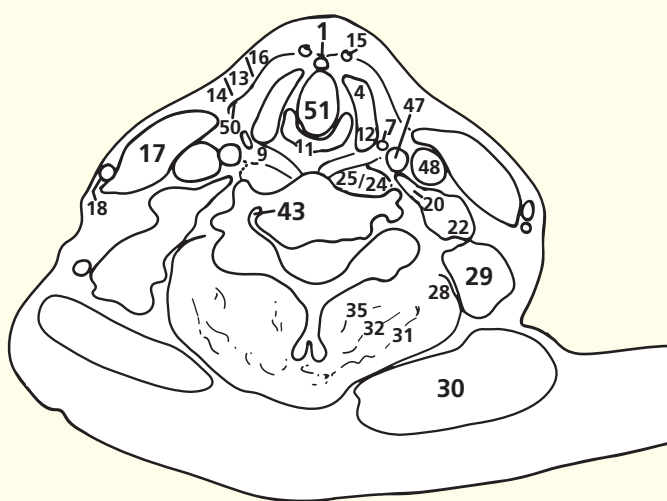
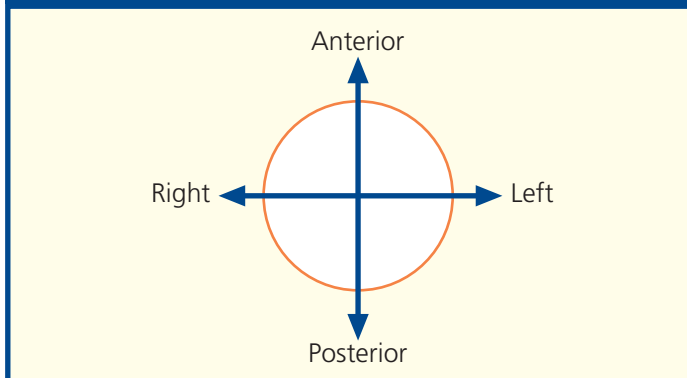
This section, together with the following section, provides a good appreciation of the relationships of the lateral lobe of the thyroid gland (6). Here, it is seen to be overlapped superficially by the strap muscles – the sternohyoid (16), omohyoid (14) and, on a deeper plane, the sternothyroid (13). Medially it lies against the larynx and laryngopharynx (8), and posteriorly it lies against the common carotid artery (47) and internal jugular vein (48). (See also CT image in Axial section 9.)

Note the demonstration of the relationship of the phrenic nerve (19) to the anterior aspect of scalenus anterior (20). The nerve is bound down to the underlying muscle by the overlying prevertebral fascia (44). Scalenus anterior (20) is thus an important landmark muscle to the surgeon. It sandwiches the subclavian artery and the brachial plexus roots between it and scalenus medius (22) and defines the phrenic nerve (19) on its anterior surface.

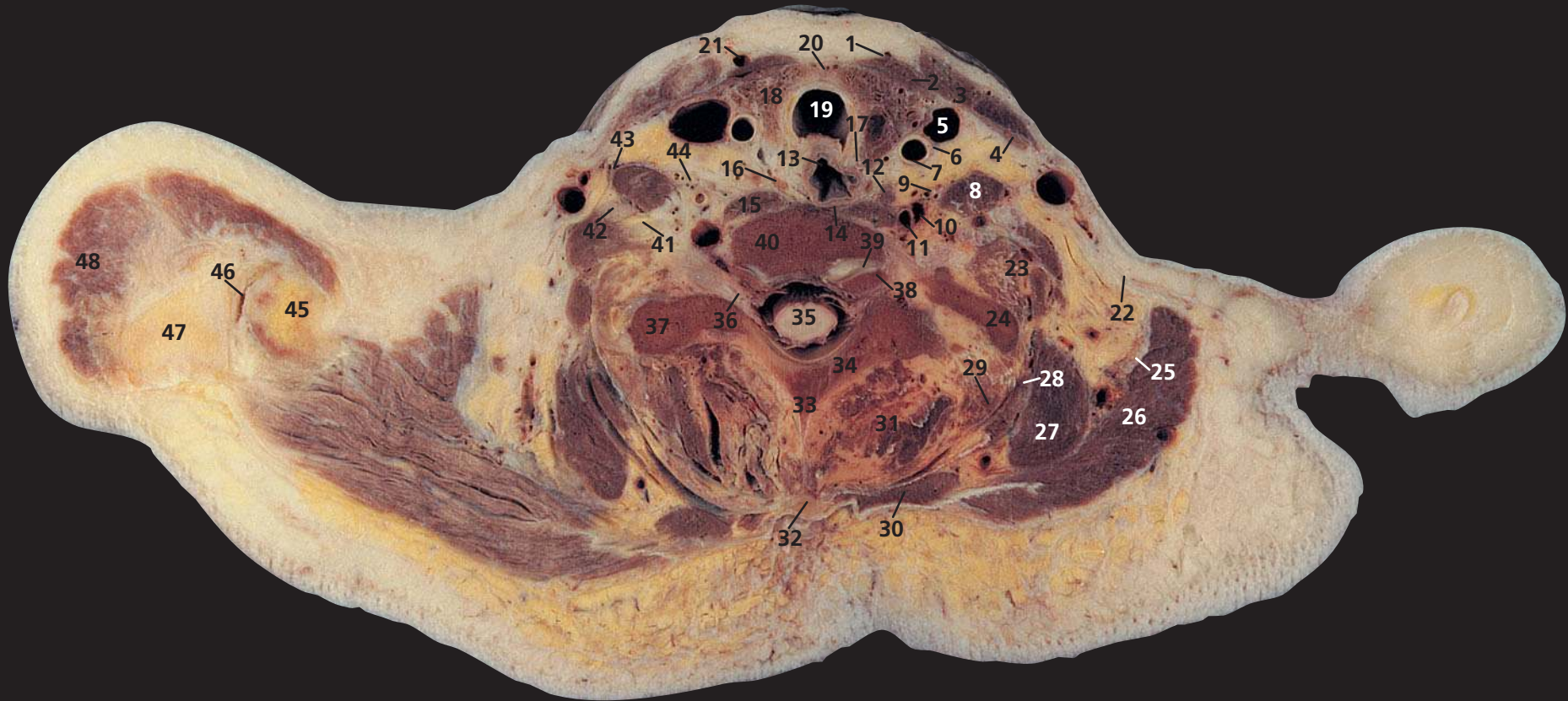
The ventral rami (21, 23) of C5 and C6, together with C7, C8 and T1, form the brachial plexus; those of C1–4 form the cervical plexus.

The inferior surfaces of the vocal folds (2) can be seen within the larynx (see CT image in Axial section 7). The vestibular folds (false cords), which lie cranial to the vestibule of the larynx, are situated more cranially to this section.

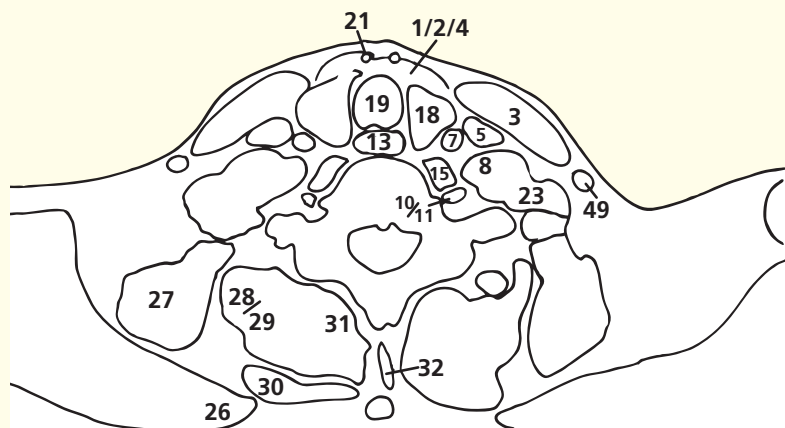
Orientation



Axial computed tomogram (CT)

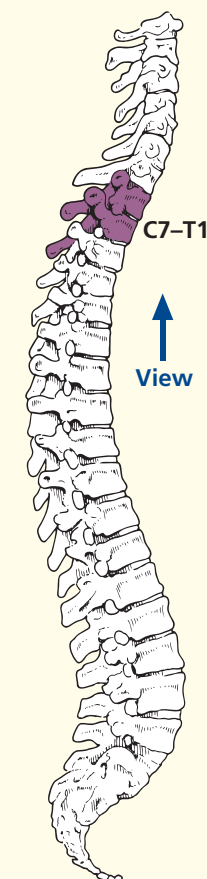


- | | | | |
|-----------------------------|----------------------------------------|----------------------------------------------------------------------------------|--------------------------------------------|
| 1 Sternohyoid | 16 Parathyroid gland | 31 Erector spinae | 40 Body of seventh cervical vertebra |
| 2 Sternothyroid | 17 Recurrent laryngeal nerve | 32 Ligamentum nuchae | 41 Ventral ramus of seventh cervical nerve |
| 3 Sternocleidomastoid | 18 Lateral lobe of thyroid gland | 33 Spinous process of first thoracic vertebra | 42 Ventral ramus of sixth cervical nerve |
| 4 Omohyoid | 19 Trachea | 34 Lamina of first thoracic vertebra | 43 Phrenic nerve |
| 5 Internal jugular vein | 20 Isthmus of thyroid gland | 35 Spinal cord within dural sheath | 44 Cervical sympathetic chain |
| 6 Vagus nerve (X) | 21 Anterior jugular vein | 36 Dorsal root ganglion of eighth cervical nerve | 45 Clavicle |
| 7 Common carotid artery | 22 Investing (deep) fascia of the neck | 37 Transverse process of first thoracic vertebra | 46 Acromioclavicular joint |
| 8 Scalenus anterior | 23 Scalenus medius and posterior | 38 Part of body of first thoracic vertebra | 47 Acromion |
| 9 Inferior thyroid artery | 24 Left first rib | 39 Uncovertebral synovial joint between lip of T1 body and inferior aspect of C7 | 48 Deltoid |
| 10 Vertebral vein | 25 Accessory nerve (XI) | | |
| 11 Vertebral artery | 26 Trapezius | | |
| 12 Deep cervical lymph node | 27 Levator scapulae | | |
| 13 Oesophagus | 28 Splenius | | |
| 14 Prevertebral fascia | 29 Semispinalis | | |
| 15 Longus colli | 30 Rhomboideus minor | | |
| | | | 49 External jugular vein |



Axial computed tomogram (CT)

Section level



Notes

This section passes through the body of the seventh cervical vertebra (40) and through the tip of the shoulder, so that a sliver of the clavicle (45) and adjacent acromioclavicular joint (46) are shown.

Taken in conjunction with the previous section, the relationships of the lateral lobe of the thyroid gland (18) are demonstrated. In this section, it is overlapped by the strap muscles (1, 2, 4) and sternocleidomastoid (3). Medially it lies against the trachea (19) and oesophagus (13), while posteriorly it rests against the common carotid artery (7) and internal jugular vein (5). The inferior thyroid artery (9) passes transversely behind the common carotid artery to reach the thyroid gland. Note also the important posterior relationship of the lobe of the thyroid gland to the recurrent laryngeal nerve (17), lying in the tracheo-oesophageal groove.

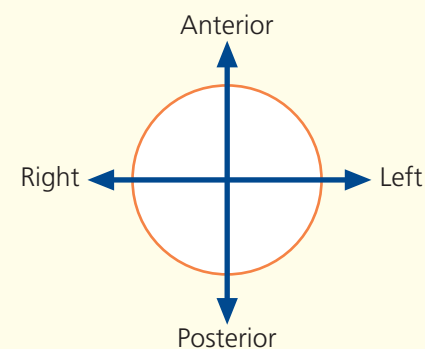
The parathyroid glands (16) are usually four in number but vary from two to six. The superior glands are fairly constant in position, at the middle of the posterior border of the

thyroid lobe above the level at which the inferior thyroid artery crosses the recurrent laryngeal nerve. The inferior glands are most usually situated near the lower pole of the thyroid gland below the inferior thyroid artery, but aberrant glands may be found in front of the trachea, behind the oesophagus, buried in the thyroid gland or descended into the superior mediastinum in company with thymic tissue.

On the CT image, the vertebral artery (11) is seen as it passes towards the gap between the foramina transversarium of the sixth and seventh cervical vertebrae.

The bodies of the cervical vertebrae and the superior aspect of T1 have raised lips (uncinate processes) on each lateral margin of their superior surfaces. These processes enclose the intervertebral disc and articulate (39) with the inferior aspect of the adjacent vertebral body; they are prone to degenerative disease, which can lead to neurological problems.

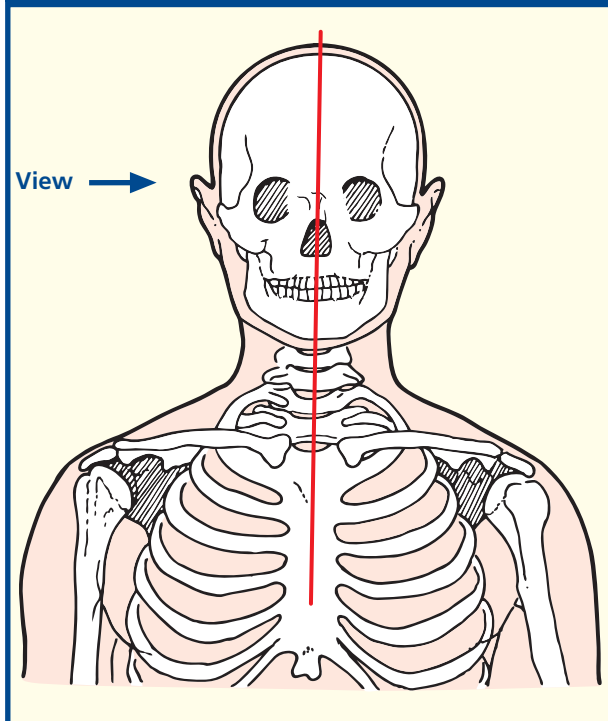
Orientation



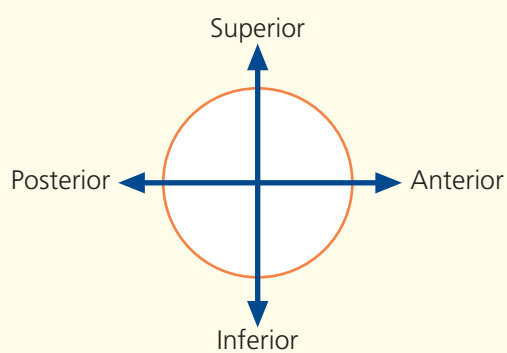


- | | | | |
|-----------------------------------------------------------|--------------------------------------|--------------------------------|---------------------------------------|
| 1 Pons | 11 External occipital protuberance | 29 Geniohyoid | 46 Second tracheal ring |
| 2 Basilar artery | 12 Occipital bone | 30 Mylohyoid | 47 Trachea |
| 3 Clivus (basi-occipital and basi-sphenoid bones) | 13 Transverse sinus | 31 Body of hyoid bone | 48 Oesophagus |
| 4 Anterior margin of foramen magnum | 14 Straight sinus | 32 Vallecula | 49 Superior lobe of left lung |
| 5 Anterior arch of atlas (first cervical vertebra) | 15 Tentorium cerebelli | 33 Epiglottis | 50 Brachiocephalic trunk |
| 6 Dens of axis (odontoid peg of second cervical vertebra) | 16 Cerebellum | 34 Laryngeal part of pharynx | 51 Brachiocephalic vein |
| 7 Nasal part of pharynx (nasopharynx) | 17 Fourth ventricle | 35 Vestibular fold | 52 Manubrium of sternum |
| 8 Oral part of pharynx (oropharynx) | 18 Cisterna magna | 36 Ventricle of larynx | 53 Anterior jugular vein |
| 9 Posterior arch of atlas (first cervical vertebra) | 19 Medulla oblongata | 37 Vocal fold (vocal cord) | 54 Posterior cricoarytenoid |
| 10 Posterior margin of foramen magnum | 20 Uvula | 38 Platysma | 55 Arytenoid cartilage |
| | 21 Soft palate | 39 Lamina of thyroid cartilage | 56 Body of third cervical vertebra |
| | 22 Hard palate | 40 Sternohyoid | 57 Spinal cord |
| | 23 Central incisor (upper and lower) | 41 Sternothyroid | 58 Spinous process of second vertebra |
| | 24 Lip (upper and lower) | 42 Isthmus of thyroid gland | 59 Semispinalis capitis |
| | 25 Body of mandible | 43 Lamina of cricoid cartilage | 60 Trapezius |
| | 26 Sublingual gland | 44 Arch of cricoid cartilage | 61 Semispinalis cervicis |
| | 27 Dorsum of tongue | 45 Lower part of larynx | 62 Occipital lobe of brain |
| | 28 Genioglossus | | |

Section level



Orientation



Notes

The nasal septum has been removed from this section in order to display the nasal conchae on the lateral wall.

Cricothyroid puncture is performed between the thyroid cartilage (39) and the isthmus of the cricoid cartilage (44). Note that a tube inserted at this site will lie below the vocal folds (37), which are therefore free of danger.

Note that the junction of the larynx and trachea (46) lies at the level of the sixth cervical vertebra. This level also marks the junction of the pharynx (34) and the oesophagus (48).

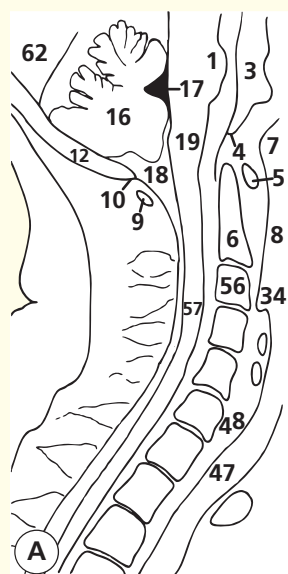
These midline sagittal magnetic resonance images – (A) T1-weighted and (B) T2-weighted – demonstrate clearly the normal relationship of the pons, medulla and cervical spinal cord to the base of the skull, foramen magnum, dens of the axis (odontoid peg) and cervical canal. The anterior and posterior margins of the foramen magnum, the tip of the basi-occipital part of the clivus and the anterior margin of the occipital bone can be well appreciated.

Note the size of the cervical cord in relation to the spinal canal compared with the ratio more caudally; of course, the cervical canal carries many more white matter fibres. On T2 weighting (image B), there is only a relatively small amount of cerebrospinal fluid surrounding the cord; hence, the diameter of the spinal canal in this region is of key importance. If the canal is too narrow, then the inevitable degenerative changes of middle/old age that occur in the vertebral column can affect nerve roots supplying the arms (brachialgia) or even affect the cord to cause upper motor neurone signs.

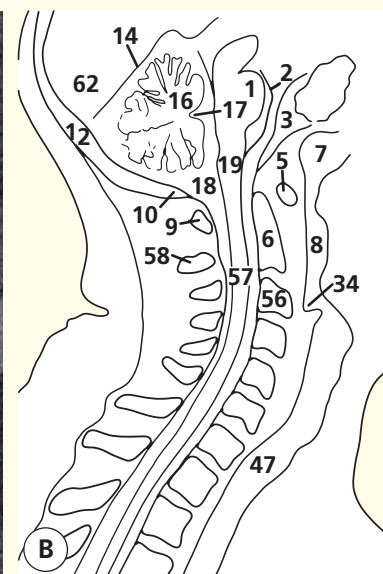
The relationship of the anterior arch of the atlas (first cervical vertebra) to the dens (odontoid peg) of the axis (the body of the first cervical vertebra assimilated on to the body of the second cervical vertebra – the axis) is shown well. This pivot synovial joint allows rotation of the head and C1 on C2 and the rest of the spinal column.



Sagittal magnetic resonance image (MRI)

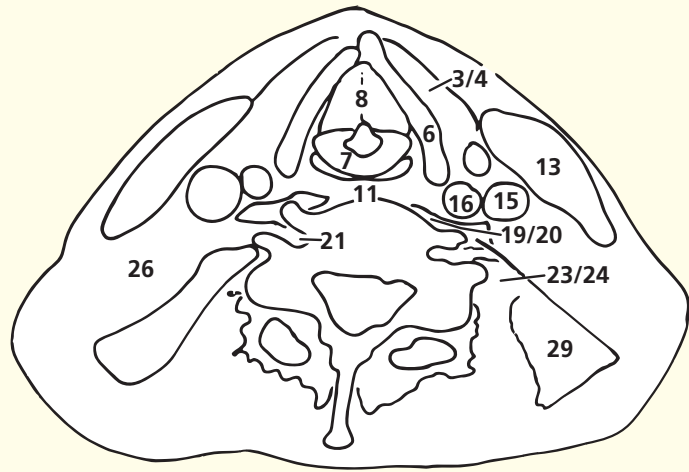


Sagittal magnetic resonance image (MRI)



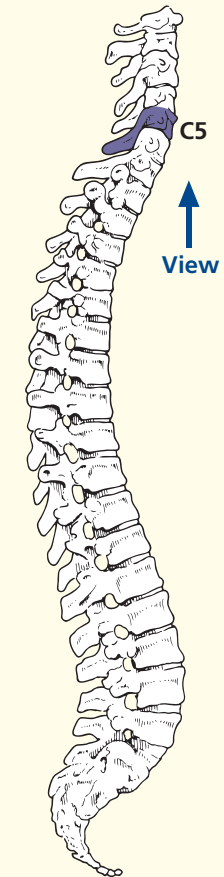


- | | | | | |
|-------------------------|-------------------------------------------|----------------------------------|-------------------------------------|------------------------------------------|
| 1 Platysma | 12 Inferior constrictor muscle of pharynx | 22 Phrenic nerve | 30 Splenius | uncovertebral synovial joint (of Lushka) |
| 2 Anterior jugular vein | 13 Sternocleidomastoid | 23 Scalenus anterior | 31 Ligamentum nuchae | 38 Lateral lobe of thyroid gland |
| 3 Sternohyoid | 14 Common facial vein | 24 Scalenus medius and posterior | 32 Spine of fifth cervical vertebra | 39 Accessory anterior jugular vein |
| 4 Omohyoid | 15 Internal jugular vein | 25 External jugular vein | 33 Erector spinae | 40 Lymph node of internal jugular chain |
| 5 Sternothyroid | 16 Common carotid artery | 26 Fat of posterior triangle | 34 Root of sixth cervical nerve | 41 Cervical lymph node |
| 6 Thyroid cartilage | 17 Vagus nerve (X) | 27 Accessory nerve (XI) | 35 Spinal cord within dural sheath | |
| 7 Cricoid cartilage | 18 Sympathetic chain | 28 Trapezius | 36 Body of fifth cervical vertebra | |
| 8 Rima glottidis | 19 Longus capitis | 29 Levator scapulae | 37 Neurocentral or | |
| 9 Arytenoid cartilage | 20 Longus colli | | | |
| 10 Thyro-arytenoid | 21 Vertebral artery and vein | | | |
| 11 Pharynx | | | | |



Axial computed tomogram (CT)

Section level



Notes

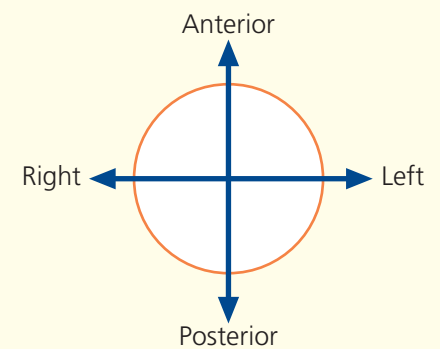
This section passes through the body of the fifth cervical vertebra (**36**), immediately above the level of the shoulder joint. Here the fibres of the trapezius (**28**) arch over the posterior extremity of the posterior triangle. Just below this level, at C6, lies the junction between the pharynx (**11**) and oesophagus, and the larynx (**6**, **7**, **9**) and the trachea. In both the section and the CT image, the pharynx (**11**) has a narrow anteroposterior diameter; it distends considerably during deglutition. On the CT image, the vocal cords of the

rima glottidis (**8**) are adducted.

The posterior triangle of the neck has, at its boundaries, the posterior border of sternocleidomastoid (**13**) anteriorly, the anterior border of trapezius (**28**) posteriorly and the middle third of the clavicle below. Its floor comprises, from above downwards, splenius capitis (**30**), levator scapulae (**29**) and scalenus medius and posterior (**24**).

Not unusually, as in this case, the external jugular vein (**39**) is double.

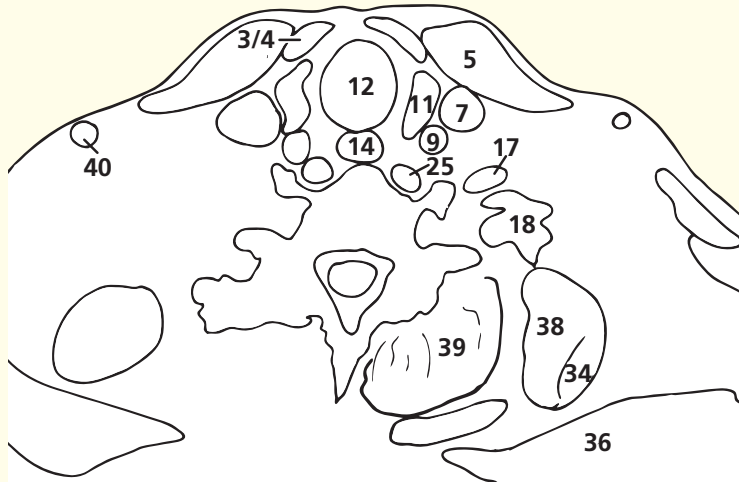
Orientation





- | | | | |
|----------------------------------|--------------------------------------------------|----------------------------------------------------------|--------------------------------|
| 1 Platysma | 13 Recurrent laryngeal nerve | vertebra prominens | 32 Capsule of shoulder joint |
| 2 Anterior jugular vein | 14 Oesophagus | 22 Spinal cord within dural sheath | 33 Supraspinatus |
| 3 Sternohyoid | 15 Lymph node | 23 Inferior articular facet of seventh cervical vertebra | 34 Spine of scapula |
| 4 Sternothyroid | 16 Ventral ramus of sixth cervical nerve | 24 Body of seventh cervical vertebra | 35 Coracoid process of scapula |
| 5 Sternocleidomastoid | 17 Scalenus anterior | 25 Longus colli | 36 Trapezius |
| 6 Omohyoid | 18 Scalenus medius | 26 Vertebral artery and vein | 37 Rhomboideus minor |
| 7 Internal jugular vein | 19 Ventral ramus of seventh cervical nerve | 27 Ascending cervical artery and vein | 38 Levator scapulae |
| 8 Vagus nerve (X) | 20 Dorsal root ganglion of eighth cervical nerve | 28 Inferior thyroid artery | 39 Erector spinae |
| 9 Common carotid artery | 21 Spine of seventh cervical vertebra – | 29 Phrenic nerve | |
| 10 Isthmus of thyroid gland | | 30 Deltoid | |
| 11 Lateral lobe of thyroid gland | | 31 Head of humerus | |
| 12 Trachea | | | |

40 External jugular vein



Axial computed tomogram (CT)

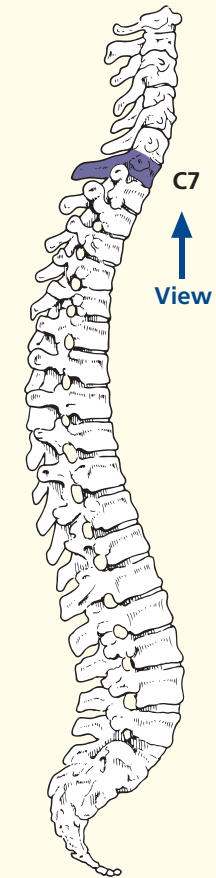
Notes

This section traverses the body of the seventh cervical vertebra, which bears the longest spine of the cervical series, the vertebra prominens (21). This is shorter, however, than the spine of T1, as can be ascertained easily by feeling the back of your own neck.

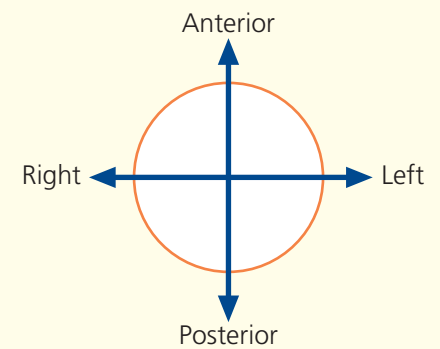
Three important relationships are demonstrated well. The recurrent laryngeal nerve (13) lies in the groove between

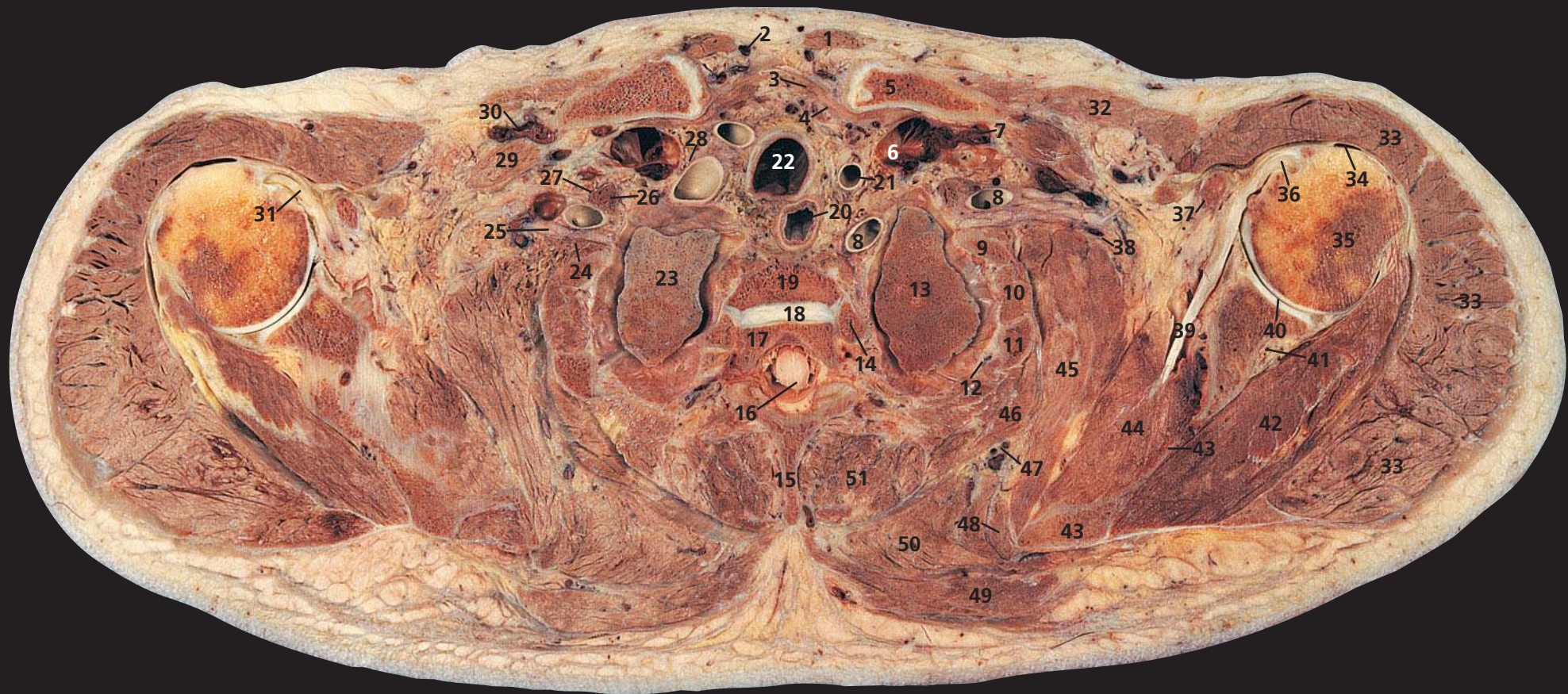
the trachea (12) and the oesophagus (14). The phrenic nerve (29) hugs the anterior aspect of scalenus anterior (17) deep to the prevertebral fascia; three structures – the common carotid artery (9), the internal jugular vein (7) and the vagus nerve (8) – lie together within the fascial carotid sheath. The deep cervical chain of lymph nodes (15) lies lateral to the carotid sheath.

Section level

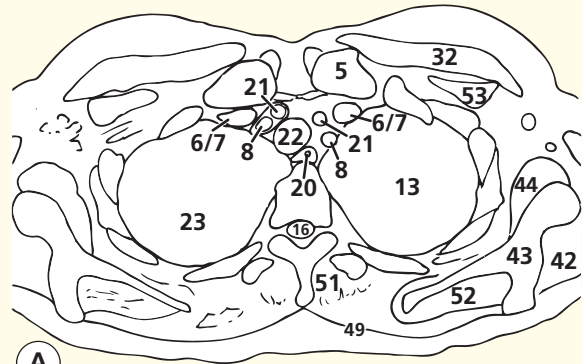


Orientation





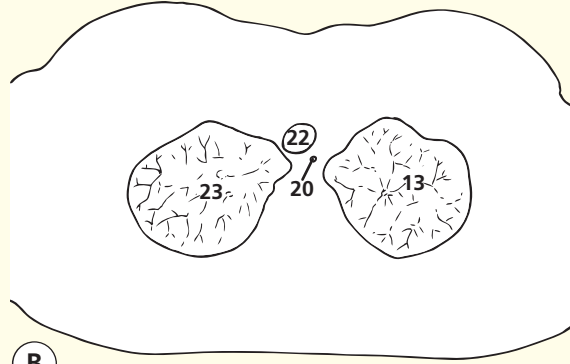
- | | | | |
|--------------------------------------------------------------|----------------------------------------------------------------------------|-------------------------------------|------------------------------------------------------|
| 1 Sternocleidomastoid sternal head | 15 Spine of first thoracic vertebra | 27 Phrenic nerve | 42 Infraspinatus |
| 2 Anterior jugular vein | 16 Spinal cord within dural sheath | 28 Vagus nerve (X) | 43 Scapula |
| 3 Sternohyoid | 17 Part of body of second thoracic vertebra | 29 Subclavius | 44 Subscapularis |
| 4 Sternothyroid | 18 Part of intervertebral disc between first and second thoracic vertebrae | 30 Right subclavian vein | 45 Serratus anterior |
| 5 Clavicle | 19 Part of body of first thoracic vertebra | 31 Tendon of right biceps long head | 46 Serratus posterior superior |
| 6 Internal jugular vein – junction with left subclavian vein | 20 Oesophagus | 32 Pectoralis major | 47 Superficial (transverse) cervical artery and vein |
| 7 Left subclavian vein | 21 Common carotid artery | 33 Deltoid | 48 Rhomboideus minor |
| 8 Subclavian artery | 22 Trachea | 34 Subdeltoid bursa | 49 Trapezius |
| 9 First rib | 23 Right lung apex | 35 Head of humerus | 50 Rhomboideus major |
| 10 Intercostal muscles | 24 Scalenus medius | 36 Tendon of left biceps long head | 51 Erector spinae |
| 11 Second rib | 25 Root of first thoracic nerve | 37 Coracoid process of scapula | 52 Supraspinatus |
| 12 Intercostal neurovascular bundle | 26 Scalenus anterior | 38 Nerve to serratus anterior | 53 Pectoralis minor |
| 13 Apex of left lung | | 39 Tendon of subscapularis | |
| 14 Head of second rib | | 40 Glenoid fossa of scapula | |
| | | 41 Suprascapular artery and vein | |



(A)



Axial computed tomogram (CT)

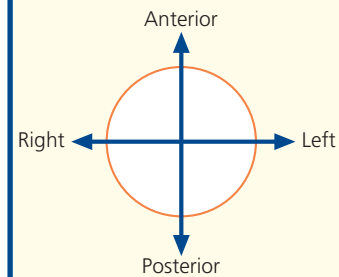


(B)

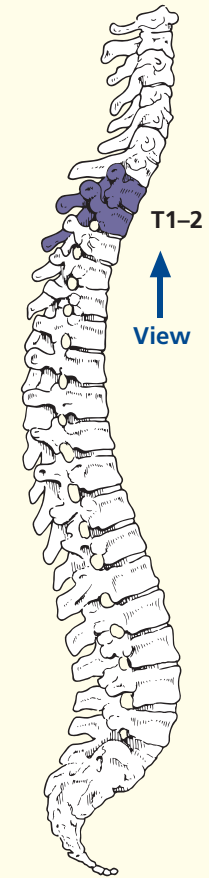


Axial computed tomogram (CT)

Orientation



Section level



Notes

This section, through the intervertebral disc between the first and second thoracic vertebrae (18), enters the apex of the thorax and traverses the apices of the upper lobes of the lungs (13, 23). There are considerable differences between the section and CT images at this level because the CT is performed with the arms elevated alongside the head in order to reduce artefacts from the humeri.

Here, posterior to the medial end of the clavicle (5), the internal jugular vein (6) joins with the subclavian vein (7) to form the brachiocephalic vein (see Axial section 4).

The intercostal neurovascular bundle (12) is seen well. Note that it comprises the intercostal vein, artery and nerve from above downwards; the nerve corresponds to the number of its

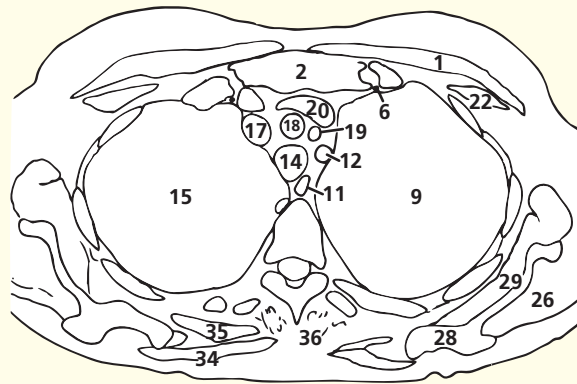
overlying rib and lies protected within the subcostal groove.

Only in transverse section is the extreme thinness of the blade of the scapula (43) appreciated fully.

One CT (A) is displayed at soft tissue settings (window level and width of grey scale), the other CT (B) at lung windows.



- | | | | |
|-----------------------------------|---------------------------------------------|-----------------------------------------------------------------------------------------------------|-----------------------------------------------------------|
| 1 Pectoralis major | 15 Upper lobe of right lung | 28 Scapula | 38 Spinal cord within dural sheath |
| 2 Manubrium of sternum | 16 Right vagus nerve (X) | 29 Subscapularis | 39 Body of third thoracic vertebra |
| 3 Sternothyroid | 17 Right brachiocephalic vein | 30 Second rib | 40 Axillary nerve |
| 4 Sternoclavicular joint | 18 Brachiocephalic artery | 31 Intercostal artery and vein and nerve | 41 Radial nerve |
| 5 First rib | 19 Left common carotid artery | 32 External and internal intercostal muscles | 42 Ulnar nerve |
| 6 Internal thoracic artery | 20 Left brachiocephalic vein | 33 Third rib | 43 Median nerve |
| 7 Left phrenic nerve | 21 Right phrenic nerve | 34 Trapezius | 44 Right axillary artery |
| 8 Left vagus nerve (X) | 22 Pectoralis minor | 35 Rhomboideus major | 45 Right axillary vein |
| 9 Upper lobe of left lung | 23 Coracobrachialis and biceps (short head) | 36 Erector spinae | 46 Axillary fat |
| 10 Thoracic duct | 24 Long head of biceps tendon | 37 Fourth rib with articulation of its head with body of third thoracic vertebra transverse process | 47 Pectoral branch of the acromiothoracic artery and vein |
| 11 Oesophagus | 25 Deltoid | | 48 Cephalic vein |
| 12 Left subclavian artery | 26 Infraspinatus | | 49 Shaft of humerus |
| 13 Left recurrent laryngeal nerve | 27 Suprascapular artery and vein | | |
| 14 Trachea | | | |

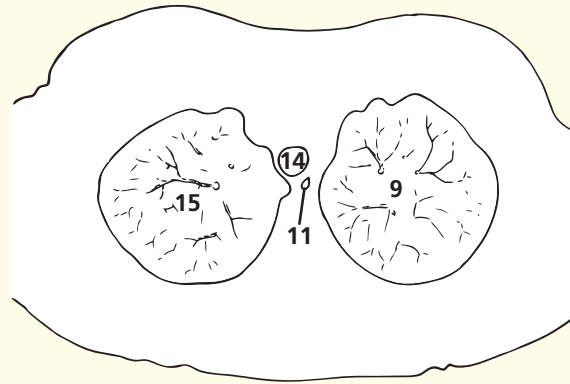


(A)

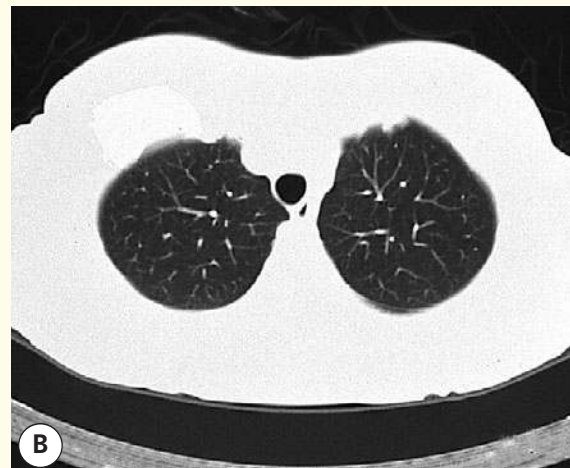


(A)

Axial computed tomogram (CT)



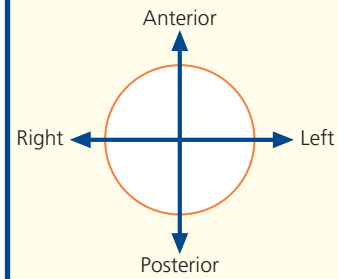
(B)



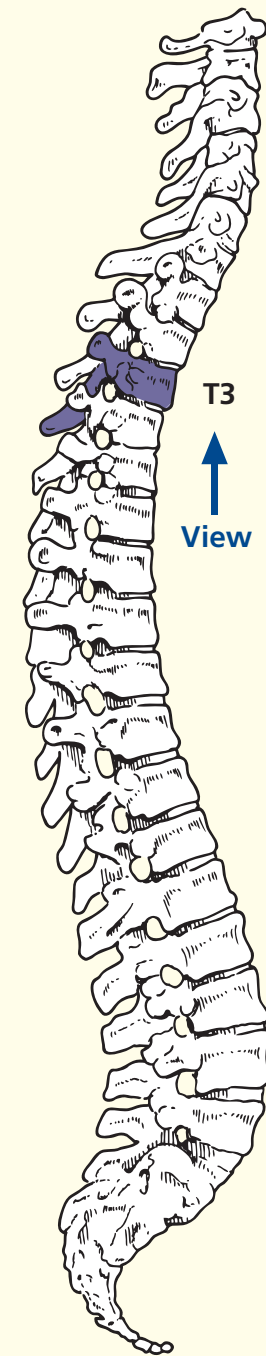
(B)

Axial computed tomogram (CT)

Orientation



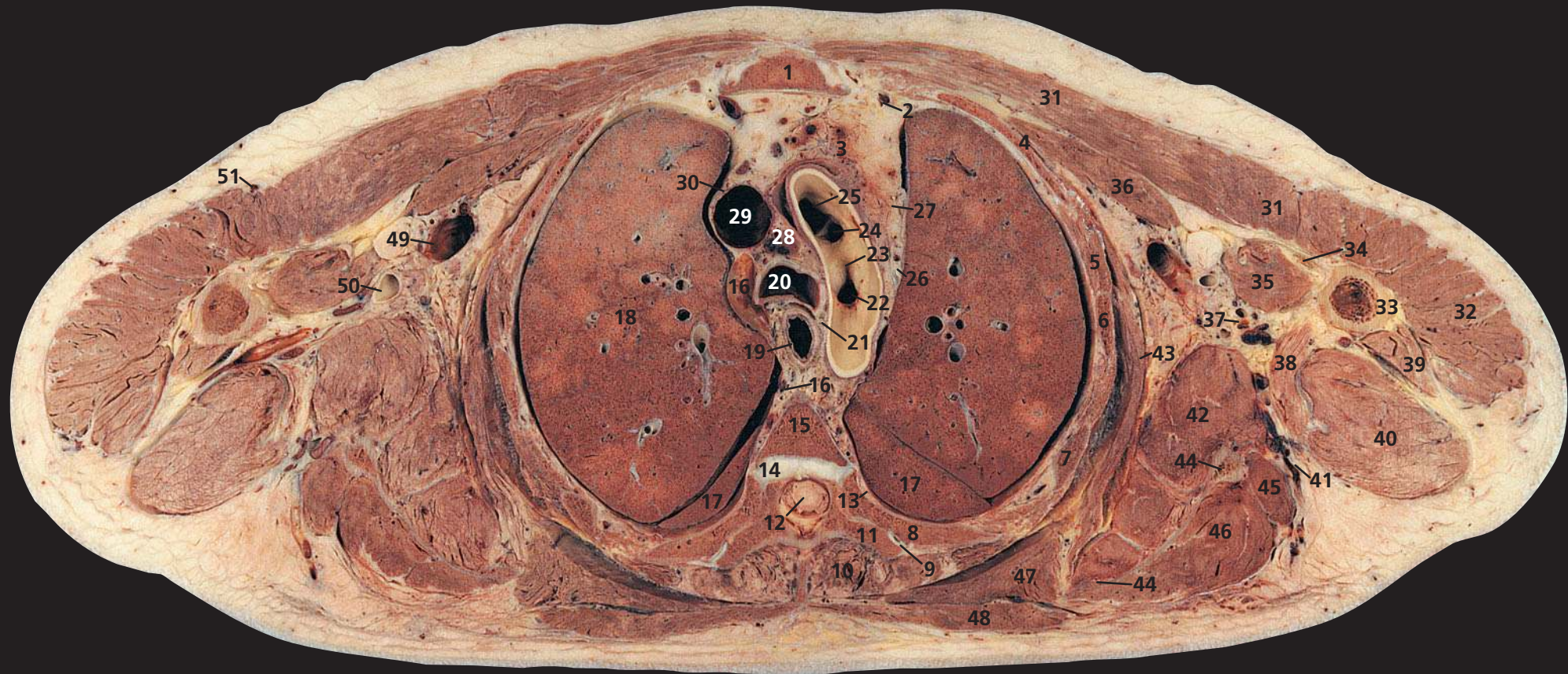
Section level



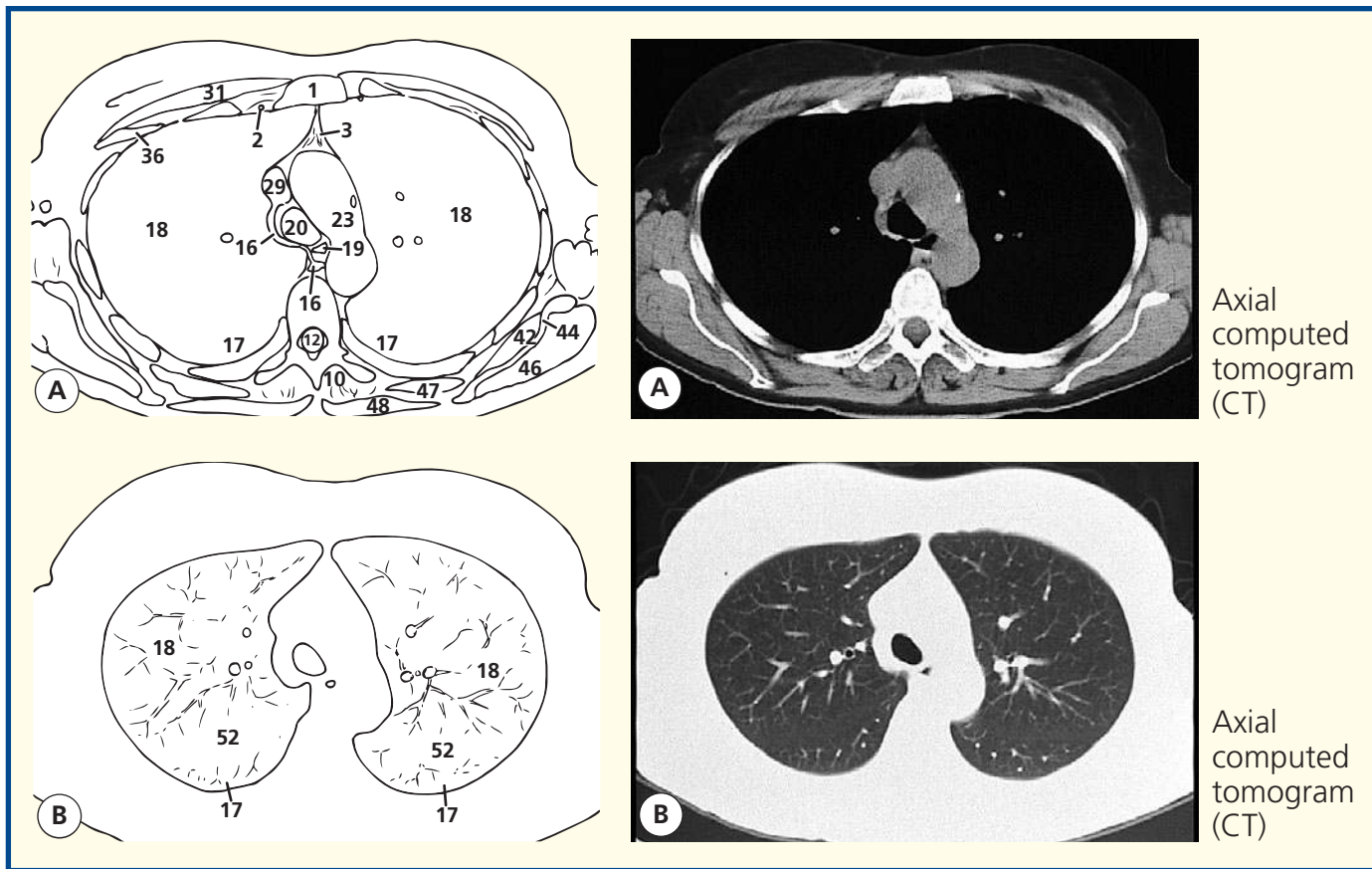
Notes

The contents of the upper mediastinum – including the oesophagus, trachea and great vessels – are demonstrated in this section, which traverses the manubrium and the third thoracic vertebra; these are also shown in Axial section 5.

This section also shows the walls and contents of the axilla. Note that the cephalic vein (48) runs in the deltopectoral groove between the medial edge of deltoid and the lateral edge of pectoralis major.

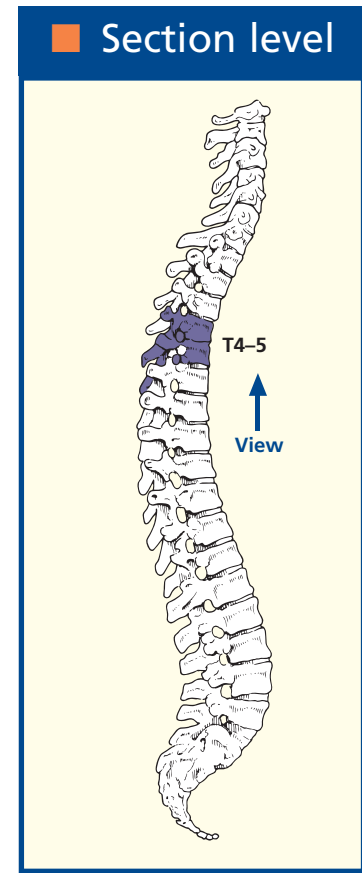
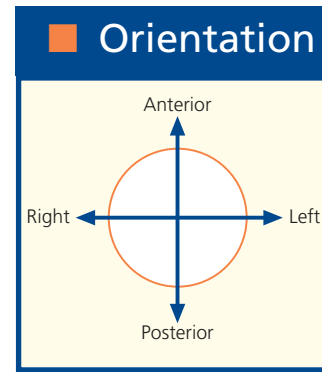


- | | | | |
|--------------------------------------------------|----------------------------------------------------------------------------|---------------------------------------------|----------------------------------------|
| 1 Manubriosternal joint (angle of Louis) | 14 Part of intervertebral disc between fourth and fifth thoracic vertebrae | 26 Left vagus nerve (X) | 41 Circumflex scapular artery and vein |
| 2 Internal thoracic artery and vein | 15 Part of body of fourth thoracic vertebra | 27 Left phrenic nerve | 42 Subscapularis |
| 3 Thymic residue within anterior mediastinal fat | 16 Azygos vein | 28 Pretracheal lymph node | 43 Serratus anterior |
| 4 Second rib | 17 Apical segment lower lobe lung separated by oblique fissure from (18) | 29 Superior vena cava | 44 Body of scapula |
| 5 Intercostal | 18 Upper lobe of lung | 30 Right phrenic nerve | 45 Teres minor |
| 6 Third rib | 19 Oesophagus | 31 Pectoralis major | 46 Infraspinatus |
| 7 Fourth rib | 20 Trachea at bifurcation | 32 Deltoid | 47 Rhomboideus |
| 8 Fifth rib | 21 Recurrent laryngeal nerve | 33 Shaft of humerus | 48 Trapezius |
| 9 Fifth costotransverse joint | 22 Left subclavian artery orifice | 34 Biceps – long head | 49 Axillary vein |
| 10 Erector spinae | 23 Aortic arch | 35 Biceps – short head and coracobrachialis | 50 Axillary artery |
| 11 Transverse process of fifth thoracic vertebra | 24 Left common carotid artery orifice | 36 Pectoralis minor | 51 Cephalic vein |
| 12 Spinal cord within dural sheath | 25 Brachiocephalic artery orifice | 37 Subscapular artery vein and nerve | 52 Oblique fissure |
| 13 Sympathetic chain | | 38 Latissimus dorsi | |
| | | 39 Triceps – lateral head | |
| | | 40 Triceps – long head | |



Axial computed tomogram (CT)

Axial computed tomogram (CT)



Notes

This section passes through the important anatomical level of the manubriosternal joint, the angle of Louis (1). At this joint articulate the second costal cartilage and rib (4), and it is from here that the ribs can be conveniently counted in clinical practice. Posteriorly this plane passes through the T4/5 intervertebral disc (14).

This plane demarcates the junction between the superior and the lower mediastinum, the latter of which is subdivided into the anterior mediastinum, in front of the pericardium, the middle mediastinum, occupied by the pericardium and its

contents, and the posterior mediastinum, behind the pericardium.

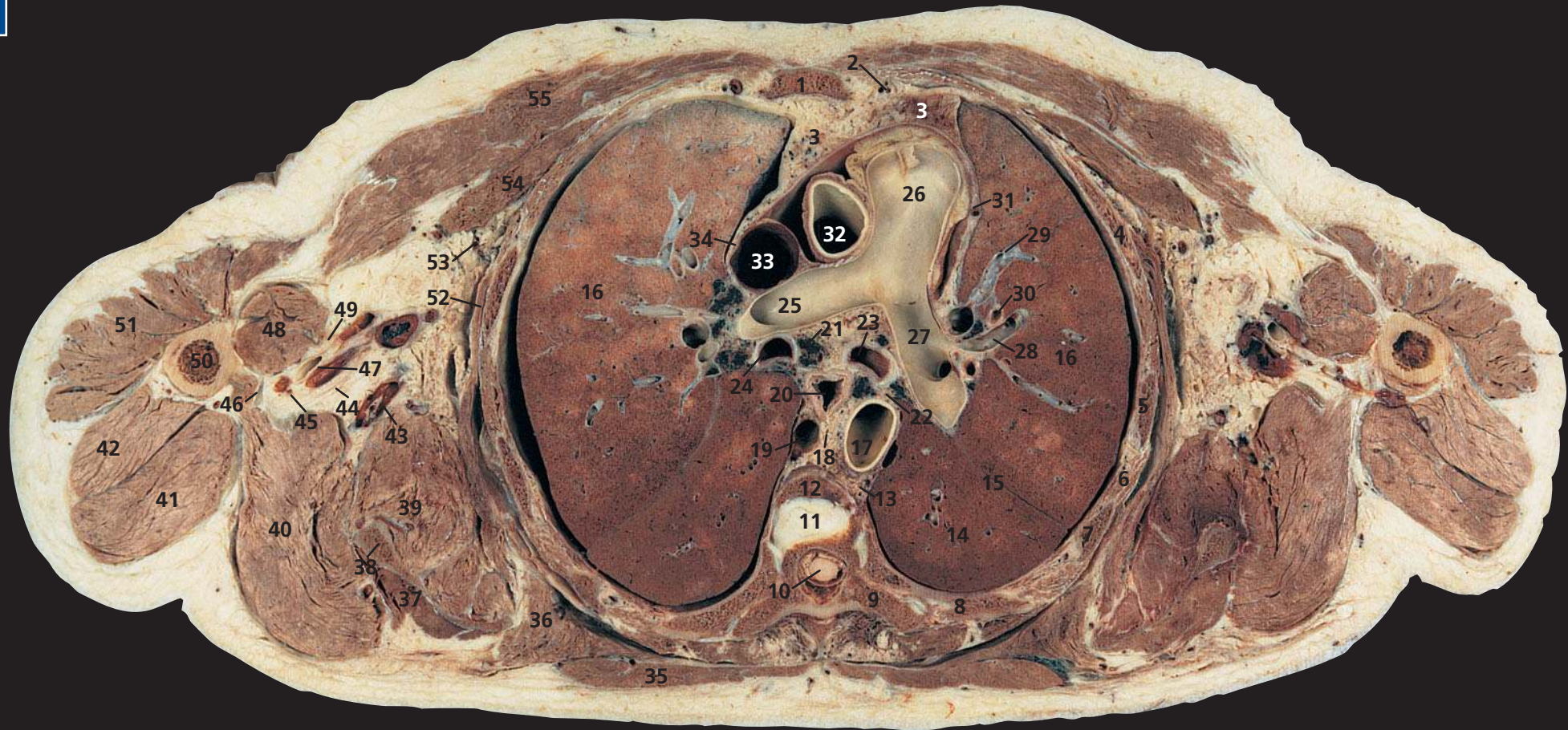
The trachea bifurcates at this level (20). In the living upright subject, however, the bifurcation may be as low as the level of T6, particularly in deep inspiration.

The cranial portions of the oblique fissures of the lungs (17, 52) are traversed on this section. The normal oblique fissures are often not seen on conventional CT images of the lung parenchyma. The position can be inferred, however (see CT b) by the paucity of blood vessels; only small terminal vessels

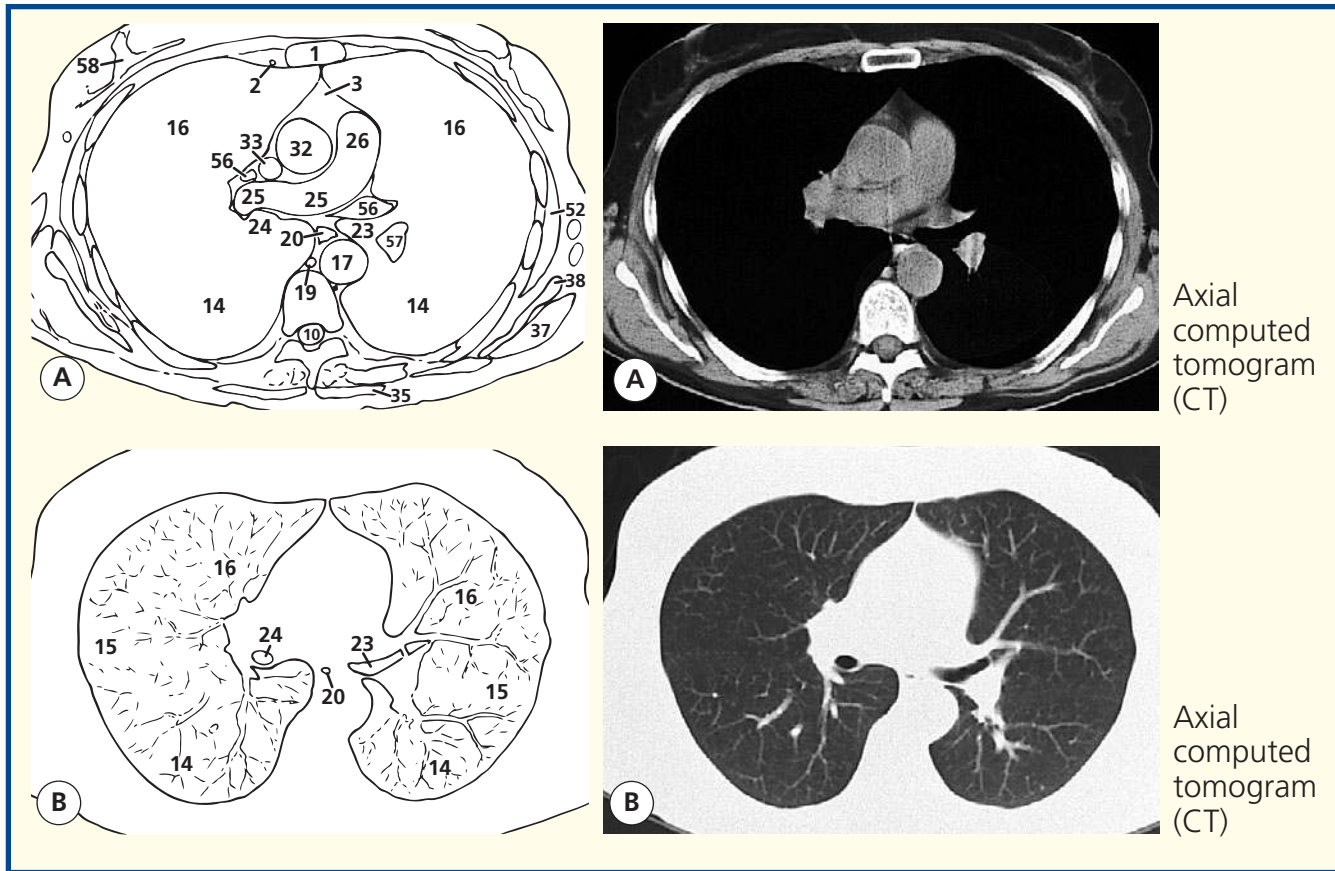
are present in the lung parenchyma adjacent to a fissure.

Pretracheal nodes (28) may become enlarged due to a wide variety of disease processes. They are accessible for biopsy via mediastinoscopy.

Subscapularis (42) arises not only from the periosteum of the medial two-thirds of the subscapular fossa of the scapula but also from tendinous laminae in the muscle itself, which are attached to prominent transverse ridges on the subscapular fossa. This is shown clearly in this section.

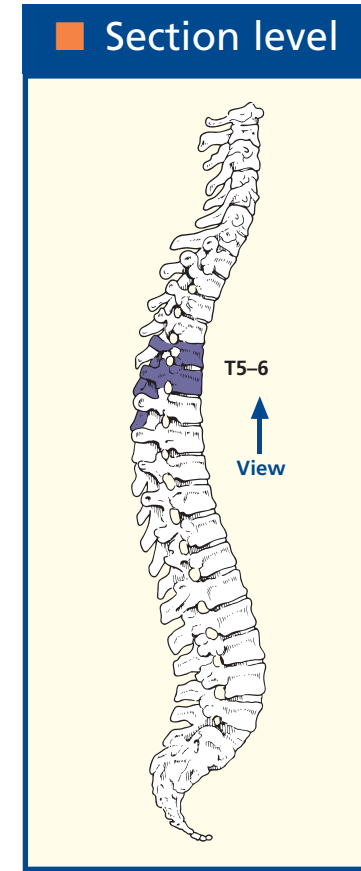
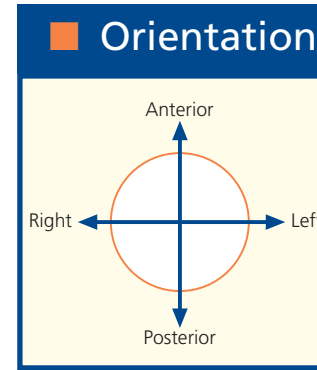


- | | | | |
|---------------------------------------------------------------------------|--------------------------------|-----------------------------------------------------|-------------------------------------|
| 1 Body of sternum | 13 Intercostal artery and vein | 29 Pulmonary vein tributary | 44 Ulnar nerve |
| 2 Internal thoracic artery and vein | 14 Lower lobe of lung | 30 Segmental bronchus | 45 Radial nerve |
| 3 Thymic residue within anterior mediastinal fat | 15 Oblique fissure | 31 Left phrenic nerve with pericardiophrenic artery | 46 Latissimus dorsi tendon |
| 4 Third rib | 16 Upper lobe of lung | 32 Ascending aorta | 47 Axillary artery and vein |
| 5 Fourth rib | 17 Descending aorta | 33 Superior vena cava | 48 Biceps and coracobrachialis |
| 6 Intercostal muscle | 18 Thoracic duct | 34 Right phrenic nerve | 49 Median nerve |
| 7 Fifth rib | 19 Azygos vein | 35 Trapezius | 50 Shaft of humerus |
| 8 Sixth rib | 20 Oesophagus | 36 Rhomboideus major | 51 Deltoid |
| 9 Transverse process of sixth thoracic vertebra | 21 Lymph node | 37 Infraspinatus | 52 Serratus anterior |
| 10 Spinal cord within dural sheath | 22 Left vagus nerve (X) | 38 Scapula | 53 Lateral thoracic artery and vein |
| 11 Part of intervertebral disc between fifth and sixth thoracic vertebrae | 23 Left main bronchus | 39 Subscapularis | 54 Pectoralis minor |
| 12 Part of body of fifth thoracic vertebra | 24 Right intermediate bronchus | 40 Teres major | 55 Pectoralis major |
| | 25 Right pulmonary artery | 41 Triceps – long head | |
| | 26 Pulmonary trunk | 42 Triceps – lateral head | |
| | 27 Left pulmonary artery | 43 Subscapular artery and vein | |
| | 28 Pulmonary artery branch | | |
| | | | 56 Superior pulmonary vein |
| | | | 57 Left basal pulmonary artery |
| | | | 58 Breast |



Axial computed tomogram (CT)

Axial computed tomogram (CT)



Notes

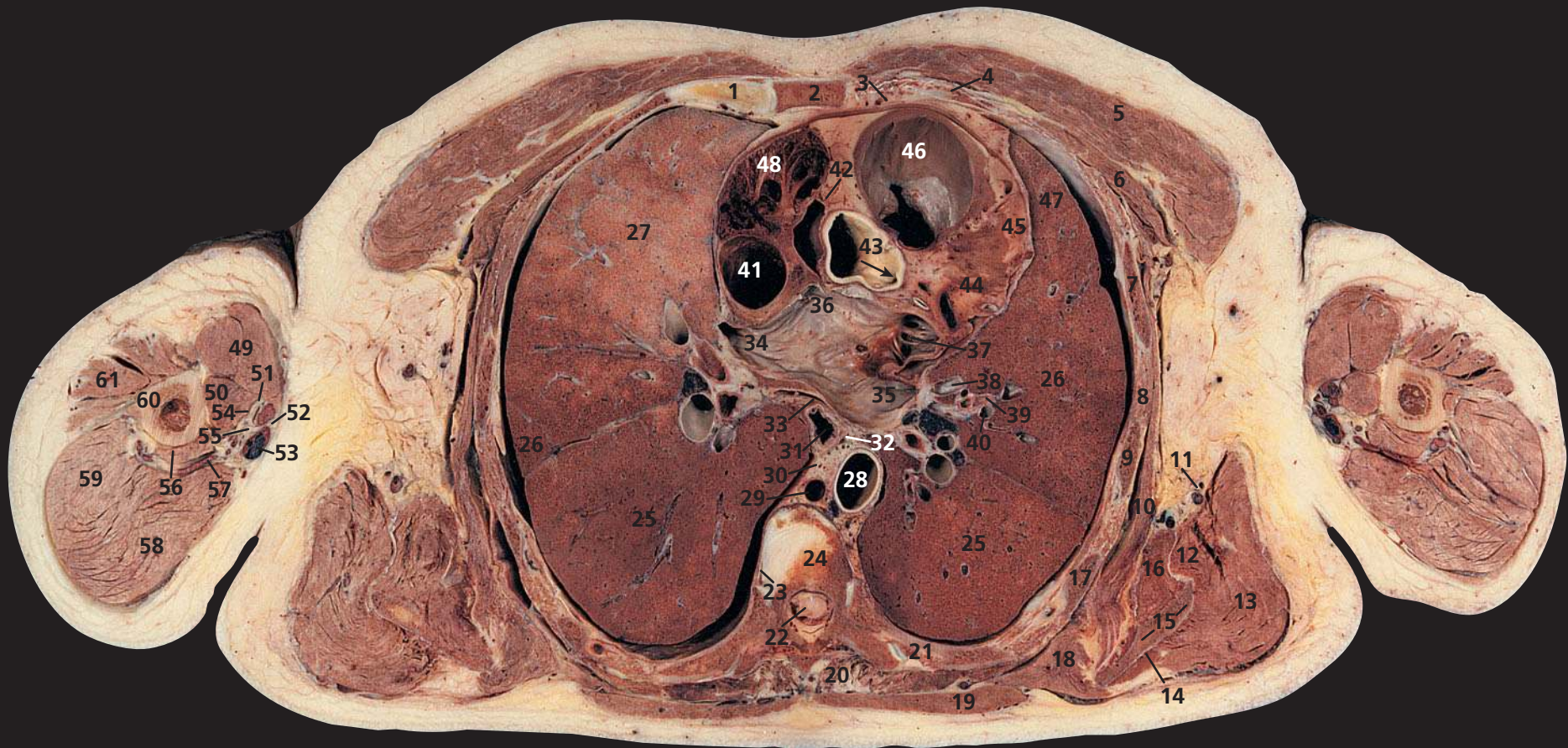
This section, traversing the upper body of the sternum (1) and the lower part of the body of the fifth thoracic vertebra (12), passes through the great arterial trunks as these emerge from the heart, the pulmonary trunk (26) and the ascending aorta (32).

On the CT image, the left main bronchus gives off its common upper lobe/lingular branch at this level. On the right, the upper lobe bronchus has already originated more cranially (on both CT images and section); hence, the term 'intermediate bronchus' (24) is applied to that portion of the right bronchus between its upper lobe and middle lobe branches.

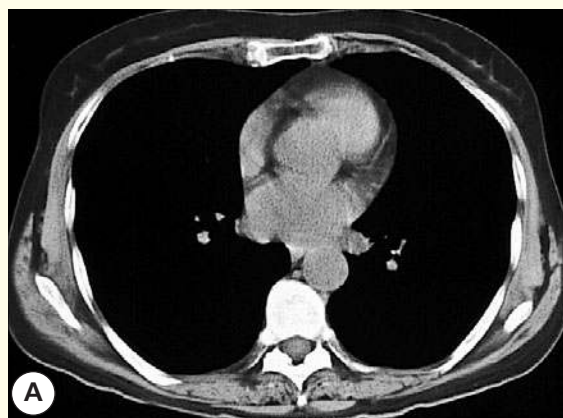
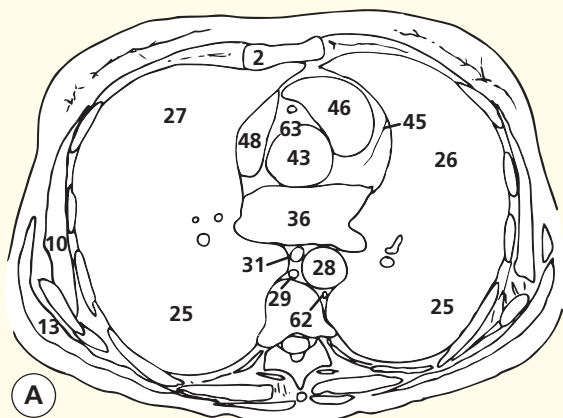
At the left hilum, the superior pulmonary vein (56) lies anterior to the bronchus (23), which in turn lies anterior to the left basal pulmonary artery (57). On the right side, the vein (56) lies anterior to the right pulmonary artery, which lies anterior to the right intermediate bronchus (24).

In this subject, the right (25) and left (27) pulmonary arteries lie in the same axial plane. In most subjects, the left pulmonary artery is at a more cranial level than the right – hence the discrepancy between the section and CT image appearances. The branches of the pulmonary artery (28) that

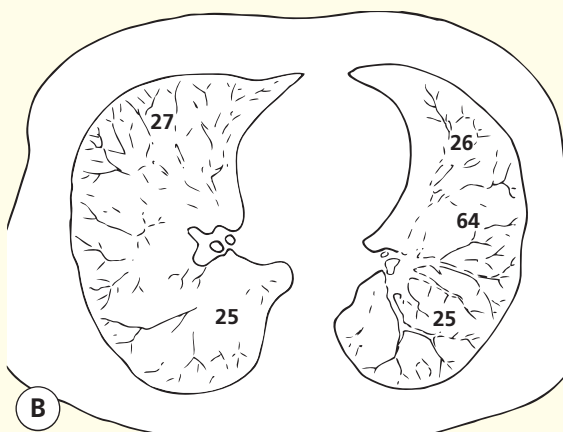
accompany the segmental and subsegmental bronchi (30) usually lie dorsolaterally to these structures; each pulmonary segment receives an independent arterial supply. The bronchi usually separate the dorsolateral pulmonary artery branch from the ventromedially situated pulmonary vein tributary (29). Peripherally, many pulmonary venous tributaries run between, and drain adjacent, pulmonary segments. Thus, an individual bronchopulmonary segment will have its own bronchus and artery but not an individual pulmonary venous drainage.



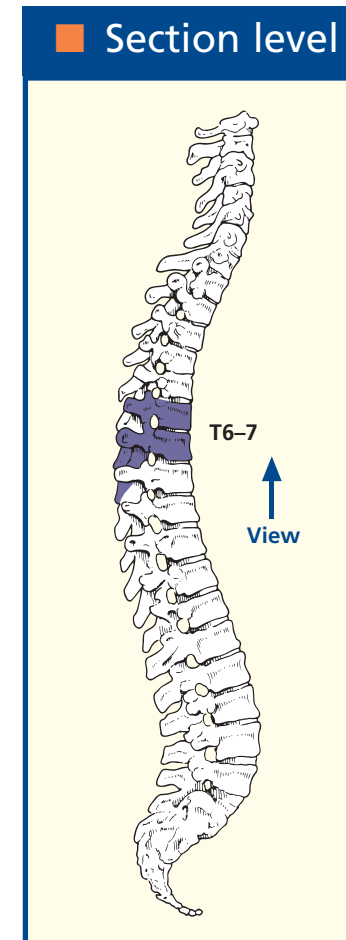
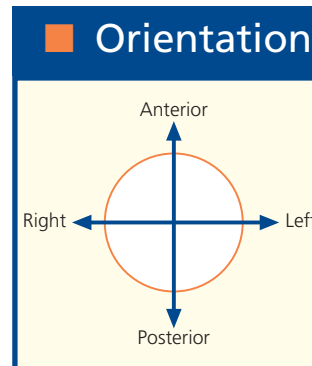
- | | | | | |
|-----------------------------------------------------------------------|-----------------------------------------------------------------------------------------------------------------------|----------------------------------------------|--------------------------------------------------------------------|-------------------------------------------------------|
| 1 Third costal cartilage with adjacent sternocostal joint (see Notes) | 15 Scapula | 26 Upper lobe of lung | 40 Left pulmonary artery branch to lingula | 50 Coracobrachialis |
| 2 Body of sternum | 16 Subscapularis | 27 Middle lobe of right lung | 41 Superior vena cava | 51 Axillary artery and vein |
| 3 Internal thoracic artery and vein | 17 Fifth rib | 28 Descending aorta | 42 Artefactual gap within the pericardial space | 52 Medial cutaneous nerves of arm and forearm |
| 4 Partially calcified third costal cartilage | 18 Rhomboideus major | 29 Azygos vein | 43 Ascending aorta, with orifice of left coronary artery (arrowed) | 53 Basilic vein |
| 5 Pectoralis major | 19 Trapezius | 30 Thoracic duct | 44 Left ventricle wall | 54 Median nerve |
| 6 Pectoralis minor | 20 Erector spinae | 31 Oesophagus | 45 Coronary artery (left anterior interventricular branch) | 55 Ulnar nerve |
| 7 Third rib | 21 Sixth rib, with adjacent costotransverse joint to transverse process of sixth thoracic vertebra | 32 Left vagal plexus | 46 Infundibulum of right ventricle with pulmonary valves | 56 Triceps – medial head |
| 8 Intercostal muscle | 22 Spinal cord within dural sheath | 33 Right vagal plexus | 47 Fibrous pericardium | 57 Radial nerve with profunda brachii artery and vein |
| 9 Fourth rib | 23 Thoracic sympathetic chain | 34 Right superior pulmonary vein | 48 Right auricle (atrial appendage) | 58 Triceps – long head |
| 10 Serratus anterior | 24 Body of sixth thoracic vertebra, with part of intervertebral disc between the sixth and seventh thoracic vertebrae | 35 Left superior pulmonary vein | 49 Biceps | 59 Triceps – lateral head |
| 11 Subscapular artery vein and nerve | 25 Lower lobe of lung | 36 Left atrium | | 60 Shaft of humerus |
| 12 Teres major | | 37 Left auricle (atrial appendage) | | 61 Deltoid |
| 13 Latissimus dorsi | | 38 Left pulmonary vein tributary to lingula | | |
| 14 Infrapinatus | | 39 Left bronchus segmental branch to lingula | | |
| | | | | 62 Hemiazygos vein |
| | | | | 63 Right coronary artery |
| | | | | 64 Oblique fissure |



Axial computed tomogram (CT)



Axial computed tomogram (CT)



Notes

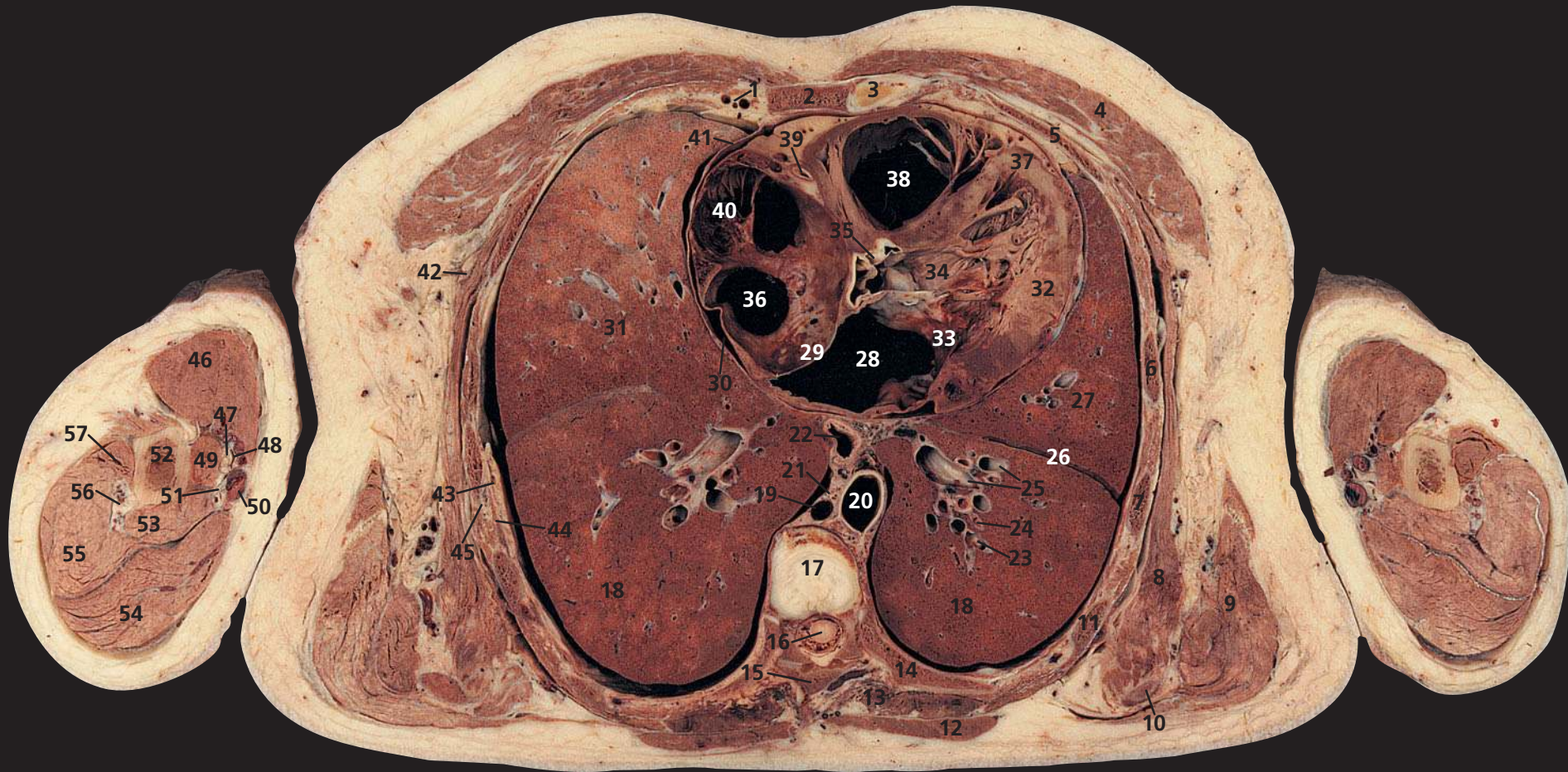
The plane of this section traverses the lower part of the body of the sixth thoracic vertebra (**24**). Anteriorly, it passes through the body of the sternum (**2**) at the level of the third costal cartilage (**1**). Note the adjacent sternocostal joint. These vary; the first lacks a synovial cavity, its costal cartilage being attached by fibrocartilage to the manubrium. The second to seventh joints are usually synovial (as in this subject), with the fibrocartilaginous articular surfaces on both the chondral and the sternal

components of the joint. In some or all of these joints, however, an arrangement may be found similar to that of the first joint.

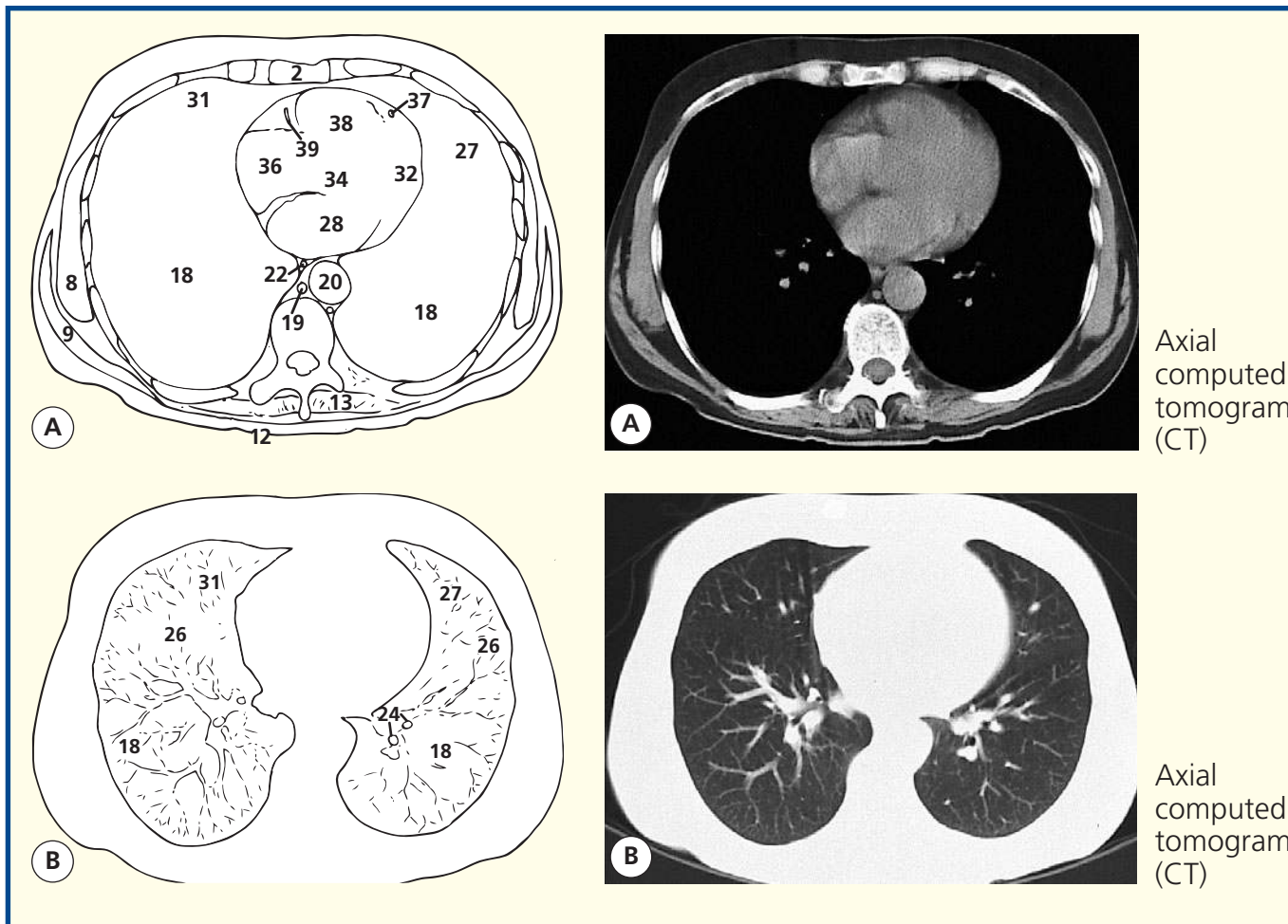
The presence of a pericardial effusion in this subject has produced an artefactual gap in the superior reflection of the pericardial space (**42**). The aorta at its origin (**43**) shows the orifice of the left coronary artery. The descending aorta (**28**) is normally more circular in outline than in this subject. Note that this section passes through the

infundibulum of the right ventricle and demonstrates the pulmonary valves (**46**).

On the CT image, both the ascending aorta (**43**) and the region of the pulmonary valves (**46**) have indistinct outlines due to pulsation (compliance) of their walls during the 1-s data-acquisition time. (See also the ascending aorta on the left-hand image in Axial section 6.)

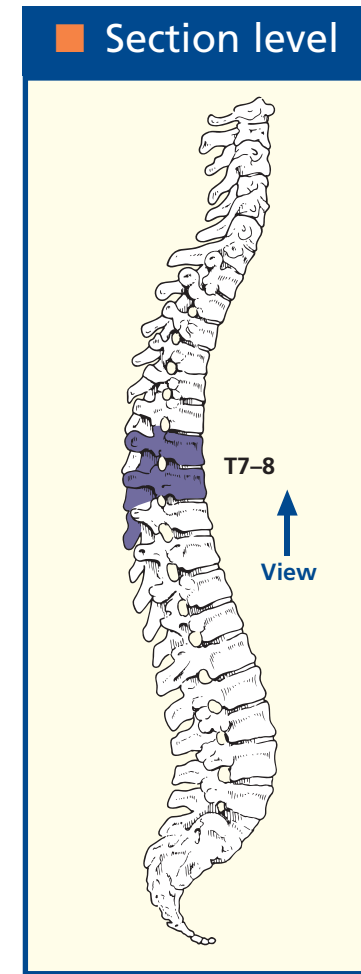
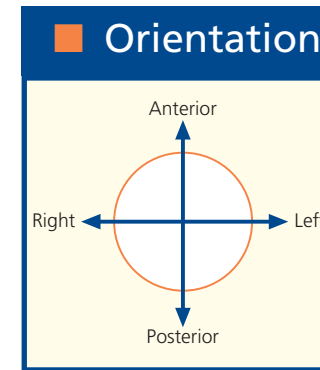


- | | | | | |
|----------------------------------------|----------------------------------------------------------------------|--------------------------------------------------------------------------|-------------------------------------------------------------|-------------------------------------------------------|
| 1 Internal thoracic artery and vein | 16 Spinal cord within dural sheath | 29 Interatrial septum | 39 Right coronary artery | 50 Basilic vein |
| 2 Body of sternum | 17 Intervertebral disc between seventh and eighth thoracic vertebrae | 30 Phrenic nerve with pericardiophrenic artery and vein | 40 Right auricle (atrial appendage) | 51 Ulnar nerve |
| 3 Fourth costal cartilage | 18 Lower lobe of lung | 31 Middle lobe of right lung | 41 Fibrous pericardium | 52 Shaft of humerus |
| 4 Pectoralis major | 19 Azygos vein | 32 Wall of left ventricle | 42 Nerve to serratus anterior | 53 Triceps – short head |
| 5 Fourth rib | 20 Descending aorta | 33 Mitral valve | 43 Intercostal neurovascular bundle | 54 Triceps – long head |
| 6 Fifth rib | 21 Thoracic duct | 34 Vestibule of left ventricle (outflow tract) leading to root of aorta | 44 Innermost intercostal | 55 Triceps – lateral head |
| 7 Sixth rib | 22 Oesophagus | 35 Divided cusp of aortic valve | 45 External and internal intercostal muscles | 56 Radial nerve with profunda brachii artery and vein |
| 8 Serratus anterior | 23 Pulmonary artery branch | 36 Right atrium | 46 Biceps | 57 Deltoid |
| 9 Latissimus dorsi | 24 Branches of left lower lobe bronchus | 37 Anterior interventricular (descending) branch of left coronary artery | 47 Median nerve with musculocutaneous nerve (lateral to it) | |
| 10 Scapula inferior angle | 25 Pulmonary vein tributaries | 38 Right ventricle cavity | 48 Brachial artery with two venae comitantes | |
| 11 Seventh rib | 26 Oblique fissure | | 49 Coracobrachialis | |
| 12 Trapezius | 27 Upper lobe of left lung | | | |
| 13 Erector spinae | 28 Left atrium | | | |
| 14 Eighth rib | | | | |
| 15 Lamina of seventh thoracic vertebra | | | | |



Axial computed tomogram (CT)

Axial computed tomogram (CT)



Notes

This section lies at the level of the intervertebral disc between the seventh and eighth thoracic vertebrae (17) and passes through the body of the sternum (2) at the level of the fourth costal cartilage (3). All four cardiac chambers can be seen and their relationships to each other appreciated. Note that the right atrium (36) forms the right border of the heart. The left atrium (28) is the major contribution to the base of the heart and lies immediately anterior to the

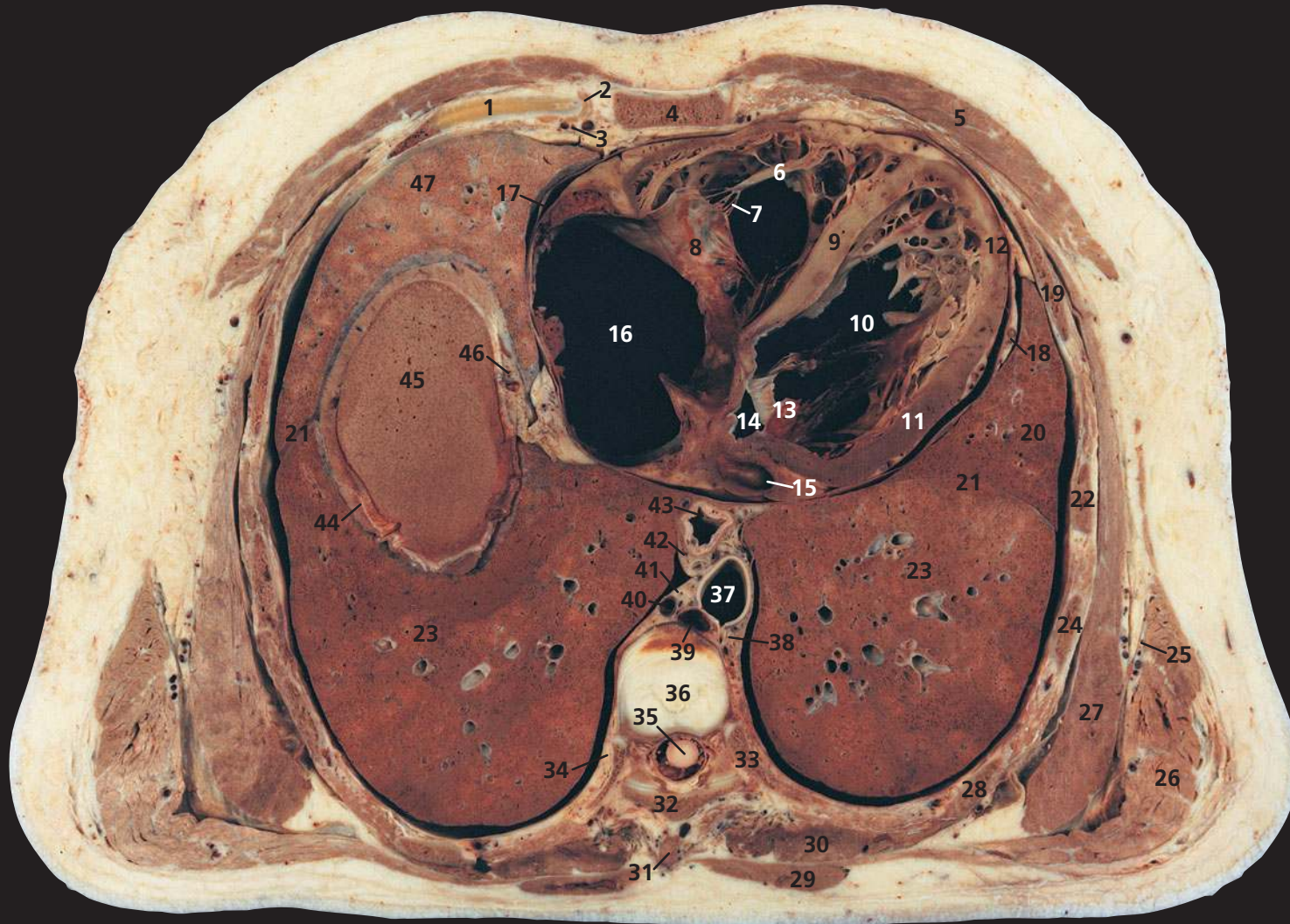
oesophagus (22), separated by the pericardium. The left ventricle (32) forms the bulk of the left border of the heart, and the right ventricle (38) constitutes the major component of the anterior cardiac surface.

In this subject, the left ventricular wall (32) becomes thinner in the region of the apex of the left ventricle, due to a previous myocardial infarction.

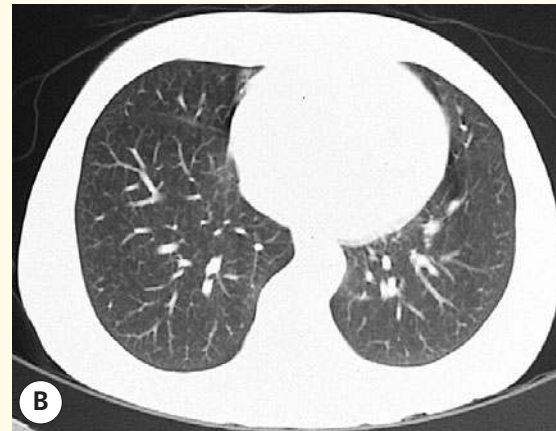
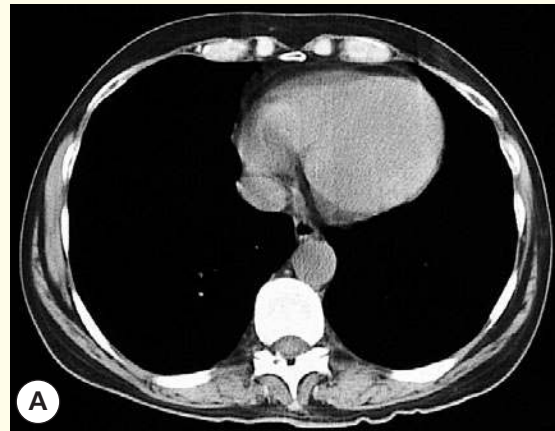
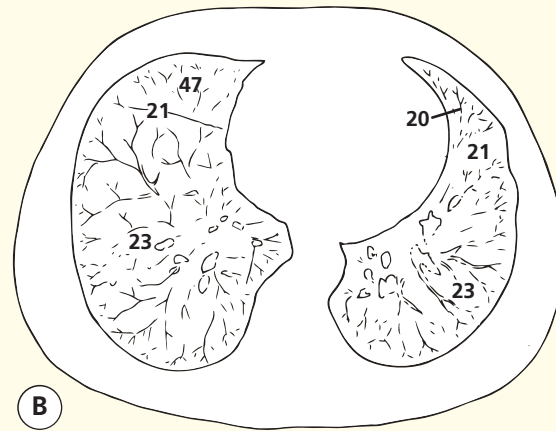
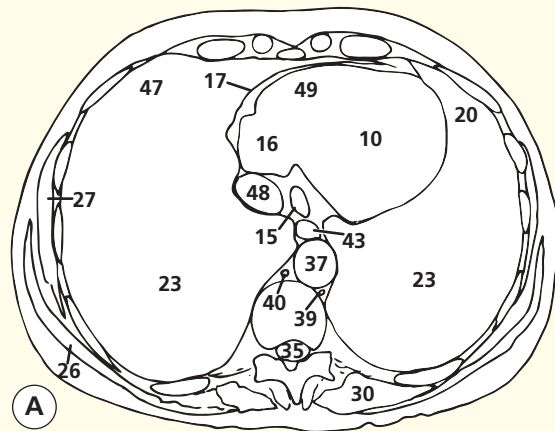
The interatrial septum (29) has a rather curious convexity. This has been caused by extensive post-

mortem thrombus in the right atrium (36). The septum is normally straighter.

The lower four or five digitations of serratus anterior (8) converge to insert on the costal aspect of the inferior angle of the scapula. This component of the muscle, together with the trapezius, powerfully pulls the inferior angle of the scapula forwards and upwards in raising the arm above the head.



- | | | | |
|----------------------------------------------------|---------------------------------------------------------------|--------------------------------------------------------------------|----------------------------------------------------------------|
| 1 Fifth costal cartilage | 14 Left atrium | 27 Serratus anterior | 40 Azygos vein |
| 2 Sternocostal joint | 15 Coronary sinus | 28 Eighth rib | 41 Thoracic duct |
| 3 Internal thoracic artery and vein | 16 Right atrium | 29 Trapezius | 42 Oesophageal vagal plexus |
| 4 Body of sternum | 17 Fibrous pericardium | 30 Erector spinae | 43 Oesophagus |
| 5 Pectoralis major | 18 Left phrenic nerve, with pericardiophrenic artery and vein | 31 Spine of eighth thoracic vertebra | 44 Dome of right hemidiaphragm |
| 6 Papillary muscle | 19 Fifth rib | 32 Lamina of eighth thoracic vertebra | 45 Apex of right lobe liver |
| 7 Chordae tendinae within right ventricular cavity | 20 Upper lobe of left lung (lingula) | 33 Ninth rib | 46 Right phrenic nerve, with pericardiophrenic artery and vein |
| 8 Tricuspid valve | 21 Oblique fissure | 34 Right sympathetic chain | 47 Middle lobe of right lung |
| 9 Interventricular septum | 22 Sixth rib | 35 Spinal cord within dural sheath | |
| 10 Left ventricular cavity | 23 Lower lobe of lung | 36 Intervertebral disc between eighth and ninth thoracic vertebrae | |
| 11 Normal left ventricular wall | 24 Seventh rib | 37 Aorta | |
| 12 Thinned left ventricular wall | 25 Lateral thoracic artery and vein | 38 Origin of eighth intercostal artery | |
| 13 Mitral valve | 26 Latissimus dorsi | 39 Hemiazygos vein | |
| | | | 48 Inferior vena cava |
| | | | 49 Right ventricular cavity |



Axial computed tomogram (CT)

Axial computed tomogram (CT)

Notes

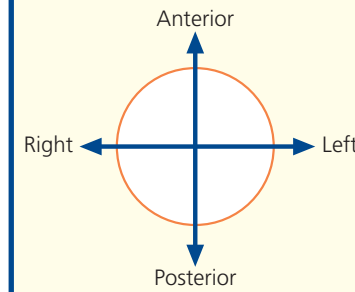
This section traverses the intervertebral disc between the eighth and ninth thoracic vertebrae (36) and slices through the dome of the right hemidiaphragm (44) and a sliver of the underlying right lobe of the liver (45).

In this section, there is considerable thinning and discoloration of the left ventricular wall at the apex (12), consistent with infarction associated with left anterior descending (interventricular) coronary arterial disease.

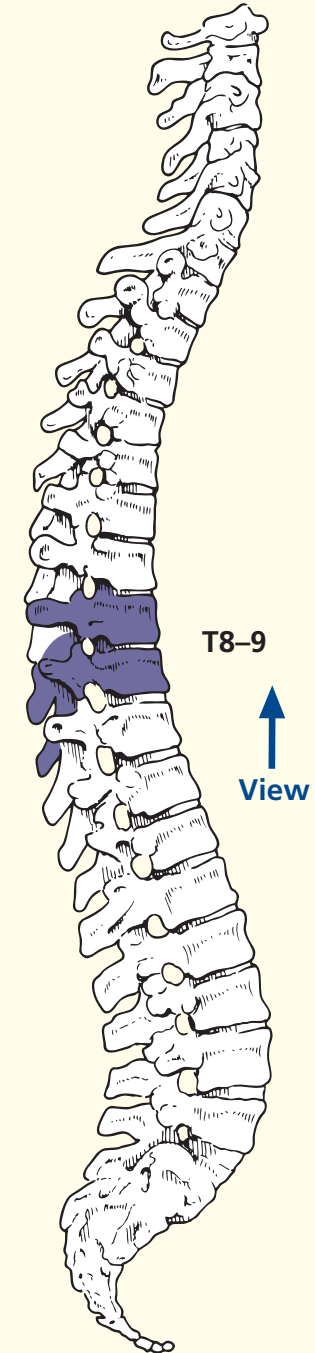
Note how only a tiny portion of the left atrium (14) is present on this section. This demonstrates that the left atrium is situated more cranially than the other three cardiac chambers.

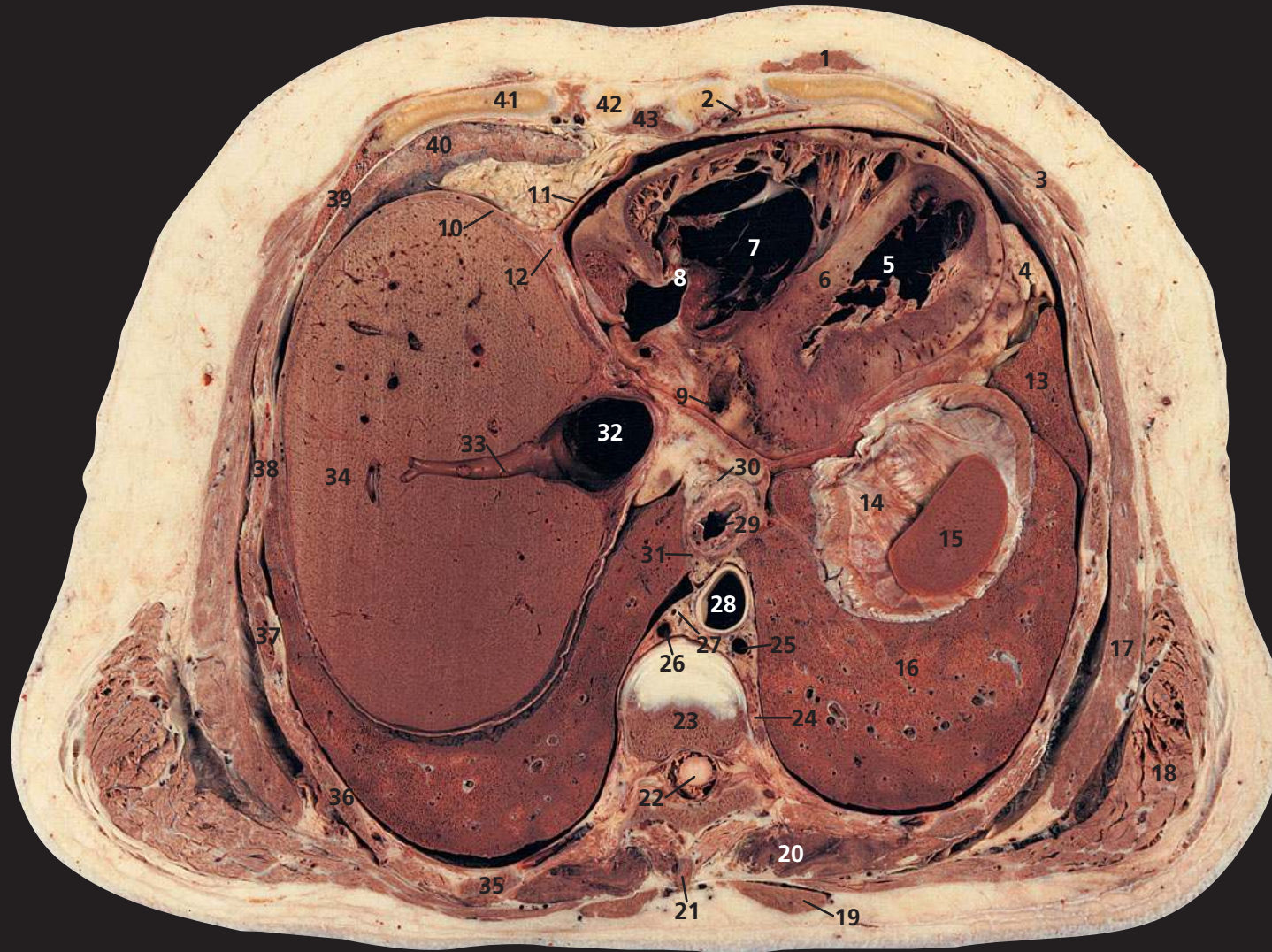
The terminal fibres of the right phrenic nerve (46) usually pass through the vena caval opening in the diaphragm but may traverse the muscle itself.

Orientation

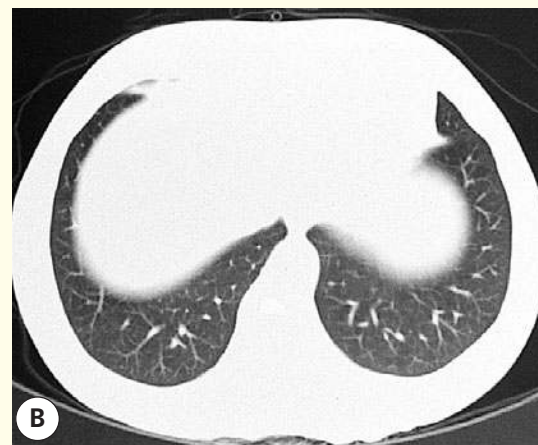
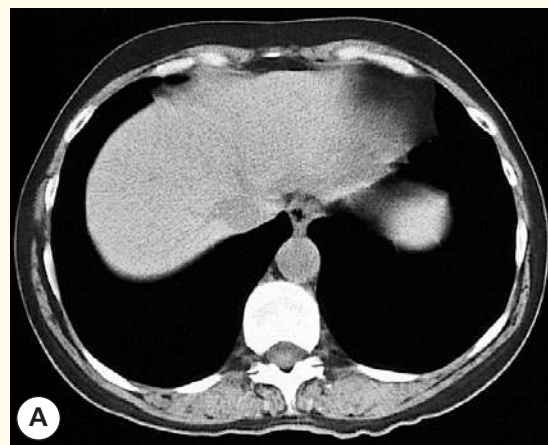
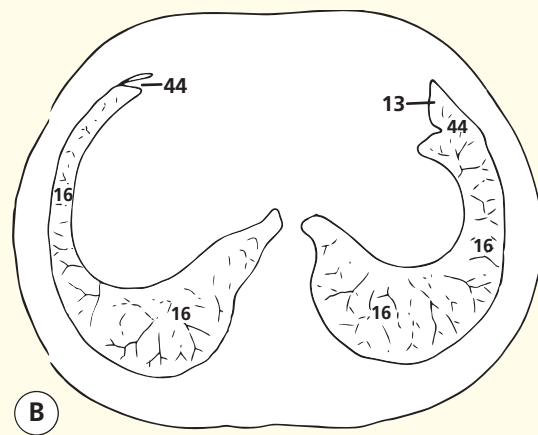
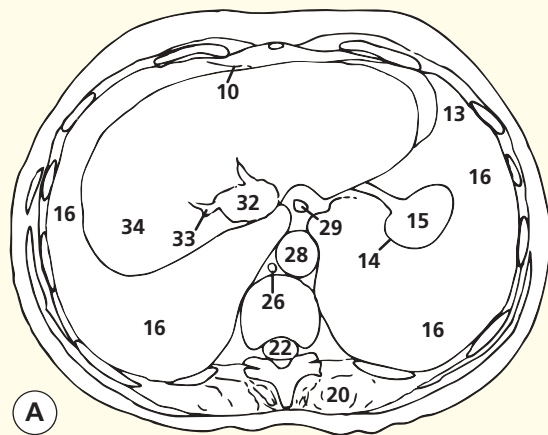


Section level





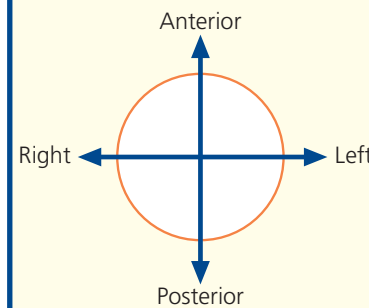
- | | | | |
|------------------------------------------------|----------------------------------------------------------------------|--------------------------------------------|------------------------------|
| 1 Pectoralis major | 13 Upper lobe of left lung (lingula) | between ninth and tenth thoracic vertebrae | 35 Tenth rib |
| 2 Internal thoracic artery and vein | 14 Left dome of diaphragm | 24 Left sympathetic chain | 36 Ninth rib |
| 3 External oblique | 15 Spleen | 25 Hemiazygos vein | 37 Eighth rib |
| 4 Extrapericardial pad of fat | 16 Lower lobe of lung | 26 Azygos vein | 38 Seventh rib |
| 5 Left ventricle | 17 Serratus anterior | 27 Thoracic duct | 39 Sixth rib |
| 6 Interventricular septum | 18 Latissimus dorsi | 28 Aorta | 40 Middle lobe of right lung |
| 7 Right ventricle | 19 Trapezius | 29 Oesophagus | 41 Sixth costal cartilage |
| 8 Tricuspid valve | 20 Erector spinae | 30 Left vagus nerve (X) | 42 Fifth costal cartilage |
| 9 Coronary sinus | 21 Tip of spine of eighth thoracic vertebra | 31 Right vagus nerve (X) | 43 Sternum |
| 10 Diaphragm | 22 Spinal cord within dural sheath | 32 Inferior vena cava | |
| 11 Fibrous pericardium | 23 Body of ninth thoracic vertebra, with part of intervertebral disc | 33 Right hepatic vein | |
| 12 Line of fusion of diaphragm and pericardium | | 34 Right lobe of liver | |
| | | | 44 Oblique fissure |



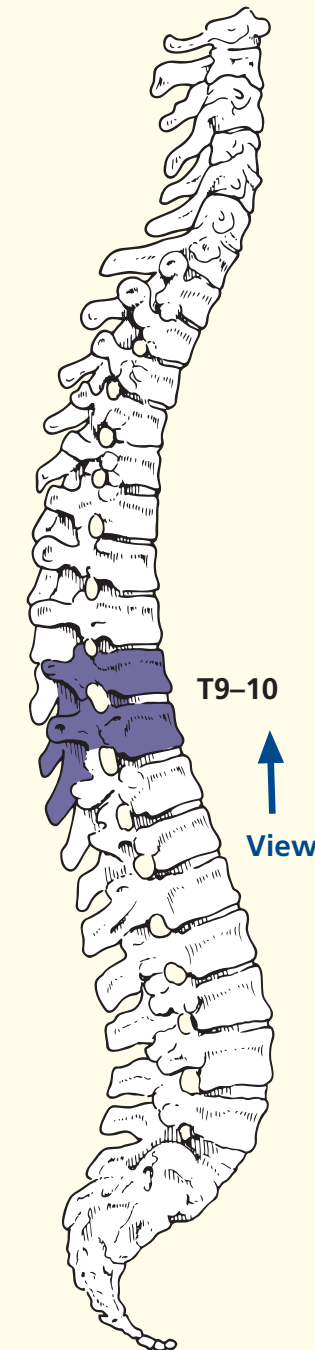
Axial computed tomogram (CT)

Axial computed tomogram (CT)

Orientation



Section level



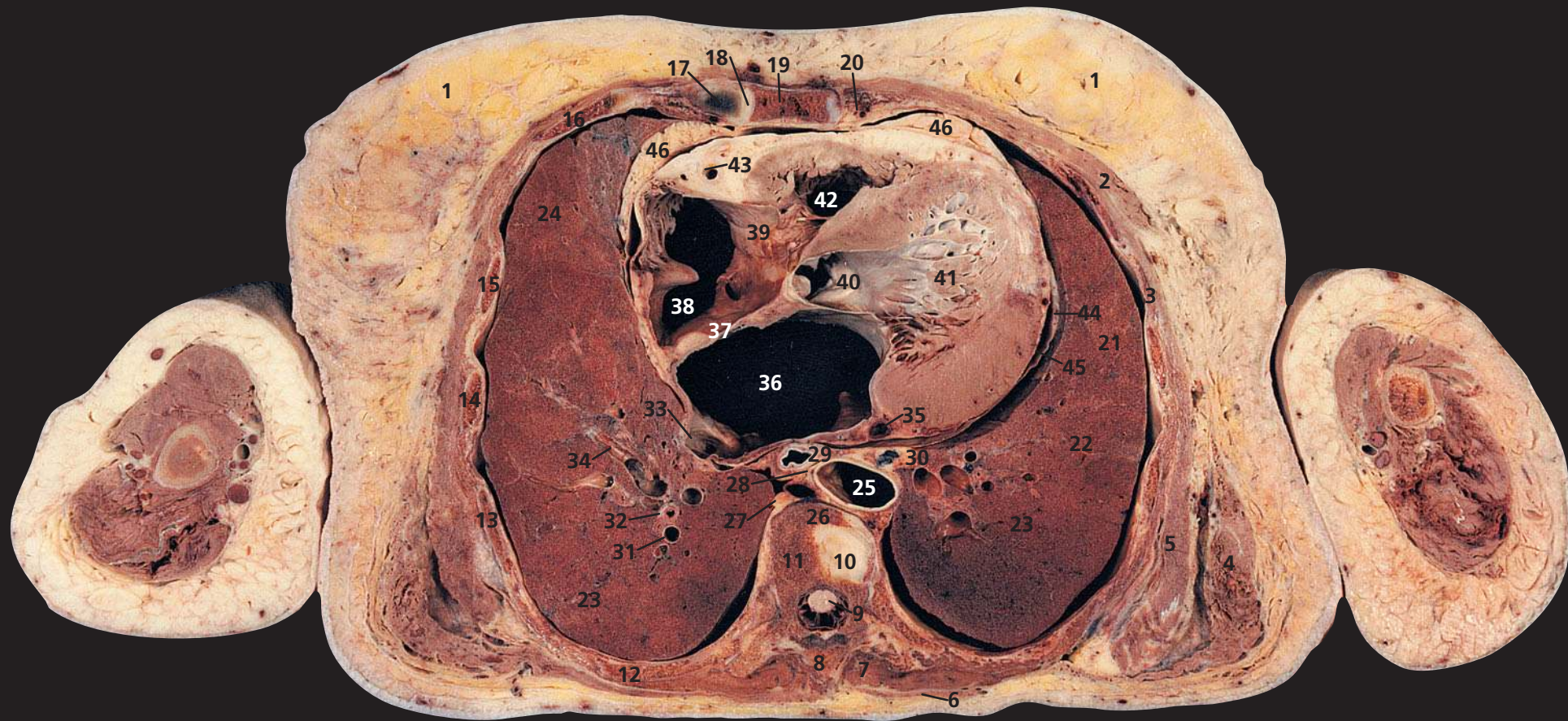
Notes

This section is at the level of the body of the ninth thoracic vertebra (**23**) and traverses the dome of the left diaphragm (**14**). The cranial portion of the spleen (**15**) is, therefore, revealed.

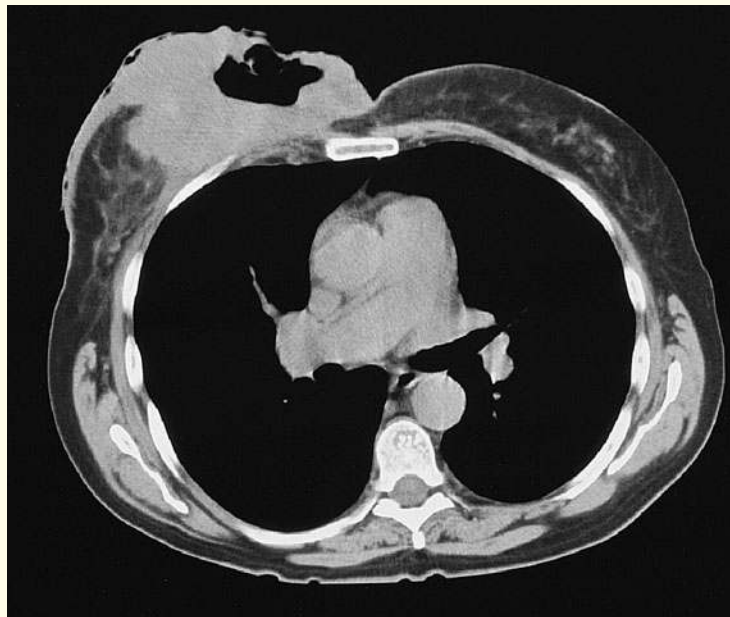
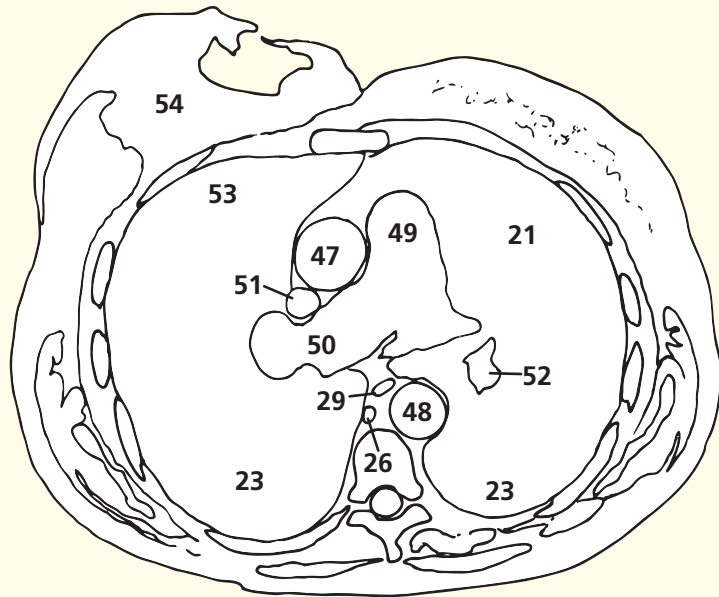
The fusion of the diaphragm (**10**) with the base of the fibrous pericardium (**11**) is shown clearly at this point.

The massive size of the hepatic veins as they drain into the inferior vena cava (**32**) is well demonstrated in this section, which passes through the right hepatic vein at its termination (**33**).

The aorta (**28**) at this level has become the immediate posterior relation of the oesophagus (**29**), just as it is about to pass through its hiatus in the diaphragm (**10**).

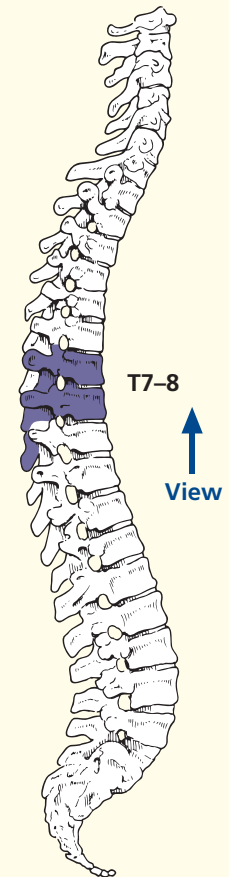


- | | | | |
|----------------------------------------------------------------------------------|--------------------------------------|----------------------------------------------|--------------------------------|
| 1 Breast | 14 Fifth rib | 29 Oesophagus | 41 Left ventricle |
| 2 Pectoralis major | 15 Fourth rib | 30 Mediastinal lymph node | 42 Right ventricle |
| 3 Intercostal muscles | 16 Third rib | 31 Pulmonary arterial branch in lower lobe | 43 Right coronary artery |
| 4 Latissimus dorsi | 17 Third costal cartilage | 32 Bronchus – segmental branch in lower lobe | 44 Left phrenic nerve |
| 5 Serratus anterior | 18 Third sternocostal joint | 33 Orifice of right inferior pulmonary vein | 45 Fibrous pericardium |
| 6 Trapezius | 19 Sternum | 34 Right inferior pulmonary vein | 46 Extrapericardial fat pad |
| 7 Erector spinae | 20 Internal thoracic artery and vein | 35 Coronary sinus | 47 Ascending aorta |
| 8 Spine of seventh thoracic vertebra | 21 Upper lobe of left lung (lingula) | 36 Left atrium | 48 Descending aorta |
| 9 Spinal cord within dural sheath | 22 Left oblique fissure | 37 Interatrial septum | 49 Pulmonary trunk |
| 10 Part of intervertebral disc between the seventh and eighth thoracic vertebrae | 23 Lower lobe of lung | 38 Right atrium | 50 Right pulmonary artery |
| 11 Body of seventh thoracic vertebra | 24 Middle lobe of right lung | 39 Tricuspid valve | 51 Superior vena cava |
| 12 Seventh rib | 25 Aorta | 40 Aortic valve | 52 Left basal pulmonary artery |
| 13 Sixth rib | 26 Azygos vein | | 53 Upper lobe of right lung |
| | 27 Right sympathetic chain | | 54 Carcinoma right breast |
| | 28 Thoracic duct | | |



Axial computed tomogram (CT)

Section level



Notes

This section of a female subject passes through the body of the seventh thoracic vertebra (**11**) and through the third sternocostal joint (**18**). Note the general smaller configuration of the female thorax and the smaller, less bulky muscles.

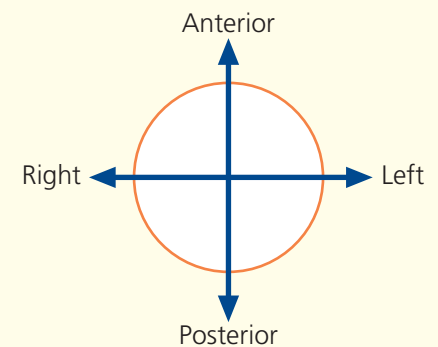
The breast (**1**) contains the mammary gland. This extends vertically from the second to the sixth rib and transversely from the side of the sternum to near the mid-axillary line. The gland is situated within the superficial fascia and is separated from the fascia covering pectoralis major, serratus anterior and the external oblique muscle by loose areolar tissue. In old age, as in this subject, the glandular

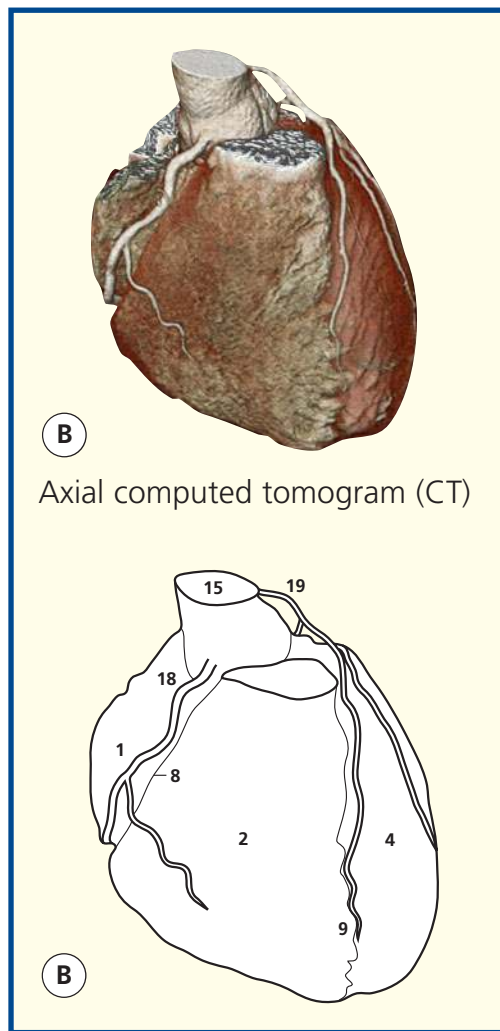
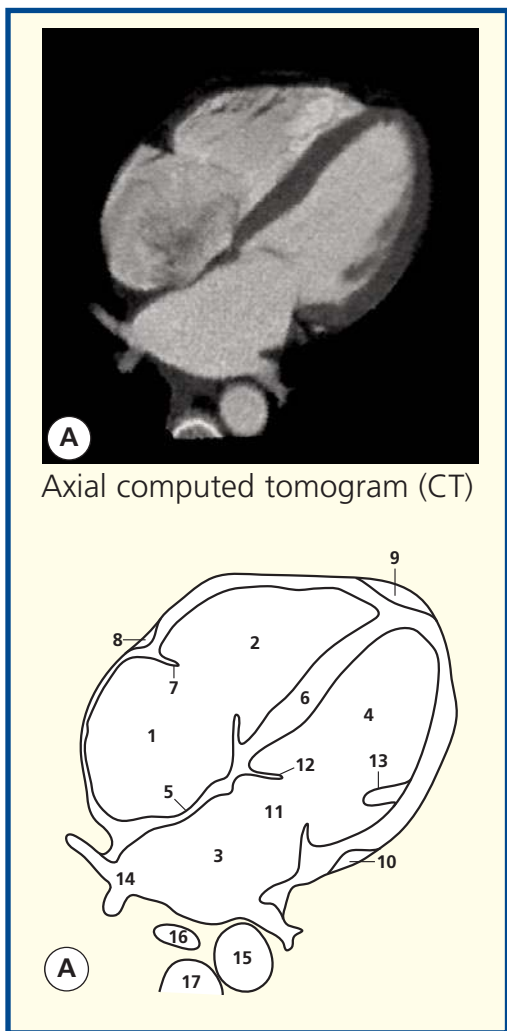
tissue becomes atrophied. The inner wall of the left ventricle, immediately proximal to the aortic valve (**40**), is smooth-walled and termed the aortic vestibule.

This CT image shows a patient with a large carcinoma of the right breast, which has ulcerated and extended into, and infiltrated, a wide area of adjacent skin. The anatomical level is considerably more cranial than the cadaveric section; it corresponds closely to that shown in Axial section 6 of the male thorax.

Note that in this section, the margin of the mass of left ventricular muscle (**41**) has been cut across; there is infarction in the anterior free wall.

Orientation





Images A–B

- 1 Right atrium
- 2 Right ventricle
- 3 Left atrium
- 4 Left ventricle
- 5 Interatrial septum
- 6 Interventricular septum

- 7 Tricuspid valve
- 8 Right atrioventricular groove for right coronary artery
- 9 Interventricular groove for anterior branch of left coronary artery
- 10 Left atrioventricular groove for circumflex branch of left coronary artery
- 11 Mitral valve
- 12 Anterior leaflet of mitral valve
- 13 Papillary muscle
- 14 Pulmonary vein

- 15 Aorta
- 16 Oesophagus
- 17 Thoracic vertebra
- 18 Right coronary artery
- 19 Left coronary artery

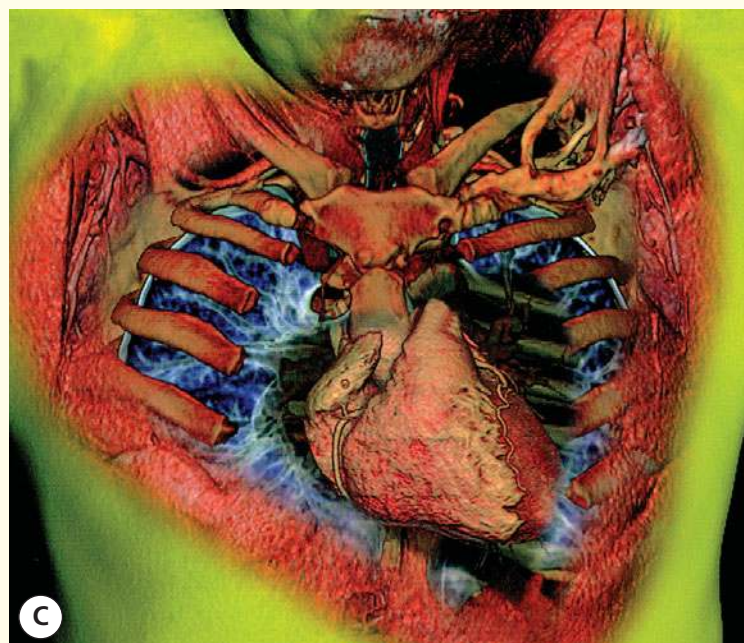
Notes

Multidetector CT with rapid data acquisition has opened up huge opportunities for imaging the heart and great vessels. If the data for a whole revolution of the CT gantry can be acquired in less than 400 ms, then a considerable amount of information can be obtained in the relatively quiescent period of the cardiac cycle. If the patient's heart rate is slow and regular, then a succession of images can be obtained during one breath-hold at the same phase of the cardiac cycle; these can be combined and a three-dimensional dataset created. This can provide exceptional anatomical (and, increasingly, functional) information.

The four-chamber view (A) is a multiplanar two-

dimensional reconstruction so that all four chambers can be seen on one oblique image. This is a standard view used in many imaging investigations, including CT, ultrasound and MRI. It allows direct comparison of the left and right sides of the heart. It elegantly shows the interventricular septum. The close relationship of the oesophagus to the posterior aspect of the left atrium explains the advantages of transoesophageal echocardiography.

The coloured three-dimensional surface rendered view of the ventricles and coronary arteries provides a good general overview but, in practice, the coronary arteries (B) are better displayed and analysed using more selective analysis tools.



C
Axial computed tomogram (CT)

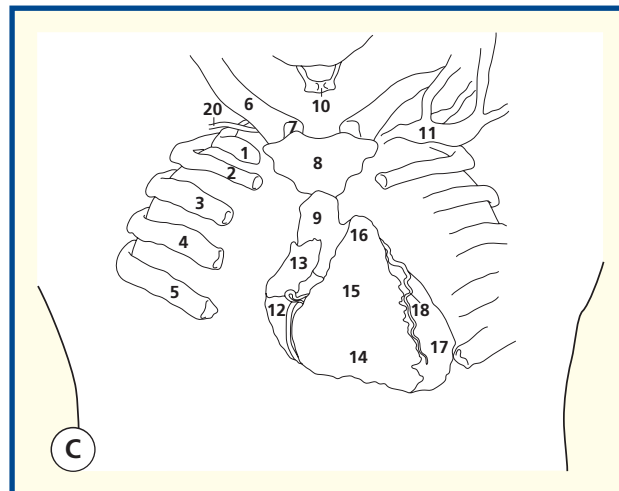
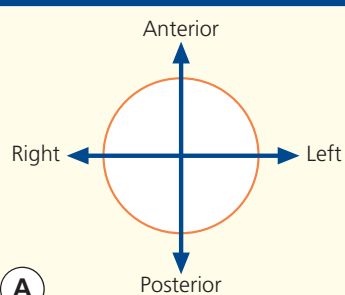


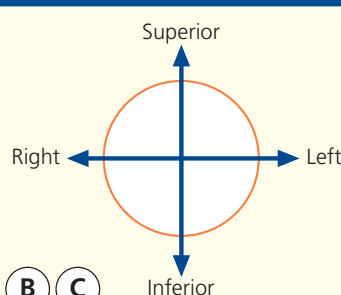
Image C

- 1 First rib (right)
- 2 Second rib
- 3 Third rib
- 4 Fourth rib
- 5 Fifth rib
- 6 Clavicle
- 7 Sternoclavicular joint
- 8 Sternum – manubrium
- 9 Sternum – body
- 10 Hyoid bone
- 11 Left subclavian vein
- 12 Right atrium
- 13 Right atrial appendage
- 14 Right ventricle
- 15 Right ventricular outflow tract
- 16 Pulmonary trunk
- 17 Left ventricle
- 18 Left anterior descending – branch of left coronary artery
- 19 Right coronary artery
- 20 Right subclavian artery

Orientation



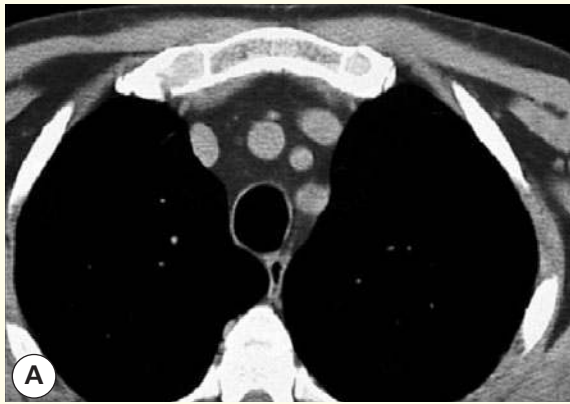
Orientation



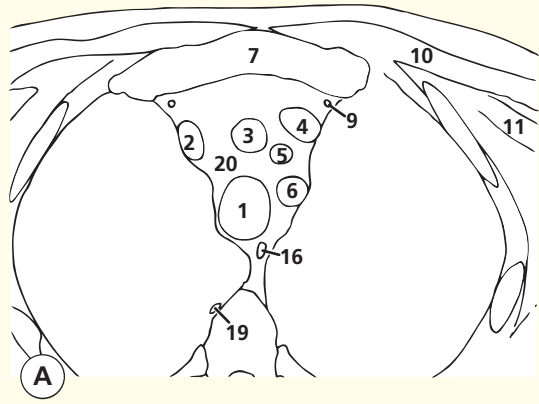
Notes

This edited 3D view of the chest (C) has been presented as a collage whereby the skin and subcutaneous tissues have been 'peeled away' to expose the internal structures of the chest. By using different window widths and colouring, it has been possible to demonstrate some lung detail in areas, which have not been obscured by overlying structures. These images were obtained during a long bolus injection of dilute iodinated contrast medium via the left arm. Hence the left subclavian vein (11) is well demonstrated but not the right. The heart, great vessels and coronary arteries are rendered opaque by

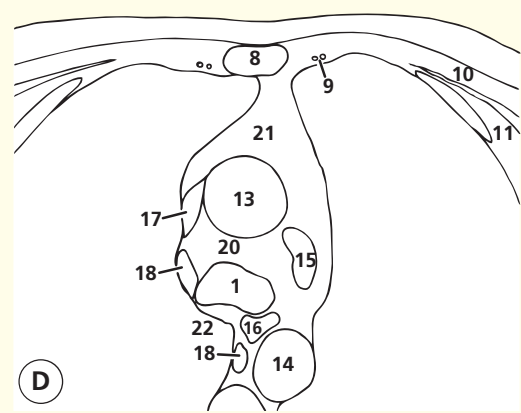
the contrast medium and are well shown. It is just possible to see the right subclavian artery (20) between the right first rib (1) and the right clavicle (6). The coronary vessels are well shown with the left anterior descending artery (LAD, 18) seen in the interventricular groove and the right coronary artery (19) seen in the right atrioventricular groove. Note the way that the 2nd rib (2) leads to the sterno-manubrial angle (of Louis). Of course the chondral part of the rib, which articulates with the sternomanubrial joint, is not sufficiently calcified to be seen at these settings.



Axial computed tomogram (CT)



A



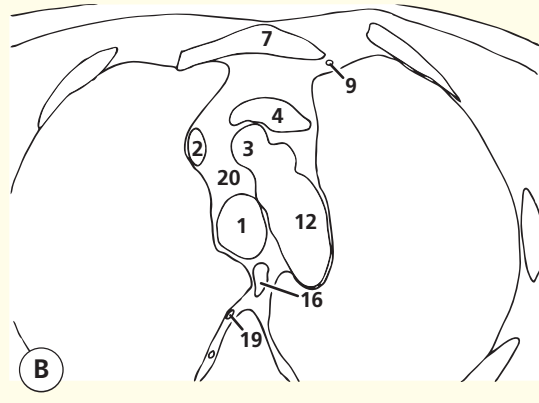
D



Axial computed tomogram (CT)



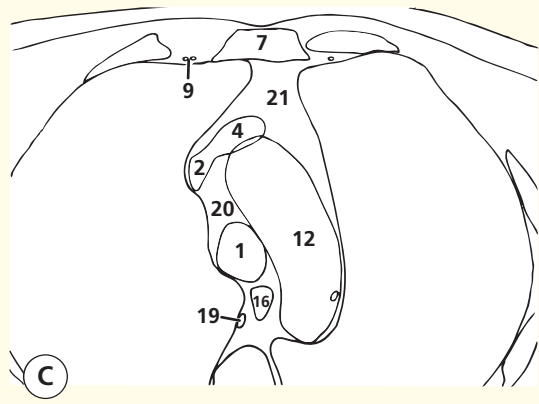
Axial computed tomogram (CT)



B



Axial computed tomogram (CT)

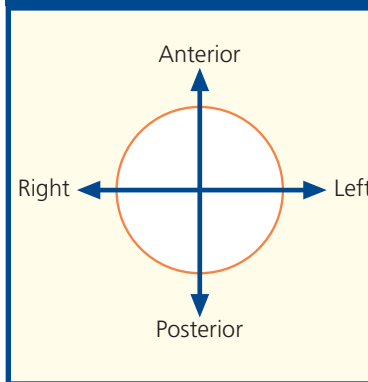


C

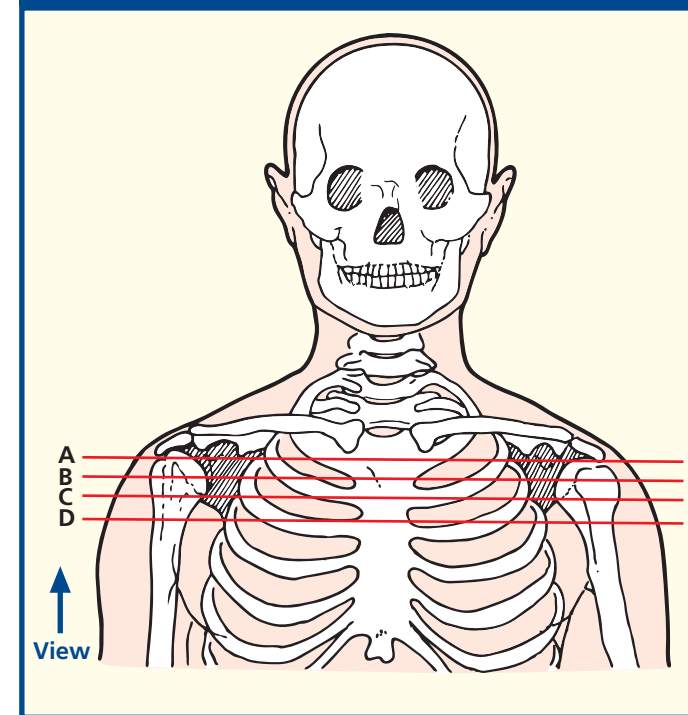
Images A–D

- | | |
|-------------------------------------|-----------------------------------------------------------------|
| 1 Trachea | 12 Aortic arch (with fleck of calcification in wall in image C) |
| 2 Right brachiocephalic vein | 13 Ascending aorta |
| 3 Brachiocephalic artery | 14 Descending aorta |
| 4 Left brachiocephalic vein | 15 Left pulmonary artery |
| 5 Left common carotid artery | 16 Oesophagus |
| 6 Left subclavian artery | 17 Superior vena cava |
| 7 Manubrium of sternum | 18 Azygos vein |
| 8 Body of sternum | 19 Right superior intercostal vein |
| 9 Internal thoracic artery and vein | 20 Fat in pretracheal space |
| 10 Pectoralis major | 21 Fat in anterior mediastinal space (with thymic remnant) |
| 11 Pectoralis minor | 22 Azygos-oesophageal recess |

Orientation



Section level



Notes

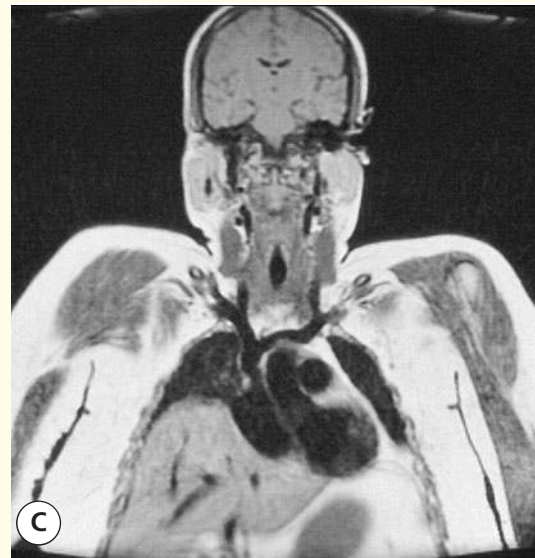
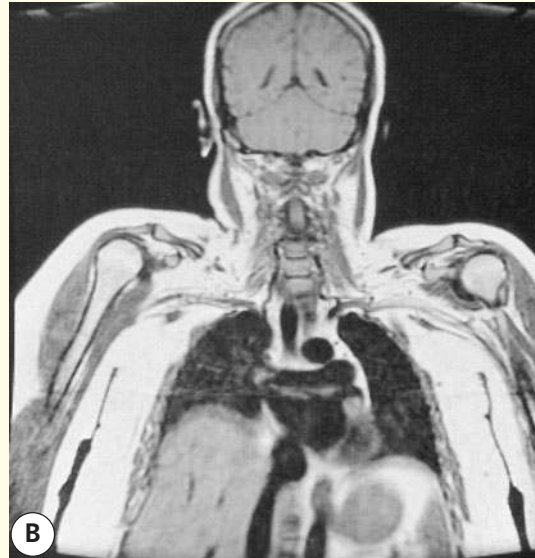
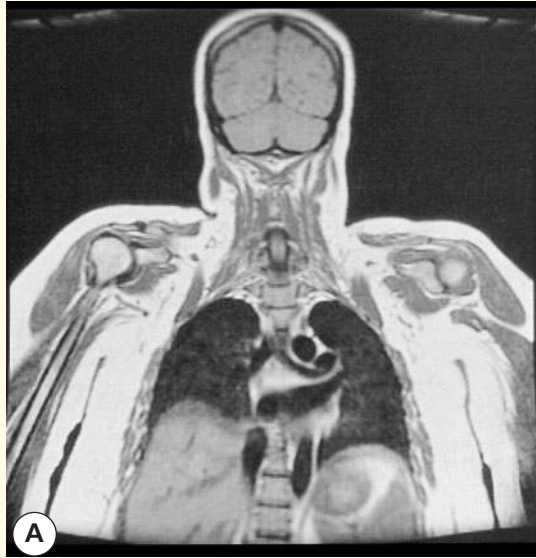
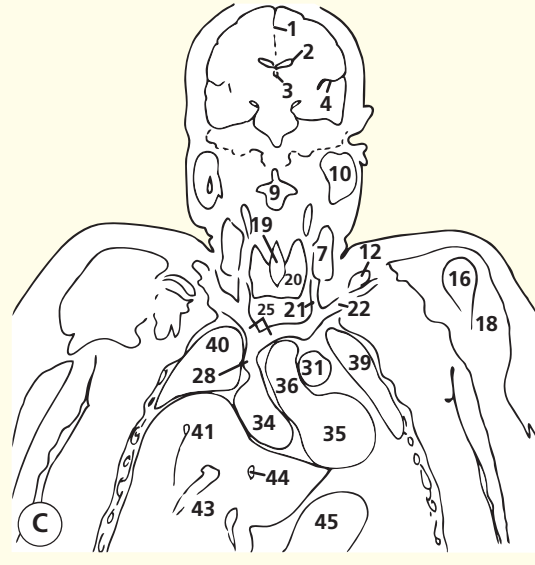
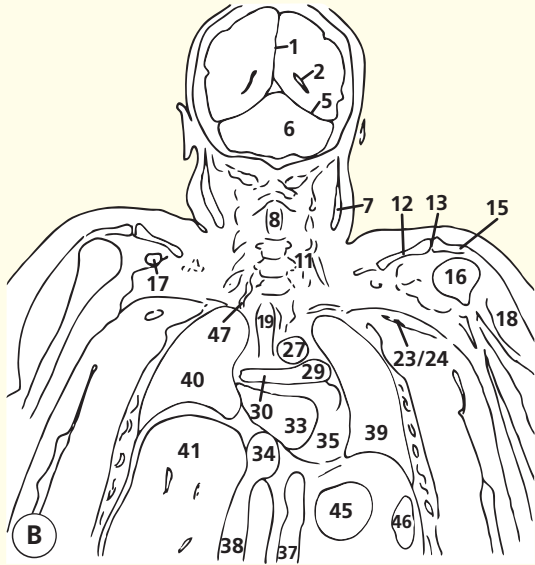
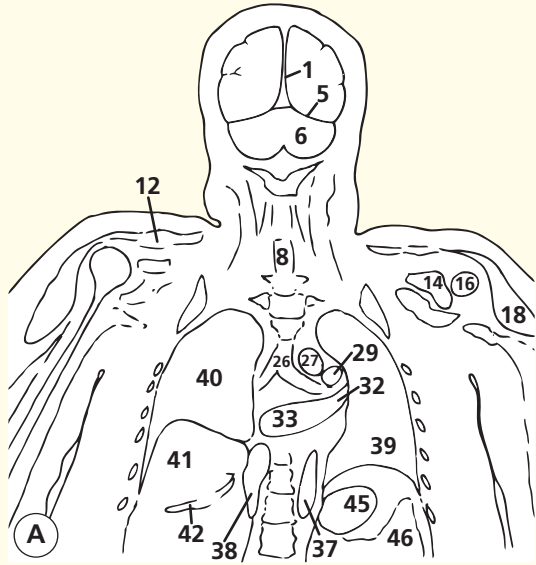
This patient has copious mediastinal fat, which makes the normal structures very conspicuous. Enlarged lymph nodes would show up well in such a patient (see Axial section 6). If such nodes lie in the pretracheal space (20), then biopsy material can be obtained via mediastinoscopy.

The trachea (1) is bifurcating on image D; this point is known as the carina. The left pulmonary artery (15) lies at a more cranial level than the right; it is just entering part of the section shown on image D. It appears indistinct because only part of the thickness of the slice is occupied by the

structure (partial volume effect). The space immediately caudal to the aortic arch and cranial to the bifurcation of the pulmonary artery is known as the subaortic fossa or aortopulmonary window. The ligamentum arteriosum (the obliterated ductus arteriosus passing from the left pulmonary artery to the aorta) runs through this space. This fossa may also contain enlarged lymph nodes.

The azygos vein (18) can be seen approaching the posterior aspect of the superior vena cava (17) on image D. This venous system, which developed at an early stage of embryological development of

the cardinal veins, is of immense importance when the vena cava becomes blocked for any reason (usually by a tumour). For example, in superior vena cava obstruction caused by mediastinal nodal enlargement secondary to carcinoma of the bronchus, the venous return from the head, neck and arms will go via collateral veins around the scapula and retrogradely in the intercostal veins into the azygos and thence back to the heart, bypassing the obstruction in the superior mediastinum.

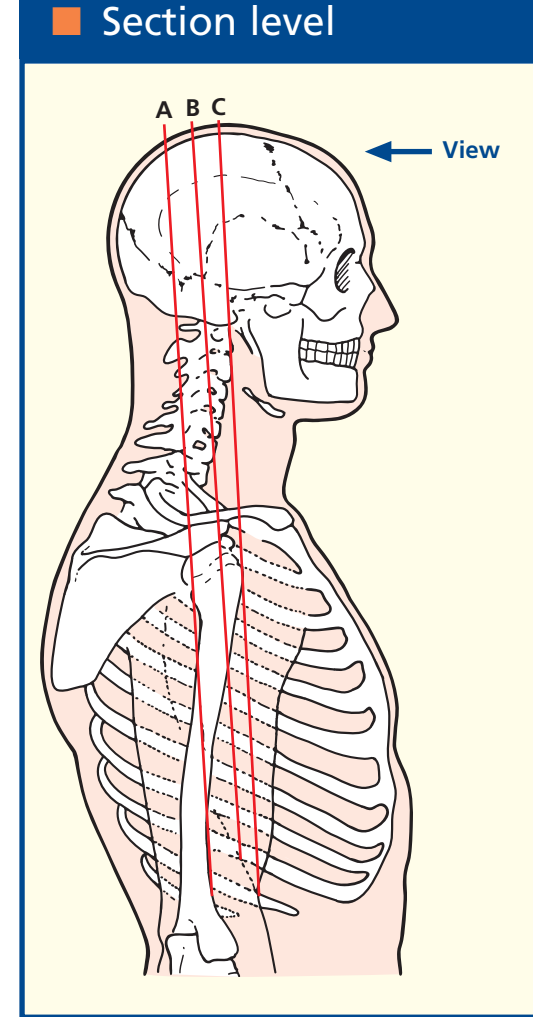
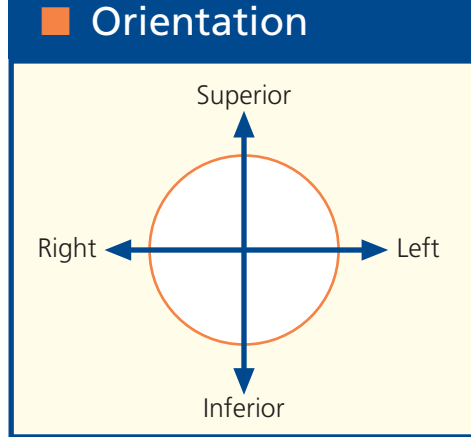


Coronal magnetic resonance image (MRI)

Coronal magnetic resonance image (MRI)

Coronal magnetic resonance image (MRI)

- | | |
|-----------------------------------------|----------------------------------------------------------|
| 1 Falx cerebri | 25 Brachiocephalic vein |
| 2 Lateral ventricle | 26 Carina (bifurcation of trachea into two main bronchi) |
| 3 Third ventricle | 27 Aortic arch |
| 4 Lateral sulcus (Sylvian fissure) | 28 Superior vena cava |
| 5 Tentorium cerebelli | 29 Left pulmonary artery |
| 6 Cerebellum | 30 Right pulmonary artery |
| 7 Sternocleidomastoid | 31 Main pulmonary artery |
| 8 Spinal cord | 32 Left superior pulmonary vein |
| 9 Second cervical vertebra (axis) | 33 Left atrium |
| 10 Parotid gland | 34 Right atrium |
| 11 Scalene muscles | 35 Left ventricle |
| 12 Clavicle | 36 Ascending aorta |
| 13 Acromioclavicular joint | 37 Descending aorta |
| 14 Glenoid fossa of scapula | 38 Inferior vena cava |
| 15 Acromion process of scapula | 39 Left lung |
| 16 Humeral head | 40 Right lung |
| 17 Coracoid process of scapula | 41 Liver |
| 18 Deltoid | 42 Right hepatic vein |
| 19 Trachea | 43 Middle hepatic vein |
| 20 Thyroid gland | 44 Left hepatic vein |
| 21 Internal jugular vein | 45 Stomach |
| 22 Subclavian vein | 46 Spleen |
| 23 Axillary vessels | 47 Vertebral artery |
| 24 Brachial plexus and resulting nerves | |



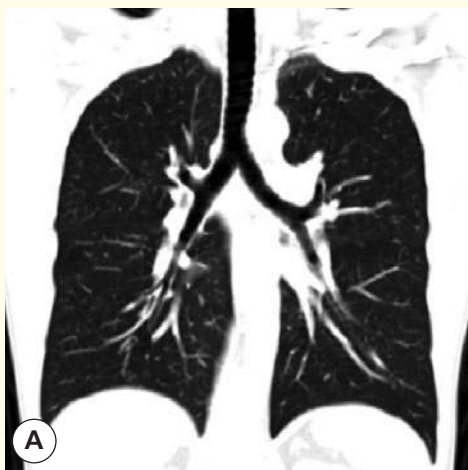
Notes

These three T1-weighted coronal magnetic resonance images are included to show the overall relations of the head, neck, thorax and upper abdomen. Only rarely would such a large field of view be used in clinical practice, as the anatomical spatial resolution is inevitably compromised. Of course, the exact relations on the coronal plane

depend much on the degree of thoracic spine kyphosis, body habitus and degree of inspiration. The relations in this relatively obese subject are fairly representative.

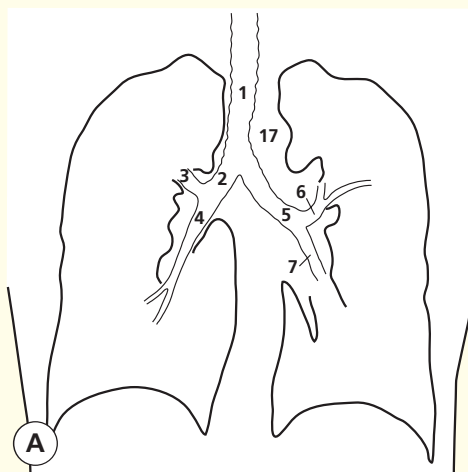
A wide field of view is used when trying to compare structures on the two sides. The brachial plexus (image B, **24**) is a case in point. In breast

cancer, the axilla may be affected both by nodal metastases and by the effects of radiotherapy. These can cause either neurological symptoms in the arm or lymphoedema. Coronal images of the two axillae together can be very helpful in this differentiation, which can be difficult on clinical grounds.

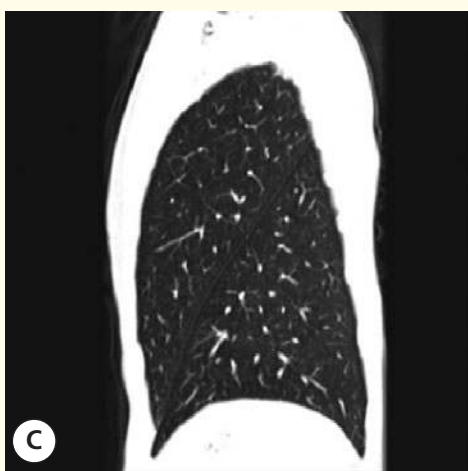


A

Coronal computed tomogram (CT)

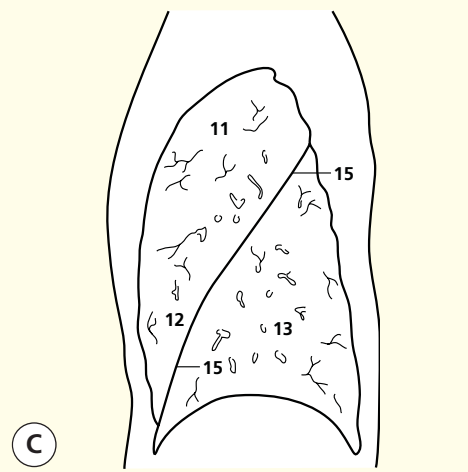


A

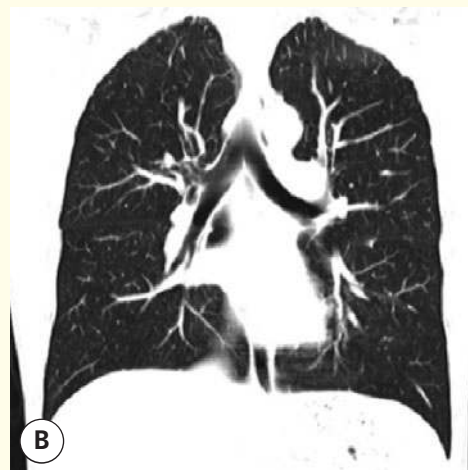


C

Sagittal computed tomogram (CT)
Left Lung

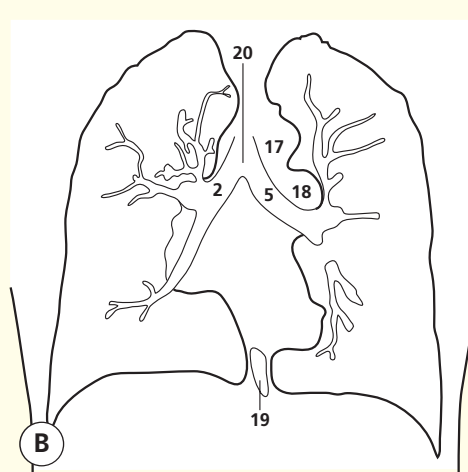


C

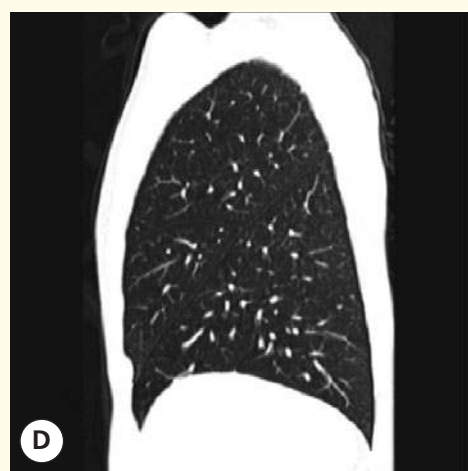


B

Coronal computed tomogram (CT)

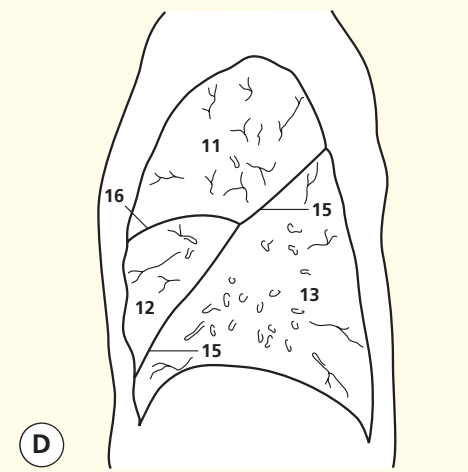


B

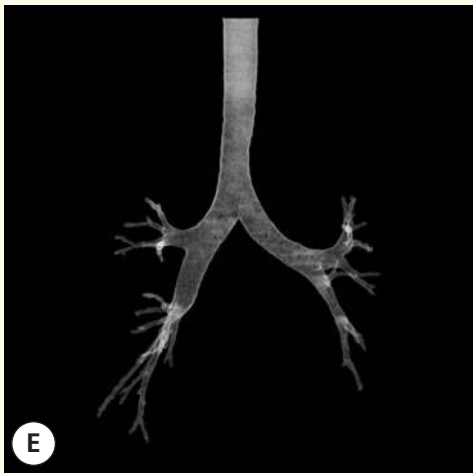


D

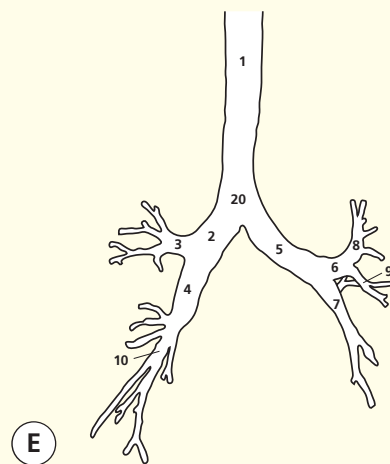
Sagittal computed tomogram (CT)
Right Lung



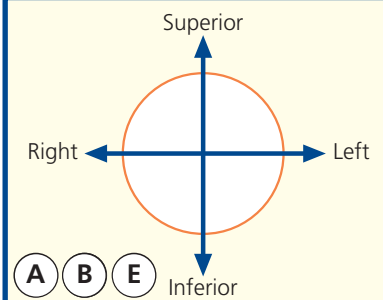
D



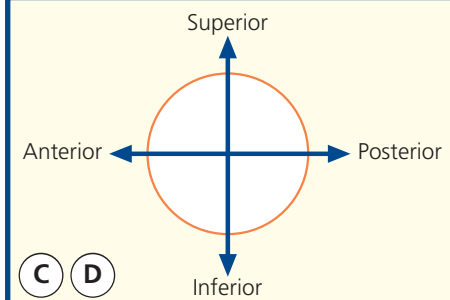
Reconstructed 3D computed tomogram (CT)



Orientation



Orientation



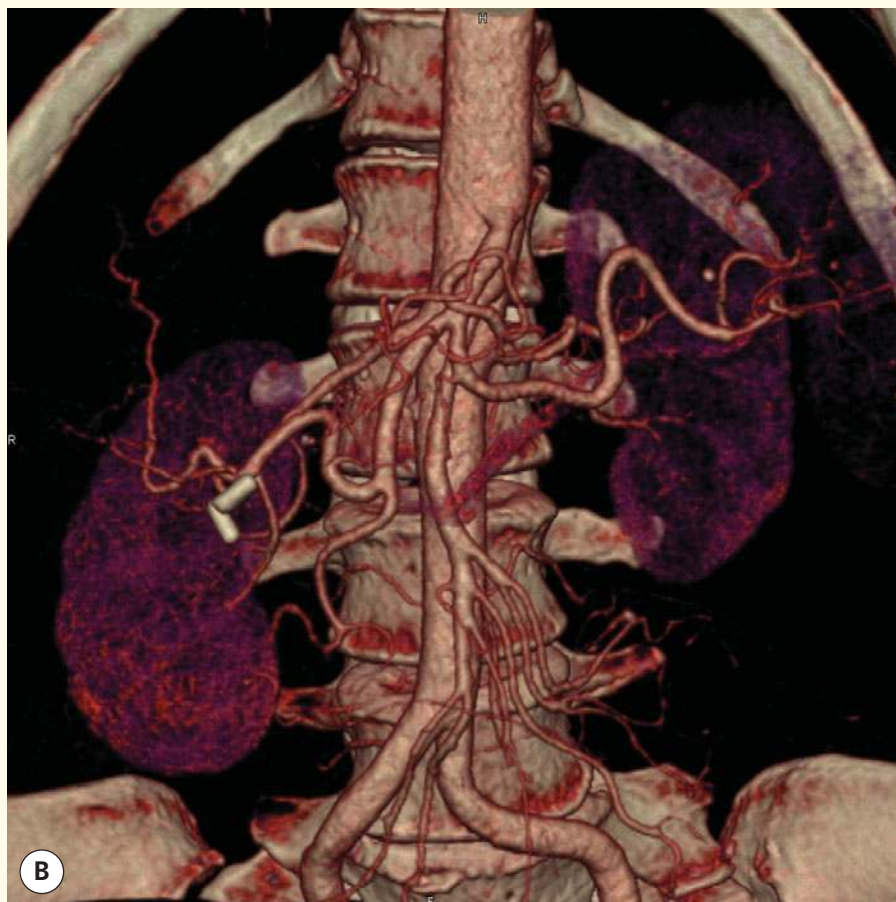
- | | |
|-------------------------------------|-----------------------------------------------|
| 1 Trachea | 12 Lingula (on the left) |
| 2 Right main bronchus | 13 Lower lobe |
| 3 Right upper lobe bronchus | 14 Middle lobe (on the right) |
| 4 Bronchus intermedius | 15 Oblique fissure |
| 5 Left main bronchus | 16 Horizontal fissure (on the right) |
| 6 Left upper lobe/lingular bronchus | 17 Aortic knuckle |
| 7 Left lower lobe bronchus | 18 Left pulmonary artery |
| 8 Left upper lobe bronchus | 19 Oesophagus (containing some swallowed air) |
| 9 Left upper lobe lingular bronchus | 20 Carina – the bifurcation of the trachea |
| 10 Right lower lobe bronchus | |
| 11 Upper lobe | |

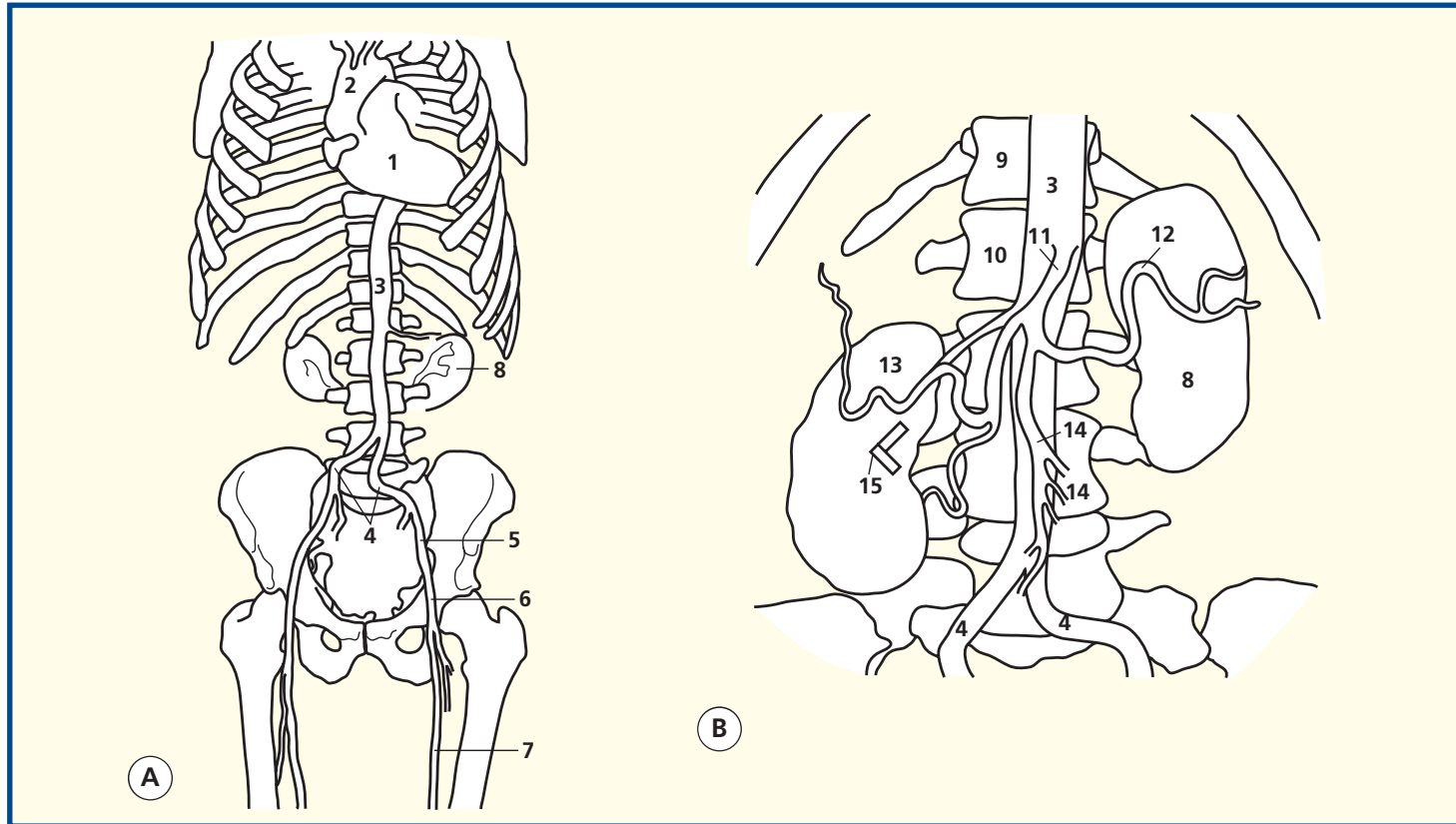
Notes

A spiral CT dataset of the chest at full inspiration has been obtained on a multidetector CT system. Next, the individual thin slices have been loaded together to form a three-dimensional volume with each voxel isometric so that the *x*, *y* and *z* resolutions of the resulting pixels are identical. This three-dimensional dataset can be analysed in a variety of ways.

The first two images show coronal multiplanar reconstructions viewed at lung settings to show the anatomy of the airways in this plane. The middle images shows sagittal reconstructions to demonstrate the lobes and fissures of the left and right lungs. The

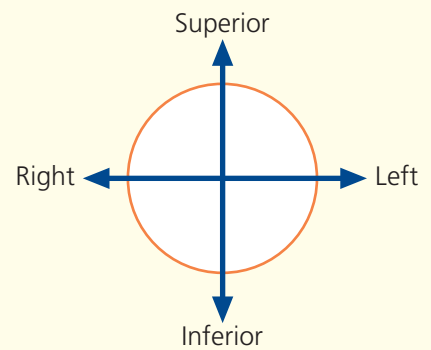
lowest image is a three-dimensional reconstruction just extracting out the airways and accentuating the interface between air and soft tissue – this provides a graphic map of the anatomy of the trachea and main bronchi. These images elegantly show the more vertical nature of the right main bronchus (2) – hence the peanut and the endotracheal tube tend to enter the right side preferentially. They also show the greater length of the left main bronchus (5); on the right, the takeoff for the upper lobe bronchus can be very close to the carina (20, the point of bifurcation of the trachea into two main bronchi).





- | | |
|-----------------------------------|------------------------------------------|
| 1 Heart | 9 Twelfth thoracic vertebra |
| 2 Ascending aorta | 10 First lumbar vertebra |
| 3 Abdominal aorta | 11 Coeliac artery |
| 4 Common iliac artery | 12 Splenic artery |
| 5 External iliac artery | 13 Hepatic artery |
| 6 Common femoral artery | 14 Superior mesenteric artery and arcade |
| 7 Superficial femoral artery | 15 Cholecystectomy clips |
| 8 Kidney and pelvicalyceal system | |

Orientation

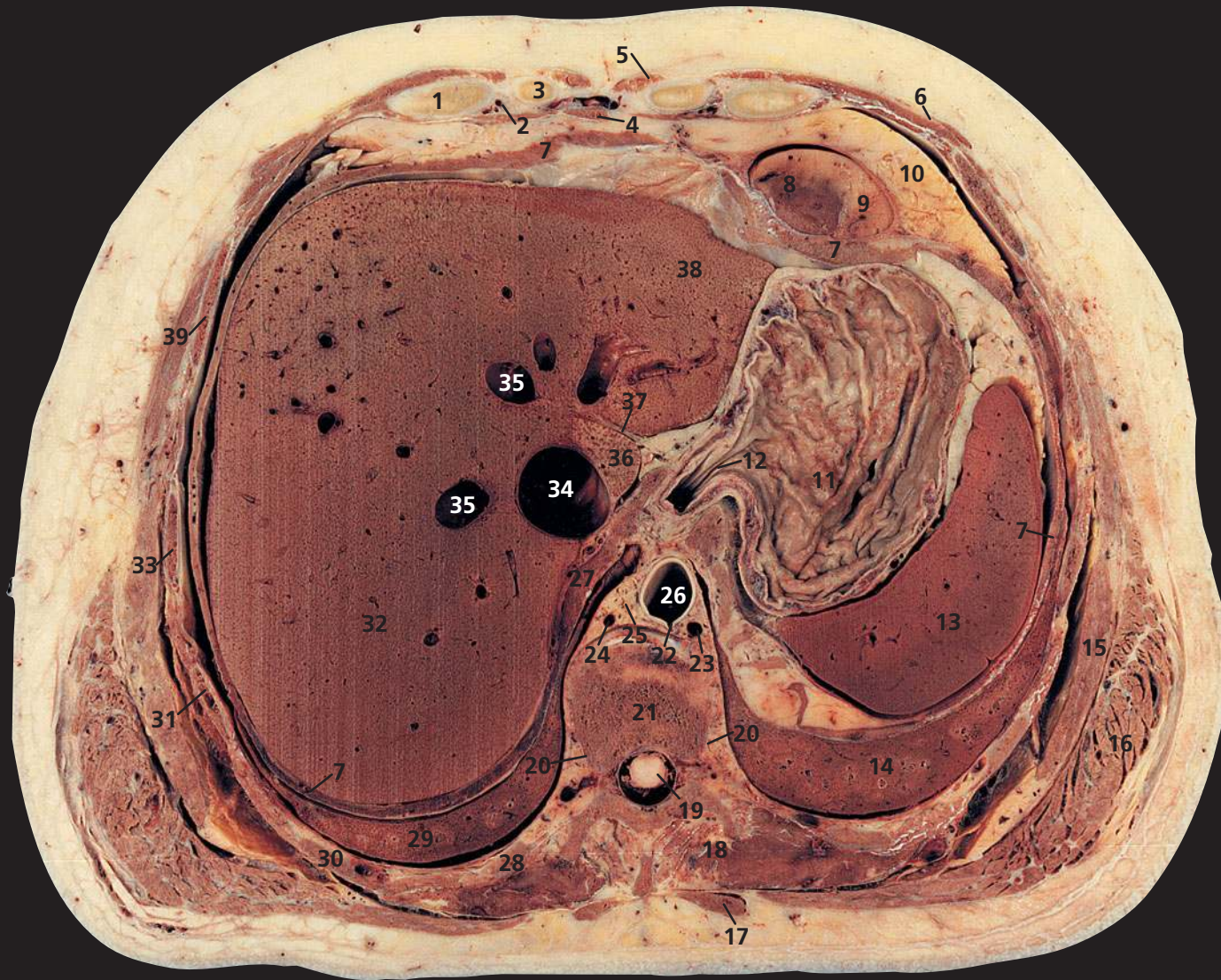


Notes

These two surface rendered 3D angiograms have been obtained on a modern CT system following the injection of standard iodinated contrast medium. The CT data were acquired during the aortic phase of the passage of contrast medium through the body and the images subsequently manipulated on the workstation.

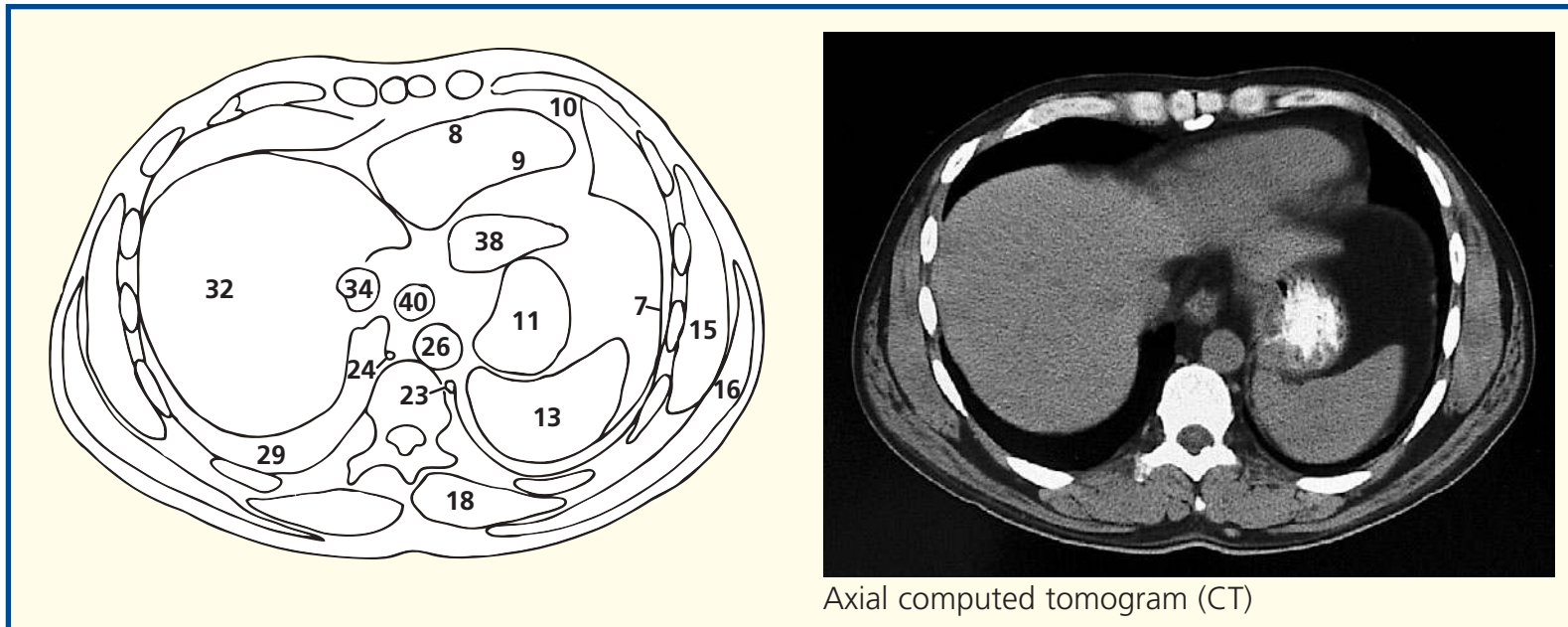
On the left image the global view allows the relationship of the heart, aorta, iliac and femoral vessels to be appreciated in relation to the skeletal structures. A test dose of contrast medium has been given sometime before and this accounts for the dense iodine being excreted from the kidneys and pelvicalyceal system (8).

On the right image the patient has had a previous laproscopic cholecystectomy and the clips (15) can readily be identified as very dense structures overlying the right kidney and close to the hepatic artery (13). Note the way the aorta changes in calibre at the L1 level; it is smaller inferior to the coeliac artery, superior mesenteric artery and the two renal arteries. The superior mesenteric arcade is beautifully demonstrated (14). The tortuosity of the iliac vessels is normal in middle age and above. The renal and splenic parenchyma are only faintly seen in this early phase.

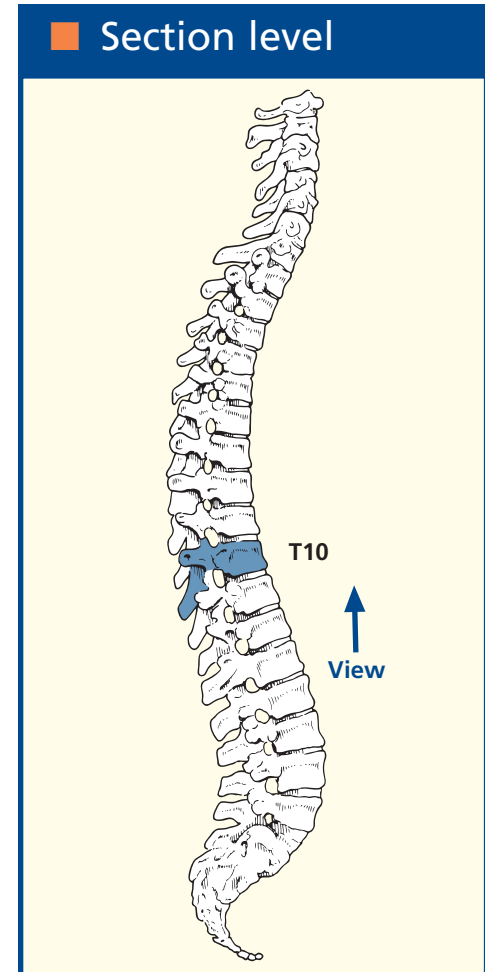


- | | | | | |
|---------------------------------------|------------------------------|------------------------------------|-----------------------------|----------------------------------------------------|
| 1 Sixth costal cartilage | 9 Left ventricle | 18 Erector spinae | 25 Thoracic duct | 34 Inferior vena cava |
| 2 Superior epigastric artery and vein | 10 Extrapericardial fat | 19 Spinal cord within dural sheath | 26 Aorta | 35 Hepatic vein |
| 3 Seventh costal cartilage | 11 Fundus of stomach | 20 Sympathetic chain | 27 Right crus of diaphragm | 36 Caudate lobe of liver |
| 4 Xiphoid | 12 Oesophagogastric junction | 21 Body of tenth thoracic vertebra | 28 Tenth rib | 37 Fissure for ligamentum venosum – lesser omentum |
| 5 Rectus abdominis | 13 Spleen | 22 Origin of intercostal artery | 29 Lower lobe of right lung | 38 Left lobe of liver |
| 6 External oblique | 14 Lower lobe of left lung | 23 Hemiazygos vein | 30 Ninth rib | 39 Sixth rib |
| 7 Diaphragm | 15 Serratus anterior | 24 Azygos vein | 31 Eighth rib | |
| 8 Right ventricle | 16 Latissimus dorsi | | 32 Right lobe of liver | |
| | 17 Trapezius | | 33 Seventh rib | |

40 Oesophagus



Axial computed tomogram (CT)



Notes

This section passes through the body of the tenth thoracic vertebra (21) and anteriorly transects the xiphoid (4).

The oesophagogastric junction (12) is seen in longitudinal section. This acts as a physiological sphincter in the prevention of reflux. The fundus of the stomach (11) contains air in the erect position but in the supine position is normally full of fluid. It is opaque in the CT image because of the ingested radio-opaque iodinated material.

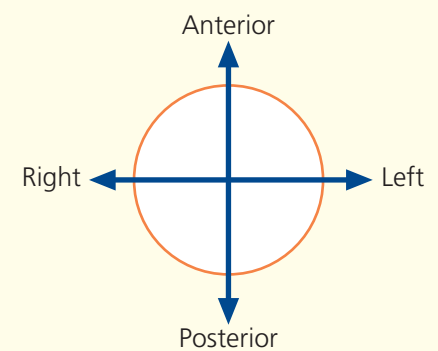
The lesser omentum is the fold of peritoneum that extends to the liver from the lesser curvature of the stomach and the commencement of the duodenum. Superiorly it attaches to the porta hepatis and to the bottom of the fissure for the ligamentum venosum (37). At

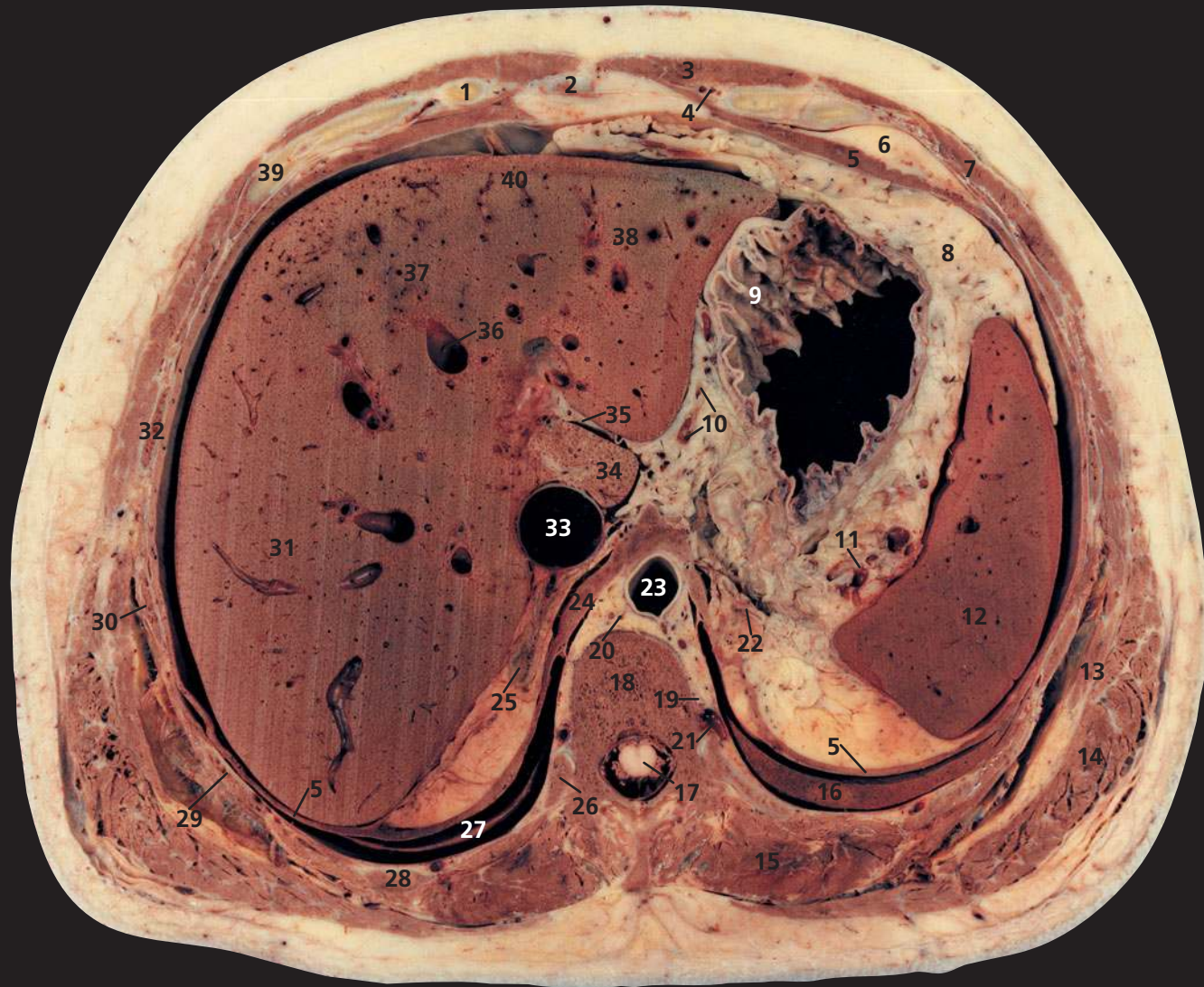
the cranial margin of this fissure, the lesser omentum reaches the diaphragm, where its two layers separate to surround the lower end of the oesophagus.

The ligamentum venosum is the thrombosed cord of the ductus venosus, which, in fetal life, connects the left portal vein to the anterior aspect of the inferior vena cava.

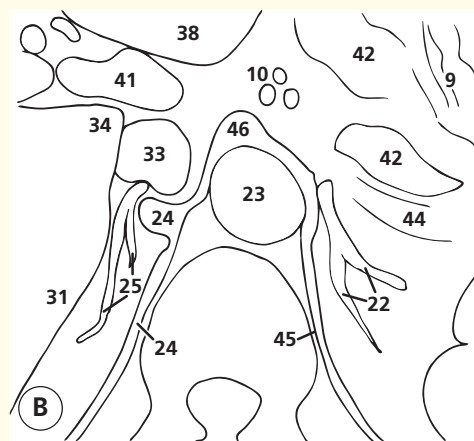
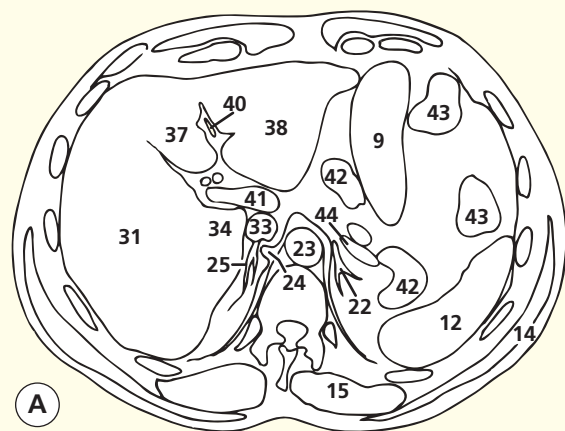
The spleen (13) lies against the diaphragm (7) opposite ribs 9 (30), 10 and 11. This section demonstrates clearly how a stab wound of the left lower chest posteriorly might traverse the pleural cavity, injure the lower lobe of the lung (14), traverse the diaphragm and lacerate the spleen. Similarly, a stab wound of the right chest at this level might injure the liver (32).

Orientation

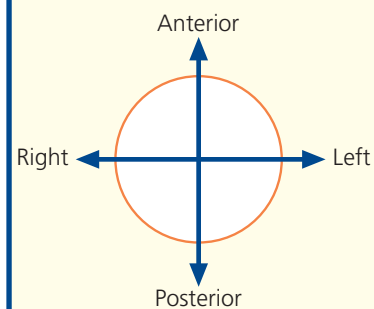




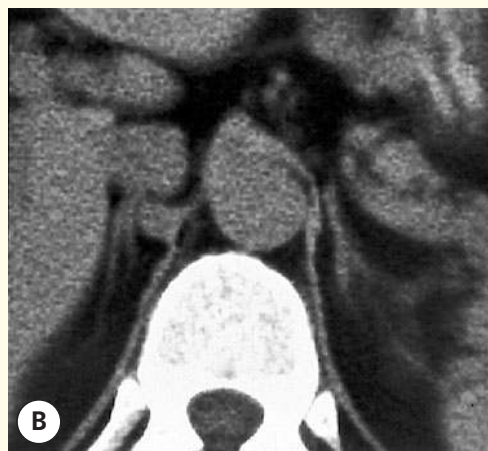
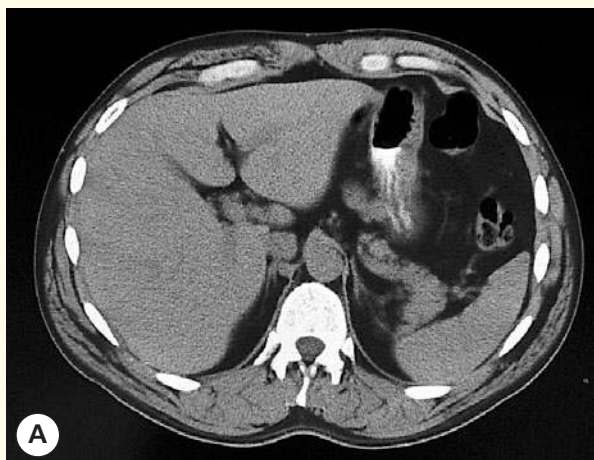
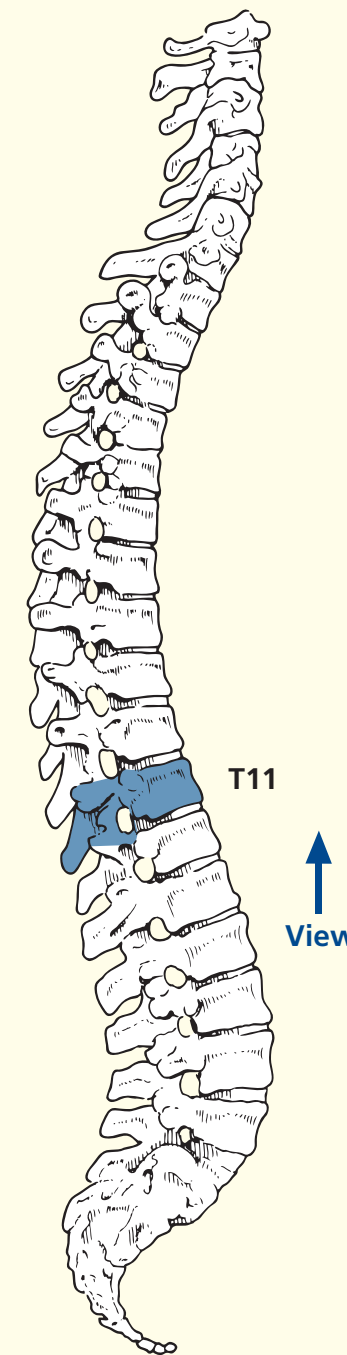
- | | | | | |
|---------------------------------------|---------------------------------------|-----------------------------|-----------------------------------------------------|-----------------------------------|
| 1 Seventh costal cartilage | 11 Splenic pedicle | 20 Thoracic duct | 31 Right lobe of liver | 39 Sixth costal cartilage and rib |
| 2 Xiphoid | 12 Spleen | 21 Intercostal vein | 32 Seventh rib | 40 Falciform ligament |
| 3 Rectus abdominis | 13 External oblique | 22 Left suprarenal gland | 33 Inferior vena cava | |
| 4 Superior epigastric artery and vein | 14 Latissimus dorsi | 23 Aorta | 34 Caudate lobe of liver | 41 Portal vein |
| 5 Diaphragm | 15 Erector spinae | 24 Right crus of diaphragm | 35 Lesser omentum in fissure for ligamentum venosum | 42 Pancreas |
| 6 Pericardial fat | 16 Lower lobe of left lung | 25 Right suprarenal gland | 36 Hepatic vein | 43 Left colic (splenic) flexure |
| 7 External oblique | 17 Spinal cord within dural sheath | 26 Head of eleventh rib | 37 Left lobe of liver medial segment | 44 Splenic vein |
| 8 Greater omentum | 18 Body of eleventh thoracic vertebra | 27 Lower lobe of right lung | 38 Left lobe of liver lateral segment | 45 Left crus of diaphragm |
| 9 Body of stomach | 19 Intercostal artery | 28 Tenth rib | | 46 Median arcuate ligament |
| 10 Left gastric artery branches | | 29 Ninth rib | | |
| | | 30 Eighth rib | | |



Orientation



Section level



Axial computed tomograms (CTs)

Notes

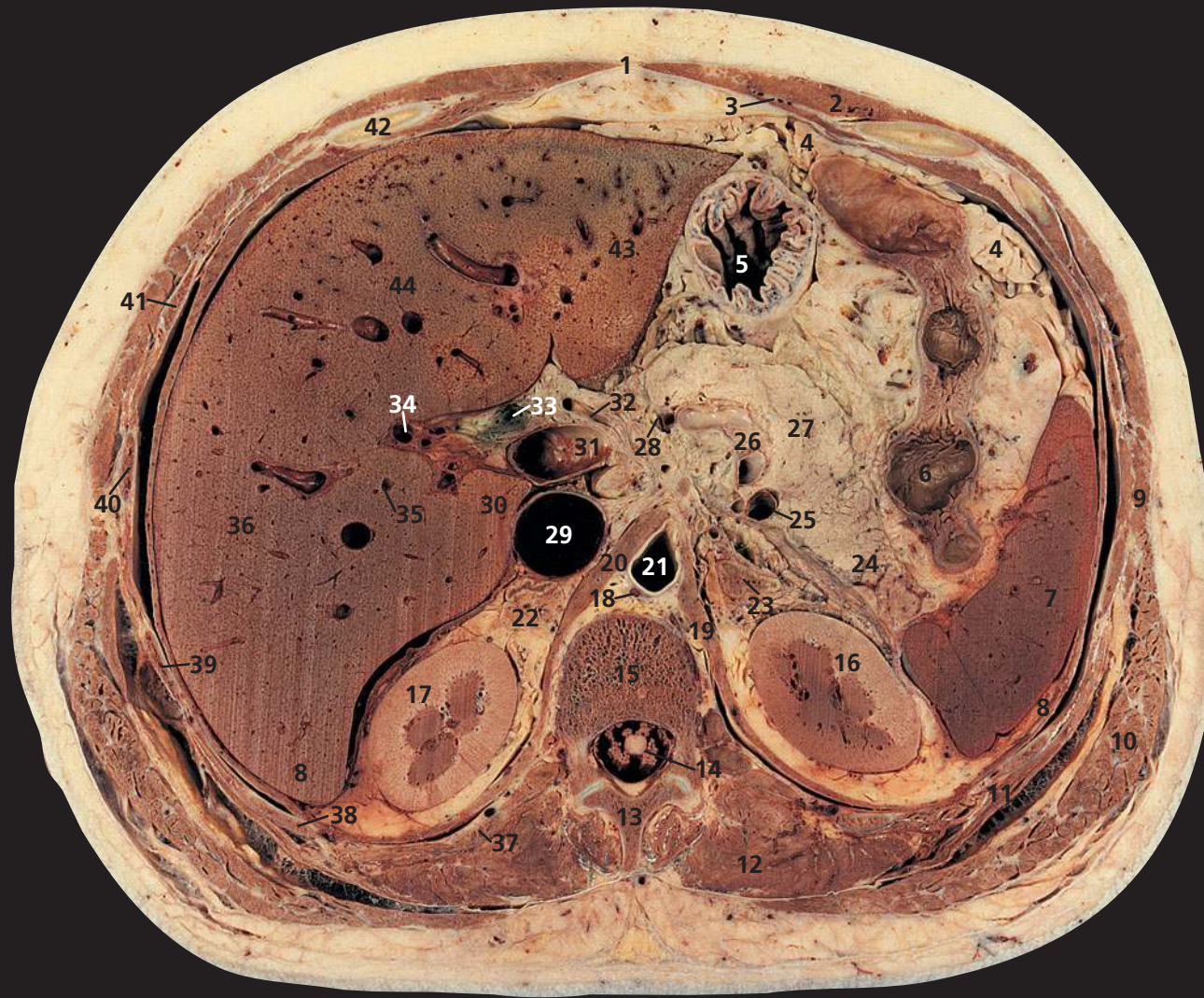
This section passes through the body of the eleventh thoracic vertebra (**18**) and the xiphoid (**2**).

This is the most caudal section that transects intrathoracic viscera – note the pericardial fat (**6**) anteriorly and the lower lobe of the left lung (**16**).

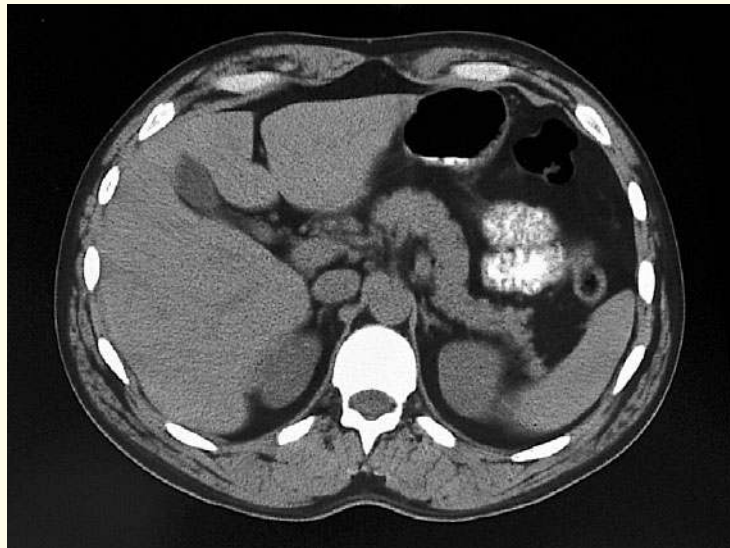
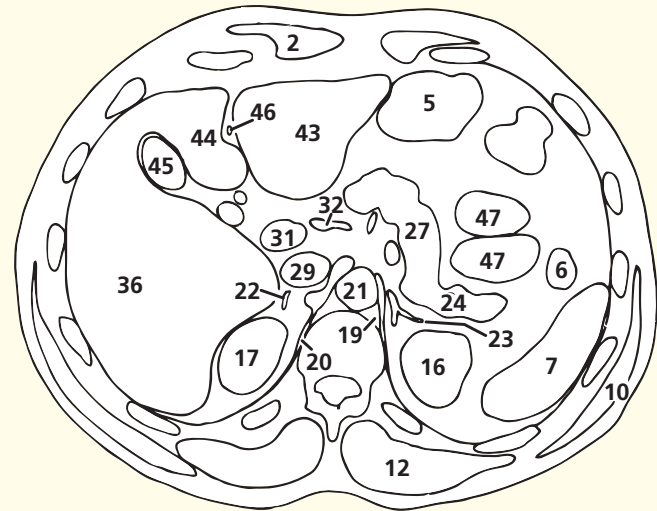
The suprarenal glands (**22**, **25**) have a constant relationship to the diaphragmatic crura (**24**, **45**). Note on the CT images that the separate limbs of the suprarenal glands are demarcated.

The right crus of the diaphragm (**24**) on the CT image is often bulky. The crura change shape during respiration; normally they are bulkier on inspiration.

On the CT image, the pancreas (**42**) is just visible as it enters the plane of this section. It is seen better in more caudal sections. As the pancreas occupies only part of the section, its outlines are not demarcated sharply. This is another example of the 'partial volume' effect.

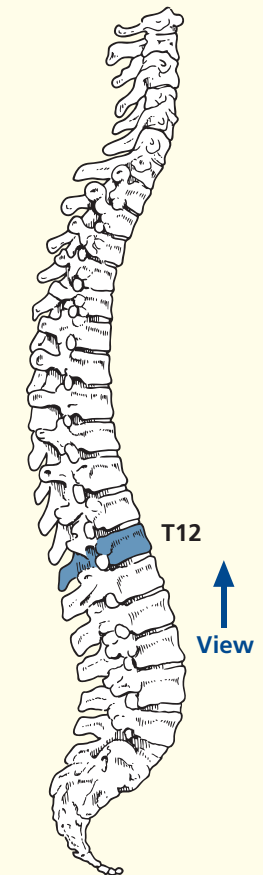


- | | | | | |
|---------------------------------------|--------------------------------------------------------------------|---------------------------------|---------------------------|-----------------------------------------|
| 1 Linea alba | 11 Serratus posterior inferior | 18 Thoracic duct | 29 Inferior vena cava | 40 Ninth rib |
| 2 Rectus abdominis | 12 Erector spinae | 19 Left crus of diaphragm | 30 Caudate lobe of liver | 41 Eighth rib |
| 3 Superior epigastric artery and vein | 13 Spine of eleventh thoracic vertebra | 20 Right crus of diaphragm | 31 Portal vein | 42 Seventh costal cartilage |
| 4 Greater omentum | 14 Conus medullaris surrounded by cauda equina within dural sheath | 21 Aorta | 32 Hepatic artery | 43 Left lobe of liver (lateral segment) |
| 5 Body of stomach | 15 Body of twelfth thoracic vertebra | 22 Right suprarenal gland | 33 Common bile duct | 44 Left lobe of liver (medial segment) |
| 6 Left colic (splenic) flexure | 16 Left kidney | 23 Left suprarenal gland | 34 Radicle of portal vein | |
| 7 Spleen | 17 Right kidney | 24 Tail of pancreas | 35 Hepatic artery branch | |
| 8 Diaphragm | | 25 Splenic vein | 36 Right lobe of liver | |
| 9 External oblique | | 26 Splenic artery | 37 Twelfth rib | |
| 10 Latissimus dorsi | | 27 Body of pancreas | 38 Eleventh rib | |
| | | 28 Left gastric artery and vein | 39 Tenth rib | |
| | | | | 45 Gall bladder |
| | | | | 46 Ligamentum teres |
| | | | | 47 Jejunum |



Axial computed tomogram (CT)

Section level



Notes

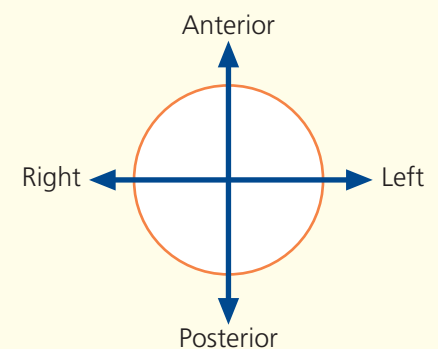
This section passes through the body of the twelfth thoracic vertebra (**15**). It demonstrates well the relationships of the structures at the porta hepatis – the common bile duct (**33**) anterior and to the right, the hepatic artery (**32**) anterior and to the left, and the portal vein (**31**) posterior to these structures. The inferior vena cava (**29**) lies immediately behind the portal vein; between the two is the epiploic foramen, or the aditus to the lesser sac (the foramen of Winslow). The division between the cortex (peripheral) and medulla (central) of the kidneys (**16**, **17**) is shown well; in the plane of this division run the small arcuate vessels, which can just be identified in this section. Post-mortem changes account for the discrepancy in the differentiation between cortex and medulla in the left kidney.

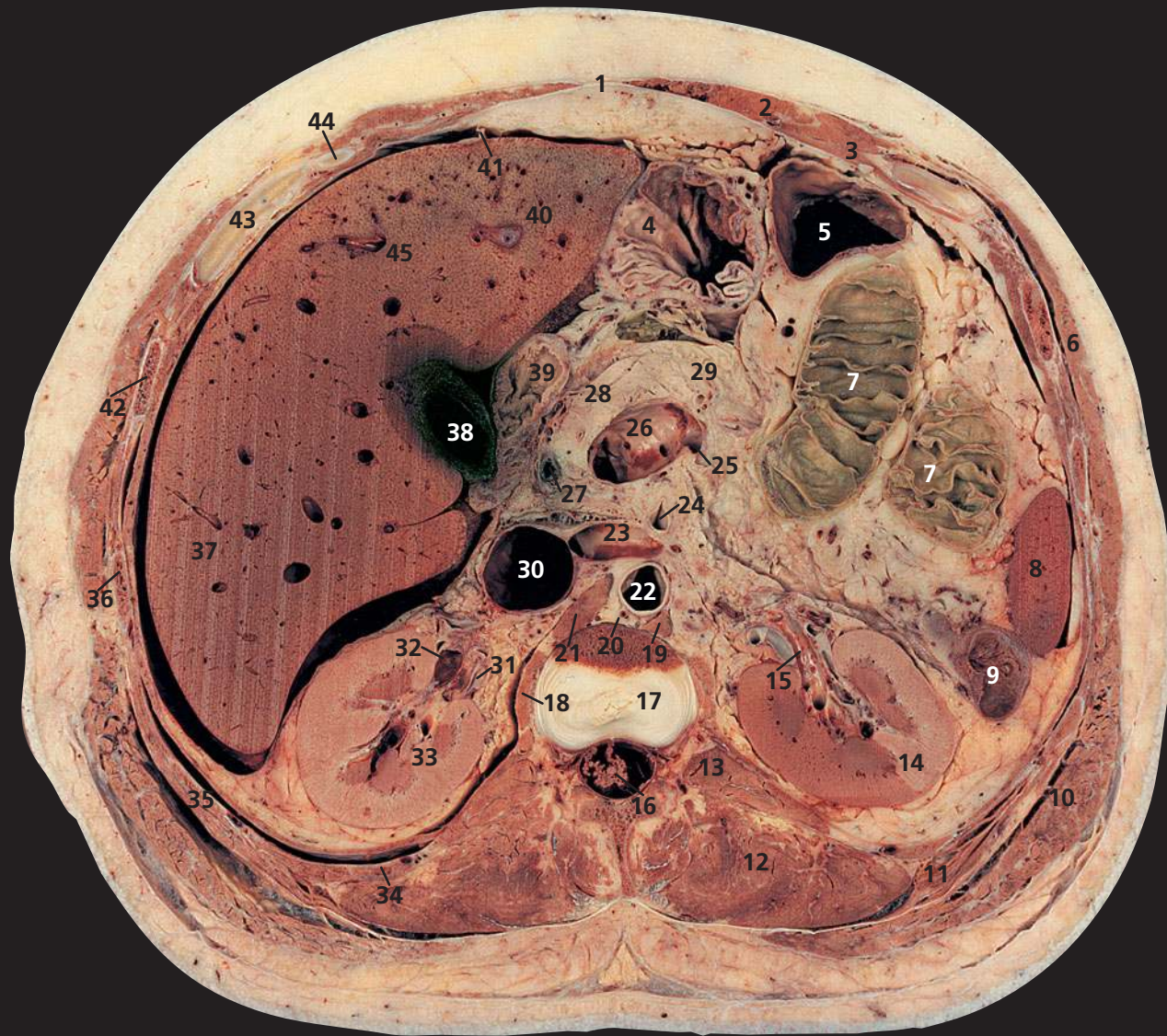
Note on the lobes of the liver

The gross anatomical division of the liver is into right and left lobes, demarcated by the attachment of the falciform ligament

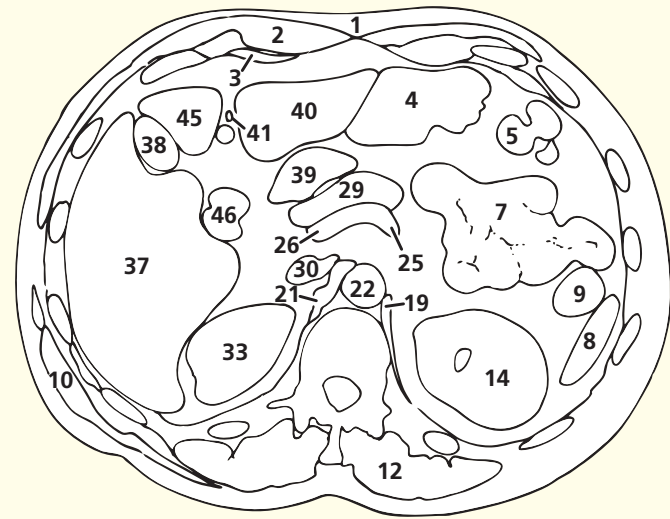
on the anterior surface and by the fissures for the ligamentum teres and ligamentum venosum on its visceral surface. This is simply a gross anatomical descriptive term, with no morphological significance. Two subsidiary additional lobes are marked out on the visceral aspect of the liver – the quadrate lobe anteriorly, between the gall bladder fossa and the fissure for the ligamentum teres, and the caudate lobe posteriorly, between the groove for the inferior vena cava and the fissure for the ligamentum venosum. The transverse fissure for the porta hepatis separates the quadrate and caudate lobes. The distribution of the right and left branches of the hepatic artery and of the hepatic duct shows that the morphological division of the liver is into a right and left lobe demarcated by a plane that passes through the fossa of the gall bladder and the fossa of the inferior vena cava (the median plane of the liver). Morphologically, the quadrate lobe and the left half of the caudate lobe are part of the morphological left lobe of the liver. Further subdivision into hepatic segments is made by the Couinaud system (segments I–VIII).

Orientation



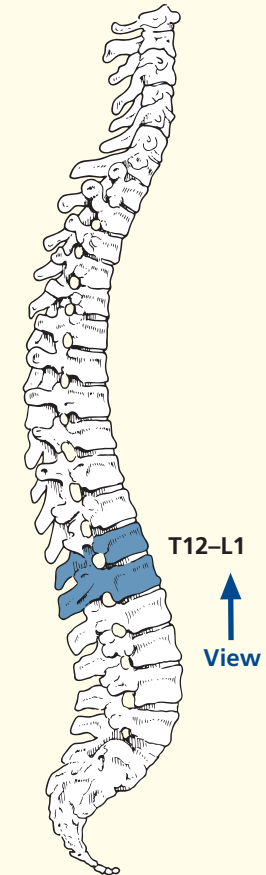


- | | | | | |
|--------------------------------|----------------------------------------------------------------------------------------------------------------------------------------|-------------------------------|-----------------------------------------|----------------------------------------|
| 1 Linea alba | 14 Left kidney | 19 Left crus of diaphragm | 31 Right renal artery | 42 Ninth rib |
| 2 Rectus abdominis | 15 Left renal vein (intrarenal portion); see also 23 | 20 Thoracic duct | 32 Right renal vein | 43 Eighth costal cartilage |
| 3 Transversus abdominis | 16 Conus medullaris surrounded by cauda equina within dural sheath | 21 Right crus of diaphragm | 33 Right kidney | 44 Ninth costal cartilage |
| 4 Stomach, body/antrum | 17 Part of intervertebral disc between the twelfth thoracic and first lumbar vertebrae, with part of body of twelfth thoracic vertebra | 22 Aorta | 34 Twelfth rib | 45 Left lobe of liver (medial segment) |
| 5 Transverse colon | 18 Psoas major | 23 Left renal vein | 35 Eleventh rib | 46 Right colic (hepatic) flexure |
| 6 External oblique | | 24 Superior mesenteric artery | 36 Tenth rib | |
| 7 Jejunum | | 25 Splenic vein | 37 Right lobe of liver | |
| 8 Lower pole of spleen | | 26 Portal vein (commencement) | 38 Gall bladder | |
| 9 Descending colon | | 27 Common bile duct | 39 First part of duodenum (cap) | |
| 10 Latissimus dorsi | | 28 Head of pancreas | 40 Left lobe of liver (lateral segment) | |
| 11 Serratus posterior inferior | | 29 Neck of pancreas | 41 Falciform ligament | |
| 12 Erector spinae | | 30 Inferior vena cava | | |
| 13 Quadratus lumborum | | | | |



Axial computed tomogram (CT)

Section level



Notes

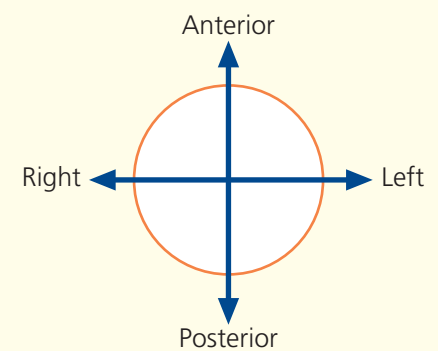
This section transects the intervertebral disc between the twelfth thoracic and the first lumbar vertebrae (**17**). The spinal cord tapers into the conus medullaris (**16**), which terminates, in this subject, at the level of the body of the first lumbar vertebra. The site of termination is variable, the range being from the disc between the twelfth thoracic and first lumbar vertebrae to the lower border of the second lumbar vertebra.

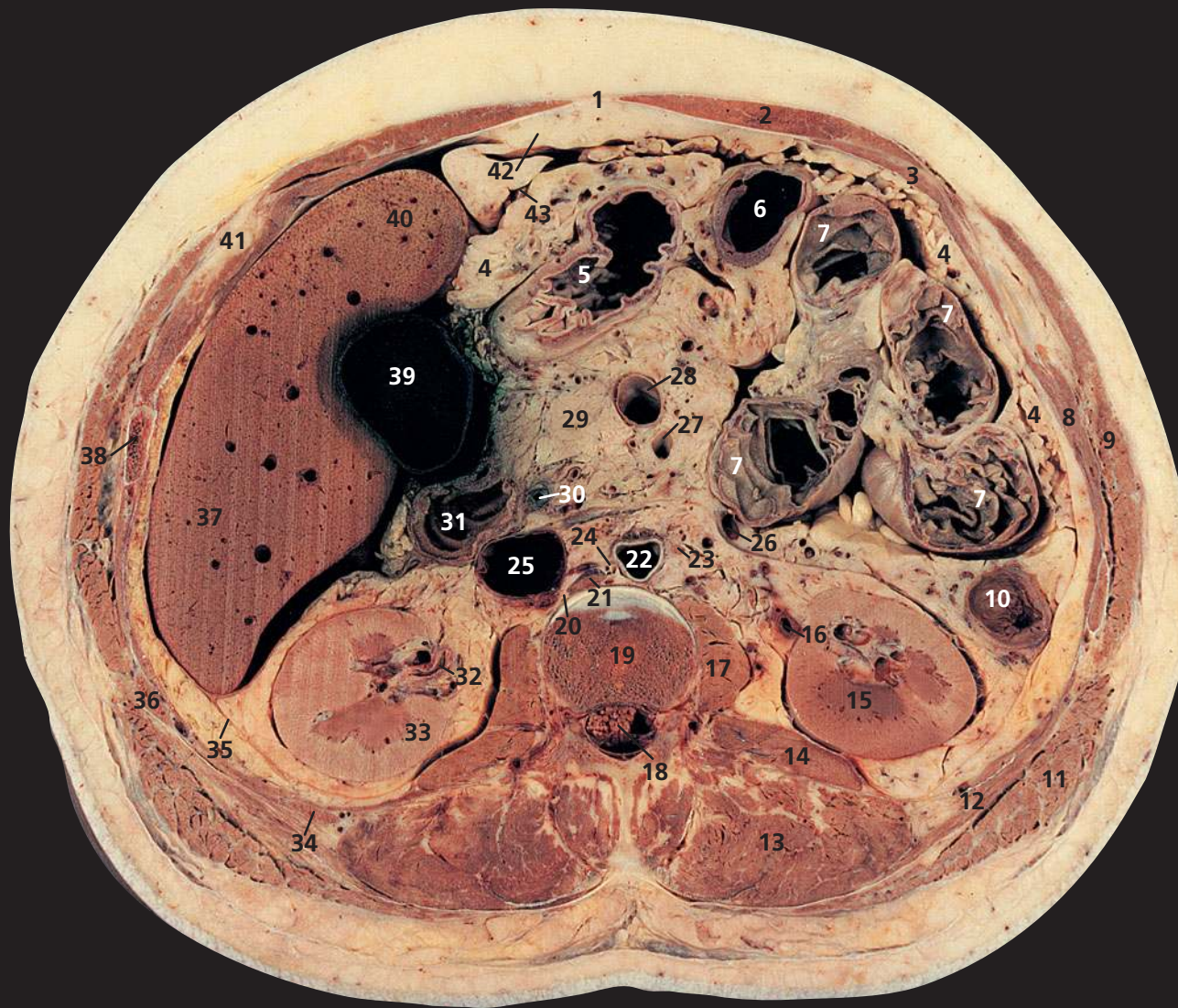
The plane of this section passes through the left renal vein (**23**) and demonstrates well the close relationship of this vein to the superior mesenteric artery (**24**), which passes forward from its aortic origin (**22**) immediately

superior to the vein. These features are demonstrated well on the CT image in Axial section 5. In exposure of the abdominal aorta (**22**), the surgeon can divide the left renal vein (**23**) in order to obtain additional access. The left kidney is not infarcted if this is done because the left renal vein receives the terminations of the left gonadal and left suprarenal veins, so that venous drainage of the left kidney can take place via collaterals from these vessels.

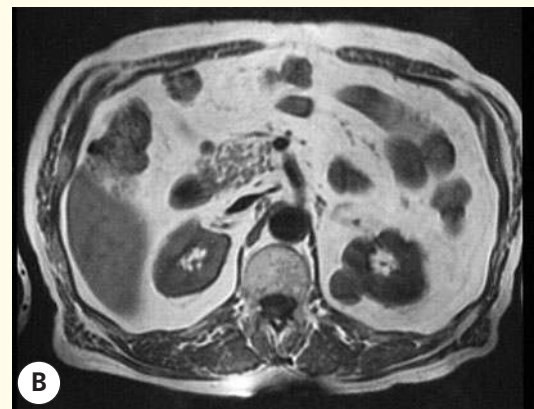
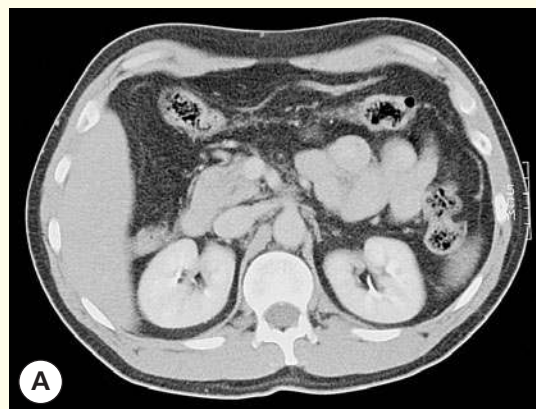
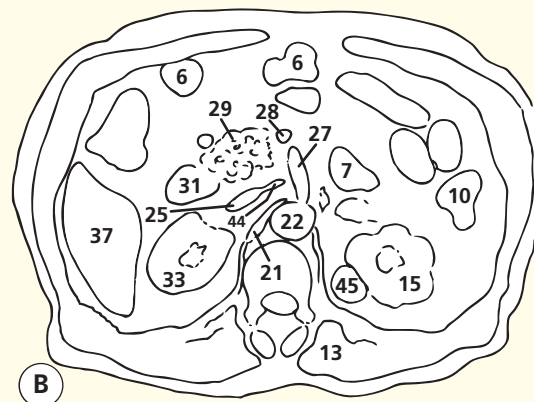
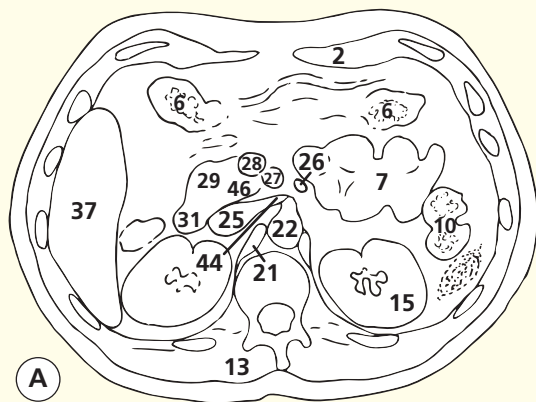
Note the circular folds of mucous membrane that project into the lumen of the small intestine transversely to its long axis (**7**). These are termed the *plicae circulares*. Radiologists and clinicians refer to these as *valvulae conniventes*.

Orientation





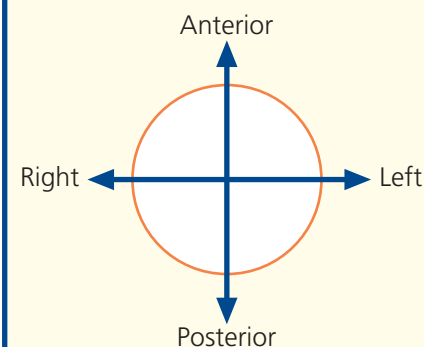
- | | | | | |
|--------------------------------|---------------------------------------------------------------------------------------------------------------------|-------------------------------|----------------------------------------|-----------------------------------------|
| 1 Linea alba | 13 Erector spinae | 20 Right sympathetic chain | 32 Commencement of right ureter | 42 Falciform ligament |
| 2 Rectus abdominis | 14 Quadratus lumborum | 21 Right crus of diaphragm | 33 Right kidney | 43 Left lobe of liver (lateral segment) |
| 3 Transversus abdominis | 15 Left kidney | 22 Aorta | 34 Twelfth rib | 44 Left renal vein |
| 4 Greater omentum | 16 Left ureter | 23 Para-aortic lymph node | 35 Renal fascia | 45 Renal cyst |
| 5 Antrum of stomach | 17 Psoas major | 24 Cisterna chyli | 36 Eleventh rib | 46 Uncinate process pancreas |
| 6 Transverse colon | 18 Cauda equina within dural sheath | 25 Inferior vena cava | 37 Right lobe of liver | |
| 7 Jejunum | 19 Body of first lumbar vertebra, with portion of intervertebral disc between the first and second lumbar vertebrae | 26 Inferior mesenteric vein | 38 Tenth rib | |
| 8 Internal oblique | | 27 Superior mesenteric artery | 39 Gall bladder | |
| 9 External oblique | | 28 Superior mesenteric vein | 40 Left lobe of liver (medial segment) | |
| 10 Descending colon | | 29 Head of pancreas | 41 Ninth costal cartilage | |
| 11 Latissimus dorsi | | 30 Common bile duct | | |
| 12 Serratus posterior inferior | | 31 Duodenum | | |



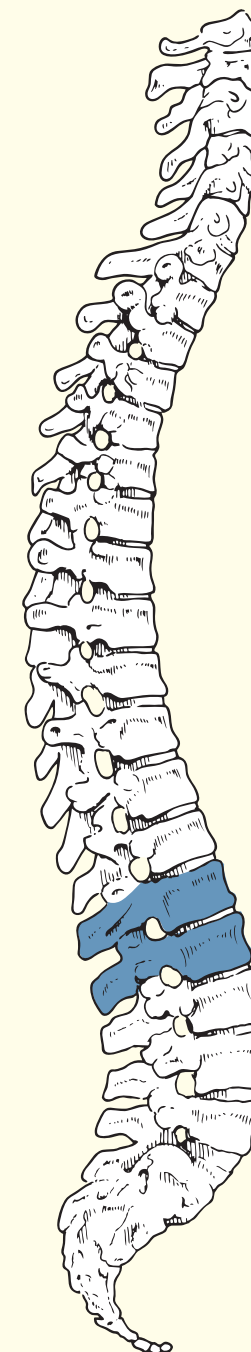
Axial computed tomogram (CT)

Axial magnetic resonance image (MRI)

Orientation



Section level



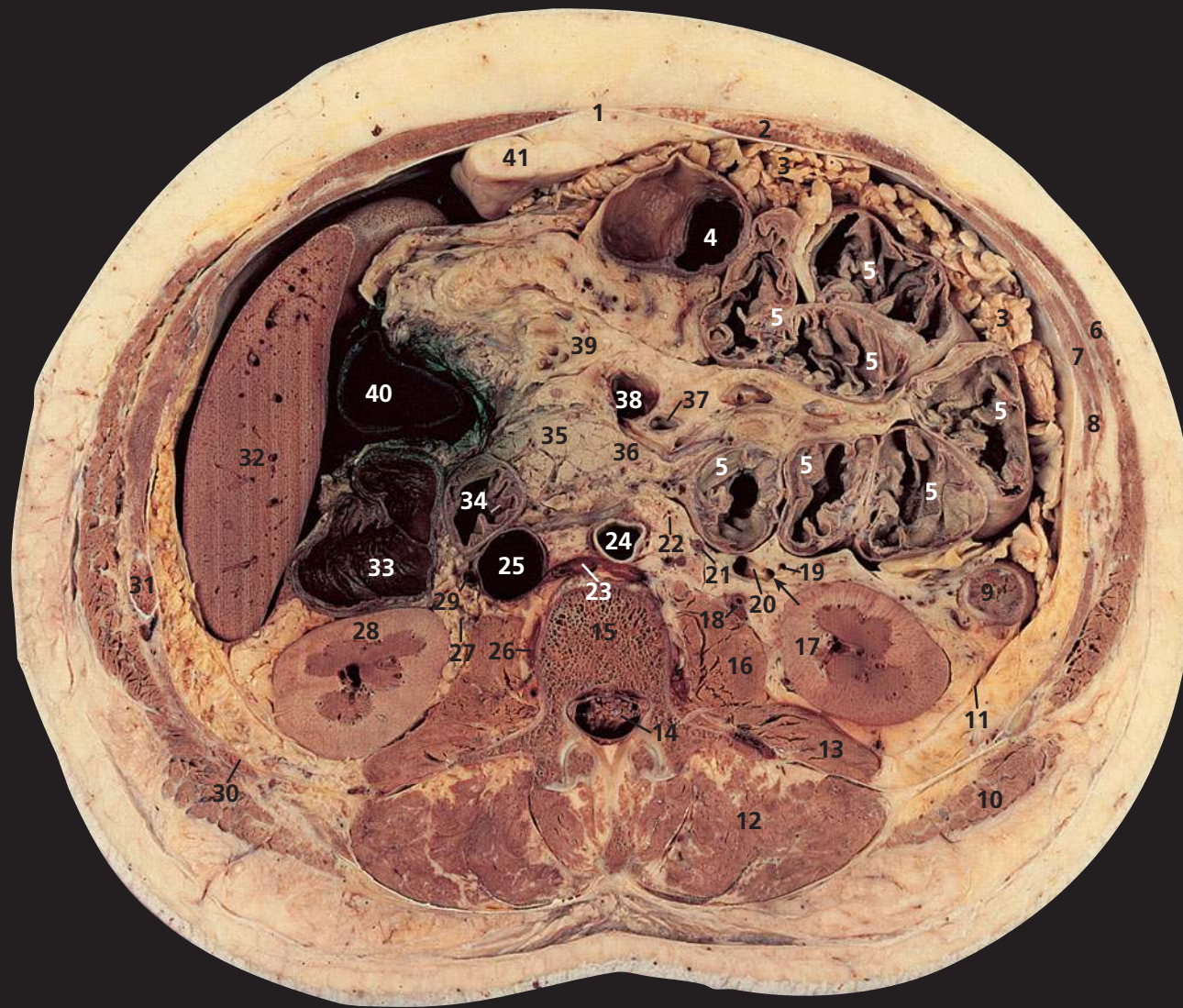
Notes

This section passes through the body of the first lumbar vertebra (**19**), with a small portion of the intervertebral disc between the first and second lumbar vertebrae.

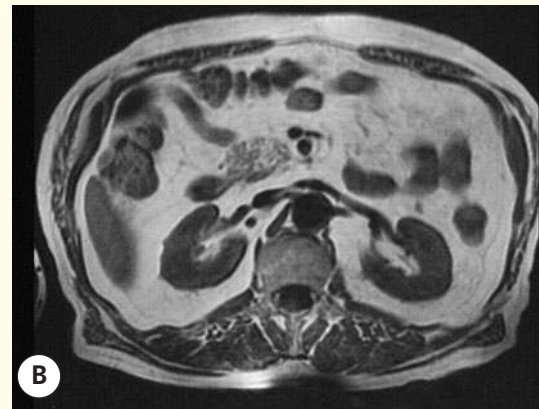
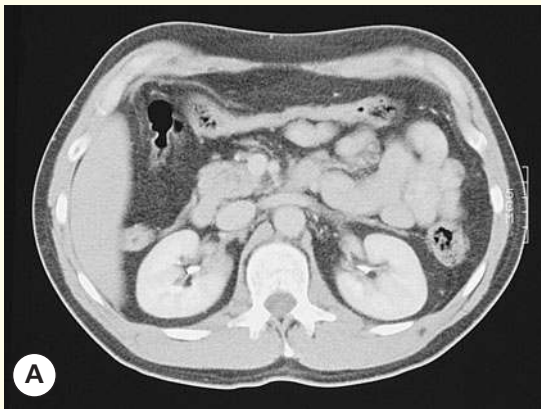
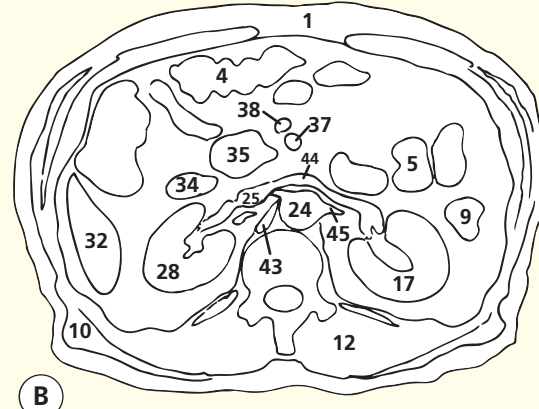
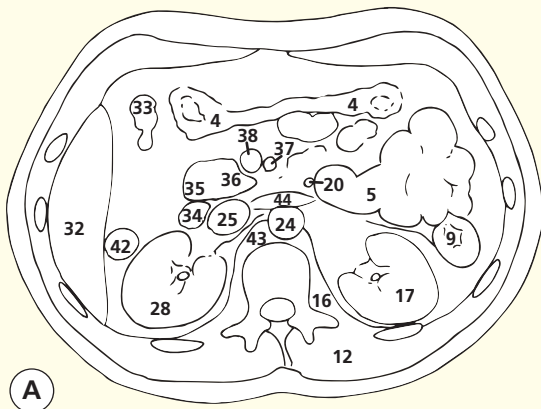
The kidneys (**15**, **33**) are embedded in a mass of fatty connective tissue termed the perirenal (perinephric) fat, which is thickest at their medial and lateral borders. The fibro-areolar tissue surrounding the kidney and perirenal fat condenses to form a sheath termed the renal fascia (**35**). At the lateral border of the kidney, the two layers of the renal fascia are fused. The anterior layer is carried medially

anterior to the kidney and its vessels and merges with the connective tissue anterior to the aorta and inferior vena cava. The posterior layer extends medially in front of the fascia covering quadratus lumborum (**14**) and psoas major (**17**) and to the vertebrae and intervertebral discs. The perirenal fat and renal fascia (**35**) are surrounded by further retroperitoneal (pararenal) fatty connective tissue. The amount varies with the relative obesity of the subject.

In this section, a tiny portion of the lateral segment of the left lobe of the liver can be seen (**43**).



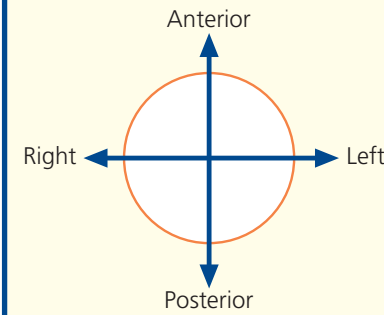
- | | | | | |
|-------------------------|-------------------------------------------------------------|---------------------------|----------------------------------------------------------------------|----------------------------|
| 1 Linea alba | 13 Quadratus lumborum | (arrowed) | 32 Right lobe of liver | 40 Gall bladder |
| 2 Rectus abdominis | 14 Cauda equina within dural sheath | 21 Left testicular vein | 33 Right colic (hepatic) flexure | 41 Falciform ligament |
| 3 Greater omentum | 15 Body of second lumbar vertebra | 22 Para-aortic lymph node | 34 Duodenum – second part (with ampulla marked with a white bristle) | 42 Ascending colon |
| 4 Transverse colon | 16 Psoas major | 23 Left lumbar vein | 35 Head of pancreas | 43 Right crus of diaphragm |
| 5 Jejunum | 17 Left kidney | 24 Aorta | 36 Uncinate process of pancreas | 44 Left renal vein |
| 6 External oblique | 18 Left ureter | 25 Inferior vena cava | 37 Superior mesenteric artery | 45 Left renal artery |
| 7 Internal oblique | 19 Left colic artery – ascending branch | 26 Right lumbar vein | 38 Superior mesenteric vein | |
| 8 Transversus abdominis | 20 Inferior mesenteric vein, with origin of left colic vein | 27 Right ureter | 39 Mesentery with mesenteric vessels | |
| 9 Descending colon | | 28 Right kidney | | |
| 10 Latissimus dorsi | | 29 Right testicular vein | | |
| 11 Renal fascia | | 30 Twelfth rib | | |
| 12 Erector spinae | | 31 Eleventh rib | | |



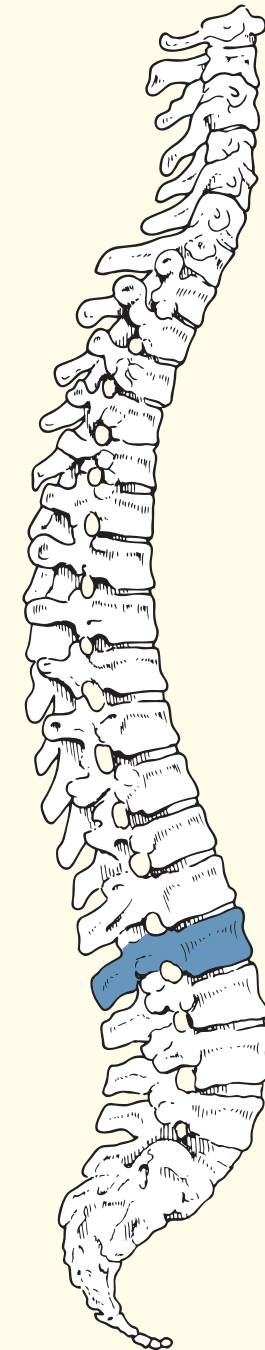
Axial computed tomogram (CT)

Axial magnetic resonance image (MRI)

Orientation



Section level



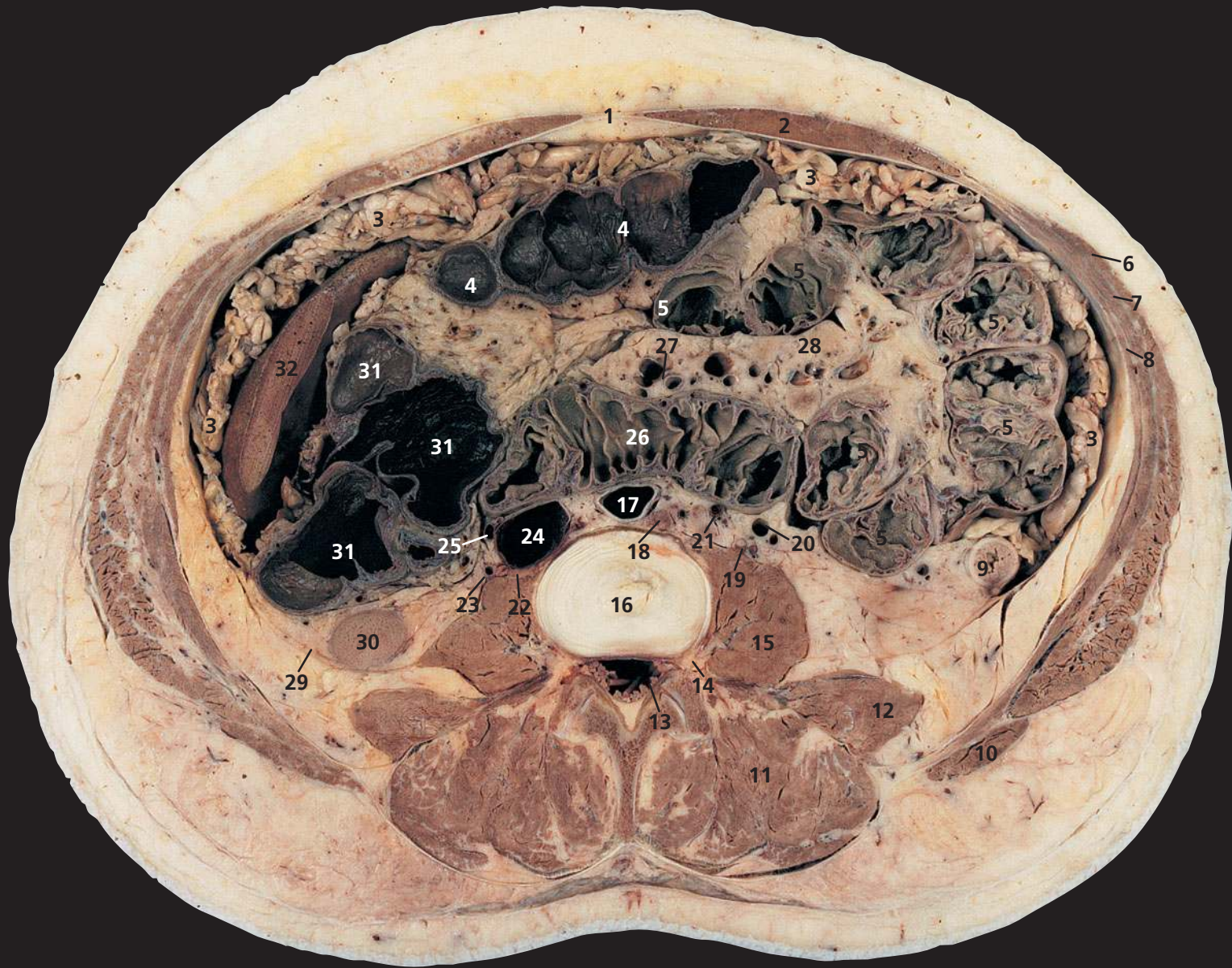
Notes

This section passes through the body of the second lumbar vertebra (**15**). The plane of section passes through a prominent left lumbar vein (**23**) as it passes posterior to the aorta (**24**) to drain into the inferior vena cava (**25**). Occasionally, it may constitute the principal venous return from the left kidney, when it is termed a retro-aortic renal vein.

The right testicular vein (**29**) drains directly into the inferior vena cava, whereas the left testicular vein (**21**) (together with the left suprarenal vein) drains into the left renal vein.

This section passes through the second part of the duodenum (**34**). The orifice of the ampulla of Vater on its papilla is marked with a white bristle.

On both the section and the CT image, the uncinate process of the pancreas (**36**) is seen clearly. This lies posterior to the superior mesenteric artery (**37**) and vein (**38**) and is related closely to the entry point of the left renal vein (**44**) into the inferior vena cava (**25**).



1 Linea alba
2 Rectus abdominis
3 Greater omentum
4 Transverse colon
5 Jejunum
6 External oblique
7 Internal oblique
8 Transversus abdominis
9 Descending colon

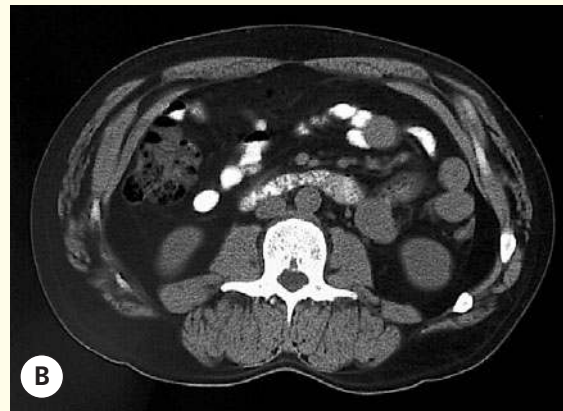
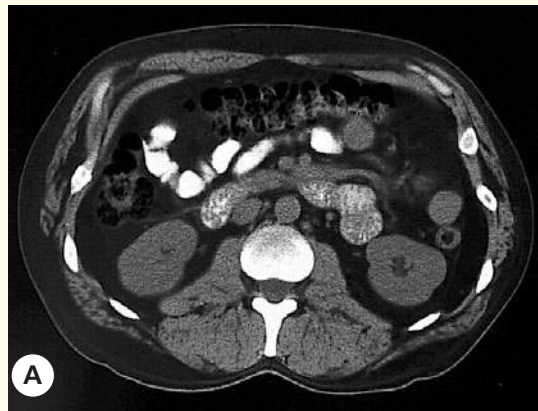
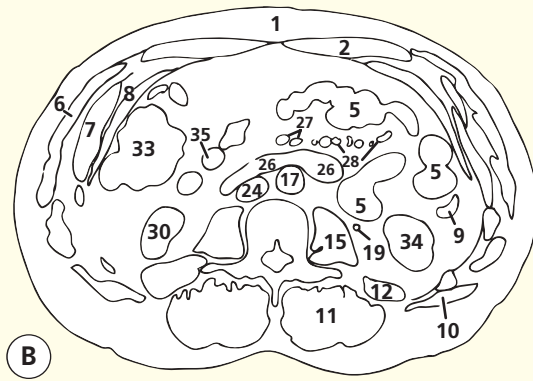
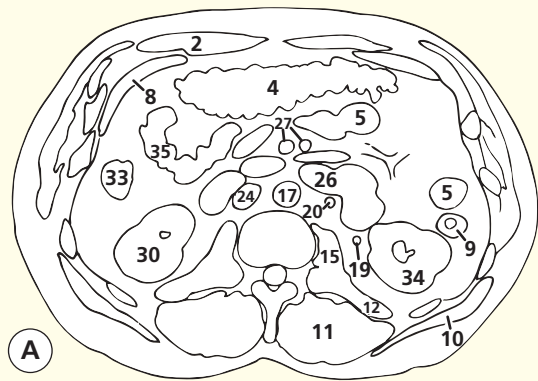
10 Latissimus dorsi
11 Erector spinae
12 Quadratus lumborum
13 Cauda equina within dural sheath
14 Root of second lumbar nerve
15 Psoas major
16 Intervertebral disc between

the second and third lumbar vertebrae
17 Aorta
18 Para-aortic lymph node
19 Left ureter
20 Inferior mesenteric vein
21 Left testicular artery and vein
22 Right sympathetic chain

23 Right ureter
24 Inferior vena cava
25 Right testicular vein
26 Duodenum, third part
27 Superior mesenteric artery and vein
28 Mesentery with mesenteric vessels
29 Renal fascia

30 Right kidney lower pole
31 Ascending colon and right colic (hepatic) flexure
32 Right lobe liver

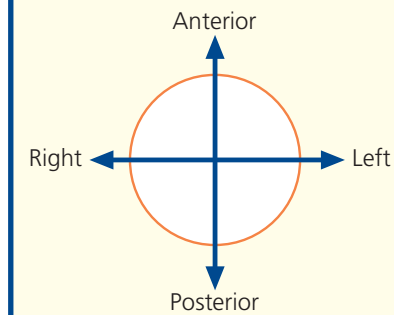
33 Ascending colon
34 Left kidney
35 Ileum



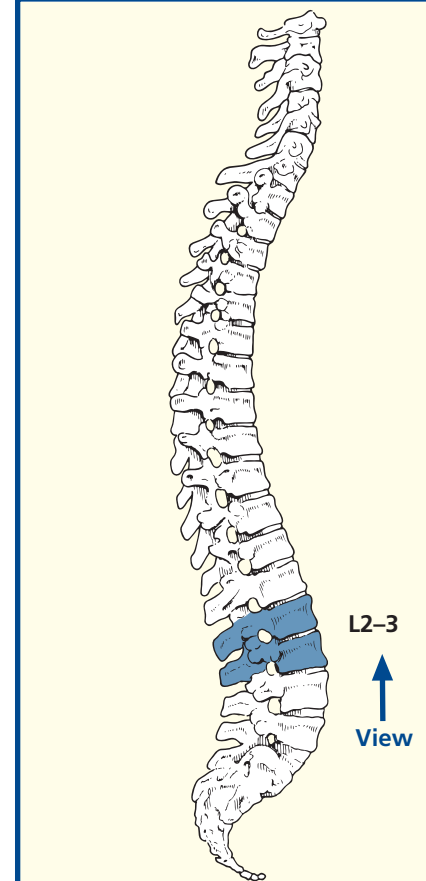
Axial computed tomogram (CT)

Axial computed tomogram (CT)

Orientation



Section level



Notes

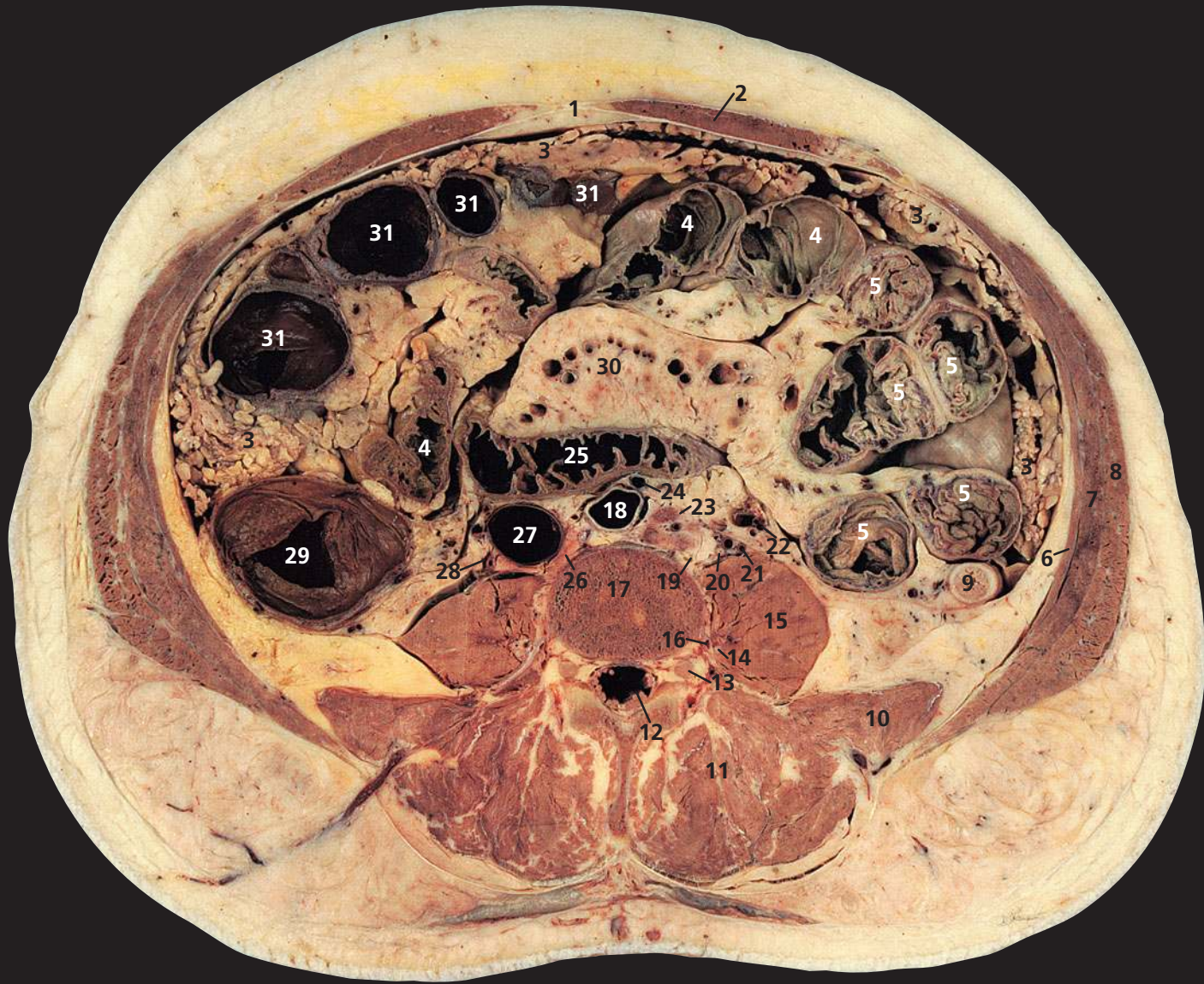
This section passes through the intervertebral disc between the second and third lumbar vertebrae (16). It transects the most caudal part of the right lobe of the liver (32). The caudal extent of this lobe is variable and may project downwards in some subjects for a considerable distance as a broad tongue-like process (Riedel's lobe).

Note the third part of the duodenum (26) lying in the inverted V between the aorta (17) and the superior mesenteric vessels (27). Occasionally, this

produces obstruction of the third part of the duodenum (duodenal ileus).

Seen clearly in this section are the three layers of muscles that constitute the lateral part of the anterior abdominal wall – the external oblique (6), internal oblique (7) and transversus abdominis (8). Medially, their aponeuroses form the sheath that surrounds the rectus abdominis (2). The anterior sheath comprises the aponeurosis of the external oblique together with the split anterior portion of

the internal oblique; the posterior sheath is made up of the aponeurosis of the transversus abdominis reinforced by the posterior portion of the internal oblique. Below a line roughly halfway between the umbilicus and the pubis, the posterior sheath is deficient and all three aponeuroses pass in front of the rectus to form the anterior sheath. These muscles are demonstrated well on the CT image in Axial section 8.

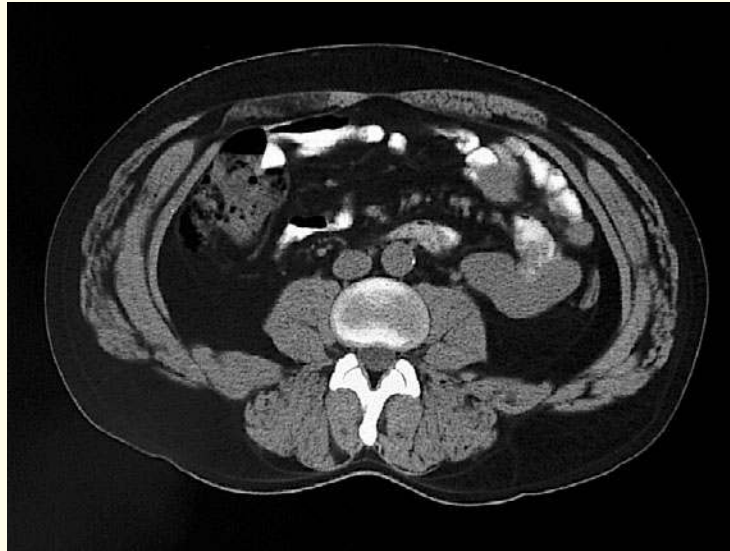
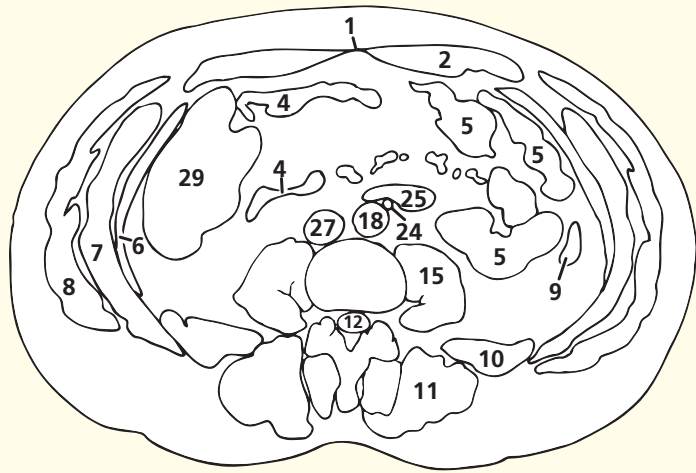


- 1 Linea alba
- 2 Rectus abdominis
- 3 Greater omentum
- 4 Ileum
- 5 Jejunum
- 6 Transversus abdominis
- 7 Internal oblique
- 8 External oblique
- 9 Descending colon

- 10 Quadratus lumborum
- 11 Erector spinae
- 12 Cauda equina within dural sheath
- 13 Dorsal root ganglion of third lumbar nerve
- 14 Ventral ramus of second lumbar nerve
- 15 Psoas major
- 16 Third lumbar artery

- 17 Body of third lumbar vertebra
- 18 Aorta
- 19 Left sympathetic chain
- 20 Left ureter
- 21 Left testicular artery and vein
- 22 Left colic artery and inferior mesenteric vein
- 23 Para-aortic lymph node
- 24 Inferior mesenteric artery

- 25 Duodenum, third part
- 26 Right sympathetic chain
- 27 Inferior vena cava
- 28 Right ureter
- 29 Ascending colon
- 30 Mesentery with mesenteric vessels
- 31 Transverse colon



Axial computed tomogram (CT)

Notes

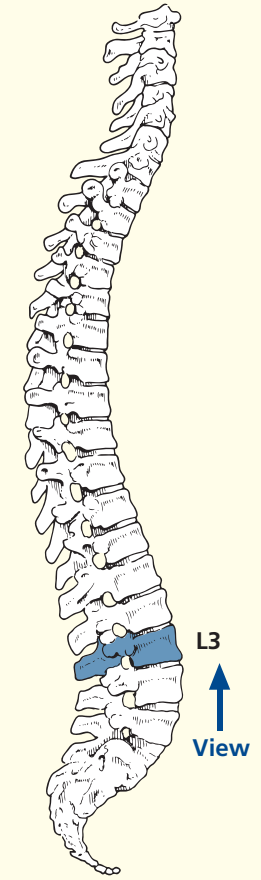
This section passes through the body of the third lumbar vertebra (17). This is just distal to the origin of the inferior mesenteric artery (24) from the anterior aspect of the aorta (18) posterior to the third part of the duodenum (25). This section is now caudal to the liver and the kidneys.

The ventral ramus of the second lumbar nerve (14) is seen in this section as it passes downwards and laterally into the psoas major (15). The first three lumbar nerves and the greater part of the fourth lumbar nerve form the lumbar plexus within the posterior part of the psoas major in front of the transverse processes of the lumbar vertebra.

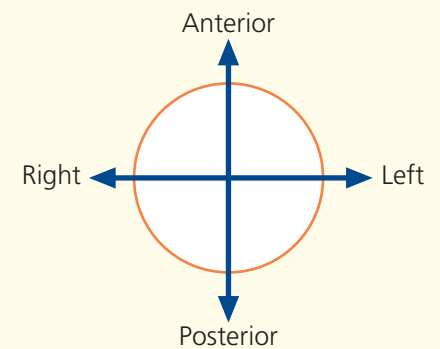
The linea alba (1) is wide above the umbilicus and becomes quite narrow below this level (see page 164). This line marks the almost avascular blending of the rectus sheaths on either side and gives the surgeon rapid access to the abdominal cavity. The incision can, if necessary, be extended from the xiphoid to the pubic symphysis. The falciform ligament (see page 152) lies to the right-hand side of the incision.

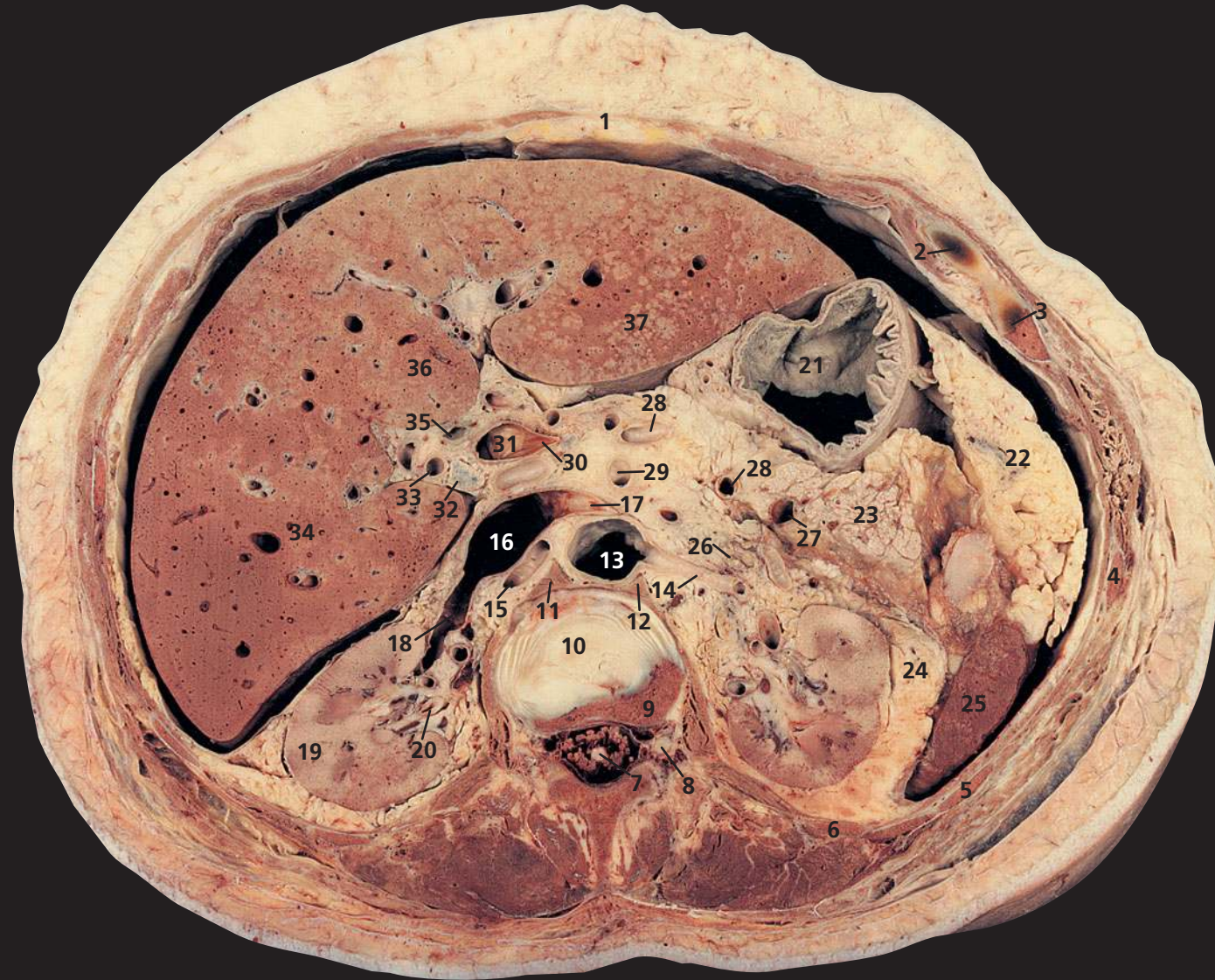
Note the marked disparity between the patulous ascending colon (29) and the thick-walled, narrow descending colon (9).

Section level

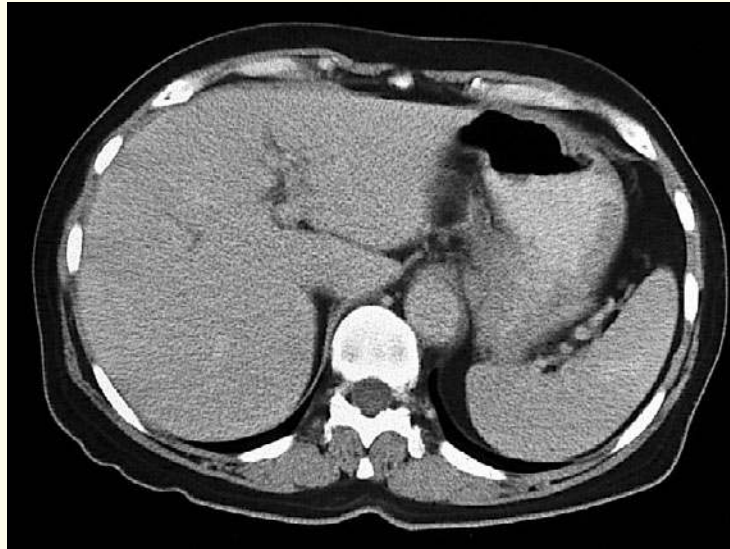
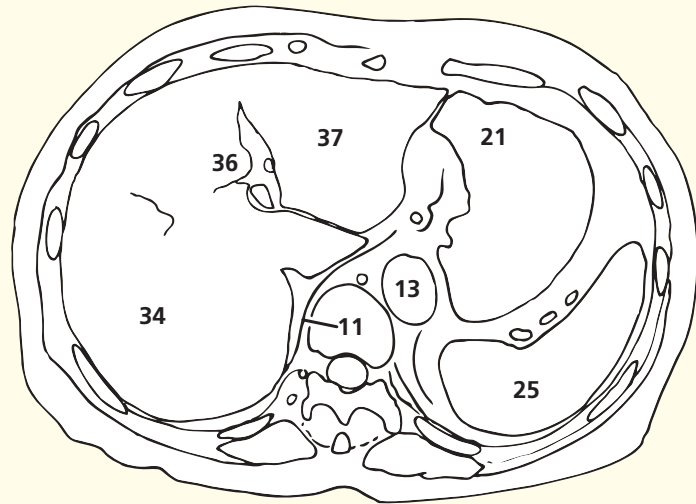


Orientation





- | | | | | |
|-------------------------------------------------------------------|------------------------------------------------------------------------------|-----------------------|--------------------------------------|----------------------------------------------------------|
| 1 Linea alba | 8 Dorsal root ganglion of first lumbar nerve | 14 Left renal artery | 24 Perirenal fat within renal fascia | 32 Lymph node in porta hepatis |
| 2 Eighth costal cartilage | 9 Part of body of first lumbar vertebra | 15 Right renal artery | 25 Spleen | 33 Hepatic artery |
| 3 Ninth rib/costal cartilage junction | 10 Part of intervertebral disc between the first and second lumbar vertebrae | 16 Inferior vena cava | 26 Left suprarenal gland | 34 Right lobe of liver |
| 4 Tenth rib | 11 Right crus of diaphragm | 17 Left renal vein | 27 Splenic vein | 35 Common bile duct |
| 5 Eleventh rib | 12 Left crus of diaphragm | 18 Right renal vein | 28 Splenic artery | 36 Quadrate lobe of medial segment of left lobe of liver |
| 6 Twelfth rib | 13 Aorta | 19 Kidney | 29 Superior mesenteric artery | 37 Left lobe of liver, lateral segment |
| 7 Cauda equina and termination of spinal cord within dural sheath | | 20 Right ureter | 30 Termination of splenic vein | |
| | | 21 Body of stomach | 31 Commencement of portal vein | |
| | | 22 Greater omentum | | |
| | | 23 Tail of pancreas | | |



Axial computed tomogram (CT)

Notes

Axial sections 1 and 2 through the female abdomen should be compared with the male abdominal sections. There are wide individual variations in both the sexes, but a comparison of the 'typical' male and female abdomens reveals a greater accumulation of subcutaneous fat in the female in contrast to a higher proportion of intraperitoneal fat in the male subject.

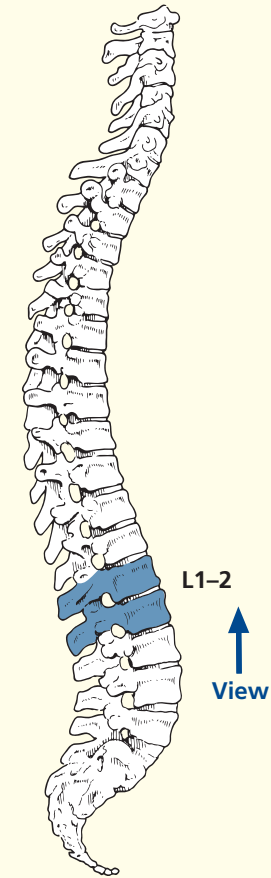
This section passes through the intervertebral disc between the first and second lumbar vertebrae. This section shows well the quadrate lobe of the liver (**36**). Although the common bile duct (**35**) is usually the most anterolateral structure in the free (right) edge of the lesser omentum, variations are common. In this elderly female, the hepatic artery (**33**) is tortuous and thus is unusually

lateral. Anomalies of the hepatic artery are common. In 12 per cent of cases, the right hepatic artery derives from the superior mesenteric artery. The left hepatic artery or an accessory hepatic artery may originate from the left gastric, splenic or superior mesenteric artery. Occasionally, one or other of these vessels derives directly from the aorta.

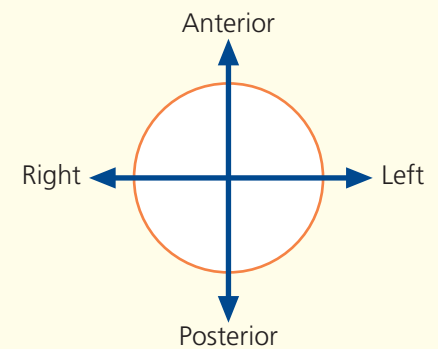
Note the caudal tip of the left suprarenal gland (**26**), which may extend down to the left renal vein.

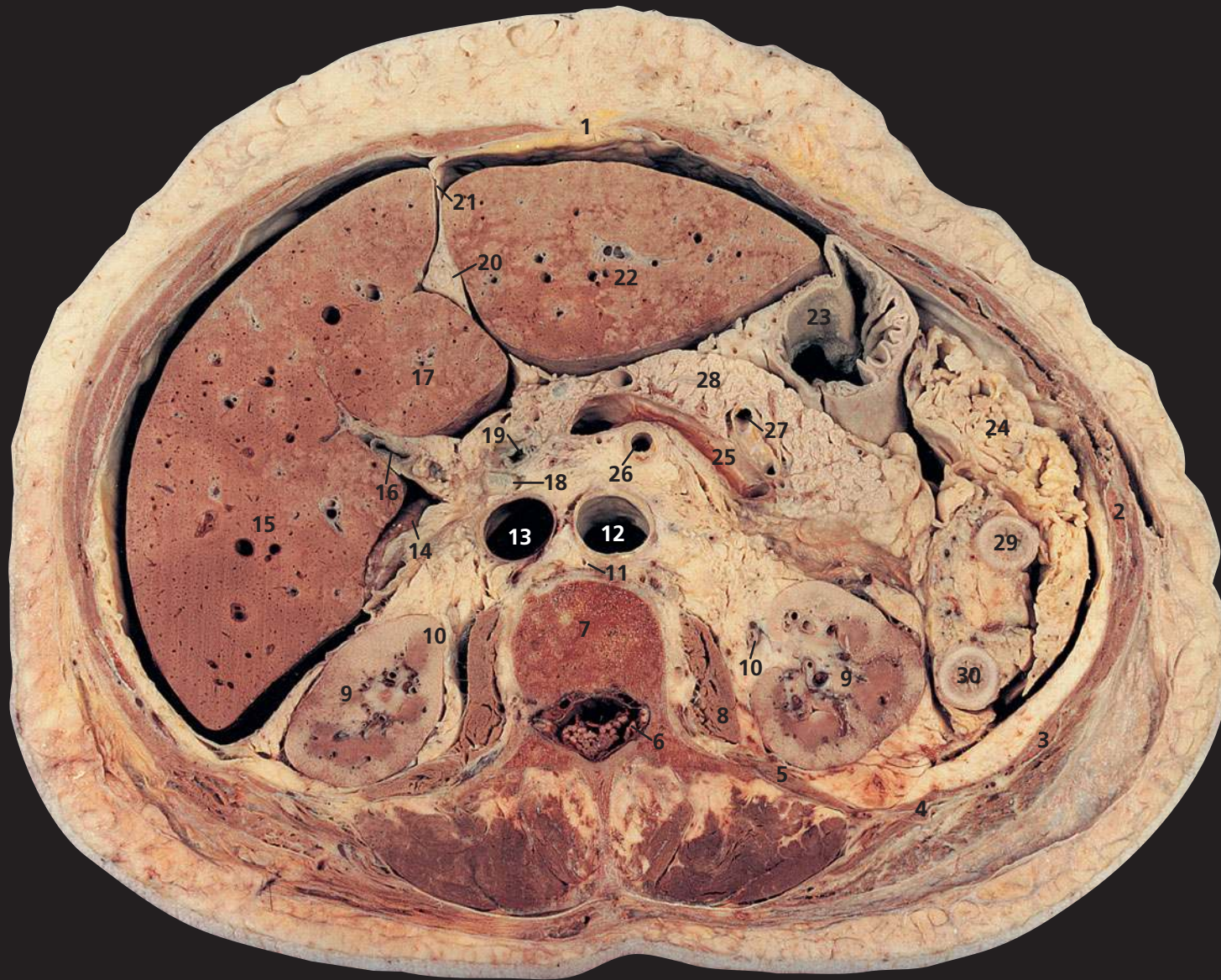
This section demonstrates the fascial layers that enclose the kidney (**19**). The kidney itself is enclosed in its renal capsule, which is readily stripped from the healthy organ. Surrounding this is the perirenal fat, contained within the renal fascia (**24**). A closed rupture of the kidney is usually contained and tamponaded by this fascial sheath.

Section level

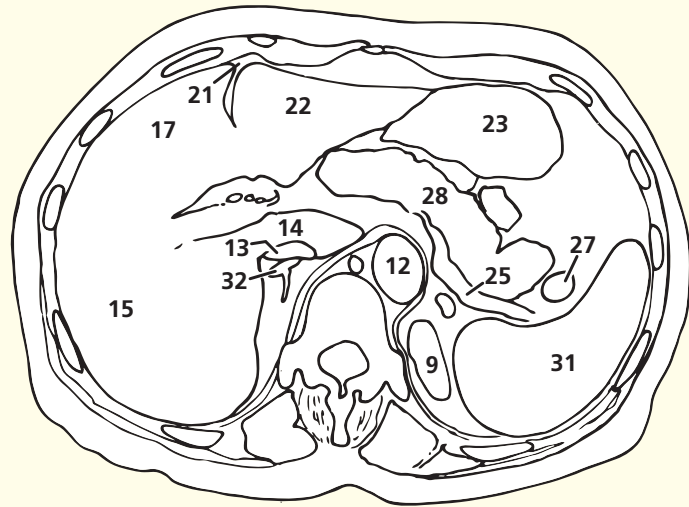


Orientation





- | | | | |
|------------------------------------|----------------------------------------|-----------------------------------------|---------------------------|
| 1 Linea alba | 10 Ureter | 19 Common bile duct | 28 Body of pancreas |
| 2 Tenth rib | 11 Cisterna chyli | 20 Ligamentum teres | 29 Transverse colon |
| 3 Eleventh rib | 12 Aorta | 21 Falciform ligament | 30 Descending colon |
| 4 Twelfth rib | 13 Inferior vena cava | 22 Left lobe of liver (lateral segment) | 31 Spleen |
| 5 Quadratus lumborum | 14 Caudate lobe of liver | 23 Body of stomach | 32 Right suprarenal gland |
| 6 Cauda equina within dural sheath | 15 Right lobe of liver | 24 Greater omentum | |
| 7 Body of second lumbar vertebra | 16 Neck of gall bladder | 25 Splenic vein | |
| 8 Psoas major | 17 Left lobe of liver (medial segment) | 26 Superior mesenteric artery | |
| 9 Kidney | 18 Lymph node in porta hepatis | 27 Splenic artery | |



Axial computed tomogram (CT)

Notes

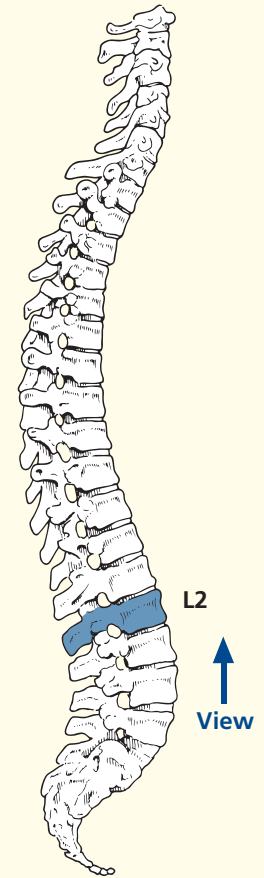
This section lies just caudal to the left colic (splenic) flexure, which joins the transverse colon (29) to the descending colon (30).

The tip of the papillary process of the caudate lobe of the liver (14) can be seen as a separate structure in the gap medial to the right lobe of the liver. The ligamentum teres (20) is the fibrotic remnant of the obliterated left umbilical vein. The falciform ligament divides the morphological left lobe of the liver into a lateral segment (22) and a medial

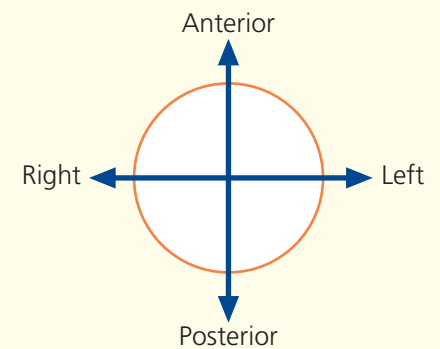
segment (17). The visceral aspect of this, between the falciform ligament and the gall-bladder bed (16), forms the anatomical quadrate lobe.

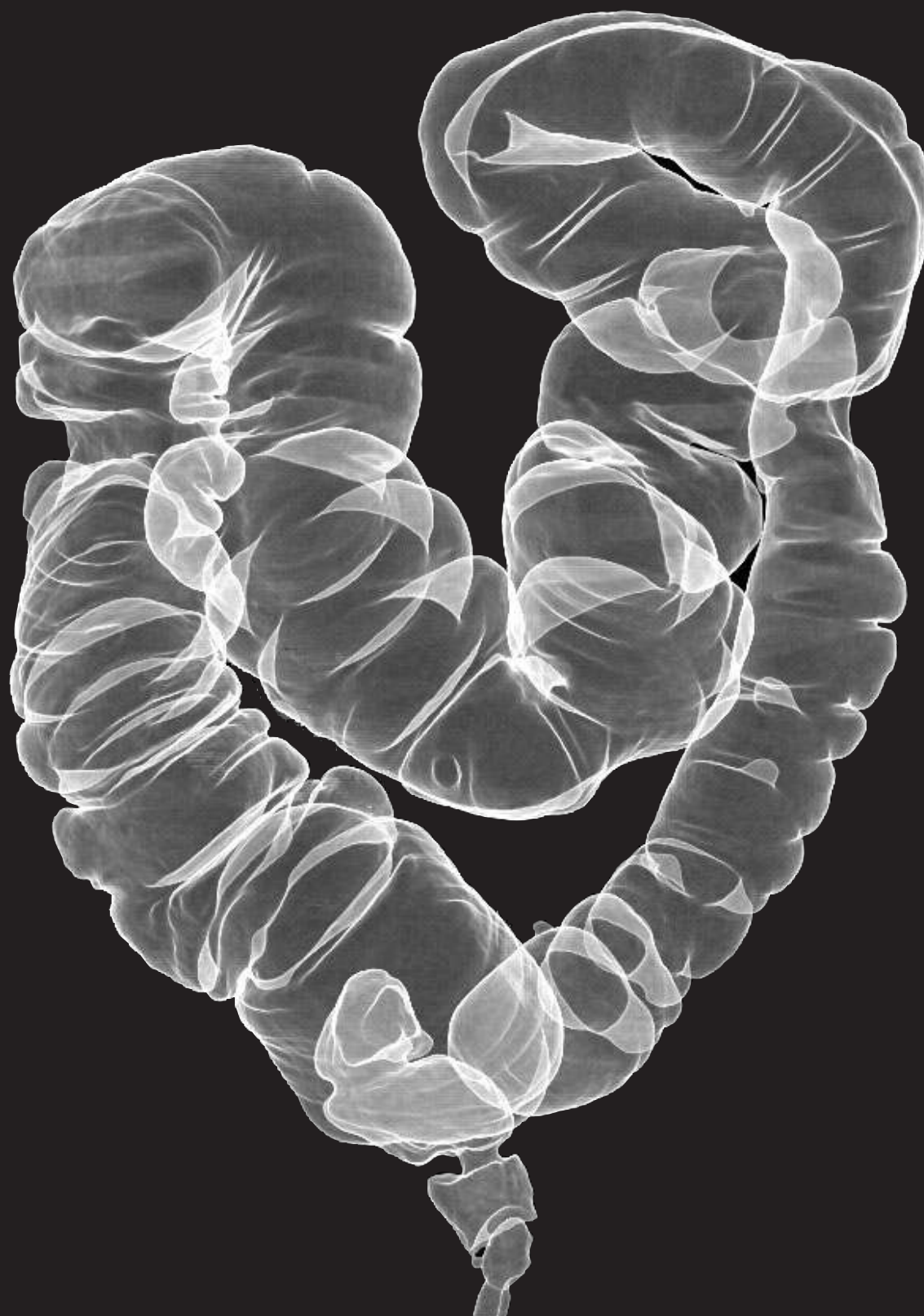
Although the left extremity of the transverse colon (29) and the upper extremity of the descending colon (30) are seen at this level, which is immediately inferior to the splenic flexure, this is above the level of the hepatic flexure of the right colon, which is displaced downwards by the right lobe of the liver.

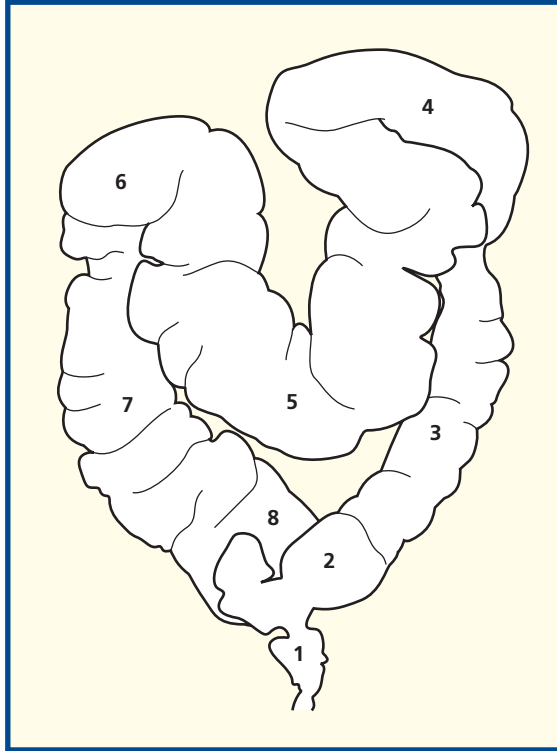
Section level



Orientation

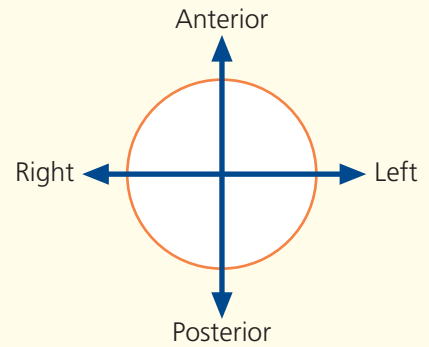






- 1 Tube in distal rectum
- 2 Sigmoid colon
- 3 Descending colon
- 4 Splenic flexure
- 5 Transverse colon
- 6 Hepatic flexure
- 7 Ascending colon
- 8 Caecum

Orientation



Notes

This CT colonogram was obtained in the following way. First, the large bowel was cleaned by the oral administration of a standard purgative. The bowel was then distended by air via a small tube inserted by rectum. The wall of the bowel was enhanced by the use of a standard iodinated contrast agent administered intravenously. A spiral CT dataset was obtained on a multidetector CT system. Next, the individual thin slices were loaded together to form a three-dimensional volume, with each voxel isometric so that the x , y and z resolution of the resulting pixels

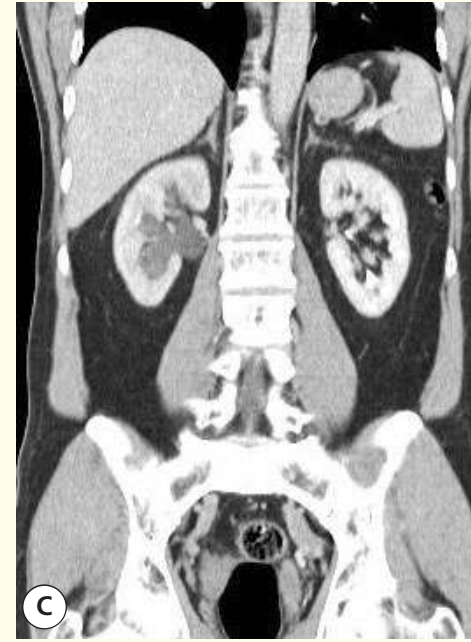
was identical. This three-dimensional dataset can be analysed in a variety of ways – many people find software-generated virtual colonoscopy images helpful, where colour-rendered images allow a ‘fly-through’ approach that simulates what the endoscopist sees at standard colonoscopy. Others find standard multiplanar two-dimensional reconstructions helpful. For all such viewing, a roadmap of the whole colon is a valuable tool for orientation – hence this reconstructed image, which looks uncannily like the double-contrast barium enema of old.



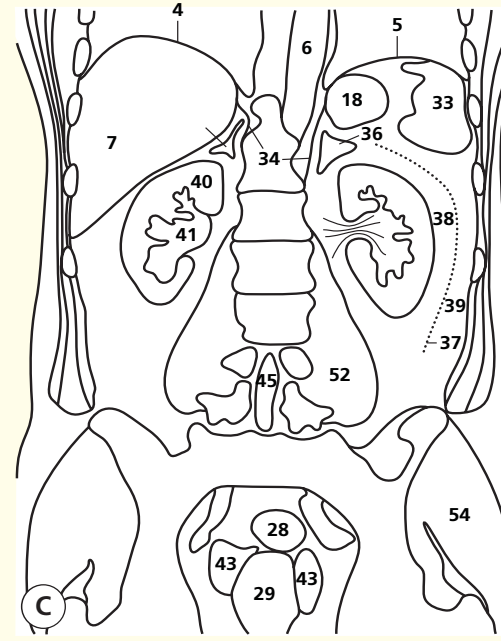
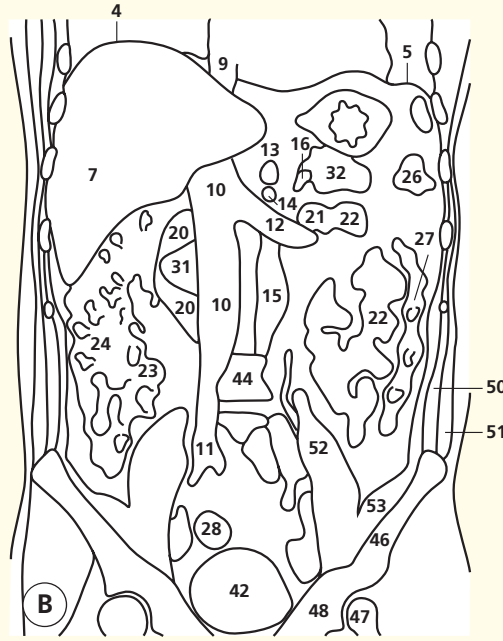
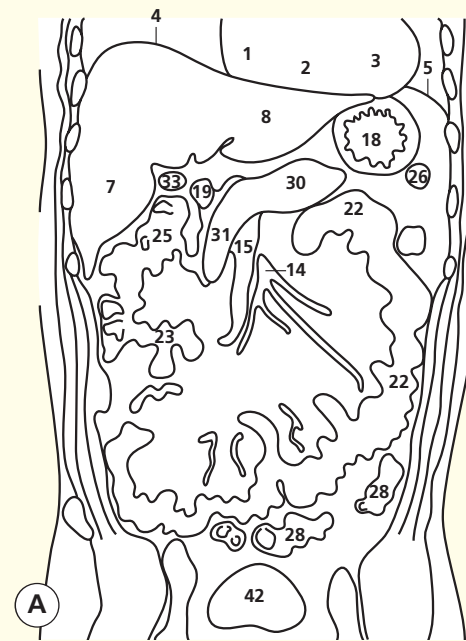
Coronal computed tomogram (CT)



Coronal computed tomogram (CT)



Coronal computed tomogram (CT)



- | | | | |
|---------------------------------------------------------------|----------------------------------------------|-------------------------------------|---------------------------------------|
| 1 Right atrium | 14 Superior mesenteric artery | 27 Colon – descending part | 41 Renal pelvis (distended on right) |
| 2 Right ventricle | 15 Abdominal aorta | 28 Sigmoid colon | 42 Bladder (urinary) |
| 3 Left ventricle | 16 Splenic vein | 29 Rectum | 43 Seminal vesicle |
| 4 Diaphragm (right side) | 17 Superior mesenteric vein | 30 Body of pancreas | 44 Body of third lumbar vertebra |
| 5 Diaphragm (left side) | 18 Fundus of stomach | 31 Head of pancreas | 45 Thecal sac containing cauda equina |
| 6 Ascending aorta | 19 Duodenum – cap (also known as D1) | 32 Tail of pancreas | 46 Ilium (and iliac crest) |
| 7 Right lobe of liver | 20 Duodenum – second part (also known as D2) | 33 Gall bladder | 47 Head of femur |
| 8 Left lobe of liver | 21 Duodenum – fourth part (also known as D4) | 34 Left and right crus of diaphragm | 48 Acetabulum |
| 9 Inferior vena cava – suprahepatic | 22 Jejunum | 35 Right suprarenal (adrenal) gland | 49 Transversus abdominis |
| 10 Inferior vena cava – infrahepatic | 23 Ileum | 36 Left suprarenal (adrenal) gland | 50 Internal oblique |
| 11 Confluence of common iliac veins | 24 Colon – ascending part | 37 Renal (Gerota) fascia | 51 External oblique |
| 12 Left renal vein | 25 Colon – hepatic flexure | 38 Perirenal space | 52 Psoas major |
| 13 Coeliac trunk – hepatic, left gastric and splenic arteries | 26 Colon – splenic flexure | 39 Pararenal space | 53 Iliacus |
| | | 40 Kidney | 54 Gluteus maximus |

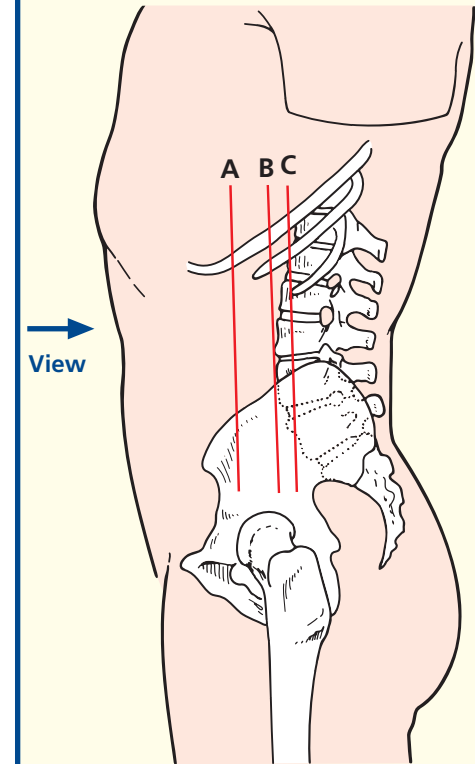
Notes

A spiral CT dataset of the abdomen was obtained on a multidetector CT system. The individual thin slices were loaded together to form a three-dimensional volume, with each voxel isometric, so that the *x*, *y* and *z* resolution of the resulting pixels is identical. This three-dimensional dataset can be analysed in a variety of ways – here in coronal multiplanar two-dimensional reformats.

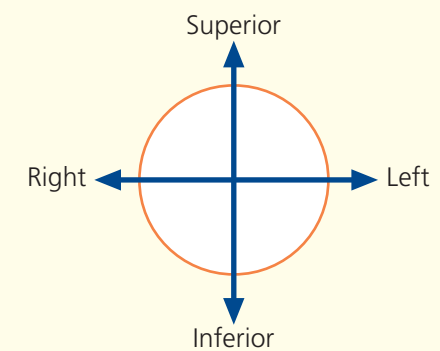
Now that CT of the abdomen has become such a

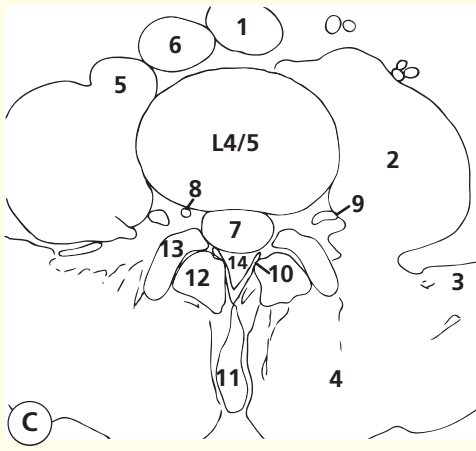
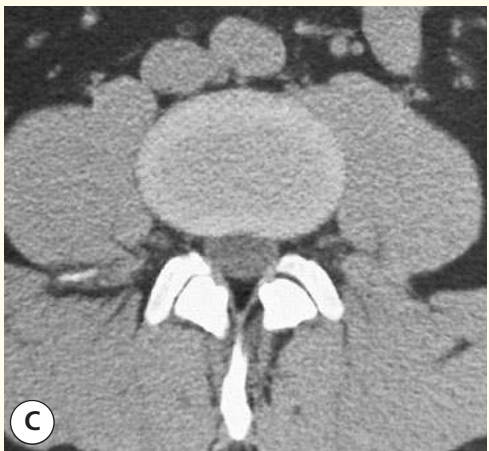
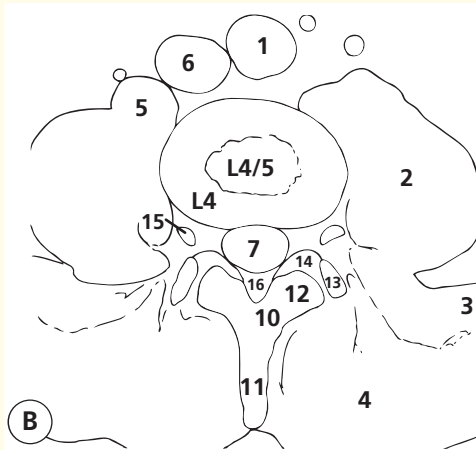
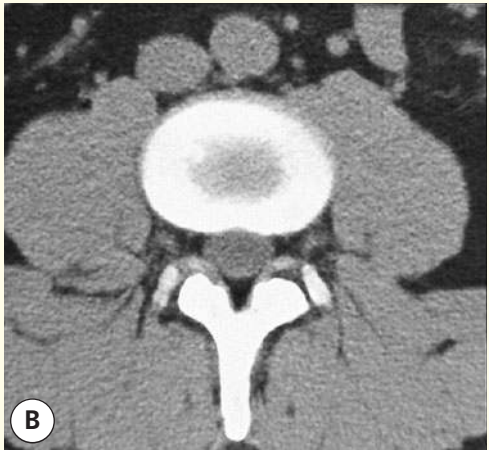
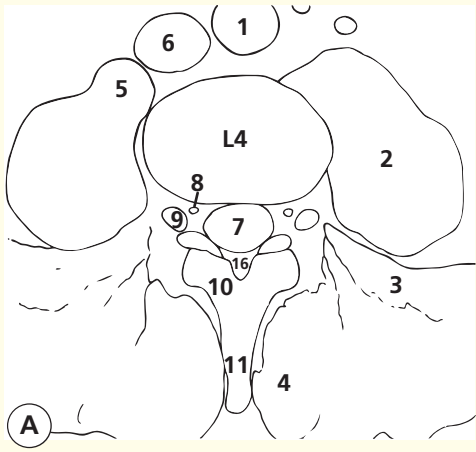
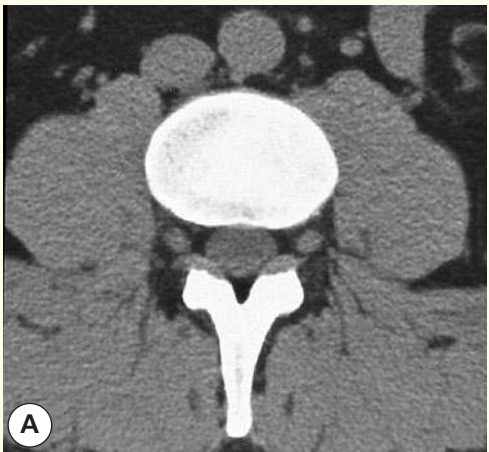
standard investigation for a wide range of abdominal conditions, the radiologist has to scroll through hundreds of axial images on a monitor. Some lesions are depicted better on coronal rather than axial images (e.g. asymmetry of the pelvicalyceal systems in the two kidneys in this case). To non-radiologists, such coronal views are a more intuitive method of looking at the abdomen than the source axial images.

Section level

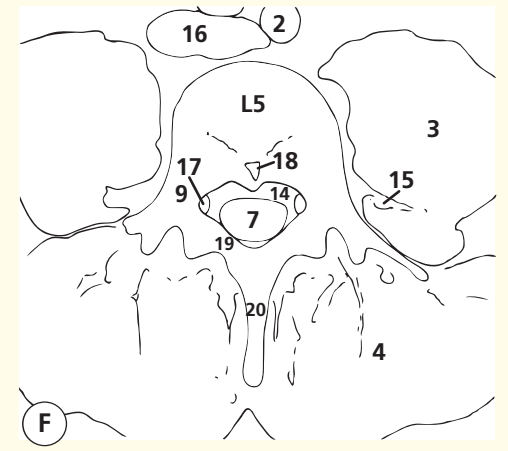
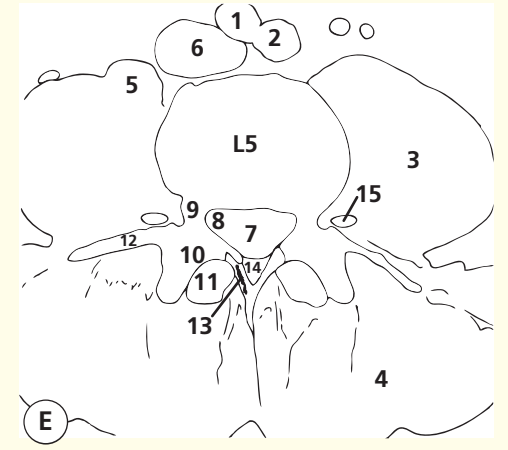
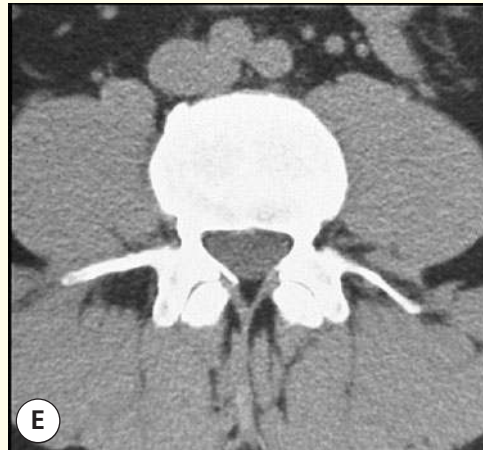
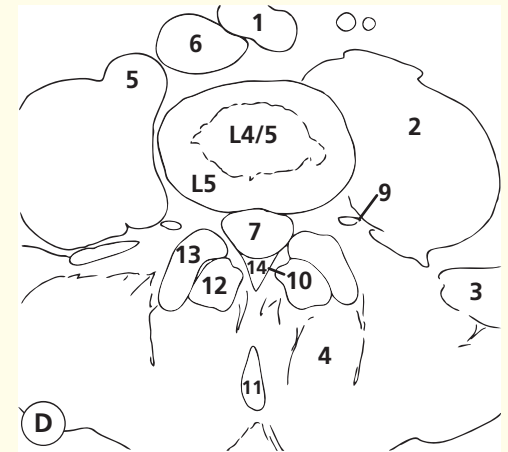
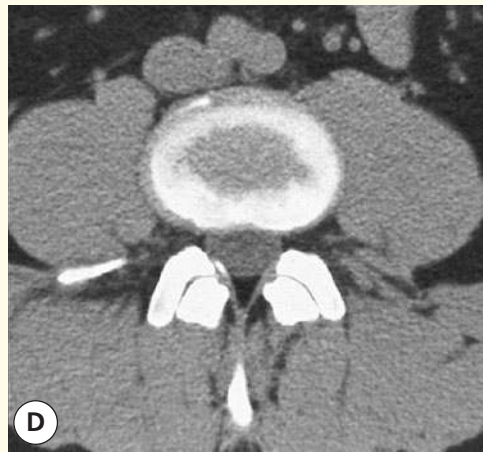


Orientation





Axial computed tomograms (CTs)



Axial computed tomograms (CTs)

Images A–B

- 1 Aorta
- 2 Psoas major
- 3 Quadratus lumborum
- 4 Erector spinae
- 5 Psoas minor
- 6 Inferior vena cava
- 7 Dural sheath
- 8 Epidural vein
- 9 Dorsal root ganglion L4 in foramen between L4 and L5
- 10 Lamina L4
- 11 Spinous process L4
- 12 Inferior facet L4

- 13 Superior facet L5
- 14 Capsule L4/L5 facet joint
- 15 L4 nerve
- 16 Epidural fat

Images C–D

- 1 Aortic bifurcation
- 2 Psoas major
- 3 Quadratus lumborum
- 4 Erector spinae
- 5 Psoas minor
- 6 Inferior vena cava
- 7 Dural sheath
- 8 Epidural vein

- 9 Ventral ramus L4
- 10 Flaval ligament
- 11 Spinous process L4
- 12 Inferior facet L4
- 13 Superior facet L5
- 14 Epidural fat

Images E–F

- 1 Right common iliac artery
- 2 Left common iliac artery
- 3 Psoas major
- 4 Erector spinae
- 5 Psoas minor

- 6 Inferior vena cava
- 7 Dural sheath
- 8 Pouch for L5 root
- 9 Pedicle L5
- 10 Superior facet L5
- 11 Inferior facet L4
- 12 Transverse process of L5
- 13 Flaval ligament
- 14 Epidural fat
- 15 Ventral ramus L4
- 16 Confluence of common iliac veins
- 17 L5 nerve root sheath
- 18 Basi-vertebral vein
- 19 Lamina L5
- 20 Spinous process L5

Notes

This series of six computed tomograms (A–F) demonstrates the key anatomical features of a segment of the lumbar spine. Although all the features can also be demonstrated by magnetic resonance imaging (MRI), which is now the preferred test, computed tomography (CT) is perhaps easier to understand: bone appears white, soft tissues appear grey and fat appears black.

Images A–B

Image a traverses the slightly sclerotic endplate of L4. The dorsal root ganglion (9) lies in the foramen, immediately caudal to the L4 pedicle. Note how the dorsal root ganglion is demarcated clearly by normal epidural fat.

Images C–D

Image C traverses the L4/L5 disc. Note that the posterior aspect of the disc is concave with respect to the dural sheath (7). A normal disc at this anatomical level has either a concave or flat interface with the sheath. A convex disc here is indicative of an annular bulge. Note how the L4 ventral ramus (9) is now heading towards the psoas muscle

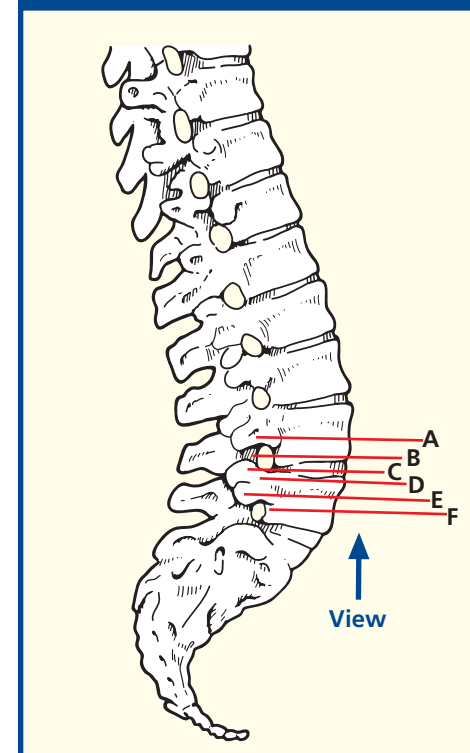
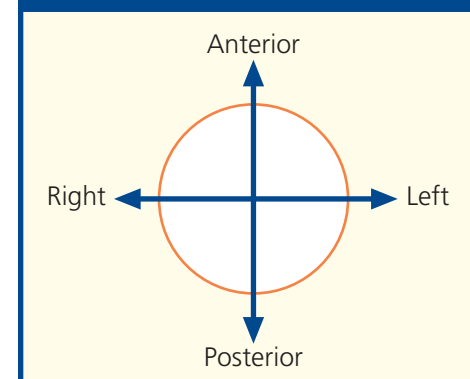
in which the lumbar plexus is formed. The dorsal ramus is too small to be resolved by CT; it would pass just lateral to the superior facet of L5.

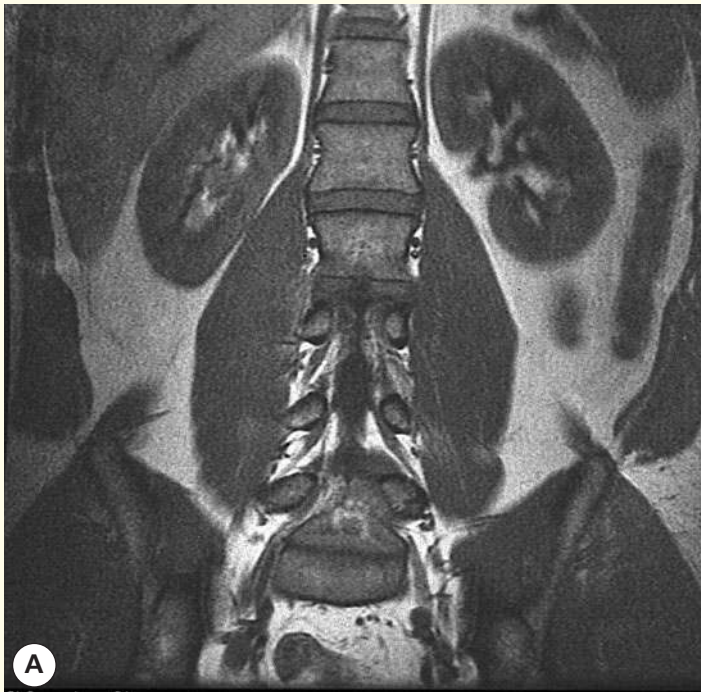
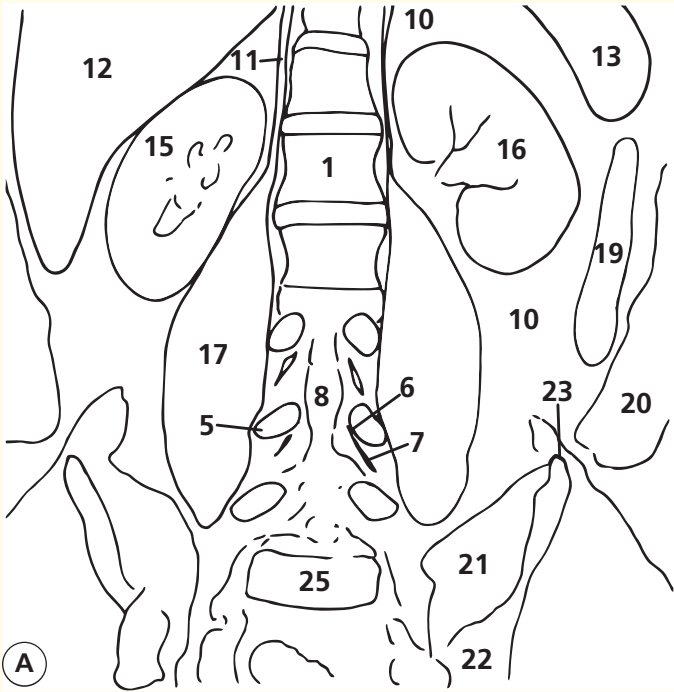
Image D shows a portion of the L5 endplate surrounding the inferior aspect of the L4/L5 disc.

Images E–F

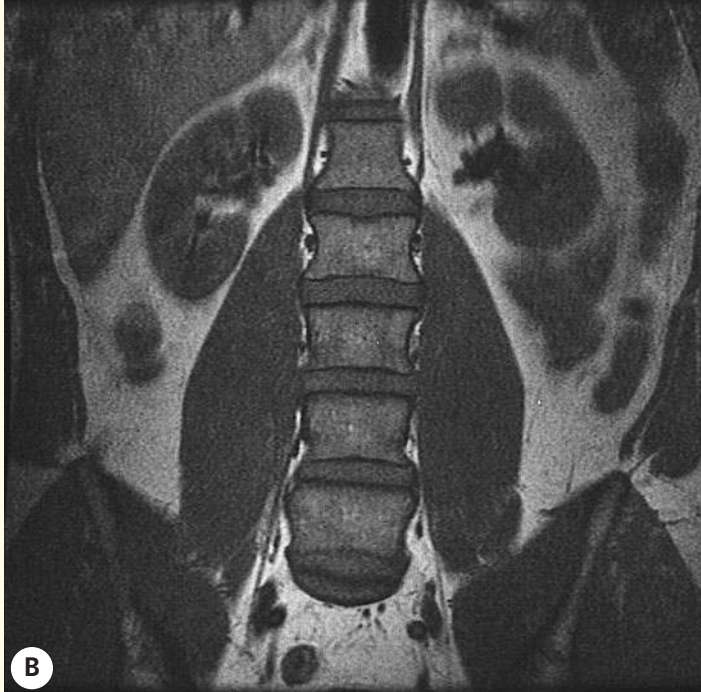
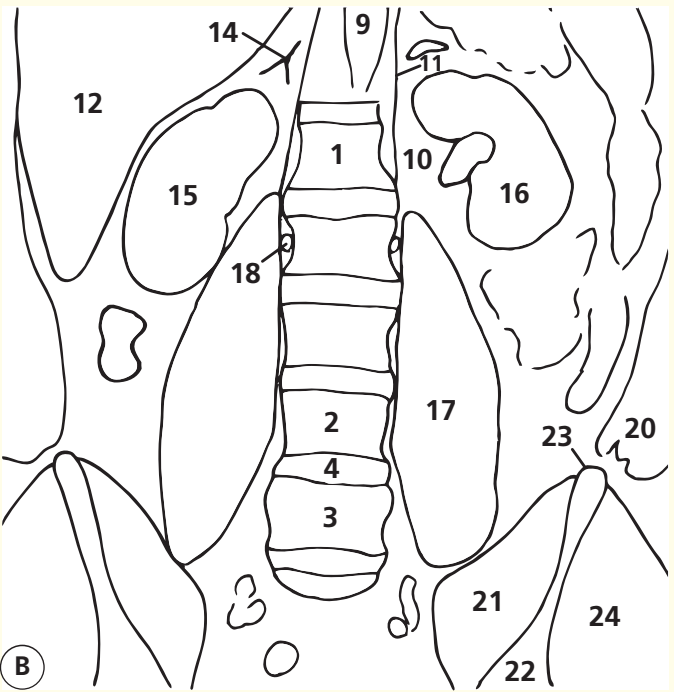
Image E transects the sclerotic endplate of L5. The flaval ligaments (13) running from the L4 to L5 laminae are shown well. Surgeons often operate through small openings in the flaval ligaments without the full laminectomy that used to be the standard approach for spinal surgery.

Image F passes through the body of the L5 vertebra – the normal bony architecture can be appreciated. The veins running through the body converge on the basi-vertebral vein (18), which has a small bony hood guarding its passage so that venous blood passes to the epidural veins (see 8 in image C). The right L5 root sheath (17) hugs the medial aspect of the pedicle (9).

Section level**Orientation**



Coronal magnetic resonance image (MRI)



Coronal magnetic resonance image (MRI)

- | | | | |
|-----------------------------|------------------------|----------------------------------------|----------------------|
| 1 L1 vertebral body | 8 Thecal sac | 15 Right kidney | 21 Iliacus |
| 2 L4 vertebral body | 9 Aorta | 16 Left kidney | 22 Ilium |
| 3 L5 vertebral body | 10 Retroperitoneal fat | 17 Psoas | 23 Iliac crest |
| 4 L4/L5 intervertebral disc | 11 Crus of diaphragm | 18 Lumbar vein | 24 Gluteal muscles |
| 5 Pedicle | 12 Liver | 19 Descending colon | 25 S1 vertebral body |
| 6 Nerve root sheath L4 | 13 Spleen | 20 Anterior abdominal-wall musculature | |
| 7 Dorsal root ganglion L4 | 14 Right adrenal gland | | |

Notes

Two coronal T1-weighted images elegantly show the relationship of the lumbar spine to the psoas muscles and kidneys (within retroperitoneal fat). Note that the kidneys lie in an oblique orientation, aligned to the lateral margins of the psoas muscles; thus, the upper poles lie in a more medial sagittal plane than the lower poles. Because of the lumbar lordosis, the upper poles lie in a more posterior coronal plane than the lower poles.

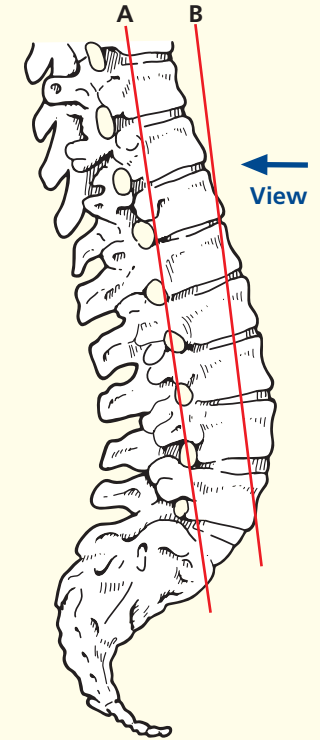
Because of the lumbar lordosis, the thecal sac and emerging nerve root sheaths can be seen in the L4 region, while vertebral bodies are demonstrated more superiorly and inferiorly. Note the way in which each nerve root sheath hugs the medial and inferior aspects of its associated pedicle (L4 root inferomedial to the L4 pedicle). The expansion for the dorsal root ganglion can just be appreciated. The fairly constant relationship of the L4/L5 disc space with the level of the superior iliac crest is shown

well; this is particularly useful in patients with lumbosacral anomalies (around 25 per cent of people).

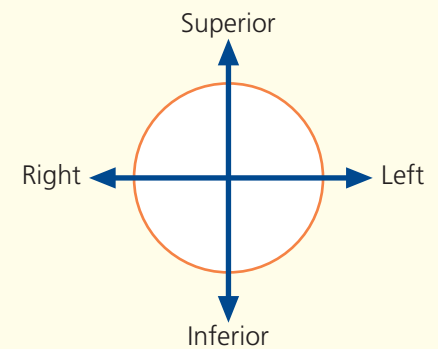
Also apparent are the segmental lumbar veins, which drain blood from the epidural veins. These run anteriorly within a narrow, but important, fat plane alongside each vertebral body.

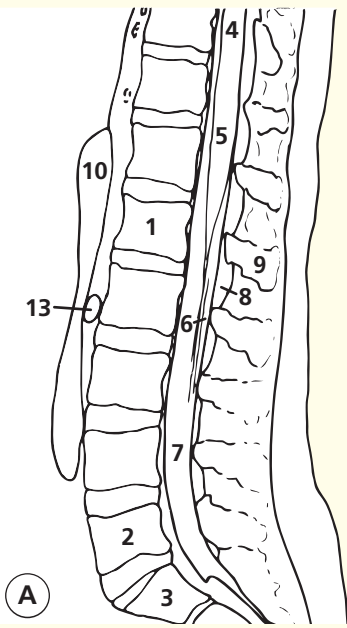
The psoas muscles (**17**) are particularly prominent in this individual. The superior attachment to the lateral aspects of the disc at the thoracolumbar junction is seen well. One can appreciate how a disc-space infection (often tuberculous) at this level could track inferiorly in and around the psoas muscle down to the iliacus and eventually present as a cold abscess in the inguinal region. The close relation of the adrenal to the right crus of the diaphragm (labelled **11** on the left) is apparent. The adrenal gland originates at this site, while the kidneys 'ascended' by differential growth during fetal life.

Section level

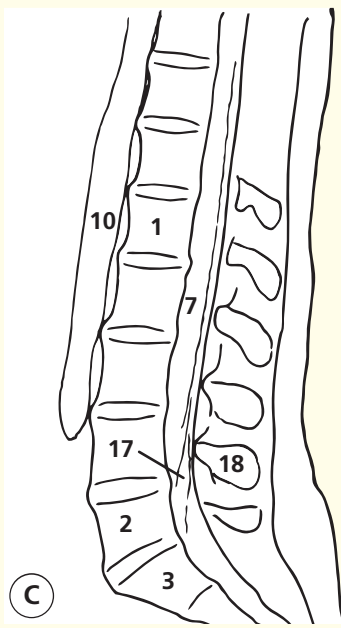


Orientation

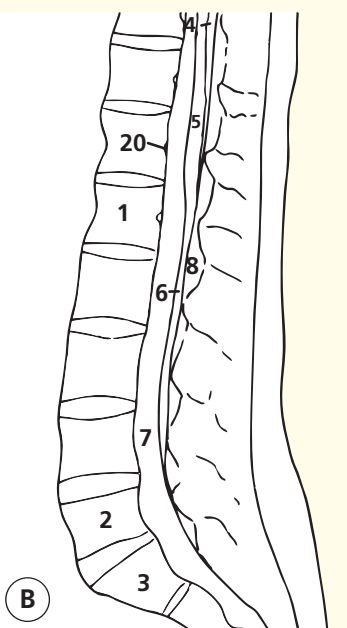




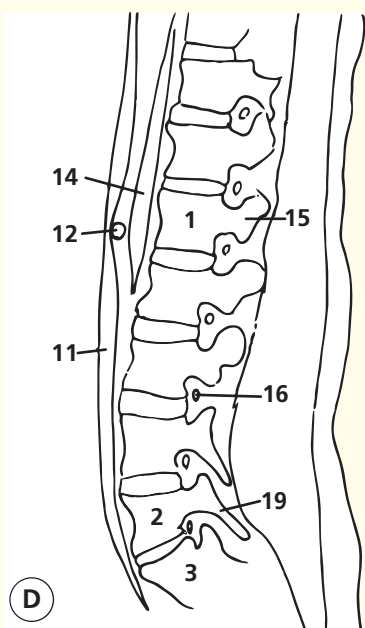
Sagittal T1-weighted magnetic resonance image (MRI)



Sagittal T2-weighted magnetic resonance image (MRI)



Sagittal T2-weighted magnetic resonance image (MRI)



Sagittal T1-weighted magnetic resonance image (MRI)

1 L1 vertebral body	7 Cerebrospinal fluid within thecal sac	11 Inferior vena cava	vertebra	18 Spinous process L4
2 L5 vertebral body		12 Right renal artery	16 L3 nerve root sheath/dorsal root ganglion	19 Pars interarticularis L5
3 S1 vertebral body		13 Retro-aortic left renal vein	17 Nerve roots within cerebrospinal fluid	20 Basi-vertebral vein
4 Spinal cord	8 Epidural fat	14 Crus of diaphragm		
5 Conus medullaris	9 Spinous process L1	15 Pedicle of L1		
6 Cauda equina	10 Aorta			

Notes

Images A–B

These midline sagittal magnetic resonance images are of key importance in evaluating the lumbar spine (one of the commonest anatomical sites examined by MRI).

The anteroposterior diameter of the spinal canal can be assessed readily. This normally measures around 15 mm from the posterior aspect of the vertebral body to the anterior aspect of the lamina arch; values under 11.5 mm indicate a degree of spinal stenosis. The height of the disc spaces can be evaluated, as can the degree of hydration within. The normal disc space yields high signal intensity on T2 weighting (image B); a degenerate disc returns low signal intensity and becomes narrower. In these images, the L5/S1 is slightly degenerate, as judged by the slight reduction of signal. There is a slight increase in fat content in the superior portion of S1 vertebral body, suggesting a longstanding disc abnormality.

These sagittal images also demonstrate clearly the slight expansion of the distal cord at the T12/L1 level (the conus medullaris). The collection of nerve roots that forms the cauda equina ('horse's tail') is seen well posteriorly within the canal when the patient lies supine (as during MRI). Because normal roots move freely within the cerebrospinal fluid, lumbar puncture is generally a very safe procedure at any level caudal to the conus medullaris.

Image C

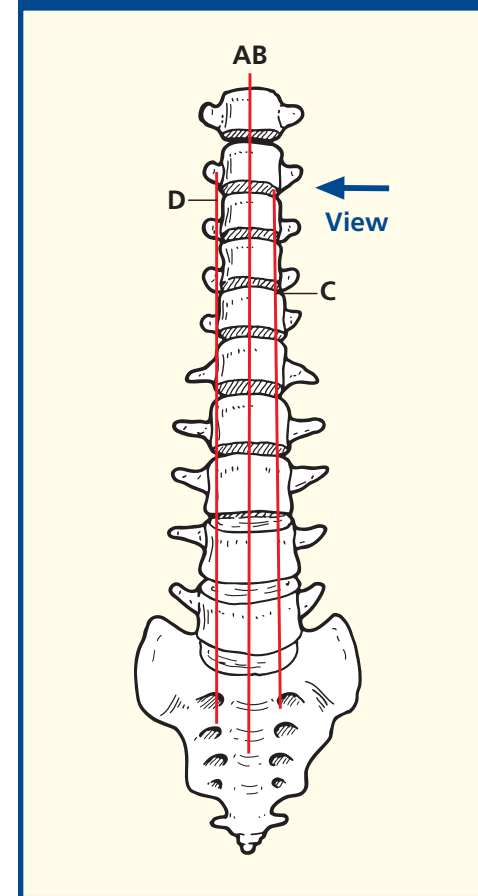
A T2-weighted magnetic resonance image about 10 mm to the left of the median sagittal plane shown in the images A and B. Here, the segmental roots can be seen traversing the cerebrospinal fluid towards their respective nerve root sheaths and exit foramina. The aorta can just be seen anterior to the vertebral bodies.

Image D

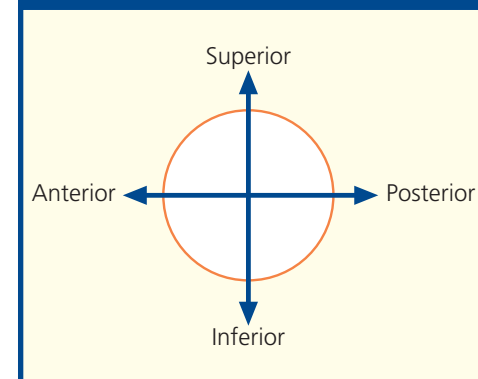
A T1-weighted sagittal magnetic resonance image even more lateral than in image C. This is to the right of the midline, however, as the right renal artery can be seen passing anterior to the diaphragmatic crus and posterior to the inferior vena cava. This plane shows the exit foramina at several segmental levels. The classical shape has been said to resemble that of the human ear. The pedicles of two adjacent vertebral bodies form the superior and inferior boundaries of the foramen. The anterior margin is formed by the vertebral body superiorly and the posterolateral portion of the intervertebral disk inferiorly. Posteriorly lie the pars interarticularis, the flaval ligament and the facet joint. Narrowing of the disc space and degenerative changes in the facet joints will reduce the capacity of the foramen, and the flaval ligament gets thicker as the disc space narrows; all of these changes can contribute to nerve-root compression.

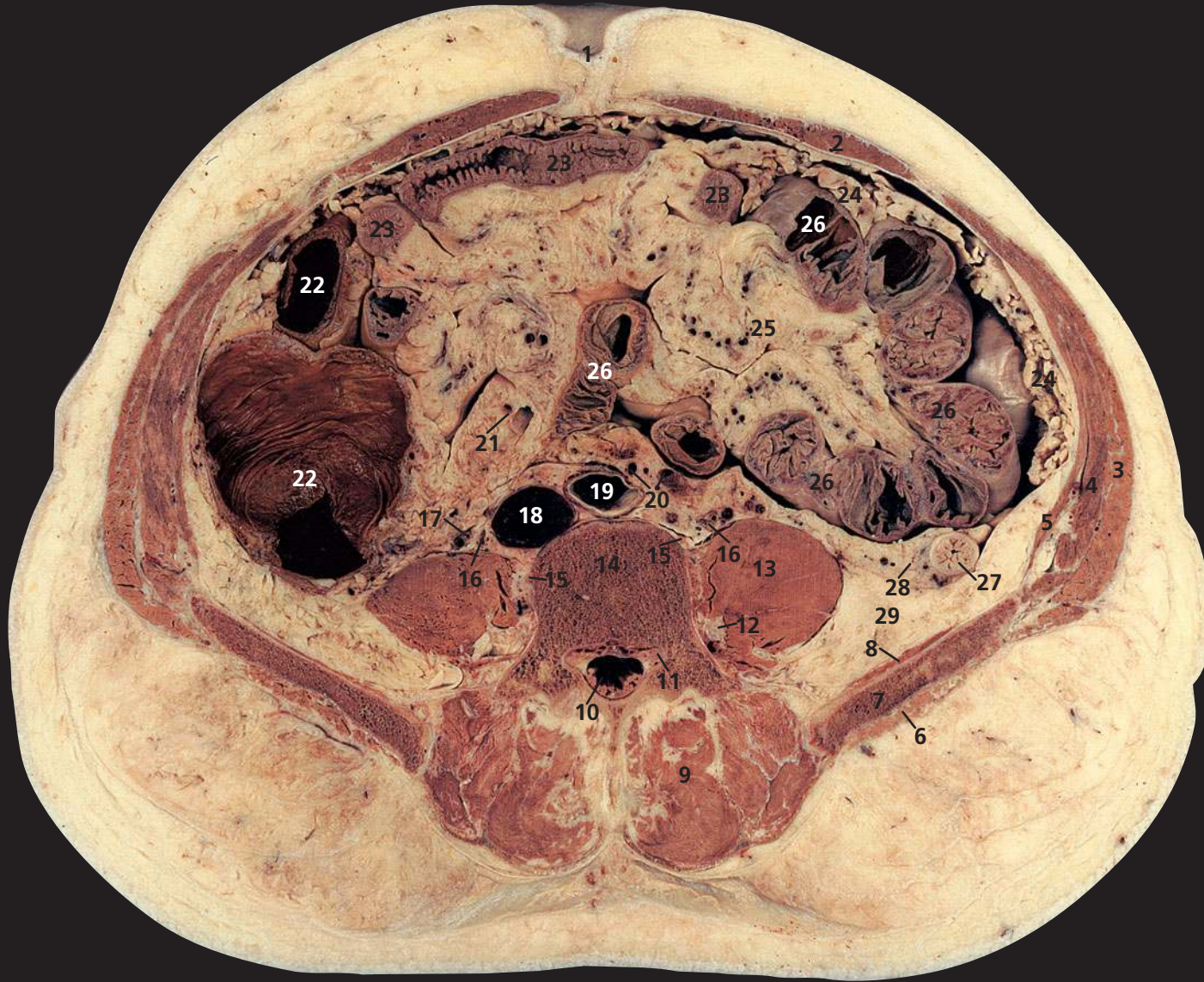
The nerve root sheaths, dorsal root ganglion and segmental nerve lie in the superior portion of the foramen. There are commonly two epidural veins in each foramen – a superior vein between the nerve root and the body/pedicle, and a second vein that usually lies much more caudally within the foramen. Remember that in the lumbar (and thoracic and sacral) spine, the segmental nerve root escapes caudal to its numbered vertebral body. For example, the L5 nerve root escapes caudal to the L5 pedicle through the L5/S1 foramen. Although the L5 root can be affected by a lateral L5/S1 disc herniation or facet joint degeneration, much more commonly it will be affected by a more central herniation at the L4/L5 level.

Section level



Orientation





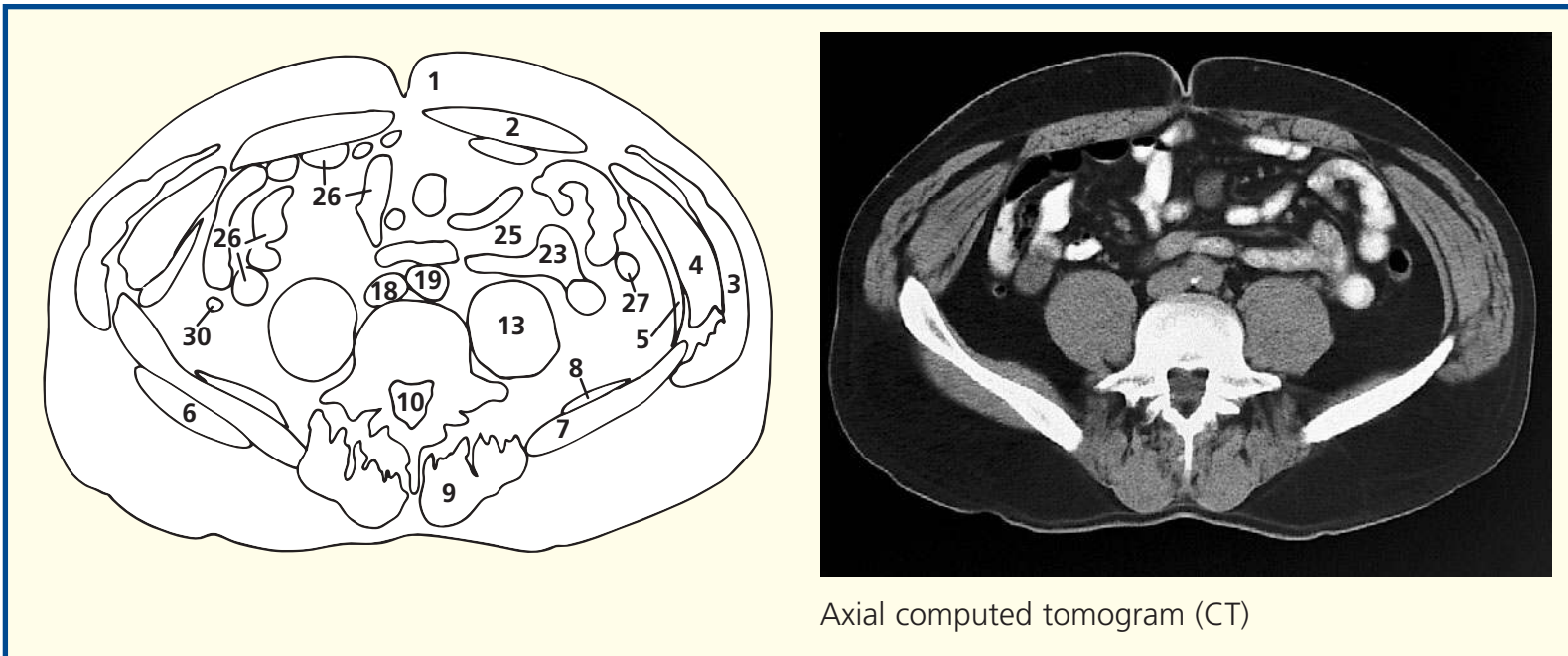
- 1 Umbilicus
- 2 Rectus abdominis
- 3 External oblique
- 4 Internal oblique
- 5 Transversus abdominis
- 6 Gluteus medius
- 7 Ilium
- 8 Iliacus
- 9 Erector spinae

- 10 Cauda equina within dural sheath
- 11 Dorsal root ganglion of fourth lumbar nerve
- 12 Ventral ramus of third lumbar nerve
- 13 Psoas major
- 14 Body of fourth lumbar vertebra
- 15 Lumbar sympathetic chain
- 16 Ureter

- 17 Testicular artery and vein
- 18 Inferior vena cava
- 19 Aorta
- 20 Inferior mesenteric artery and vein
- 21 Right colic artery and vein
- 22 Ascending colon
- 23 Jejunum
- 24 Greater omentum
- 25 Mesentery of small intestine

- 26 Ileum
- 27 Descending colon
- 28 Anterior pararenal fat of retroperitoneum
- 29 Posterior pararenal fat of retroperitoneum

- 30 Appendix vermiformis



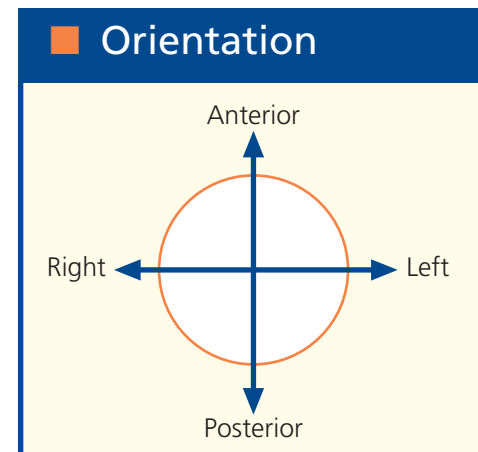
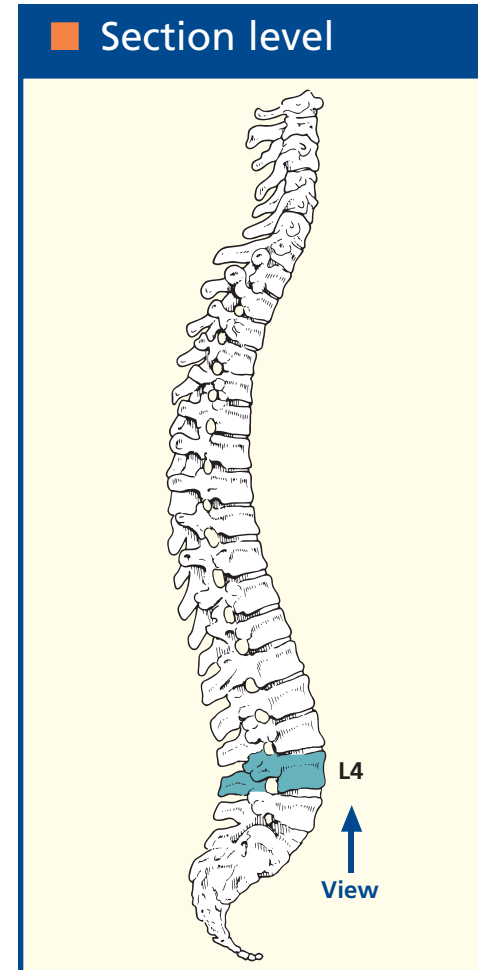
Notes

This section passes through the body of the fourth lumbar vertebra (**14**), the cranial portion of the iliac crests (**7**) and the umbilicus (**1**). There are wide individual variations in these landmarks, but the umbilicus is usually around the level of L4.

The inferior mesenteric artery (**20**) has just arisen from the aorta at the level of the third lumbar vertebra. More caudally, it will give rise to the superior rectal artery (see

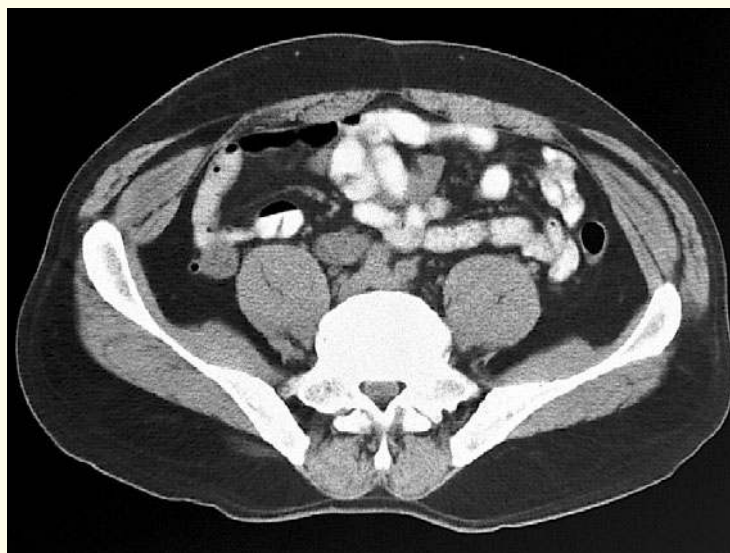
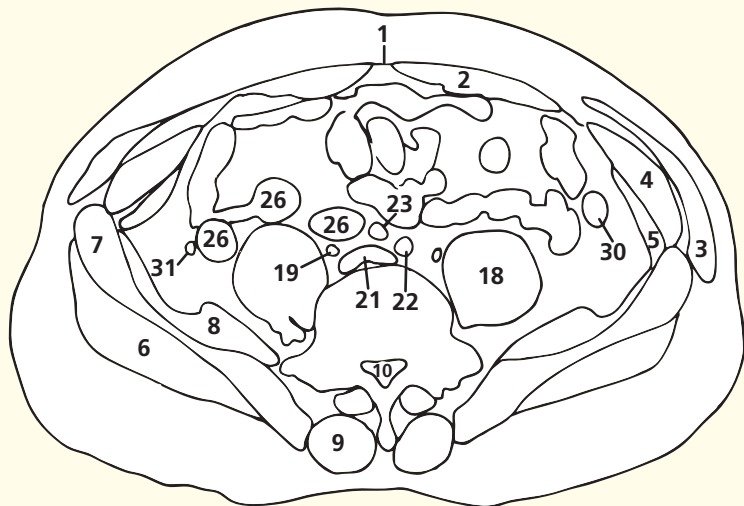
Axial section 2, **24**). The accompanying inferior mesenteric vein (**20**) has a long ascending retroperitoneal course to enter the splenic vein.

The aorta (**19**) is commencing to bifurcate on both the section and the CT image. This level of bifurcation, anterior to the fourth lumbar vertebra, is surprisingly constant, even in subjects with gross arteriosclerosis or with aneurysmal dilation of the aorta.





- | | | | |
|-------------------------|--------------------------------------------------------------------------|------------------------------------|-----------------------------|
| 1 Linea alba | 10 Cauda equina within dural sheath | 16 Femoral nerve | 25 Ascending colon |
| 2 Rectus abdominis | 11 Root of fifth lumbar nerve | 17 Obturator nerve | 26 Ileum |
| 3 External oblique | 12 Transverse process of fifth lumbar vertebra | 18 Psoas major | 27 Jejunum |
| 4 Internal oblique | 13 Part of intervertebral disc between fourth and fifth lumbar vertebrae | 19 Uretra | 28 Greater omentum |
| 5 Transversus abdominis | 14 Part of body of fourth lumbar vertebra | 20 Testicular artery and vein | 29 Mesentery of small bowel |
| 6 Gluteus medius | 15 Lumbar sympathetic chain | 21 Inferior vena cava at origin | 30 Descending colon |
| 7 Ilium | | 22 Left common iliac artery | |
| 8 Iliacus | | 23 Right common iliac artery | |
| 9 Erector spinae | | 24 Superior rectal artery and vein | |
| | | | 31 Appendix vermiformis |



Axial computed tomogram (CT)

Notes

This section transects the intervertebral disc between the fourth and fifth lumbar vertebrae (**13**). The lumbar sympathetic chain (**15**) is visualized well as it lies on the fourth lumbar vertebral body (**14**); it is overlapped on the right by the inferior vena cava (**21**) and on the left by the common iliac artery (**22**). More cranially, it lies just lateral to the aorta.

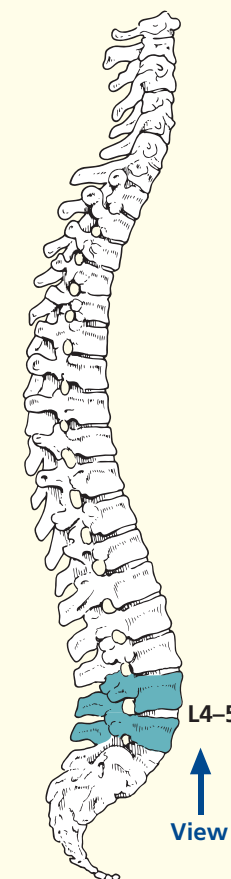
The transverse processes of the fifth lumbar vertebra (**12**) are bulky and all but reach the sacrum, particularly (in this subject) on the left side. Reference to Axial section 3 shows partial sacralization of L5, a very common variation.

The superior rectal artery (**24**) is the continuation of the inferior mesenteric artery after this has given off its left colic branch (see Axial section 1).

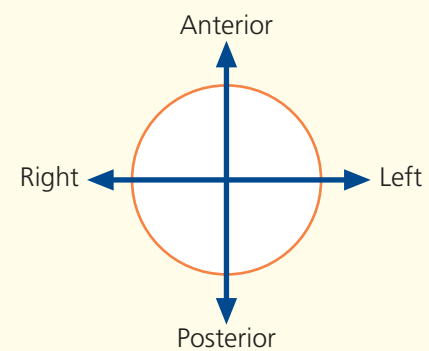
The inferior vena cava (**21**) is seen at its commencement. Its oval shape in the section (more markedly oval in the CT image) is produced by the convergence of the two common iliac veins at this level.

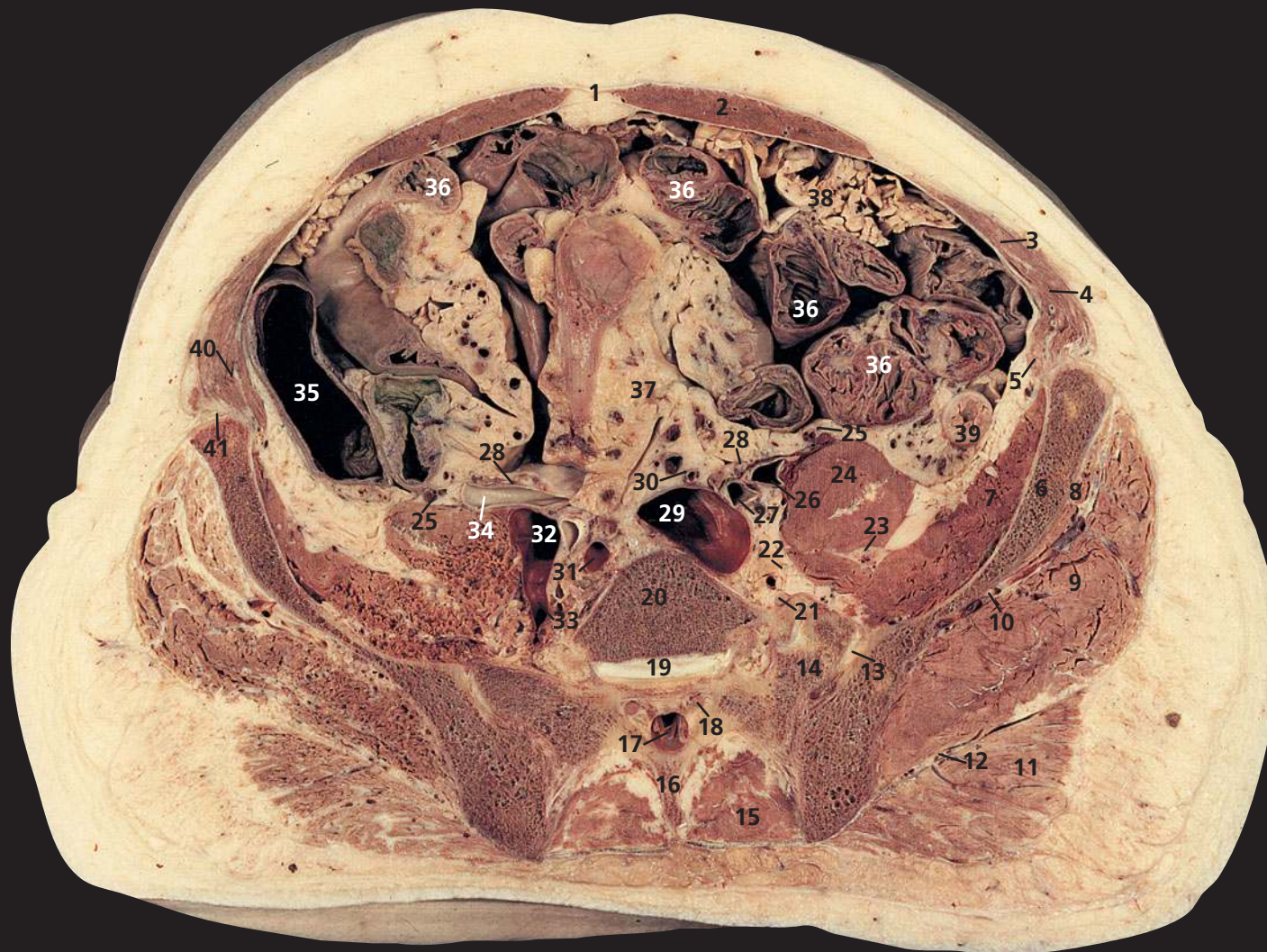
The intervertebral discs (**13**) account for nearly 25 per cent of the total length of the spinal column. They are composed at their circumference of laminae of fibrous tissue, forming the annulus fibrosus. At their centre is the soft, pulpy, highly elastic nucleus pulposus, which is especially prominent in the lumbar region. This is considered to represent the remains of the fetal notochord. With increasing age, the nucleus becomes progressively less differentiated from the annulus and is gradually replaced with fibrocartilage.

Section level

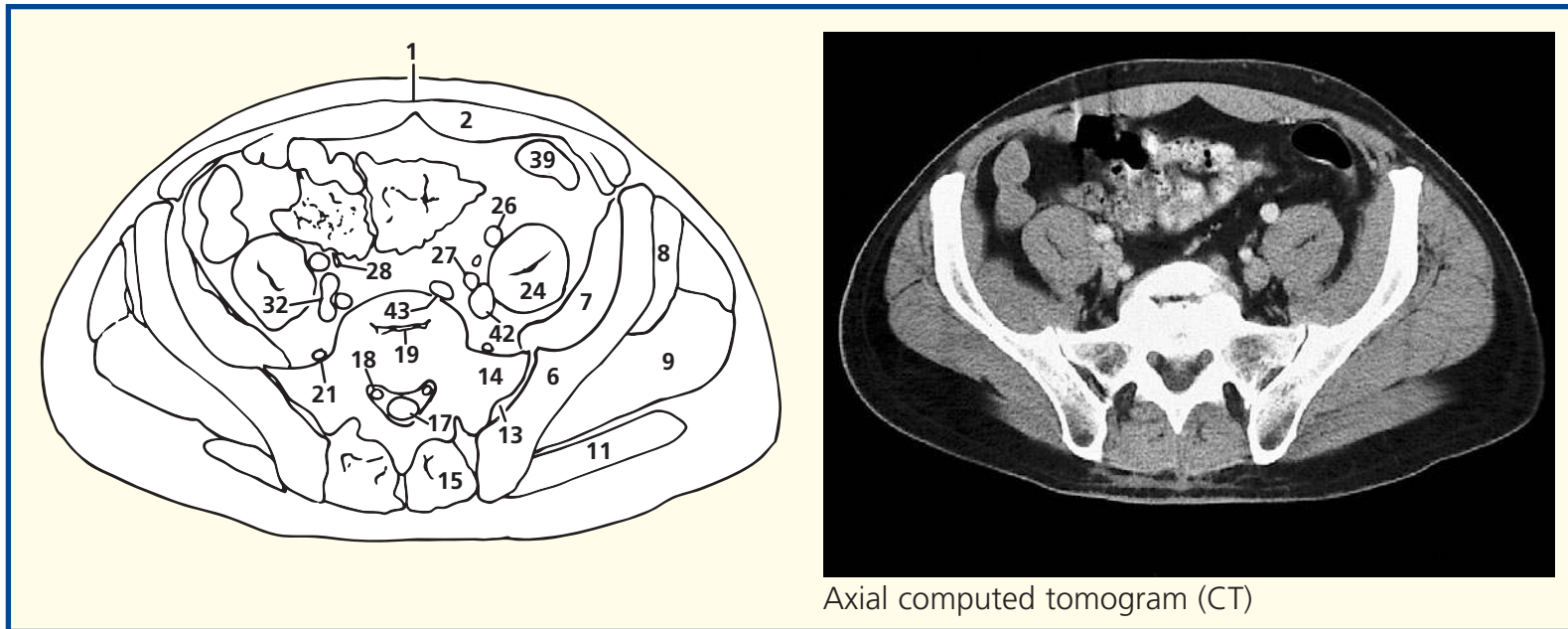


Orientation





- | | | | | |
|-------------------------------------------|-------------------------------------------|------------------------------------------|---------------------------------------------------|-------------------------------------------------------------------|
| 1 Linea alba | 11 Gluteus maximus | 19 Part of lumbosacral disc | 28 Ureter | 36 Ileum |
| 2 Rectus abdominis | 12 Inferior gluteal artery vein and nerve | 20 Part of body of fifth lumbar vertebra | 29 Left common iliac vein | 37 Mesentery of small bowel |
| 3 External oblique | 13 Sacroiliac joint | 21 Ventral ramus of fifth lumbar nerve | 30 Superior rectal artery and vein | 38 Greater omentum |
| 4 Internal oblique | 14 Lateral mass of sacrum | 22 Obturator nerve | 31 Superior gluteal artery and vein within pelvis | 39 Descending colon |
| 5 Transversus abdominis | 15 Erector spinae | 23 Femoral nerve | 32 Right common iliac vein | 40 Iliohypogastric nerve |
| 6 Ilium | 16 Spine of first segment of sacrum | 24 Psoas major | 33 Right internal iliac vein | 41 Ilioinguinal nerve, with deep circumflex iliac artery and vein |
| 7 Iliacus | 17 Cauda equina within dural sheath | 25 Testicular artery and vein | 34 Right common iliac artery at bifurcation | |
| 8 Gluteus minimus | 18 Root of first sacral nerve | 26 Left external iliac artery | 35 Ascending colon | |
| 9 Gluteus medius | | 27 Left internal iliac artery | | |
| 10 Superior gluteal artery vein and nerve | | | | 42 Left external iliac vein |
| | | | | 43 Left internal iliac vein |



Axial computed tomogram (CT)

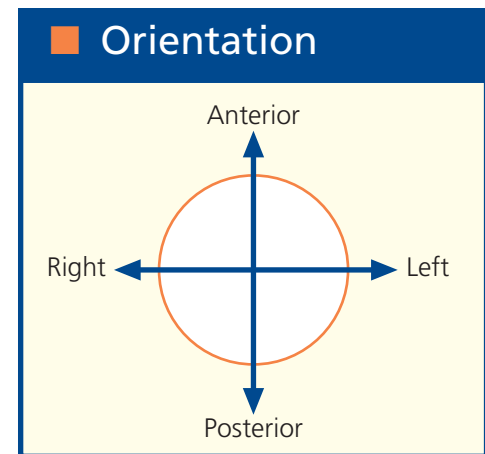
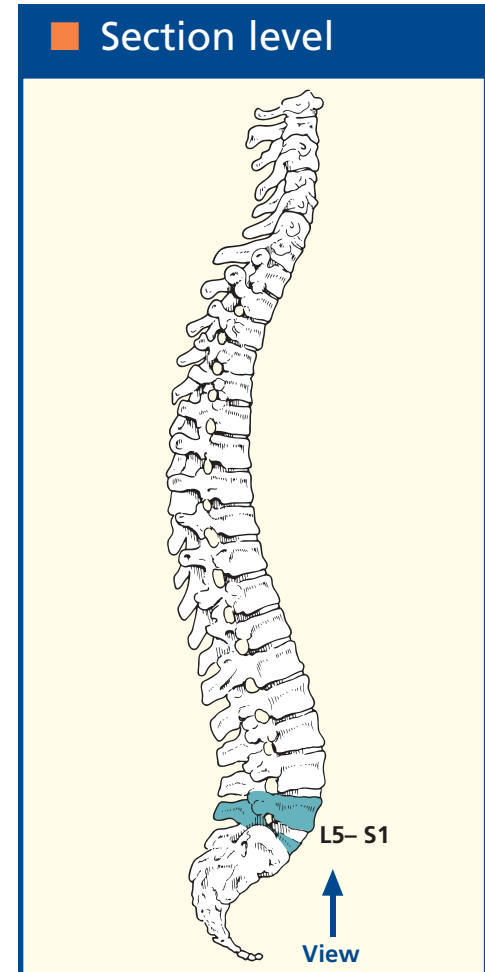
Notes

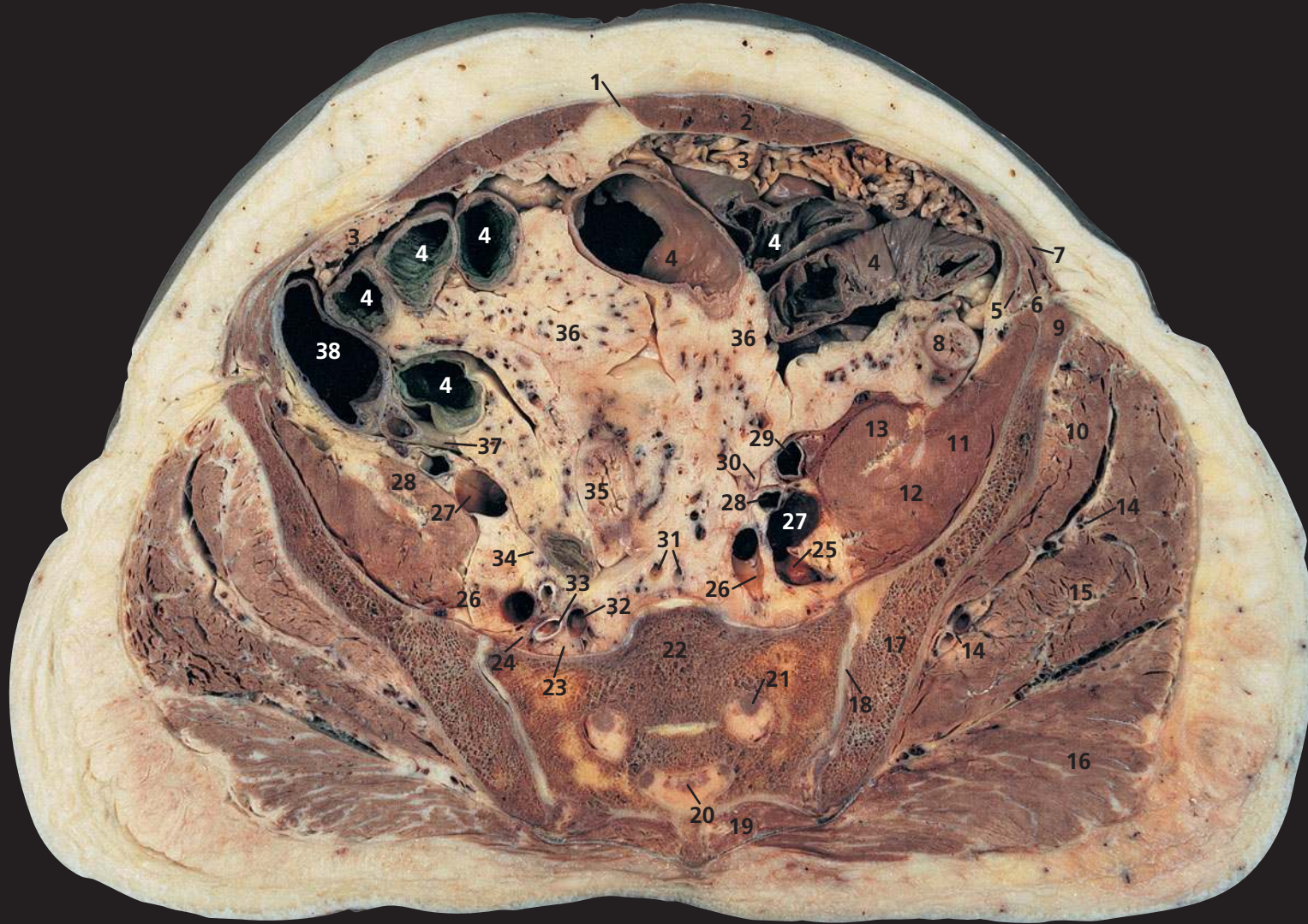
This section traverses the sacroiliac joint (**13**), the lumbosacral disc (**19**) and a lower part of the body of the fifth lumbar vertebra (**20**). There is some asymmetry of the lateral mass of the sacrum (**14**) in this subject, the left side being larger. This is because there is a small articulation (just visible) between the left sacral mass and the sacralized left L5 transverse process (see also Axial section 2). These variations are very common.

An intravenous injection of contrast medium was given

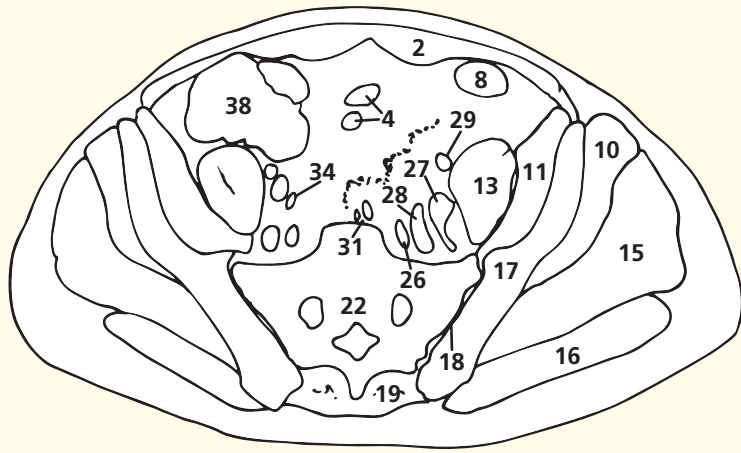
before the CT image series, hence the opacification of the blood vessels.

The superior gluteal vessels (**31**) arise from the internal iliac vessels. Together with the superior gluteal nerve (**10**), they emerge from the pelvis through the greater sciatic foramen above piriformis and then run between and supply gluteus medius (**9**) and gluteus minimus (**8**). The inferior gluteal artery, vein and nerve (**12**) emerge below piriformis and supply gluteus maximus (**11**).



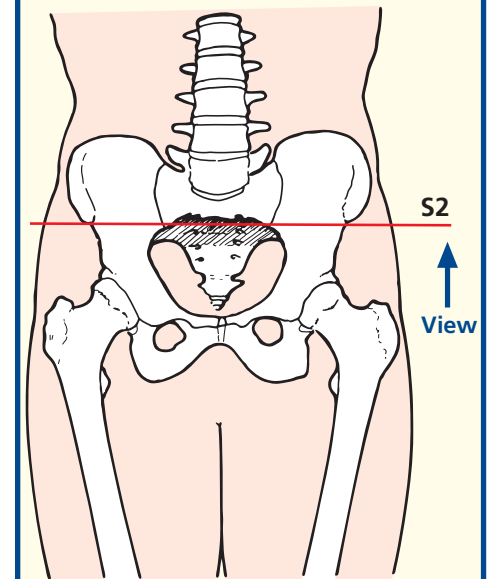


- | | | | |
|---------------------------------|----------------------------------------|-----------------------------|----------------------------------|
| 1 Linea alba | 11 Iliacus | 21 Second sacral nerve root | 31 Median sacral artery and vein |
| 2 Rectus abdominis | 12 Femoral nerve | 22 Sacrum, second segment | 32 Superior gluteal vein |
| 3 Greater omentum | 13 Psoas major | 23 Lumbosacral trunk | 33 Superior gluteal artery |
| 4 Ileum | 14 Superior gluteal artery and vein | 24 Obturator nerve | 34 Right ureter |
| 5 Transversus abdominis | 15 Gluteus medius | 25 Iliolumbar vein | 35 Sigmoid colon |
| 6 Internal oblique | 16 Gluteus maximus | 26 Internal iliac vein | 36 Mesentery of ileum |
| 7 External oblique aponeurosis | 17 Ilium | 27 External iliac vein | 37 Appendix vermiformis |
| 8 Descending colon | 18 Sacroiliac joint | 28 Internal iliac artery | 38 Caecum |
| 9 Anterior superior iliac spine | 19 Erector spinae | 29 External iliac artery | |
| 10 Gluteus minimus | 20 Filum terminale within sacral canal | 30 Left ureter | |



Axial computed tomogram (CT)

Section level



Notes

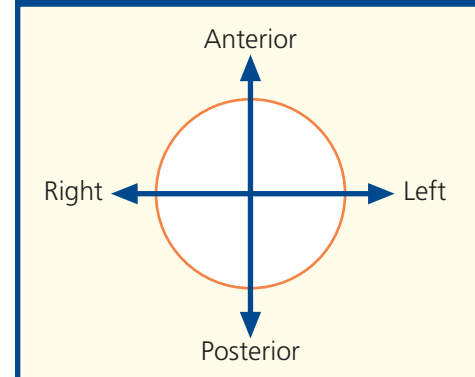
This section transects the second segment of the sacrum (**22**). Note that in this subject, the gluteal muscles on the right side are smaller and paler than those on the left (**10, 15, 16**). This subject had suffered a cerebrovascular accident that resulted in a right-sided paresis.

The sacroiliac joint (**18**) is a synovial joint. Since, as can be seen in this section, the sacral component is markedly wider anteriorly than posteriorly, the weight of the body tends to project it forward. This is resisted by the powerful posterior sacroiliac ligament on either side.

The appendix vermiformis (**37**) lies posterior to the ileum (**4**) in this section – the retro-ileal position. Much more commonly, the post-mortem appendix lies behind the caecum (65 per cent of cases) or descends into the pelvis (30 per cent of cases) (see the CT images in Axial sections 1 and 2).

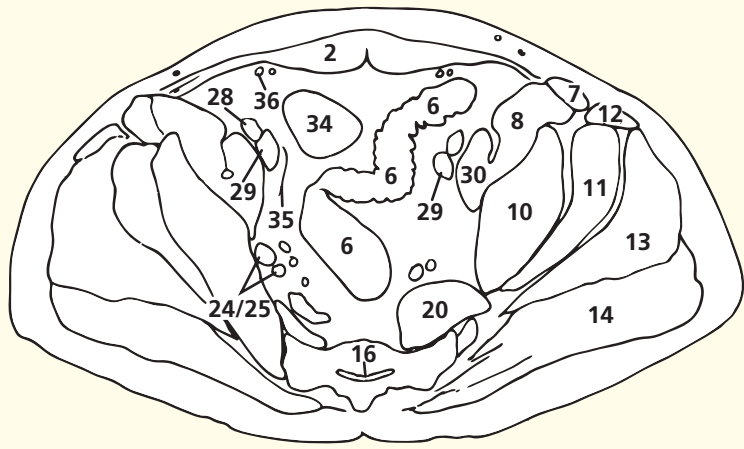
The superior gluteal vessels in their pelvic (**32, 33**) and gluteal (**14**) course are demonstrated clearly (see also Axial section 3).

Orientation



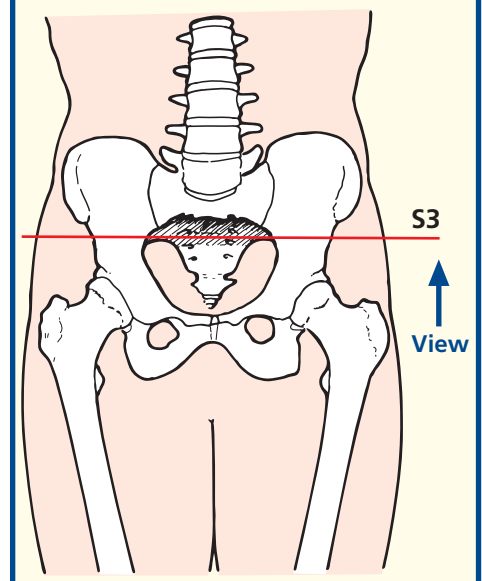


- | | | | |
|-------------------------|-----------------------------------|-------------------------------------|-------------------------------|
| 1 Linea alba | 11 Gluteus minimus | 21 Sciatic nerve | 31 Sigmoid mesocolon |
| 2 Rectus abdominis | 12 Tensor fasciae latae | 22 Superior gluteal artery and vein | 32 Right ureter |
| 3 Greater omentum | 13 Gluteus medius | 23 Obturator artery and vein | 33 Ileum |
| 4 Internal oblique | 14 Gluteus maximus | 24 Internal iliac vein | 34 Bladder |
| 5 Transversus abdominis | 15 Erector spinae | 25 Internal iliac artery | 35 Vas deferens |
| 6 Sigmoid colon | 16 Sacral canal | 26 Left ureter | 36 Inferior epigastric artery |
| 7 Sartorius | 17 Sacrum, third segment | 27 Lymph node | |
| 8 Iliacus | 18 Median sacral artery and vein | 28 External iliac vein | |
| 9 Femoral nerve | 19 Lateral sacral artery and vein | 29 External iliac artery | |
| 10 Ilium | 20 Piriformis | 30 Psoas major | |



Axial computed tomogram (CT)

Section level



Notes

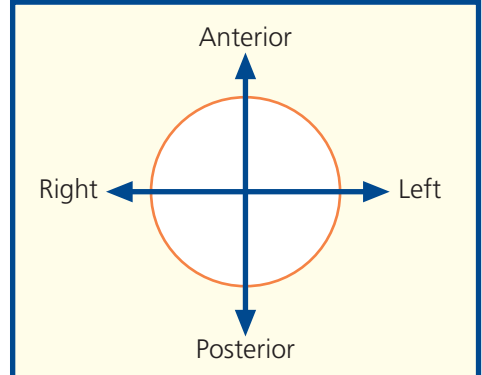
This section passes through the sacrum at its third segment (17). At this level, the sacral canal (16) lies below the termination of the dural sac, which ends at the second segment of the sacrum. The sacral canal now contains only the filum terminale and the lowermost sacral nerve roots, together with loose extradural fat. The sacral hiatus is, therefore, a useful portal of entry for the performance of an extradural nerve block.

Piriformis (20) arises from the front of the sacrum by three digitations, attached to the portions of bone between the pelvic sacral foramina and also to the grooves leading laterally from these foramina. The superior gluteal vessels (22), together with the superior gluteal nerve, pass above

piriformis through the greater sciatic foramen. In this subject, piriformis is paler and less bulky on the right side than on the left side as a result of a previous cerebrovascular accident (see Axial section 4). Piriformis is a bulky muscle that must be traversed when using the greater sciatic foramen as a route for percutaneous pelvic aspiration. On the CT image, there is asymmetry of the piriformis muscles due to a degree of scoliosis.

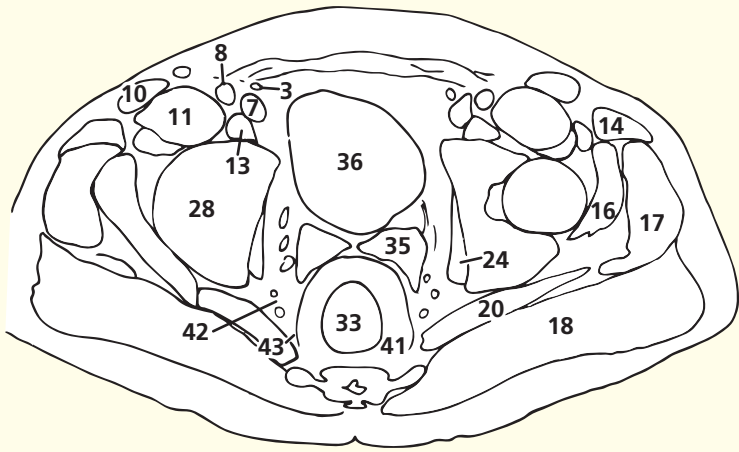
The ureter (26) descends into the pelvis characteristically immediately anterior to the internal iliac artery (25). It lies immediately deep to the pelvic peritoneum, crossed only by the vas deferens, which is seen in Axial section 6.

Orientation



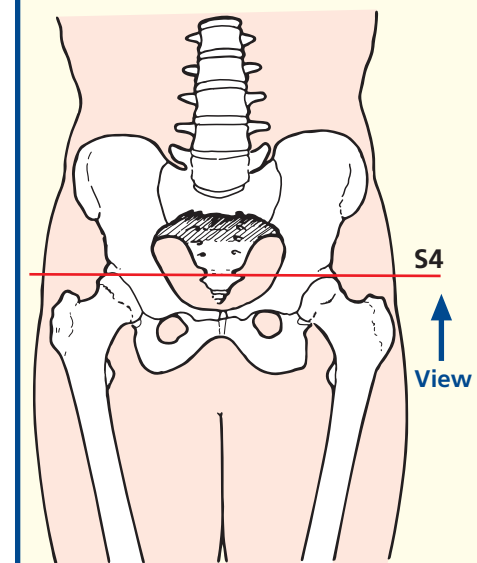


- | | | | |
|----------------------------------------|-------------------------------------|------------------------------------|---------------------------------------------------------------------|
| 1 Linea alba | 13 Psoas major and tendon | 25 Obturator vein | 37 Ileum |
| 2 Rectus abdominis | 14 Tensor fasciae latae | 26 Obturator artery | 38 Transversus abdominis |
| 3 Inferior epigastric artery and vein | 15 Iliofemoral ligament | 27 Obturator nerve | 39 Internal oblique |
| 4 Greater omentum | 16 Gluteus minimus | 28 Acetabulum (ilial portion) | 40 External oblique |
| 5 Sigmoid colon | 17 Gluteus medius | 29 Sacrum, fourth segment | |
| 6 Vas deferens | 18 Gluteus maximus | 30 Median sacral artery and vein | |
| 7 External iliac vein | 19 Sciatic nerve | 31 Superior rectal artery and vein | |
| 8 External iliac artery | 20 Piriformis | 32 Lateral sacral artery and vein | |
| 9 Femoral nerve | 21 Inferior gluteal artery and vein | 33 Rectum | |
| 10 Sartorius | 22 Pudendal nerve | 34 Rectosigmoid junction | |
| 11 Iliacus | 23 Internal pudendal artery | 35 Seminal vesicle | |
| 12 Rectus femoris straight head tendon | 24 Obturator internus | 36 Fundus of bladder | |
| | | | 41 Perirectal (mesorectal) fat |
| | | | 42 Pararectal fat (with branches of internal iliac artery and vein) |
| | | | 43 Perirectal (mesorectal) fascia |



Axial computed tomogram (CT)

Section level

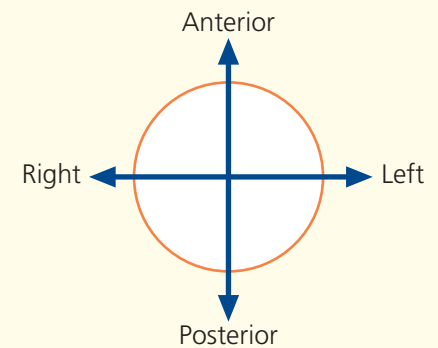


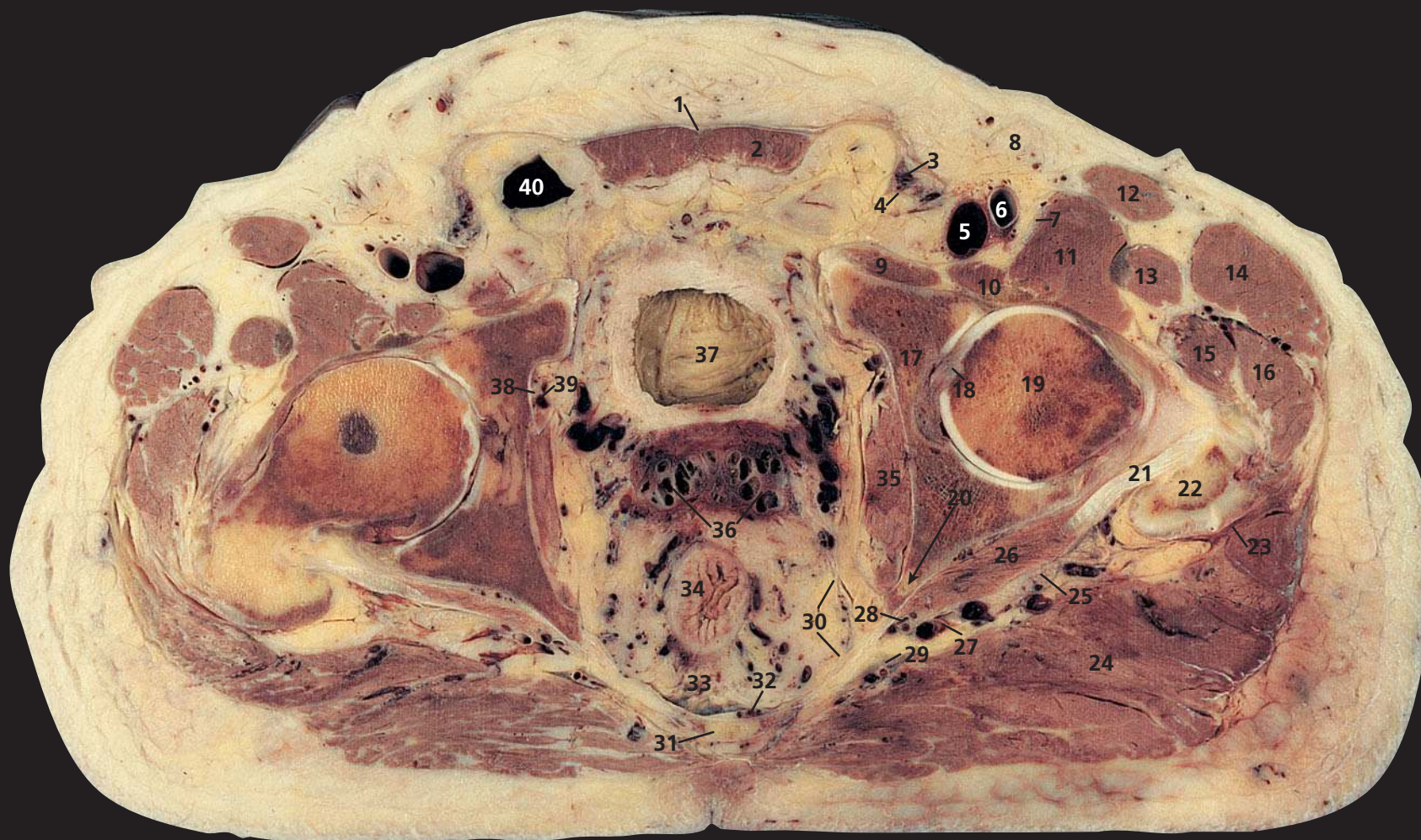
Notes

This section passes through the fourth segment of the sacrum (**29**), the superior portion of the acetabulum (**28**) and the fundus of the bladder (**36**). The rectum (**33**) lies immediately in front of the sacrum, separated by the median sacral vessels (**30**); it commences just cranial to this line of section on the third sacral segment. The rectosigmoid junction is also seen (**34**).

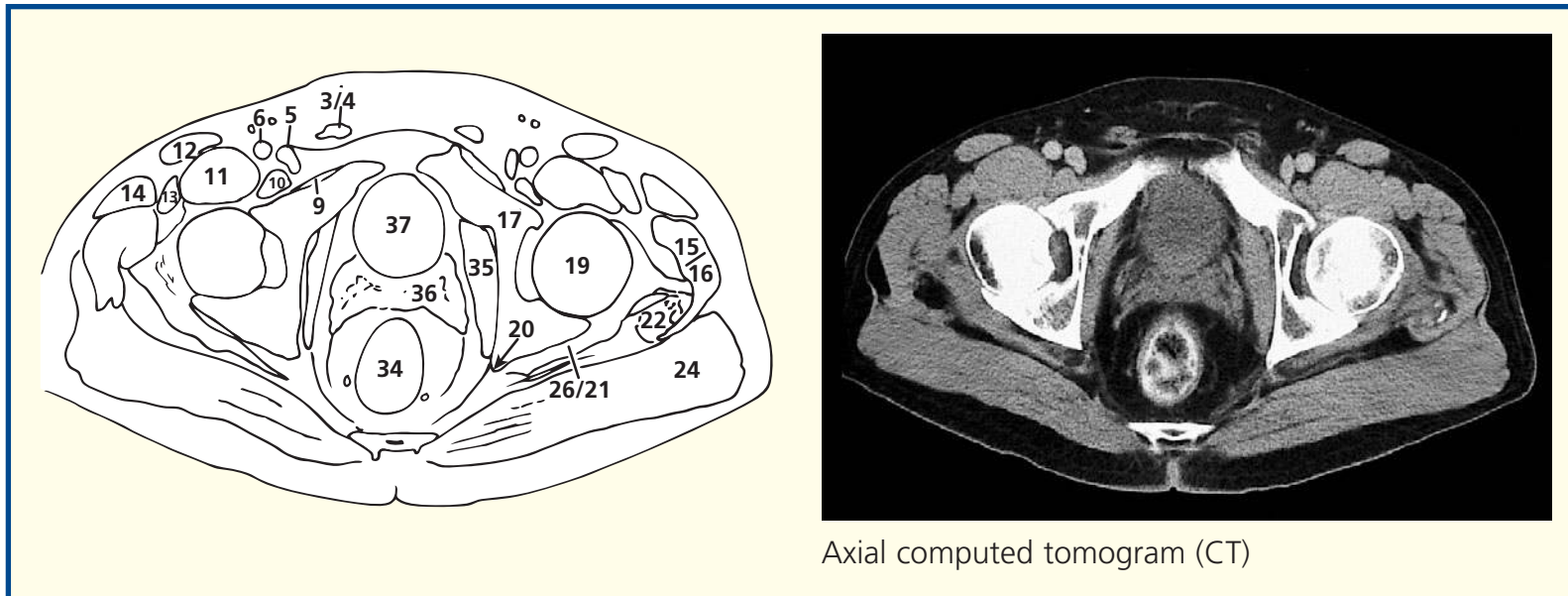
The vas deferens (**6**) is the most medial structure crossing the side wall of the pelvis immediately deep to the pelvic peritoneum. More caudally, it will join the seminal vesicle (**35**) to form the ejaculatory duct.

Orientation

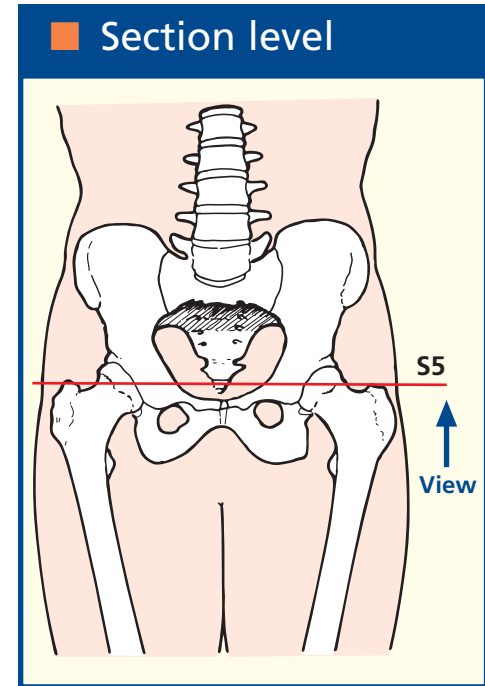




- | | | | |
|---------------------------|------------------------------------------------|---------------------------------------------------------------------------------|-------------------------------------------------------------------|
| 1 Linea alba | 13 Rectus femoris | 24 Gluteus maximus | 33 Superior rectal artery and vein in perirectal (mesorectal) fat |
| 2 Rectus abdominis | 14 Tensor fasciae latae | 25 Sciatic nerve | 34 Rectum |
| 3 Spermatic cord | 15 Gluteus minimus | 26 Gemellus superior | 35 Obturator internus |
| 4 Vas deferens | 16 Gluteus medius | 27 Inferior gluteal artery and vein | 36 Seminal vesicle |
| 5 Femoral vein | 17 Acetabulum (pubic portion) | 28 Pudendal nerve and inferior pudendal artery and vein | 37 Bladder |
| 6 Femoral artery | 18 Ligamentum teres | 29 Sacrospinous ligament | 38 Obturator nerve |
| 7 Femoral nerve | 19 Femoral head | 30 Perirectal (mesorectal) fascia separating perirectal fat from pararectal fat | 39 Obturator artery and vein |
| 8 Lymph node | 20 Ischium, leading to ischial spine (arrowed) | 31 Sacrum, fifth segment | 40 Patent processus vaginalis (indirect inguinal hernia sac) |
| 9 Pectineus | 21 Obturator internus tendon | 32 Lateral sacral artery and vein | |
| 10 Psoas major and tendon | 22 Greater trochanter | | |
| 11 Iliacus | 23 Trochanteric bursa | | |
| 12 Sartorius | | | |



Axial computed tomogram (CT)



Notes

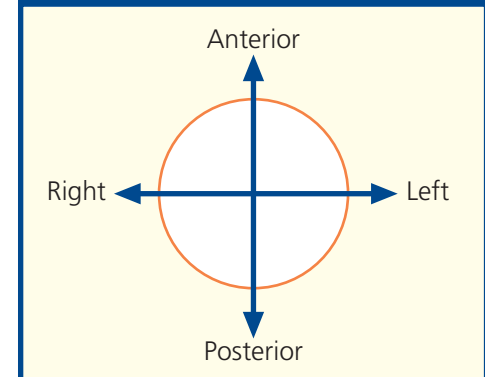
This section traverses the last (fifth) segment of the sacrum (**31**). The sacrospinous ligament (**29**) is transected as it passes forward to the ischial spine (**20**).

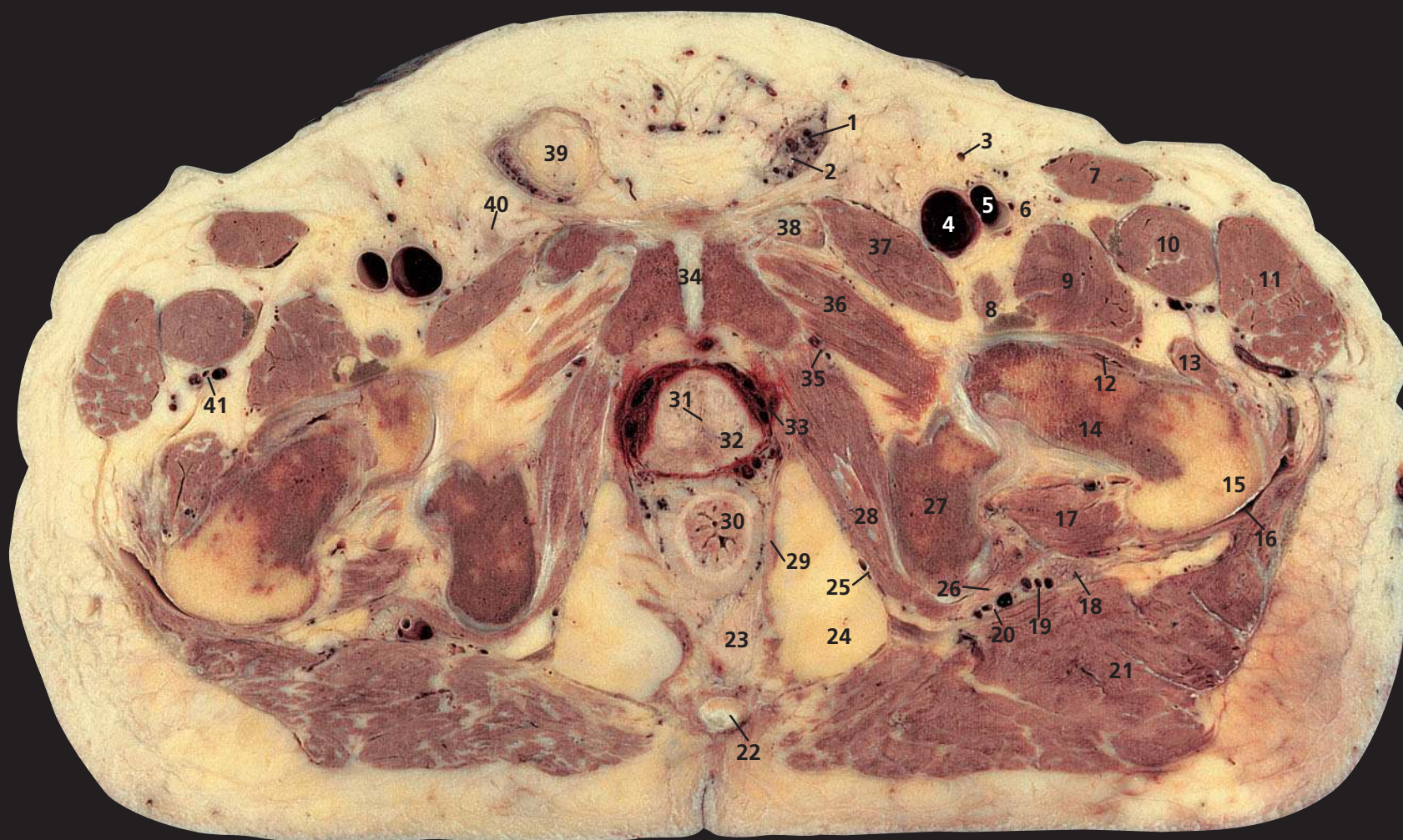
This section gives an excellent illustration of the hip joint at the level of the ligamentum teres (**18**). The ligamentum teres (**18**) transmits an artery, a branch of the obturator artery, to the femoral head, which is its sole source of blood in childhood. Damage to this vessel (Perthes' disease or slipped femoral epiphysis) may lead to avascular necrosis of the femoral head.

The superior rectal vessels (**33**) can be seen as they lie in the loose perirectal (mesorectal) fat, which also contains lymphatic vessels, lymph nodes and the pelvic plexuses lying on the rectal wall. The perirectal fat is separated from the pararectal fat by the perirectal (mesorectal) fascia (**30**).

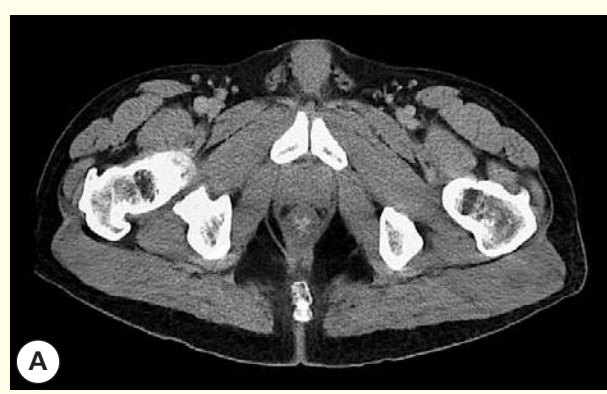
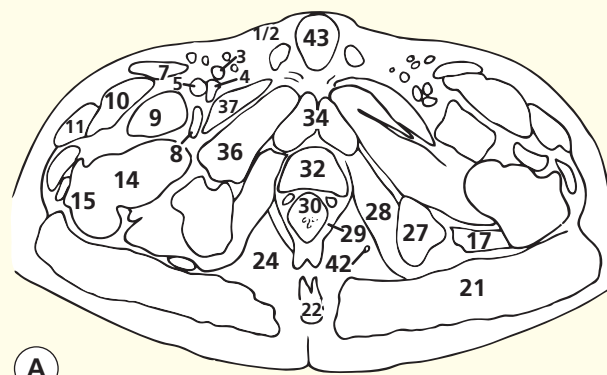
Note that this subject has an indirect inguinal hernia sac on the right side (**40**).

Orientation

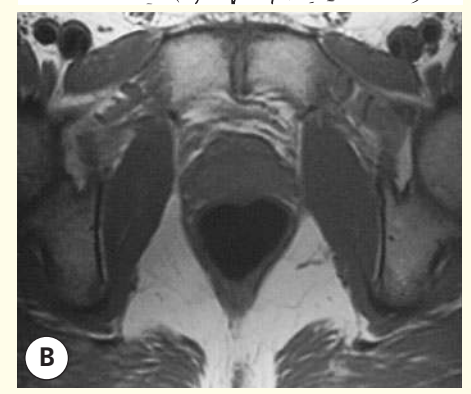
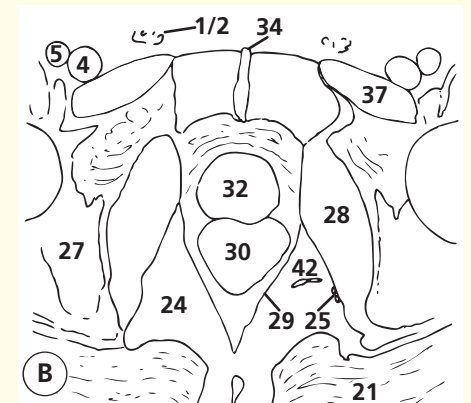




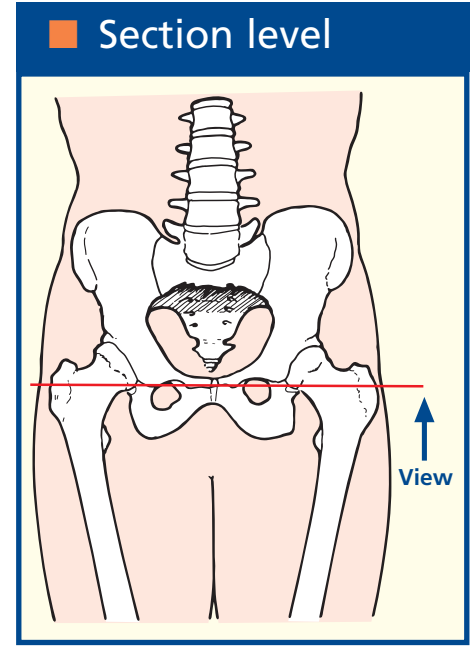
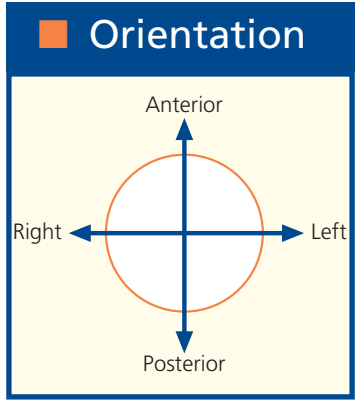
- | | | | |
|--------------------------|-----------------------------------------------------------------------|---------------------------------------|-----------------------------------------------|
| 1 Spermatic cord | 13 Vastus lateralis | 24 Ischiorectal fossa | 36 Obturator externus |
| 2 Vas deferens | 14 Femoral neck | 25 Pudendal (Alcock's) canal | 37 Pectineus |
| 3 Great saphenous vein | 15 Greater trochanter | 26 Obturator internus tendon | 38 Superior ramus of pubis |
| 4 Femoral vein | 16 Trochanteric bursa | 27 Ischium | 39 Extraperitoneal fat related to hernia sac |
| 5 Femoral artery | 17 Quadratus femoris | 28 Obturator internus | 40 Inguinal lymph node |
| 6 Femoral nerve | 18 Sciatic nerve | 29 Levator ani (puborectalis portion) | 41 Lateral circumflex femoral artery and vein |
| 7 Sartorius | 19 Inferior gluteal artery and vein | 30 Rectum | |
| 8 Psoas major and tendon | 20 Internal pudendal artery and vein and pudendal nerve (see also 25) | 31 Prostatic urethra | |
| 9 Iliacus | 21 Gluteus maximus | 32 Prostate | |
| 10 Rectus femoris | 22 Coccyx | 33 Prostatic venous plexus | 42 Inferior rectal artery |
| 11 Tensor fasciae latae | 23 Mesorectum | 34 Symphysis pubis | 43 Body of penis |
| 12 Hip joint capsule | | 35 Obturator artery and vein | |



Axial computed tomogram (CT)



Axial magnetic resonance image (MRI)



Notes

This section passes through the coccyx (22) and the symphysis pubis (34). In the standing position, the horizontal plane that passes through the coccyx corresponds to the superior margin of the symphysis.

The ischiorectal fossa (24) is wedge-shaped; its base points to the surface of the perineum, while its apex is the junction of obturator internus (28) and levator ani (29), covered respectively by the obturator fascia and the inferior fascia of the pelvic diaphragm. Medially it is bounded by the external anal sphincter and levator ani, laterally by the

tuberosity of the ischium and the obturator fascia, and posteriorly by the lower border of gluteus maximus (21) and the sacrotuberous ligament. Anteriorly lies the urogenital diaphragm, but the fossa is prolonged as a narrow recess above this diaphragm, where it is limited by the fusion between the inferior fascia of the pelvic diaphragm and the superior fascia of the urogenital diaphragm.

The internal pudendal vessels and the pudendal nerve (20) enter the perineum through the lesser sciatic foramen and then traverse the pudendal canal of Alcock (25). This canal comprises a special

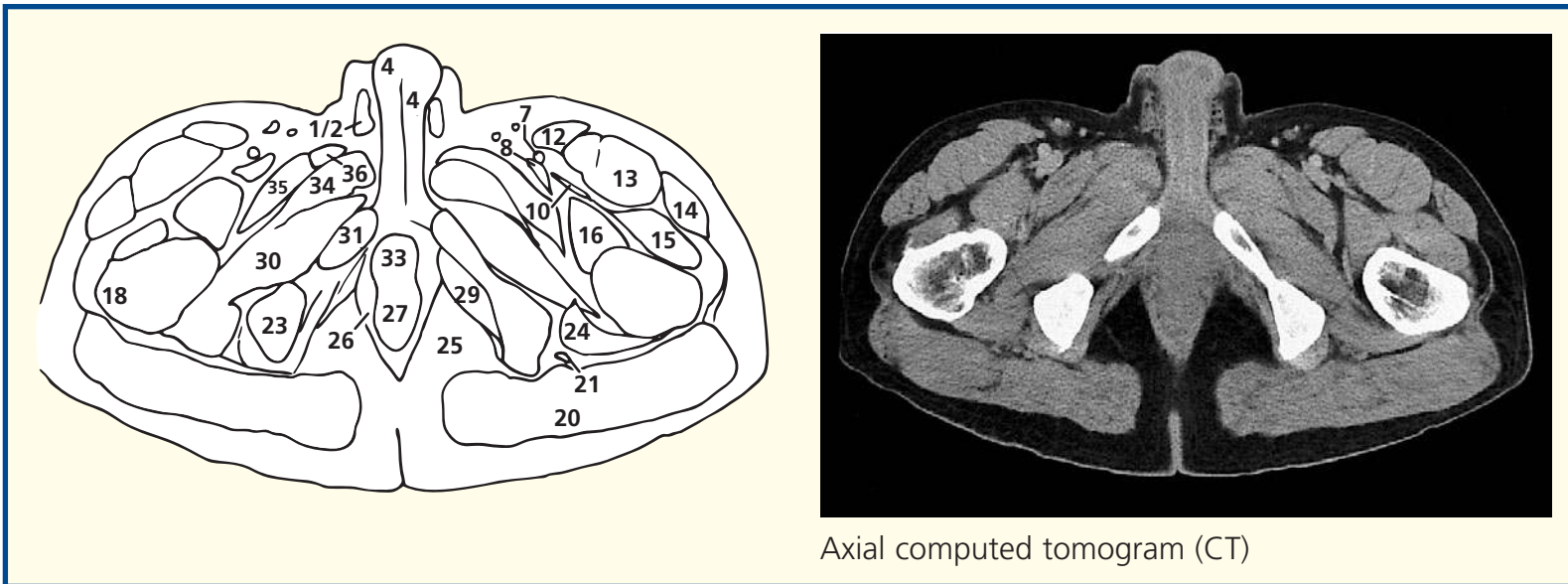
sheath of fascia fused with the lower part of the obturator fascia.

The left common femoral artery (5) is about to divide into the superficial femoral and profunda femoris on the section. On the CT image, this has already taken place.

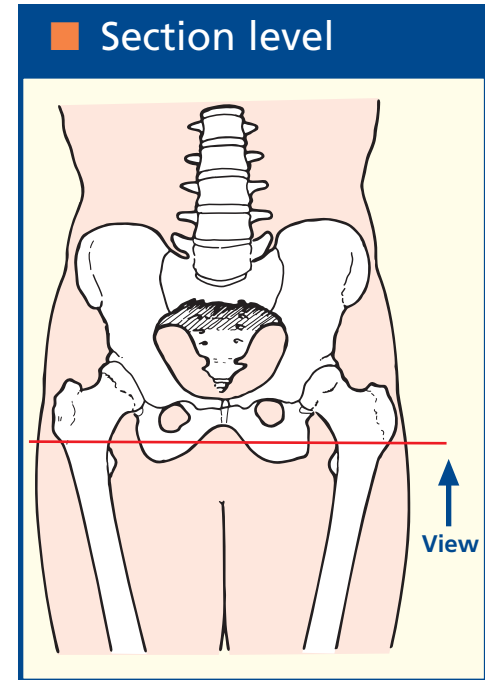
The spermatic cord (1) and vas deferens (2) are seen clearly on the left-hand side. On the right, these are compressed by extraperitoneal fat related to this subject's indirect inguinal hernia (39). This hernia is seen well in Axial section 7.



- | | | | |
|------------------------------|------------------------------------|--------------------------|---------------------------------|
| 1 Spermatic cord | 10 Profunda femoris artery | 19 Trochanteric bursa | 28 Pudendal canal |
| 2 Vas deferens | 11 Lateral circumflex femoral vein | 20 Gluteus maximus | 29 Obturator internus |
| 3 Tunica albuginea of penis | 12 Sartorius | 21 Sciatic nerve | 30 Obturator externus |
| 4 Corpus cavernosum (body) | 13 Rectus femoris | 22 Biceps femoris tendon | 31 Pubis-inferior ramus |
| 5 Inguinal lymph node | 14 Tensor fasciae latae | 23 Ischial tuberosity | 32 Corpus cavernosum (crus) |
| 6 Great saphenous vein | 15 Vastus lateralis | 24 Quadratus femoris | 33 Urethra (in distal prostate) |
| 7 Superficial femoral artery | 16 Iliacus | 25 Ischiorectal fat | 34 Adductor brevis |
| 8 Femoral vein | 17 Tendon of psoas major | 26 Levator ani | 35 Pectineus |
| 9 Femoral nerve | 18 Greater trochanter | 27 Anorectal junction | 36 Adductor longus |

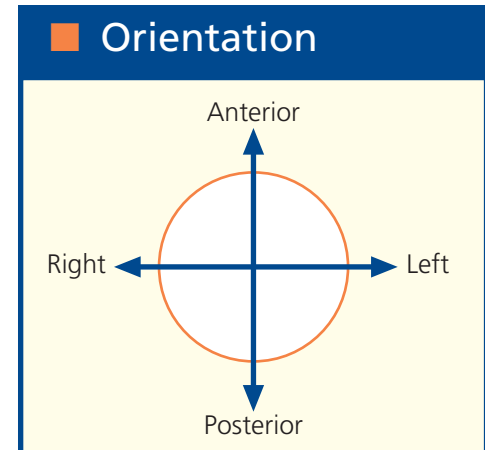


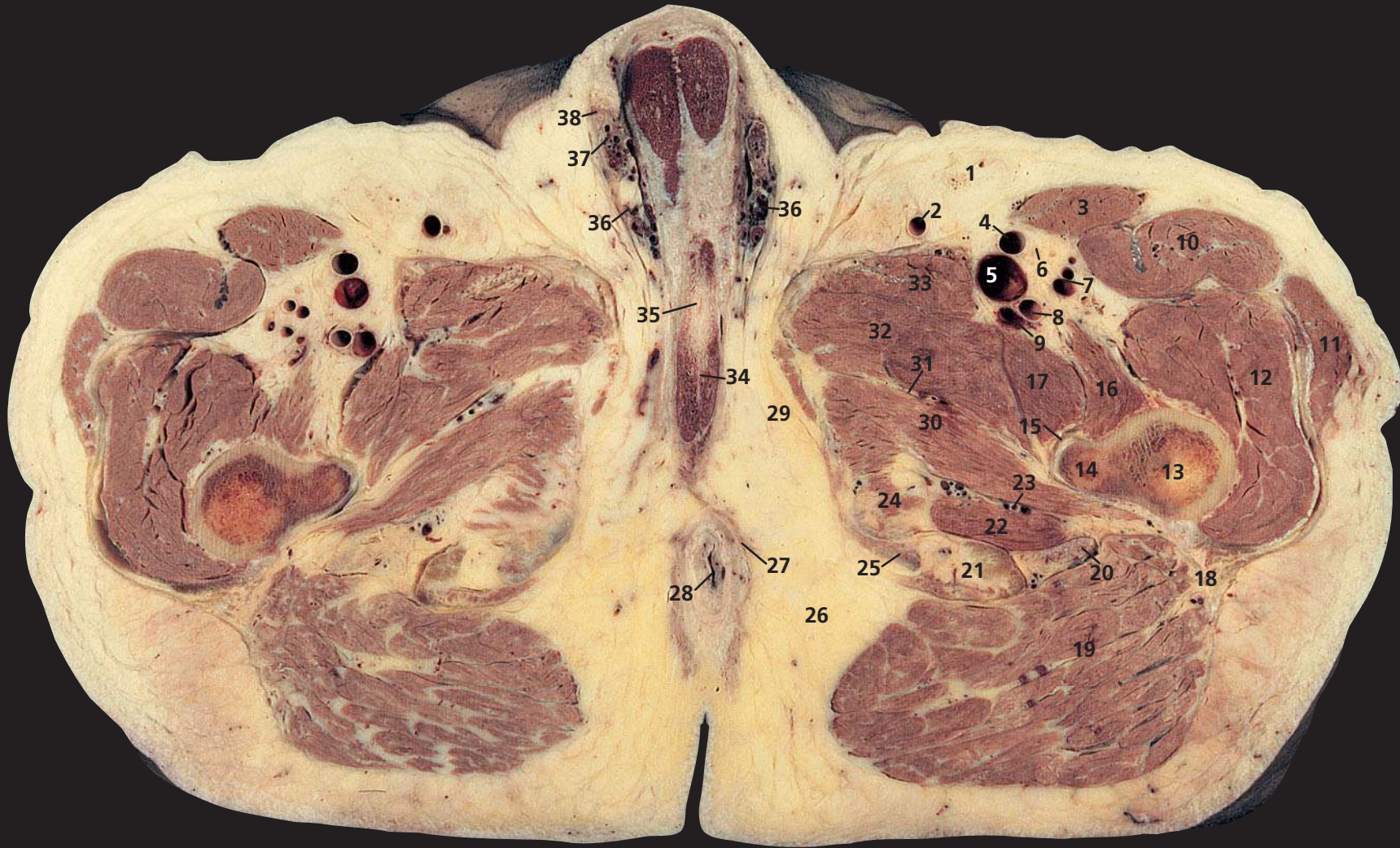
Axial computed tomogram (CT)



Notes

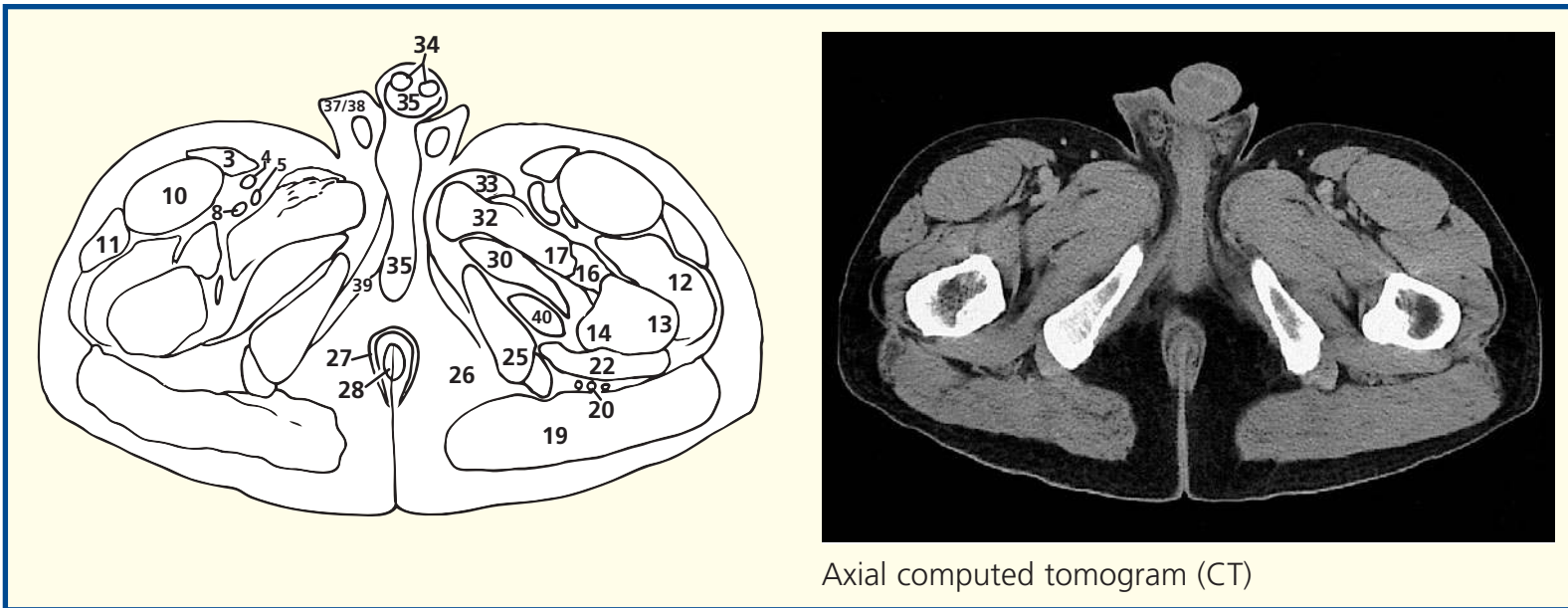
This section lies caudal to the coccyx and pubis but passes through the level of the ischial tuberosity (23). The plane of section cuts through the anorectal junction (27), around which lies levator ani (26). The ischiorectal fossa, filled with fat (25), which is described in Axial section 8, can be seen to communicate with the fossa on the other side, posterior to the anal canal. The inferior rectal artery is seen clearly in the centre of the fossa on the left-hand side.



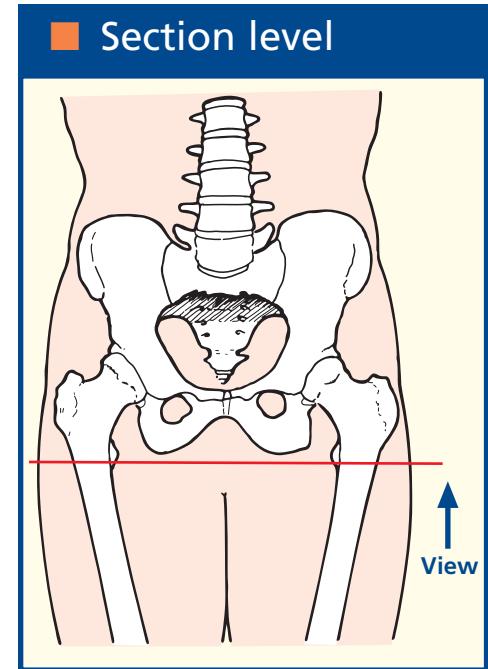


- | | | | |
|-------------------------------------------------|-------------------------------------------------|-------------------------------------------------------------------|-----------------------|
| 1 Inguinal lymph node | 12 Vastus lateralis | 23 Profunda femoris artery and vein
first perforating branches | 34 Corpus cavernosum |
| 2 Great saphenous vein | 13 Femur | 24 Semimembranosus | 35 Urethra |
| 3 Sartorius | 14 Lesser trochanter | 25 Ischium | 36 Pampiniform plexus |
| 4 Superficial femoral artery | 15 Tendon of psoas major | 26 Ischiorectal fat | 37 Spermatic cord |
| 5 Superficial femoral vein | 16 Iliacus | 27 Levator ani | 38 Vas deferens |
| 6 Femoral nerve | 17 Pectineus | 28 Anal canal | |
| 7 Lateral circumflex femoral artery
and vein | 18 Gluteus maximus tendon | 29 Gracilis | |
| 8 Profunda femoris artery | 19 Gluteus maximus | 30 Adductor magnus | |
| 9 Profunda femoris vein | 20 Sciatic nerve | 31 Obturator nerve, deep branch | |
| 10 Rectus femoris | 21 Biceps femoris and semitendinosus
tendons | 32 Adductor brevis | |
| 11 Tensor fasciae latae | 22 Quadratus femoris | 33 Adductor longus | |

- 39 Corpus cavernosum (crus)
- 40 Obturator externus

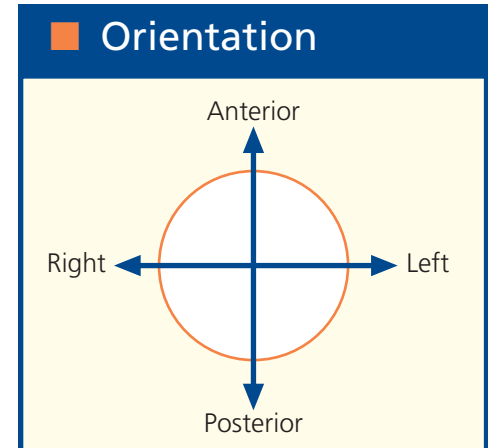


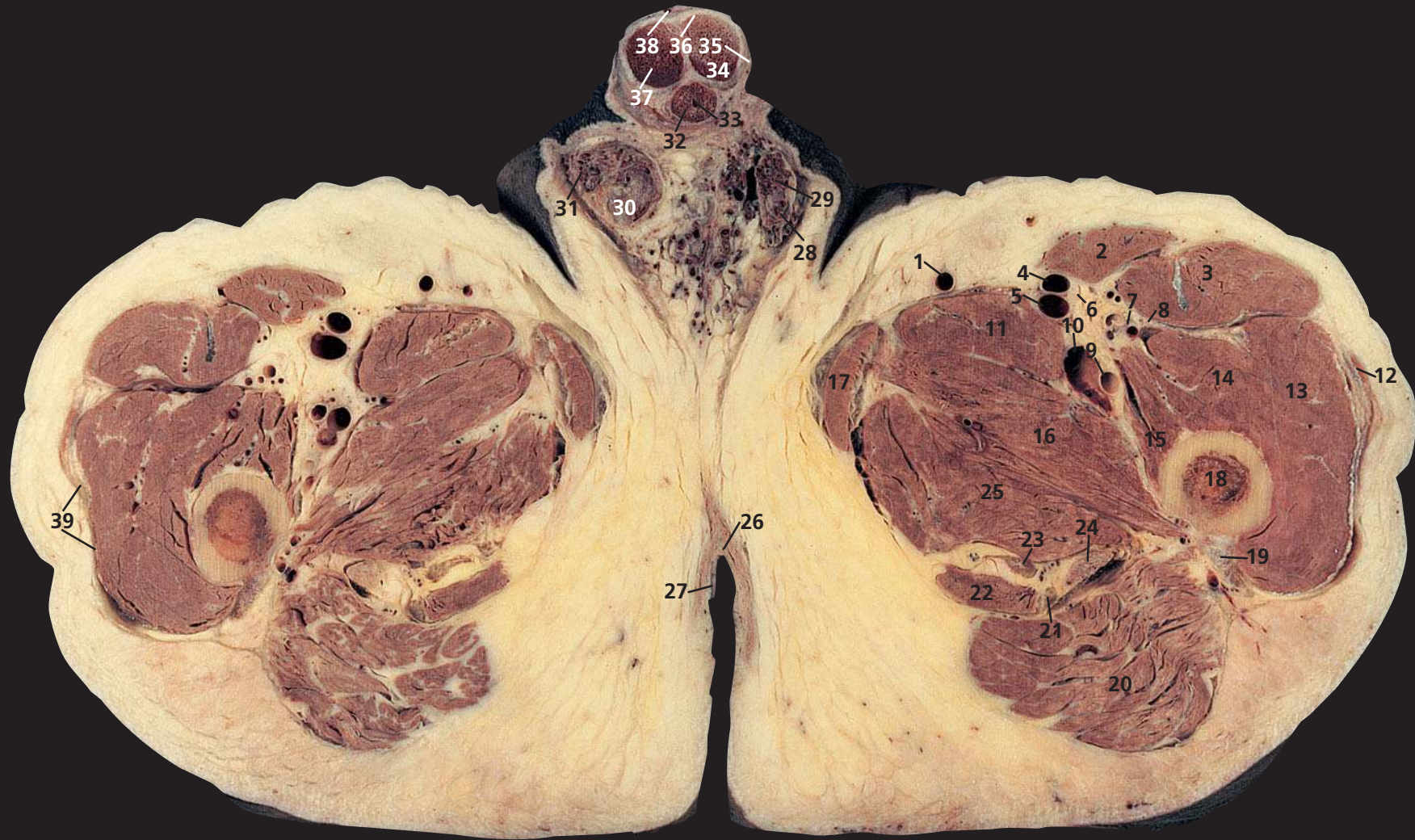
Axial computed tomogram (CT)



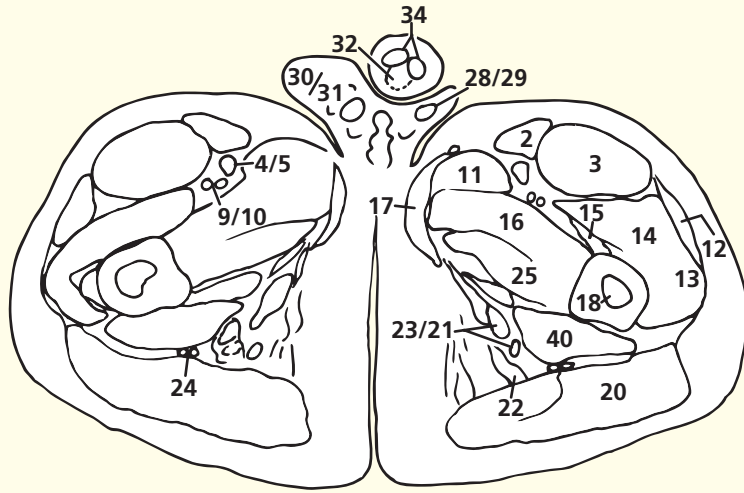
Notes

This section is completely below the pelvic girdle and transects the upper ends of the femoral shafts (**13**) at the level of the lesser trochanter (**14**). It transects the anal canal (**28**). The bulky gluteus maximus provides a good target for intramuscular injections of medications. It is worth considering the site of the sciatic nerve (**20**). Many patients have so much fat overlying the gluteal muscles that supposedly intramuscular injections are in fact placed in overlying adipose tissue!



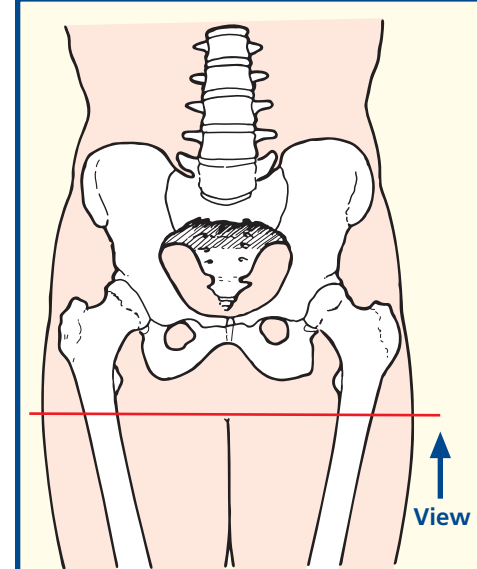


- | | | | |
|----------------------------------------------------------------|-----------------------------------------|----------------------------|--------------------------------------------|
| 1 Great saphenous vein | 11 Adductor longus | 22 Semimembranosus | 34 Corpus cavernosum |
| 2 Sartorius | 12 Tensor fasciae latae | 23 Semitendinosus tendon | 35 Penile fascia |
| 3 Rectus femoris | 13 Vastus lateralis | 24 Sciatic nerve | 36 Tunica albuginea of penis |
| 4 Superficial femoral artery | 14 Vastus intermedius | 25 Adductor magnus | 37 Deep artery of penis |
| 5 Superficial femoral vein | 15 Vastus medialis | 26 External anal sphincter | 38 Dorsal vein of penis |
| 6 Saphenous nerve | 16 Adductor brevis | 27 Anal verge | 39 Investing fascia of thigh – fascia lata |
| 7 Lateral circumflex femoral artery and vein (inferior branch) | 17 Gracilis | 28 Vas deferens | |
| 8 Femoral nerve (branch to quadriceps) | 18 Femoral shaft | 29 Spermatic cord | |
| 9 Profunda femoris artery | 19 Gluteus maximus tendon | 30 Testis – upper pole | |
| 10 Profunda femoris vein | 20 Gluteus maximus | 31 Pampiniform plexus | |
| | 21 Biceps femoris – tendon of long head | 32 Corpus spongiosum | |
| | | 33 Urethra | |
| | | | 40 Quadratus femoris |



Axial computed tomogram (CT)

Section level



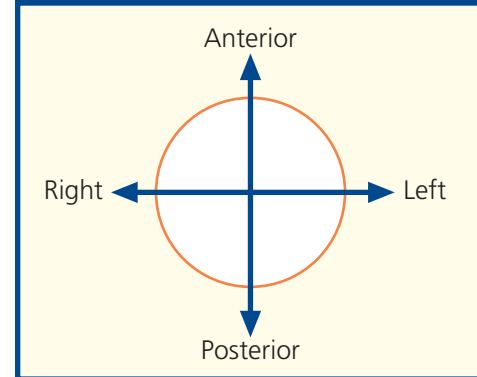
Notes

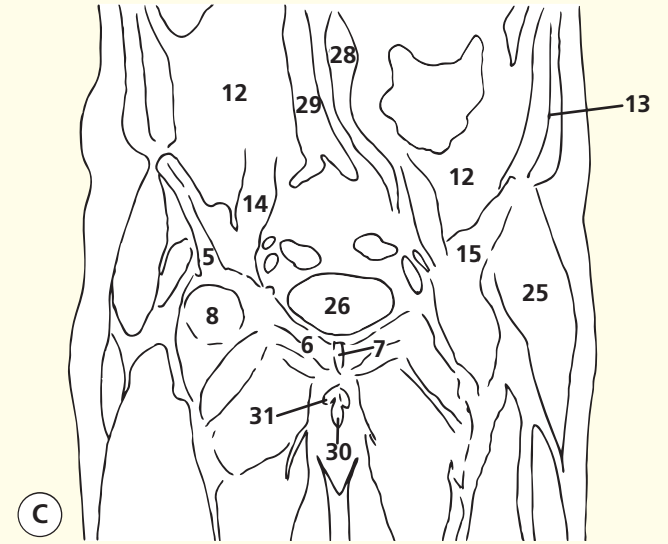
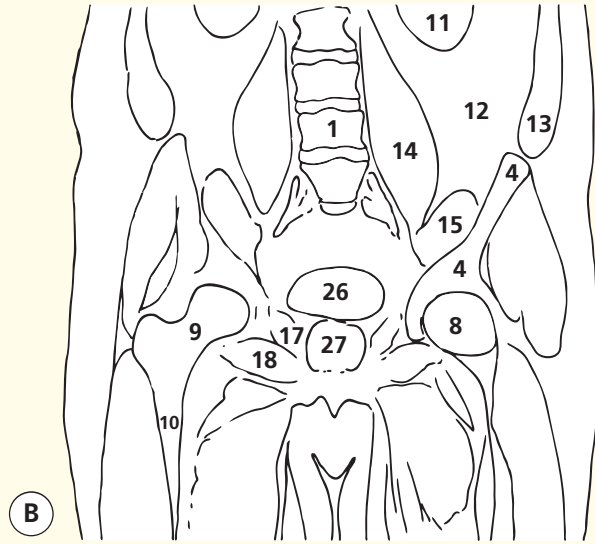
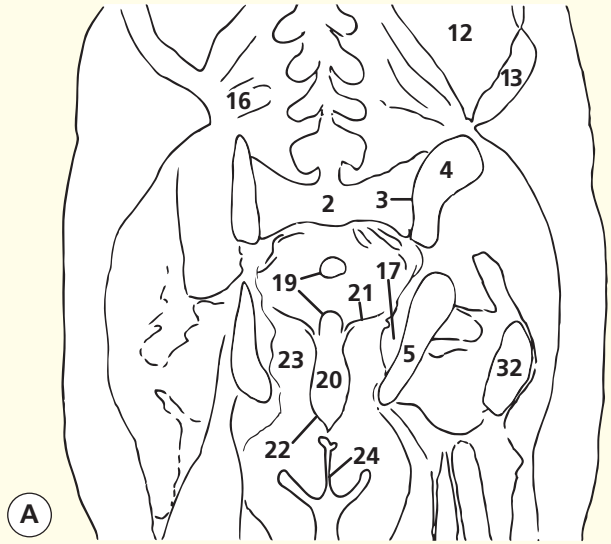
This section passes through the anal verge (**27**), surrounded by the external anal sphincter (**26**). It demonstrates well the structure of the penis in transverse section. The penile urethra (**33**) is surrounded by the corpus spongiosum (**32**). Above and lateral to this, on either side, are the corpora cavernosa (**34**). These structures are bound together within the penile fascia (**35**). The deep artery of the penis (**37**) is a branch of the internal pudendal artery, which ends in the deep perineal pouch by dividing into the deep and the dorsal arteries of the penis and the artery to the bulb. The deep artery supplies the corpus cavernosum, the dorsal artery supplies the prepuce and glans, and the artery to the bulb supplies the corpus spongiosum.

This section also demonstrates the upper pole of the testis (**30**), surrounded by its tunica albuginea, and also the vas deferens (**28**), surrounded by the pampiniform plexus (**31**).

The saphenous nerve (**6**), a branch of the femoral nerve, is seen here entering the adductor, or subsartorial, canal (Hunter's canal). This is an aponeurotic tunnel in the middle third of the thigh, formed posteriorly by adductor longus (**11**), more distally by adductor magnus (**25**), anterolaterally by vastus medialis (**15**) and anteromedially by sartorius (**2**). Its contents are the superficial femoral artery (**4**) and vein (**5**), the saphenous nerve (**6**) and the nerve to vastus medialis. (See also Lower limb – Thigh – Axial section 3.) The saphenous nerve (**6**) itself is of clinical interest. It is entirely sensory and is a branch of the femoral nerve just distal to the inguinal ligament. It becomes subcutaneous by emerging from the femoral canal at the posterior aspect of sartorius above the knee and descends, in company with the great saphenous vein, to the medial side of the foot as far as the base of the hallux. It is the longest cutaneous nerve in the body.

Orientation





Coronal magnetic resonance image (MRI)



Coronal magnetic resonance image (MRI)



Coronal magnetic resonance image (MRI)

- | | | |
|---------------------|------------------------------------------------------------------------|-------------------------------------|
| 1 L4 vertebral body | 13 Anterior wall musculature (transversus, internal/external obliques) | 23 Ischio-rectal (ischioanal) fossa |
| 2 Sacrum | 14 Psoas major | 24 Natal cleft |
| 3 Sacroiliac joint | 15 Iliacus | 25 Gluteal muscles |
| 4 Ilium | 16 Quadratus lumborum | 26 Bladder |
| 5 Ischium | 17 Obturator internus | 27 Prostate |
| 6 Pubis | 18 Obturator externus | 28 Aorta |
| 7 Pubic symphysis | 19 Rectum | 29 Inferior vena cava |
| 8 Femoral head | 20 Anal canal | 30 Corpus spongiosum |
| 9 Neck of femur | 21 Levator ani | 31 Corpus cavernosum |
| 10 Shaft of femur | 22 Anal sphincters | 32 Greater trochanter of femur |

Notes

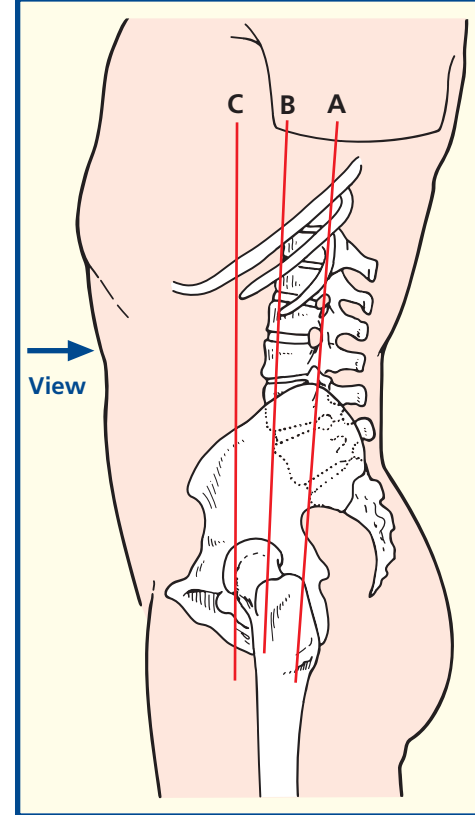
These three T1 MR coronal images provide a good overview of the relationships of the structures within the male pelvis. In particular, the way in which the anatomy relates to the pelvic floor is demonstrated well. So too is the way in which the anterior wall musculature merges with the bony pelvis. The copious quantity of intra-abdominal fat in men is also apparent; women have relatively much more fat in the subcutaneous tissues.

In image C, the confluence of the two common iliac veins forming the inferior vena cava (29) can be appreciated. So too can the continuation of the aorta (28) as the left common iliac artery; the right common iliac

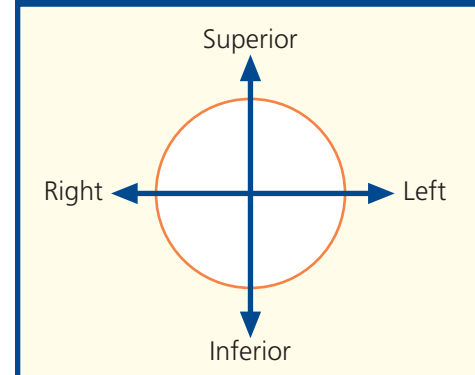
artery cannot be seen on this image, as it lies in a more anterior position as it passes anterior to the confluence of the common iliac veins. This is an important point, as the veins usually lie posterior to the arteries in this region – this is also true for the external iliac and popliteal vessels. More superiorly in the body (brachiocephalic, pulmonary and renal), the veins lie anterior to the arteries.

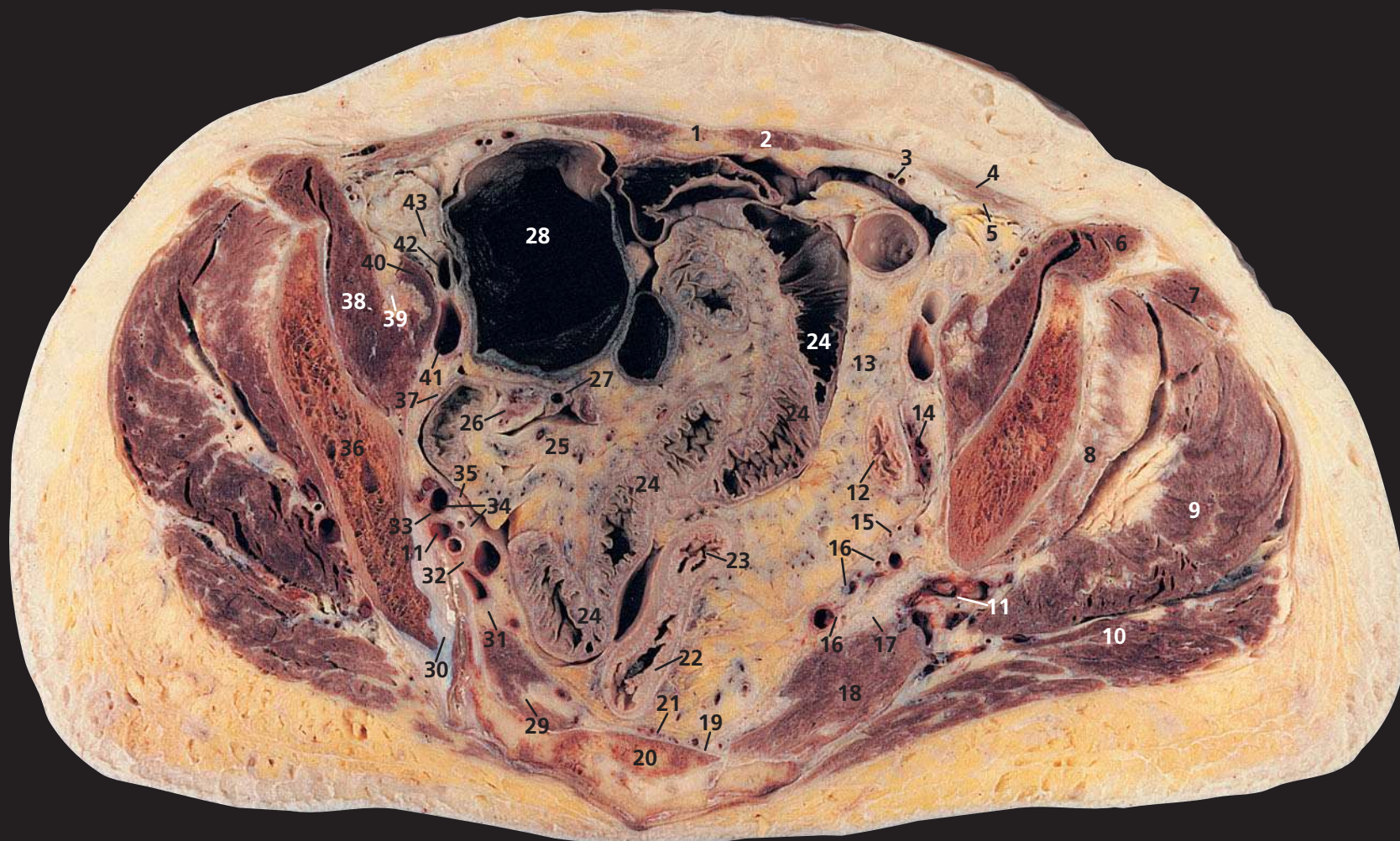
Such coronal images also provide a very useful overview when assessing the musculoskeletal system. The hips and sacroiliac joints are seen well, although smaller fields of view are used for more detailed imaging of a particular joint.

Section level

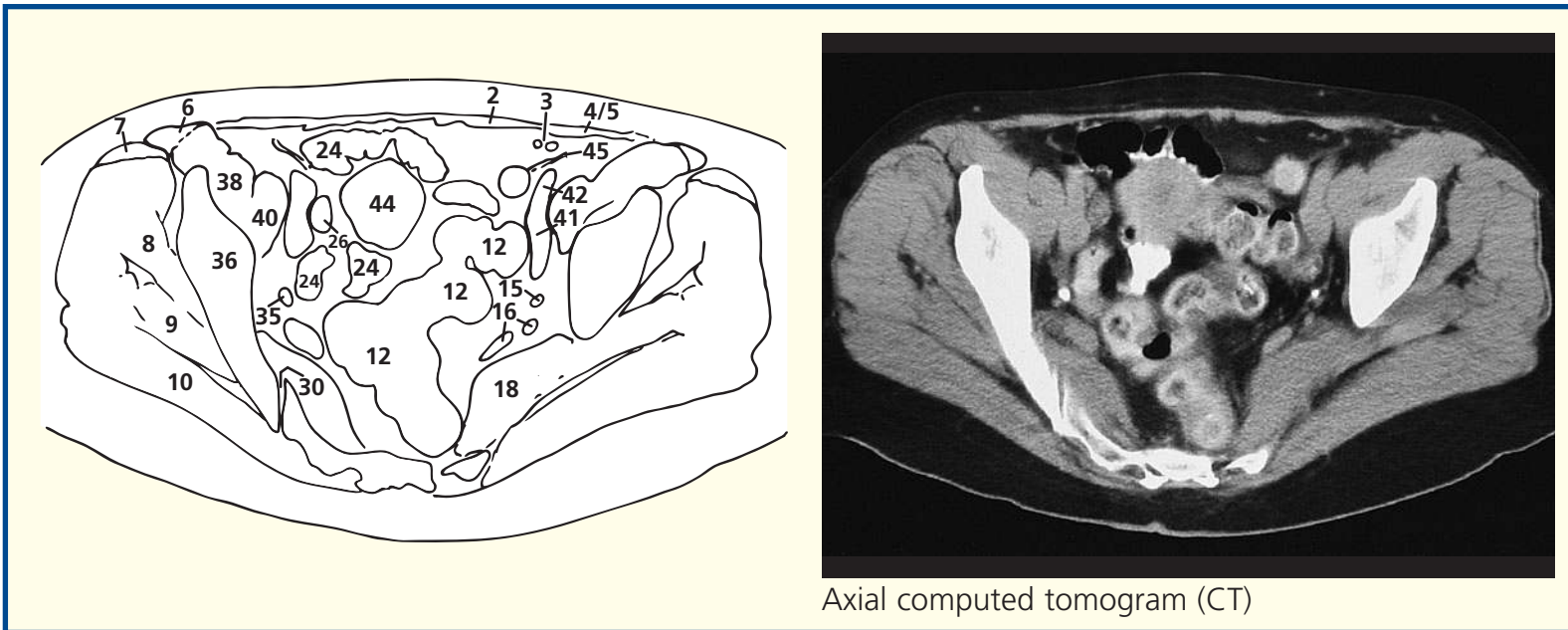


Orientation

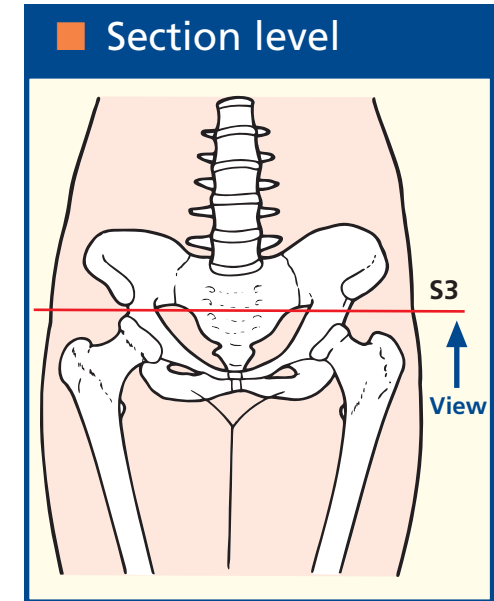




- | | | | |
|--------------------------------------------------------------|-----------------------------------------------|-----------------------------------------|--------------------------|
| 1 Linea alba | 13 Sigmoid mesocolon | 25 Mesentery of small bowel | 37 Obturator nerve |
| 2 Rectus abdominis | 14 Left ovary | 26 Right ovary | 38 Iliacus |
| 3 Inferior epigastric artery and vein | 15 Left ureter | 27 Right uterine (fallopian) tube | 39 Femoral nerve |
| 4 Fused aponeurosis of external and internal oblique muscles | 16 Branches of internal iliac artery and vein | 28 Caecum | 40 Psoas major |
| 5 Transversus abdominis | 17 Sciatic nerve | 29 Ventral ramus of third sacral nerve | 41 External iliac vein |
| 6 Sartorius | 18 Piriformis | 30 Sacroiliac joint | 42 External iliac artery |
| 7 Tensor fasciae latae | 19 Lateral sacral artery and vein | 31 Ventral ramus of second sacral nerve | 43 Lymph node |
| 8 Gluteus minimus | 20 Sacrum, third segment | 32 Ventral ramus of first sacral nerve | 44 Uterus (fundus) |
| 9 Gluteus medius | 21 Median sacral artery and vein | 33 Lumbosacral trunk | 45 Round ligament |
| 10 Gluteus maximus | 22 Rectum | 34 Uterine artery and vein | |
| 11 Superior gluteal artery and vein | 23 Rectosigmoid junction | 35 Right ureter | |
| 12 Sigmoid colon | 24 Ileum | 36 Ilium | |



Axial computed tomogram (CT)



Notes

This section through the female pelvis transects the third segment of the sacrum (**20**), which delimits the commencement of the rectum (**22**) at its junction with the sigmoid colon (**23**). The rectosigmoid junction demonstrates a marked change – the rectum, unlike the colon, is free of appendices epiploicae, and the taenia coli disappear from its wall.

The left ovary is seen at (**14**) and the right ovary at (**26**); in this elderly subject, they are atrophic.

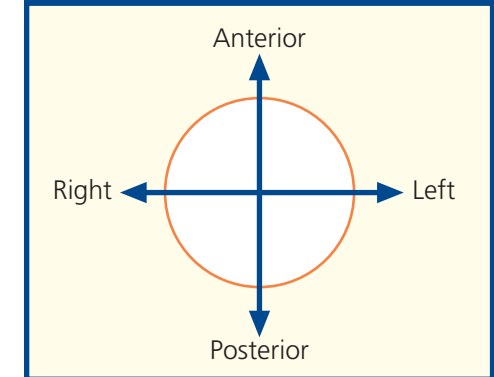
Along the internal iliac vessels (**16**) lies a rich lymphatic plexus, together with the internal iliac lymph nodes. These receive afferents from all the pelvic viscera, the deeper parts of the perineum and the muscles of the buttock.

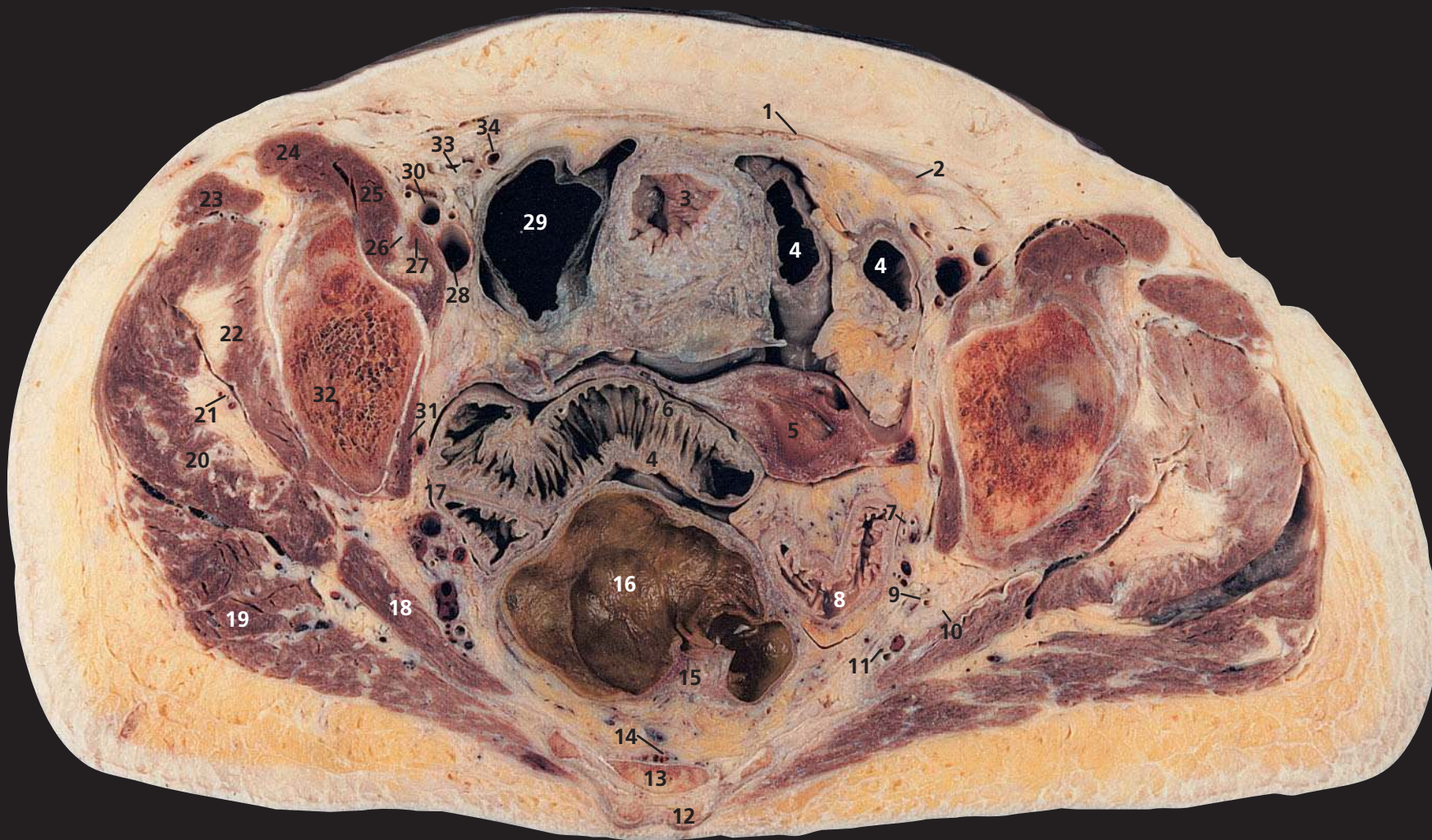
Their efferents pass through the common iliac nodes.

The sciatic nerve (**17**) at its origin is lying on piriformis (**18**). Its important relationships can be traced in subsequent sections as it emerges through the greater sciatic foramen below piriformis to cross, in turn, obturator internus tendon with its accompanying gemelli, quadratus femoris and, finally, adductor magnus. It is covered superficially by gluteus maximus and is crossed by the long head of biceps.

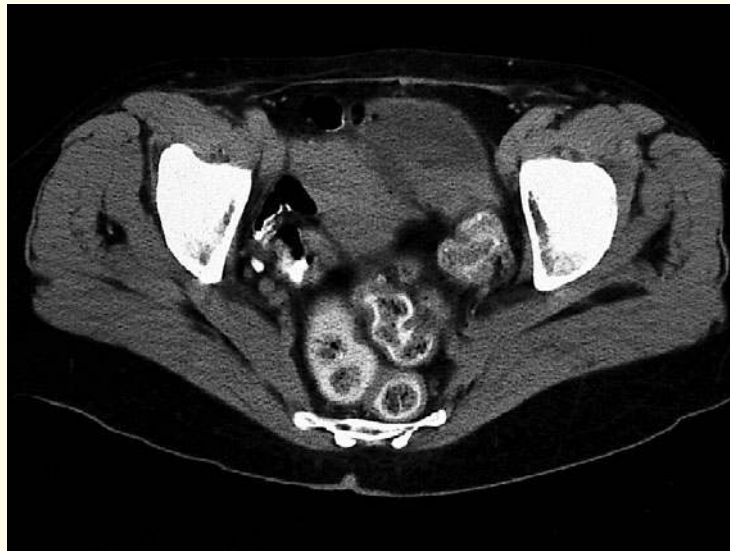
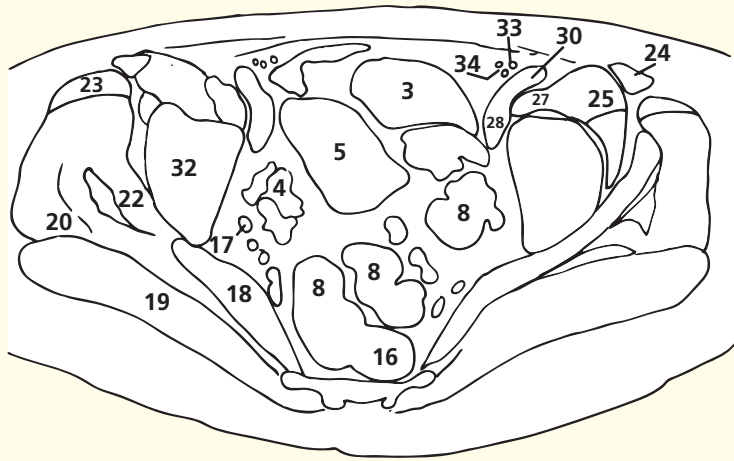
Note that a degree of scoliosis in this subject explains the asymmetry of the sciatic nerve and other structures on the two sides of this section.

Orientation



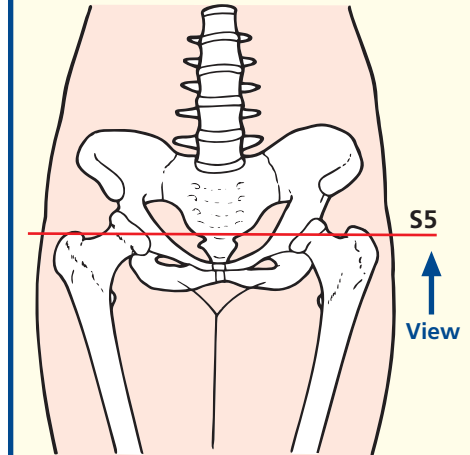


- | | | | |
|------------------------------------------|------------------------------------------------------|-------------------------------------|----------------------------------------|
| 1 Rectus sheath | 10 Sciatic nerve | 18 Piriformis | 28 External iliac vein |
| 2 Transversus abdominis | 11 Internal pudendal artery, vein and pudendal nerve | 19 Gluteus maximus | 29 Caecum |
| 3 Fundus of bladder | 12 Superior sacral cornu | 20 Gluteus medius | 30 External iliac artery |
| 4 Ileum | 13 Sacrum, fifth segment | 21 Superior gluteal artery and vein | 31 Obturator internus |
| 5 Fundus of uterus | 14 Median sacral artery and vein | 22 Gluteus minimus | 32 Ilium |
| 6 Broad ligament | 15 Mesorectum with superior rectal artery and vein | 23 Tensor fasciae latae | 33 Round ligament |
| 7 Left ureter | 16 Rectum | 24 Sartorius | 34 Inferior epigastric artery and vein |
| 8 Sigmoid colon | 17 Right ureter | 25 Iliacus | |
| 9 Inferior gluteal artery vein and nerve | | 26 Femoral nerve | |
| | | 27 Psoas major | |



Axial computed tomogram (CT)

Section level



Notes

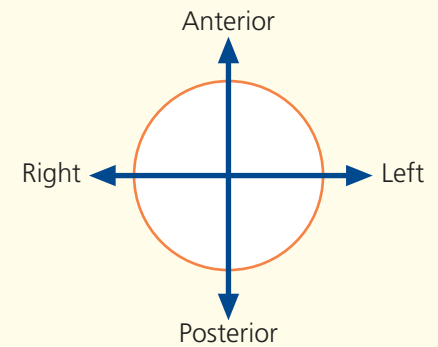
This section passes through the lowest (fifth) segment of the sacrum (**13**) and shaves through the fundus of the bladder (**3**) and of the uterus (**5**), together with the upper part of the broad ligament (**6**).

There is wide normal variation in the relative positions of the pelvic organs. For example, on the CT images, the fundus of the uterus was first encountered in the image on page 185. On this CT image, the body of the uterus is traversed. Conversely, the rectosigmoid junction lies at a

more caudal level on the CT images than on the sections.

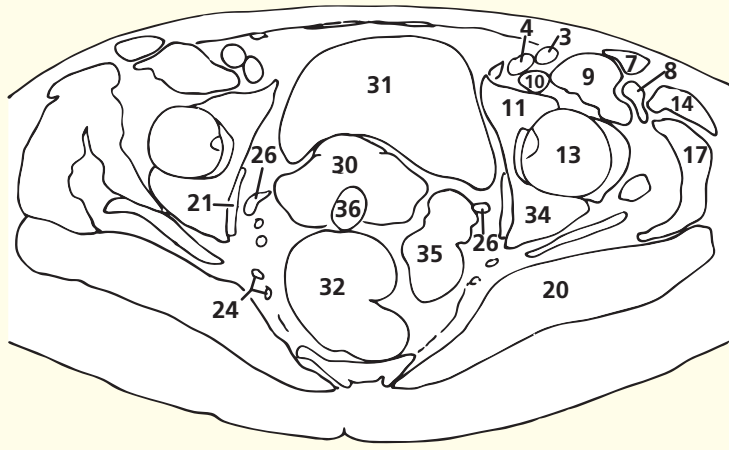
The rectum, from its narrow lumen at its origin, shown in the previous section, has widened into its patulous ampulla (**16**). Between the posterior aspect of the rectum (covered by its fascia propria) and the fascia covering the anterior aspect of the sacrum (**13**), the presacral fascia, is the connective tissue plane, which is developed in the surgical mobilization of the rectum and its vascular pedicle.

Orientation



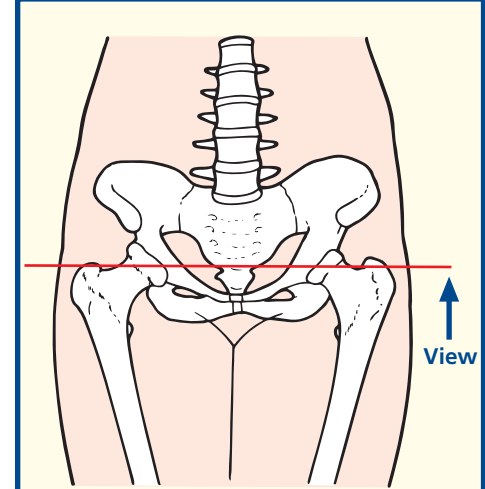


- | | | | |
|-------------------------------------------------|----------------------------------|-------------------------------------------|------------------------------------|
| 1 Inguinal ligament | 10 Psoas major tendon | 20 Gluteus maximus | 29 Uterine artery and vein |
| 2 Femoral hernia containing extraperitoneal fat | 11 Pubic component of acetabulum | 21 Obturator internus | 30 Internal os of cervix |
| 3 Femoral artery | 12 Ligamentum teres | 22 Sciatic nerve | 31 Bladder |
| 4 Femoral vein | 13 Head of femur | 23 Ischial spine | 32 Ampulla of rectum |
| 5 Femoral nerve | 14 Tensor fasciae latae | 24 Inferior gluteal artery vein and nerve | 33 Coccyx |
| 6 Pectineus | 15 Iliofemoral ligament | 25 Sacrospinous ligament | 34 Ischial component of acetabulum |
| 7 Sartorius | 16 Iliotibial tract | 26 Ureter | 35 Sigmoid colon |
| 8 Rectus femoris | 17 Gluteus medius | 27 Acetabulum | 36 Vault of vagina (with tampon) |
| 9 Iliacus | 18 Tendon of gluteus minimus | 28 Obturator artery, vein and nerve | |
| | 19 Greater trochanter | | |



Axial computed tomogram (CT)

Section level



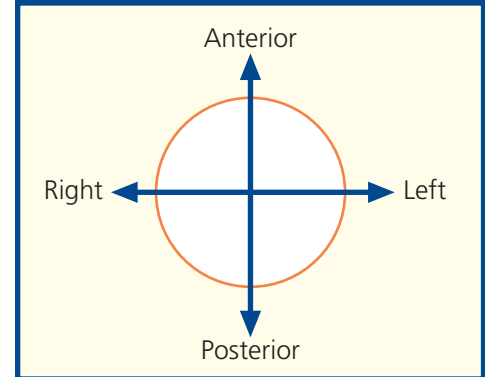
Notes

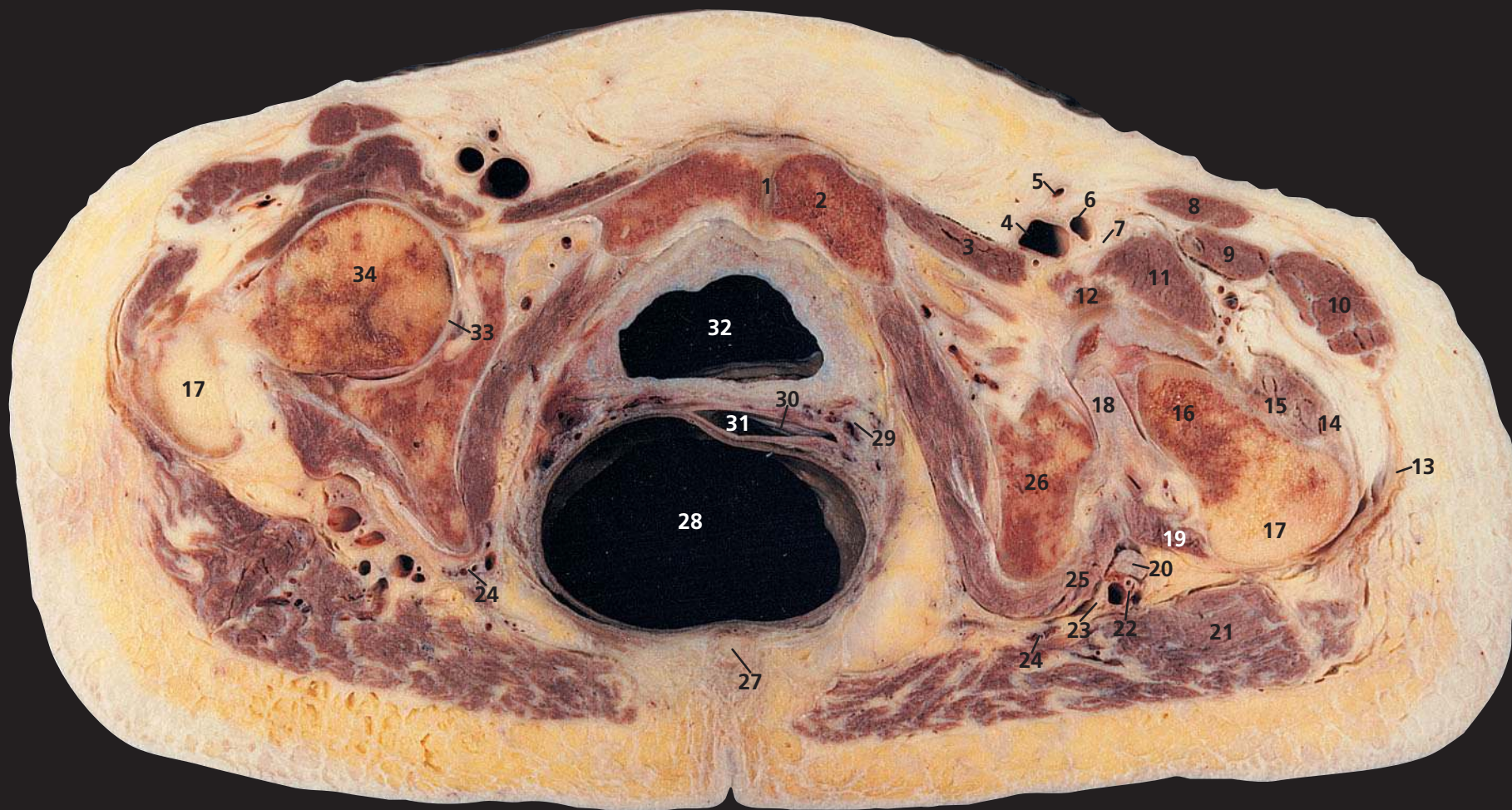
This section passes through the coccyx (**33**) and transects the femoral head (**13**). In this elderly subject, the uterus is atrophic; note the small size of the cervix, here divided through its internal os (**30**).

Some CT units prepare all female patients undergoing pelvic CT by giving dilute iodinated contrast medium per rectum, as here; this renders the lumen of the rectosigmoid opaque. Sometimes a tampon is present in the vagina; the air trapped by its fibres is readily recognized (**36**). This allows appreciation of the level of the vaginal vault and the external os of the cervix (**30**), even though neither structure is demonstrated directly.

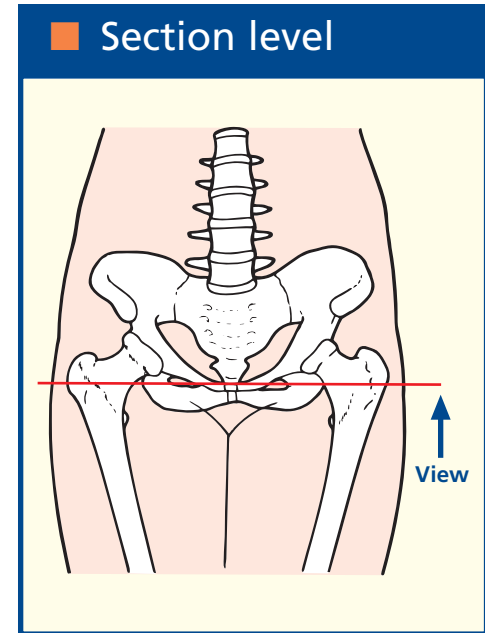
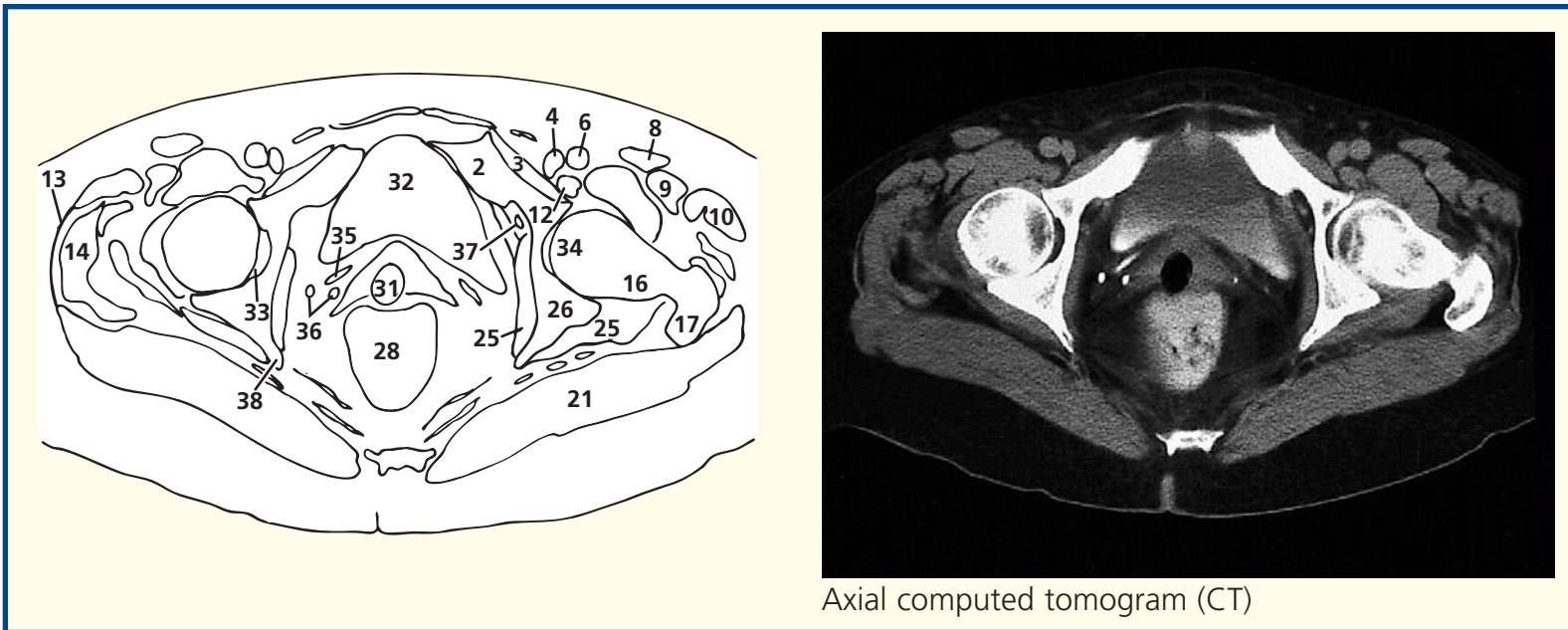
The uterine artery (**29**) arises from the internal iliac artery, runs medially on levator ani towards the cervix of the uterus, and crosses above and in front of the ureter (**26**) above the lateral vaginal fornix to reach the side of the uterus, where it ascends in the broad ligament. The corresponding uterine veins (**29**), usually two in number, drain a uterine plexus along the lateral side of the uterus within the broad ligament and open into the internal iliac vein. The close relationship between the uterine vessels and the ureter is of immense importance to the gynaecological surgeon when performing a hysterectomy (see also the CT image in Axial section 4).

Orientation





- | | | | |
|-------------------------|-------------------------------------|---------------------------------------------------------|-------------------------------------|
| 1 Pubic symphysis | 12 Psoas major tendon | 23 Posterior cutaneous nerve of thigh | 33 Acetabulum |
| 2 Body of pubis | 13 Iliotibial tract | 24 Internal pudendal artery and vein and pudendal nerve | 34 Femoral head |
| 3 Pectineus | 14 Gluteus medius | 25 Obturator internus | 35 Ureter |
| 4 Femoral vein | 15 Gluteus minimus | 26 Ischium | 36 Calcified phleboliths |
| 5 Great saphenous vein | 16 Neck of femur | 27 Coccyx | 37 Obturator artery, vein and nerve |
| 6 Femoral artery | 17 Greater trochanter | 28 Ampulla of rectum | 38 Ischial spine |
| 7 Femoral nerve | 18 Ischiofemoral ligament | 29 Vaginal artery and vein | |
| 8 Sartorius | 19 Quadratus femoris | 30 External os of cervix | |
| 9 Rectus femoris | 20 Sciatic nerve | 31 Vagina | |
| 10 Tensor fasciae latae | 21 Gluteus maximus | 32 Bladder | |
| 11 Iliacus | 22 Inferior gluteal artery and vein | | |

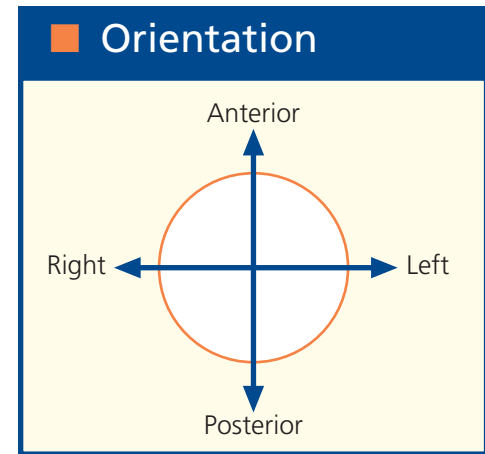


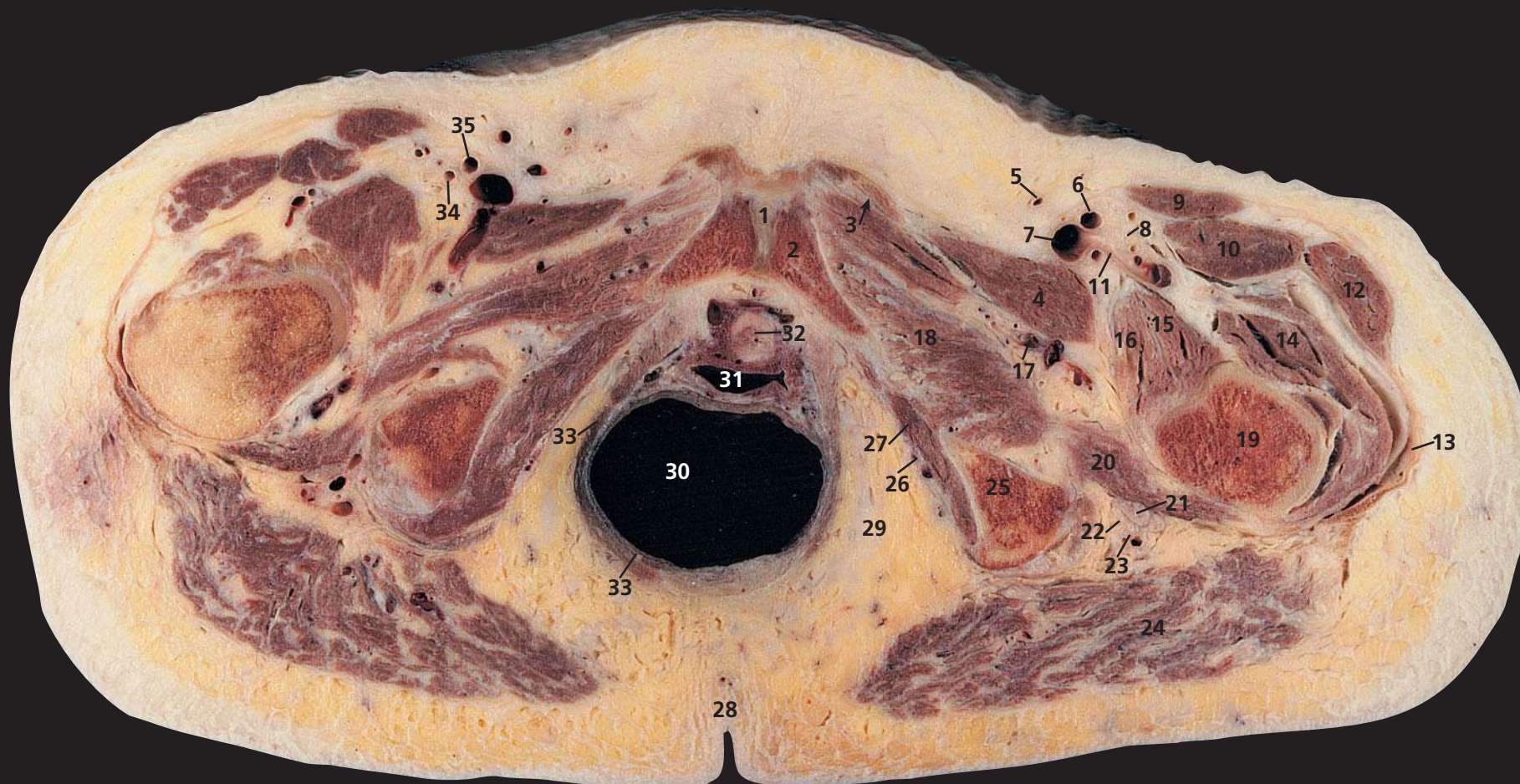
Notes

This section traverses the tip of the coccyx (**27**) and passes through the pubic symphysis in its upper part (**1**). Note that the vagina (**31**) is transected in its upper part so that the external os of the cervix (**30**) can be seen peeping through, with the posterior fornix of the vagina behind it. Alongside the vagina are the vaginal vessels (**29**). The vaginal artery usually corresponds to the inferior vesical artery in the male and is a branch of the internal iliac artery. It is frequently double or triple. It supplies the vagina as well as the fundus of the bladder and the adjacent part of the rectum and anastomoses with branches of the uterine artery.

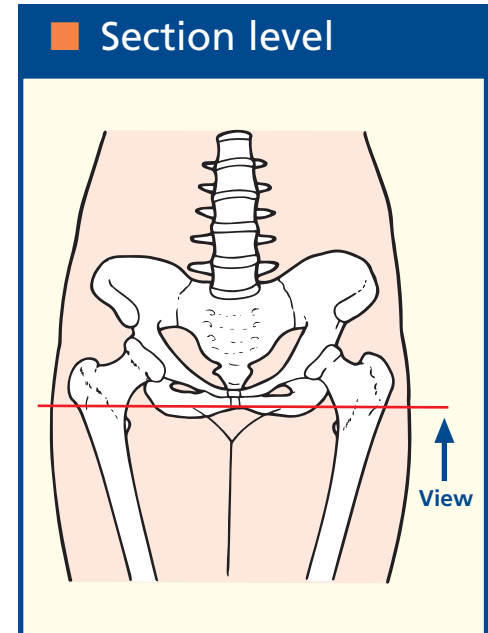
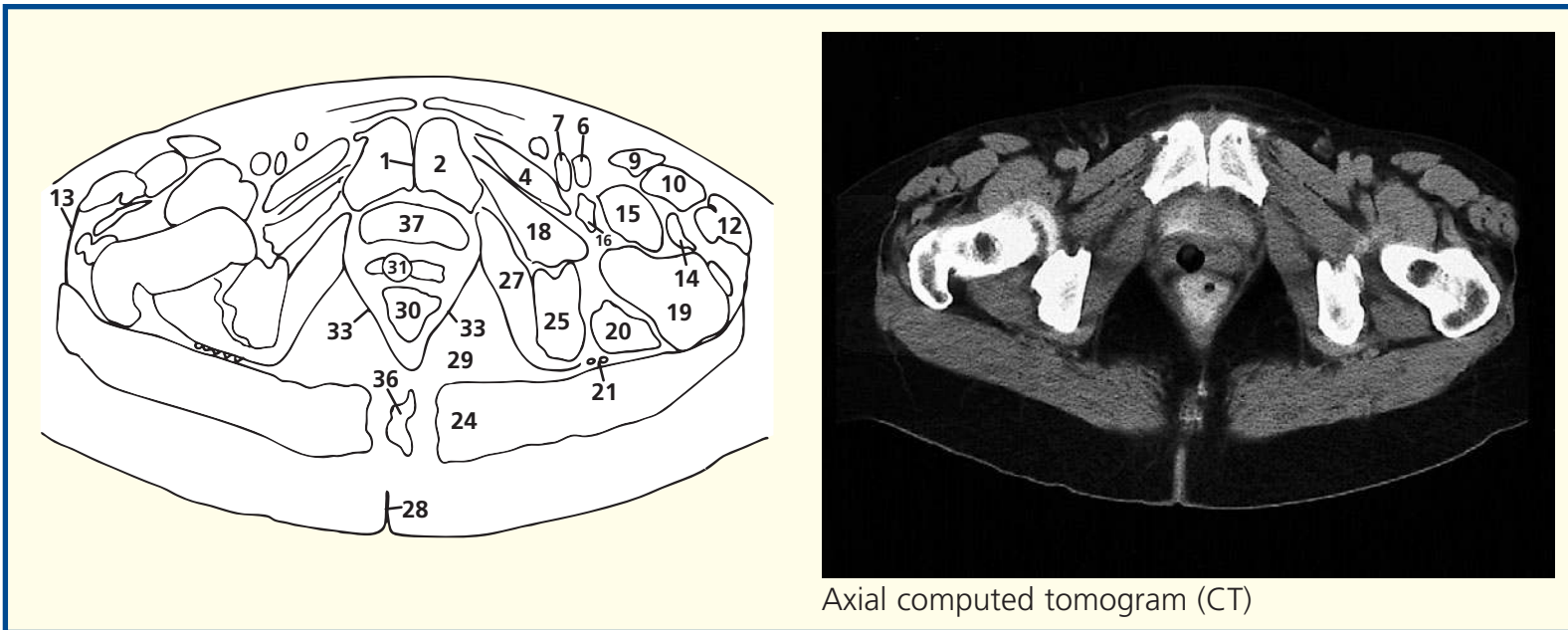
This section shows well the obturator internus muscle (**25**) as it sweeps around the lesser sciatic foramen, with the sciatic nerve (**20**) lying on its superficial (posterior) face, covered posteriorly by gluteus maximus (**21**).

Many patients develop small out-pouchings, or diverticula, in the extensive plexus of small pelvic veins. These diverticula often contain calcified thrombus to form phleboliths, as demonstrated on this CT image (**36**). On plain pelvic radiographs, these may simulate ureteric calculi.





- | | | | |
|----------------------------------------------------------|------------------------------------|-----------------------------------------------------------------------------------------------|-------------------------------------|
| 1 Symphysis pubis | 11 Lateral circumflex femoral vein | 22 Posterior cutaneous nerve of thigh | 31 Vagina |
| 2 Body of pubis | 12 Tensor fasciae latae | 23 Inferior gluteal artery and vein | 32 Urethra |
| 3 Adductor brevis, with adductor longus origin (arrowed) | 13 Iliotibial tract | 24 Gluteus maximus | 33 Levator ani |
| 4 Pectineus | 14 Vastus lateralis | 25 Ischial tuberosity | 34 Right profunda femoris artery |
| 5 Great saphenous vein | 15 Iliacus | 26 Pudendal (Alcock's) canal, containing internal pudendal artery and vein and pudendal nerve | 35 Right superficial femoral artery |
| 6 Left femoral artery | 16 Psoas major tendon | 27 Obturator internus | |
| 7 Femoral vein | 17 Obturator artery and vein | 28 Natal cleft | 36 Coccyx |
| 8 Femoral nerve | 18 Obturator externus | 29 Ischiorectal fossa | 37 Bladder |
| 9 Sartorius | 19 Femur | 30 Rectum | |
| 10 Rectus femoris | 20 Quadratus femoris | | |
| | 21 Sciatic nerve | | |

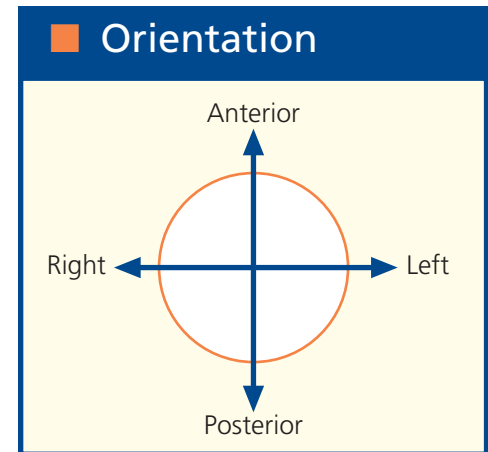


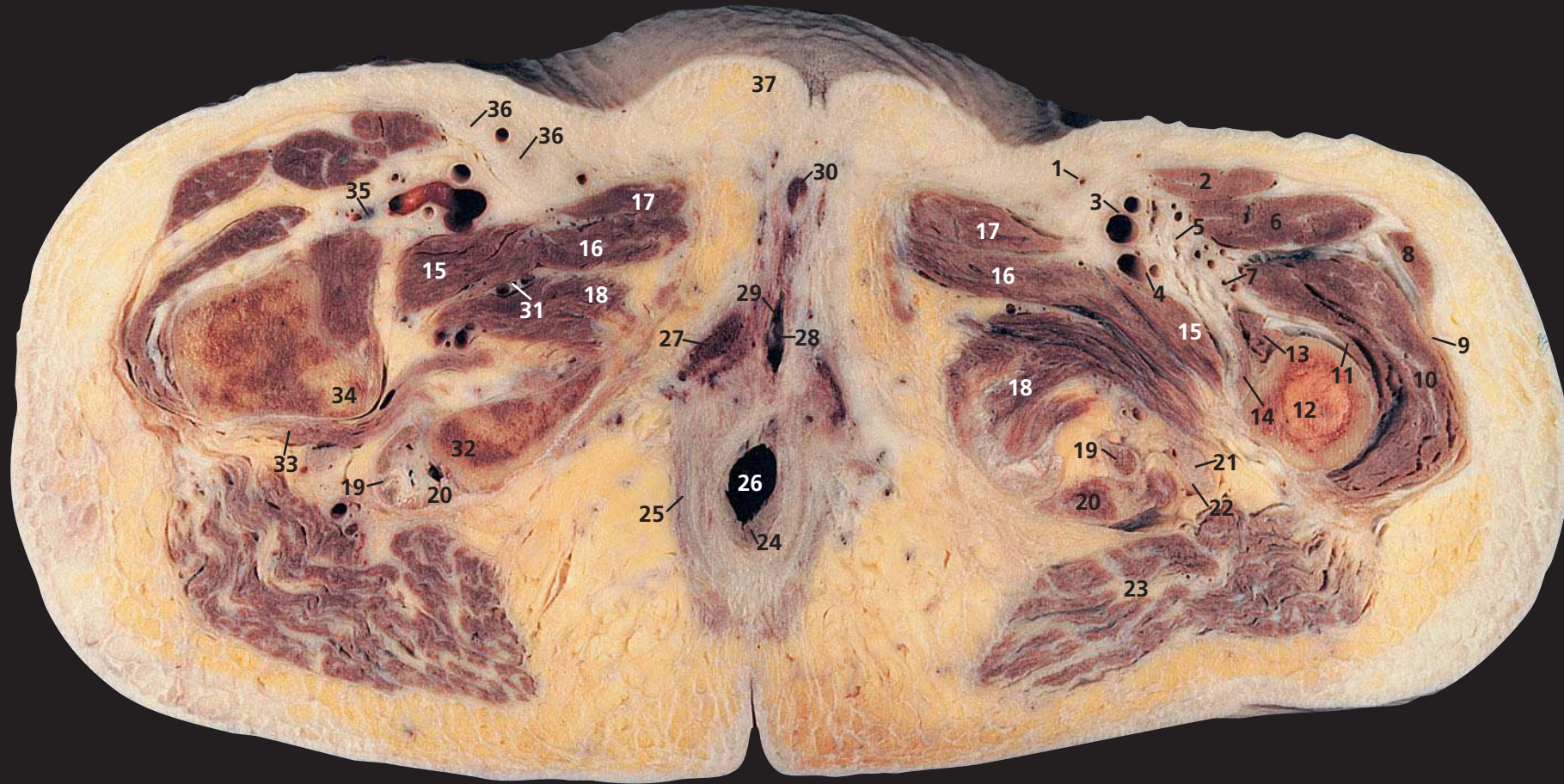
Notes

This section passes through the upper part of the natal cleft (28) and the body of the pubis (2). The intimate relationship between the female urethra (32) and vagina (31) is shown well; the former is actually embedded in the anterior wall of the latter.

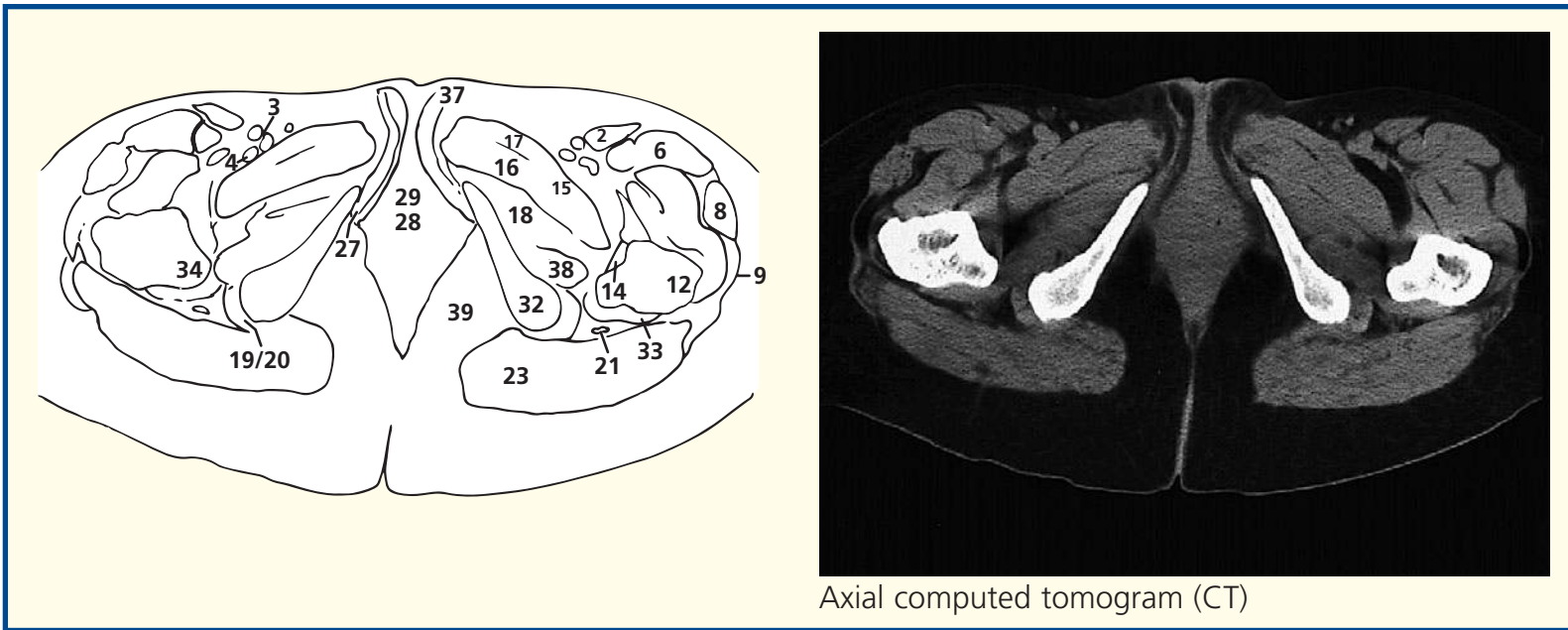
Unusually, the lateral circumflex femoral vein (11) in this subject arises from the common femoral vein (7); more usually, the circumflex vessels arise from the profunda femoris artery and vein. The right common femoral artery has divided into its profunda (34) and superficial (35) branches. On the left-hand side, the femoral artery (6) has not yet divided.

The anatomy of the ischiorectal fossa (29) is demonstrated well. It lies between levator ani (33) and obturator internus (27), on which can be seen the pudendal canal (26) and its contents. (See also Axial section 8 – male.)

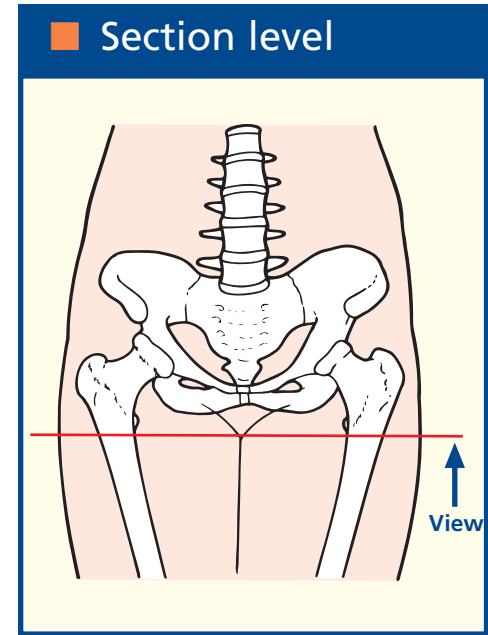




- | | | | |
|----------------------------------------------|------------------------------------------------------------|--------------------------------------------------------|------------------------------------|
| 1 Great saphenous vein | 11 Vastus intermedius | 21 Sciatic nerve | 32 Ischial tuberosity |
| 2 Sartorius | 12 Shaft of femur | 22 Posterior cutaneous nerve of thigh | 33 Quadratus femoris |
| 3 Superficial femoral artery and vein | 13 Vastus medialis | 23 Gluteus maximus | 34 Lesser trochanter of femur |
| 4 Deep femoral artery and vein | 14 Psoas major insertion to lesser trochanter with iliacus | 24 External anal sphincter | 35 Lateral circumflex femoral vein |
| 5 Femoral nerve (dividing into branches) | 15 Pectineus | 25 Levator ani | 36 Inguinal lymph node |
| 6 Rectus femoris | 16 Adductor brevis | 26 Anal canal | 37 Mons pubis |
| 7 Lateral circumflex femoral artery and vein | 17 Adductor longus | 27 Crus of clitoris | |
| 8 Tensor fasciae latae | 18 Adductor magnus | 28 Vaginal orifice | |
| 9 Iliotibial tract | 19 Tendon of semimembranosus | 29 Urethral orifice | |
| 10 Vastus lateralis | 20 Origin of semitendinosus and biceps femoris muscles | 30 Clitoris | |
| | | 31 Obturator artery, vein and nerve (posterior branch) | |
| | | | 38 Obturator externus |
| | | | 39 Ischiorectal fossa |



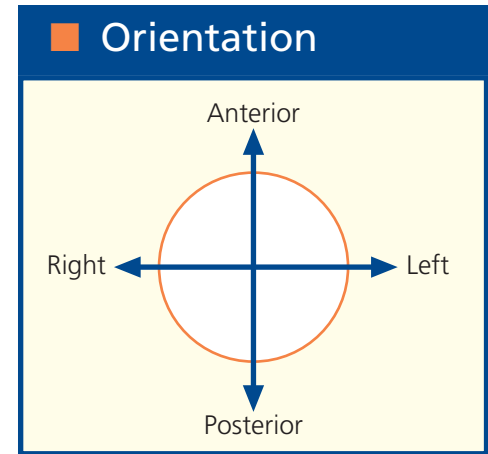
Axial computed tomogram (CT)



Notes

This section passes through mons pubis (**37**) anteriorly and the anal canal (**26**) posteriorly. Note the close relationship between the vaginal (**28**) and urethral (**29**) orifices.

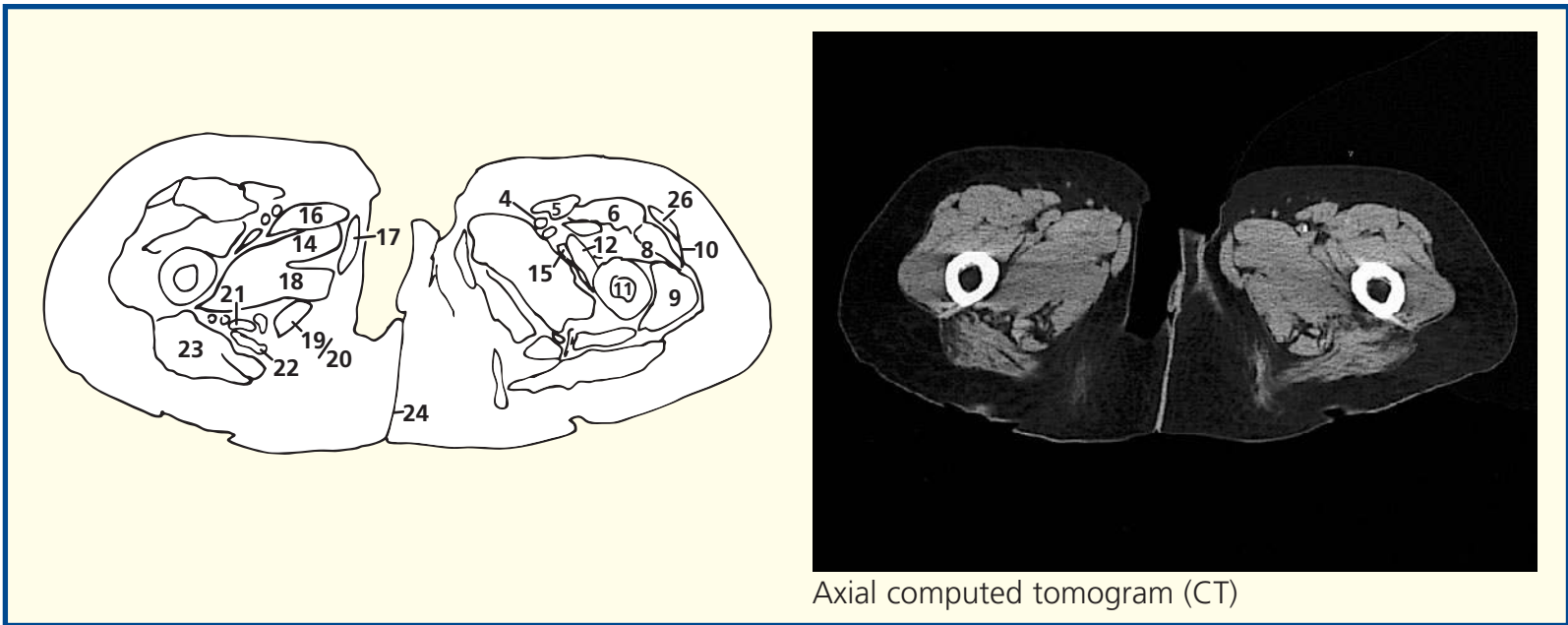
The sciatic nerve (**21**), with its accompanying posterior cutaneous nerve of the thigh (**22**) immediately superficial to it, can now be seen as it lies on quadratus femoris (**33**).



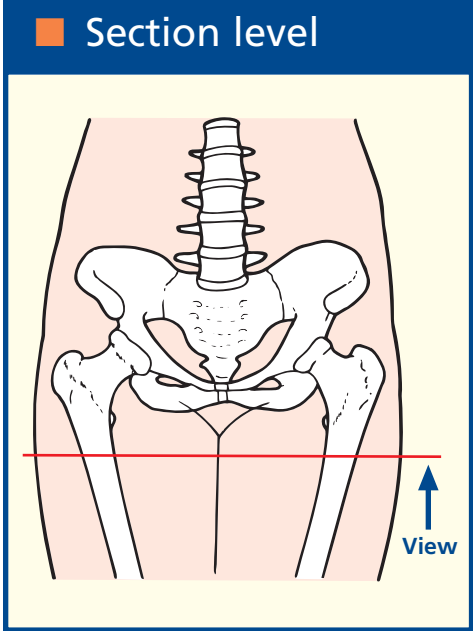


- | | | | |
|------------------------------------------------|--------------------------------------------------------------------------|-------------------------------------|--------------------|
| 1 Prepuce of clitoris | 8 Vastus intermedius | 15 Profunda femoris artery and vein | 23 Gluteus maximus |
| 2 Glans clitoridis | 9 Vastus lateralis | 16 Adductor longus | 24 Natal cleft |
| 3 Great saphenous vein | 10 Iliotibial tract | 17 Gracilis | 25 Anal verge |
| 4 Superficial femoral artery and vein | 11 Shaft of femur | 18 Adductor magnus | |
| 5 Sartorius | 12 Vastus medialis | 19 Semimembranosus tendon | |
| 6 Rectus femoris | 13 First perforating artery and vein of profunda femoris artery and vein | 20 Semitendinosus | |
| 7 Femoral nerve (branch to quadratus femoris) | 14 Adductor brevis | 21 Sciatic nerve | |
| | | 22 Long head of biceps | |

26 Tensor fasciae latae



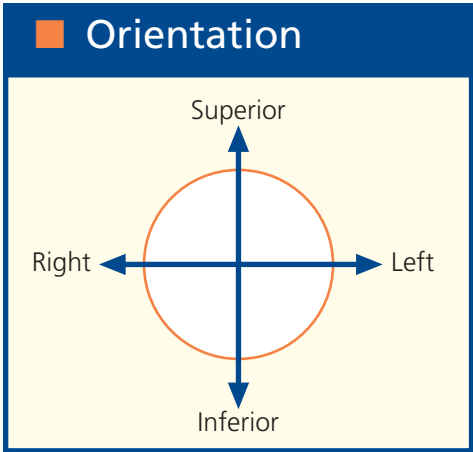
Axial computed tomogram (CT)

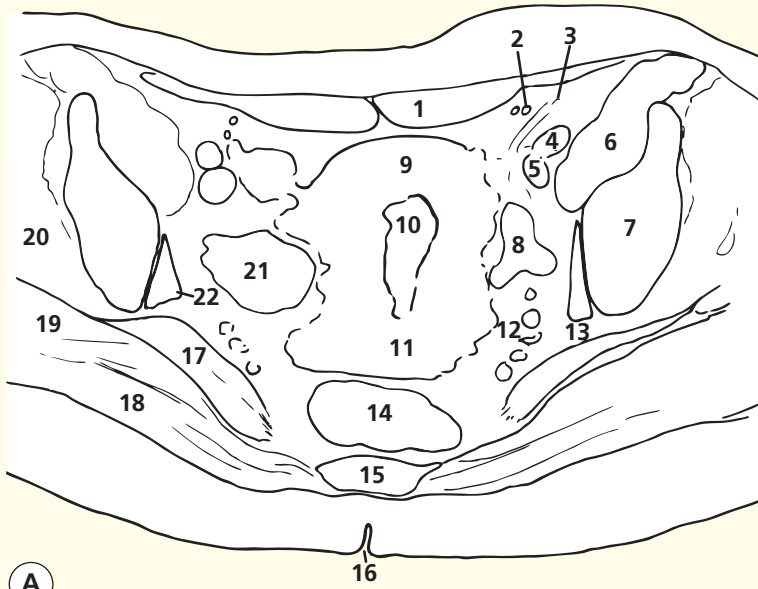


Notes

This section passes through the upper thigh but demonstrates the prepuce (**1**) and glans (**2**) of the clitoris. The anal verge (**25**) can be seen within the natal cleft (**24**).

The sciatic nerve (**21**) now lies on adductor magnus (**18**) and is crossed superficially by the long head of biceps (**22**).



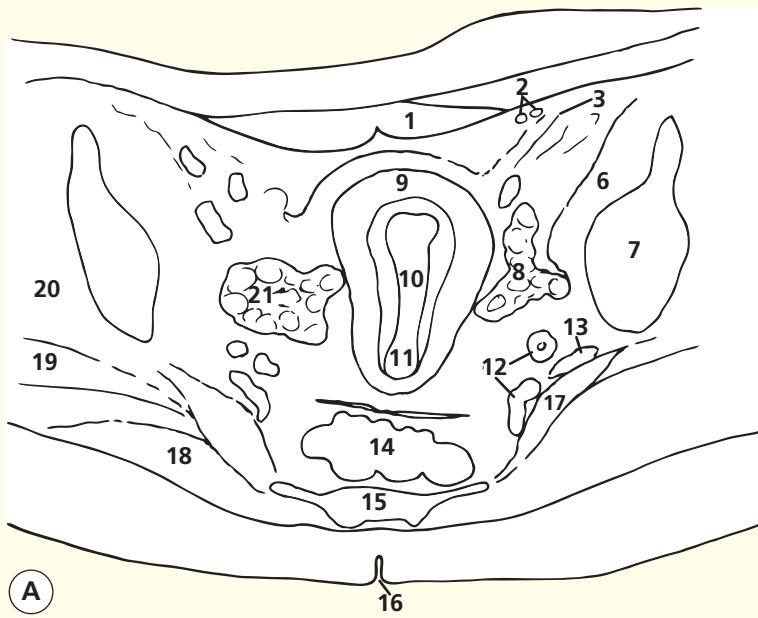


A

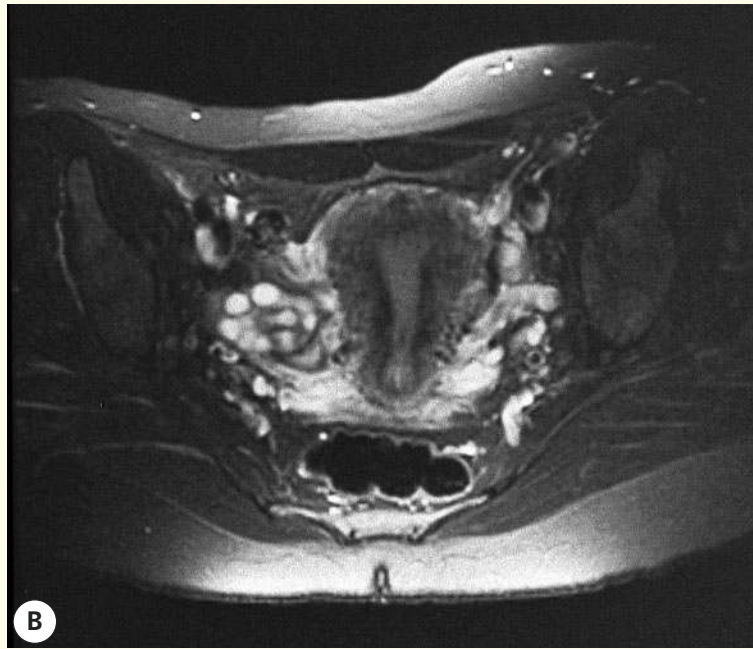


B

Axial magnetic resonance image (MRI) T1-weighted



A



B

Axial magnetic resonance image (MRI) T2-weighted

- 1 Rectus abdominis
- 2 Inferior epigastric vessels
- 3 Round ligament
- 4 External iliac artery
- 5 External iliac vein
- 6 Iliopsoas
- 7 Ilium
- 8 Left ovary
- 9 Fundus of uterus
- 10 Uterine cavity
- 11 Cervix of uterus
- 12 Internal iliac vessels
- 13 Plane of sciatic nerve
- 14 Rectum
- 15 Sacrum
- 16 Natal cleft
- 17 Piriformis
- 18 Gluteus maximus
- 19 Gluteus medius
- 20 Gluteus minimus
- 21 Right ovary
- 22 Obturator internus

Notes

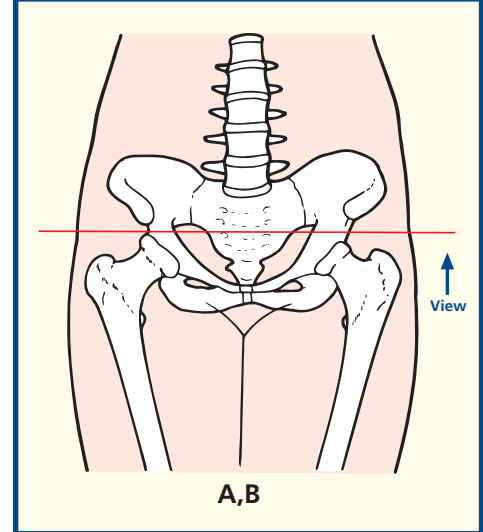
T1- (A) and T2- (B) weighted axial magnetic resonance images using a pelvic phased-array coil. The design of the coil accounts for the higher signal intensity within the subcutaneous fat anteriorly and posteriorly. Note the way in which T2 weighting demonstrates the internal anatomy of the uterus and the individual follicles within the ovary.

Note how there is a normal plane of fat lateral to each ovary and internal to the ilium and obturator internus. Any enlarged obturator nodes would be seen immediately posterior to the external iliac vein and would tend to disrupt the fat plane just internal to the ilium. The way in which the external iliac artery (4) lies anterior to the vein (5) is appreciated well. The femoral nerve may be just identifiable anterior to the external iliac artery on the right, having just emerged from the gap in the iliopsoas (6). At the base of the gap in the medial aspect of the right iliopsoas is the low-signal-intensity iliopsoas tendon, which will continue down to the distal attachment on the lesser trochanter. In diseases of the psoas (e.g. psoas abscess), the femoral nerve (L2,3,4) is often involved. This will lead to an absent patellar tendon reflex and difficulty with full extension of the hip.

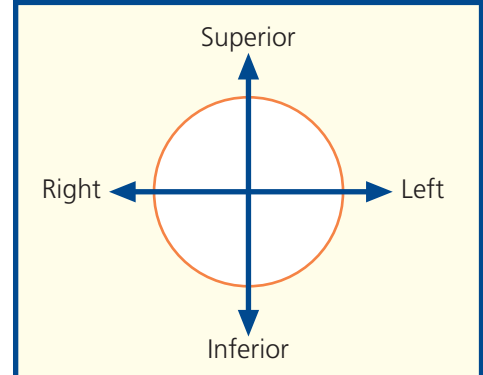
On the T1-weighted images, the epigastric vessels return low signal intensity (signal void). On T2-weighted images, they return high signal.

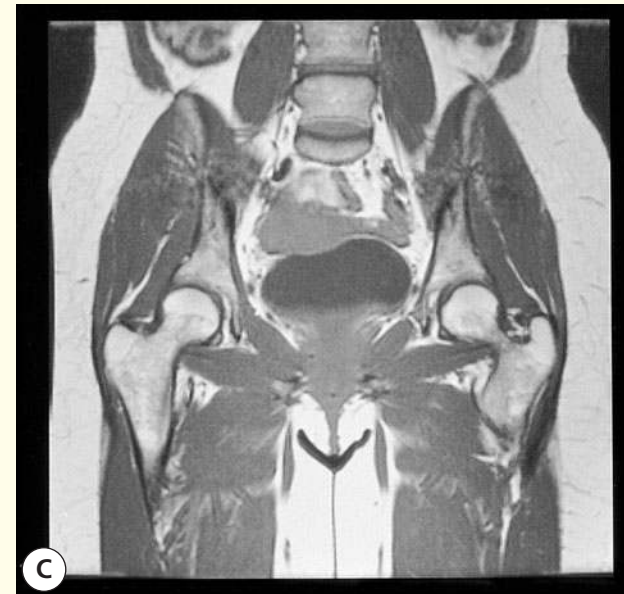
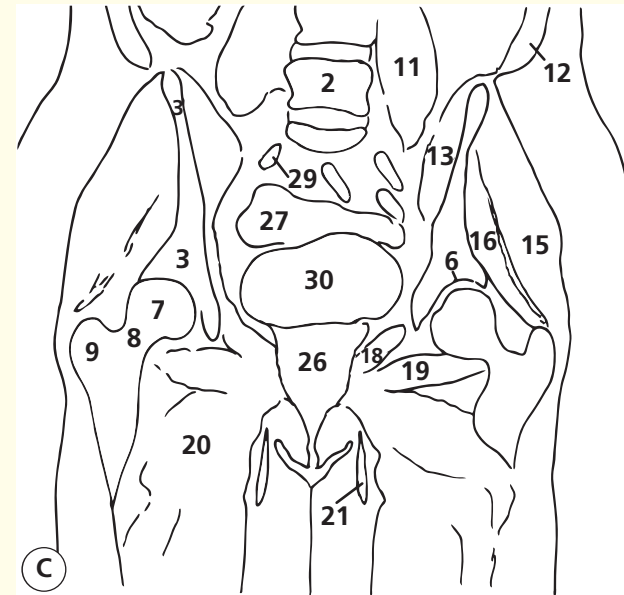
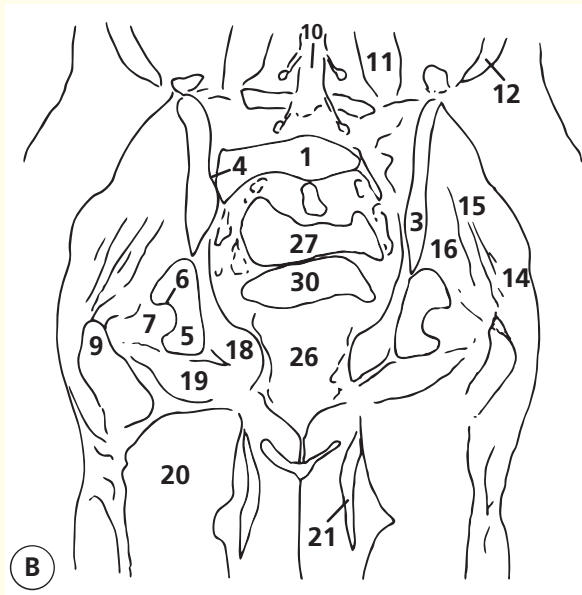
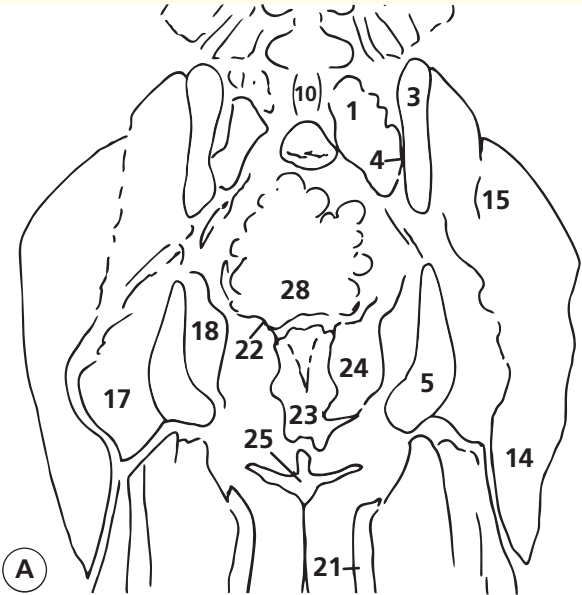
Note the way in which the round ligament passes lateral to the epigastric vessels en route to the inguinal canal. This course is exactly analogous to that of the vas deferens in the male patient. The round ligament contributes to keeping the uterus anteverted. Contrary to what might be thought, however, the main support for the uterus is not due to any of its ligaments; rather, it is the integrity of the pelvic-floor musculature that is important.

Section level



Orientation





Coronal magnetic resonance image (MRI)

Coronal magnetic resonance image (MRI)

Coronal magnetic resonance image (MRI)

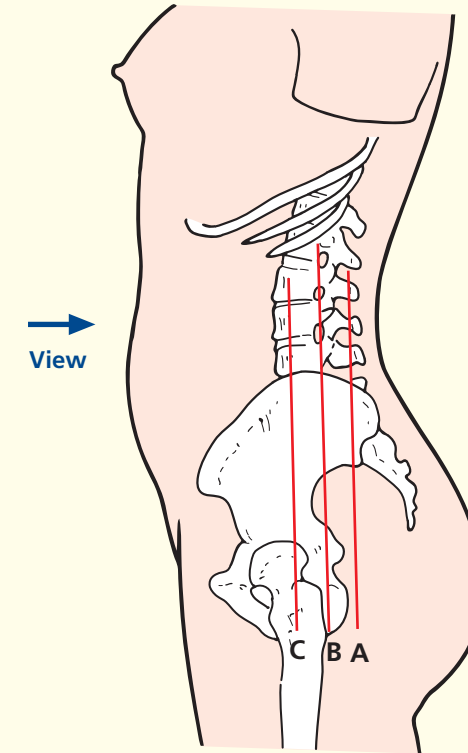
- | | | |
|-----------------------------|----------------------------------------|------------------------------------|
| 1 Sacrum | 12 Anterior abdominal-wall musculature | 22 Levator ani |
| 2 L5 vertebral body | 13 Iliacus | 23 Anal canal |
| 3 Ilium | 14 Gluteus maximus | 24 Ischiorectal (ischioanal) canal |
| 4 Sacroiliac joint | 15 Gluteus medius | 25 Natal cleft |
| 5 Ischium | 16 Gluteus minimus | 26 Vagina |
| 6 Acetabulum | 17 Quadratus femoris | 27 Uterus (body) |
| 7 Femoral head | 18 Obturator internus | 28 Uterus (cervix) |
| 8 Femoral neck | 19 Obterator externus | 29 Common iliac vessels |
| 9 Femur, greater trochanter | 20 Adductor group of muscles | 30 Bladder |
| 10 Thecal sac | 21 Gracilis | |

Notes

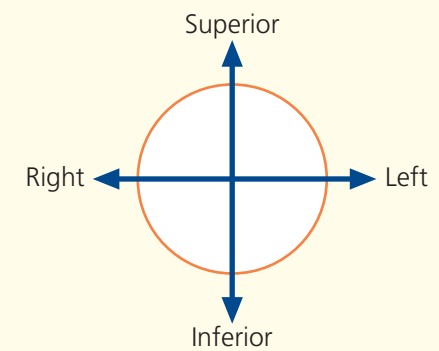
These coronal T1-weighted images elegantly demonstrate the way in which the anteverted uterine body rests on the bladder. It is important to realize that the support for the pelvic organs comes mainly from the tone in the pelvis musculature. The levator ani are important; so too are the collective contributions of all the muscles attached to the

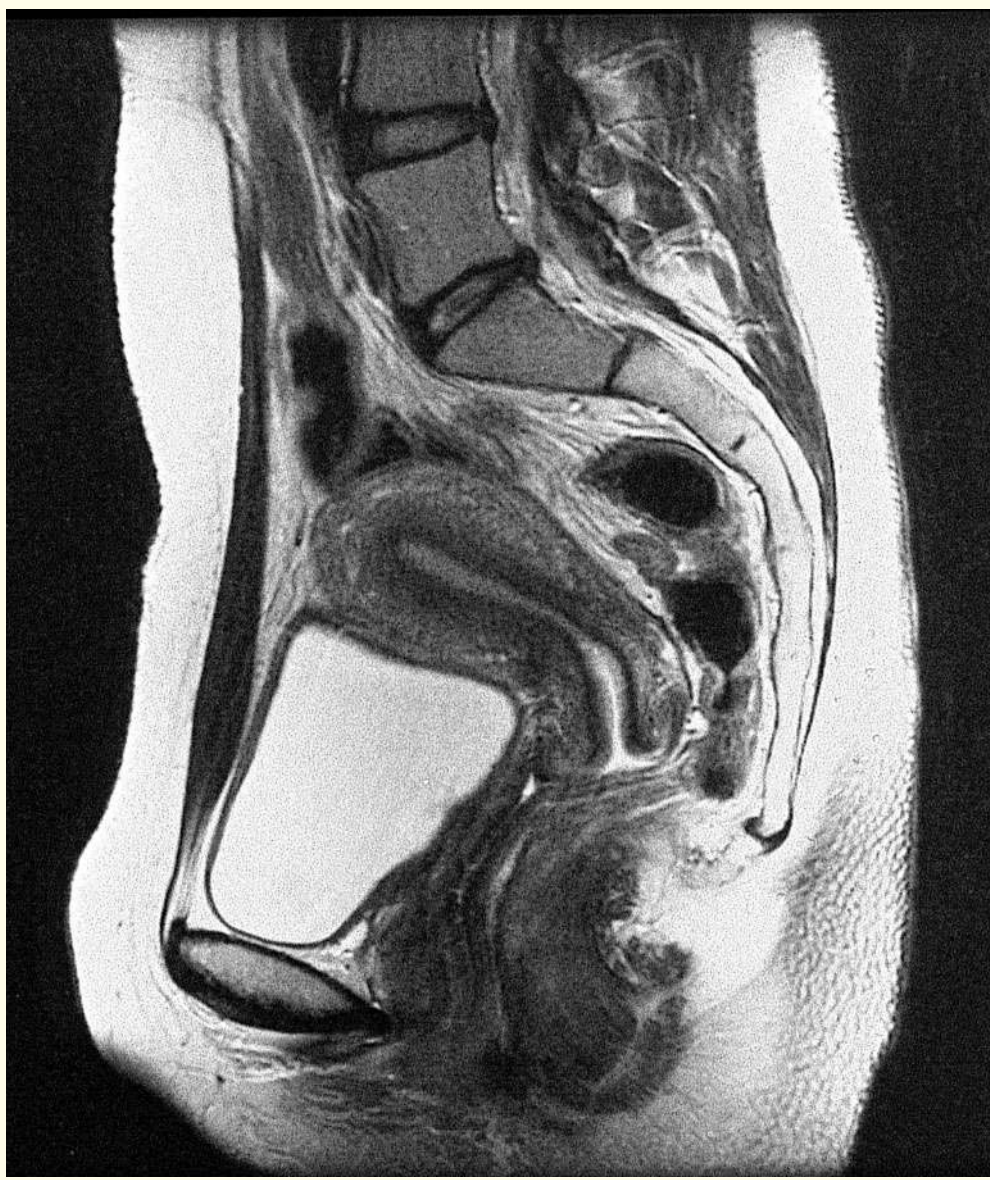
inferior bony pelvis, many of which converge directly or indirectly on the region of the perineal body. All of these muscles play a part in supporting the pelvic organs and ultimately preventing prolapse and incontinence – hence the importance of practising pelvic-floor exercises before and after pregnancy.

Section level

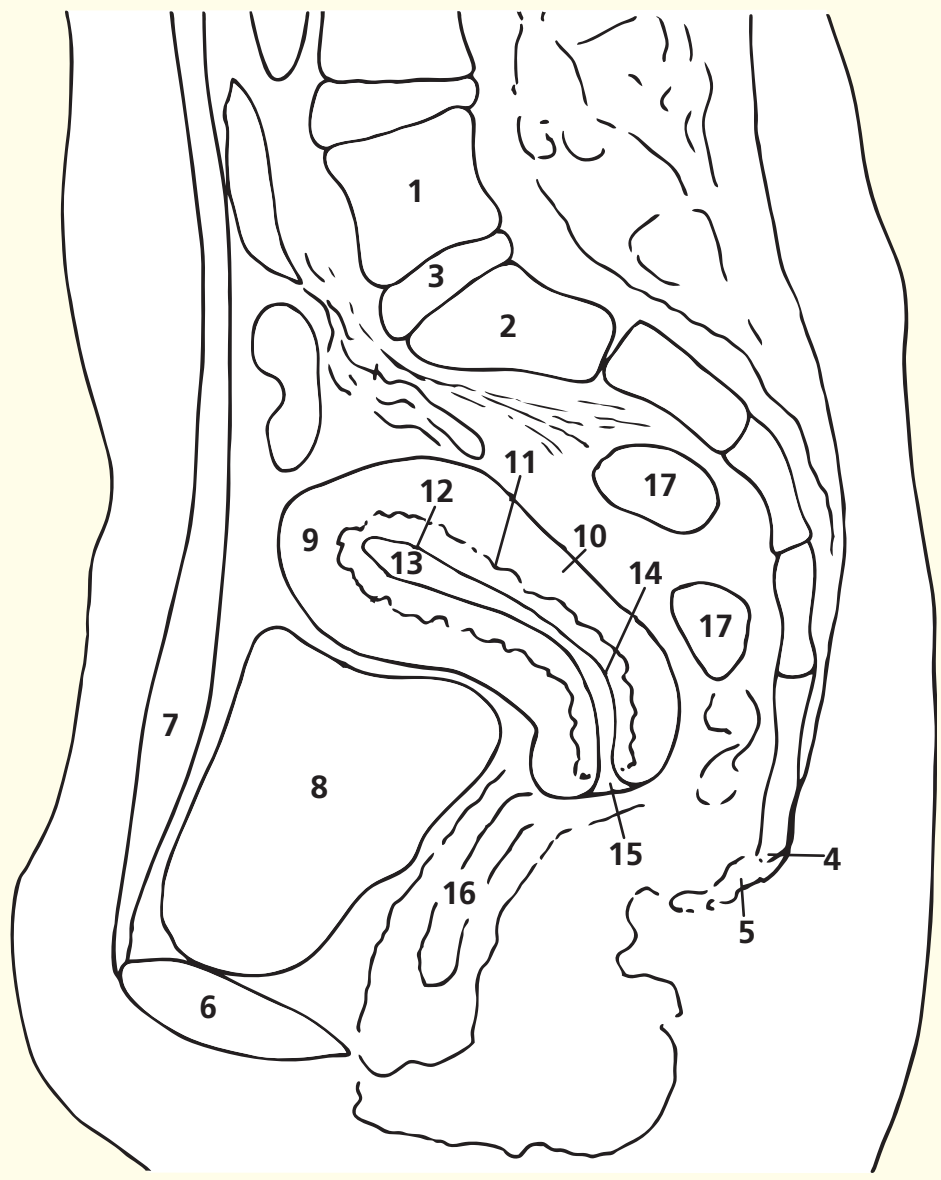


Orientation





Sagittal magnetic resonance image (MRI)



- 1 L5 vertebral body
- 2 S1 vertebral body
- 3 L5/S1 intervertebral disc
- 4 Lowest fixed point of sacrococcygeal region (here probably coccyx 1/2)
- 5 Rest of coccyx (mobile)
- 6 Pubic symphysis
- 7 Rectus abdominis
- 8 Bladder
- 9 Fundus of uterus

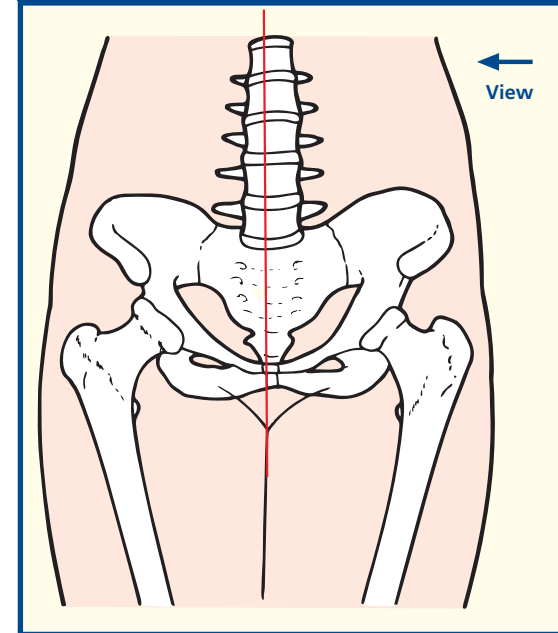
- 10 Myometrium of uterus
- 11 Junctional zone between myometrium and endometrium
- 12 Endometrium of uterus
- 13 Cavity of uterus
- 14 Internal os of uterus
- 15 External os of uterus
- 16 Vagina
- 17 Rectum

Notes

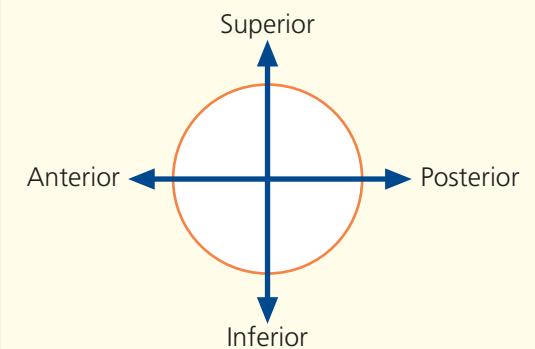
This midline sagittal T2-weighted magnetic resonance image illustrates many of the important features of the female pelvis. The bony dimensions can be assessed easily. The anteroposterior (AP) diameter of the pelvic inlet (from the superoposterior aspect of the pubic symphysis to the anterior aspect of the promontory on S1) is of key importance for obstetrics; ideally, this should be about 12 cm – the fetal head has a diameter of about 10.5 cm. The AP diameter of the mid-pelvis is usually somewhat larger; this is where rotation of the fetal head occurs during childbirth – much depends on the shape of the sacrum. The AP diameter of the pelvic outlet (from the inferior posterior aspect of the pubic symphysis to the anterior aspect of the lowest fixed point of the sacrum – usually the sacrococcygeal junction) should be similar to that of the inlet or sacrum; only rarely do the common anomalies at this site cause problems during childbirth.

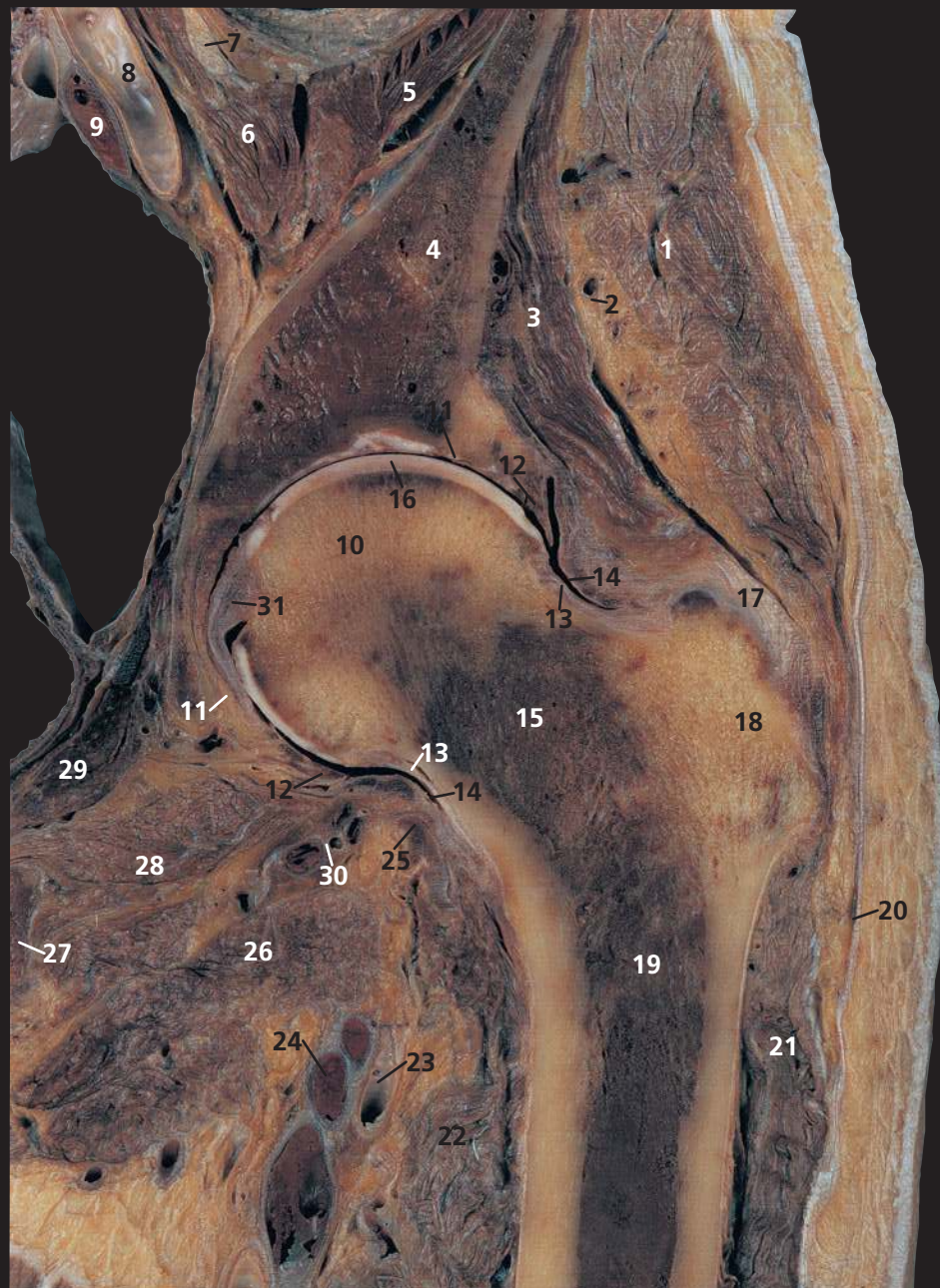
The anatomy of the uterus is shown well. This anteverted uterus (the common arrangement) is seen clearly resting on a semi-distended bladder. The cavity is defined sharply by the endometrium, and then by the junctional zone and the myometrium peripherally. The relationship of the internal and external ostia of the cervix to the vaginal vault is shown well, as is the close relationship of the vagina and the rectum. It is important to realize that many of these relationships vary according to the degree of distension of the urinary bladder and rectum and the strength of the pelvic-floor muscles on a semi-distended bladder. The body of the uterus is usually found to be flexed forwards on the cervix, as in this section, in the so-called anteflexed position.

Section level



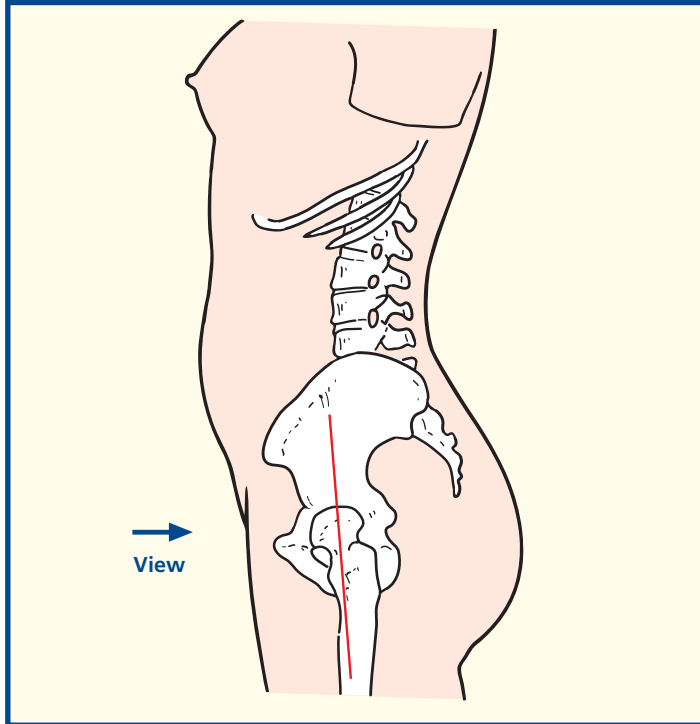
Orientation





- | | |
|-----------------------------------------|-------------------------------------------------|
| 1 Gluteus medius | 17 Iliofemoral ligament |
| 2 Superior gluteal neurovascular bundle | 18 Greater trochanter |
| 3 Gluteus minimus | 19 Shaft of femur |
| 4 Ilium | 20 Iliotibial tract |
| 5 Iliacus | 21 Vastus lateralis |
| 6 Psoas major | 22 Vastus medialis |
| 7 Femoral nerve | 23 Profunda femoris artery |
| 8 External iliac artery | 24 Profunda femoris vein |
| 9 External iliac vein | 25 Iliopsoas tendon |
| 10 Head of femur | 26 Adductor longus |
| 11 Rim of acetabulum | 27 Ischiopubic ramus |
| 12 Acetabular labrum | 28 Obturator externus |
| 13 Zona orbicularis of capsule | 29 Obturator internus |
| 14 Capsule of hip joint | 30 Medial circumflex femoral artery and vein |
| 15 Neck of femur | 31 Ligament of head of femur (ligamentum teres) |
| 16 Articular cartilage | |

Section level

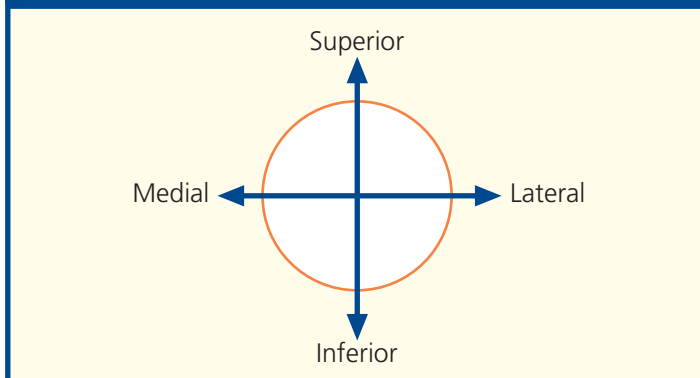


Notes

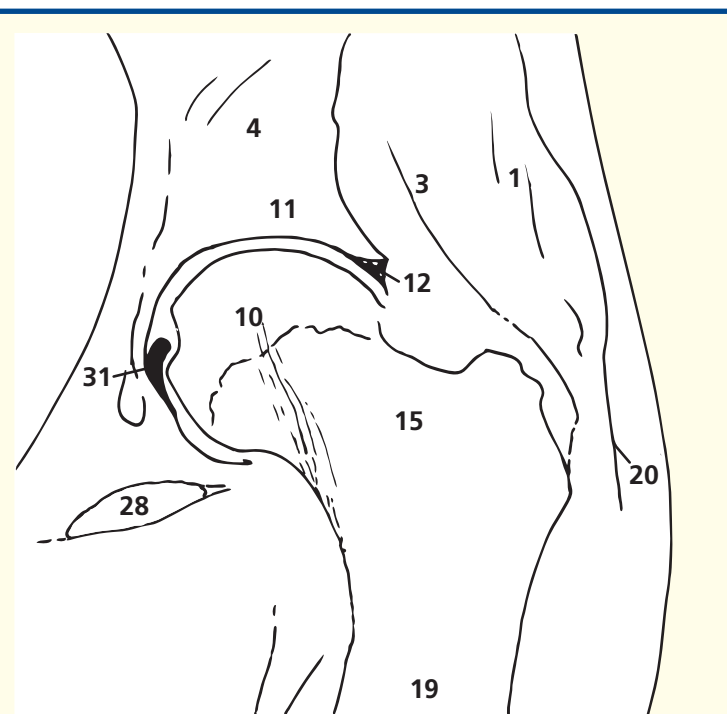
This coronal section through the hip illustrates the 'ball-and-socket' arrangement of the joint. This socket is much deeper and the ball much rounder than at the shoulder. Stability is an important function here. The two powerful abductors of the hip – gluteus medius (1) and minimus (3) – have their own neurovascular bundle (the superior gluteal nerve, artery and vein), and these can be seen between the two sheets of muscle (2).

The ligament of the head of the femur, the ligamentum teres (31), is the important source of blood supply to the femoral head in the fetus and infant. It transmits the acetabular branch of the obturator artery. It becomes obliterated during early childhood, when periosteal vessels are of key importance before vessels traverse the epiphyseal plate. The blood supply to the femoral head remains of importance throughout life: avascular necrosis has many causes. The zona orbicularis of the capsule of the hip joint (13) transmits vessels from the lateral and medial circumflex femoral branches of the deep femoral artery (profunda femoris) to the head and neck of the femur (10). A subcapital fracture of the femoral head thus deprives the head of its blood supply and often leads to avascular necrosis.

Orientation



Coronal magnetic resonance image (MRI)

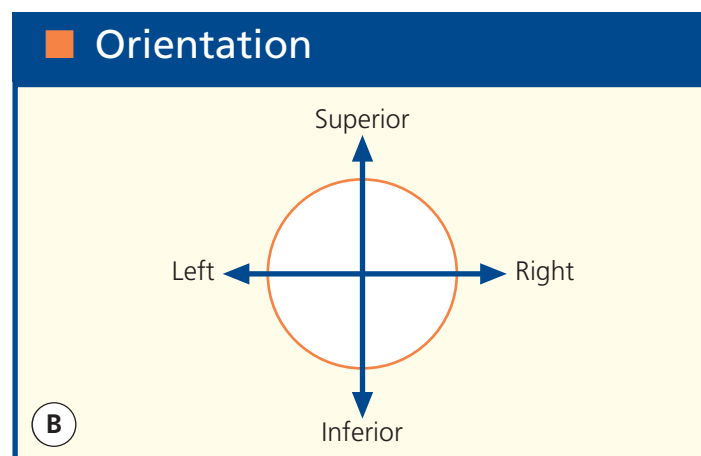
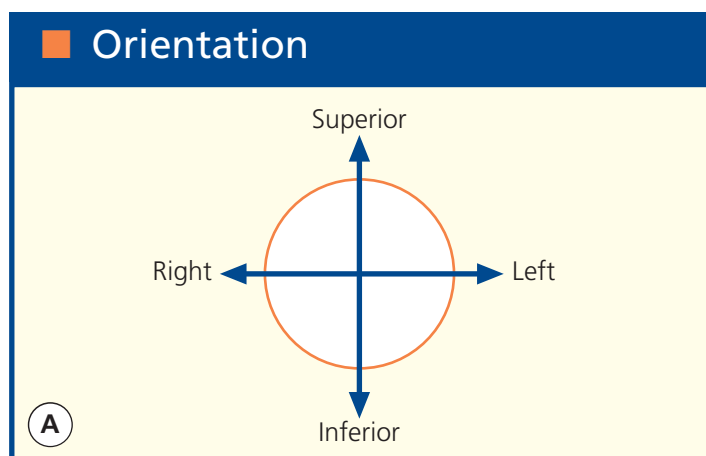
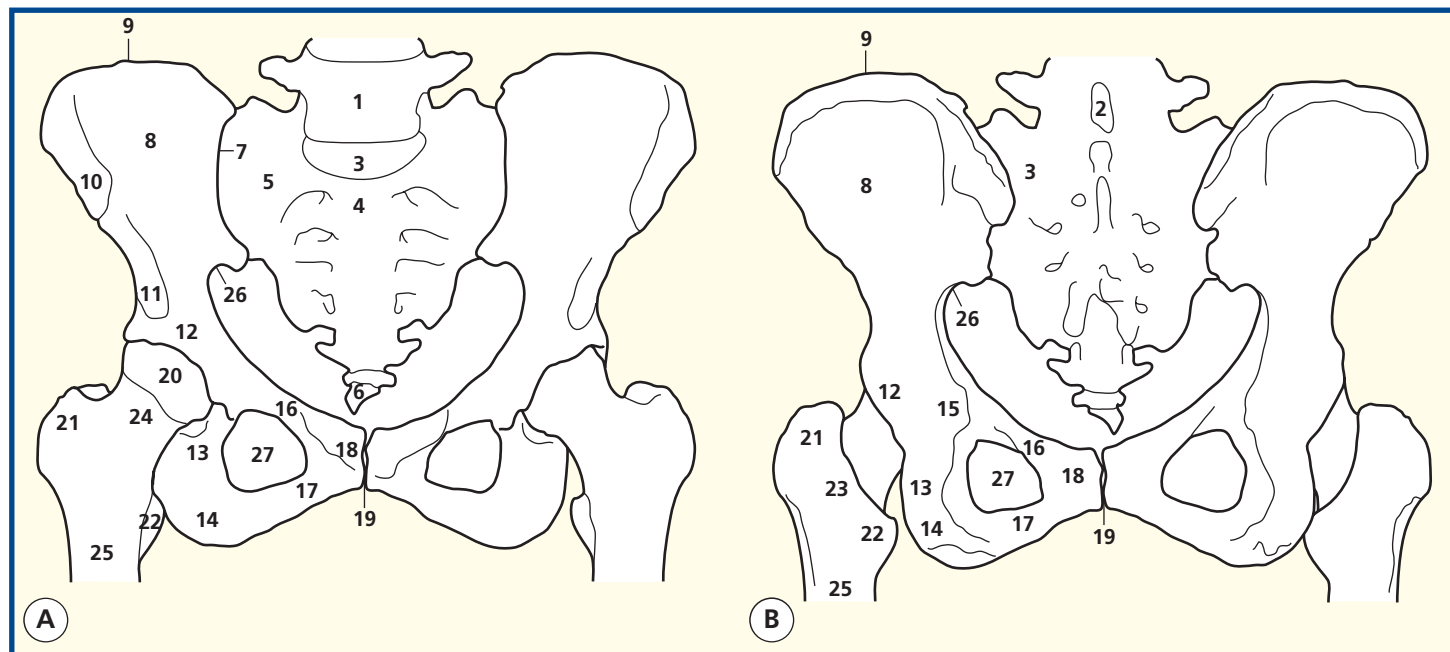




3D computed tomogram (CT)



3D computed tomogram (CT)

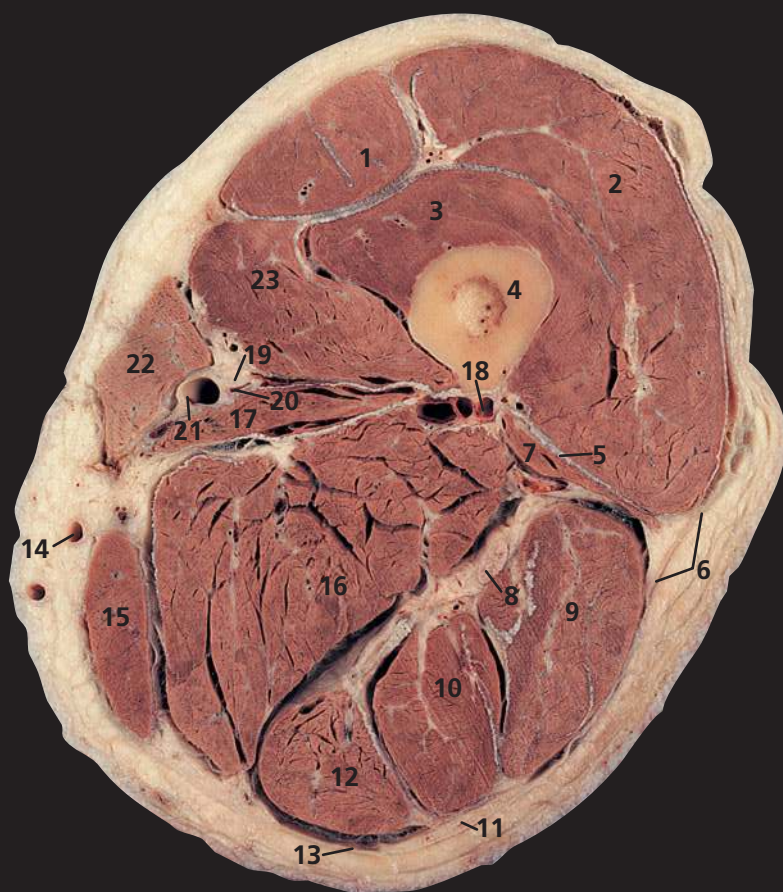


Notes

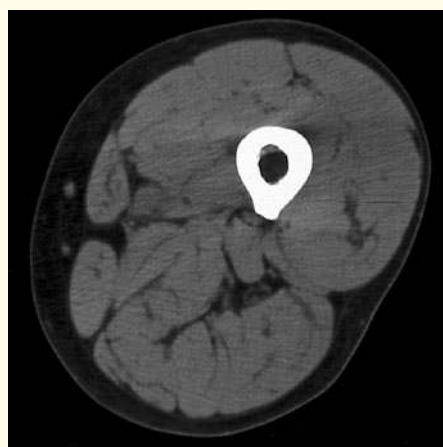
Surface-shaded three-dimensional volume-rendered CT images. Because bone attenuates the X-ray beam so much, its CT attenuation value (around +1000 HU) is much greater than that of the surrounding soft tissues. Thus, the bones can be ‘extracted’, with no overlying artefacts, to provide information equivalent to that from a cadaveric skeleton.

These two views, anterior and posterior, show the general principles of the pelvic girdle well. Note how the femoral head (two-thirds of a hemisphere) is much better contained within the acetabular fossa than the humeral head, thereby providing stability at the expense of mobility. The obliquity of the acetabulum means that the femoral head can just be seen on the anterior view, but not posteriorly.

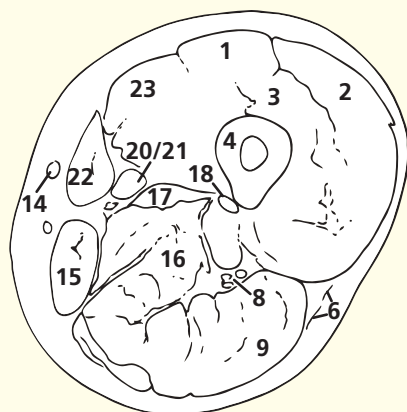
- | | | |
|---------------------------------------------------------------------------------|----------------------------------|----------------------------|
| 1 Body of fifth lumbar vertebra | 8 Ilium | 19 Pubic symphysis |
| 2 Spinous process of fifth lumbar vertebra | 9 Iliac crest | 20 Head of femur |
| 3 Intervertebral disc between fifth lumbar vertebra and first segment of sacrum | 10 Anterior superior iliac spine | 21 Greater trochanter |
| 4 Promontory of sacrum | 11 Anterior inferior iliac spine | 22 Lesser trochanter |
| 5 Upper surface of latter part of sacrum (ala) | 12 Acetabulum | 23 Intertrochanteric crest |
| 6 Coccyx | 13 Ischium | 24 Neck of femur |
| 7 Sacroiliac joint | 14 Ischial tuberosity | 25 Shaft of femur |
| | 15 Ischial spine | 26 Greater sciatic notch |
| | 16 Superior pubic ramus | 27 Obturator foramen |
| | 17 Inferior pubic ramus | |
| | 18 Body of pubic bone | |



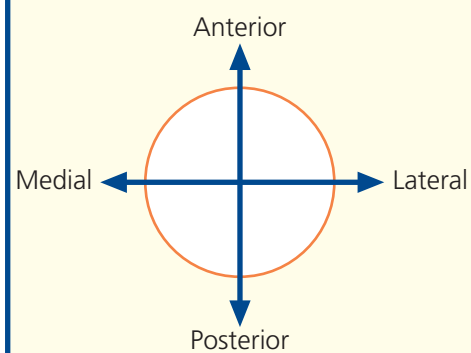
- | | |
|---------------------------------------|---------------------------------------|
| 1 Rectus femoris | 12 Semimembranosus |
| 2 Vastus lateralis | 13 Fascia lata (deep fascia of thigh) |
| 3 Vastus intermedius | 14 Great saphenous vein |
| 4 Femur | 15 Gracilis |
| 5 Lateral intermuscular septum | 16 Adductor magnus |
| 6 Iliotibial tract | 17 Adductor longus |
| 7 Biceps femoris – short head | 18 Profunda femoris artery |
| 8 Sciatic nerve | 19 Saphenous nerve |
| 9 Biceps femoris – long head | 20 Femoral vein |
| 10 Semitendinosus | 21 Femoral artery |
| 11 Posterior cutaneous nerve of thigh | 22 Sartorius |
| | 23 Vastus medialis |



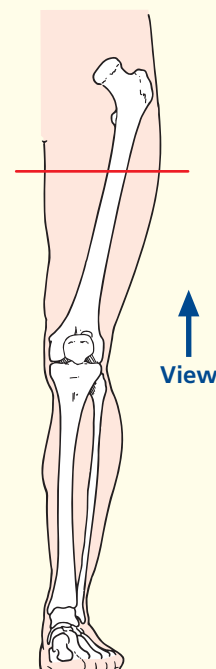
Axial computed tomogram (CT)



Orientation



Section level

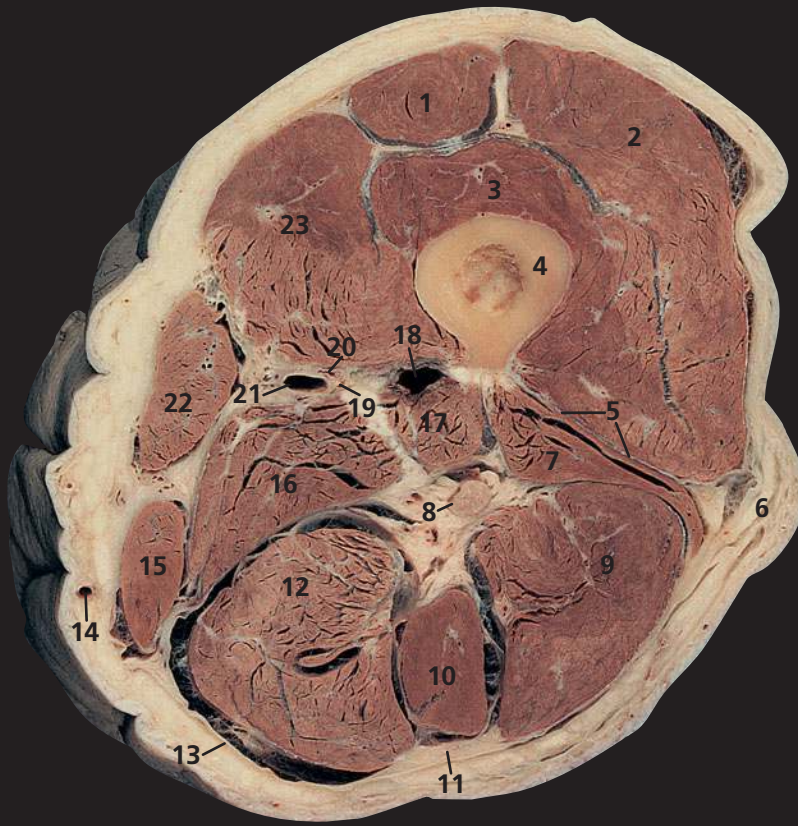


Notes

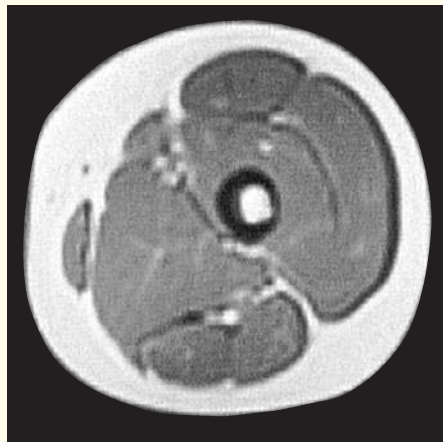
This section passes through the upper third of the thigh and provides a useful view of the three muscular compartments of the thigh:

- The **anterior compartment**, containing quadriceps femoris, made up of the vasti (2, 3, 23) and rectus femoris (1), supplied by the femoral nerve.
- The **adductor compartment**, containing the three adductors (of which only adductor magnus (16) and adductor longus (17) are present at this level, brevis having already found insertion into the femoral shaft), together with gracilis (15). These muscles are supplied by the obturator nerve; in addition, adductor magnus receives innervation from the sciatic nerve.
- The **posterior compartment** contains the hamstrings, the biceps with its long (9) and short heads (7), semitendinosus (10) and semimembranosus (12), all supplied by the sciatic nerve.

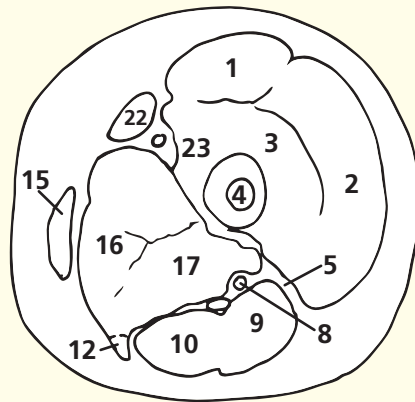
Sartorius (22) lies in a separate fascial sheath.



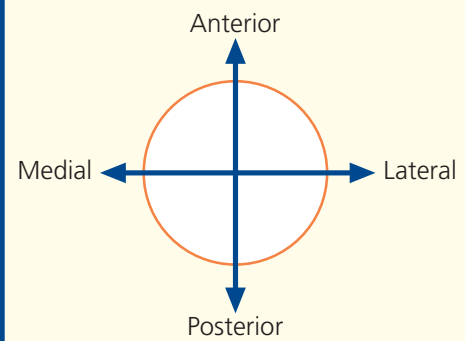
- | | |
|---------------------------------------|-----------------------------------|
| 1 Rectus femoris | 14 Great saphenous vein |
| 2 Vastus lateralis | 15 Gracilis |
| 3 Vastus intermedius | 16 Adductor magnus – medial part |
| 4 Femur | 17 Adductor magnus – lateral part |
| 5 Lateral intermuscular septum | 18 Profunda femoris artery |
| 6 Iliotibial tract | 19 Saphenous nerve |
| 7 Biceps femoris – short head | 20 Superficial femoral vein |
| 8 Sciatic nerve | 21 Superficial femoral artery |
| 9 Biceps femoris – long head | 22 Sartorius |
| 10 Semitendinosus | 23 Vastus medialis |
| 11 Posterior cutaneous nerve of thigh | |
| 12 Semimembranosus | |
| 13 Fascia lata (deep fascia of thigh) | |



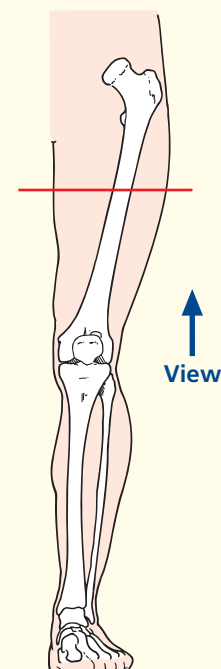
Axial magnetic resonance image (MRI)



Orientation



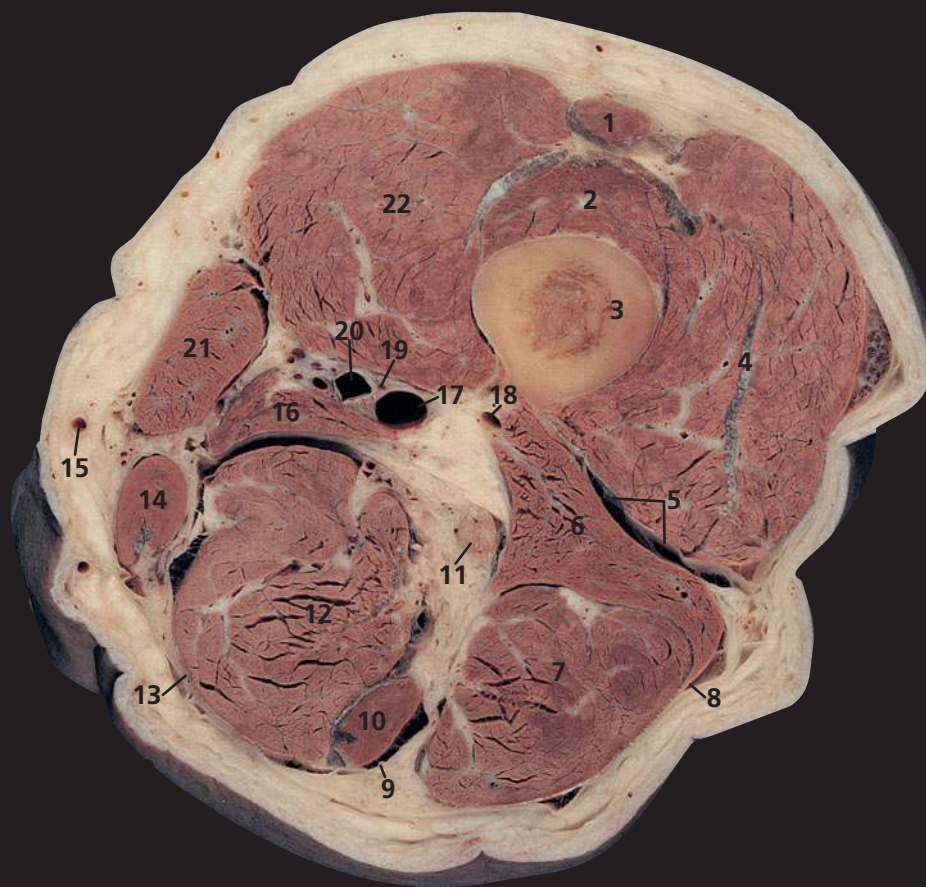
Section level



Notes

This section passes through the mid-shaft of the femur (4). Note that at this level, adductor magnus is dividing into two sections. Its lateral part (17), which arises from the ischial ramus, forms a broad aponeurosis, which inserts along the linea aspera along the posterior border of the femoral shaft (4). The medial part (16), which arises mainly from the ischial tuberosity, descends almost vertically to a tendinous attachment to the adductor tubercle of the medial condyle of the femur. Between the two parts distally is the osseo-aponeurotic adductor hiatus, which admits the femoral vessels to the popliteal fossa.

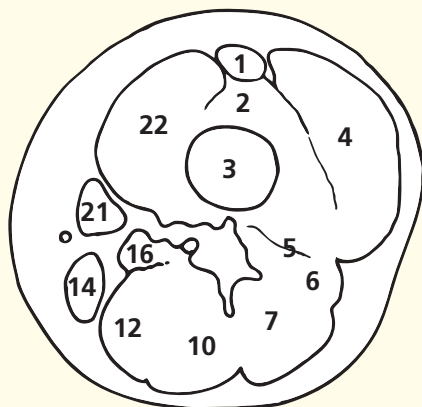
Being a composite muscle, adductor magnus also has a composite nerve supply; the medial part is innervated by the tibial division of the sciatic nerve (8) and the lateral part by the obturator nerve.



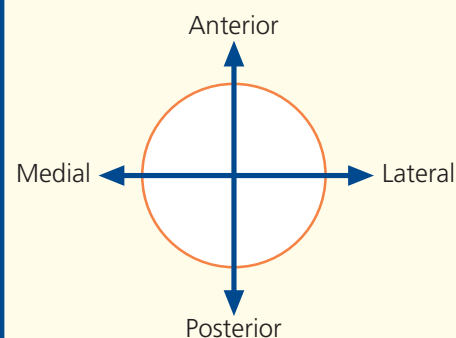
- | | |
|--------------------------------------|---------------------------------------|
| 1 Rectus femoris | 12 Semimembranosus |
| 2 Vastus intermedius | 13 Fascia lata (deep fascia of thigh) |
| 3 Femur | 14 Gracilis |
| 4 Vastus lateralis | 15 Great saphenous vein |
| 5 Lateral intermuscular septum | 16 Adductor magnus |
| 6 Biceps femoris – short head | 17 Superficial femoral vein |
| 7 Biceps femoris – long head | 18 Profunda femoris artery and vein |
| 8 Iliotibial tract | 19 Saphenous nerve |
| 9 Posterior cutaneous nerve of thigh | 20 Superficial femoral artery |
| 10 Semitendinosus | 21 Sartorius |
| 11 Sciatic nerve | 22 Vastus medialis |



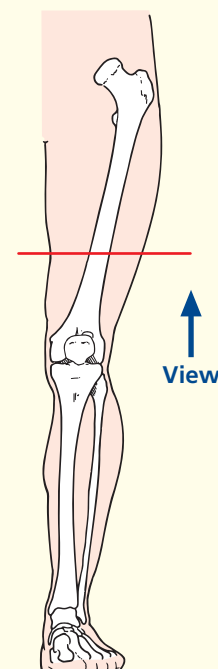
Axial magnetic resonance image (MRI)



Orientation



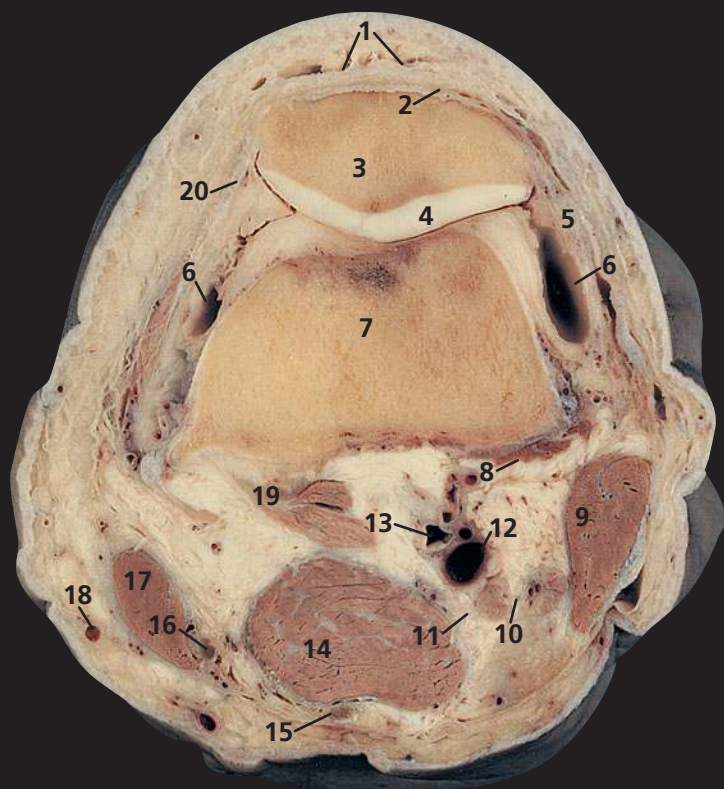
Section level



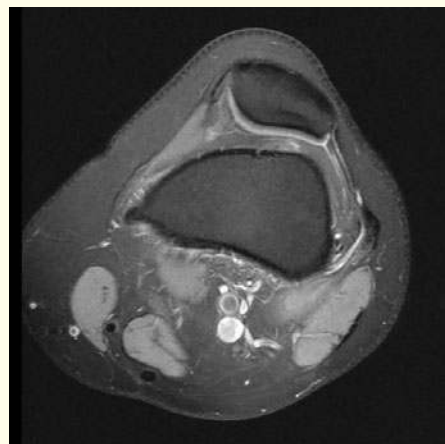
Notes

This section transects the lower third of the thigh. This and the previous two sections demonstrate the anatomy of the adductor, or subsartorial, canal (Hunter’s canal). This is formed as a triangular aponeurotic tunnel, which leads from the femoral triangle above to the popliteal fossa below, via the hiatus in adductor magnus. The canal lies between sartorius (**21**) anteromedially, adductor longus and, more distally, adductor magnus (**16**) posteriorly and vastus medialis (**22**) anterolaterally. Its contents are the femoral artery (**20**) and vein (**17**), the saphenous nerve (**19**) and the nerve to vastus medialis until this enters and supplies this muscle.

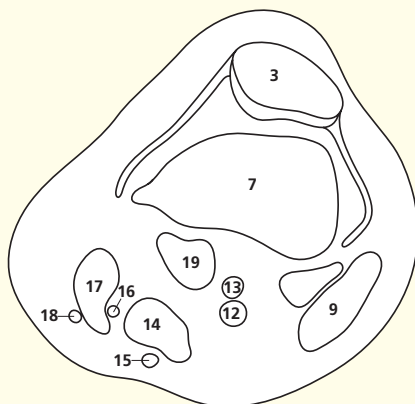
John Hunter (1728–93) described ligation of the femoral artery within this canal in the treatment of popliteal aneurysm, and his name is now used to describe the canal.



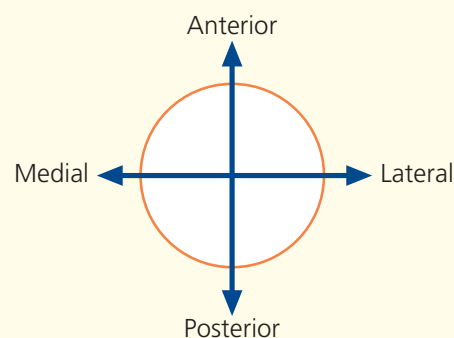
- | | |
|------------------------------------|------------------------------|
| 1 Prepatellar bursa | 11 Tibial nerve |
| 2 Tendon of quadriceps femoris | 12 Popliteal vein |
| 3 Patella | 13 Popliteal artery |
| 4 Articular cartilage of patella | 14 Semimembranosus |
| 5 Lateral patellar retinaculum | 15 Semitendinosus |
| 6 Capsule of knee joint | 16 Gracilis tendon |
| 7 Femur | 17 Sartorius |
| 8 Plantaris origin | 18 Great saphenous vein |
| 9 Biceps femoris | 19 Gastrocnemius |
| 10 Common fibular (peroneal) nerve | 20 Tendon of vastus medialis |
| | 21 Vastus medialis |



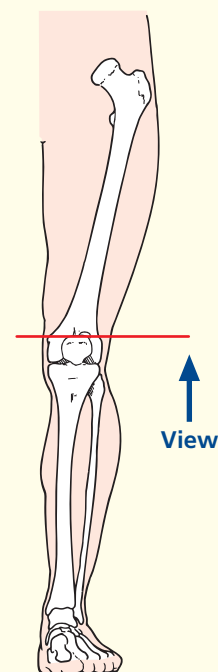
Axial magnetic resonance image (MRI)



Orientation



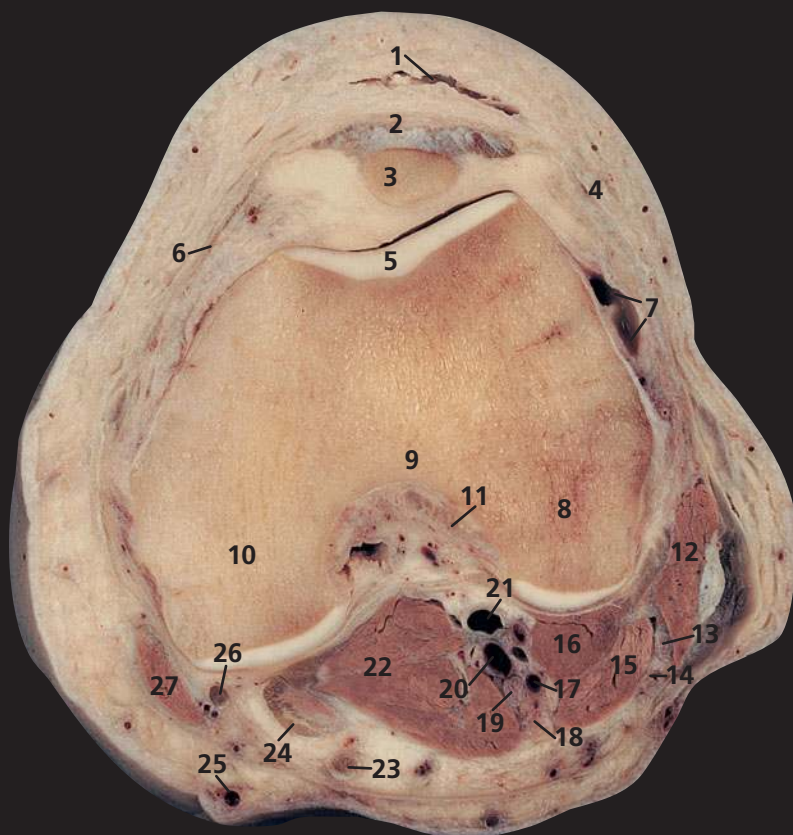
Section level



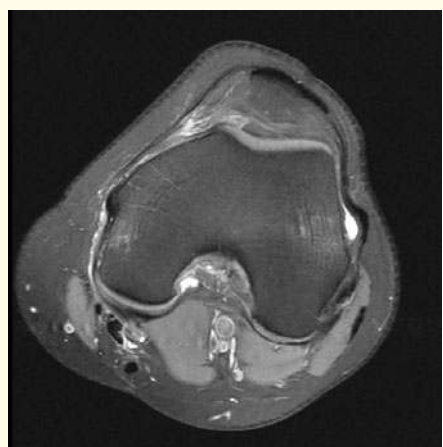
Notes

This section passes through the upper part of the patella (3) and the femur just as this widens into its condyles (7). Note how the lateral portion of the patella (3) has a larger and flatter articular surface than the medial surface. This, together with the low insertion of vastus medialis (20) into the medial side of the patella, helps to prevent lateral dislocation of the patella. The exact alignment of the patella depends on the relative contributions of the vasti muscles via their tendons (medial and lateral retinacula).

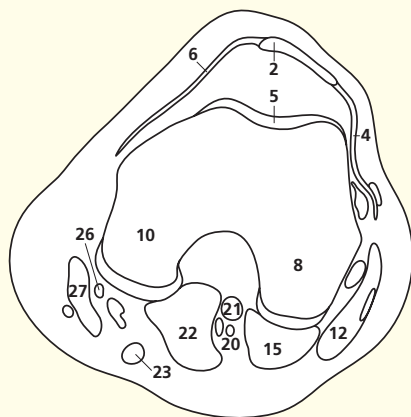
The sciatic nerve has now divided into the common fibular (peroneal) nerve (10) and tibial nerve (11); the latter is usually about twice the size of the former. Division usually takes place just proximal to the knee, but the sciatic nerve may divide anywhere along its course. Indeed, its division may take place at the sciatic plexus, when the common fibular (peroneal) nerve usually pierces the piriformis muscle in the greater sciatic foramen and the tibial division emerges caudal to this muscle.



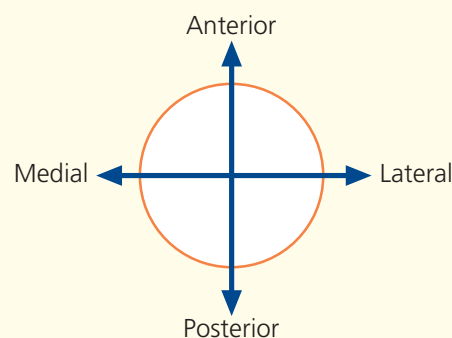
- | | |
|------------------------------------|---------------------------------------|
| 1 Prepatellar bursa | 14 Sural communicating nerve |
| 2 Ligamentum patellae | 15 Gastrocnemius – lateral head |
| 3 Patella | 16 Plantaris |
| 4 Lateral patellar retinaculum | 17 Small saphenous vein – termination |
| 5 Articular cartilage of femur | 18 Sural nerve |
| 6 Medial patellar retinaculum | 19 Tibial nerve |
| 7 Capsule of knee joint | 20 Popliteal vein |
| 8 Lateral condyle of femur | 21 Popliteal artery |
| 9 Intercondylar fossa | 22 Gastrocnemius – medial head |
| 10 Medial condyle of femur | 23 Semitendinosus tendon |
| 11 Anterior cruciate ligament | 24 Semimembranosus tendon |
| 12 Biceps femoris | 25 Great saphenous vein |
| 13 Common fibular (peroneal) nerve | 26 Gracilis tendon |
| | 27 Sartorius |



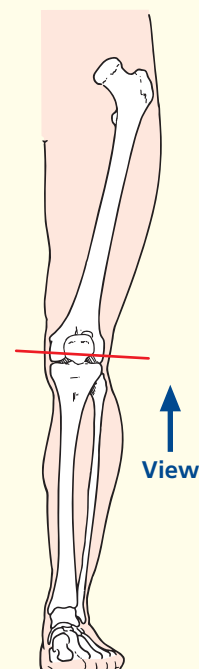
Axial magnetic resonance image (MRI)



Orientation



Section level

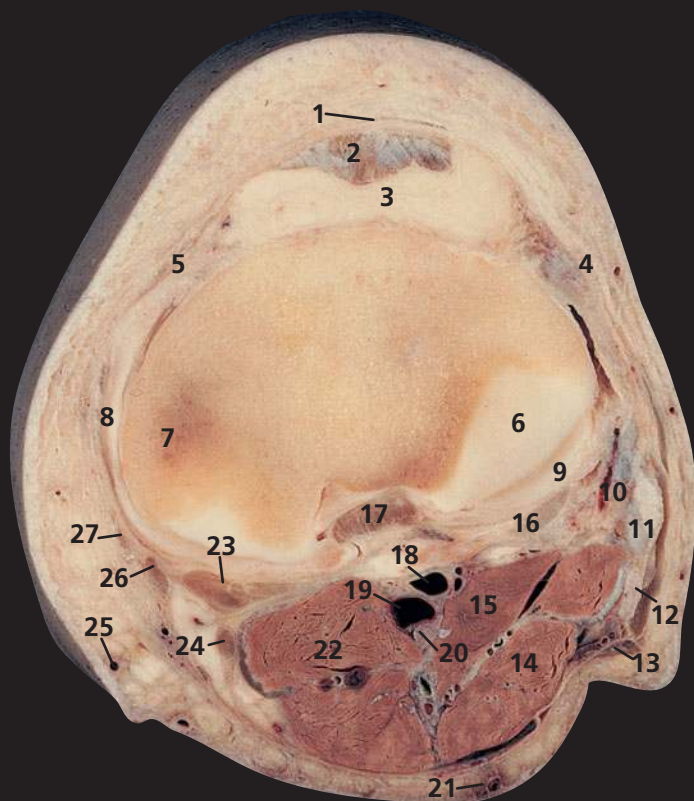


Notes

This section passes through the distal extremity of the patella (3) and the femoral condyles (8, 10).

The anterior cruciate ligament (11) arises from the intercondylar fossa (9) of the femur laterally and slightly more proximally than the posterior cruciate ligament, whose attachment is seen better in the next cadaveric section. The anterior cruciate ligament passes downwards and forwards laterally to the posterior cruciate ligament, to attach to the anterior intercondylar area of the tibia.

The small saphenous vein (17), which will be seen in later sections as it lies in the superficial fascia of the back of the calf, has here pierced the deep fascia of the popliteal fossa and is about to drain into the popliteal vein (20). On the magnetic resonance images, these veins are joining.

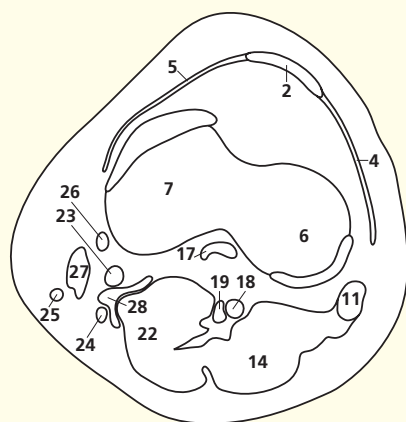


- 1 Infrapatellar bursa
- 2 Ligamentum patellae
- 3 Infrapatellar fat pad
- 4 Lateral patellar retinaculum
- 5 Medial patellar retinaculum
- 6 Sliver of cartilage over lateral condyle of tibia
- 7 Medial condyle of tibia
- 8 Medial collateral ligament
- 9 Lateral meniscus
- 10 Lateral collateral ligament
- 11 Tendon of biceps femoris
- 12 Common fibular (peroneal) nerve
- 13 Lateral cutaneous nerve of calf
- 14 Gastrocnemius lateral head
- 15 Plantaris
- 16 Popliteus
- 17 Posterior cruciate ligament
- 18 Popliteal artery
- 19 Popliteal vein
- 20 Tibial nerve
- 21 Small saphenous vein
- 22 Gastrocnemius – medial head
- 23 Semimembranosus tendon
- 24 Semitendinosus tendon
- 25 Great saphenous vein
- 26 Gracilis tendon
- 27 Sartorius tendon

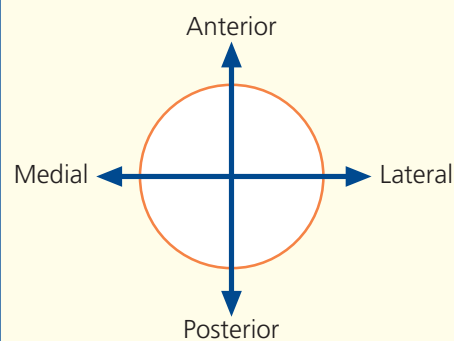
28 Semimembranosus bursa



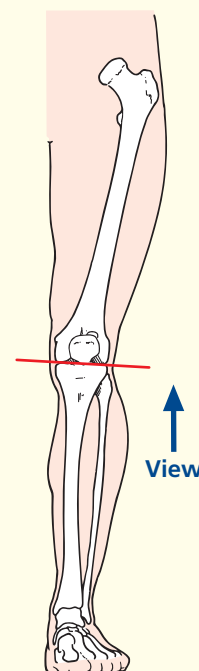
Axial magnetic resonance image (MRI)



Orientation



Section level

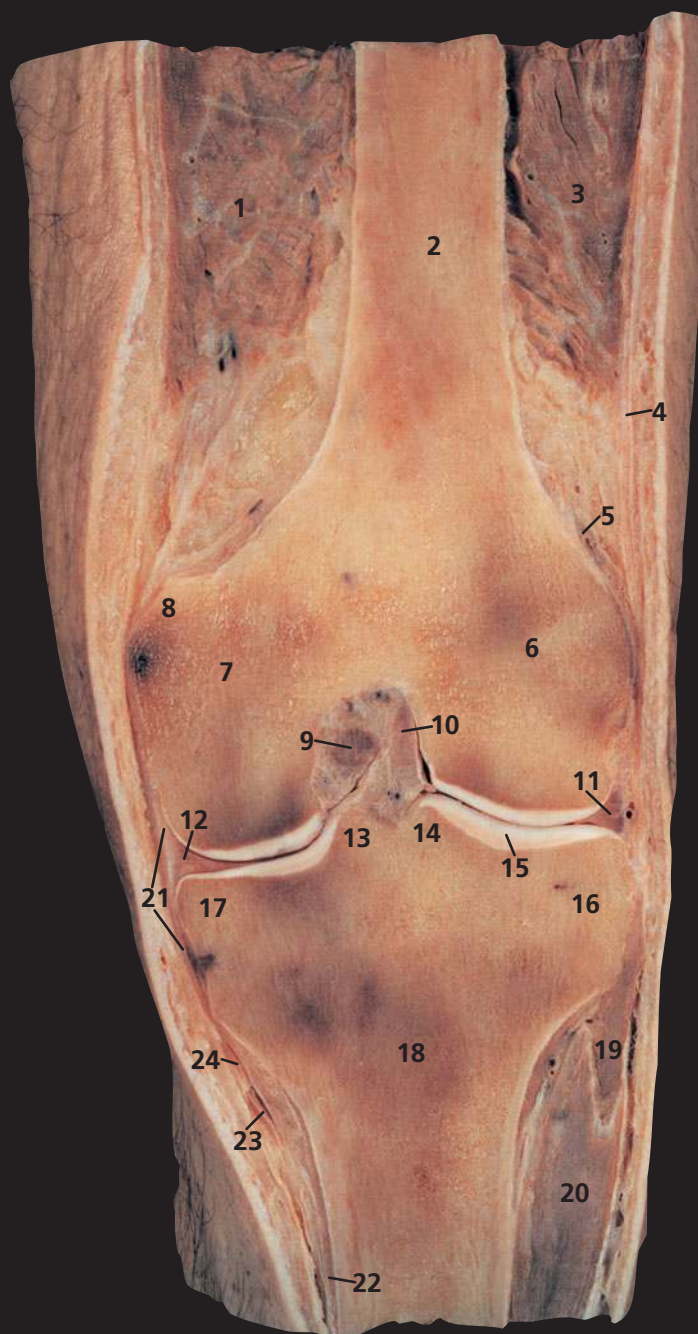


Notes

This section passes through the tibial condyles (6, 7). The posterior cruciate ligament (17) is here finding attachment to the posterior intercondylar area of the proximal articular surface of the tibia.

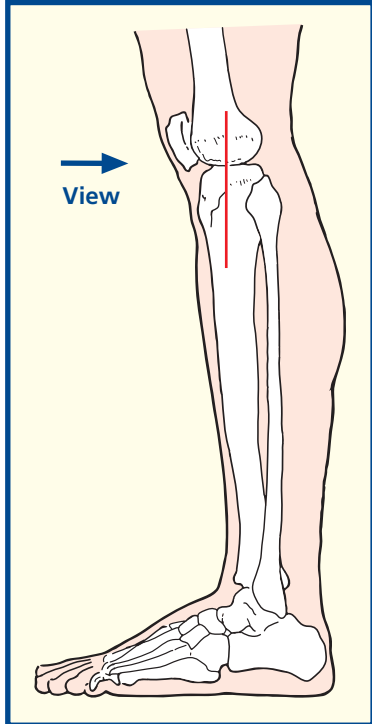
The popliteus tendon (16), which inserts on to the femur in a depression immediately distal to the lateral epicondyle, passes between the lateral meniscus (9) and the lateral collateral ligament (10) of the knee. In contrast, the medial collateral ligament (8) is applied closely to the medial meniscus, which lies just proximal to this plane of section. This tethering of the medial meniscus probably accounts for the much higher incidence of tears of the medial compared with the lateral meniscus.

The semimembranosus bursa contains a trace of fluid on the magnetic resonance image (28). It can enlarge greatly to form a popliteal cyst (a misnomer).



- | | |
|------------------------------------------------------------------|---------------------------------------|
| 1 Vastus medialis | 16 Lateral condyle (plateau) of tibia |
| 2 Shaft of femur | 17 Medial condyle (plateau) of tibia |
| 3 Vastus lateralis | 18 Tibia |
| 4 Fascia lata | 19 Extensor digitorum longus |
| 5 Superior lateral genicular artery | 20 Tibialis anterior |
| 6 Lateral condyle of femur | 21 Medial collateral ligament |
| 7 Medial condyle of femur | 22 Popliteus (most medial fibres) |
| 8 Adductor tubercle of femur | 23 Tendon of gracilis |
| 9 Posterior cruciate ligament | 24 Tendon of sartorius |
| 10 Anterior cruciate ligament | |
| 11 Lateral meniscus | 25 Popliteus tendon |
| 12 Medial meniscus | 26 Lateral collateral ligament |
| 13 Medial intercondylar eminence/tubercle (also known as spine) | 27 Head of fibula |
| 14 Lateral intercondylar eminence/tubercle (also known as spine) | 28 Great saphenous vein |
| 15 Articular cartilage | 29 Medial gastrocnemius |
| | 30 Biceps femoris |

Section level



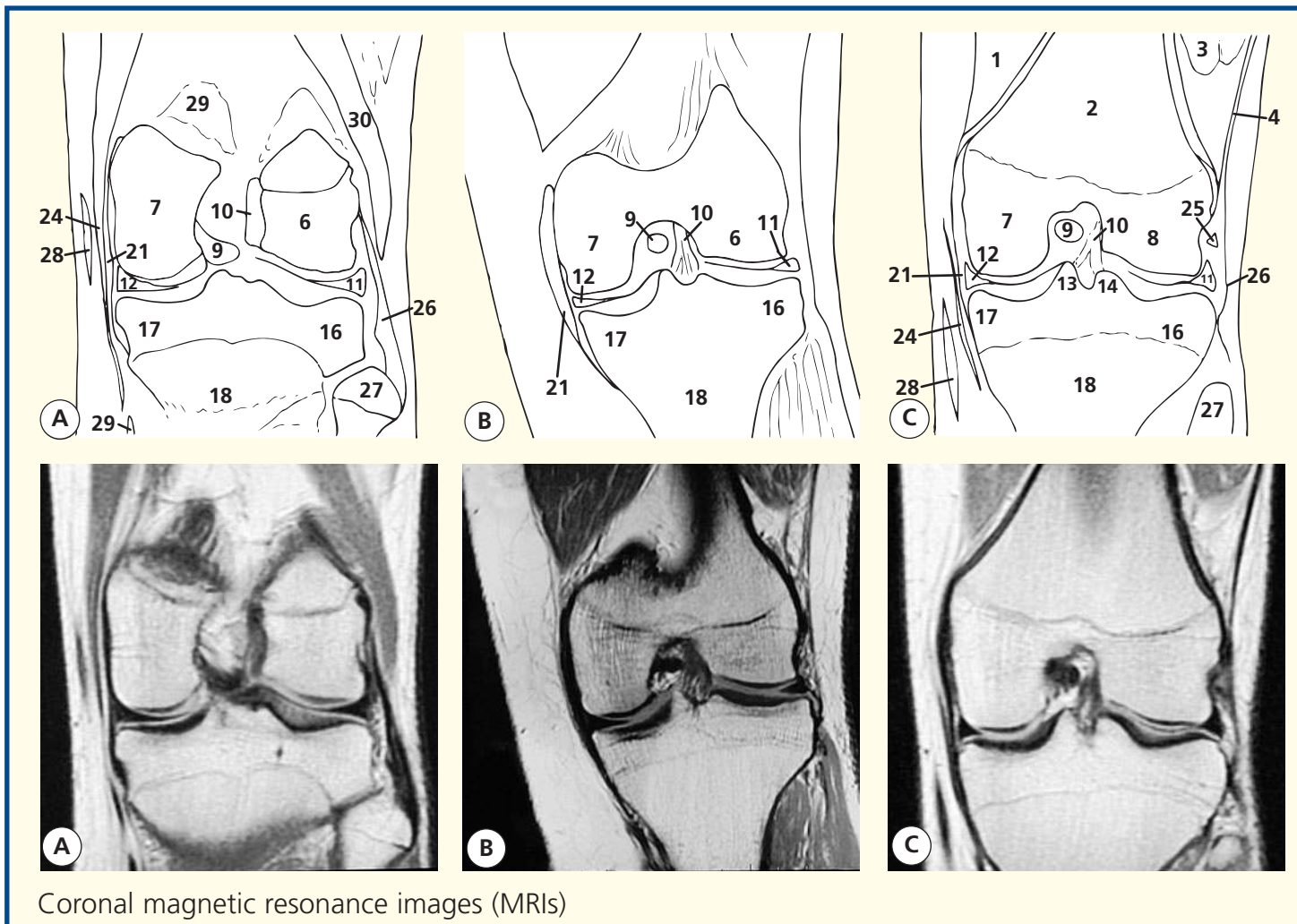
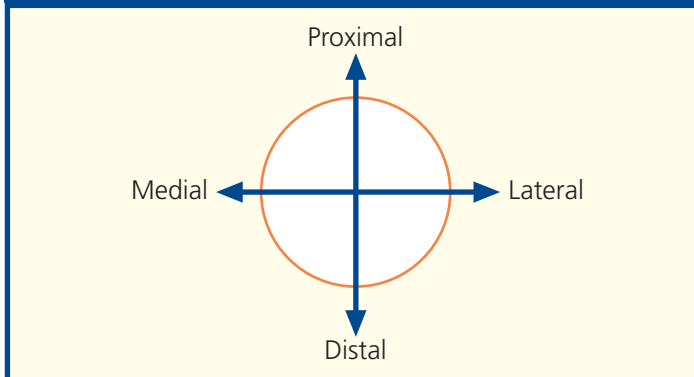
Notes

The posterior cruciate ligament (9) lies on the medial side of the anterior cruciate ligament (10). The former prevents posterior sliding movement of the tibia on the femur, while the latter prevents anterior displacement and resists torsional movement at the knee joint. They may be torn in violent torsional injury of the knee especially in the flexed position, when the collateral ligaments (21) are less tense.

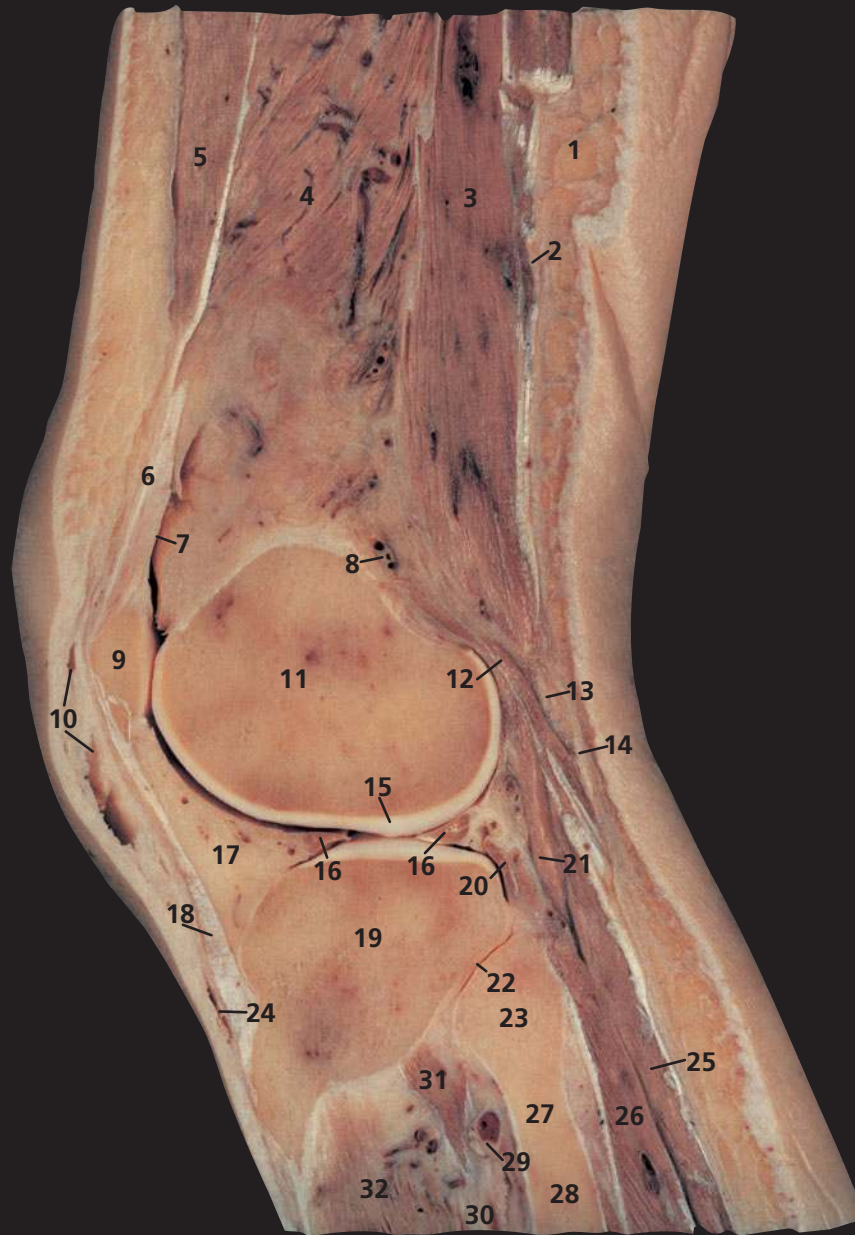
It can be seen that the menisci (11, 12) do little to deepen the concavity of the knee joint on either side. They do act, however, as 'shock absorbers' at the knee, for example when jumping from a height.

Note that the medial collateral ligament is continuous with the medial meniscus, whereas the lateral collateral ligament is discontinuous with the lateral meniscus. This contributes to the medial meniscus being more static and being injured more commonly; the lateral meniscus is more mobile.

Orientation

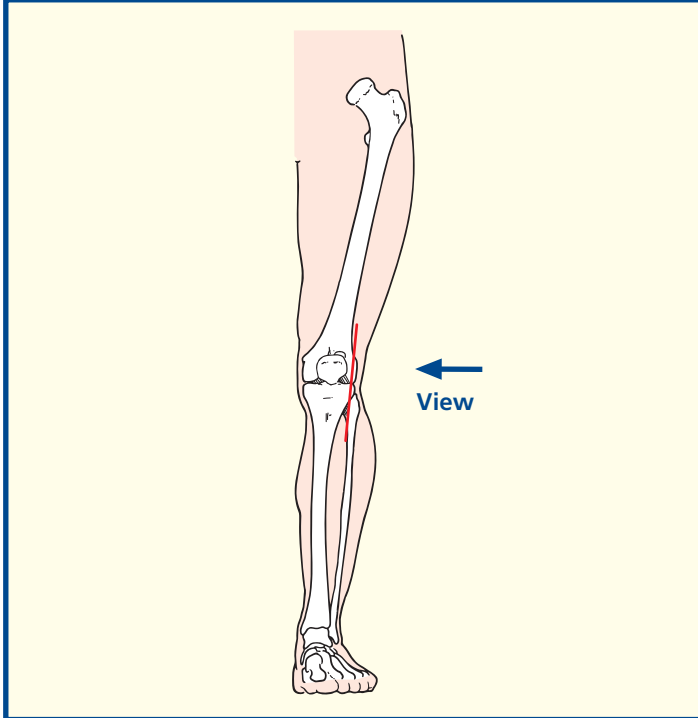


Coronal magnetic resonance images (MRIs)



- | | |
|-----------------------------------------------|---------------------------------------------------------------|
| 1 Superficial fascia | 17 Infrapatellar pad of fat extending into infrapatellar fold |
| 2 Deep fascia | 18 Ligamentum patellae |
| 3 Biceps femoris | 19 Lateral condyle (plateau) of tibia |
| 4 Vastus intermedius | 20 Tendon of popliteus |
| 5 Vastus lateralis | 21 Plantaris |
| 6 Tendon of quadriceps femoris | 22 Superior tibiofibular joint |
| 7 Suprapatellar bursa | 23 Head of fibula |
| 8 Lateral superior geniculate artery and vein | 24 Infrapatellar bursa |
| 9 Patella | 25 Gastrocnemius lateral |
| 10 Prepatellar bursa | 26 Soleus |
| 11 Lateral condyle of femur | 27 Neck of fibula |
| 12 Fibrous capsule of knee joint | 28 Shaft of fibula |
| 13 Common fibular (peroneal) nerve | 29 Anterior tibial artery and vein |
| 14 Lateral cutaneous nerve of calf | 30 Interosseous membrane |
| 15 Articular cartilage | 31 Tibialis posterior |
| 16 Lateral meniscus | 32 Tibialis anterior |

Section level



Notes

The prepatellar bursa (10) and infrapatellar bursa (24) are both subcutaneous. Either may become inflamed by continual kneeling, which produces a traumatic bursitis. A prepatellar bursa comes into contact with the ground on scrubbing the floor (hence 'housemaid's knee'), while the infrapatellar bursa does so when kneeling to pray (hence 'clergyman's knee').

The communication of the suprapatellar bursa (7) with the main synovial cavity of the knee is demonstrated well. It extends a hand's breadth superior to the border of the patella (9) and lies posterior to the quadriceps tendon (6). It becomes distended when there is an effusion into the knee joint. A puncture wound within a hand's breadth of the superior border of the patella must always be suspected of having penetrated the knee joint. Failure to do so may result in septic arthritis of the knee.

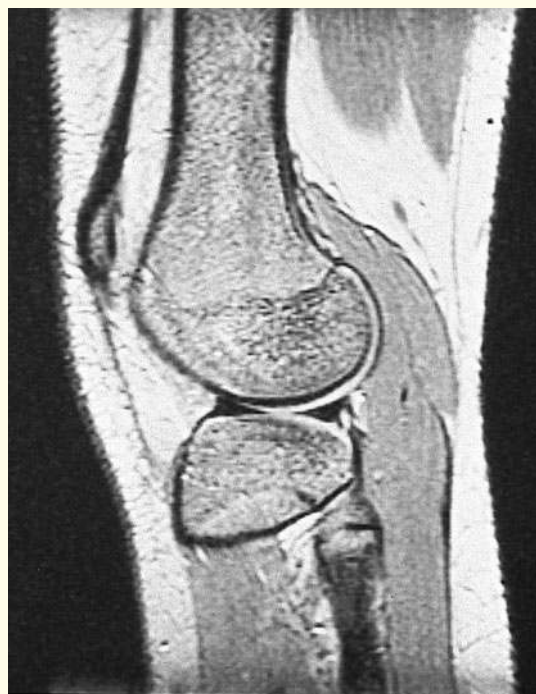
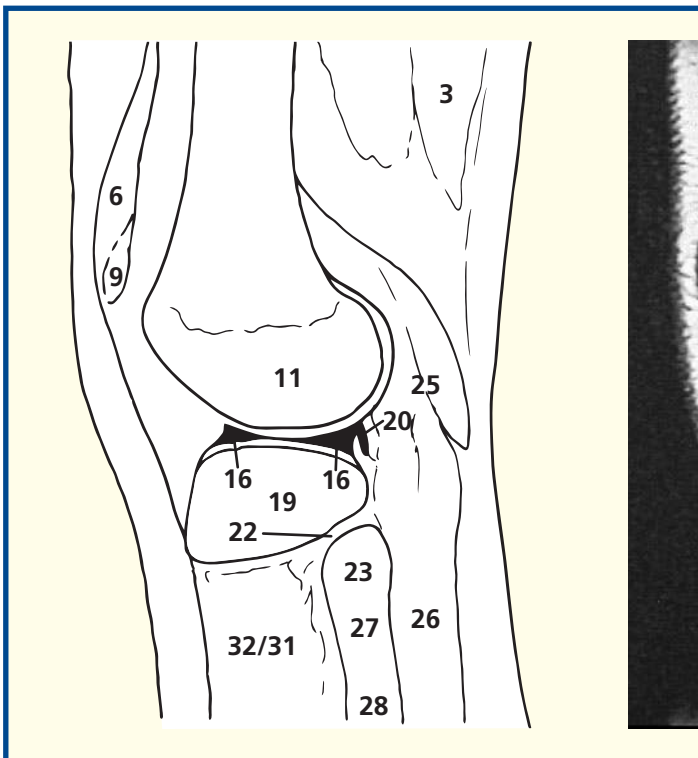
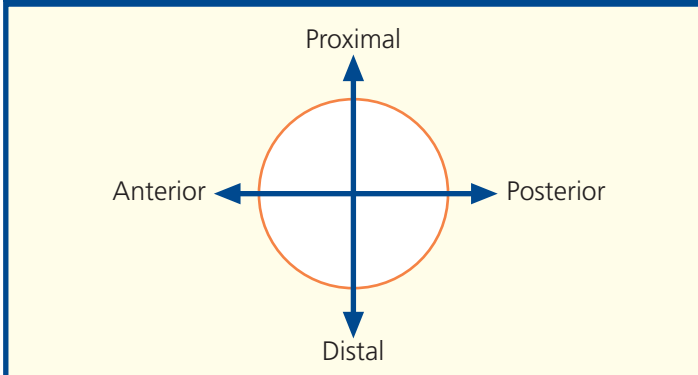
Plantaris (21) is absent in about ten per cent of subjects. Very rarely, it has two heads.

The tendon of popliteus (20) is connected to the lateral meniscus (16). It may thus retract and protect the mobile lateral meniscus during lateral rotation of the femur in flexion of the knee joint, protecting the meniscus from being crushed between the femoral and tibial condyles during this movement.

The superior tibiofibular joint (22) is a plane synovial joint, in contrast to the fibrous inferior tibiofibular joint.

The lateral meniscus is of even thickness throughout. Thus, a lateral sagittal slice creates a bowtie appearance to this portion of the lateral meniscus.

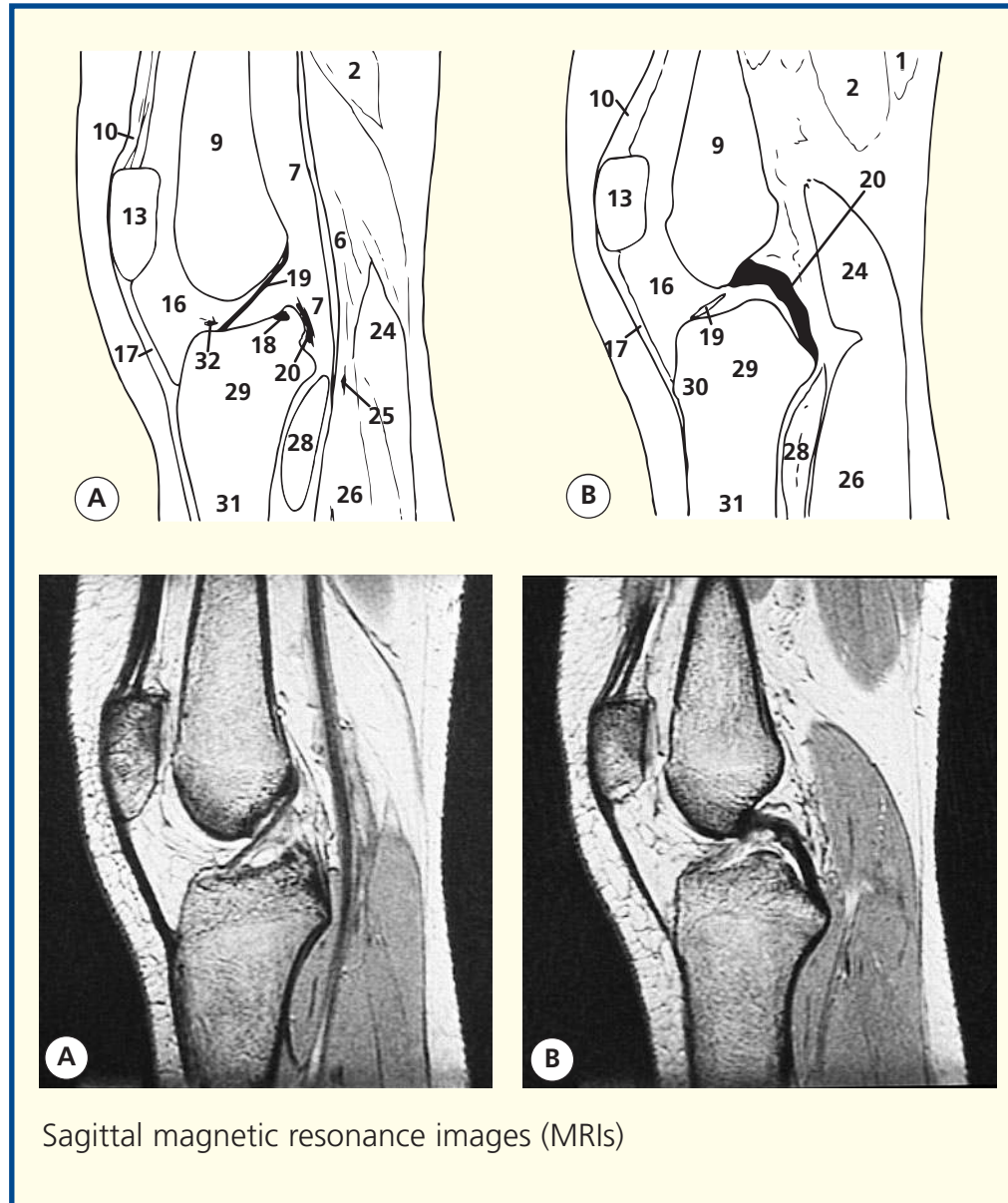
Orientation



Sagittal magnetic resonance image (MRI)

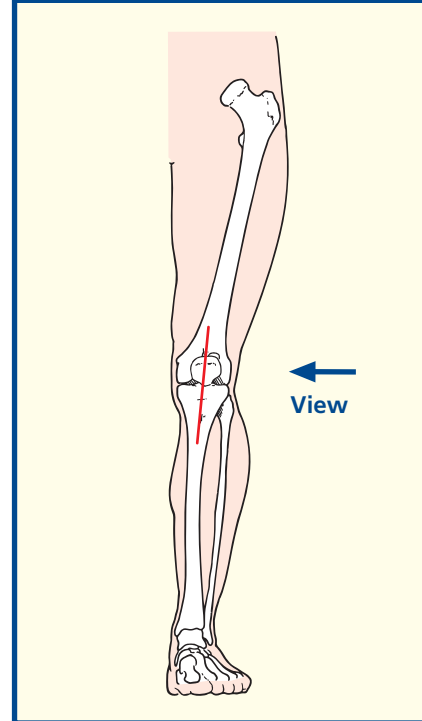


- | | |
|-----------------------------------------------------------------------|--------------------------------------|
| 1 Semitendinosus | 17 Ligamentum patellae |
| 2 Semimembranosus | 18 Medial meniscus |
| 3 Sciatic nerve | 19 Anterior cruciate ligament |
| 4 Vastus intermedius | 20 Posterior cruciate ligament |
| 5 Rectus femoris | 21 Fibrous capsule of knee joint |
| 6 Popliteal vein | 22 Superficial fascia |
| 7 Popliteal artery | 23 Deep fascia |
| 8 Popliteal surface of femur | 24 Gastrocnemius |
| 9 Shaft of femur | 25 Tendon of plantaris |
| 10 Tendon of quadriceps femoris | 26 Soleus |
| 11 Suprapatellar bursa | 27 Tibial nerve |
| 12 Popliteal pad of fat | 28 Popliteus |
| 13 Patella | 29 Proximal end of tibia |
| 14 Prepatellar bursa | 30 Tibial tuberosity |
| 15 Articular cartilage | 31 Shaft of tibia |
| 16 Infrapatellar pad of fat (Hoffa) extending into infrapatellar fold | 32 Transverse intermeniscal ligament |

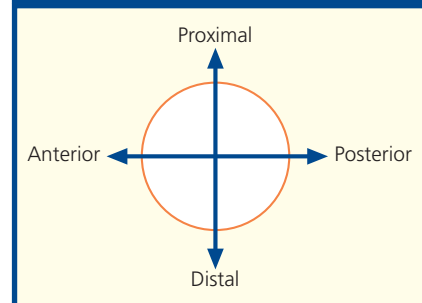


Sagittal magnetic resonance images (MRIs)

Section level



Orientation



Notes

The relationships in the popliteal fossa comprise the tibial nerve (27) most superficially, the popliteal vein (6) and then, more deeply, the popliteal artery (7). The valves in the vein are shown well. It is within these large veins that postoperative (or post-immobilization) thrombosis of the deep veins of the lower limb usually commences.

The fossa contains a large amount of fat (12) as well as the rather insignificant popliteal lymph nodes, usually five or six in number. Note the composition of the floor of the popliteal fossa comprises superiorly the popliteal surface of the femur (8), the capsule of the knee joint (21) and finally popliteus (28).

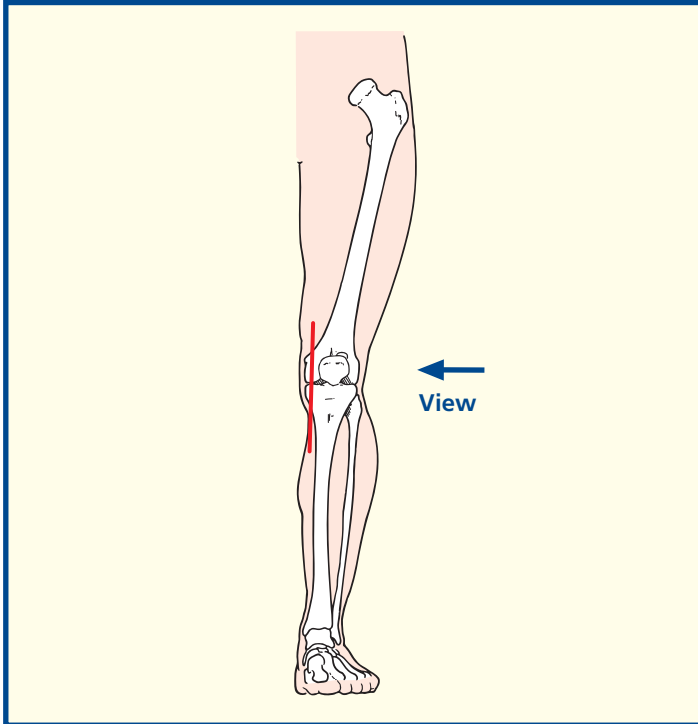
Both gastrocnemius (24) and soleus (26) contain large veins, an important component of the calf pump mechanism in venous return from the lower limb. Note also the density of the deep fascia (23), which assists the pumping action of the muscles.

Note that with the knee in the extended position, the anterior cruciate ligament is taut and straight; there is less tension on the posterior cruciate, which appears curved in that position. The cruciate ligaments take their names (anterior and posterior) from the site of attachment to the tibia. The anterior cruciate passes lateral to the posterior ligament.



- | | |
|---------------------------------|---------------------------------------|
| 1 Semimembranosus | 9 Medial head/tendon of gastrocnemius |
| 2 Adductor magnus | 10 Tendon of semitendinosus |
| 3 Femoral artery | 11 Superficial fascia |
| 4 Vastus medialis | 12 Deep fascia |
| 5 Medial gastrocnemius | 13 Medial meniscus |
| 6 Suprapatellar bursa | 14 Articular cartilage |
| 7 Medial condyle of femur | 15 Medial condyle (plateau of tibia) |
| 8 Fibrous capsule of knee joint | |

Section level



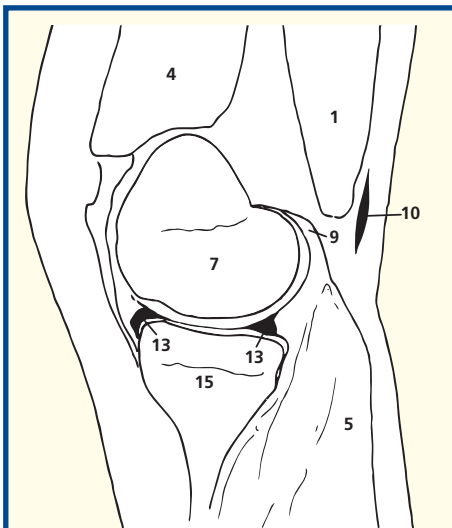
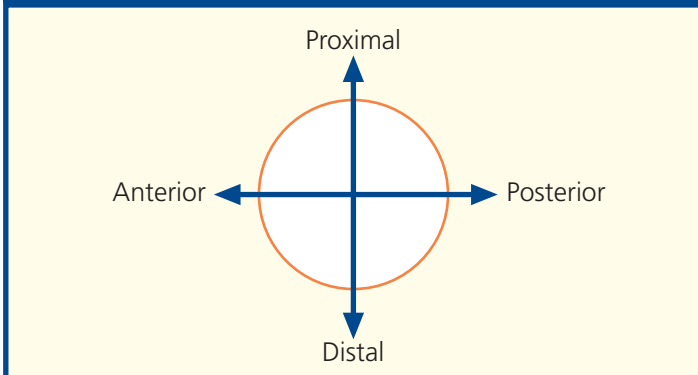
Notes

The femoral artery (3) passes through the hiatus in adductor magnus (2) to become the popliteal artery about two-thirds of the distance along a line that joins the femoral pulse at the groin, with the adductor tubercle on the medial condyle of the femur.

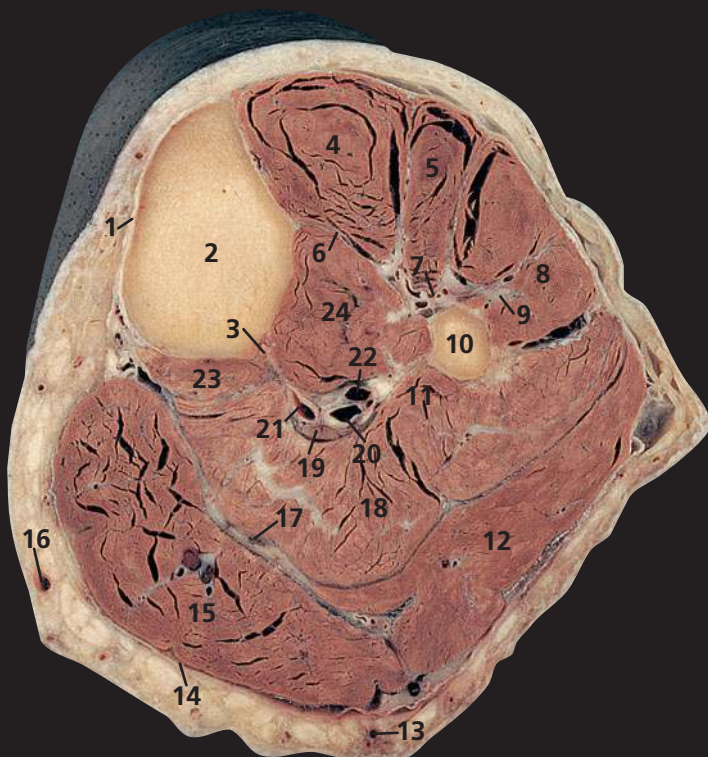
The posterior third of the medial meniscus is usually a little thicker than the mid and anterior thirds, in contrast to the lateral meniscus, which is of constant thickness around its circumference. Furthermore, the posterior third frequently undergoes myxoid change during early middle age; thus, this part of the medial meniscus often appears rather heterogeneous in consistency.

This section shows the possible consequence of a fracture of the shaft of the femur at its lower extremity. The medial (9) and lateral heads of gastrocnemius tilt the otherwise unsupported distal femoral fragment posteriorly. This may well injure the popliteal vessels, lying immediately behind. (See also Sagittal section 2.)

Orientation



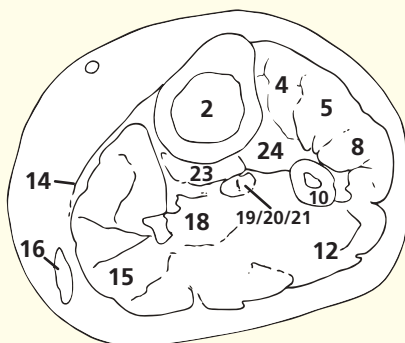
Sagittal magnetic resonance image (MRI)



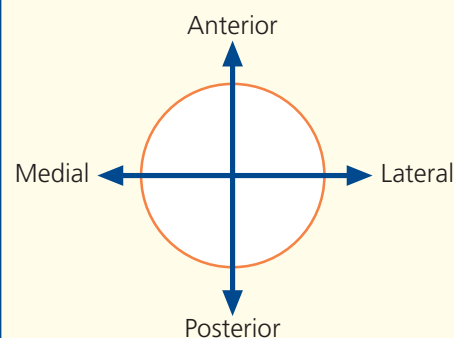
- | | |
|-----------------------------------------------------------------------|---------------------------------|
| 1 Subcutaneous surface of tibia | 12 Gastrocnemius – lateral head |
| 2 Tibia | 13 Small saphenous vein |
| 3 Vertical ridge of tibia | 14 Deep fascia of calf |
| 4 Tibialis anterior | 15 Gastrocnemius – medial head |
| 5 Extensor digitorum longus | 16 Great saphenous vein |
| 6 Interosseous membrane | 17 Plantaris tendon |
| 7 Anterior tibial artery and vein, with deep fibular (peroneal) nerve | 18 Soleus |
| 8 Fibularis (peroneus) longus | 19 Tibial nerve |
| 9 Superficial fibular (peroneal) nerve | 20 Posterior tibial artery |
| 10 Fibula | 21 Posterior tibial vein |
| 11 Medial crest of fibula | 22 Fibular (peroneal) artery |
| | 23 Popliteus |
| | 24 Tibialis posterior |



Axial computed tomogram (CT)



Orientation



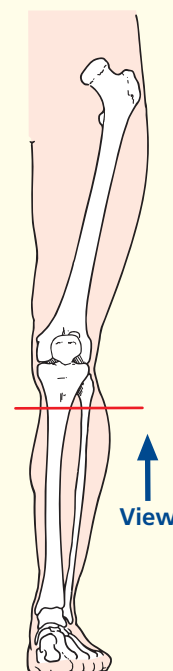
Notes

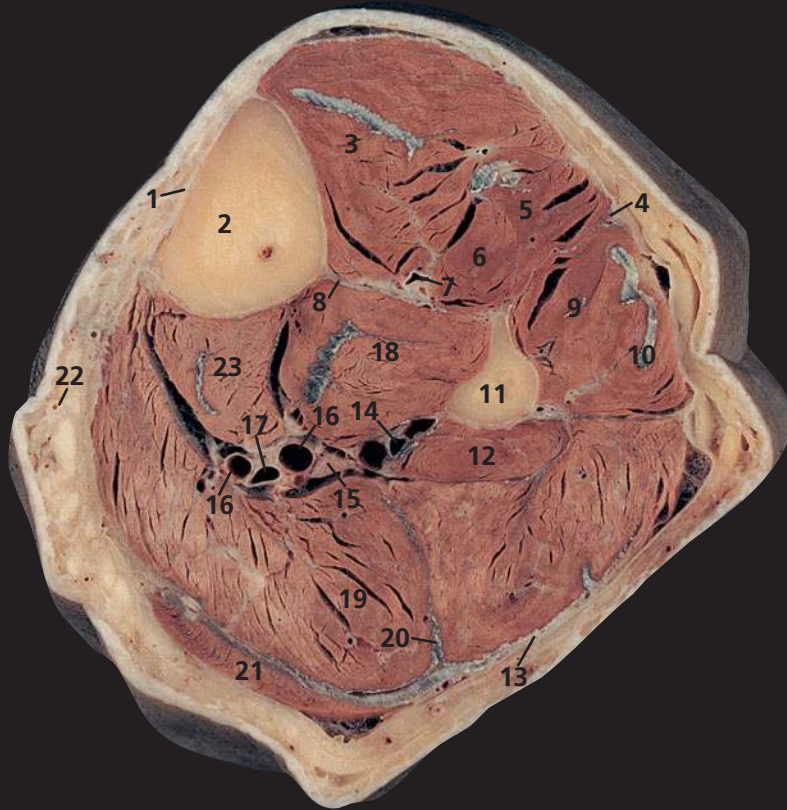
This section traverses the proximal end of the tibial shaft (2) and the shaft of the fibula (10) immediately distal to the neck of the fibula.

At this level, the common fibular (peroneal) nerve, which sweeps around the neck of the fibula deep to fibularis (peroneus) longus (8), has divided into its superficial fibular (peroneal) (9) and deep fibular (peroneal) (7) branches. The superficial fibular (peroneal) nerve lies deep to fibularis (peroneus) longus. The deep fibular (peroneal) nerve passes obliquely forwards, deep to extensor digitorum longus (5), to descend with the anterior tibial vessels (7).

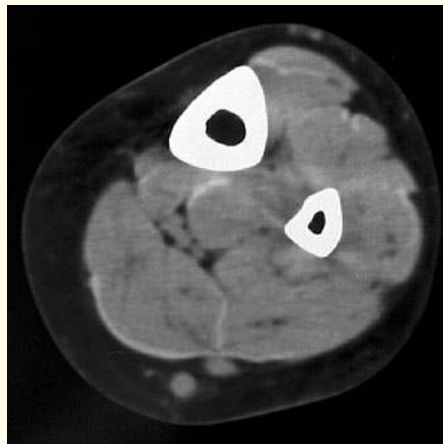
The tendon of plantaris (17) lies in a well-defined tissue plane between soleus (18) and gastrocnemius (12, 15). Fluid enters this plane following rupture of a semimembranosus bursa (Baker's cyst).

Section level

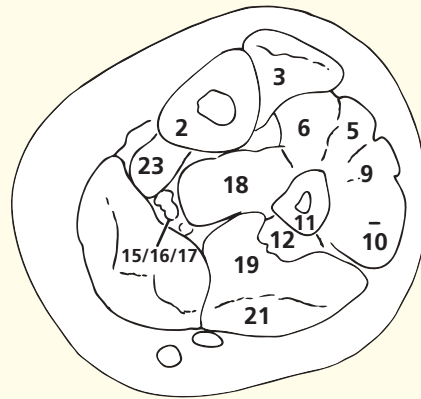




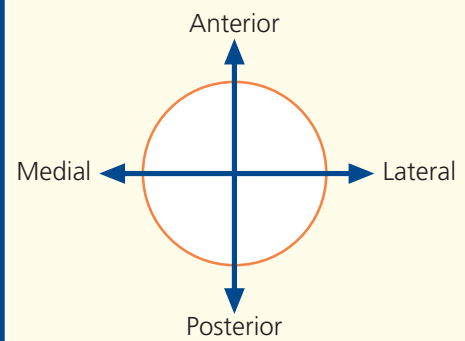
- | | |
|-----------------------------------------------------------------------|-----------------------------------------------------|
| 1 Subcutaneous border of tibia | 12 Flexor hallucis longus |
| 2 Tibia | 13 Deep fascia of calf |
| 3 Tibialis anterior | 14 Fibular (peroneal) artery, with venae comitantes |
| 4 Superficial fibular (peroneal) nerve | 15 Tibial nerve |
| 5 Extensor digitorum longus | 16 Venae comitantes of posterior tibial artery |
| 6 Extensor hallucis longus | 17 Posterior tibial artery |
| 7 Anterior tibial artery and vein, with deep fibular (peroneal) nerve | 18 Tibialis posterior |
| 8 Interosseous membrane | 19 Soleus |
| 9 Fibularis (peroneus) brevis | 20 Plantaris tendon |
| 10 Fibularis (peroneus) longus | 21 Gastrocnemius |
| 11 Fibula | 22 Great saphenous vein |
| | 23 Flexor digitorum longus |



Axial computed tomogram (CT)



Orientation



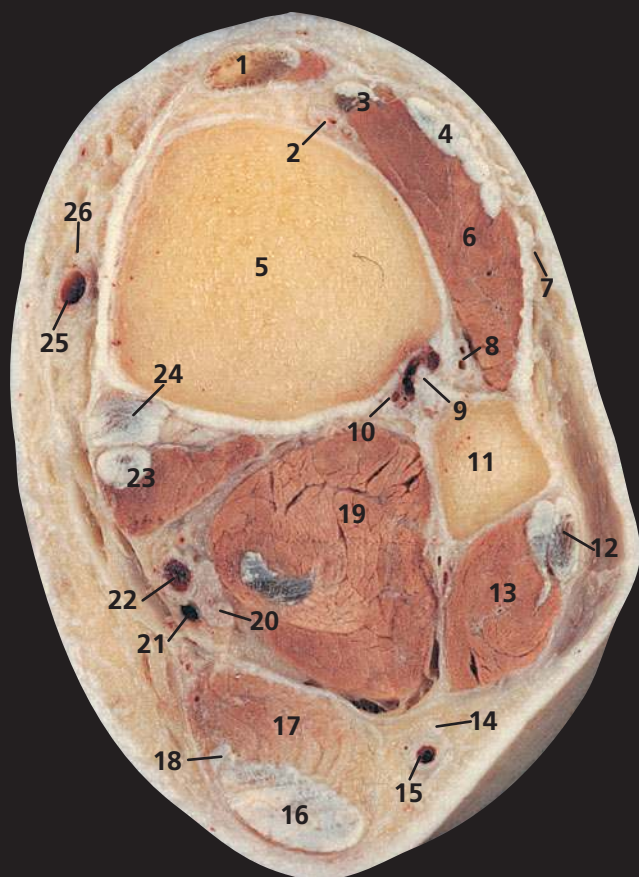
Section level



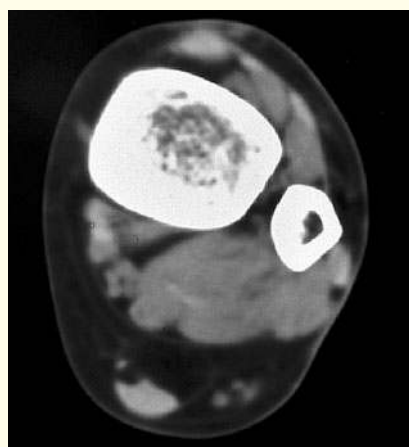
Notes

This section traverses the mid-calf. Note that the whole of the anteromedial aspect of the shaft of the tibia (1) is subcutaneous, covered only by skin, superficial fascia and periosteum, and crossed, in its lower part, only by the great saphenous vein (22) and saphenous nerve.

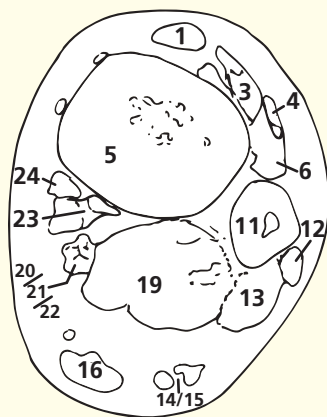
The neurovascular bundle of the anterior tibial vessels and deep fibular (peroneal) nerve (7), having descended first between extensor digitorum longus (5) and tibialis anterior (3), now runs between the latter and extensor hallucis longus (6), as this takes origin from the anterior aspect of the fibular shaft (11).



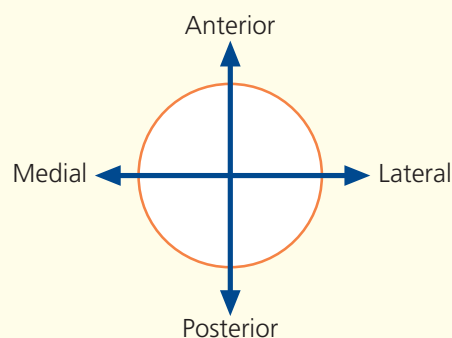
- | | |
|-----------------------------------------------------------------------------------|---------------------------------------|
| 1 Tibialis anterior tendon | 11 Fibula |
| 2 Anterior tibial artery, with venae comitantes and deep fibular (peroneal) nerve | 12 Fibularis (peroneus) longus tendon |
| 3 Extensor hallucis longus and tendon | 13 Fibularis (peroneus) brevis |
| 4 Extensor digitorum longus tendon | 14 Sural nerve |
| 5 Tibia | 15 Small saphenous vein |
| 6 Fibularis (peroneus) tertius | 16 Tendo calcaneus (Achilles tendon) |
| 7 Superficial fibular (peroneal) nerve | 17 Soleus |
| 8 Perforating branch of fibular (peroneal) artery | 18 Plantaris tendon |
| 9 Inferior tibiofibular joint (interosseous ligament) | 19 Flexor hallucis longus |
| 10 Fibular (peroneal) artery | 20 Tibial nerve |
| | 21 Posterior tibial vein |
| | 22 Posterior tibial artery |
| | 23 Flexor digitorum longus and tendon |
| | 24 Tibialis posterior tendon |
| | 25 Great saphenous vein |
| | 26 Saphenous nerve |



Axial computed tomogram (CT)



Orientation



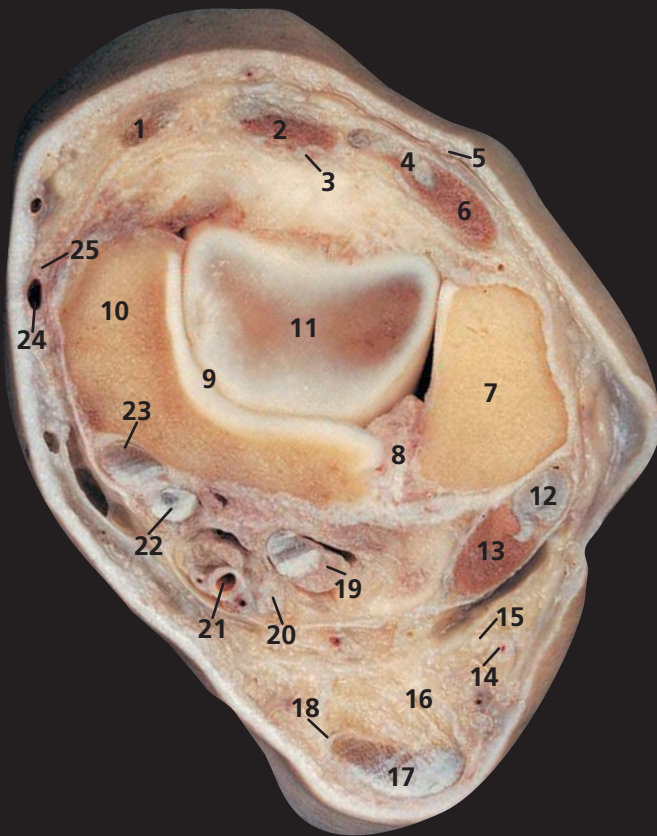
Section level



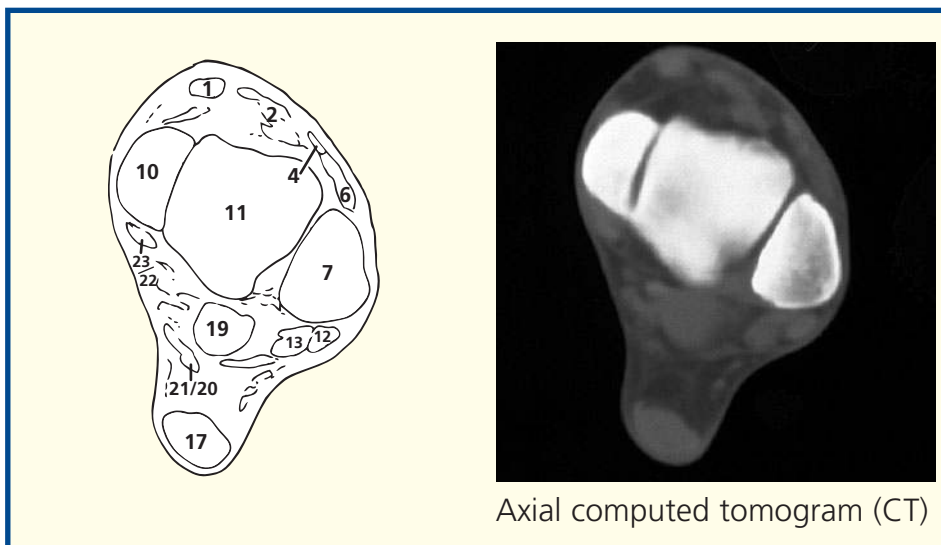
Notes

This section passes immediately above the ankle joint at the level of the inferior tibiofibular joint (9). This is the only fibrous joint, apart from the skull sutures, and represents the thickened distal extremity of the interosseous membrane. (See also Axial section 2.)

At this level, gastrocnemius has already become tendinous (16), although soleus (17) still displays muscle fibres. A little more distally, this too will become tendinous and fuse into the tendo calcaneus (tendo Achilles tendon).

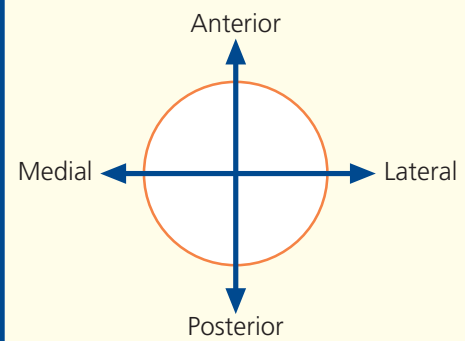


- | | |
|-----------------------------------------------------------------------------------|---------------------------------------------------|
| 1 Tibialis anterior tendon | 13 Fibularis (peroneus) longus |
| 2 Extensor hallucis longus and tendon | 14 Small saphenous vein |
| 3 Anterior tibial artery and venae comitantes, with deep fibular (peroneal) nerve | 15 Sural nerve |
| 4 Extensor digitorum tendon | 16 Fat |
| 5 Superficial fibular (peroneal) nerve | 17 Tendo calcaneus |
| 6 Fibularis (peroneus) tertius and tendon | 18 Plantaris tendon |
| 7 Lateral malleolus | 19 Flexor hallucis longus tendon |
| 8 Inferior tibiofibular joint | 20 Tibial nerve |
| 9 Ankle joint | 21 Posterior tibial artery, with venae comitantes |
| 10 Medial malleolus | 22 Flexor digitorum longus tendon |
| 11 Talus | 23 Tibialis posterior tendon |
| 12 Fibularis (peroneus) brevis tendon | 24 Great saphenous vein |
| | 25 Saphenous nerve |



Axial computed tomogram (CT)

Orientation



Section level

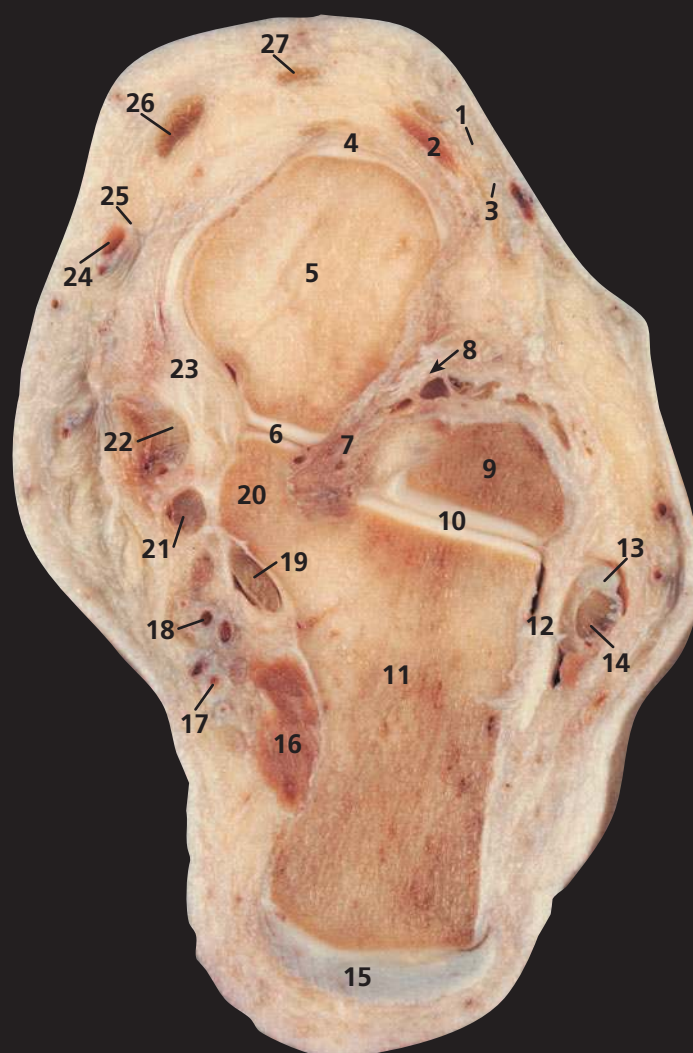


Notes

This section passes through the ankle joint (9) and the inferior tibiofibular joint (8). Note that this section illustrates the fibrous nature of the inferior tibiofibular joint.

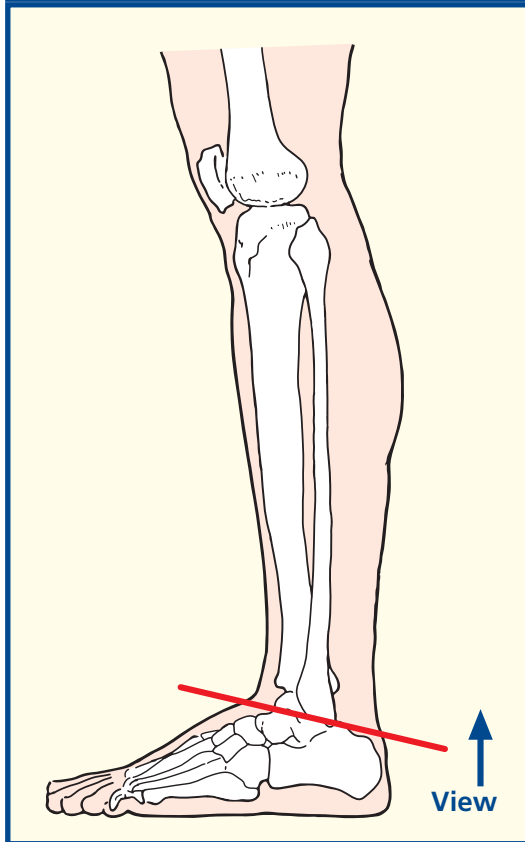
Fibularis (peroneus) brevis (12) and fibularis (peroneus) longus (13) pass behind the lateral malleolus (7) of the fibula and will groove the bone a little more distally to form the malleolar fossa.

This section demonstrates the order of structures that pass behind the medial malleolus (10). These are, from the medial to the lateral side, the tendon of tibialis posterior (23), the tendon of flexor digitorum longus (22), the posterior tibial artery with its venae comitantes (21), the tibial nerve (20) and, most laterally, the tendon of flexor hallucis longus (19).

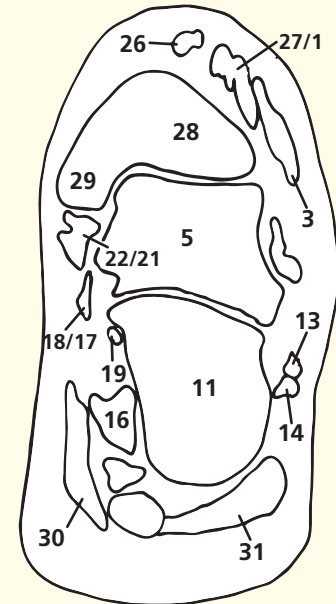


- | | |
|-------------------------------------------------------------|-----------------------------------------|
| 1 Extensor digitorum longus tendon | 17 Lateral plantar neurovascular bundle |
| 2 Extensor digitorum brevis | 18 Medial plantar neurovascular bundle |
| 3 Fibularis (peroneus) tertius tendon | 19 Flexor hallucis longus tendon |
| 4 Talocalcaneonavicular joint (anterior talonavicular part) | 20 Sustentaculum tali |
| 5 Head of talus | 21 Flexor digitorum longus tendon |
| 6 Talocalcaneonavicular joint (posterior part) | 22 Tibialis posterior tendon |
| 7 Interosseous talocalcanean ligament | 23 Deltoid ligament of ankle |
| 8 Sulcus tali (arrowed) | 24 Great saphenous vein |
| 9 Lateral process of talus | 25 Saphenous nerve |
| 10 Talocalcanean (subtalar) joint | 26 Tibialis anterior tendon |
| 11 Calcaneus | 27 Extensor hallucis longus tendon |
| 12 Capsule of talocalcanean joint | 28 Tibia |
| 13 Fibularis (peroneus) brevis tendon | 29 Medial malleolus |
| 14 Fibularis (peroneus) longus tendon | 30 Abductor hallucis |
| 15 Tendo Achilles | 31 Abductor digiti minimi |
| 16 Quadratus plantae (flexor accessorius) | |

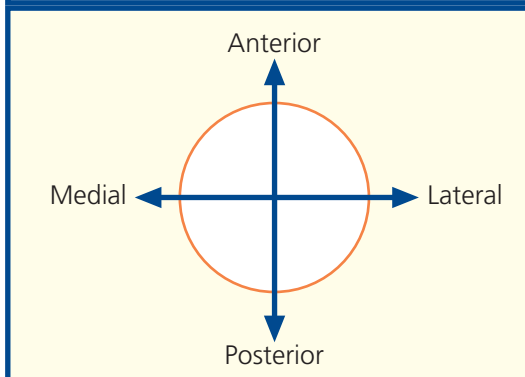
Section level



Axial computed tomogram (CT)



Orientation



Notes

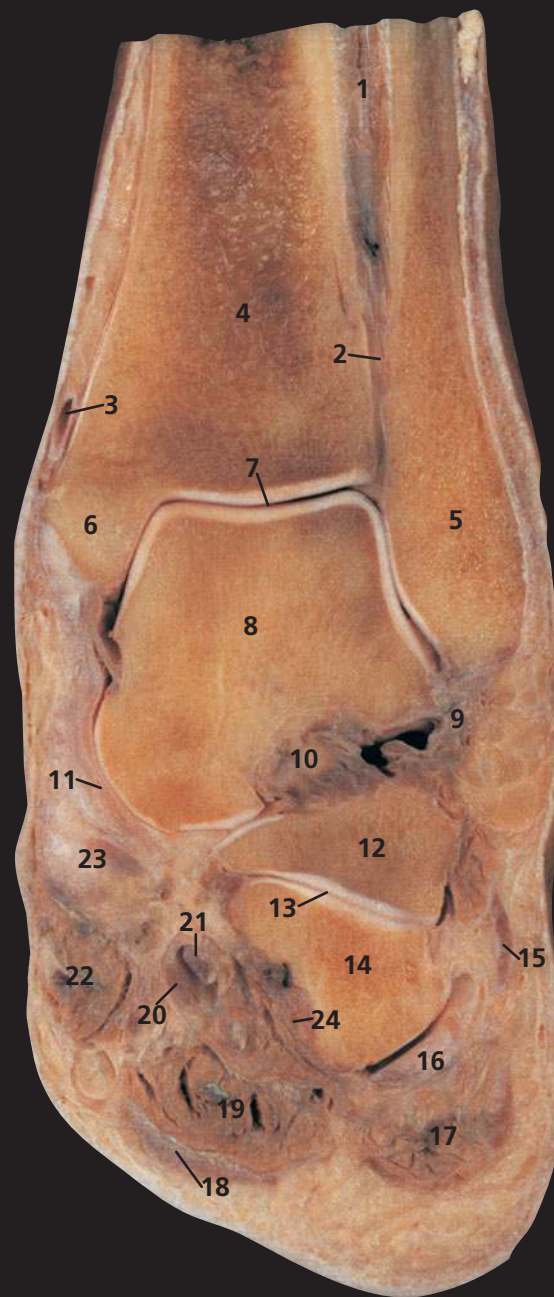
This section passes through the head (5) and lateral process (9) of the talus and the calcaneus (11). The CT image is in a more coronal plane, and hence the tibia (28) is seen with its articulation with the talus (5).

The tendon of flexor hallucis longus (19) passes behind the sustentaculum tali (20) and, more distally, grooves its inferior aspect. The sulcus tali (8), with its corresponding sulcus calcanei, forms the sinus tarsi and contains the strong interosseous talocalcaneal ligament.

The talocalcaneal joint (10), also termed the subtalar joint, lies between the convex posterior facet on the inferior surface of the talus and the

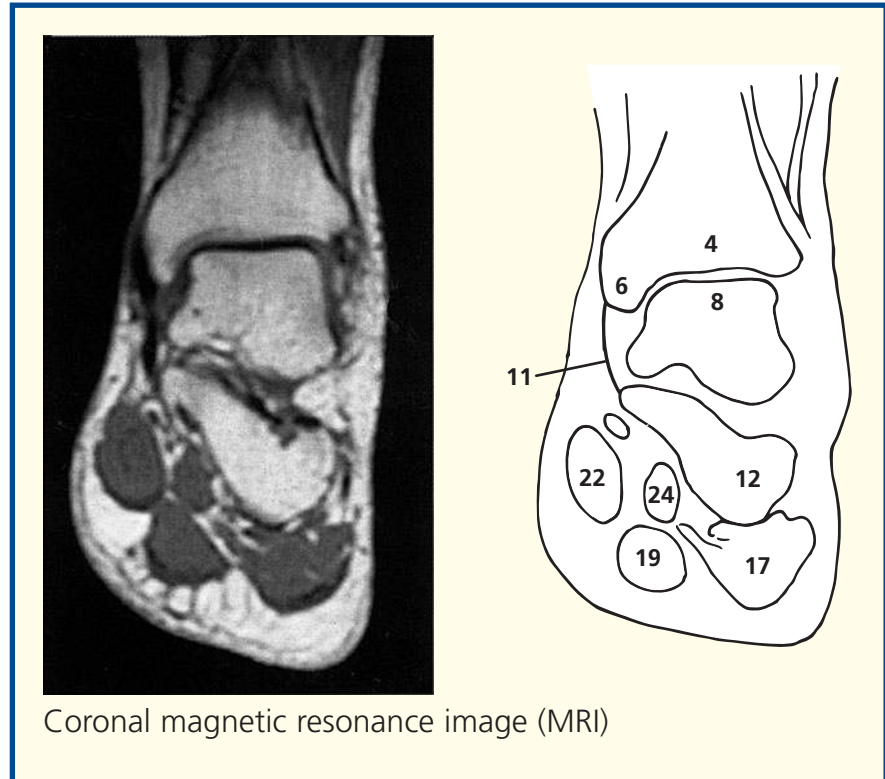
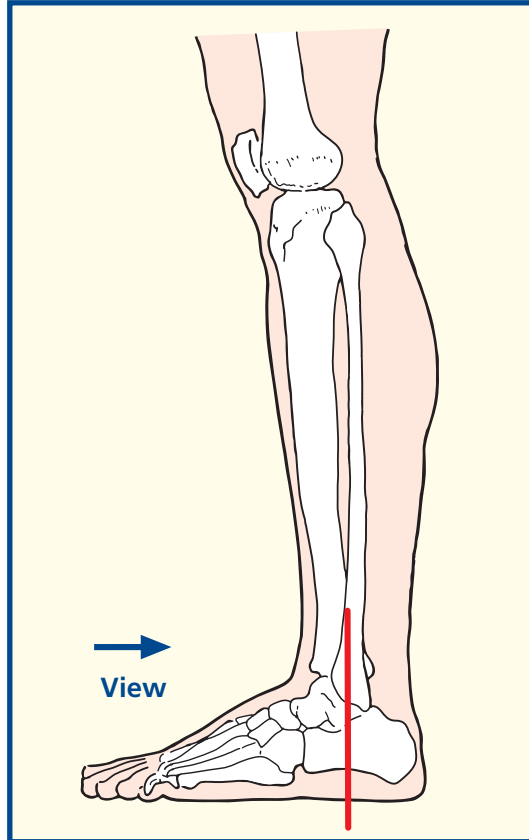
concave posterior facet on the inferior surface of the talus. The talocalcaneonavicular joint is complex. It is formed by the rounded head of the talus (5), which fits into the concavity on the posterior aspect of the navicular, the upper surface of the plantar calcaneonavicular ligament (the spring ligament), which runs between the sustentaculum tali and the inferior aspect of the navicular, and the anterior and middle facets for the talus on the calcaneus. The anterior (4) and posterior (6) portions of this joint are shown.

A considerable degree of inversion and eversion of the foot takes place at the talocalcaneal and talocalcaneonavicular joints.



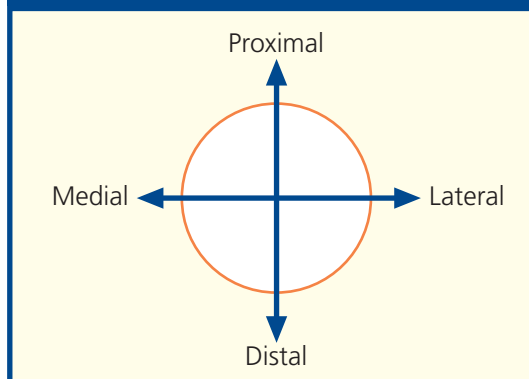
- | | |
|--------------------------------------------------|-------------------------------------------|
| 1 Tibialis posterior | 14 Cuboid |
| 2 Inferior tibiofibular joint | 15 Tendon of fibularis (peroneus) brevis |
| 3 Small saphenous vein | 16 Tendon of fibularis (peroneus) longus |
| 4 Tibia | 17 Abductor digiti minimi |
| 5 Lateral malleolus of fibula | 18 Plantar aponeurosis |
| 6 Medial malleolus of tibia | 19 Flexor digitorum brevis |
| 7 Ankle joint | 20 Tendon of flexor digitorum longus |
| 8 Body of talus (talar dome) | 21 Tendon of flexor hallucis longus |
| 9 Lateral collateral ligament of ankle | 22 Abductor hallucis |
| 10 Talocalcaneal interosseous ligament | 23 Tendon of tibialis posterior |
| 11 Deltoid ligament (medial collateral ligament) | 24 Quadratus plantae (flexor accessories) |
| 12 Body of calcaneus | |
| 13 Calcaneocuboid joint | |

Section level



Coronal magnetic resonance image (MRI)

Orientation



Notes

By convention, the articulation between the lower end of the fibula and the tibia is described as the inferior tibiofibular joint (**2**) and is stated to be the only fibrous joint apart from those pertaining to the skull. In effect, this 'joint' represents the considerable thickening of the lowermost part of the interosseous membrane between the shafts of these two bones.

The mortice joint of the ankle (**7**) is demonstrated well. The lateral collateral ligament (**9**), especially its anterior talofibular component, is commonly injured.

The plantar aponeurosis (**18**) is thick and tough. It adheres closely to flexor digitorum brevis (**19**).

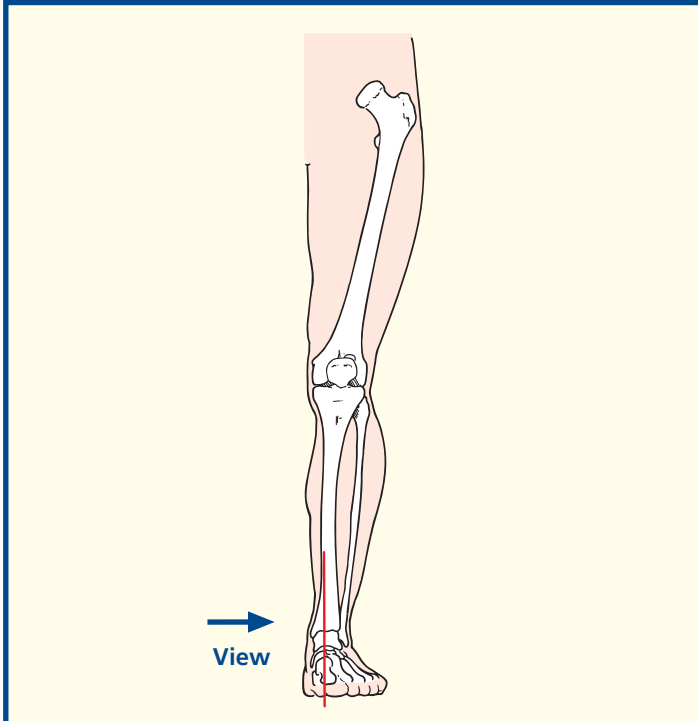
The hyaline cartilage and subchondral bone of the talar dome (**8**) is commonly damaged by relatively minor trauma. Loose fragments may break off and cause symptoms. Cystic degenerative change may follow in later life.

In spite of the fact that the talocalcaneal ligament (**10**) is thick and powerful, the major part of the movements of inversion and eversion of the foot take place at this joint.



- | | | |
|--------------------------------------------------------------------------------------|------------------------------------------------------------|------------------------------------------------|
| 1 Gastrocnemius | 13 Interosseous talocalcanean ligament | 26 Abductor hallucis |
| 2 Soleus | 14 Head of talus | 27 Plantar aponeurosis |
| 3 Flexor digitorum longus | 15 Sustentaculum tali | 28 Dense subcutaneous fibrofatty tissue |
| 4 Tibia | 16 Navicular | 29 Abductor digiti minimi |
| 5 Tendon of flexor hallucis longus (posterior relation to ankle joint – see also 25) | 17 Medial cuneiform | 30 Lateral plantar artery, vein and nerve |
| 6 Tendo calcaneus (Achilles tendon) | 18 First metatarsal bone | 31 Quadratus plantae (flexor accessories) |
| 7 Fat deep to tendo calcaneus | 19 Tributary of great saphenous vein | 32 Medial process of tuberosity of calcaneus |
| 8 Bursa deep to tendo calcaneus | 20 Extensor hallucis longus | 33 Calcaneus |
| 9 Medial tubercle of posterior process of talus | 21 Proximal phalanx of hallux | 34 Plantar calcaneonavicular (spring) ligament |
| 10 Ankle joint | 22 Distal phalanx of hallux | 35 Tendon of tibialis posterior |
| 11 Body of talus | 23 Nail bed | |
| 12 Tendon of tibialis anterior | 24 Sesamoid bone | |
| | 25 Tendon of flexor hallucis longus (in foot – see also 5) | |

Section level

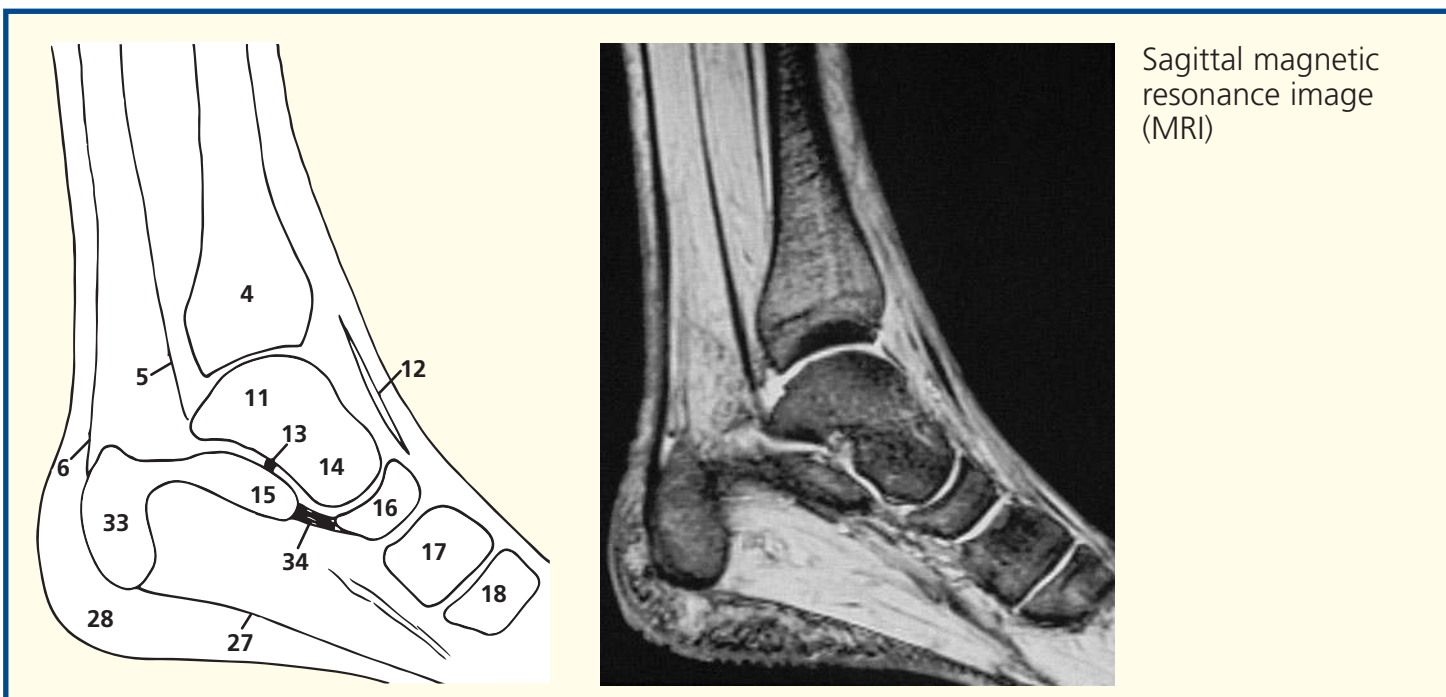
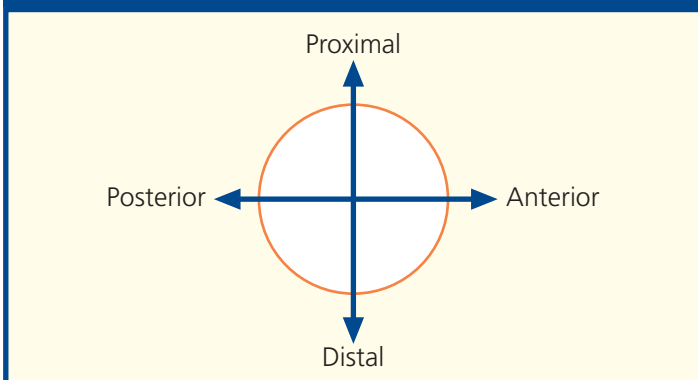


Notes

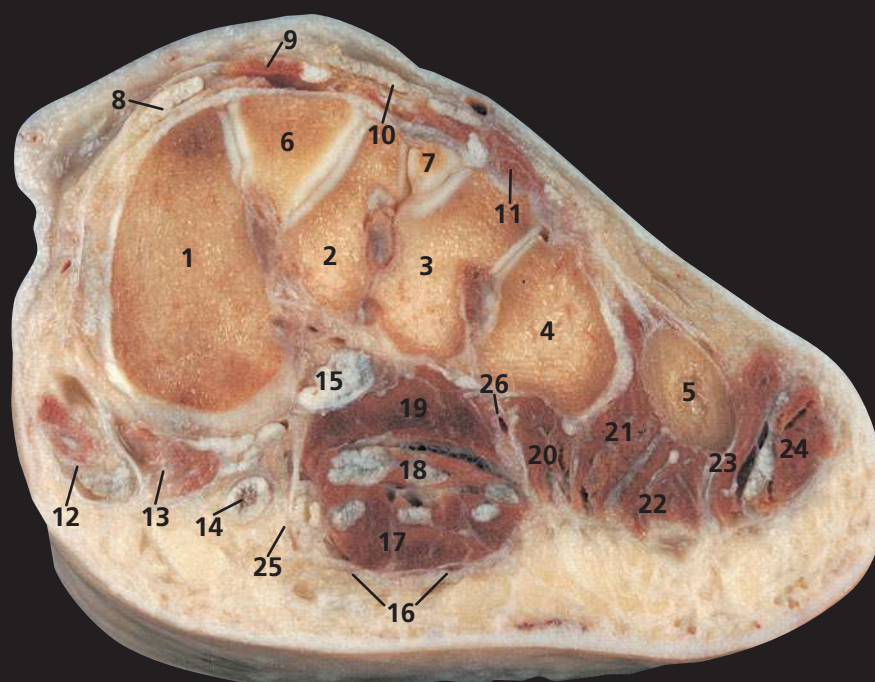
Flexor hallucis longus (5) is the immediate posterior relation of the ankle joint. It grooves the posterior aspect of the lower extremity of the tibia (4); then, distal to the capsule of the ankle joint (10), it grooves the posterior process of the talus between its medial (9) and lateral tubercle. The tendon (25) grooves a third bone as it passes beneath the sustentaculum tali of the calcaneus (15). Surprisingly, the flexor hallucis longus at this point is lateral to the flexor digitorum longus; they cross on the foot.

This section shows clearly the role of the plantar calcaneonavicular (or spring) ligament (34) as this passes from the sustentaculum tali (15) to the navicular (16). It supports the head of the talus (14). In standing, the weight of the body is borne on the medial (32) and lateral processes of the posterior tuberosity of the calcaneus behind, and on the heads of the metatarsals anteriorly. That of the first metatarsal, the hallux, bears two sesamoid bones (24), each within a tendon of flexor hallucis brevis. This section demonstrates well the dense subcutaneous fibrofatty tissue (28), which is developed particularly well over these two areas of contact of the foot with the ground on standing.

Orientation

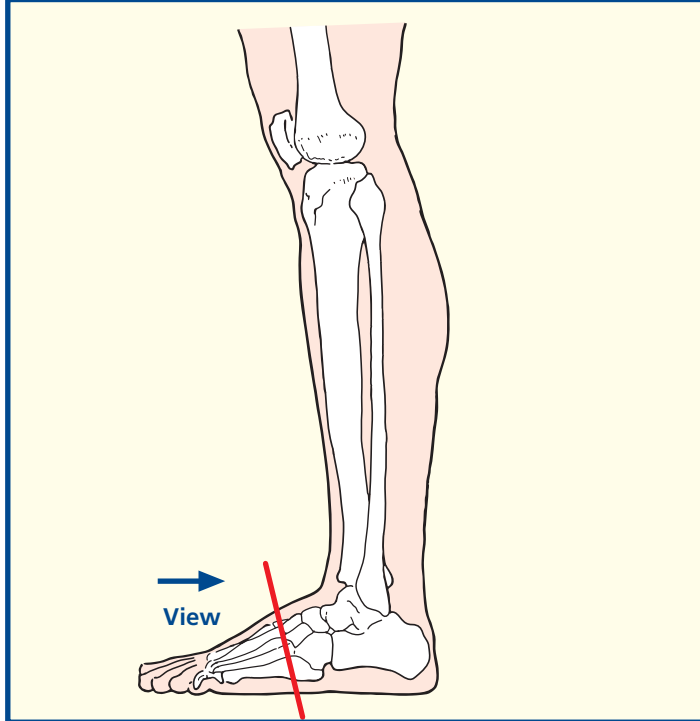


Sagittal magnetic resonance image (MRI)

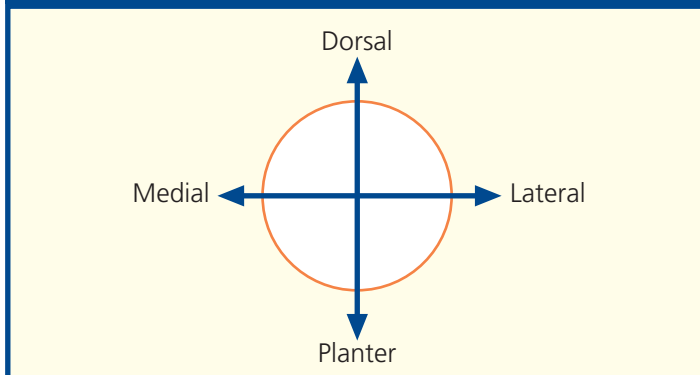


- | | |
|-------------------------------------|---------------------------------------|
| 1 First metatarsal | 15 Fibularis (peroneus) longus tendon |
| 2 Second metatarsal | 16 Plantar aponeurosis |
| 3 Third metatarsal | 17 Flexor digitorum brevis |
| 4 Fourth metatarsal | 18 Flexor digitorum longus tendon |
| 5 Fifth metatarsal | 19 Adductor hallucis (oblique head) |
| 6 Medial cuneiform | 20 Second plantar interosseous |
| 7 Fragment of lateral cuneiform | 21 Third plantar interosseous |
| 8 Extensor hallucis longus tendon | 22 Flexor digiti minimi |
| 9 Extensor hallucis brevis | 23 Opponens digiti minimi |
| 10 Extensor digitorum longus tendon | 24 Abductor digiti minimi |
| 11 Extensor digitorum brevis | 25 Medial plantar artery and nerve |
| 12 Abductor hallucis | 26 Lateral plantar artery and nerve |
| 13 Flexor hallucis brevis | |
| 14 Flexor hallucis longus tendon | |

Section level



Orientation

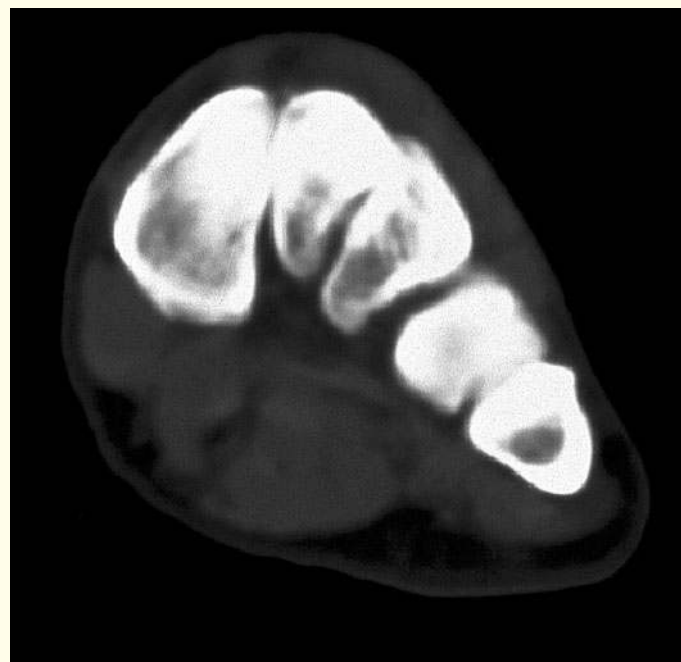
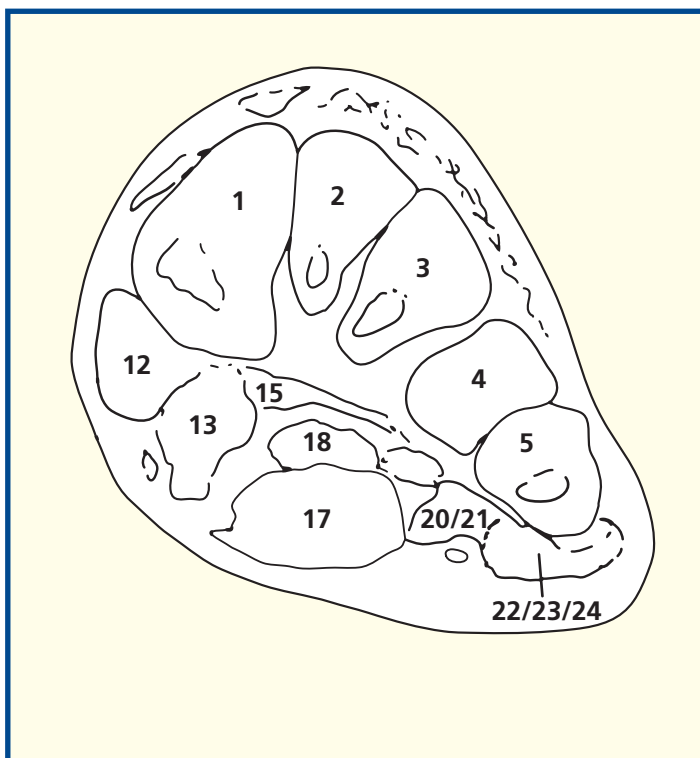


Notes

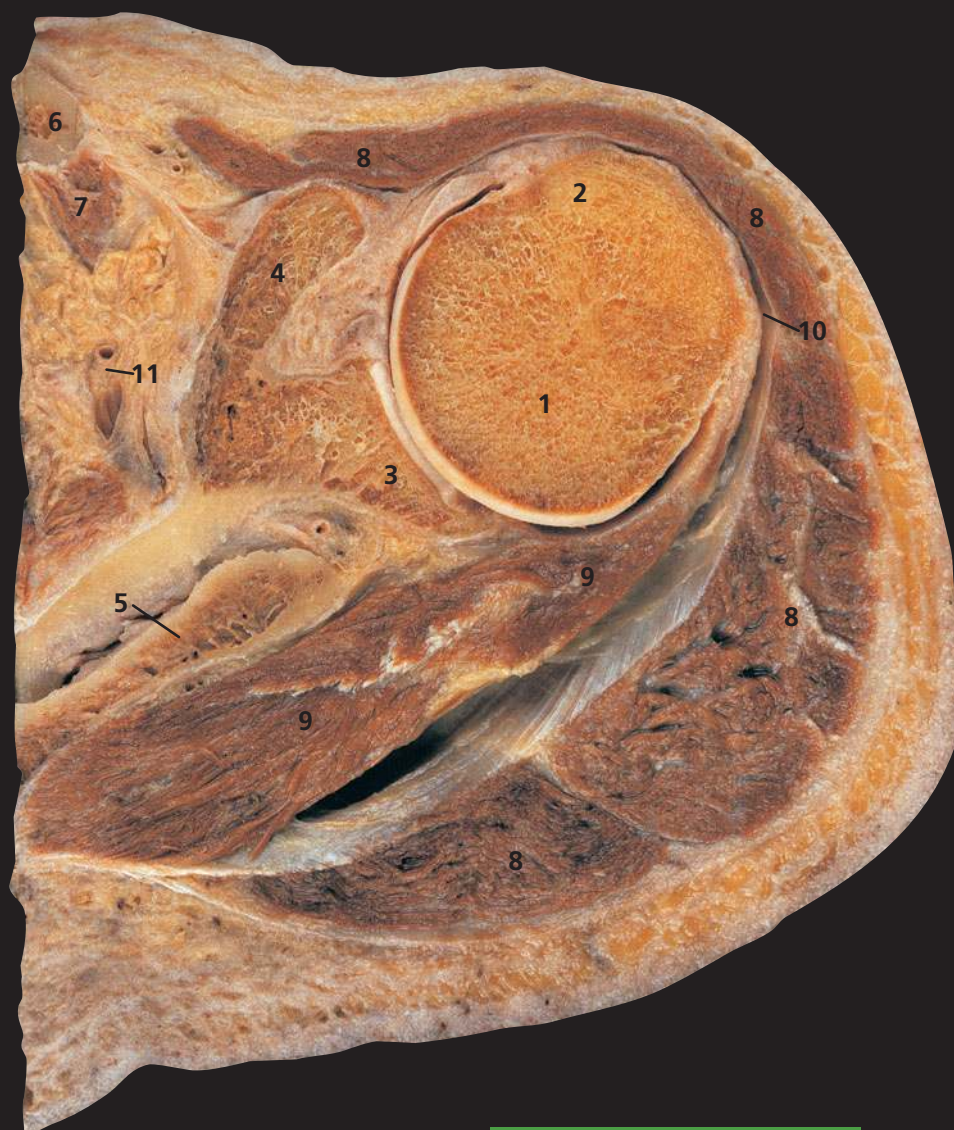
This section of the lower limb passes through the forefoot and the bases of the metatarsal bones. It demonstrates the appearance of the transverse arch of the foot.

The tendon of fibularis (peroneus) longus (**15**), having grooved the inferior aspect of the cuboid, passes forward and medially to insert into the inferolateral aspect of the medial cuneiform (**6**) and the base of the first metatarsal (**1**). The sling-like action of this tendon helps maintain the transverse arch.

The medial plantar nerve (**25**) has a cutaneous distribution that closely resembles that of the median nerve of the hand – that is, the medial two-thirds of the sole of the foot and plantar aspects of the medial three and a half toes. Similarly, the lateral plantar nerve supplies the lateral third of the skin of the sole and the plantar aspects of the later one and a half toes, similar to the distribution of the ulnar nerve to the palm of the hand and fingers.

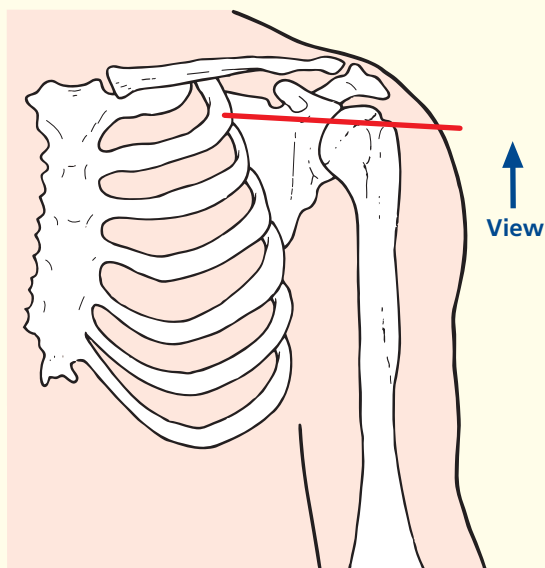


Coronal computed tomogram (CT)

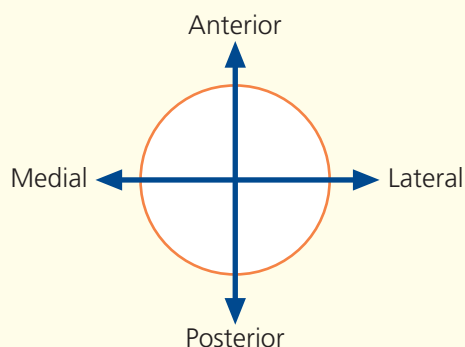


- | | |
|----------------------------------|----------------------------------------------------------------------------|
| 1 Head of humerus | 12 Labrum of glenoid |
| 2 Greater tubercle of humerus | 13 Subscapularis tendon |
| 3 Glenoid fossa of scapula | 14 Middle glenohumeral ligament |
| 4 Coracoid process of scapula | 15 Long head of biceps tendon in bicipital groove (intertubercular groove) |
| 5 Spine of scapula | 16 Attachment of coraco-acromial and coraco-humeral ligaments |
| 6 Clavicle | 17 Lesser tubercle of humerus |
| 7 Subclavius | 18 Transverse humeral ligament |
| 8 Deltoid | |
| 9 Infraspinatus | |
| 10 Subdeltoid bursa | |
| 11 Suprascapular artery and vein | |

Section level



Orientation



Notes

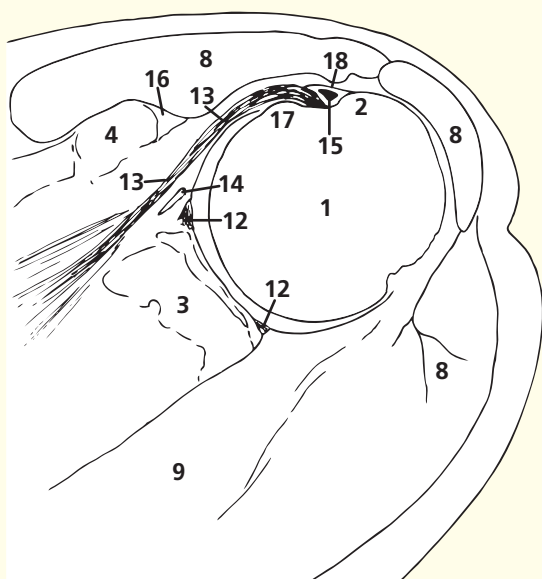
The greater tubercle of the humerus (2) is the most lateral bony landmark around the shoulder. The subacromial bursa passes below the acromion and above supraspinatus to continue into the subdeltoid bursa (10) between the upper shaft of the humerus and the deltoid muscle (8).

Infraspinatus (9), together with supraspinatus, teres minor and subscapularis, forms a protective rotator cuff around the shoulder joint, which, as can be seen in this section, has little stability afforded by either its bony configuration or its capsular strength.

The shallow glenoid is in sharp contrast to the deep acetabulum in the hip; stability has been sacrificed for mobility in order to allow a greater range of movement.

The orientation and shape of the coracoid process is an important feature; the coraco-acromial ligament can impinge on the rotator cuff.

The tendon of subscapularis attaches mainly to the lesser tubercle, but some slips attach to the floor of the intertubercular sulcus. Furthermore, the transverse humeral ligament, which retains the long head of biceps tendon, could be regarded as fibres from the subscapular's attachment on the lesser tubercle extending on towards the greater tubercle.

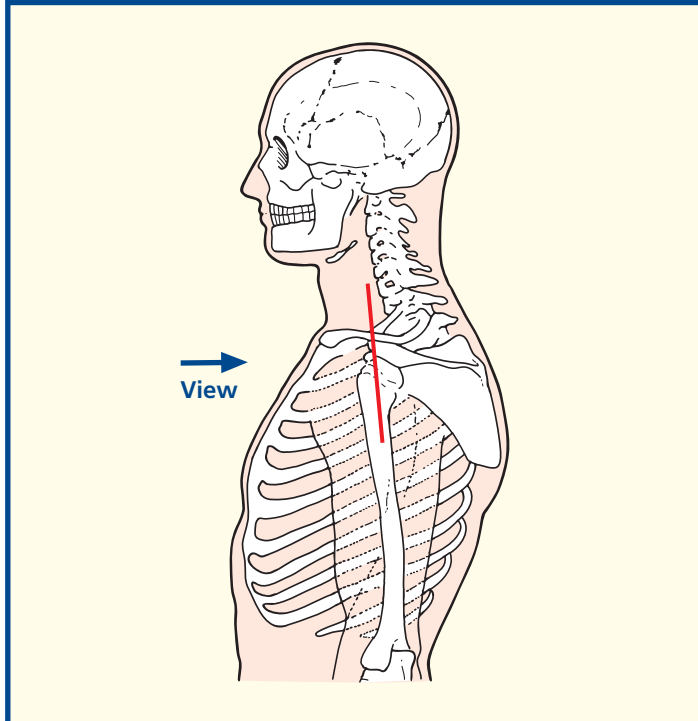


Axial magnetic resonance image (MRI)

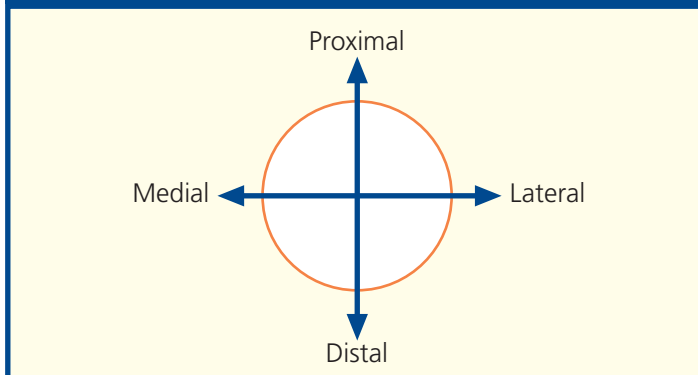


- | | |
|-------------------------------------------------------------------------------|-------------------------------|
| 1 Clavicle | 13 Latissimus dorsi |
| 2 Acromioclavicular joint | 14 Brachial artery and vein |
| 3 Acromion of scapula | 15 Nerves of brachial plexus |
| 4 Supraspinatus | 16 Tendon of teres major |
| 5 Glenoid labrum | 17 Teres minor |
| 6 Shoulder joint cavity | 18 Long head of triceps |
| 7 Anatomical neck of humerus | 19 Head of scapula |
| 8 Greater tubercle of humerus | 20 Neck of scapula |
| 9 Deltoid | 21 Glenoid fossa of scapula |
| 10 Axillary nerve accompanied by posterior circumflex humeral artery and vein | 22 Subscapularis |
| 11 Shaft of humerus | 23 Long head of biceps tendon |
| 12 Medial circumflex artery and vein | 24 Surgical neck of humerus |

Section level



Orientation

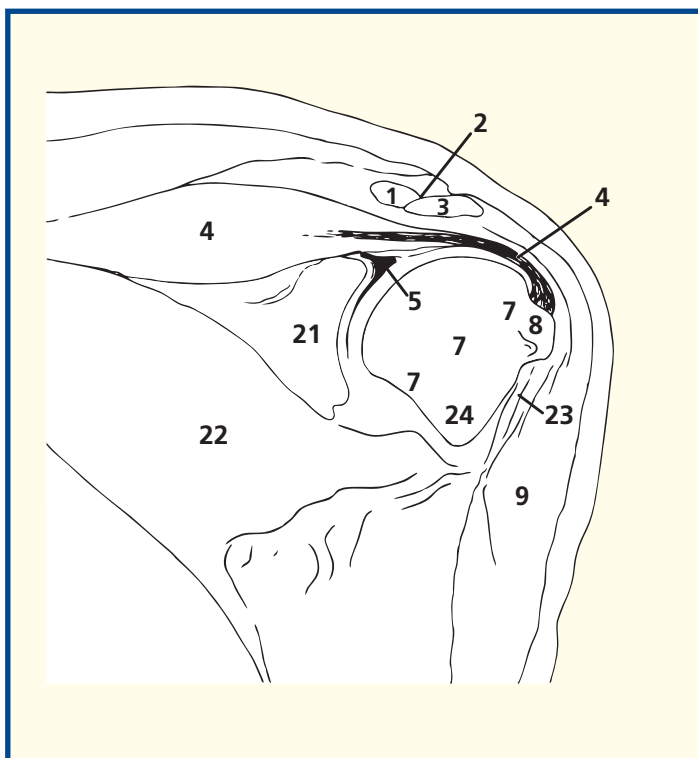


Notes

The important relationship of the supraspinatus tendon (**4**) to the acromion process (**3**) and clavicle (**1**) is demonstrated well. This muscle initiates abduction of the shoulder, which is then continued powerfully by deltoid (**9**). Degenerative changes in the acromioclavicular joint frequently cause impingement on the musculotendinous junction of supraspinatus; tendonitis and a tear in the rotator cuff may follow.

Note the close relationship of the axillary nerve (**10**), together with its accompanying vessels, the posterior circumflex humeral artery and vein, to the surgical neck of the humerus (**24**). Fractures commonly occur in the region of the surgical neck; the axillary nerve may be affected. The axillary nerve may also be damaged in dislocation of the shoulder. The resultant paralysis of the deltoid muscle is demonstrated by the patient being unable to abduct the affected shoulder. There is also characteristic anaesthesia over the lateral aspect of the deltoid.

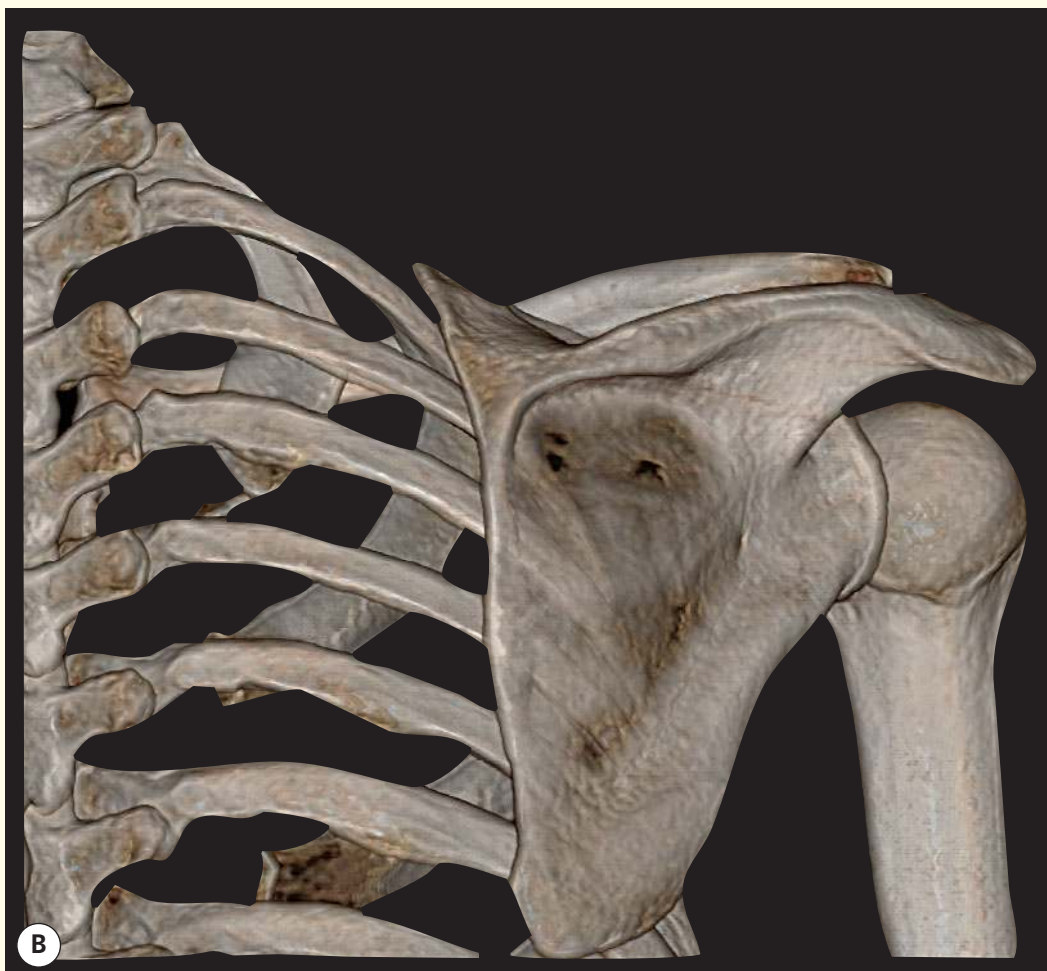
This magnetic resonance image is in a somewhat coronal oblique plane in order to demonstrate the supraspinatus muscle, tendon and insertion as a continuum.



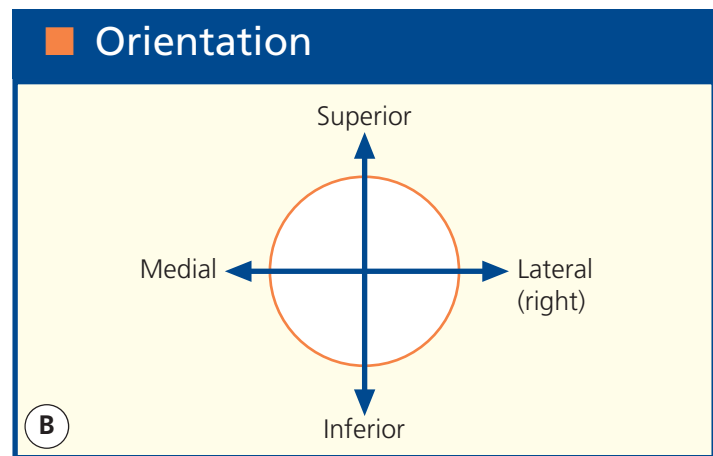
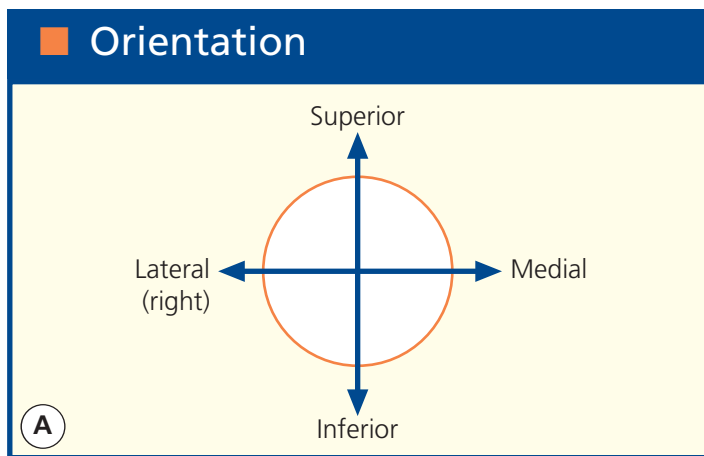
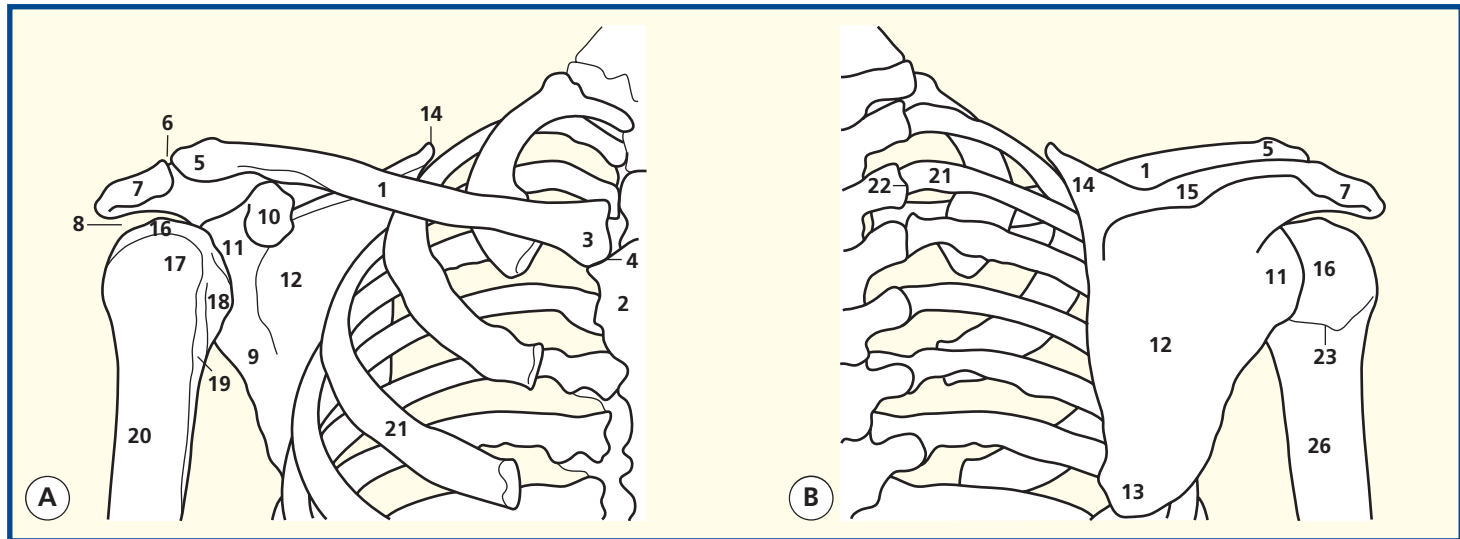
Coronal magnetic resonance image (MRI)



3D computed tomogram (CT)



3D computed tomogram (CT)



- 1 Shaft of clavicle
- 2 Body of sternum
- 3 Sternal end of clavicle
- 4 Sternoclavicular joint
- 5 Acromial end of clavicle
- 6 Acromioclavicular joint
- 7 Subacromial space
- 8 Acromion of scapula
- 9 Lateral border of scapula
- 10 Coracoid process of scapula

- 11 Neck of scapula
- 12 Subscapular fossa of scapula
- 13 Inferior angle of scapula
- 14 Superior angle of scapula
- 15 Spine of scapula
- 16 Head of humerus
- 17 Greater tubercle of humerus
- 18 Lesser tubercle of humerus
- 19 Intertubercular sulcus of humerus

- 20 Shaft (proximal third) of humerus
- 21 Surgical neck of humerus
- 22 Costotransverse joint between third rib and transverse process of third thoracic vertebra
- 23 Third rib
- 24 Infrapinous fossa

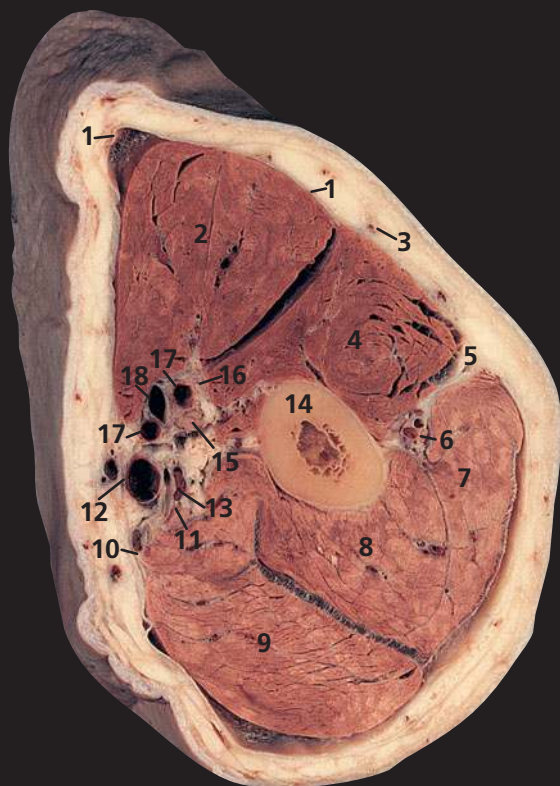
Notes

Surface-shaded three-dimensional volume-rendered CT images. Because bone attenuates the X-ray beam so much, its CT attenuation value (around +1000 HU) is much greater than that of the surrounding soft tissues. Thus, the bones can be 'extracted', with no overlying artefacts, to provide information equivalent to that from a cadaveric skeleton. This subject is holding the upper arm in mild internal rotation, which means that the bicipital groove (the groove for the tendon of the long head of biceps – also known as the intertubercular sulcus) (19) is directed medially rather than anteriorly.

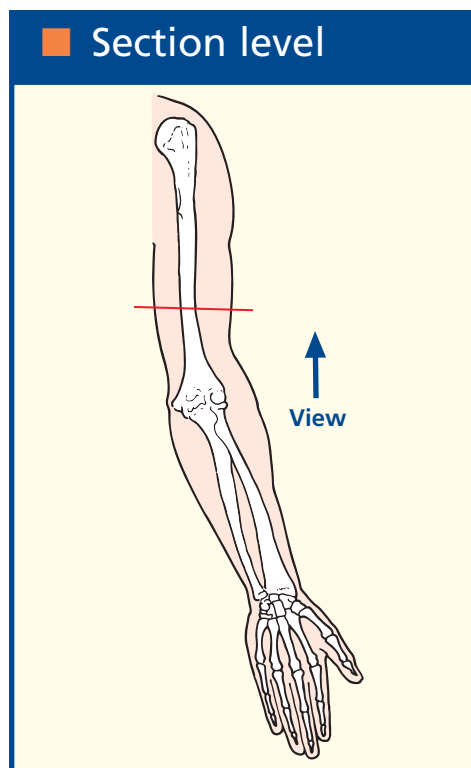
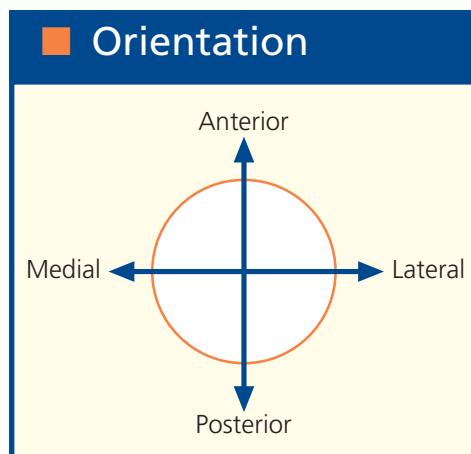
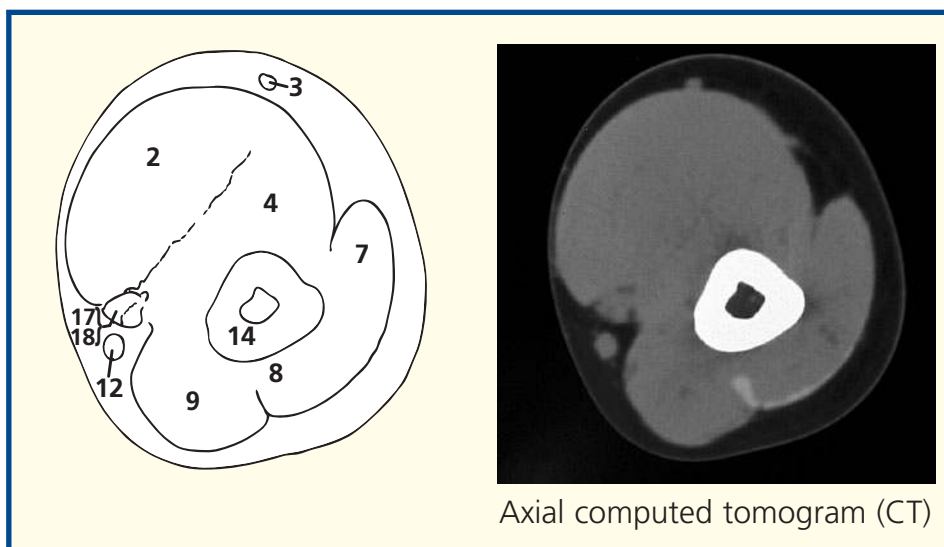
The relationship of the acromioclavicular joint (6) to the humeral head is well appreciated, along with the

important subacromial space (8) (normal in this subject). The rotator cuff tendons (especially supraspinatus) have to pass through this limited space. Mild congenital variations in anatomy and the inevitable degenerative changes in the acromioclavicular joint combine to impinge on this tendon. A high percentage of elderly people have damaged rotator cuffs – one of the design flaws associated with man's evolution to a biped.

Note the thinness of the scapula (12), which is translucent in places. The strength of the scapula lies in the border and processes; the lateral border (9) is especially thick and strong for the attachment of muscles.



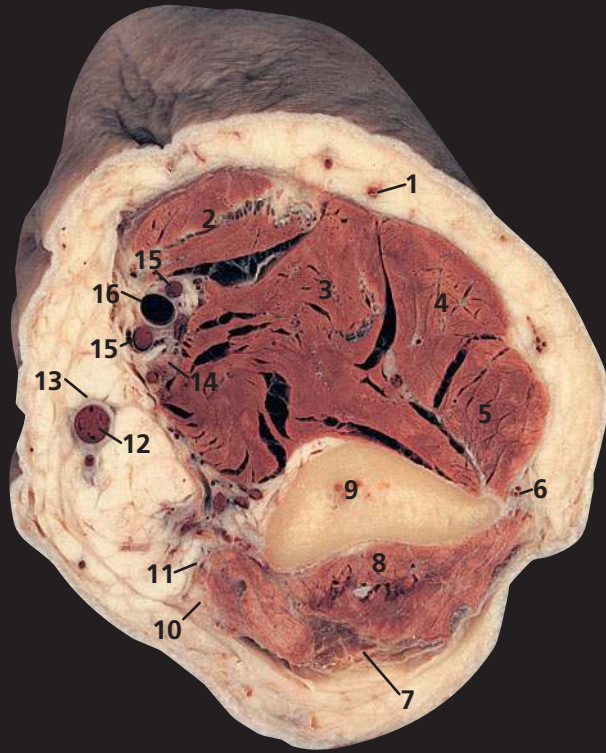
- | | |
|-------------------------------------------------------|----------------------------------------------|
| 1 Deep fascia of arm | 10 Medial intermuscular septum |
| 2 Biceps | 11 Ulnar nerve |
| 3 Cephalic vein | 12 Basilic vein |
| 4 Brachialis | 13 Superior ulnar collateral artery and vein |
| 5 Lateral intermuscular septum | 14 Humerus shaft |
| 6 Radial nerve, with profunda brachii artery and vein | 15 Median nerve |
| 7 Triceps – lateral head | 16 Musculocutaneous nerve |
| 8 Triceps – medial head | 17 Venae comitantes of brachial artery |
| 9 Triceps – long head | 18 Brachial artery |



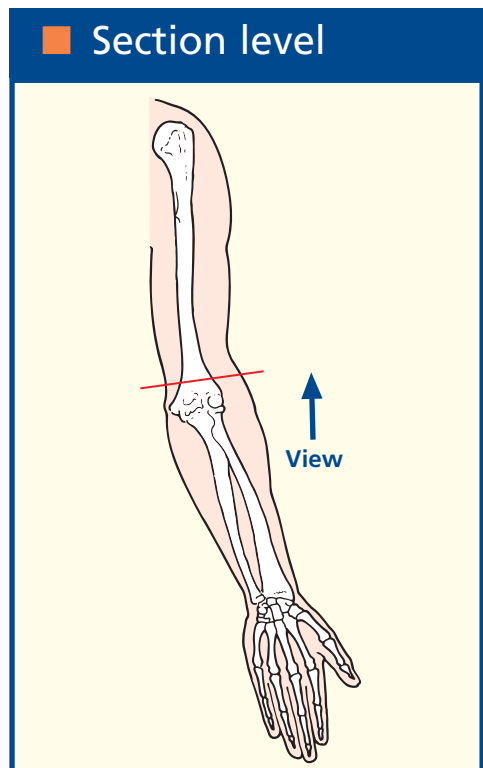
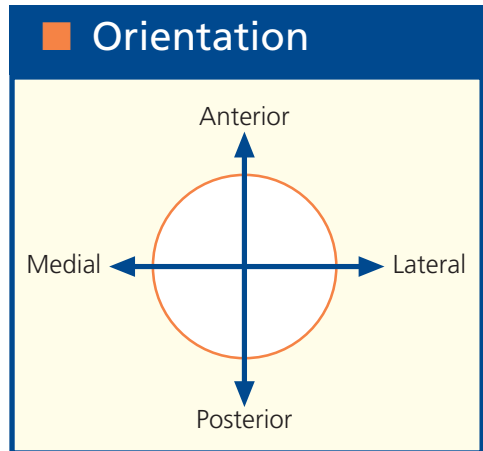
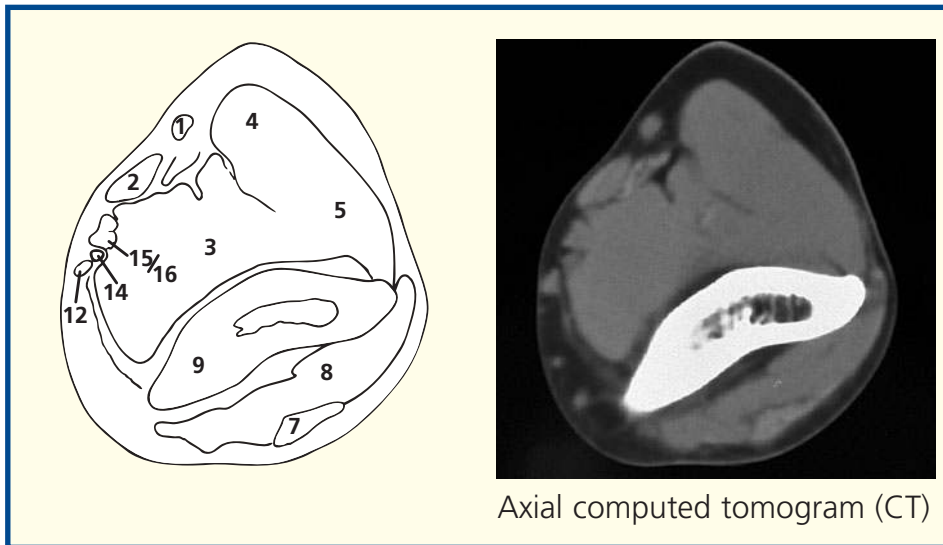
Notes

This section passes through the mid-shaft of the humerus (14). It gives a clear view of the fascial arrangements of the upper arm – the investing sheath of the deep fascia (1), with its lateral (5) and medial (10) intermuscular septa, which attach to the humeral shaft. These septa divide the extensor group of muscles, the triceps (7, 8, 9), from the anterior flexor group. The medial septum is pierced by the ulnar nerve (11) and its accompanying vessels (13); the lateral septum is pierced by the radial nerve with its accompanying profunda brachii artery and vein (6).

The median nerve (15) and brachial artery (18) bear a close relationship to each other in the upper arm, as shown in this section. Superiorly, the nerve lies on the lateral side of the artery. At the mid-humerus level, the artery is crossed superficially (sometimes deeply) by the nerve, which then descends on its medial side.



- | | |
|----------------------------------|----------------------------------------|
| 1 Cephalic vein | 10 Ulnar nerve |
| 2 Biceps | 11 Medial intermuscular septum |
| 3 Brachialis | 12 Basilic vein |
| 4 Brachioradialis | 13 Medial cutaneous nerve of forearm |
| 5 Extensor carpi radialis longus | 14 Median nerve |
| 6 Lateral intermuscular septum | 15 Venae comitantes of brachial artery |
| 7 Triceps tendon | 16 Brachial artery |
| 8 Triceps | |
| 9 Humerus | |

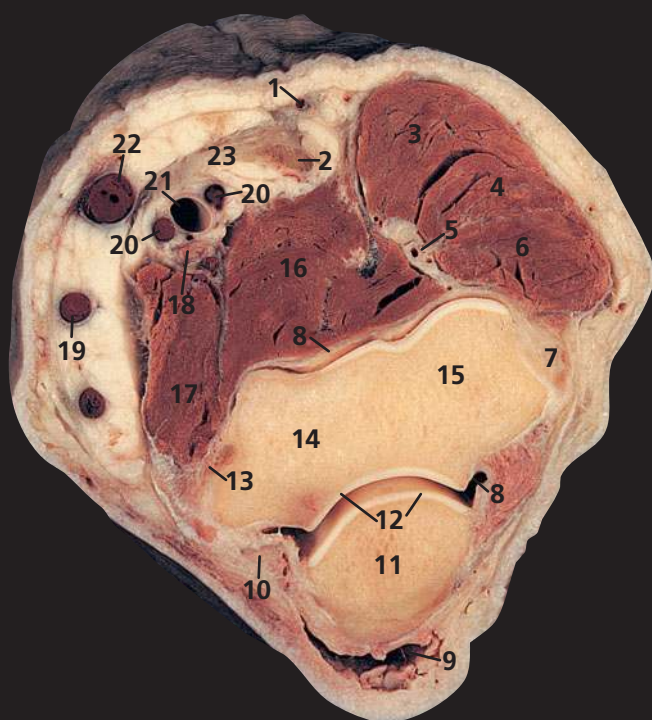


Notes

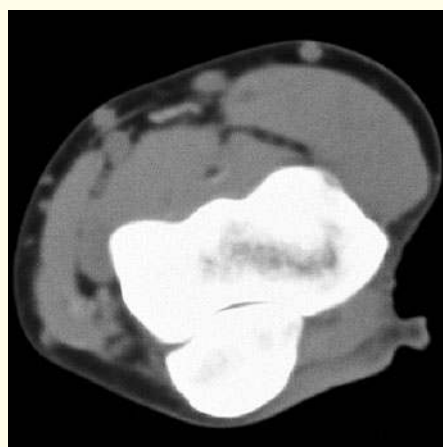
This section transects the lower end of the humeral shaft as it expands to form its medial and lateral supracondylar ridges.

The origin of extensor carpi radialis longus (5) is from the upper part of the lateral ridge, and this muscle arises superior to, and separate from, the remaining extensor muscles of the forearm, which originate from a common origin from the lateral epicondyle of the humerus.

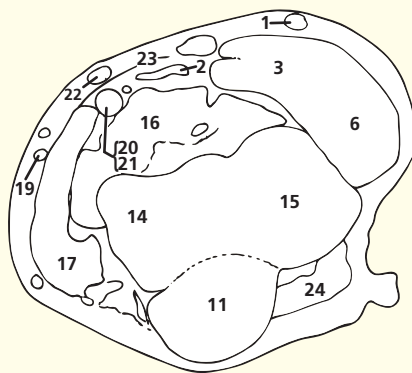
The ulnar nerve (10), just distal to the line of this section, will pass behind the medial epicondyle of the humerus; pressure here will elicit discomfort and often paraesthesia.



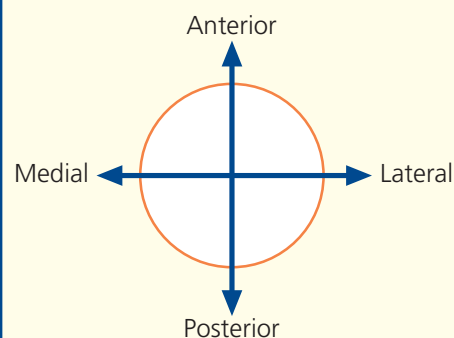
- | | |
|------------------------------------------------------|----------------------------------------|
| 1 Cephalic vein | 12 Articular cartilage |
| 2 Biceps tendon | 13 Medial collateral ligament of elbow |
| 3 Brachioradialis | 14 Trochlea of humerus |
| 4 Extensor carpi radialis longus | 15 Capitulum of humerus |
| 5 Radial nerve with profunda brachii artery and vein | 16 Brachialis |
| 6 Common extensor origin | 17 Common flexor origin |
| 7 Lateral collateral ligament of elbow | 18 Median nerve |
| 8 Joint capsule of elbow | 19 Basilic vein |
| 9 Olecranon bursa | 20 Venae comitantes of brachial artery |
| 10 Ulnar nerve | 21 Brachial artery |
| 11 Olecranon process of ulna | 22 Median cubital vein |
| | 23 Bicipital aponeurosis |
| | 24 Anconeus |



Axial computed tomogram (CT)



Orientation



Section level



Notes

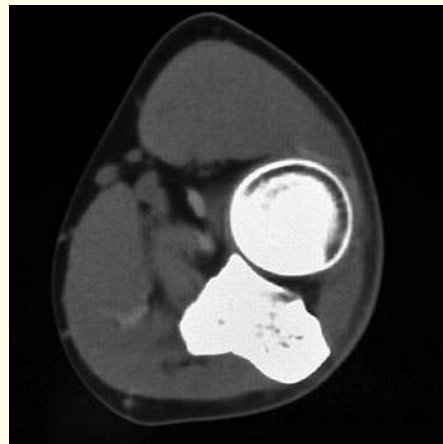
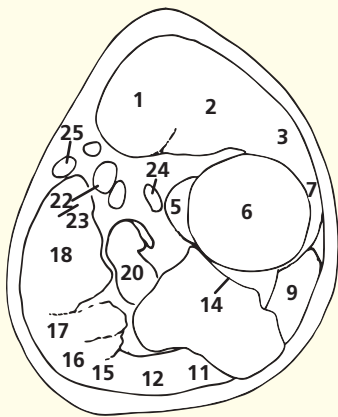
This section transects the elbow joint. The cartilage (12) covering the articular surfaces of the lower end of the humerus (14, 15) and the olecranon process of the ulna (11), together with the joint cavity and collateral ligaments (8), are readily appreciated.

The posterior surface of the olecranon process of the ulna is separated from the skin by a bursa (9). This is a common site for bursitis ('student's elbow', 'miner's elbow').

The median nerve (18), here lying medial to the brachial artery (21) (see note on page 244) is well-named. It lies in the median position throughout its course in the upper arm, at the elbow, in the forearm and at the wrist as it passes into the carpal tunnel below the flexor retinaculum.

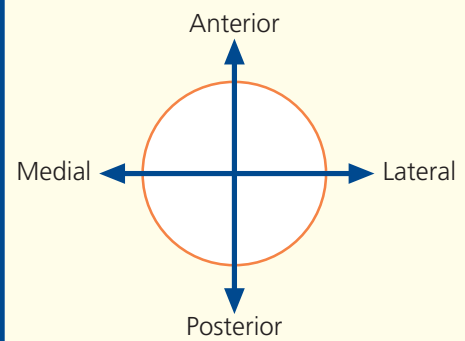


- | | |
|--------------------------------------------------|----------------------------------------------------------------|
| 1 Brachioradialis | 12 Flexor carpi ulnaris |
| 2 Extensor carpi radialis longus | 13 Ulnar nerve, with posterior recurrent ulnar artery and vein |
| 3 Extensor carpi radialis brevis | 14 Radial notch of ulna |
| 4 Radial nerve with radial recurrent artery | 15 Flexor digitorum superficialis |
| 5 Supinator | 16 Palmaris longus |
| 6 Head of radius | 17 Flexor carpi radialis |
| 7 Common extensor origin | 18 Pronator teres |
| 8 Annular ligament of superior radio-ulnar joint | 19 Basilic vein |
| 9 Anconeus | 20 Brachialis |
| 10 Deep fascia of the forearm | 21 Median nerve |
| 11 Flexor digitorum profundus | 22 Venae comitantes of brachial artery |
| | 23 Brachial artery |
| | 24 Tendon of biceps |
| | 25 Median cubital vein |
| | 26 Cephalic vein |

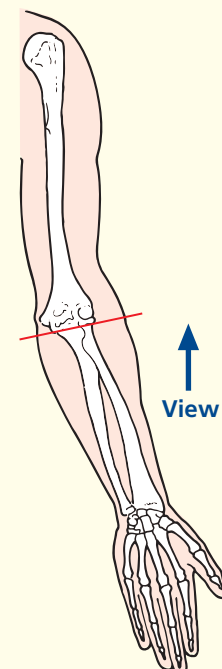


Axial computed tomogram (CT)

Orientation



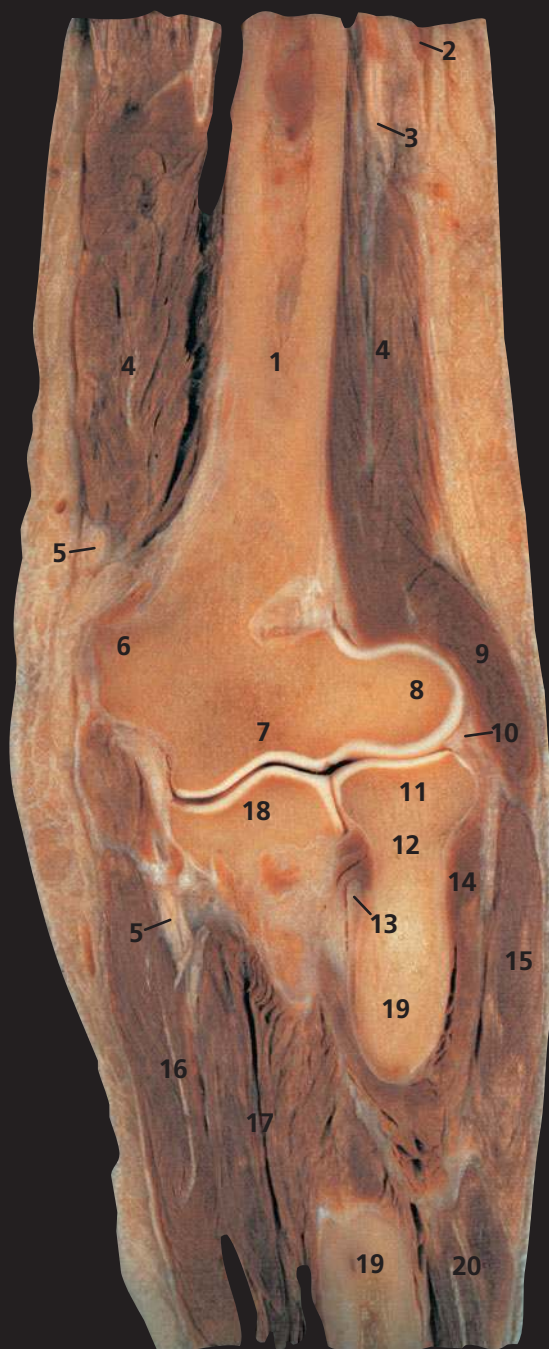
Section level



Notes

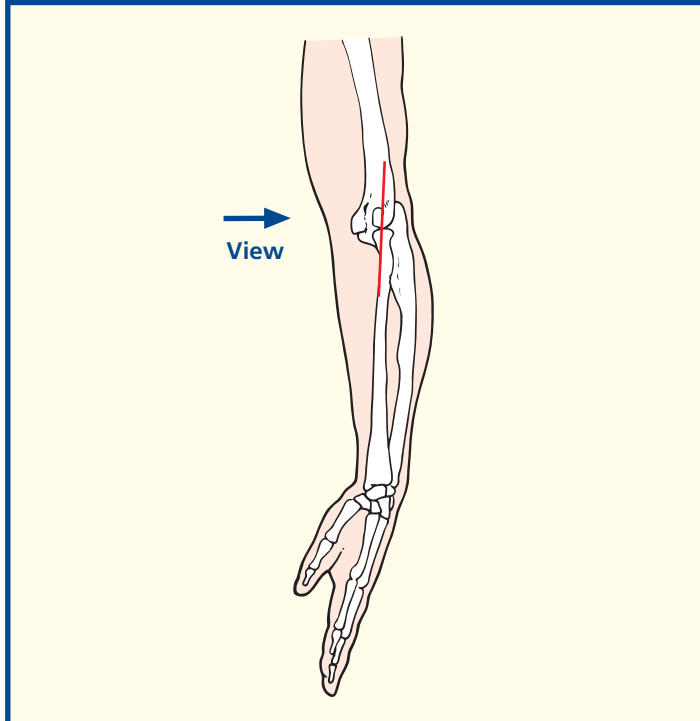
This section passes through the superior radio-ulnar joint between the head of the radius (**6**) and the radial notch of the ulna (**14**). The annular ligament (**8**), which maintains the congruity of this pivot joint, is shown well. In this CT image, the hand is in the neutral position alongside the body.

The median cubital vein (**25**) passes obliquely across the front of the elbow between the cephalic vein (**26**) and the basilic vein (**19**). It is separated from the underlying brachial artery (**23**) by a condensation of the deep fascia (**10**) termed the bicipital aponeurosis. Occasionally, in high division of the brachial artery, an abnormal ulnar artery may lie immediately below the median cubital vein in the superficial fascia. This vein is therefore best avoided for intravenous injections in order to protect against inadvertent intra-arterial injection.



- | | |
|--------------------------------|-----------------------------------|
| 1 Shaft of humerus | 15 Extensor carpi radialis longus |
| 2 Lateral head of triceps | 16 Flexor carpi ulnaris |
| 3 Radial nerve | 17 Flexor digitorum profundus |
| 4 Medial head of triceps | 18 Coronoid process of ulna |
| 5 Ulnar nerve | 19 Shaft of radius |
| 6 Medial epicondyle of humerus | 20 Extensor carpi radialis brevis |
| 7 Trochlea of humerus | 21 Olecranon fossa of humerus |
| 8 Capitulum of humerus | 22 Lateral epicondyle of humerus |
| 9 Brachioradialis | |
| 10 Annular ligament | |
| 11 Head of radius | |
| 12 Neck of radius | |
| 13 Tendon of biceps | |
| 14 Supinator | |

Section level



Notes

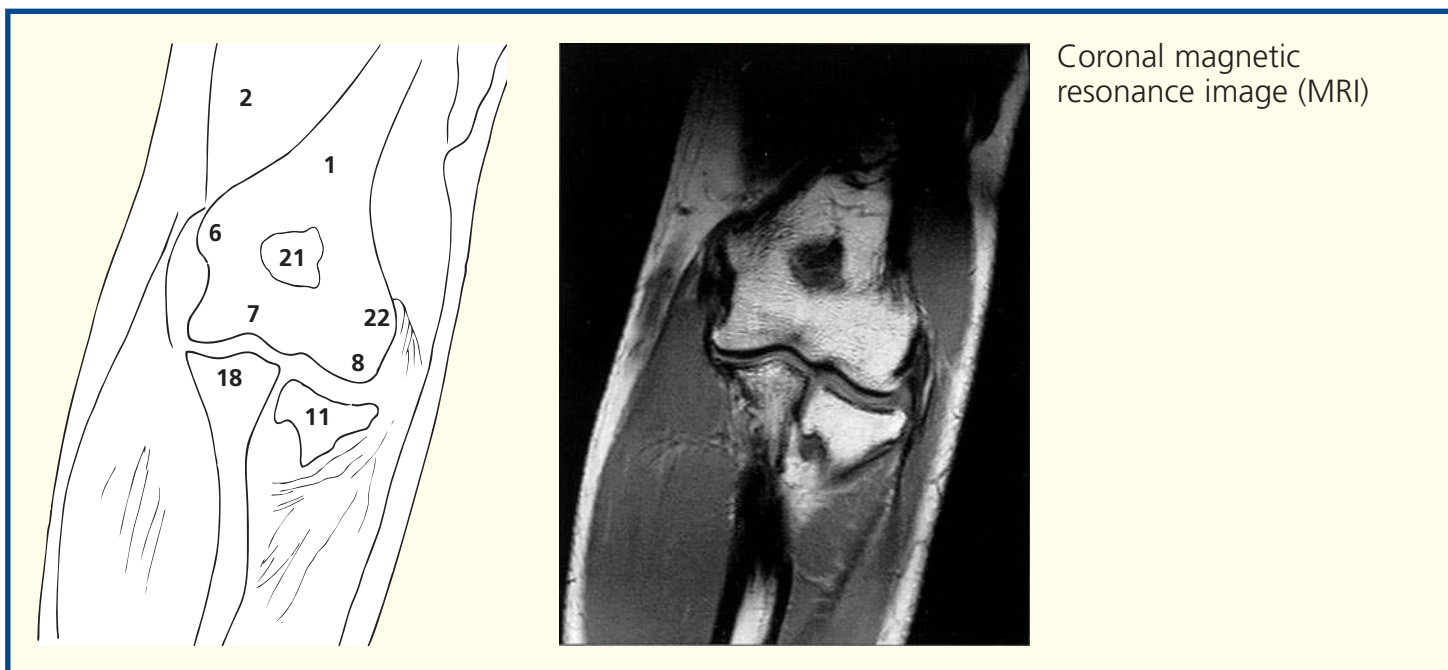
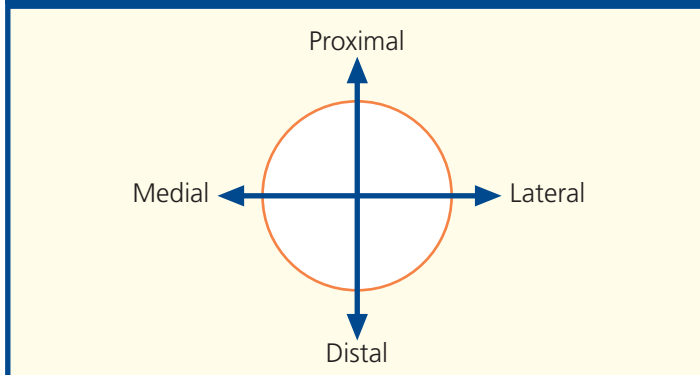
The ulnar nerve (5) passes posterior to the medial epicondyle of the humerus (6), where it may be palpated. It may be injured at this site in fractures or dislocations around the elbow, or stretched in valgus deformity of this joint.

The tendon of biceps (13) inserts into the posterior lip of the tuberosity of the radius. It is a powerful supinator of the radio-ulnar joints and a flexor of the elbow joint.

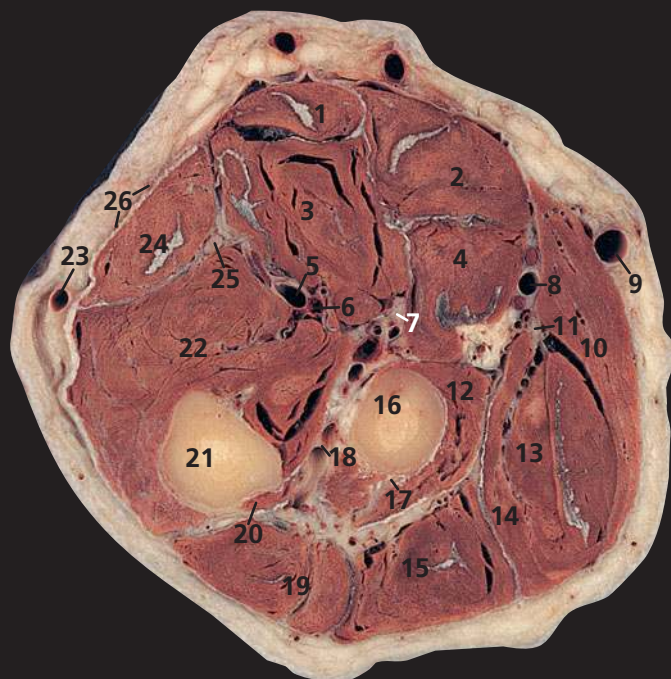
The brachial vessels are in close anterior proximity to the elbow joint; the artery may be compromised in supracondylar fractures, which are relatively common in children.

The epicondyles have developed to provide attachment of the common extensor (lateral epicondyle) and flexor (medial epicondyle) muscle groups. Inflammation of the extensor origin on the lateral epicondyle (22) is known as 'tennis elbow'. This section provides an excellent view of the superior radio-ulnar joint between the head of the radius (11) and the radial notch of the ulna (18). It communicates freely with the elbow joint. Together with the inferior radio-ulnar joint, it allows the movements of pronation and supination of the forearm, which are unique to the primate upper limb.

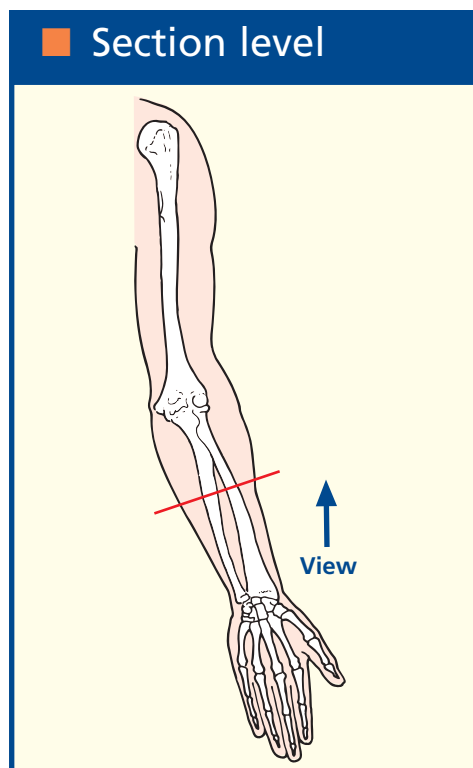
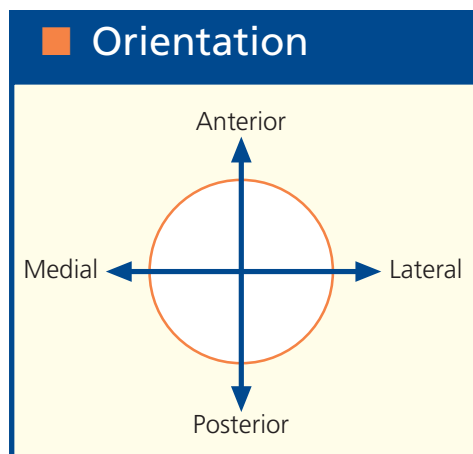
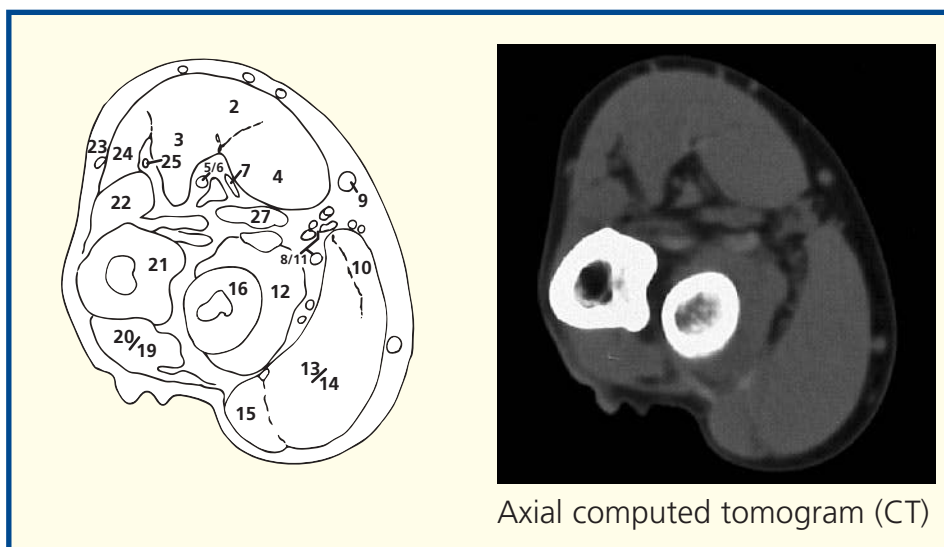
Orientation



Coronal magnetic resonance image (MRI)

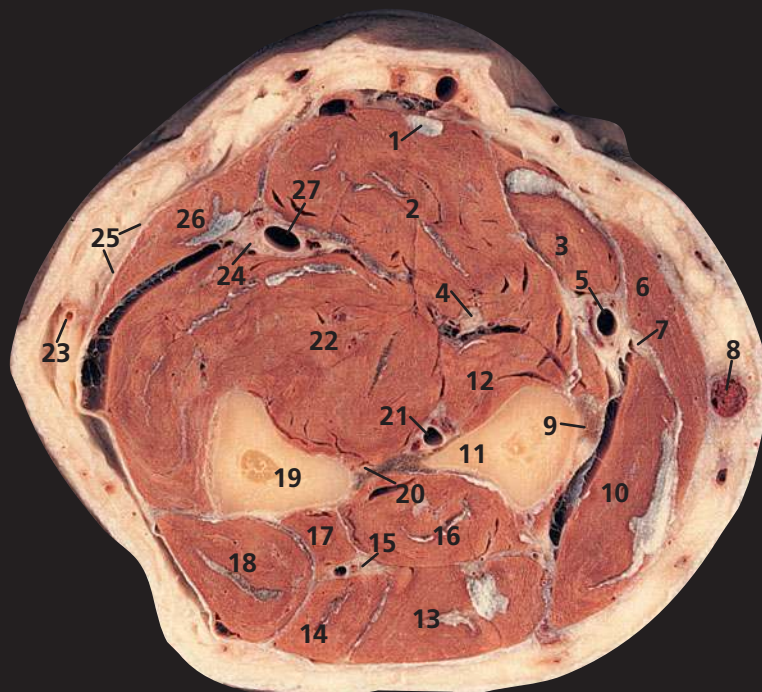


- | | |
|------------------------------------------------------------|-------------------------------------------|
| 1 Palmaris longus | 15 Extensor digitorum |
| 2 Flexor carpi radialis | 16 Radius |
| 3 Flexor digitorum superficialis | 17 Posterior interosseous nerve |
| 4 Pronator teres – humeral head | 18 Posterior interosseous artery and vein |
| 5 Ulnar artery | 19 Extensor carpi ulnaris |
| 6 Ulnar vein | 20 Anconeus |
| 7 Median nerve, with anterior interosseous artery and vein | 21 Ulna |
| 8 Radial artery, with venae comitantes | 22 Flexor digitorum profundus |
| 9 Cephalic vein | 23 Basilic vein |
| 10 Brachioradialis | 24 Flexor carpi ulnaris |
| 11 Radial nerve | 25 Ulnar nerve |
| 12 Supinator | 26 Deep fascia of forearm |
| 13 Extensor carpi radialis longus | |
| 14 Extensor carpi radialis brevis | 27 Pronator teres (ulnar head) |



Notes

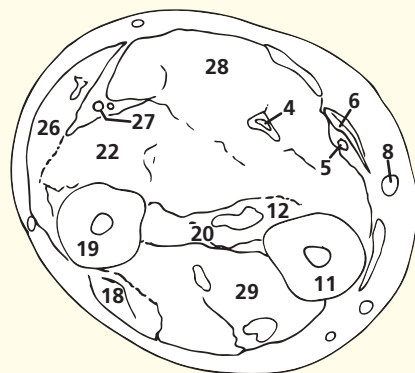
This section passes through the mid forearm. In both the section and the CT image, the forearm is viewed in the supinated position. Note how the median nerve (7) characteristically hugs the deep aspect of flexor digitorum superficialis (3). The ulnar nerve (25) lies sandwiched between flexor carpi ulnaris (24) and flexor digitorum profundus (22), and the radial nerve (11) lies beneath brachioradialis (10).



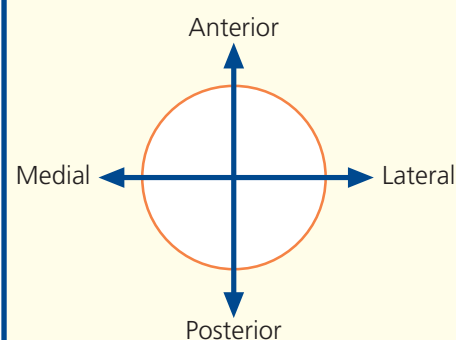
- | | |
|-------------------------------------------------------|-------------------------------------------------|
| 1 Palmaris longus tendon | 17 Extensor pollicis longus |
| 2 Flexor digitorum superficialis | 18 Extensor carpi ulnaris |
| 3 Flexor carpi radialis | 19 Ulna |
| 4 Median nerve | 20 Interosseous membrane |
| 5 Radial artery | 21 Anterior interosseous artery, vein and nerve |
| 6 Brachioradialis | 22 Flexor digitorum profundus |
| 7 Radial nerve | 23 Basilic vein |
| 8 Cephalic vein | 24 Ulnar nerve |
| 9 Pronator teres tendon | 25 Deep fascia of forearm |
| 10 Extensor carpi radialis longus and brevis | 26 Flexor carpi ulnaris |
| 11 Radius | 27 Ulnar artery with venae comitantes |
| 12 Flexor pollicis longus | 28 Superficial flexor group of muscles |
| 13 Extensor digitorum | 29 Extensor group of muscles |
| 14 Extensor digiti minimi | |
| 15 Posterior interosseous nerve, with artery and vein | |
| 16 Abductor pollicis longus | |



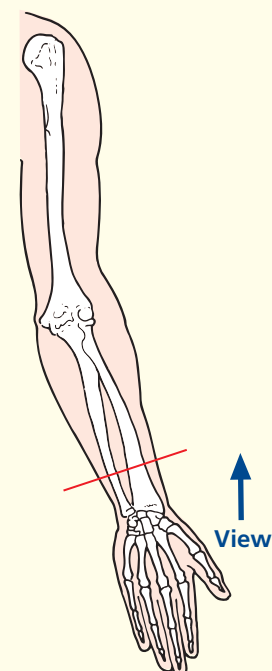
Axial computed tomogram (CT)



Orientation

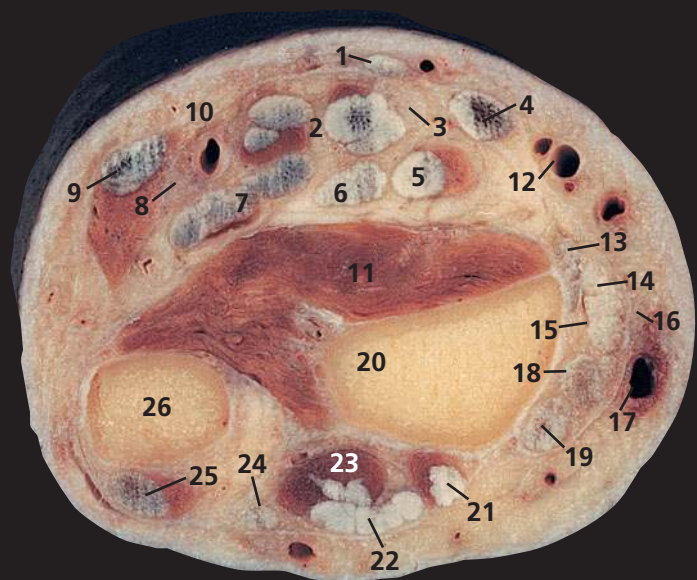


Section level



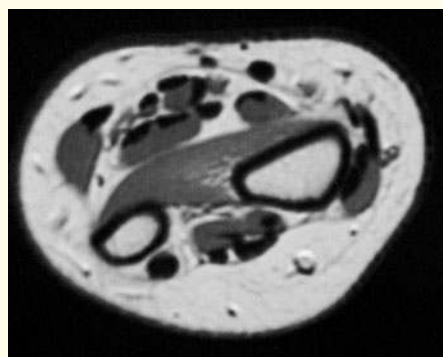
Notes

This section transects the supinated forearm at the junction of its upper two-thirds and lower one-third. Note that the very extensive origin of flexor digitorum profundus (**22**) is demonstrated clearly by this section. It arises from both the anterior and medial surfaces of the upper three-quarters of the ulna (**19**), from the ulnar half of the interosseous membrane (**20**) and also from the superior three-quarters of the posterior border of the ulna by an aponeurosis that is in common with that of flexor carpi ulnaris (**26**) and extensor carpi ulnaris (**18**).

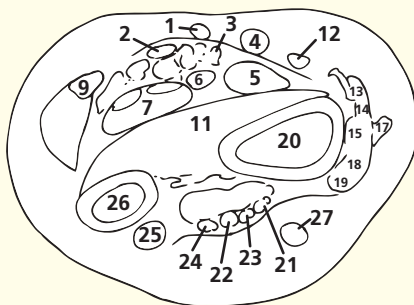


- | | |
|----------------------------------------------------------|------------------------------------------|
| 1 Palmaris longus tendon | 15 Extensor pollicis brevis tendon |
| 2 Flexor digitorum superficialis tendons | 16 Radial nerve |
| 3 Median nerve | 17 Cephalic vein |
| 4 Flexor carpi radialis tendon | 18 Extensor carpi radialis longus tendon |
| 5 Flexor pollicis longus tendon | 19 Extensor carpi radialis brevis tendon |
| 6 Flexor digitorum profundus tendon to index finger | 20 Radius |
| 7 Flexor digitorum profundus tendon to remaining fingers | 21 Extensor pollicis longus tendon |
| 8 Ulnar nerve | 22 Extensor digitorum tendon |
| 9 Flexor carpi ulnaris tendon | 23 Extensor indicis |
| 10 Ulnar artery | 24 Extensor digiti minimi tendon |
| 11 Pronator quadratus | 25 Extensor carpi ulnaris tendon |
| 12 Radial artery | 26 Ulna |
| 13 Brachioradialis insertion | |
| 14 Abductor pollicis longus tendon | |

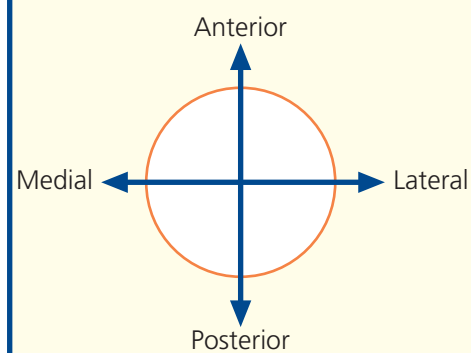
27 Superficial vein



Axial magnetic resonance image (MRI)



Orientation



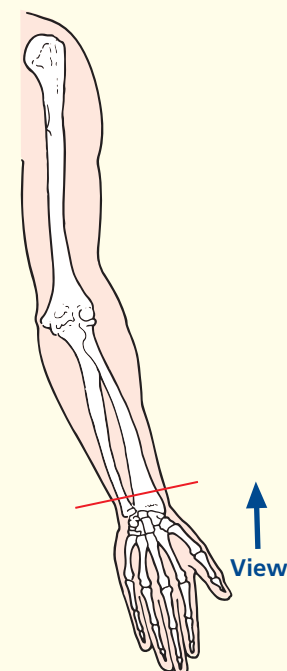
Notes

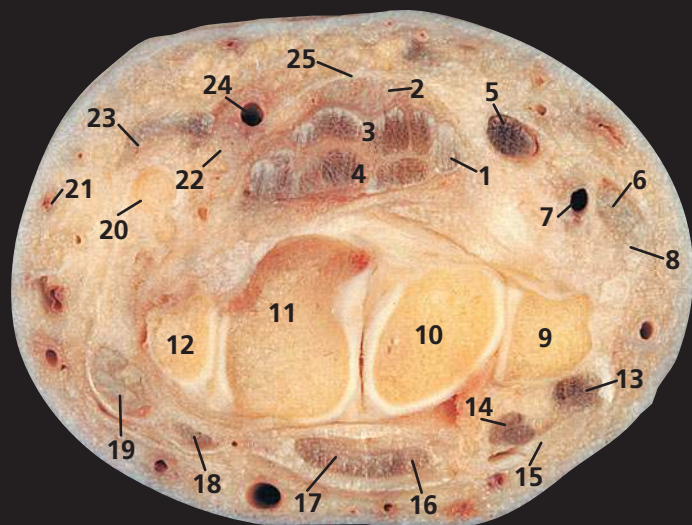
This section transects the forearm immediately proximal to the wrist joint. The arrangement of the extensor tendons on the posterior and radial aspects of the wrist can be appreciated clearly. Note that extensor carpi ulnaris tendon (**25**) grooves the dorsal aspect of the distal ulna (**26**).

At this level, flexor digitorum profundus has given off a separate tendon to the index finger (**6**), while those for the remaining three fingers are still closely applied to each other (**7**).

Usually the cephalic vein (**17**) is easily visible at this site; here, it is a common locus for venous cannulation.

Section level



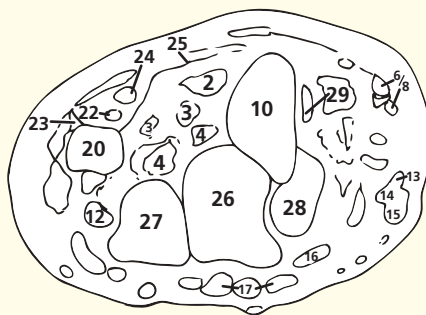


- | | |
|------------------------------------------|------------------------------------|
| 1 Flexor pollicis longus tendon | 15 Extensor pollicis longus tendon |
| 2 Median nerve | 16 Extensor indicis tendon |
| 3 Flexor digitorum superficialis tendons | 17 Extensor digitorum tendon |
| 4 Flexor digitorum profundus tendons | 18 Extensor digiti minimi tendon |
| 5 Flexor carpi radialis tendon | 19 Extensor carpi ulnaris tendon |
| 6 Abductor pollicis longus tendon | 20 Pisiform |
| 7 Radial artery | 21 Basilic vein |
| 8 Extensor pollicis brevis tendon | 22 Ulnar nerve |
| 9 Styloid process of radius | 23 Flexor carpi ulnaris tendon |
| 10 Scaphoid | 24 Ulnar artery |
| 11 Lunate | 25 Flexor retinaculum |
| 12 Triquetral | |
| 13 Extensor carpi radialis longus tendon | |
| 14 Extensor carpi radialis brevis tendon | |

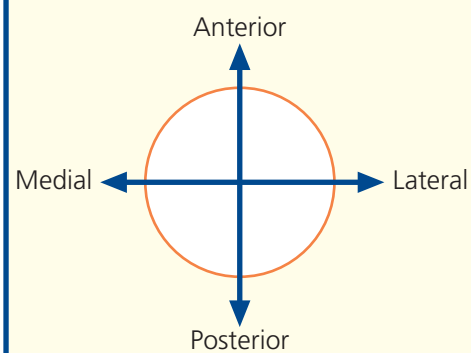
- 26 Capitate
- 27 Hamate
- 28 Trapezoid
- 29 Trapezium



Axial computed tomogram (CT)



Orientation



Notes

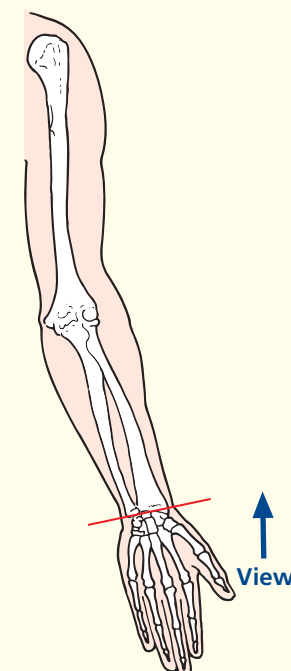
This section passes through the proximal row of carpal bones and the radial styloid process. The CT image is at a more distal level.

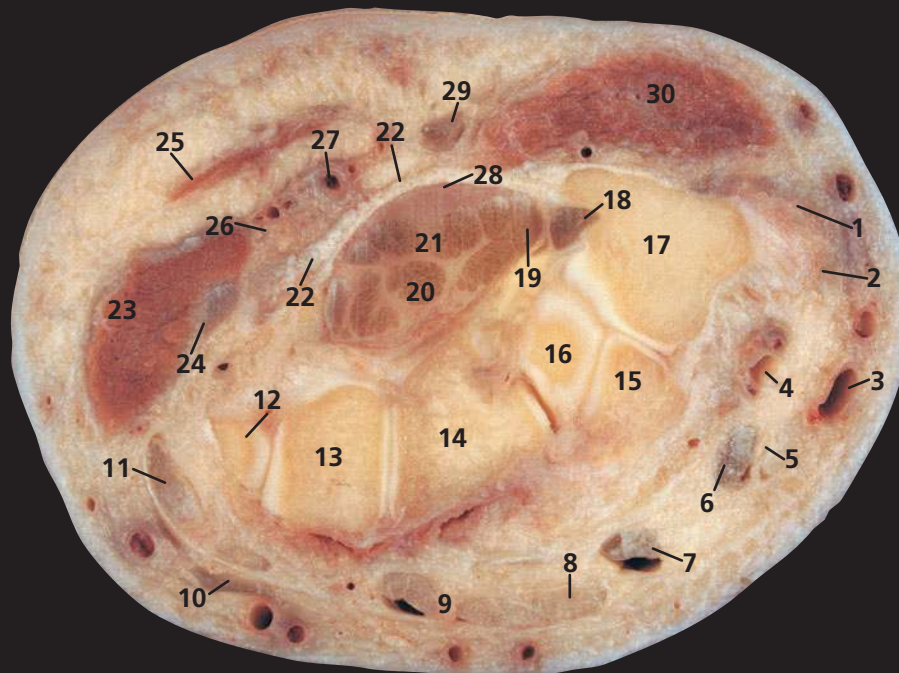
The radius (9) extends more distally than the ulna; thus, abduction of the wrist is more limited than adduction.

The pisiform bone (20) can be considered as a sesamoid within the termination of the tendon of flexor carpi ulnaris (23), which anchors via the pisohamate ligament to the hook of the hamate and via the pisometacarpal ligament to the base of the fifth metacarpal bone.

The flexor retinaculum (25) is a tough fibrous band across the front of the carpus, which converts its concavity into the carpal tunnel, transmitting the flexor tendons of the digits together with the median nerve (2). Its attachments can be seen in this section and on page 254, medially to the pisiform (20) and to the hook of the hamate (27), laterally as two laminae, the more superficial one being attached to the tubercles of the scaphoid (10) and the trapezium (29) and the deep lamina to the medial lip of the groove on the latter.

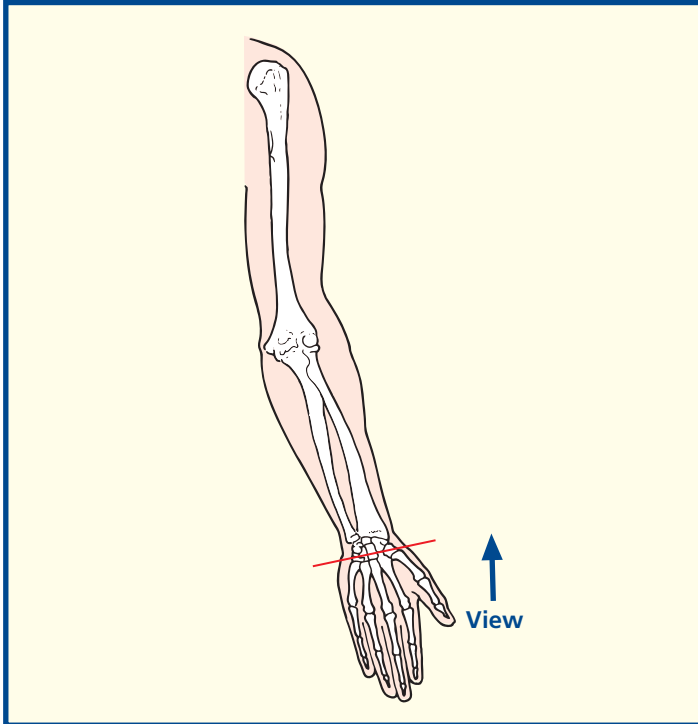
Section level





- | | |
|-----------------------------------------|-------------------------------------------|
| 1 Abductor pollicis longus tendon | 18 Flexor carpi radialis tendon |
| 2 Extensor pollicis brevis tendon | 19 Flexor pollicis longus tendon |
| 3 Cephalic vein | 20 Flexor digitorum profundus tendons |
| 4 Radial artery | 21 Flexor digitorum superficialis tendons |
| 5 Extensor pollicis longus tendon | 22 Flexor retinaculum |
| 6 Extensor carpi radialis longus tendon | 23 Muscles of hypothenar eminence |
| 7 Extensor carpi radialis brevis tendon | 24 Pisometacarpal ligament |
| 8 Extensor indicis tendon | 25 Palmaris brevis |
| 9 Extensor digitorum tendons | 26 Ulnar nerve |
| 10 Extensor digiti minimi tendon | 27 Ulnar artery |
| 11 Extensor carpi ulnaris tendon | 28 Median nerve |
| 12 Triquetral | 29 Palmaris longus tendon |
| 13 Hamate | 30 Muscles of thenar eminence |
| 14 Capitate | |
| 15 Trapezoid | |
| 16 Scaphoid | |
| 17 Trapezium | |
| | 31 Base of thumb metacarpal |

Section level

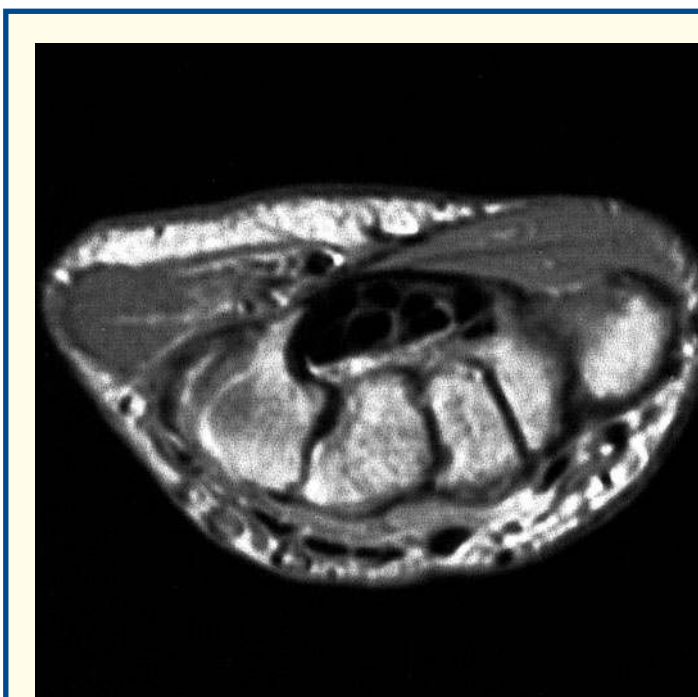
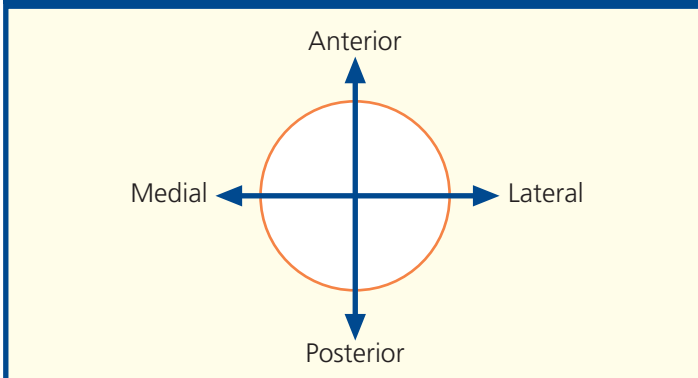


Notes

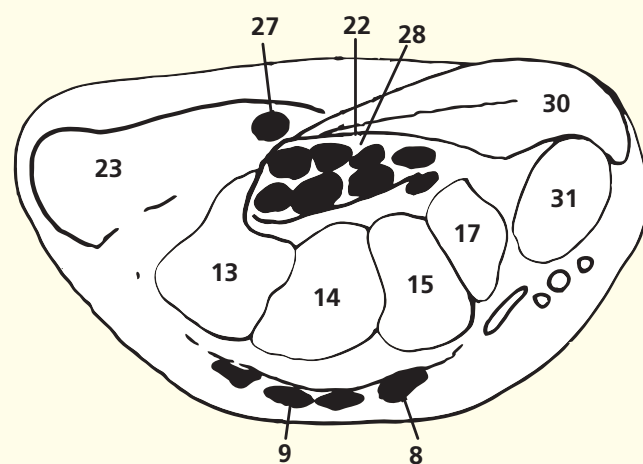
This section passes through the distal part of the carpus. The bony arch is seen well. The flexor retinaculum (22) has already been described (see page 253). Here, its distal attachment to the trapezium (17) and the hook of the hamate (13) can be seen. Note the tendon of flexor carpi radialis (18) lying in the tunnel formed by the groove on the trapezium and the two laminae of the lateral attachment of the retinaculum.

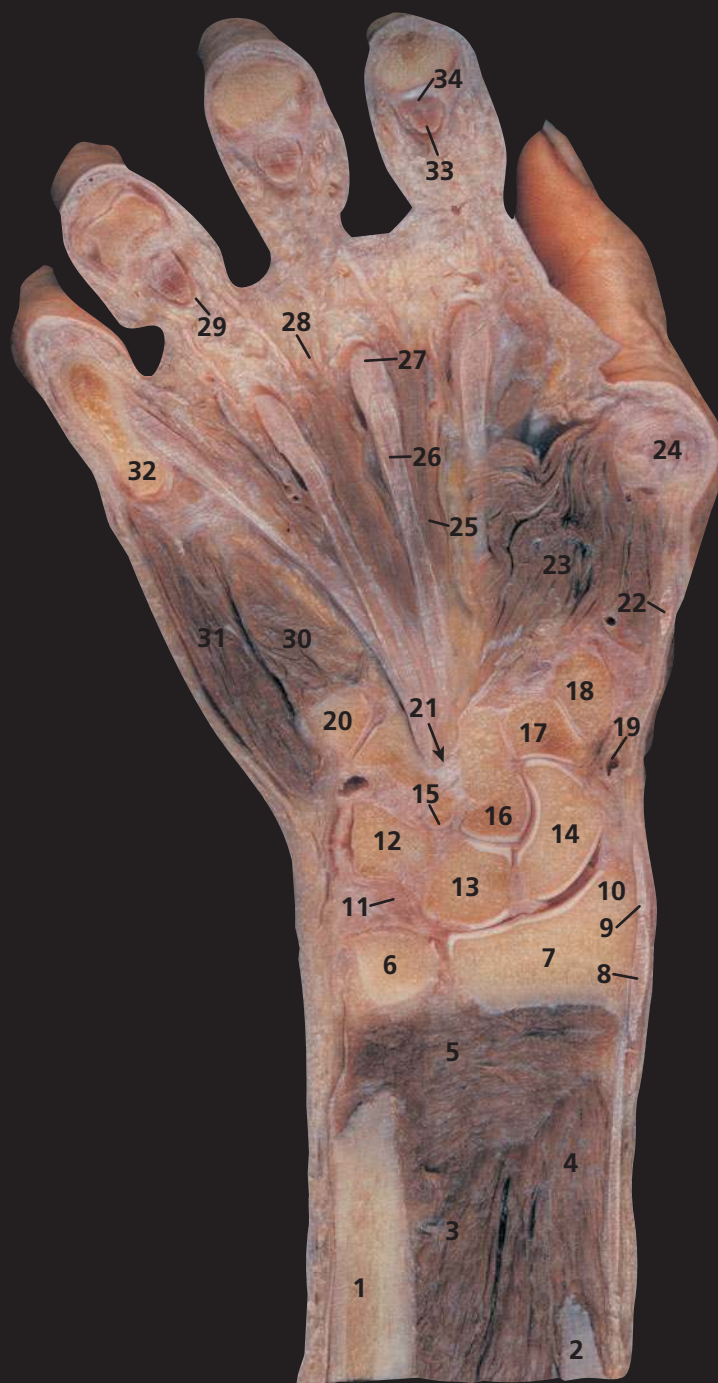
Swelling or deformity within the carpal tunnel compresses the median nerve (28) and produces carpal tunnel syndrome. The ulnar nerve (26) – part of a neurovascular bundle with the ulnar artery and its venae comitantes (27) – passes superficially to the flexor retinaculum and is, therefore, not implicated in this syndrome.

Orientation



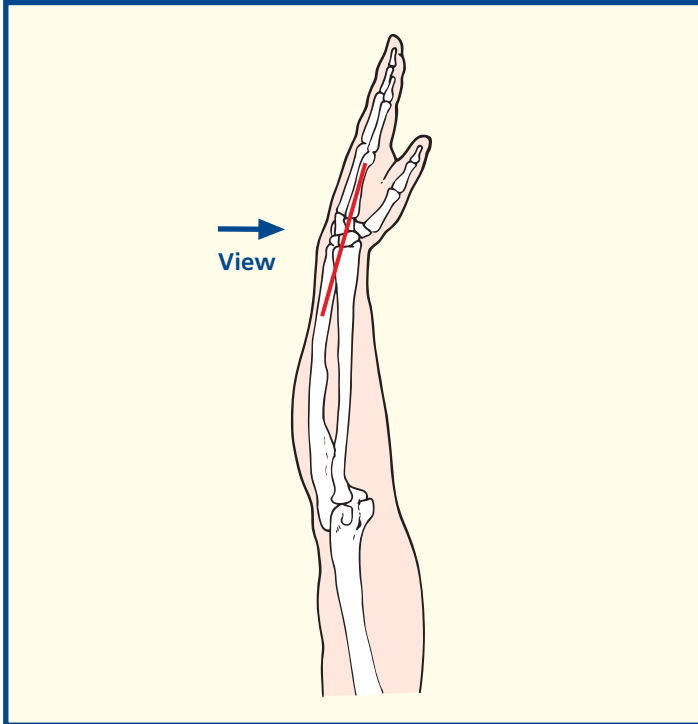
Axial magnetic resonance image (MRI)





- | | | |
|-----------------------------------------------------------------|----------------------------------------------|----------------------------------------------------------------------|
| 1 Shaft of ulna | 15 Hamate | 28 Common digital artery, vein and nerve |
| 2 Shaft of radius | 16 Capitate | 29 Digital fibrous sheath of ring finger |
| 3 Flexor digitorum profundus (see also 33) | 17 Trapezoid | 30 Flexor digiti minimi |
| 4 Flexor pollicis longus | 18 Trapezium | 31 Abductor digiti minimi |
| 5 Pronator quadratus | 19 Radial artery in anatomical snuffbox | 32 Base of proximal phalanx of little finger |
| 6 Head of ulna | 20 Base of little finger bone | 33 Tendon of flexor digitorum profundus of index finger (see also 3) |
| 7 Distal end of radius | 21 Distal opening of carpal tunnel (arrowed) | 34 Tendon of flexor digitorum superficialis of index finger |
| 8 Abductor pollicis longus | 22 Extensor pollicis longus | |
| 9 Extensor pollicis brevis | 23 Abductor pollicis | |
| 10 Radial styloid process | 24 Head of first metacarpal | |
| 11 Articular disc (triangular fibrocartilaginous complex, TFCC) | 25 Second lumbrical | |
| 12 Triquetrum | 26 Tendon of flexor digitorum profundus | |
| 13 Lunate | 27 Tendon of flexor digitorum superficialis | |
| 14 Scaphoid | | |
| | | 35 Ulnar styloid |
| | | 36 Base of index metacarpal bone |

Section level



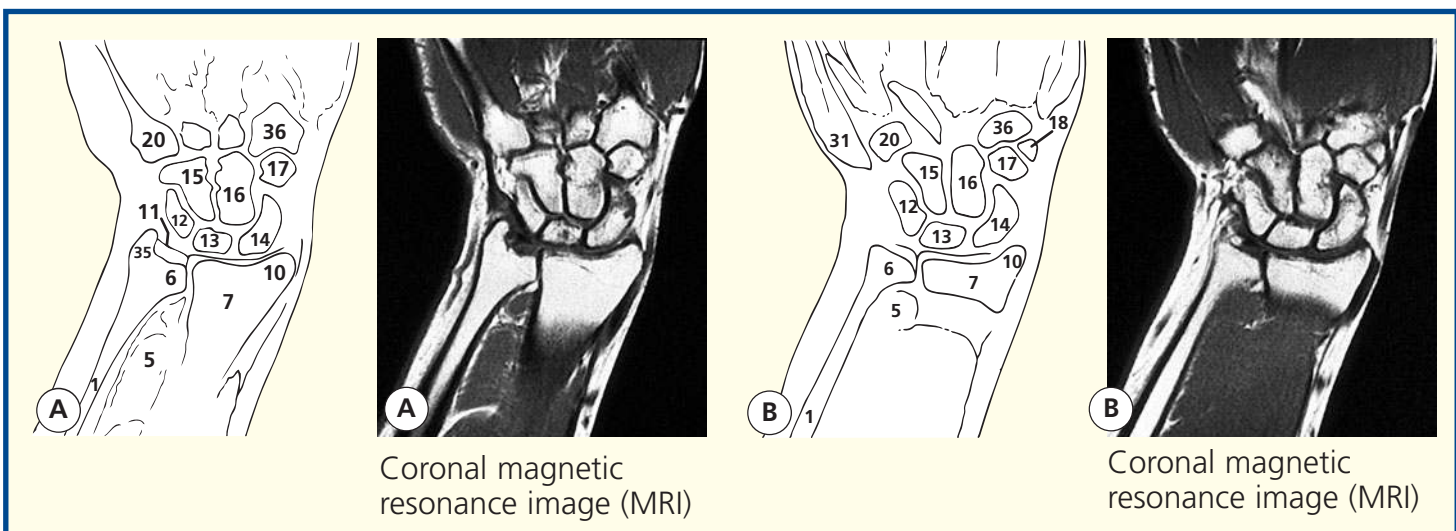
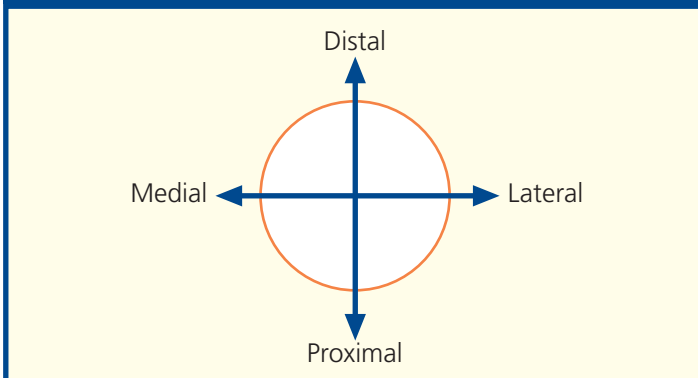
Notes

Note that in the anatomical position of the wrist joint, the scaphoid (14) and lunate (13) are in contact with the distal end of the radius (7). The triquetrum (12) articulates against the articular disc (11) only when the hand is adducted. The triquetrum is, therefore, almost never injured in falls on the hand.

The pulse of the radial artery (19) is readily palpated in the anatomical snuffbox as the artery lies against the underlying scaphoid (14).

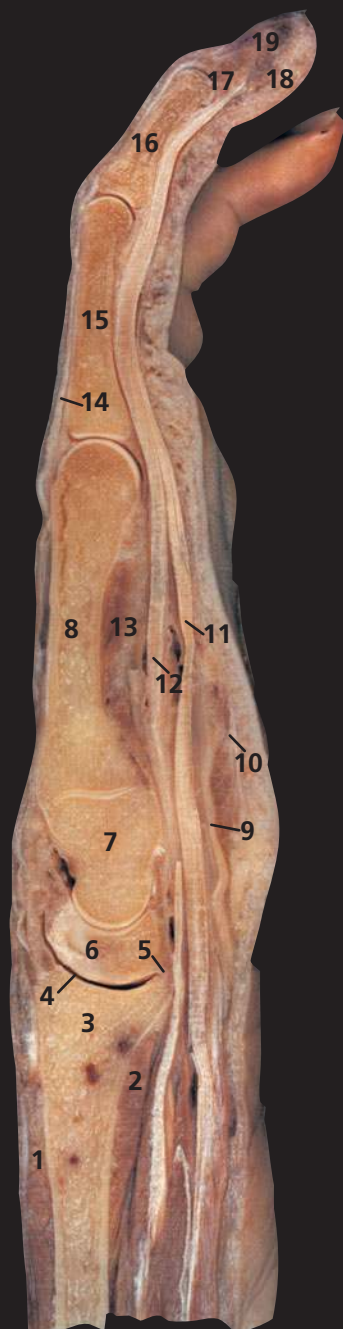
The distal end of the ulna is fractionally shorter than that of the radius. Thus, an articular disc (the triangular fibrocartilaginous complex, TFCC) runs from the ulnar styloid to the radius to complete the proximal part of the ellipsoid wrist joint. An articular disc implies two types of movement: the radius supinates and pronates around the ulna proximal to the disc. Minor variance in ulnar length probably contributes to damage to the TFCC in later life.

Orientation



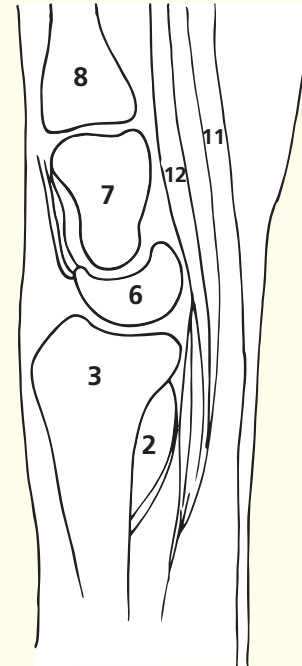
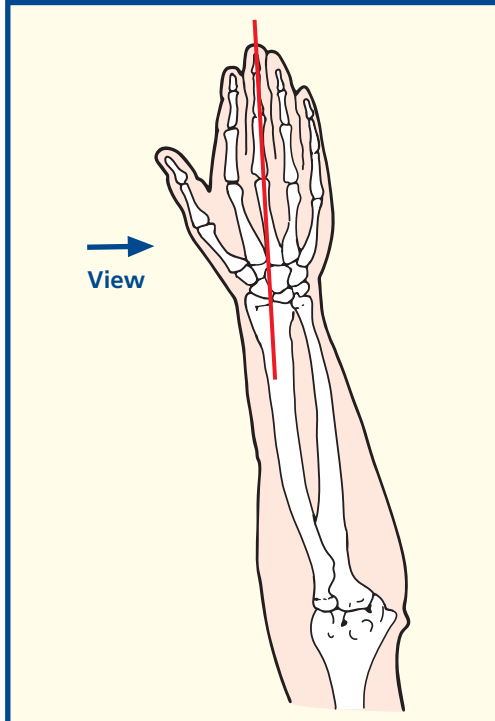
Coronal magnetic resonance image (MRI)

Coronal magnetic resonance image (MRI)



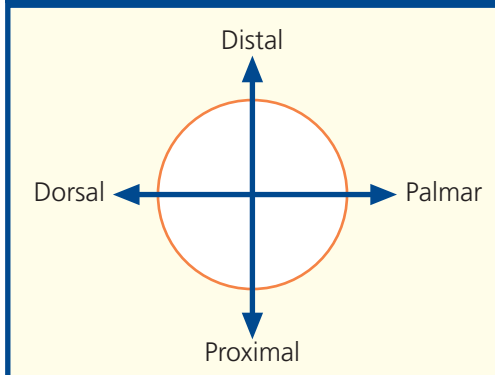
- | | |
|---------------------------------------------|-----------------------------------------|
| 1 Extensor digitorum | 12 Tendon of flexor digitorum profundus |
| 2 Pronator quadratus | 13 Adductor pollicis |
| 3 Distal end of radius | 14 Extensor expansion |
| 4 Wrist joint | 15 Proximal phalanx of middle finger |
| 5 Capsule of wrist joint | 16 Middle phalanx of middle finger |
| 6 Lunate | 17 Distal phalanx of middle finger |
| 7 Capitate | 18 Pulp space of distal phalanx |
| 8 Metacarpal bone of middle finger | 19 Nail bed |
| 9 Flexor retinaculum | |
| 10 Palmar aponeurosis | |
| 11 Tendon of flexor digitorum superficialis | |

Section level



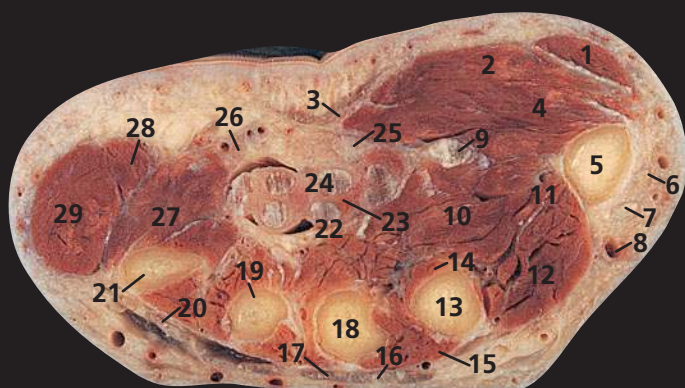
Sagittal magnetic resonance image (MRI)

Orientation

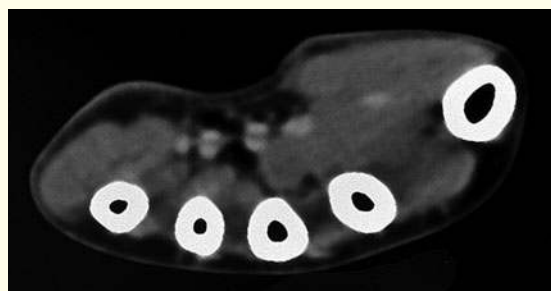


Notes

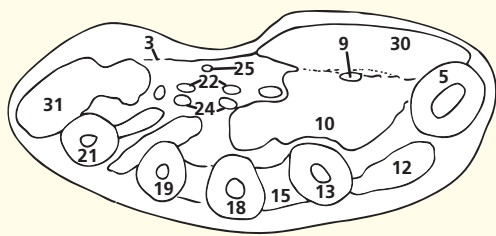
The 'half-moon' of the lunate (**6**) is demonstrated well in this sagittal section. This characteristic appearance enables it to be identified readily in a lateral radiograph of the hand. Lateral radiographs are needed to assess lunate or perilunate dislocations, which are often missed on anteroposterior radiographs. Note the continuous alignment of the radius, lunate, capitate and metacarpal bones.



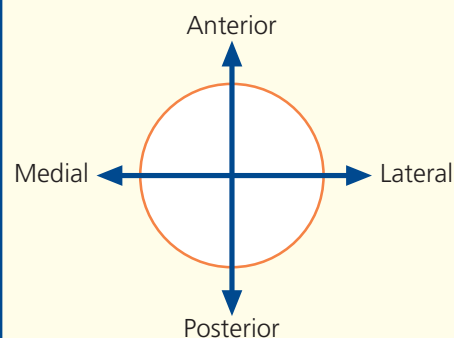
- 1 Abductor pollicis brevis
 - 2 Flexor pollicis brevis
 - 3 Palmar aponeurosis
 - 4 Opponens pollicis brevis
 - 5 First metacarpal
 - 6 Extensor pollicis brevis tendon
 - 7 Extensor pollicis longus tendon
 - 8 Cephalic vein
 - 9 Flexor pollicis longus tendon
 - 10 Adductor pollicis
 - 11 Radial artery
 - 12 First dorsal interosseous
 - 13 Second metacarpal
 - 14 Second palmar interosseous
 - 15 Second dorsal interosseous
 - 16 Extensor indicis tendon
 - 17 Extensor digitorum tendon
 - 18 Third metacarpal
 - 19 Fourth metacarpal
 - 20 Extensor digiti minimi tendon
 - 21 Fifth metacarpal
 - 22 Flexor digitorum profundus tendons
 - 23 Lumbrical
 - 24 Flexor digitorum superficialis tendons
 - 25 Median nerve
 - 26 Ulnar artery and nerve
 - 27 Opponens digiti minimi
 - 28 Flexor digiti minimi
 - 29 Abductor digiti minimi
- 30 Muscles of thenar eminence
 - 31 Muscles of hypothenar eminence



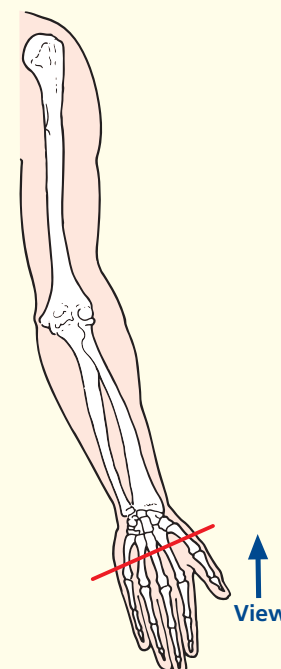
Axial computed tomogram (CT)



Orientation



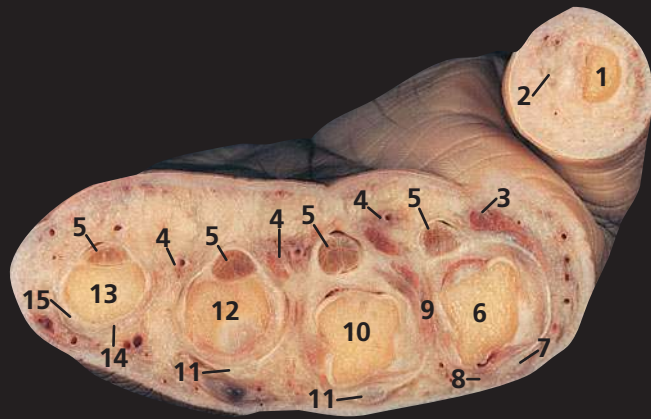
Section level



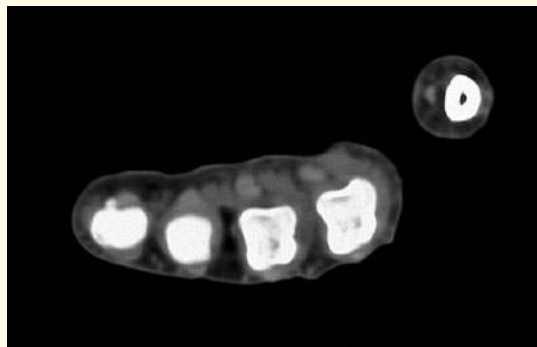
Notes

This section passes through the proximal shafts of the metacarpals.

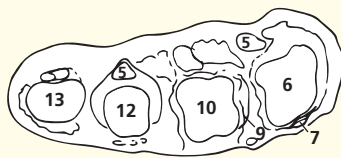
The dense central part of the palmar aponeurosis (**3**) is triangular, its apex being continuous with the distal margin of the flexor retinaculum (see pages 253 and 254). The expanded tendon of palmaris longus (see page 252) is attached to it. It is bound strongly to the overlying skin by dense fibro-areolar tissue. Compare this with the loose superficial fascia over the extensor aspect of the hand. Oedema of the hand thus occurs only on its dorsal aspect. The lateral and medial extensions of the palmar aponeurosis are the thin superficial coverings of the thenar and hypothenar muscles, respectively.



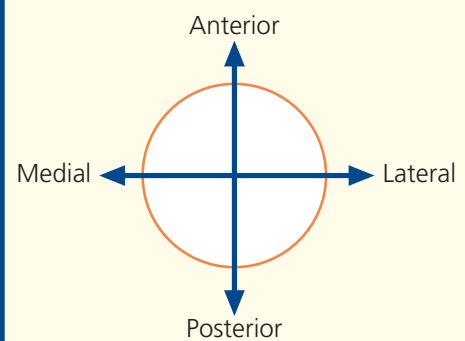
- 1 Proximal phalanx of thumb
- 2 Flexor pollicis longus tendon
- 3 First lumbrical
- 4 Neurovascular bundle
- 5 Flexor tendons within sheath
- 6 Second metacarpal head
- 7 Extensor digitorum tendon to index finger
- 8 Extensor indicis tendon
- 9 Interosseous muscles
- 10 Third metacarpal head
- 11 Extensor digitorum tendon
- 12 Fourth metacarpal head
- 13 Fifth metacarpal head
- 14 Extensor digitorum tendon to little finger
- 15 Extensor indicis tendon



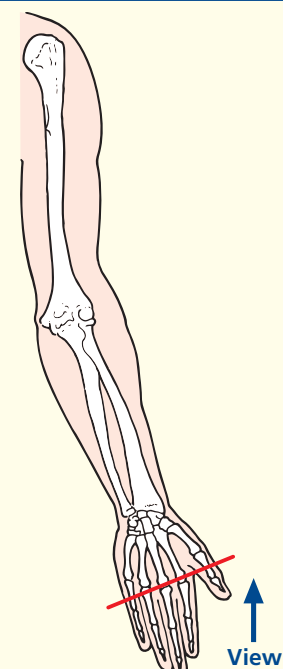
Axial computed tomogram (CT)



Orientation



Section level



Notes

This section passes through the heads of the metacarpals of the fingers and through the proximal phalanx of the thumb (1). In the distal part of the palm, the digital arteries pass deeply between the divisions of the digital nerves so that, on the sides of the digits, the neurovascular bundle (4) has the digital nerve lying anterior to the digital artery and vein. The bundles lie adjacent to the tendon sheaths anterior to the metacarpal heads; this relationship is also maintained in the fingers. Thus, an incision along the anterior border of the bone will avoid these important structures.

The majority of entries are those mentioned in the notes section with bold numbers in brackets. These are mainly on the right (odd numbered) pages of double-page spreads. The words 'odd nos.' appearing in brackets following a page range reference are for CT or MRI images appearing over a number of consecutive odd numbered pages. Roman numerals indicate references in the preface and introduction.

abdomen xvi–xvii, 134–63
 axial section
 female 150–3
 male 134–49
 CT see computed tomography
 accessory nerve 33
 acetabulum 175, 211
 Achilles tendon 228
 acoustic meatus see auditory meatus
 acoustic neuroma 61
 acromioclavicular joint 99
 acromion process 241
 adductor compartment of thigh 212
 adductor longus 185, 212
 adductor magnus 185, 201, 212, 214, 225
 adipose tissue see fat
 adrenal (suprarenal) gland 151, 161
 Alcock's canal see pudendal canal (Alcock's canal)
 alveolar process of maxilla 85
 alveolus (dentalis) 87
 anal canal
 female 199
 male 183
 anal sphincter, external 185
 anal verge
 female 201
 male 185
 angle of Louis 111
 ankle and ankle joint 228–33, 235
 annular ligament of radius 247
 anorectal junction 181
 anterior compartment of thigh 212
 anus see anorectal junction *and entries under anal*
 aorta 121
 abdominal xvi, 141, 145, 147, 149, 165, 187
 thoracic
 ascending 113, 115
 descending 115
 aortic valve 123
 aponeurosis
 epicranial 15, 53
 palmar 260
 plantar 233
 appendix vermiformis 171
 aqueduct of Sylvius 25
 arachnoid mater 13
 arm 244
 arterial system, thorax 132–3
 see *also specific arteries*
 articular cartilage, elbow joint 246

articular disc see disc
 atlanto-axial joint 39, 87
 atlanto-occipital joint 39, 57
 atlas (C1) 37, 39, 59, 63, 87, 101
 atrium
 left 117, 119
 right 117
 septum 117
 auditory meatus/canal (acoustic meatus)
 external 33, 63
 internal 49, 61, 79
 auditory nerve see vestibulocochlear nerve
 auditory ossicles 79
 auditory tube 67, 85
 axial images, orientation xi–xii
 axial section
 abdomen see abdomen
 head 10–47
 lower limb
 ankle 228–31
 knee 215–17
 leg 226–7
 thigh 212–14
 neck 82–99
 pelvis see pelvis
 thorax see thorax
 upper limb
 arm 245
 elbow 245–7
 forearm 250–1
 hand 260–1
 shoulder 238–9
 wrist 252–5
 axis (C2) 37, 39, 41, 43, 53, 89, 101
 dens 37, 39, 57, 63, 77, 87, 101
 azygos vein 127

basilar artery 9, 31, 49
 basilic vein 247
 basi-occiput 33, 83
 basi-vertebral vein 159
 biceps brachii tendon 249
 biceps femoris
 long head 201, 212
 short head 212
 bicipital groove 243
 bile duct, common 139, 151
 bladder
 female 191, 205
 male 175
 brachial artery 244, 246, 247
 brachial vein 244
 brachioradialis 250
 brain 2–9
 axial section 10–35
 coronal section 50–75
 images 8–9
 sagittal section 76–7
 superficial dissection 2–7
 breast 123
 broad ligament 191
 bronchi 113, 131
 buccal fat pad 75
 buccinator 75, 85

cadaver preservation ix
 calcaneonavicular ligament 235
 calcaneus 231, 235
 sustentaculum tali of 231, 235
 calcified phlebolith 195
 capsule
 fibrous, knee joint 223
 internal see internal capsule
 carotid artery
 common 93, 97, 99, 105
 external 37, 47
 internal 9, 49, 87, 91, 93
 cartilage(s)
 costal 115
 elbow joint 246
 laryngeal 95, 97, 101
 caudate nucleus 23, 61, 63
 caval veins see vena cava
 cavernous sinus 67
 cephalic vein 109, 247, 252
 cerebello-medullary cistern 57
 cerebello-pontine angle syndrome 31
 cerebellum 31, 55, 85
 dentate nucleus 57
 peduncles 29
 tentorium 27, 57
 tonsil 35
 cerebral arteries 9
 cerebral veins 57
 cerebrospinal fluid 13
 cervical lymph nodes 105
 cervical spinal canal 101
 cervical spinal cord 35, 37, 59
 cervical spine 37, 45
 vertebrae see vertebrae
 cervical vein, deep 43
 cervix
 external os 195
 internal os 193
 chest see thorax
 cholecystectomy clips 133
 chorda tympani 35
 choroid plexus 21
 cisterna ambiens 25
 cisterna cerebello-medullaris 57
 claustrum 23
 clavicle 99, 107, 125
 clinoid process, posterior 9
 clitoris 201
 coccyx
 female 193, 195
 male 179
 collateral ligaments
 ankle, lateral 233
 elbow 246
 knee 217, 219
 colliculi, inferior 27
 colon xvii
 ascending 149
 descending 149, 153
 transverse 153
 see *also rectosigmoid junction*
 colonogram, CT 154–5
 commissures (corpus callosum) 19
 communicating arteries 9

- computed tomography (CT) ix, x
 abdomen
 axial 135–41(odd nos.), 147–53(odd nos.), 158, 159
 coronal 156–7
 lower limb
 ankle, axial 228, 229, 231
 foot, coronal 237
 leg, axial 226, 227
 thigh, axial 212
 neck, axial 91–9(odd nos.)
 pelvis
 3D 210
 axial, female 189–201
 axial, male 165–85
 skull/brain
 3D 8
 axial 11–19(odd nos.), 25, 29, 33–47(odd nos.), 69–75(odd nos.), 81
 coronal 69–75(odd nos.), 79
 thorax 125
 axial 103–23(odd nos.), 124, 126–7
 coronal 130, 131
 sagittal 130, 131
 upper limb
 arm, axial 244
 elbow, axial 245, 246, 247
 forearm, axial 250, 251
 hand, axial 260, 261
 shoulder, 3D 242, 243
 computed tomography angiography
 brain 9
 thorax 132–3
 computed tomography colonogram 154–5
 concha see nasal concha
 conus medularis 141
 cornea 29
 corona radiata 17, 19
 coronal images, orientation xii
 coronal section
 head 50–75
 lower limb
 ankle 232–3
 foot 236–7
 hip 208–9
 knee 218–19
 upper limb
 elbow 249
 shoulder 240–1
 wrist/hand 256–7
 coronary arteries 125
 corpus callosum 19
 corpus cavernosum 185
 corpus spongiosum 185
 costal cartilage 115
 cranial nerves 31, 33, 61, 67, 79, 85, 87
 cranium see skull
 cricoid cartilage 97, 101
 cruciate ligaments
 anterior 216, 219, 223
 posterior 217, 219, 223
 cubital vein, median 247
 cuneiform, medial 237
 cutaneous nerve of thigh, lateral 199

 da Vinci, Leonardo viii
 De Riemer viii
 deep artery of penis 185
 deep fascia
 arm 244
 elbow 247
 leg 223
 deltoid 239, 241
 dens 37, 39, 57, 63, 77, 87, 101
 dentate nucleus 57
 denticulate ligament 95
 descending (coronary) artery, left anterior 125
 diaphragm (and hemidiaphragm) 119, 121, 135
 crura 137, 161
 digital neurovascular bundles 261
 diploic veins 11
 disc (intra-articular)
 intervertebral see intervertebral disc
 temporomandibular joint 65
 wrist joint 257
 dorsal root(s), cervical 59
 dorsal root ganglion
 cervical 59
 lumbar 159
 duodenum 145, 147, 149
 dura mater, brain 11, 13, 15, 37, 57
 dural sheath, lumbar 159

 ear
 inner 78–81
 middle 79
 eardrum (tympanic membrane) 63, 79
 elbow 245–9
 endocranium 11
 epicondyles, humeral 249
 epicranial aponeurosis 15, 53
 epiglottis 95
 ethmoid bone 75
 ethmoidal sinuses 29, 71
 Eustachian (auditory) tube 67, 85
 extensor carpi radialis longus 245
 extensor carpi ulnaris 251
 tendon 252
 extensor digitorum longus 226, 227
 extensor hallucis longus 227
 extraocular muscles 29, 71
 eye/eyeball/globe 29
 MRI 49

 facial artery 47
 facial bones 8
 facial nerve 31, 61, 79, 85, 87
 falx cerebri 13, 27, 57
 fascia
 deep see deep fascia
 penile 185
 renal 143, 151
 fast imaging sequences x
 fat (adipose tissue) xvii
 in imaging
 in CT x
 suppression in MRI xi
 pericardial 137
 perirenal 151
 fat pad
 buccal 75
 popliteal 223
 femoral artery 225
 common 179, 197
 superficial 185, 214
 femoral nerve 203
 femoral vein
 common 197
 lateral circumflex 197
 superficial 185, 214
 femur
 condyles 215, 216
 head 193, 209, 211
 ligament of (ligamentum teres) 177, 209
 popliteal surface 223
 shaft 183, 214
 fibula, shaft 226, 227
 fibular (peroneal) nerve
 common 215
 deep 226, 227
 superficial 226
 fibularis (peroneus) brevis 229
 fibularis (peroneus) longus 226
 tendon 237
 fissures, lung 111
 flaval ligaments 159
 flexor carpi radialis tendon 255
 flexor carpi ulnaris 250, 251
 tendon 253
 flexor digitorum brevis 233
 flexor digitorum longus tendon 229
 flexor digitorum profundus 250, 251
 tendon 252
 flexor digitorum superficialis 250
 flexor hallucis longus 235
 tendon 229, 231, 235
 flexor retinaculum 253, 255
 foot 234–7
 foramen magnum 9, 39, 59
 foramen ovale (skull) 33
 foramen transversarium 41, 45, 89
 forearm 250–1
 formalin-hardened material viii
 frontal bone 11
 frontal sinus 77
 frontalis 53
 fundus
 bladder 175, 191
 stomach 135

 galea aponeurotica (epicranial aponeurosis) 15, 53
 gallbladder 153
 see also cholecystectomy clips
 gastric fundus 135
 gastrocnemius 223, 225, 226
 tendon 228
 genioglossus 47, 91
 glans of clitoris 201
 globus pallidus 23, 61

- glossopharyngeal nerve 33
 gluteal nerve
 inferior 169
 superior 169, 209
 gluteal vessels
 inferior 169
 superior 169, 171, 173, 209
 gluteus maximus 169, 171, 179, 195
 gluteus medius 169, 171, 209
 gluteus minimus 169, 171, 209
 gracilis 212
 grey matter 15
 gyri 17
- hamate 253, 255
 hamstrings 212
 hand 256–61
 hardening fluids viii
 head
 axial section 10–47
 coronal section 50–75
 sagittal section 76–7
 heart 117, 119, 124–5
 helical (spiral) CT x
 hemidiaphragm *see* diaphragm
 hepatic artery 133, 139, 151
 hepatic vein, right 121
 hip, coronal section 208–9
 history of sectional anatomy viii
 Hounsfield scale x
 humerus
 epicondyles 249
 greater tubercle 239
 mid-shaft 244
 neck 241
 hyoid bone 67, 93
 hypoglossus 93
- ileum 171
 iliac artery
 common 167
 external 203
 internal 173, 189
 iliac crests 165
 iliac vein
 external 203
 internal 189
 iliopsoas 203
 see also psoas muscles
 images
 imaging techniques ix, x–xi
 orientation xi–xii
 incus 79
 infrahyoid (strap) muscles 97, 99
 infrapatellar bursa 221
 infraspinatus 239
 inguinal hernia, direct 177, 179
 interatrial septum 117
 intercostal neurovascular bundle 107
 internal capsule
 anterior limb 23, 63
 posterior limb 61
 interosseous membrane of forearm 251
- intertubercular sulcus 243
 interventricular foramen 23
 intervertebral discs
 lumbar 147, 167
 lumbosacral 169
 thoracic 107, 111, 117, 119
 thoracolumbar 141
 ischiorectal fossa
 female 197
 male 179, 181
 ischium
 spine 177
 tuberosity 181
- jaw *see* mandible; maxilla
 jejunum 141
 jugular vein
 external 93, 103
 internal 33, 35, 87, 97, 99, 105, 107
- kidney xvi, 133, 139
 fascia 143, 151
 knee
 axial section 215–17
 coronal section 218–19
 sagittal section 220–7
- labial mucous glands 41
 labial vessels and nerves 41
 labyrinthine artery 31
 lacrimal gland 75
 large intestine *see* colon; rectum
 laryngeal nerve, recurrent 99, 105
 laryngopharynx 93, 97, 101, 103
 larynx 101, 103
 cartilages 95, 97, 101
 lateral collateral ligament
 of ankle 233
 of knee 217
 leg 226–7
 lens 29
 Leonardo da Vinci viii
 levator ani
 female 197
 male 179, 181
 levator palpebrae superioris 75
 levator scapulae 103
 ligament(s)
 of ankle 233
 of elbow 246, 247
 flaval 159
 of foot 235
 of knee 216, 217, 219, 223
 sacrospinous 177
 of uterus
 broad 191
 round 203
 ligamentum denticulatum 95
 ligamentum nuchae 55
 ligamentum teres femoris 177, 209
 ligamentum teres hepatis 153
 ligamentum venosum 135
- limbs
 lower 208–37
 upper 238–61
 linea alba 149
 lingual artery 93
 lingual nerve 35
 lips 41, 43, 45, 47
 liver xvii, 135
 lobes 139
 caudate 153
 left 143, 153
 quadrate 151
 right 119, 147
 Louis' angle 111
 lower limbs 208–37
 lumbar nerve, 2nd 149
 lumbar spine 158–63
 intervertebral disc 147
 vertebrae *see* vertebrae
 lumbar sympathetic chain 165
 lumbar vein 145
 lumbosacral discs 169
 lunata 257, 259
 lung 107
 fissures 111
 lower lobes 135, 137
 lymph nodes
 cervical 105
 occipital 55
 pretracheal 111, 127
- Macewen, Sir William viii
 magnetic resonance imaging (MRI) ix
 abdomen
 axial 143, 145
 coronal 160–1
 sagittal 162–3
 ankle, coronal 233
 elbow, coronal 249
 foot, sagittal 235
 head
 axial 21, 23, 27, 29, 48–9
 coronal 51–67(odd nos.)
 sagittal 77
 hip, coronal 209
 knee
 axial 215, 216, 217
 coronal 219
 sagittal 221, 223, 225
 neck
 axial 83–9(odd nos.)
 coronal 101
 pelvis 202–7
 axial 165, 202–3
 coronal 186–7, 204–5
 female 202–7
 male 165, 186–7
 sagittal 206–7
 shoulder
 axial 239
 coronal 241
 thigh, axial 213, 214
 thorax, coronal 128–9

- wrist/hand
axial 255
coronal 257
sagittal 259
- malleolus, medial 229
- malleus 79
- mandible 47, 65, 91
canal 89
ramus 85
- mandibular nerve 33
- manubriosternal joint 111
- masseter 69
- mastoid sinus/air cells 85
- maxilla (upper jaw) 41
alveolar process 85
- maxillary artery 37
- maxillary nerve 33
- maxillary sinus/antrum 33, 39, 73, 83, 85
- medial collateral ligament of knee 217, 219
- median cubital vein 247
- median nerve 244, 246, 250, 253, 255
- median sacral vessels 175
- mediastinum 109, 126–7
- medulla oblongata 31, 59, 85
- meningeal artery, middle 25
- meninges 11, 53
- meniscus
lateral 217, 219, 221
medial 219
- mesenteric artery
inferior 149, 165
superior 133, 141, 145, 147
- mesenteric vein
inferior 165
superior 145, 147
- metacarpals 260, 261
- metatarsal, first 237
- Monro's foramen 23
- mons pubis 199
- mucous glands 69
labial 41
- muscles
abdominal 147
extraocular 29, 71
strap 97, 99
tongue 43, 67
see also individual muscles
- nasal cavity 31, 37
- nasal concha
inferior 37, 71, 83
middle 33, 71, 73
superior 71
- nasal septum 35, 69
- nasal vestibule 83
- nasolacrimal duct 29, 35
- nasopharynx 39, 67
- natal cleft 197, 201
- navicular bone (foot) 235
- neck 82–101
axial section 82–99
sagittal section 100–1
- nerve(s), *see specific nerves*
- nerve roots and root sheaths
cervical 59
lumbar 159
- neurovascular bundles
digital (hand) 261
intercostal 107
superior gluteal 209
- nose *see entries under nasal*
- nuchal ligament 55
- oblique muscles of abdomen 147
- obliquus capitis inferior 39
- obturator internus 179, 195, 197
- occipital bone
basilar part (basi-occiput) 33, 83
external occipital protuberance 31
posterior part 51
squamous part 23
- occipital lobe 55, 83, 85
- occipital lymph nodes 55
- occipitofrontalis 53
- oculomotor nerve 67
- odontoid peg (dens) 37, 39, 57, 63, 77, 87, 101
- oesophagogastric junction 135
- oesophagus 99, 101, 105, 117, 121
- olecranon bursa 246
- olecranon process 246
- olfactory bulb 73
- omohyoid muscle 97
- optic chiasma 27
- optic nerve 27, 29, 71
- orbicularis oris 41
- orbit 27, 29, 71
MRI 49
- oropharynx 43, 47, 91
- ossicles, auditory 79
- ovary 189
- palate 37, 39, 69, 73, 77, 83
- palatine bone 37
- palatine tonsil 89
- palatopharyngeal arch 43
- palmar aponeurosis 260
- pampiniform plexus 185
- pancreas xvii, 137
uncinate process 145
- paranasal sinuses 29, 31, 33, 39, 63, 69, 71, 73, 83
MRI 49
- parathyroid gland 97
- parietal bone 11, 53
- parotid duct 69, 73, 83
- parotid gland 45, 63, 85, 87, 89
accessory 69, 83
- patella 215, 216, 221
- pedicle, L5 159
- pelviclyceal system 133
- pelvis 164–207
axial sections
female 188–201
male 164–85
CT *see computed tomography*
- penis 185
- pericardium 119
fat 137
space between layers 113
- pericranium (periosteum of skull) 11, 15, 53
- periosteum of skull 11, 15, 53
- perirenal fat 151
- peroneal nerve *see fibular nerve*
- peroneus brevis 229
- peroneus longus *see fibularis longus*
- petrous temporal bone 61, 79
- phalanx, thumb 261
- pharyngeal recess 83
- pharynx 47, 101
laryngeal part (laryngopharynx) 91, 95, 97, 101
nasal part (nasopharynx) 39, 67
oral part (oropharynx) 43, 47, 89
- phlebolith, calcified 195
- phrenic nerve 95, 103, 117
- pia mater 13
- piriformis 173, 189
- pisiform bone 253
- pituitary fossa 9
- pituitary gland 27, 63, 77
- plantar aponeurosis 233
- plantar nerve, medial 237
- plantaris 221
tendon 226
- pons 29, 59, 61, 83
MRI 49
- popliteal artery 223
- popliteal pad of fat 223
- popliteal vein 216, 227
- popliteus 223
tendon 217, 221
- portal vein 139
- posterior compartment of thigh 212
- postnasal space 83
- prepatellar bursa 221
- prepuce of clitoris 201
- preservation of cadavers ix
- pretracheal space 127
lymph nodes 109, 127
- prevertebral fascia 47, 63
- prevertebral muscles 47
- proton density images x
- psoas muscles 143, 149, 161
see also iliopsoas
- pterygoid muscle
lateral 83
medial 45
- pterygopalatine fossa 33
- pubis
body 197
symphysis 179, 195
see also mons pubis
- pubic canal (Alcock's canal)
female 197
male 179
- pubic nerve 179
- pubic vessels, internal 179
- pulmonary arteries 111, 127
- pulmonary trunk 111
- pulmonary valves 113

- pulmonary vein
superior 111
tributaries 111
putamen 23, 61, 63
- quadratus femoris 199, 212
tendon 221
quadratus lumborum 143
- radial artery 257
radial nerve 244, 250
radial notch 247, 249
radiology *see* images
radio-ulnar joint, superior 249
radius
distal 253, 257
head 247
ramus of mandible 83
rectal artery, superior 165, 167, 177
rectal vein, superior 177
rectosigmoid junction
female 189
male 175
rectum
female 189, 191
male 175
see also anorectal junction
rectus abdominis 147
rectus capitis posterior major 55
rectus femoris 212
recurrent laryngeal nerve 97, 103
renal vein 141, 145
retromandibular vein 85
rib
1st 125
2nd 109
9th 135
round ligament
liver (ligamentum teres hepatis) 153
uterus 203
- sacral vessels, median 175
sacroiliac joint 169, 171
sacrospinous ligament 177
sacrum
2nd segment 171
3rd segment 173, 189
4th segment 175
5th segment 177, 191
lateral mass 169
safety considerations ix
sagittal images, orientation xii
sagittal section
foot 234–5
head 76–7
knee 220–7
neck 100–1
wrist/hand 258–9
sagittal sinus, superior 11, 55
salivary glands
accessory/minor 41, 69
major 45, 47, 63
- saphenous nerve 185, 214
saphenous vein
great 227
small 216
sartorius 185, 212, 214
scalenus (scalene muscles) 47, 63, 103, 105
scalp (skin + subcutaneous tissue) 15, 53
scaphoid 253, 257
scapula 107, 243
acromion process 241
sciatic nerve
female 189, 195, 199, 201
male 183
sclera 29
section(s), orientation xi–xii
sectioning ix–x
semimembranosus bursa 217
semimembranosus muscle 212
seminal vesicle 175
semispinalis capitis 43
semispinalis cervicis 43
semitendinosus 212
septum
interatrial 117
nasal 35, 69
septum pellucidum 21
serratus anterior 117
sesamoid bones 235
shoulder 238–43
sigmoid sinus 33
skin, cranial 15, 53
skull (cranium)
images 8, 9
periosteum 11, 15, 53
sutures 21
small intestine 141, 171
soleus 223, 226
spermatic cord 179
sphenoid bone, lesser wing 69
sphenoidal sinus 29, 31, 65, 69, 77
MRI 49
spinal accessory nerve 33
spinal canal, cervical 101
spinal cord, cervical 35, 37, 59
spine *see specific regions and vertebrae*
spiral CT x
spleen xvii, 121, 135
splenium of corpus callosum 19
splenius capitis 103
spring ligament 235
squamous part
occipital bone 23
temporal bone 25, 61
stapes 79
sternal (Louis') angle 111
sternocleidomastoid muscle 99, 103
sternocostal joint, third 123
sternohyoid muscle 97
sternothyroid muscle 97
sternum 113, 115, 117
stomach, fundus 135
straight sinus 27, 85
strap muscles 97, 99
styloid process of temporal bone 85
subacromial space 243
- subarachnoid space 13, 53, 55, 57
subclavian artery 125
subclavian vein 107, 125
subcutaneous (connective) tissue, cranial 15, 53
subdeltoid process 239
subdural space 53
submandibular gland 45, 47, 63
subscapularis 111
subtalar joint 231
sulcus (sulci)
cerebral 17, 19
intertubercular 243
talar 231
suprapatellar bursa 221
suprarenal (adrenal) gland 151, 161
supraspinatus tendon 241
sustentaculum tali 231, 235
sutures, cranial 21
Sylvian aqueduct 25
sympathetic chain, lumbar 165
symphysis pubis 179, 195
- T1 and T2–weighted density images x
talocalcanean joint 231
talocalcanean ligament 233
talocalcaneonavicular joint 231
talus 231, 233, 235
temporal artery, superficial 17
temporal bone
CT 78–81
petrous ridge 61, 79
squamous part 25, 61
styloid process 85
zygomatic process 67
temporal lobe 69
temporalis muscle 25
temporomandibular joint 65, 83
tendons, *see specific tendons*
tentorium cerebelli 27, 57
terminology xiii
testicular vein 145
testis 185
thalamus 61
thigh, axial section 212–14
thoracic vertebrae *see vertebrae*
thorax 103–33
axial section
female 122–3
male 102–21
thumb, phalanx 261
thyroid artery, inferior 99
thyroid cartilage 95, 101
thyroid gland 97, 99
tibia 231
condyles 217
lower extremity 235
shaft 226, 227
tibial artery
anterior 226
posterior 229
tibial nerve 215, 223, 229
tibial vein, anterior 226
tibialis anterior 227

- tibialis posterior, tendon 229
- tibiofibular joint
 inferior 228, 229, 233
 superior 221
- tissue-specific MRI techniques x
- tongue 43, 47, 67
- tonsil
 cerebellar 35
 palatine 91
- trachea 99, 101, 105, 111, 127
 carina 131
- transverse colon 153
- transverse foramen 41, 45, 76
- transverse ligament of atlas 39, 63
- transverse process 41, 45
- transverse sinus 55, 85
- transversus abdominis 147
- trapezium 253, 255
- trapezius 103
- triangular fibrocartilaginous complex of wrist 257
- triceps 244
- trigeminal nerve 31
- triquetral 257
- trochanter, lesser 183
- tympanic cavity 79
- tympanic membrane 63, 79
- ulna 251
 distal 252
 olecranon process 246
 radial notch 247, 249
- ulnar nerve 244, 245, 249, 250, 255
- ulnar vessels 244, 255
- umbilicus 165
- uncinate process, pancreas 145
- upper limb 238–61
- ureter 173, 193
- urethra
 female 197, 199
 penile 185
- uterine vessels 193
- uterus 191, 205, 207
 broad ligament 191
- uvula 43
- vagina 193, 195, 197, 199
- vaginal vessels 195
- vagus nerve 33, 105
- vas deferens 175, 179, 185
- vastus intermedius 212
- vastus lateralis 212
- vastus medialis 185, 212, 214, 215
- veins *see specific veins*
- vena cava
 inferior xvii, 121, 145, 167, 187
 superior 127
- venous ligament 135
- ventral nerve roots, cervical 59
- ventral rami
 cervical 97
 lumbar 149, 159
- ventricles (cerebral)
 fourth 29, 49
 lateral 19, 21, 51, 55
 third 21, 23
- ventricles (heart)
 left 117, 119, 123
 right 117
- vertebrae
 cervical 47
 C1/1st (atlas) 37, 39, 59, 63, 87, 101
 C2 *see axis*
 C3 45, 91
 C4 93
 C5 59, 95, 103
- C6 97
 C7 45, 105
- lumbar
 L2 145
 L3 149
 L4 159, 165, 167
 L5 159, 167
- sacral *see sacrum*
- thoracic
 T1–T2 107
 T4–T5 111
 T5 113
 T6 115
 T7 123
 T7–T8 117
 T8–T9 119
 T9 121
 T10 135
 T11 137
 thoracolumbar, T12–L1 141
- vertebral arteries 33, 39, 41, 45, 59, 87, 99
- vertebral canal (spinal canal), cervical 101
- vertebral vein 91
- vestibule of nose 83
- vestibulocochlear (auditory) nerve 31, 61, 79
 MRI 49
- vitreous humour 29
- vocal folds 97, 101
- white matter 15
- wrist 252–9
- zona orbicularis 209
- zygomatic arch 69
- zygomatic process of temporal bone 67